Plant Genetics and Genomics: Crops and Models 4

Hank W. Bass
James A. Birchler *Editors*

Plant Cytogenetics

Genome Structure and Chromosome Function

Springer

Plant Genetics and Genomics: Crops and Models

Volume 9

Series Editor
Richard A. Jorgensen

For further volumes:
http://www.springer.com/series/7397

Hank W. Bass · James A. Birchler
Editors

Plant Cytogenetics

Genome Structure and Chromosome Function

Springer

Editors
Hank W. Bass
Institute of Molecular Biophysics
The Florida State University
Tallahassee, FL, USA
and
Department of Biological Science
Florida State University
Tallahassee, FL, USA
bass@bio.fsu.edu

James A. Birchler, Ph.D
Division of Biological Sciences
University of Missouri-Columbia
MO, USA
birchlerJ@missouri.edu

ISBN 978-0-387-70868-3 e-ISBN 978-0-387-70869-0
DOI 10.1007/978-0-387-70869-0
Springer New York Dordrecht Heidelberg London

Library of Congress Control Number: 2011939210

Preface

This reference book is intended to provide information for students, instructors, and researchers on a range of topics in plant cytogenetics, including classical cytogenetics of plant genomes and chromosomes from structural or functional perspectives, modern molecular cytology and cytogenetics in the twenty-first century, recent methods, and laboratory exercises suitable for undergraduate or graduate instruction. The book is divided into three sections, each with chapters contributed by leading international scholars in the field. Our hope is that these chapters will supplement the many excellent review articles on plant cytogenetics published in the last 10 years and will provide a lasting contribution as a reference book on this important topic.

The first section, "Structure, Variation, and Mapping in Plant Cytogenetics," covers classical cytology, chromosome aberrations, plant B chromosomes, and cytogenetic mapping by conventional or modern DNA or chromatin-fiber-based techniques. The role of plant chromosomal rearrangements, such as deletions, insertions, and rearrangements, is described, and research tools are explored. The production, detection, and impact of aneuploidy in plants are reviewed in relation to gene dosage and breeding through introgressions. In addition, the supernumerary B chromosomes are reviewed, and their potential research applications examined. This section ends with two chapters on the use of cytogenetics to map plant genomes, from historical cytology with G-banding to fluorescence in situ hybridization (FISH) on chromosome spreads. High-resolution FISH-based mapping using DNA or chromatin fibers highlights the state of the art in plant cytogenetic mapping.

The second section, "Function, Organization, and Dynamics in Plant Cytogenetics," covers the basic elements of chromosomes, their behavior in meiosis, and the epigenetic landscape as surveyed by analysis of DNA methylation and histone modifications. Chapters on plant centromeres and plant telomeres are followed by a chapter on meiotic chromosomes, with emphasis on prophase of meiosis I. The last chapter in this section reviews epigenetic code in plants and a comparison of plants and nonplant eukaryotes.

The third section, "Methods, Informatics, and Instruction in Plant Cytogenetics," provides breadth to the book by covering several major methods used by leading

laboratories as well as including chapters on informatics and laboratory exercises for aspiring or practiced instructors. The techniques for chromosome microdissection and descriptions of their use in several plant genetic applications are covered in the first of four chapters in this section. The next chapter provides detailed methods for the use of antibodies in plant cytogenetics, including immunolocalization and the chromatin immunoprecipitation (ChIP) technique. The next two chapters cover advanced methods in FISH, including extended DNA fiber-FISH and in situ PCR. A chapter on plant cytology in genome databases addresses the growing role of online resources and databases in our access to and comprehension of plant cytogenetics in relation to classic genetic and modern genomic resources. Finally, a chapter for instructors is included to encourage the development or continuation of laboratory courses in plant cytogenetics, an activity deemed important for training future plant cytogeneticists. The chapter includes several modular exercises that can serve as a resource for instructors of new or ongoing courses.

Overall, the book is designed to cover many foundational topics in plant cytogenetics, while reviewing modern research and new techniques that represent the current growth and momentum in the field today. Inclusion of methods and instruction provides a distinct advantage to this reference book. We hope it will stimulate new research and facilitate the hands-on transmission of plant cytogenetic knowledge to students and teachers alike.

Finally, we would like to acknowledge the extraordinary editorial assistance of Dr. Anne B. Thistle. We are deeply appreciative of her dedication and attention to detail.

Tallahassee, FL — Hank W. Bass
Columbia, MO — James A. Birchler

Contents

Part III Methods, Informatics, and Instruction in Plant Cytogenetics

Contributors

Ina E. Amarillo Department of Pathology and Laboratory Medicine, David Geffen School of Medicine at UCLA, Los Angeles, CA, USA

Donald L. Auger Department of Biology and Microbiology, South Dakota State University, Brookings, SD, USA

Hank W. Bass Institute of Molecular Biophysics, The Florida State University, Tallahassee, FL, USA

Department of Biological Science, Florida State University, Tallahassee, FL, USA

James A. Birchler Division of Biological Sciences, University of Missouri-Columbia, Columbia, MO, USA

Mariana Carchilan Leibniz-Institute of Plant Genetics and Crop Plant Research (IPK), Chromosome Structure and Function Laboratory, Gatersleben, Germany

Tatiana V. Danilova Division of Biological Sciences, University of Missouri-Columbia, Columbia, MO, USA

R.K. Dawe Department of Plant Biology, University of Georgia, Athens, GA, USA

Debbie M. Figueroa Department of Biological Science, Florida State University, Tallahassee, FL, USA

Jörg Fuchs Leibniz-Institute of Plant Genetics and Crop Plant Research, Chromosome Structure and Function Laboratory, Gatersleben, Germany

Zhi Gao Division of Biological Sciences, University of Missouri-Columbia, Columbia, MO, USA

Fangpu Han Division of Biological Sciences, University of Missouri, Columbia, MO, USA

Department of Molecular Agrobiology, Institute of Genetics and Developmental Biology, Chinese Academy of Sciences, Beijing, China

Lisa C. Harper USDA-ARS-PGEC, Albany, CA, USA

Khwaja G. Hossain Division of Science and Mathematics, Mayville State University, Mayville, ND, USA

Andreas Houben Leibniz-Institute of Plant Genetics and Crop Plant Research (IPK), Chromosome Structure and Function Laboratory, Gatersleben, Germany

Scott A. Jackson Department of Agronomy, Purdue University, West Lafayette, IN, USA

Jiming Jiang Department of Horticulture, University of Wisconsin, Madison, WI, USA

Shahryar F. Kianian Department of Plant Sciences, North Dakota State University, Fargo, ND, USA

Jonathan C. Lamb Department of Biochemistry and Biophysics, Texas A&M University, College Station, TX, USA

Monsanto Corporation, St. Louis, MO, USA

Carolyn J. Lawrence Corn Insects and Crop Genetics Research Unit, USDA-ARS, Iowa State University, Ames, IA, USA

X. Li Department of Plant Biology, University of Georgia, Athens, GA, USA

Shaun P. Murphy Institute of Molecular Biophysics, The Florida State University, Tallahassee, FL, USA

Ingo Schubert Leibniz-Institute of Plant Genetics and Crop Plant Research, Chromosome Structure and Function Laboratory, Gatersleben, Germany

Taner Z. Sen USDA-ARS, 1025 Crop Genome Informatics Lab, Iowa State University, Ames, IA, USA

Eugene V. Shakirov Department of Biochemistry and Biophysics, Texas A&M University, College Station, TX, USA

William F. Sheridan Department of Biology, University of North Dakota, Grand Forks, ND, USA

Dorothy E. Shippen Department of Biochemistry and Biophysics, Texas A&M University, College Station, TX, USA

Robert M. Stupar Department of Agronomy and Plant Genetics, University of Minnesota, St. Paul, MN, USA

C.N. Topp Department of Plant Biology, University of Georgia, Athens, GA, USA

Jason G. Walling Department of Horticulture, University of Wisconsin, Madison, WI, USA

Part I
Structure, Variation, and Mapping in Plant Cytogenetics

Chapter 1
Plant Chromosomal Deletions, Insertions, and Rearrangements

Donald L. Auger and William F. Sheridan

Abstract With the exception of a small subset found within mitochondria and chloroplasts, the genes of plants are arranged along an essential set of chromosomes that are found in the nucleus. Within a species, the placement of genes along the chromosomes is expected to be the same in all individuals. This chapter is a primer on several major aberrations of gene order. These aberrations have consequences not only to the individual that harbors them but also to the population at large in terms of genome evolution. Here, we limit our discussion mainly to the effects on the individual. We are particularly interested in the use of these aberrations as experimental tools and include some discussions to that effect.

Keywords Cytogenetics · Deletions · Deficiencies · Insertions · Duplications · Inversions · Reciprocal translocations · Maize B-A chromosomes

Abbreviations

Ctr	Centromeres
Df	Deficiency
Dp	Duplication
EMS	Ethyl methanesulfonate
FISH	Fluorescent in situ hybridization

D.L. Auger (✉)
Department of Biology and Microbiology, South Dakota State University, Brookings, SD 57007-2142, USA
e-mail: donald.auger@sdstate.edu

W.F. Sheridan
Department of Biology, University of North Dakota, Grand Forks, ND 58202, USA

H.W. Bass and J.A. Birchler (eds.), *Plant Cytogenetics*, Plant Genetics and Genomics: Crops and Models 4, DOI 10.1007/978-0-387-70869-0_1,

In	Inversion
N	Normal
SBE	Starch branching enzymes
TE	Transposable elements

Contents

1.1 Introduction

An analogy useful for explaining genetics to a layperson is to describe the genome as an encyclopedia of instructions necessary to make an organism, in which each gene represents an instruction. Like a traditional encyclopedia, the genome is divided among several volumes or books, which are called chromosomes. Encyclopedias are organized so as to make the data readily available. Chromosomes must be organized as well, so that the cell can access the information correctly and efficiently, when and where needed, but this system of organization is not completely clear. Among members of any given species, the order of genes on a chromosome is generally regarded as canonical – exceptions are considered aberrations. Interestingly, Barbara McClintock, who developed her career and reputation helping to establish this dogma, became one of the earliest dissenters when she described DNA elements capable of being transposed to new sites along the same or even another chromosome. Indeed, extensive sequencing data and other recent techniques are demonstrating that chromosomes are much more labile than was believed even a decade ago. The biological implications of a labile genome affect everything from the individual to the evolution of populations. Here, we offer a primer on some common aberrations from canonical chromosome organization: deficiencies, duplications, and rearrangements.

1.2 Deletions/Deficiencies

Deletion of a chromosomal segment results in a deficiency. When it occurs in a diploid cell, then that cell and its progeny will be hemizygous i.e., it has only one copy of, any gene or locus included in the deficiency. When a whole chromosome is

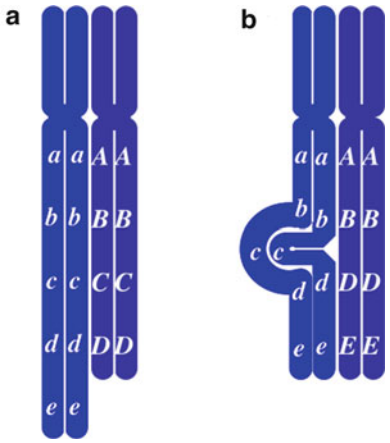

Fig. 1.1 Simple deficiencies. Homologues are lined up as in pachytene with a normal chromosome to the left and deletion chromosome to the right. (**a**) Terminal deficiency. (**b**) Internal deficiency

lost, the resulting cell is said to be monosomic for the remaining homologous chromosome. The word monosomic has also been used to describe larger chromosomal segments that are homologous to large deleted segments. The following discussion focuses on segmental deficiencies rather than losses of whole chromosomes.

A simple case of a chromosomal deficiency is breakage without reunion (Fig. 1.1a). The segment without a centromere is lost quickly in subsequent cell cycles, so the progeny cells are deficient for all loci distal to the breakpoint. In plants with diffuse centromeres, e.g., *Luzula*, a broken piece can be maintained and will not result in a deficiency (Nordenskjold 1961). Internal (interstitial) deficiencies occur when two breaks occur simultaneously in one chromosome, the proximal and distal segments rejoin, and the intervening segment is lost (Fig. 1.1b). McClintock (1931) uses the term "deletion" to describe only this form of deficiency, but the two terms are commonly used interchangeably (see e.g., Burnham 1962, p. 20). Although the deficiency is obvious as shown in Fig. 1.1, small deficiencies are difficult to visualize at pachytene, but larger ones may be visible.

Breaks that occur for unknown reasons are said to occur spontaneously. Breaks can be induced experimentally by means of heat, high-energy radiation, and certain chemicals. Deficiencies seem to be the mode for X-ray-induced mutations. Stadler and Roman (1948), Nuffer (1957), and Mottinger (1970) could not find evidence of base-change mutations when using X-rays; instead these mutations were apparently short deficiencies. Interestingly, the form of induction affects the locations of breaks. Breakages induced by high-energy radiation are more likely to occur in centromeric and heterochromatic regions (Evans and Bigger 1961). X-ray-induced breaks are more likely to be found in heterochromatin both in tomato (Gottschalk 1951; Khush and Rick 1968) and in maize (Longley 1961). In maize exposed to nuclear explosions, the bias toward breaks in heterochromatic regions was not as pronounced (Longley 1961), indicating that fast neutrons are more efficient in producing breaks in euchromatin.

Deficiencies can also be induced by one of the several genetic conditions. For example, in maize, an allele of the *r1* locus, called *r-X1*, induces deficiencies but is better known for inducing monosomies and trisomies in maize (Weber 1973; Lin et al. 1990; Weber and Chao 1994). This allele is itself a small deletion and can only be transmitted maternally. Deficiencies can also result from transposable elements (McClintock 1950) that are oriented in specific ways on a chromosome (Weil and Wessler 1993; English et al. 1995; Martínez-Férez and Dooner 1997). Another source of deficiencies is uneven crossovers or crossovers involving chromosomes with rearrangements. As these conditions are also associated with duplications, they will be explained later.

The rates of spontaneous breaks and other chromosomal abnormalities are high in various interspecific hybrids, where they seem to act as genetic barriers (Ehrendorfer 1959; Endo 1990). For example, certain chromosomes in some wild relatives of wheat possess one or more factors that induce chromosomal breakage of common wheat (*Triticum aestivum* L.) chromosomes (Endo 1990). The chromosomes that bear these factors are called Gc (gametocidal) chromosomes because their effect takes place immediately after meiosis. They somehow condition meiosis so that any of the spores that lack the Gc chromosome undergo chromosomal breaks, which are usually lethal to the gametophyte. The chromosomal aberrations found in surviving gametophytes can be transmitted and stabilized in the subsequent sporophyte generation. As a result, Gc chromosomes have been used as a tool for genetic analysis and manipulation (Endo 2007).

Deficiencies are often lethal in the gametophyte generation and so cannot be transmitted to a subsequent generation, especially in diploid plants. For example, small deficiencies are lethal to the gametophyte of *Vicia faba* L. (Schubert and Reiger 1990). In a study on tomato, the only deficiencies transmitted were smaller deletions in heterochromatin; no euchromatic deficiencies would transmit (Khush and Rick 1967). In maize, McClintock (1944) found that no deficiencies of the short arm of chromosome 9 (9S) were transmitted though the male, but a loss of the distal one-third of 9S was transmitted through the female gametophyte. Later, several very small deletions on 9S involving *shrunken1* (*sh1*) and *bronze1* (*bz1*) were found that were transmissible through both female and male and were also homozygous viable in the sporophyte (Mottinger 1970). Stadler (1933, 1935) described a haploviable deficiency in maize. It was a relatively large terminal deficiency of the long arm of chromosome 10. Although this deficiency could not be transmitted through the male, it could be through the female. It affected the phenotype of both the male and female gametophyte. About half of the pollen grains from plants heterozygous for this deficiency were small but starch-filled. The embryo sacs were also smaller, but seed set was nearly normal. The rule appears to be that female transmission of a deficiency is more likely than male transmission. Deficiencies transmissible in both egg and pollen are rare (McClintock 1944; Mottinger 1970; Patterson 1978). In polyploid plants, the situation is different, ostensibly because the gametophyte carries multiple homologues or homeologues. For example, about 67% of wheat deficiencies are transmitted normally and can be made homozygous (Endo and Gill 1996).

Deficiencies can also affect the phenotype of the sporophyte plant. The effects depend upon which loci are deleted, what alleles remain in a hemizygous condition, and whether the deficiency is transmissible to future generations. Homozygous deficiencies in maize have been demonstrated to yield phenotypes like those of recessives (Creighton 1937; McClintock 1938a, b, 1941, 1944). Indeed, transmissible deficiencies crossed with known recessive alleles result in expression of the recessive allele. This phenomenon, traditionally called pseudodominance, is the basis for correlating genetic maps, which are based on linkage, with cytological maps, which are based on observations of the chromosomes. Deficiencies have been used as a tool for mapping genes not only in maize but also in other plants such as tomato (Rick and Khush 1961; Khush and Rick 1967, 1968). More recently, deficiencies have been employed for the physical mapping of molecular traits and quantitative traits (Gill et al. 1996; Sutka et al. 1999; Tsujimoto et al. 2001).

1.3 Insertions/Duplications

Insertions involve the transposition of a chromosomal segment to another position on the same chromosome or onto a different chromosome. An insertion without concomitant deletion of that chromosomal region results in duplication and alters the copy number of the duplicated region. Three examples of simple insertions are portrayed in Fig. 1.2, each paired with a progenitor chromosome. Figure 1.2a shows a tandem duplication of the segment *AB*, Fig. 1.2b shows an inverted duplication involving the same segment, and Fig. 1.2c an insertion of a segment that originated from a nonhomologous chromosome. In the heterozygous condition, large insertions are visible at pachytene as unpaired loops or bulges, but small insertions may be undetectable. Of course, chromosomes homozygous for an insertion would be expected to align normally. Segmental duplications seem to be quite common in plants and are often fixed in populations. Different studies have estimated that from 15 to 62% of the rice genome consists of segmental duplications (Vandepoele et al. 2003; Paterson et al. 2004; Wang et al. 2005; Lin et al. 2006).

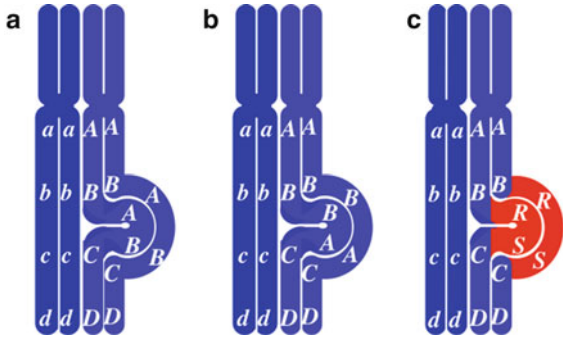

Fig. 1.2 Simple insertions. Homologues are lined up as in pachytene with normal chromosome to the left and insertion chromosome to the right. (**a**) Tandem duplication. (**b**) Inverted duplication. (**c**) Insertion from nonhomologous chromosome

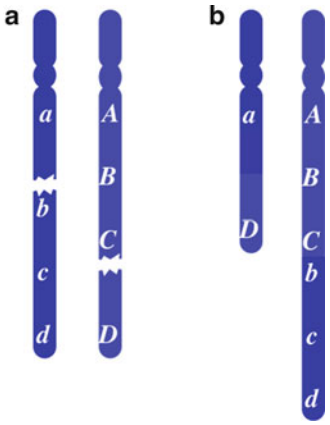

Fig. 1.3 Tandem repeat: simultaneous breaks. (**a**) Breaks in homologues or sister chromatids. (**b**) Ligation with exchange

Several mechanisms for insertions have been proposed. The most direct production of a tandem repeat results from the simultaneous breakage of homologues (Fig. 1.3) or sister chromatids at different locations along the chromosome and exchange and ligation of the broken pieces (Beard 1960). Another results from unequal crossovers (Fig. 1.4), in which nonhomologous loci of homologous chromosomes cross over, a process facilitated by the presence of similar sequences in the two segments. The presence of similar sequences could result from an earlier duplication or from the presence of repetitive sequences such as transposable elements. Note that, if a duplication is produced by either of these two mechanisms, a concomitant deficiency will also result (Figs. 1.3b and 1.4b).

Some models involving aberrant transposition of transposable elements have been developed, and the evidence is strong that these events actually occur (English et al. 1995; Zhang and Peterson 1999). Normally, DNA transposable elements (TE) are flanked by terminal inverted repeats (Fig. 1.5). They are mobilized by a transposase that cleaves the DNA immediately flanking the inverted repeats, causing those flanking ends to be joined to each other. The excised TE is then reinserted at another chromosomal location – the chromosome is cleaved at that location, and the ends of the TE are joined to the ends of the freshly cleaved DNA. In some cases, TE transposition is abnormal, and relatively large chromosomal regions can be rearranged. One example is portrayed in Fig. 1.6, where the terminal repeats are in the same orientation rather than the inverted; this situation can arise when one TE is inserted into another of its own kind. If the transposase uses one terminus from each of the sister chromatids (Fig. 1.6a), the result will be bridging of the sister chromatids at the point of excision (Fig. 1.6b). The excised termini, along with the distal chromosomal regions, are subject to transposition to a new chromosomal location. If the integration site is on the same chromosome arm, proximal to the excision site, it will produce one chromatid with an inverted repeat and another with a deficiency (Fig. 1.6c). Transposition to any other chromosomal region would result in major chromosomal imbalances that are unlikely to be heritable.

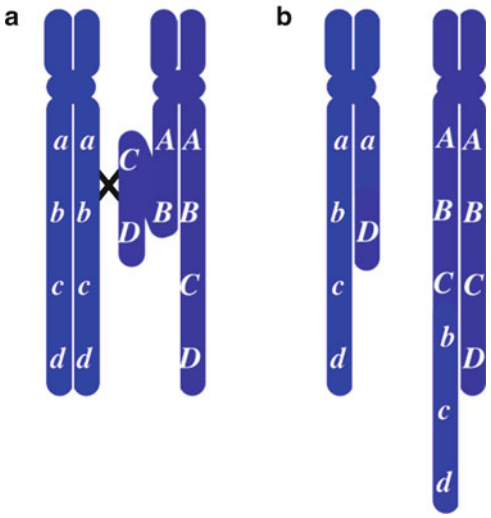

Fig. 1.4 Tandem repeat: uneven crossover. (**a**) Homologues with crossover in nonhomologous region. (**b**) Products of first meiotic division

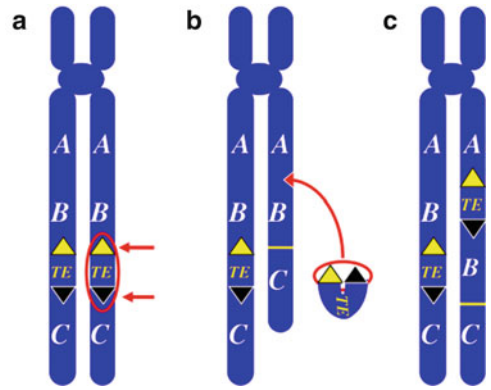

Fig. 1.5 Normal transposition of a transposable element (TE). In this cartoon, the TE is very large relative to the chromosomes. (**a**) Sister chromatids with transposase excising TE at complementary inverted repeats. (**b**) Excised TE with donor locus ligated (*yellow line*). Insertion of TE into new locus. (**c**) Resulting chromosome following transposition of the TE from one location to another within a single sister chromatid

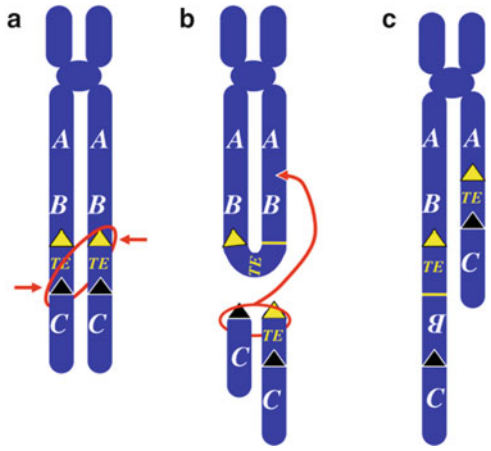

Fig. 1.6 Inverted duplication: transposon mediated. (**a**) Sister chromatids with abnormal DNA transposons having terminal repeats in direct orientation rather than inverted. In this case two ends from sisters interact in transposition. (**b**) Excision site anneals; transposing ends attack proximal site. (**c**) Resulting deletion/duplication with inverted repeat

Insertions such as those portrayed by Fig. 1.2c are more difficult to explain but appear to be common. Pairing between nonhomologous chromosomes in haploid plants of *Antirrhinum majus* L. (Reiger 1957) and *Oenothera blandina* de Vries (Catcheside 1932) indicates the existence of larger interchromosomal duplications. Smaller insertions of one or few loci are also detected. Notable are reports of insertions of organellar DNA into the nuclear chromosomes of *Arabidopsis* (Lin et al. 1999; Stupar et al. 2001), rice (International Rice Genome Sequencing Project 2005), and maize (Lough et al. 2008). The study in maize is especially interesting because it suggests that the insertion of mitochondrial DNA into the nuclear genome is frequent and ongoing (Lough et al. 2008).

Duplications tend to be less deleterious than deficiencies and can regularly be transmitted through the female gametophyte. Male transmission is often inhibited, ostensibly by the inability of aneuploid pollen to compete with euploid pollen (Buchholz and Blakeslee 1932). Whether or not a duplication can be transmitted through the pollen seems to be related to size. Transmission of large duplications and deficiencies typically fails (see e.g., Rhoades and Dempsey 1953; Patterson 1978), but some large duplications are known to be transmitted (Carlson and Curtis 1986; Auger and Birchler 2002). Duplications whose transmission through pollen fails probably include genes that have a dosage-sensitive effect that inhibits the efficient elongation of the pollen tube (Auger and Birchler 2002). Therefore, the longer the duplicated region, the more likely it is to possess such a factor.

A duplication can cause a pollen grain to be noncompetitive because it causes the pollen grain to be essentially aneuploid. Aneuploidy is often associated with abnormal development or function, and this phenomenon is known as an aneuploid syndrome. To understand why aneuploidy might have such effects, consider that, with the exception of organelles, all of the necessary structural and regulatory genes are distributed among an essential complement of chromosomes. For example, all the genes of tomatoes are distributed among 12 chromosomes ($n = 12$). Euploidy is the state of having exact complementary sets. A cell that possesses only one copy of each member of the essential complement is called monoploid (1n) and is considered euploid. Having exactly two copies of each member of the essential complement is diploidy (2n) and is also euploid. The same can be said for any multiple (3n = triploid, 4n = tetraploid, etc.) of the monoploid set as long as it is a perfect multiple; different species have optimal ploidy levels for both the sporophyte and the gametophyte generations. If one (or more) chromosome has a copy number different from those of the other members of the essential complement, the cell is said to be aneuploid. For example, if one chromosome is missing in an otherwise diploid cell ($2n - 1$), the cell is said to be monosomic because one of the essential chromosomes is represented by only one copy. Trisomy ($2n + 1$) describes the condition in which one chromosome exists as three copies in an otherwise diploid cell. Although aneuploidies are aberrant conditions, they are mitotically stable. Therefore, an aneuploid zygote will grow into an organism in which essentially all the cells retain the aneuploidy, and the resulting organism is described as being aneuploid.

Aneuploidy generally has a negative effect on the development and vigor of an individual. A gene that is in a duplicated or deleted segment may yield an amount

of gene product that is altered relative to other gene products in the same cell. Although stoichiometric changes in the products of structural genes, such as enzymes, may contribute to aneuploid syndromes, the copy numbers of regulatory genes appear to be most important (Guo and Birchler 1994). Regulatory proteins typically interact with a collection of target genes, thereby amplifying the potential of regulatory genes to affect the phenotype. To the extent that any one of the downstream products being regulated is rate limiting in some process, alteration of the expression of this downstream product can affect the phenotype. The rate-limiting effects of a deficiency are easier to appreciate, but duplications also affect development and reduce vigor. Duplications may have this effect because many regulatory factors act to down-regulate target genes.

Another effect of duplications is that they can alter the rules of genetic segregation. For example, in *Pisum*, five different genes were shown to behave as duplicates with 15:1 ratios or 9:7 ratios (Lamprecht 1953). Ancient duplications can confound both forward and reverse genetic analysis. Consider mutation analysis, which remains a powerful tool for the analysis of gene function. When genes are duplicated, the ability to detect mutant alleles is exponentially diminished. Spontaneous mutations occur at a rate of about 10^{-6} mutations per locus tested (Walbot 1992), whereas ethyl methanesulfonate (EMS)-induced mutation rates can range around 10^{-3} mutations per locus tested (Neuffer et al. 1997). Clearly, having to knock out duplicated genes simultaneously with EMS would lower detection rate below the spontaneous mutation rate of a single gene. An example in which duplicated genes were detected is *orange pericarp* (*orp*) in maize (Wright and Neuffer 1989). The phenotype, in which the pericarp reacts with indole emanating from the mutant endosperm, occurs when two genes, *orp1* and *orp2*, are homozygous for the mutant alleles. Both genes encode the β subunit of tryptophan synthase, but they are found on nonhomologous chromosomes (Wright et al. 1992). The duplication of the *orp* genes appears to have resulted from an ancient polyploidization (Ma et al. 2005). Although the mutations were found in an EMS screen, only the mutation in *orp2* was EMS-induced (Wright and Neuffer 1989). Fortunately, the mutation in *orp1* was previously segregating in the northern flint lines used in the study (Wright 1991).

Gene duplications are important evolutionarily in that they allow for mutations to accumulate that will result in new functions (neofunctionalization) or more specialized functions (subfunctionalization) of one or the other paralogue (Paterson et al. 2004; Wang et al. 2005). Examples of the latter are genes for starch branching enzymes (SBE). Unbranched starch, amylose, becomes branched when enzymes break α-1,4 glycosidic bonds of the linear starch molecules and reattach the starch fragments using an α-1,6 glycosidic bond. Two classes of SBEs are known in plants: one (SBEI) acts preferentially on amylose directly and the other (SBEII) on the partially branched starch (Morell et al. 1997). Cereals have two isoforms of SBEII, which are further subfunctionalized. In maize and rice, SBEIIb is more important for the accumulation of branched starch, amylopectin, in the endosperm (Yamanouchi and Nakamura 1992; Gao et al. 1997), whereas SBEIIa is more active in the leaves. In wheat, the SBEIIa isoform is the one more highly accumulated in the endosperm (Rahman et al. 2001).

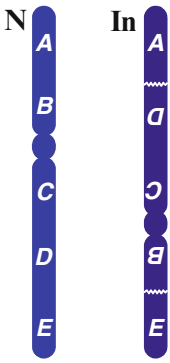

Fig. 1.7 Pericentric inversion. *N* normal (progenitor) chromosome; *In* inversion

1.4 Chromosomal Rearrangements

Chromosomal breakage does not necessarily lead to either a deficiency or a duplication but instead may result in a chromosomal rearrangement in which no chromatin is lost or gained. This process involves two simultaneous breaks followed by reattachment of the segments but not with the original partners. The nature of the chromosomal rearrangement depends on whether the two breaks occur in one chromosome, producing an inversion, or in two different chromosomes, producing a reciprocal translocation. We will first consider inversions.

1.4.1 Inversions

Inversions were first detected in *Drosophila* as "crossover reducers"; certain chromosomes were found to reduce recombination dramatically when heterozygous with their normal homologues. They were given the name inversions after the discovery that the regions between the breaks were inverted relative to the normal progenitor chromosome (Sturtevant 1926).

When two breaks occur on opposite arms of a chromosome, the segments may be reattached so that the centric fragment is reincorporated as an inversion (Fig. 1.7). These cases, in which the centromere is flanked by the breakpoints and is within the inverted region, are known as pericentric inversions (Muller 1940). In Fig. 1.7, the centromere is indicated by a constriction, and loci are designated by letters. Note that no chromatin is lost but that the loci between the breaks have been reattached in inverted positions relative to those of the progenitor chromosome. A pericentric inversion can shift the centromere position and therefore arm ratio. In some cases, the shift is sufficient to allow for the cytological identification of these chromosomes in mitotic cells.

Alternatively, when two breaks occur in one arm of a chromosome, the segments can reattach so that the fragment flanked by the two breaks is incorporated as an

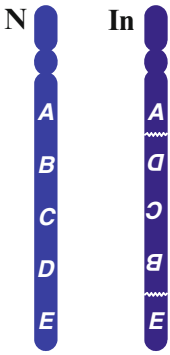

Fig. 1.8 Paracentric inversion. *N* normal (progenitor) chromosome; *In* inversion

inversion (Fig. 1.8). These cases, in which the centromere is outside the inverted region, are known as paracentric inversions (Muller 1940). Again, no chromatin was lost, but the loci between the breaks become inverted relative to those on the progenitor chromosome. In paracentric inversions, the arm ratios remain unchanged.

Because no chromatin is lost, inversions typically have no effect on gene expression. Exceptions are cases in which the breakpoints occur within a gene or in which the rearrangement causes a position effect. Ostensibly, a position effect arises when a gene is placed adjacent to chromatin that will have a *cis*-acting effect on gene expression, most probably heterochromatin. Position effects are apparently rare in plants, although *O. blandina* (Catcheside 1939, 1947) is often cited as an example. Nevertheless, inversion chromosomes can have genetic consequences when they are heterozygous with normal chromosomes. Although paracentric inversions appear to be more common, we will first consider a pericentric inversion because the genetics are more straightforward.

Inversions behave well in mitosis, but in meiosis homologous chromosomes must pair and align. Inversions cannot properly align linearly with their normal homologues. Compare the normal (N) and pericentric-inversion (In) chromosomes portrayed in Fig. 1.7. The letters in the inverted region are shown upside down to emphasize that loci are not just in a different position but are also in the opposite orientation. For the chromosomes to be paired in a completely linear fashion, either the region between the breakpoints or the ends must be paired to nonhomologous regions. Indeed, nonhomologous pairing is common when the inverted region is relatively small (McClintock 1932). Alternatively, either the distal or inverted regions may remain unpaired, i.e., asynaptic (McClintock 1933). Asynapsis between inversions and their normal homologues also appears to be common (Doyle 1994). Clearly, neither paired nonhomologous regions nor asynaptic regions are subject to genetic recombination, as is reflected by a marked decrease in expected genetic map distances within and immediately adjacent to the inverted region. Interestingly, inverted segments may increase crossover rates elsewhere on the chromosome or even other chromosomes (Stephens 1961). Nonhomologous pairing and asynapsis are not the only causes of map distortion. To see why, we must consider how inversions can align with normal chromosomes with high fidelity.

Fig. 1.9 A pericentric inversion paired with a normal homologue. The centromere is located between *B* and *C*. A crossover is indicated between loci *C* and *D*

When the inverted region is large, the alignment mechanism commonly causes the two chromosomes to pair in a way that is not linear, in what McClintock (1931, 1933) called a reverse loop (Fig. 1.9). In meiosis, each homologue has two chromatids, and in Fig. 1.9, these are separated and distorted so that they can be more easily traced. The centromeres are again shown as constrictions, but the centromeres of sister chromatids are bound to each other. The loci of the normal chromosome are shown with lower-case letters. When a loop configuration is formed in prophase I of meiosis, essentially all loci are correctly aligned and are eligible for genetic crossovers. The exceptions are the inversion breakpoints and the corresponding loci of the normal homologue; the reasons will be explained later in the discussion of reciprocal translocations.

Although the loop formation allows for homologous pairing and recombination along the lengths of the chromosomes, only the crossovers that occur outside the inverted region are readily recovered, because those outside the inverted region result in balanced exchanges just as they do with two normal chromosomes. A crossover between the breakpoints, however, will result in an unbalanced exchange – the two recombinant chromatids will each have a duplication (Dp) and a deficiency (Df). Note that Fig. 1.9 portrays a crossover between loci *C* and *D*. When these four chromatids are separated in meiosis II, they yield one N chromosome, one In chromosome, and two alternative Dp-Df chromosomes (Fig. 1.10). Monoploid spores that possess the Dp-Df chromosomes typically abort. Indeed, pollen and ovule abortion are characteristic of plants that are heterozygous for inversions. Even in the case of reverse loops, therefore, where the degree of homologous pairing is high, the occurrence of a crossover in the inverted region results in recombinant chromatids that are usually lost as a result of gametophyte abortion, and the result is distortion of map distances.

The proportion of gametophytes that abort varies according to the rate of crossovers in the inverted region (Doyle 1994). Some inversion heterozygotes have nearly 50% pollen and ovule abortion, whereas in others abortion rates are hardly detectable. For example, pollen abortion was reported to be nearly 50% in two pericentric inversions in *Vicia faba* (Sjodin 1971) and four pericentric inversions in *Scilla scilloides* (Noda 1974). One determinant appears to be the proportion of linear to

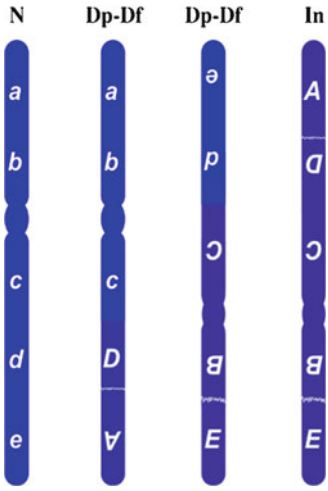

Fig. 1.10 Meiotic products from a single crossover within a pericentric inversion loop

looped meiotic pairings. Recall that linear bivalents are possible only when pairing of the inverted region is nonhomologous, precluding crossovers and Dp-Df products. Such nonhomologous pairing appears to be common for some inversions (see e.g., McClintock 1931, 1933). In some cases, the inverted region may fail to pair at all with the normal homologue (asynapsis; Russell and Burnham 1950), again precluding crossover and production of Dp-Df recombinant chromosomes.

Double crossovers within the inverted region of pericentric inversions can occur but should have little effect on rates of abortion. Two-strand double crossovers produce no Dp-Df chromosomes, whereas four-strand double crossovers cause all four chromosomes to be Dp-Df, and three-strand double crossovers have the same result as single crossovers, i.e., one N, one In, and two Dp-Df (Burnham 1962). Any crossovers that take place outside the inverted region and are concomitant with either single or double crossovers within the inverted region have no effect on the generation of Dp-Df chromosomes.

In maize, pericentric inversion heterozygotes experience abortion rates in the male (pollen) and female (embryo sacs) gametophytes that are generally similar (Anderson 1941; Morgan 1950). The slightly higher rates of male abortion are attributed to the higher crossover rates in male meiosis for the region in question (Rhoades 1941; Morgan 1950). Pollen abortion can be used as a dominant phenotypic trait to identify inversion heterozygotes in gene mapping. Because of the issues of pairing discussed above, map distances will probably be greatly distorted, but information about the placement of the breakpoints relative to other genetic markers can be obtained. A strong reduction in crossovers indicates that a marker is within or near the inversion, whereas considerable recombination indicates that the marker is outside the inversion (Burnham 1962). Although inversions have often been used to map genes (e.g., by Morgan 1950; Russell and Burnham 1950; Rhoades and Dempsey 1953; Ekberg 1974), more recently, extensive mapping projects (e.g., by Bonierbale et al. 1988; Mickelson-Young et al. 1995; Livingstone et al. 1999; Dubcovsky et al. 1996) have commonly revealed previously undetected inversions.

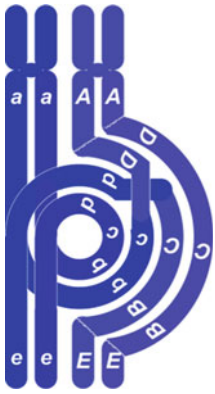

Fig. 1.11 A paracentric inversion paired with a normal homologue. The centromere is located above *A*. A crossover is indicated between loci *C* and *D*

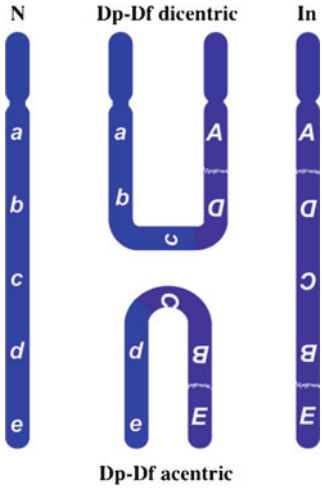

Fig. 1.12 Meiotic products from a single crossover in a paracentric inversion loop

The behavior of paracentric inversions as heterozygotes is essentially the same as that of pericentric inversions, but the genetic consequences are somewhat different. The issues involving nonhomologous pairing, asynapsis, and the formation of a reverse loop are similar. The difference is the consequence of crossovers within a reverse loop. Again, Fig. 1.11 portrays all four chromatids in a separated and distorted fashion to facilitate tracing of the products of a crossover between the *C* and *D* loci. Not only will the two chromatids that are generated by a single crossover be Dp-Df, but also one will have no centromeres (acentric) and the other will have two centromeres (dicentric) (Fig. 1.12). The acentric fragment is typically lost in meiosis I. The dicentric is also Dp-Df, and because the centromeres of the dicentric are from different homologues, they segregate at anaphase I, causing the chromatin between them to bridge and ultimately break. Although the spores that receive the broken remnants of the dicentric typically abort, a deficiency may occasionally be transmissible through the female gametophyte.

When only double crossovers within the inverted region are considered, the results are analogous to those of pericentric inversions. Two-strand double crossovers yield no Dp-Df products, three-strand double crossovers yield products similar to those of a single crossover, and four-strand double crossovers yield two Dp-Df acentrics and two Dp-Df dicentrics. In all of these cases where dicentrics are formed, bridging takes place in anaphase I.

With one exception, crossovers outside of the inverted region have no effect on the generation of acentric and dicentric Dp-Df chromosomes. The exception is the case in which the crossover occurs in the region between the inverted region and the centromere, i.e., the interstitial region. In Fig. 1.11, the *A* locus is located in the interstitial region. A crossover in the interstitial region occurring concomitantly with one or more crossovers within the inverted region creates the opportunity for bridging at anaphase II. Anaphase I bridges result because dicentrics have two centromeres from different homologues, which separate at anaphase I. Depending on which strands are involved in multiple crossovers, a crossover in the interstitial region (not shown) produces a dicentric in which the two centromeres are from sister chromatids; these are separated at anaphase II. More complete discussions of the products of multiple crossovers in paracentric inversions are given by Burnham (1962) and Moore (1976).

The level of pollen abortion experienced by paracentric inversion heterozygotes, like that of pericentric inversions, is expected to be a function of the amount of crossing over that takes place within the inverted segment. Interestingly, in maize the level of ovule abortion is often much less than that of pollen abortion. The explanation appears to be the bridges that occur at anaphase I (Beadle and Sturtevant 1935). In plants, female meiosis tends to produce megaspores in a linear fashion. The embryo sac of maize, like many plants, is monosporic in development; i.e., it develops from just one of the spores (Maheshwari 1950). Monosporic embryo sacs develop from one of the outermost megaspores: in maize, the megaspore most distal to the micropyle. Bridges are believed to cause the Dp-Df chromosomes to be oriented toward the center of the pole at the first division, such that they will be nonrandomly included in the centermost megaspores after the second division. Therefore, the megaspore that develops into the embryo sac will nonrandomly receive either the N or an In chromosome that was not Dp-Df. In male meiosis, the nonrandom distribution of Dp-Df chromosomes is not expected to occur, because divisions are not linear and, more importantly, all four microspores develop into pollen grains.

The use of inversions for genetic analysis and manipulation has been limited, probably by the difficulty of their use. For example, cytological verification of inversions by observation of bridges at anaphase is much easier than observations of reverse loops at pachytene. Even so, bridges and acentric fragments are no guarantee of an intact inversion. Some inversions are capable of producing Dp-Df chromosomes that can be transmitted, though usually through the female. Moore (1976) indicates that bridges and fragment should not be indiscriminately accepted as proof of paracentric inversion heterozygosity. Bridges and acentrics can emerge from breakage and repair in meiosis (Rees and Thompson 1955; Lewis and John 1966). Therefore, care must be taken to observe that bridges and fragments are of uniform sizes.

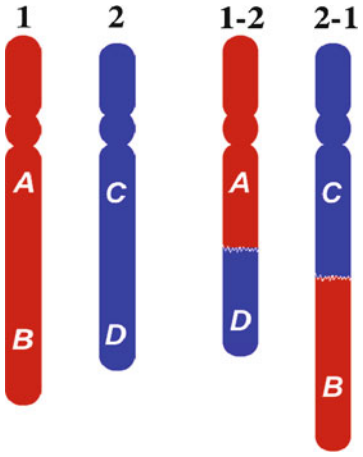

Fig. 1.13 Reciprocal translocations (1-2 and 2-1) with normal progenitors (1 and 2)

1.4.2 Reciprocal Translocations

As explained earlier, reciprocal translocations result from the breakage of two nonhomologous chromosomes and exchange of the broken pieces. Reciprocal translocations are also called translocations, segmental chromosome interchanges, or interchanges (Burnham 1956). Figure 1.13 portrays two nonhomologous chromosomes, numbered 1 and 2. Next to them are two reciprocal translocations, numbered 1-2 and 2-1. The 1-2 chromosome was generated by a break in the long arm of chromosome 1; the lost segment was replaced by a segment produced by a break in the long arm of chromosome 2. The 2-1 chromosome was reciprocally generated. Typically each member of a translocation is designated by the number of the chromosome from which the centromere was derived followed by the number of the chromosome from which the translocated piece was derived. Here we separate the two numbers with a hyphen, but often the second number is presented as a superscript or separated from the first by a comma, e.g., 1^2 and 2^1 or 1,2 and 2,1.

Like the other chromosomal abnormalities, reciprocal translocations can arise spontaneously in a population, or they can be induced by chemical mutagens or irradiation. Other contributory factors that have been noted are age of seed (Gunthardt et al. 1953) and genetic conditions (Beadle 1937; McClintock 1950). The most extensive collection of reciprocal translocations is probably that in maize (Longley 1961). These translocations were induced by various types of radiation, notably that from nuclear-blast testing in the Pacific after the World War II. More than 800 of these translocations still exist and are available through the Maize Genetics Cooperation Stock Center (http://maizecoop.cropsci.uiuc.edu/).

Reciprocal translocations, like inversions, produce no loss of chromatin, so they also have no effect on phenotype. In plants, mutations at the breakpoints, e.g., a chlorophyll mutation in barley (Tuleen 1962), or position effects, e.g., color variegation in *Oenothera* (Catcheside 1939, 1947), are relatively rarely detected. In one experiment, 13 X-ray-induced translocations produced no overt dominant or recessive

mutations, although a number of significant differences for quantitative traits were apparent (Roberts 1942). The low frequency of concomitant mutations in plants may be due to the immediate loss of deleterious mutations at the gametophyte stage (Burnham 1962). In contrast, the majority of translocations in *Drosophila* are lethal or extremely detrimental when homozygous (Bridges and Brehme 1944). Even without mutations, reciprocal translocations have genetic consequences, especially when heterozygous with normal progenitors. The first genetic consequence is new linkage relationships. Note that in the example above (Fig. 1.13), the *A* and *B* loci are linked on the normal chromosome 1 and *C* and *D* are linked on the normal chromosome 2. On the translocations, A is no longer linked with *B* but instead with *D* on the 1-2 translocation chromosome. On the 2-1 chromosome, *C* is linked with *B*. Note also that the dimensions of the chromosomes have changed. Cytologists use the overall length and the short arm/long arm ratio of mitotically and meiotically condensed chromosomes to aid in identification. In Fig. 1.13, the translocation chromosomes clearly differ in both. Unfortunately, the lengths and arm ratios often are not sufficiently reliable for chromosome identification, especially in mitosis. More recently, fluorescent in situ hybridization (FISH) techniques have made chromosome identification more reliable (see e.g., Kato et al. 2004), and these techniques have been employed to identify newly generated reciprocal translocations (Zhang et al. 2009).

In plants that are homozygous for reciprocal translocations, meiosis proceeds normally because each translocation chromosome has a structural homologue with which to pair. The story is different for translocation heterozygotes. At meiosis, reciprocal translocations cannot be correctly paired with normal chromosomes in a linear fashion. Correct pairing requires that one member of the translocation pair with the segments of the normal chromosomes with which it shares homology and that the other pair with the remaining segments of the same two normal chromosomes. Instead of a linear bivalent, the chromosomes form a cross-shaped quadrivalent (Fig. 1.14; again the four chromatids are laid out in a distorted fashion to allow easier tracing). In Fig. 1.14, the chromosomes are identified by the numbers adjacent to the centromeres; letters indicate genetic loci. For the following discussion, the spindle poles are to the left and right.

Plants heterozygous for reciprocal translocations experience pollen and ovule abortion, but the mechanics are different from those of inversions. The two reciprocal members of a translocation are not considered Dp or Df as long as they are together in the same cell. At meiosis, the opportunity arises for the two reciprocals to segregate to different daughter cells and segregate with one of the normal homologues. The daughter cell that receives such a combination will be Dp-Df and will nearly always abort. For a spore produced by meiosis to avoid being Dp-Df, it must receive either both reciprocal members of the translocation or two normal chromosomes. This pattern would result at anaphase I if the 1-2 translocation chromosome at the upper right segregated with its 2-1 reciprocal partner at the lower left and the normal chromosome 1 at the upper left cosegregated with normal chromosome 2 at the lower right (Fig. 1.15). This is called alternate segregation; when chromosomes are drawn out on a flat plane, the alternate nonhomologous centromeres cosegregate.

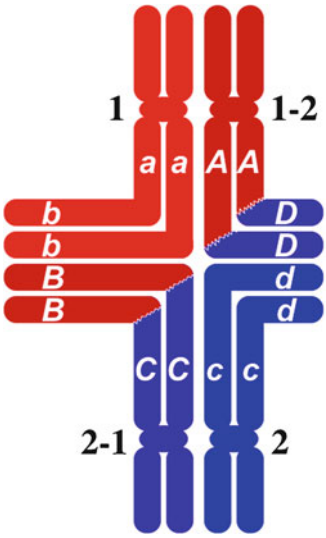

Fig. 1.14 Reciprocal translocation paired with normal homologues

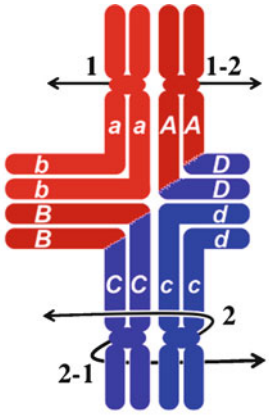

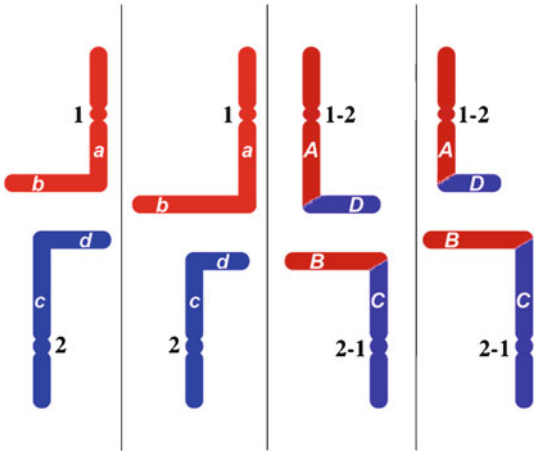

Fig. 1.15 Alternate segregation and products (no crossovers)

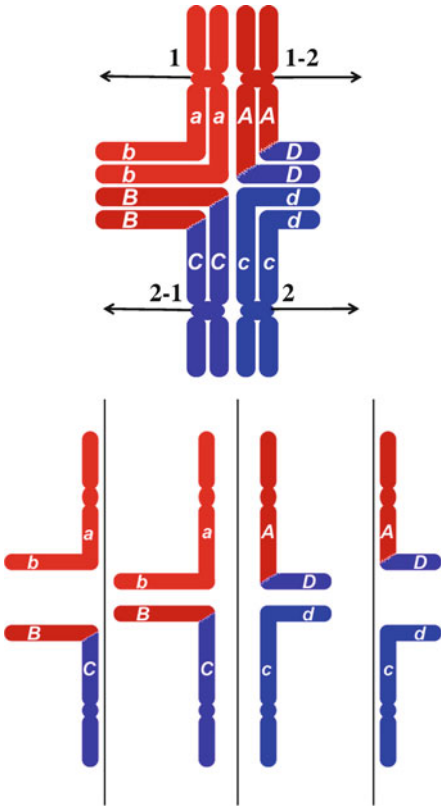

Fig. 1.16 Adjacent I segregation and products (no crossovers)

In meiosis II, the sister chromatids separate and are deposited in four daughter cells. The chromosomes of the daughter spores are separated by vertical lines. Note that each spore has a balanced complement.

Consider the result if the two leftmost chromosomes (1 and 2-1) segregated to one pole and the two to the right (1-2 and 2) segregated to the other pole (Fig. 1.16). This pattern is called adjacent segregation or, more precisely, adjacent I segregation. This time each spore is balanced only to the breakpoint. Distal to that, each spore is Dp for one chromosome and Df for the other, a configuration that would result in abortion of the gametophyte.

Another segregation pattern is possible: adjacent II, in which the homologous centromeres cosegregate. This pattern is easier to imagine if the cartoon of the quadrivalent chromosomes is turned sideways (Fig. 1.17). In this case, normal chromosome 1 cosegregates with the 1-2 translocation and normal 2 with 2-1. The failure of homologous centromeres to segregate may seem odd, but the spindle mechanism at meiosis I seems to function to separate bivalents, which are homologues. This machinery apparently has difficulty distinguishing homologous centromeres from nonhomologues in these quadrivalents. Interestingly, crossovers in either interstitial segment appear to eliminate adjacent II segregation (Burnham 1962, p. 76).

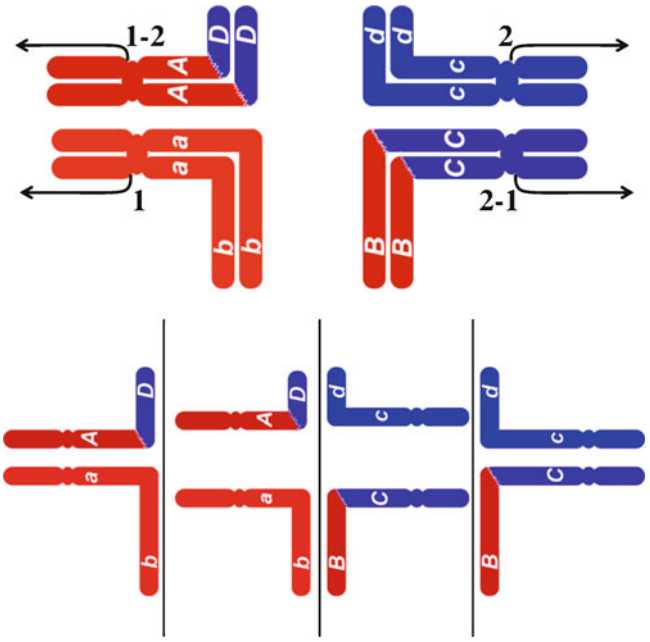

Fig. 1.17 Adjacent II segregation and products (no crossovers)

The interstitial segment of a translocation is the segment between the centromere and the breakpoint. In our example of the 1-2 chromosome, the *A* locus is situated in that segment; on the 2-1 chromosome the *C* locus is located there. Therefore, the length of the interstitial segment is an important determinant of the rate of adjacent II segregation. Short interstitial segments are associated with higher rates of adjacent II segregation and longer segments with lower rates. Adjacent II segregation results in spores that are also Dp and Df. Figure 1.17 shows the meiotic products expected to result in the absence of crossovers between markers and centromeres. The difference here is that the spores are balanced for the chromosomal segments *distal* to the breakpoint and Dp-Df for the *proximal* regions, i.e., the segments that include the centromeres. Again, all four spores are expected to abort.

Diploid plants that are heterozygous for translocations are typically semisterile; i.e., both pollen and ovules experience about 50% abortion (Burnham 1962). Although only one type of alternate segregation and two types of adjacent are apparent, the ratio of adjacent to alternate is usually 1:1, because the random distribution of the two pairs of kinetochores at anaphase generally results in an equal rate of alternate and adjacent segregations (Endrizzi 1974; Rickards 1983). That alternate segregation (Fig. 1.15) and adjacent I segregation (Fig. 1.16) are alternatives to each other is easier to imagine, but alternate segregation is also the alternative to adjacent II segregation, as is clear from a reexamination of Fig. 1.17. In this cartoon of adjacent II segregation, reversing the polarity of movements of chromosomes 1-2 and 2

will result in alternate segregation, which could also be described as alternate II segregation (Endrizzi 1974).

Polyploid plants are not so subject to semisterility (Brown 1980; Baker and McIntosh 1966; Singh and Kolb 1991), and in some cases Dp-Df pollen can be transmitted (Menzel and Dougherty 1987). Some diploid plants, when heterozygous for translocations, do not experience such high spore-abortion rates, e.g., *Datura stramonium* L. (Blakeslee 1928), *Triticum monococcum* L. (Thompson and Hutcheson 1942), *Hordeum vulgare* L. (Smith 1941), *Lycopersicon esculentum* Mill. (Barton 1954), and *Oenothera* (Cleland 1929). Among these plants alternate segregation seems to be favored (Burnham 1962, pp. 83–84).

Unlike that of inversions, the rate of pollen and ovule abortion in translocation heterozygotes is rarely tied to the rate of crossovers in some region of the chromosome. Still, crossovers can affect segregation outcomes. Crossovers are most relevant in the interstitial segments. Recall that these crossovers reduce the frequency of adjacent II segregation. Crossovers in the interstitial region also change the rules for the production of Dp-Df spores. Without such a crossover, all products of alternate segregation will be balanced and viable, and all products of alternate I segregation will be Dp-Df. With a single crossover in one of the interstitial segments, either alternate or adjacent I segregation will instead yield two balanced spores and two Dp-Df spores. The fate of adjacent II segregation products is not substantially changed by such crossovers; all four will still be Dp-Df. A demonstration of how an interstitial crossover affects adjacent I segregation is shown in Fig. 1.18. Inspection of the four products reveals that two spores that receive the crossover chromosomes are balanced and viable, even though this was adjacent I segregation. In a similar fashion (not shown), this kind of crossover before alternate segregation will cause the two spores that receive the crossover chromosomes to be Dp-Df. Recall that some plants favor alternate segregation. In these cases, the rate of spore abortion is affected by the rate of crossovers in the interstitial segments. Also, because crossovers in these cases would be lost in Dp-Df spores, it reduces map distances for the interstitial region (Burnham 1962, p. 76).

Even in plants that do not favor alternate segregation, translocation heterozygotes experience marked reductions in crossover rates near the breakpoints. This result is explained by the observations by cytologists that the fidelity of pachytene pairing is not nearly as precise as indicated in Fig. 1.14. When the four chromosomes form a quadrivalent, some asynapsed region is usually present at the center of the "cross" (Fig. 1.19), and the center of the cross can vary considerably from cell to cell, depending on the translocation involved (McClintock 1932; Burnham 1932, 1934, 1948). Indeed, observations of chromosomes with recognizable features have confirmed that nonhomologous pairings are also not uncommon. Either asynapsis or nonhomologous pairing causes major regions near the breakpoints to be ineligible for crossovers, thus reducing the map distances between nearby markers. Still, translocations have been used in mapping experiments. The breakpoints of reciprocal translocations act as a dominant marker because their presence is associated with spore abortion (Anderson 1956). Even though a distortion of map distances is observed, the order of loci is expected to be reliable (Patterson 1994).

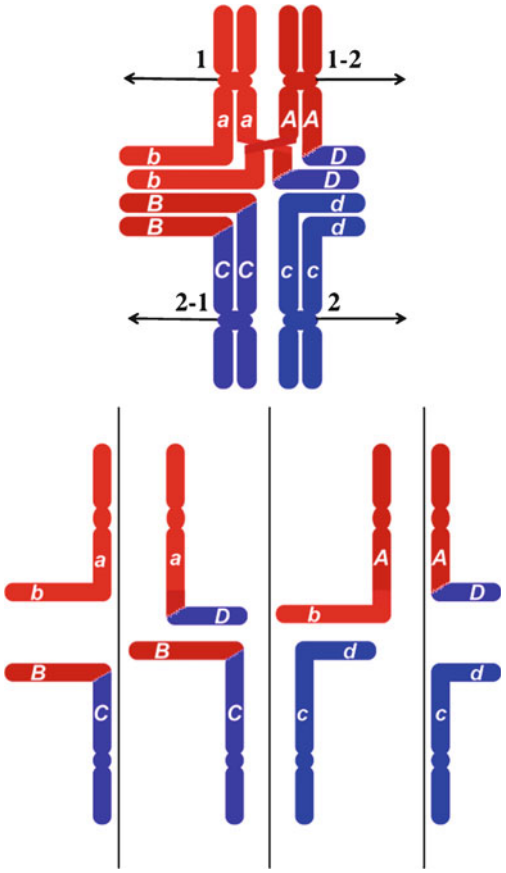

Fig. 1.18 One crossover in an interstitial segment changes fate of alternate I segregation

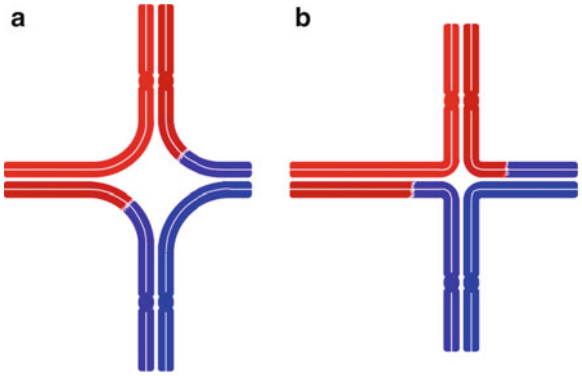

Fig. 1.19 Asynapsis and nonhomologous pairing. (**a**) Large asynaptic region. (**b**) Nonhomologous pairing

Even so, caution is advised when the map distances obtained from translocation heterozygotes are quite small. The reduction of single crossovers appears to be greater than that of double crossovers (Auger and Sheridan 2001). The coefficient of coincidence can easily exceed one, indicating more observed double crossovers than would be expected from the observed crossover rate of two intervals. High coincidence levels can be problematic because they can cause incorrect conclusions about gene order.

Another aberration of linkage seen in translocation heterozygotes is pseudolinkage, in which two loci appear to be linked, even though they reside on chromosomes that share no homology. Reconsider Fig. 1.14; note that *a* and *b* are physically linked on normal chromosome 1 and *A* and *D* are physically linked on the 1-2 translocation, neither *A* nor *a* is physically linked to either *C* or *c* on either a normal or a translocation chromosome. Therefore, the *A* allele on the 1-2 chromosome can segregate with either the *C* allele on the 2-1 chromosome or the *c* allele on normal chromosome 2. Without a crossover in the interstitial segments, the cosegregation of *A* and *C* requires alternate segregation, which yields viable spores, and the cosegregation of *A* and *c* requires adjacent I segregation, which results in a Dp-Df spore that aborts. Therefore, the rate of crossovers in the interstitial segments determines how often *A* and *C* cosegregate into viable spores, with the result that these two loci are effectively linked in recombination experiments.

Novel linkage and pseudolinkage allowed for the development of the collection of maize stocks that were used to place new mutations to chromosomes. Each stock was homozygous for a translocation that involves the short arm of chromosome 9 (9S) and one of the other maize chromosome arms (Anderson 1943, 1956). In each case, 9S was modified to carry a recessive endosperm marker, *waxy1* (*wx1*). The stock can be crossed to individuals who carry an unplaced mutation; these parents are homozygous starchy (*Wx1*). The progeny are grown and self-pollinated, producing a population segregating for waxy and starchy kernels. These are grown separately and scored for the mutant phenotype, which can be either dominant or recessive. Higher rate of segregation of the mutant phenotype among the starchy kernels than among the waxy kernels in one of these translocation lines indicates that the mutant gene is on the non-9S chromosome involved with that translocation.

Two independently arising translocations that involve the same chromosomal regions, i.e., overlapping translocations, afford the opportunity to produce interstitial deletions and duplications (Gopinath and Burnham 1956). This situation is particularly useful in generating deficiencies that are lethal in the gametophyte generation and thus lost after meiosis, because they can be regenerated on demand in future generations. Consider a reciprocal translocation (T1-2a) in which both breakpoints are distal to markers *A* and *B* (Fig. 1.20, 1-2a and 2-1a) and another translocation (T1-2b) that has breakpoints that are both proximal to markers *A* and *B* (Fig. 1.21, 1-2b and 2-1b). If a plant is heterozygous for these two pairs of translocations, the resulting spores can either be fully balanced (Fig. 1.20, two pairs on the left side) or unbalanced Dp-Df pairs (two pairs on the right). The sizes and locations of the Dp-Df regions depend on relative positions of the breakpoints on each arm. Even so, as long as one of the balanced translocation pairs has both breakpoints

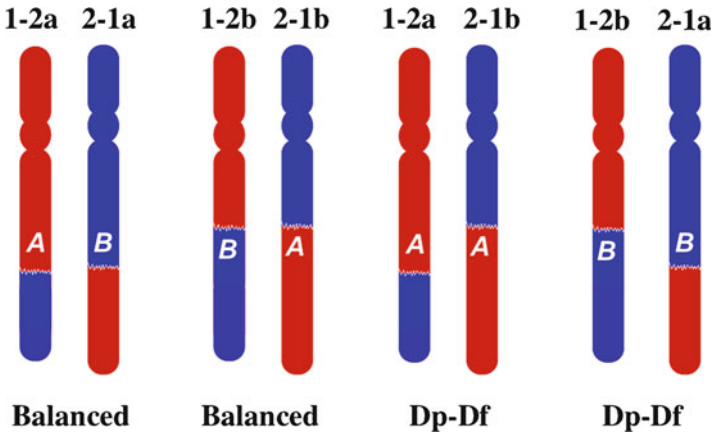

Fig. 1.20 Balanced and unbalanced translocation pairs: I. In T1-2b, both breakpoints are distal to those in T1-2a

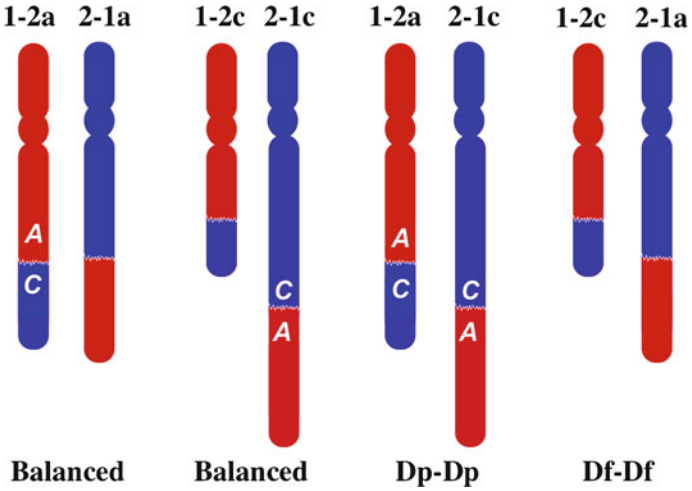

Fig. 1.21 Balanced and unbalanced translocation pairs: II. In T1-2c one breakpoint is distal to those in T1-2a, and one is proximal

distal to the breakpoints on the other pair of translocations, both of the unbalanced pairs will be Dp-Df.

The outcome is different for overlapping translocations when one of the balanced translocations has one breakpoint proximal and the other distal to the other balanced translocations. This situation is shown in Fig. 1.21, where T1-2a (first pair of chromosomes on the left) is the same as in the previous example, but showing marker *C*, which is distal to the breakpoint on chromosome 2. Consider T1-2c (Fig. 1.21, second pair of chromosomes from the left), where the breakpoint on

chromosome 1 is proximal to *A* and the breakpoint on chromosome 2 is distal to *C*. Here, neither of the unbalanced pairs is Dp-Df, one pair is duplicate for two segments (Fig. 1.21, Dp-Dp) and the other deficient (Fig. 1.21, Df-Df) for those same segments. Birchler (1980) used such constructs to locate *alcohol dehydrogenase-1* cytologically in maize. Interstitial deletions generated by overlapping translocations have also been used to study the development of the female gametophyte (Vollbrecht and Hake 1995). Birchler and Levin (1991) suggested that interstitial duplications can allow for the transmission of mutations that would otherwise be lethal to the gametophyte. A more detailed description of constructing duplications and deficiencies with overlapping translocations is given by Birchler (1994).

1.4.3 Maize B-A Chromosomes and Their Uses

Supernumerary chromosomes, known as B chromosomes, occur in various plant species. In maize, they have been extensively exploited for production of cytogenetic tools because of their peculiar behavior during pollen development. As will be explained, reciprocal translocations of B chromosomes with members of the essential chromosome complement afford the opportunity to generate individuals with known duplications and deficiencies on demand.

The presence of B chromosomes in maize was first noted by Longley (1927) and Randolph (1941) examined their genetic characteristics, but Roman (1947) was the one who clarified the anomalous behavior of maize B chromosomes, whereby they tend to accumulate in maize stocks (Randolph 1941). Roman noted that the cytological analyses by Longley and Randolph showed that plants containing two B chromosomes or no B chromosomes could be obtained from crosses of a plant containing no B chromosomes with a pollen parent plant containing two B chromosomes. Therefore, microspores containing one B chromosome must have produced some gametes containing two B chromosomes and others containing no B chromosomes. These investigators obtained the same results when plants with no B chromosomes were crossed as females with plants having one B. Roman hypothesized that these results "support the possibility that the B chromosome is undergoing 'mitotic nondisjunction' in one, perhaps rarely in both, of the divisions which produce the gametes." Although he noted that a direct cytological or genetic determination of what happens during microspore divisions was not technically feasible, Roman reasoned that, through interchanges with the standard set of A chromosomes, the B chromosomes could be genetically marked and he could thereby follow the behavior of the B chromosomes. By use of X-ray treatment of mature pollen, Roman was able to obtain eight B-A interchanges (translocations), and he reported a detailed analysis of TB-4Sa (Fig. 1.22). Reciprocal crosses involving a normal chromosome tester stock homozygous for the *su1* allele and a B-A (i.e., B-4Sa) chromosome bearing the dominant *Su1* allele demonstrated that the B-A chromosome underwent nondisjunction in the second division of the microspore, producing one sperm nucleus containing two of the B-A chromosomes as well as an A-B (4-B)

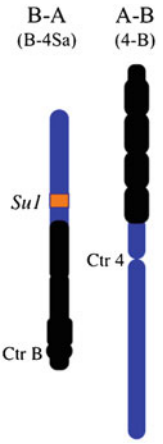

Fig. 1.22 B-A reciprocal translocation. TB-4Sa is used as an example. The A chromosomal segments are shown in *blue*, B chromosome segments in *black*. Centromeres (Ctr) are labeled

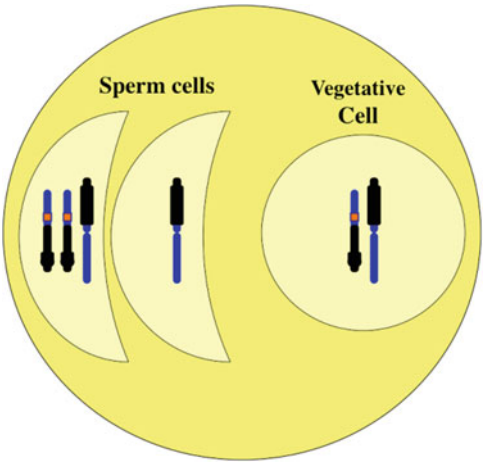

Fig. 1.23 Maize pollen grain showing fate of nondisjoined B-A chromosomes

chromosome and the other sperm containing no B-A chromosome but only the A-B chromosome (Fig. 1.23). When a plant containing the B-4Sa chromosome and the 4-B chromosome was used as a pollen parent, three kinds of kernels resulted on ears of homozygous *su1* tester plants (Fig. 1.24). One kind had a hypoploid (i.e., deficient) sugary endosperm (*su1*, *su1*, –, 4-B) with a hyperploid (i.e., possessing a duplicate chromosomal region) embryo containing two TB-4Sa chromosomes and a 4-B; a second kind had a hyperploid starchy endosperm (*su1*, *su1*, B-4Sa, B-4Sa, 4-B) and a hypoploid embryo (*su1*, –,4-B); and a third had a euploid starchy endosperm (*su1*, *su1*, TB-4Sa, 4-B) and an embryo containing a single TB-4Sa and a 4-B chromosome. (The student might be reminded that angiosperms have double fertilization; one sperm fertilizes the egg to produce the embryo, and the other fuses with the two polar nuclei to produce the endosperm.) See Carlson (1986) and Beckett (1991) for a review of the genetic control of B chromosome behavior.

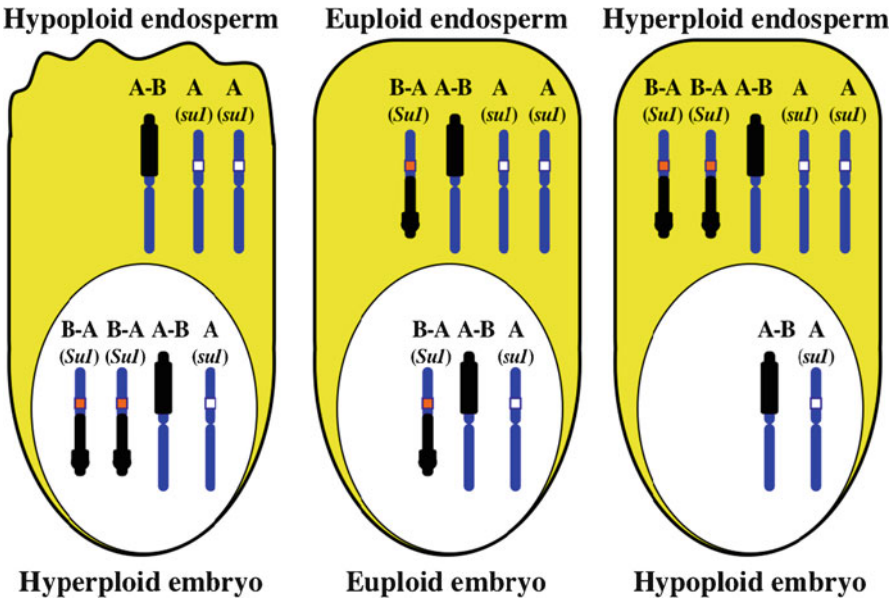

Fig. 1.24 Three classes of kernels resulting from TB-4Sa crossed onto a *su1*/*su1* female. *Yellow* represents endosperm; *white* is embryo

B-A translocations have several uses, but the most frequent, by far, is in locating recessive factors to chromosome arm. This use involves the formation of hypoploid sperm and was presaged in Roman's initial report. He said, "The production of functional deficient gametes may also be utilized to locate recessive genes within the chromosome. A plant which contains the recessive gene is crossed as the seed parent with a plant carrying an A-B interchange and homozygous for the dominant allele. The deficient progeny will show the recessive character if the locus of the gene is distal to the point of breakage in the A chromosome" (Roman 1947). This was shown to be the case by Roman's use of TB-4Sa in locating the *su1* locus. The locating of recessive factors was further described by Roman and Ullstrup (1951) and Beckett (1978). The cytogenetic, genetic, and plant-breeding applications of B-A translocations in maize were reviewed by Beckett (1991). In this extensive summary Beckett listed 101 B-A translocations that included 84 simple and 17 compound B-A-A (see description below) translocations, including the regions of the chromosome arms uncovered in hypoploid tissues and the references for their origins (see Table 1 of Beckett 1991). At that time B-A translocations were available for 19 of 20 maize chromosome arms; the exception was the short arm of Chromosome 8. Beckett (1991) identified a basic set of 15 B-A translocations and four compound translocations that could be used for most studies.

The initial investigation by Roman (1947) was intended to create B-A translocations to mark the B chromosome so that the behavior of the B chromosome could be analyzed during spore and gamete development, but as stated above, Roman noted

in his initial report that he had located the recessive *su1* allele using one of the B-A interchanges he had produced. To a large extent, it was this use that drove the subsequent efforts to produce B-A translocations. Most of these were produced during the 1970s and 1980s. Several investigators contributed to the production of new B-A translocations, but Beckett (1978, 1991, 1993) was a major contributor and source of these cytogenetic tools.

The most productive use of B-A translocations has been the analysis of chromosome arm locations of gene loci affecting kernel development. These include large-scale analysis of *defective kernel* (*dek*) mutants. The initial reports by Neuffer and Sheridan (1980) and Sheridan and Neuffer (1980) described the arm locations of 90 EMS)-induced mutations, and Scanlon et al. (1994) reported on the arm location of 63 *dek* mutants isolated from active *Mutator* transposable element stocks. Many additional EMS-induced *dek* mutations were analyzed, and their arm locations were reported (Chang et al. 1984; Neuffer and England 1995). These arm-location data and the complete list of the available B-A translocation stocks are available at the Maize Genetics and Genomics Database website (http://www.maizegdb.org). In addition, simple B-A translocations were used to analyze 51 embryo-specific mutations isolated from active *Mutator* stocks, and 24 of these were located to chromosome arm (Clark and Sheridan 1991).

By 1970, simple B-A translocations were available for many but not all of the maize chromosome arms. In that year Rakha and Robertson (1970) described a method for producing compound B-A-A translocations, by bringing together a simple B-A translocation with an A-A translocation in which breakpoints in the A-A and B-A translocation are in the same arm. A recombination event can yield a B-A-A compound translocation (for details on constructing B-A-A translocations, see Sheridan and Auger 2006 and references therein). In their report Rakha and Robertson (1970) described six B-A-A translocations, and subsequent reports (Robertson 1975a, b; Birchler 1980; Shadley and Weber 1984) increased the total to 17 compound translocations. The number of reported B-A-A translocation stocks was increased to 81 with the report by Sheridan and Auger (2006). Recent studies have enlarged this number to over 100 with the creation of approximately 20 additional B-A-A translocation stocks (Sheridan and Auger, unpublished results).

Roman (1947) noted that "The mechanism of mitotic nondisjunction thus provides a method for the study of the effect of specific chromosomal segments in various numbers." The reduced dosage of several chromosome segments occurring in kernels with hypoploid endosperm results in a reduced endosperm size. This "small kernel effect" is most obvious when chromosome arms 1S, 1L, 4S, 5S, 7S, 7L, and 10L are involved (Birchler and Hart 1987; Birchler 1993) and has also been analyzed by Lin (1982) and Beckett (1983). Simple B-A translocations have also been used to examine gene dosage effects on the expression of nuclear and mitochondrial genes (Guo and Birchler 1994; Auger et al. 2001). The effects of aneuploidy for several chromosome-arm segments have revealed that hypoploid plants are more severely reduced in their growth and vigor than their hyperploid counterparts, when simple B-A translocations are used to

produce the aneuploid plants (Chang et al. 1987; Beckett 1991; Lee et al. 1996; Neuffer et al. 1997).

The B-A-A translocations offer the greatest potential for systematic manipulation of the karyotype in any plant system. They permit simultaneous evaluation of the possible dosage effects of two nonhomologous segments on maize plant development. During the propagation of the new B-A-A translocations, Sheridan and Auger (2008) observed that, in some cases, hyperploid plants differed in appearance from nonhyperploid plants. They studied 20 paired families that involved B-A-A translocations bearing one of the chromosome arms 1S, 1L, 4L, 5S, and 10L. Their analysis revealed that one or more of seven measured morphological traits displayed dosage sensitivity among 17 of the 20 B-A-A translocations evaluated. These effects may be either the additive effects of hyperploidy for the two chromosome segments borne on each B-A-A translocation or a result of gene interaction between them (Sheridan and Auger 2008).

References

Anderson EG (1941) Long inversion on chromosome 2. *Maize Genet Coop Newslett* 15:4

Anderson EG (1943) Utilization of translocations with endosperm markers in the study of economic traits. *Maize Genet Coop Newslett* 17:4–5

Anderson EG (1956) The application of chromosomal techniques to maize improvement. In: *Genetics in Plant Breeding*. Brookhaven Symposia in Biology No. 9, Upton, New York, pp. 23–36

Auger DA, Birchler JA (2002) Maize tertiary trisomic stocks derived from B-A translocations. *J Hered* 93:42–47

Auger DL, Sheridan WF (2001) Negative crossover interference in maize translocation heterozygotes. *Genetics* 159:1717–1726

Auger DL, Newton KJ, Birchler JA (2001) Nuclear gene dosage effects upon the expression of maize mitochondrial genes. *Genetics* 157:1711–1721

Baker EP, McIntosh RA (1966) Chromosome translocations identified in varieties of common wheat. *Can J Genet Cytol* 8:592–599

Barton DW (1954) Comparative effects of X-ray and ultraviolet radiation on the differentiated chromosomes of the tomato. *Cytologia* 19:157–175

Beadle GW (1937) Chromosome aberration and gene mutation in sticky chromosome plants of *Zea mays*. *Cytologia Fujii Jubilee Volume,* 1, pp. 43–56

Beadle GW, Sturtevant AH (1935) X-chromosome inversion and meiosis in *Drosophila melanogaster*. *Proc Natl Acad Sci USA* 21:384–390

Beard BH (1960) The seed industry in the age of radiation. *Proc 5th Annual Farm Seed Research Conf* 5:25–30

Beckett JB (1978) B-A translocations in maize I. Use in locating genes by chromosome arm. *J Hered* 69:27–36

Beckett JB (1983) Kernel weight effects and transmission of a partial trisome involving the long arm of chromosome 5 in maize. *Can J Genet Cytol* 25:346–353

Beckett J (1991) Cytogenetic, genetic and plant breeding applications of B-A translocations in maize. In: Gupta PK, Tsuchiya T (eds), *Chromosome Engineering in Plants*: *Genetics, Breeding, Evolution, Vol. 2A*. Elsevier, Amsterdam, pp. 493–529

Beckett JB (1993) Locating recessive genes to chromosome arm with B-A translocations. In: Freeling M, Walbot V (eds), *The Maize Handbook*. Springer-Verlag, New York, pp. 315–327

Birchler JA (1980) The cytogenetic localization of the *alcohol dehydrogenase-1* locus in maize. *Genetics* 94:687–700
Birchler JA (1993) Dosage analysis of maize endosperm development. *Ann Rev Genet* 27:181–204
Birchler JA (1994) Segmental aneuploid analysis. In: Freeling M, Walbot V (eds), *The Maize Handbook*. Springer-Verlag, New York, pp. 377–383
Birchler JA, Hart JA (1987) Interaction of endosperm size factors in maize. *Genetics* 117:309–317
Birchler JA, Levin DM (1991) Directed synthesis of a segmental chromosomal transposition: an approach to the study of chromosomes lethal to the gametophyte generation of maize. *Genetics* 127:609–618
Blakeslee AF (1928). *Genetics of* Datura. Verh V Int Kongr Vererbungswiss, Berlin, pp. 117–130
Bonierbale MW, Plaisted RL, Tanksley SD (1988) RFLP maps based on a common set of clones reveal modes of chromosomal evolution in potato and tomato. *Genetics* 120:1095–1103
Bridges CB, Brehme KS (1944) The mutants of *Drosophila melanogaster*. Carnegie Institute of Washington Publ. 552, Washington, DC
Brown MS (1980) Identification of the chromosomes of *Gossypium hirsutum* L. by means of translocations. *J Hered* 71:266–274.
Buchholz JT., Blakeslee AF (1932) Pollen-tube growth in primary and secondary 2n + 1 *Datura*. *Am J Bot* 19:604–646
Burnham CR (1932) The association of non-homologous parts in a chromosomal interchange in maize. *Proc Natl Acad Sci USA* 18:430–447
Burnham CR (1934) Chromosomal interchanges in maize, reduction of crossing-over and the association of non-homologous parts. *Am Nat* 68:81–82
Burnham CR (1948) Cytogenetic studies of a translocation between chromosomes 1 and 7 in maize. *Genetics* 33:5–21
Burnham CR (1956) Chromosome interchanges in plants. *Bot Rev* 22:419–557
Burnham CR (1962) *Discussions in Cytogenetics*. Burgess Publishing, Minneapolis, MN
Carlson WR (1986) The B chromosome of maize. *CRC Crit Rev Plant Sci* 3:201–226
Carlson WR, Curtis CA (1986) A new method for producing homozygous duplications in maize. *Can J Genet Cytol* 28:1034–1040
Catcheside DG (1932) The chromosomes of a new haploid *Oenothera. Cytologia* 4:68–113
Catcheside DG (1939) A position effect in *Oenothera*. *J Genet* 38:345–352
Catcheside DG (1947) The *P*-locus position effect in *Oenothera*. *J Genet* 48:31–42
Chang M, Neuffer MG, Sheridan W (1984) Confirmation of chromosome arm locations for seedling and kernel mutants. *Maize Genetics Coop Newslett* 58:60–62
Chang M-T, Coe EH, Beckett JB (1987) Genetic effects of hypoploidy on kernel weight, plant height and leaf width. *Maize Genet Coop Newslett* 61:91–92
Clark JK, Sheridan WF (1991) Isolation and characterization of 51 embryo-specific mutations of maize. *Plant Cell* 3:935–951
Cleland RE (1929) Meiosis in the pollen mother cells of *Oenothera*s, and its probable bearing upon certain genetical problems. *Proc Intl Congr Plant Sci, Ithaca* (*1926*) 1:317–331
Creighton HB (1937) White seedlings due to homozygosity of deficiency in chromosome IX of *Zea mays*. *Genetics* 22:189–190
Doyle GG (1994) Inversions and list of inversions available. In: Freeling M, Walbot V (eds), *The Maize Handbook*. Springer-Verlag, New York, pp. 346–349
Dubcovsky J, Luo MC, Zhong GY, Bransteitter R, Desai A, Kilian A, Kleinhofs A, Dvorak J (1996) Genetic map of diploid wheat, *Triticum monococcum* L., and its comparison with maps of *Hordeum vulgare* L. *Genetics* 143:983–999
Ehrendorfer F (1959) Differentiation-hybridization cycles and polyploidy in *Achillea*. *Cold Spring Harbor Symp Quant Biol* 24:141–152
Ekberg I (1974) Cytogenetic studies of three paracentric inversions in barley. *Hereditas* 76:1–30
Endo TR (1990) Gc chromosomes and their induction of chromosome mutations in wheat. *Japan J Genet* 65:135–152

Endo TR (2007) The gametocidal chromosome as a tool for chromosome manipulation in wheat. *Chromosome Res* 15:67–75

Endo TR, Gill BS (1996) The deletion stocks of common wheat. *J Hered* 87:295–307

Endrizzi JE (1974) Alternate-1 and alternate-2 disjunctions in heterozygous reciprocal translocations. *Genetics* 77:55–60

English JJ, Harrison K, Jones J (1995) Aberrant transpositions of maize double *Ds*-like elements usually involve *Ds* ends on sister chromatids. *Plant Cell* 7:1235–1247

Evans HJ, Bigger TRL (1961) Chromatid aberrations induced by gamma irradiation II. Non randomness in the distribution of chromatid aberrations in relation to chromosome length in *Vicia faba* root-tip cells. *Genetics* 46:277–289

Gao M, Fisher DK, Kim KN, Shannon JC, Guiltinan MJ (1997) Independent genetic control of maize starch-branching enzymes IIa and IIb (isolation and characterization of a Sbe2a cDNA). *Plant Physiol* 114:69–78

Gill KS, Gill BS, Endo TR, Boyko EV (1996) Identification and high-density mapping of gene-rich regions in chromosome group 5 of wheat. *Genetics* 143:1001–1012

Gopinath DM, Burnham CR (1956) A cytogenetic study in maize of deficiency-duplication produce by crossing interchanges involving the same chromosome. *Genetics* 41:382–395

Gottschalk W (1951) Untersuchungen am Pachytän normaler und Röntgenbestrahlter Pollenmutterzellen von *Solanum lycopersicum*. *Chromosoma* 4:298–341

Gunthardt H, Smith L, Haferkamp ME, Nilan RA (1953). Studies on aged seed II. Relation of aged seeds to cytogenetic effects. *Agron J* 45:438–441

Guo M, Birchler JA (1994) Trans-acting dosage effects on the expression of model gene systems in maize aneuploids. *Science* 266:1999–2002

International Rice Genome Sequencing Project (2005) The map-based sequence of the rice genome. *Nature* 436:793–800

Kato K, Lamb JC, Birchler JA (2004) Chromosome painting using repetitive DNA sequences as probes for somatic chromosome identification in maize. *Proc Natl Acad Sci USA* 101: 13554–13559

Khush GS, Rick CM (1967) Studies on the linkage map of chromosome 4 of the tomato and on the transmission of induced deficiencies. *Genetica* 38:74–94

Khush FS, Rick CM (1968) Cytogenetic analysis of the tomato genome by means of induced deficiencies. *Chromosoma* 23:452–484

Lamprecht H (1953) New and hitherto known polymeric genes of *Pisum*. *Agric Hort Genetica* 11:40–54.

Lee EA, Darrah L, Coe E (1996) Dosage effects on morphological and quantitative traits in maize aneuploids. *Genome* 39:898–908

Lewis KR, John B (1966) The meiotic consequences of spontaneous chromosome breakage. *Chromosoma* 18:287–304

Lin B-Y (1982) Association of endosperm reduction with parental imprinting in maize. *Genetics* 100:475–486

Lin B-Y, Marquette K, Sallee P (1990) Characterization of deficiencies generated by *r-X1* in maize. *J Hered* 81:359–364

Lin H, Zhu W, Silva JC, Gu X, Buell CR (2006) Intron gain and loss in segmentally duplicated genes in rice. *Genome Biol* 7:R41

Lin X, Kaul S, Rounsley S, Shea TP, Benito ML, Town CD, Fujii CY, Mason T, Bowman CL, Barnstead M, Feldblyum TV, Buell CR, Ketchum KA, Lee J, Ronning CM, Koo HL, Moffat KS, Cronin LA, Shen M, Pai G, Van Aken S, Umayam L, Tallon LJ, Gill JE, Adams MD, Carrera AJ, Creasy TH, Goodman HM, Somerville CR, Copenhaver GP, Preuss D, Nierman WC, White O, Eisen JA, Salzberg SL, Fraser CM, Venter JC (1999) Sequence and analysis of chromosome 2 of the plant *Arabidopsis thaliana*. *Nature* 402:761–768

Livingstone KD, Lackneya VK, Blautha JR, van Wijkb R, Jahna MK (1999) Genome mapping in *Capsicum* and the evolution of genome structure in the Solanaceae. *Genetics* 152:1183–1202

Longley AE (1927) Supernumerary chromosomes in *Zea mays*. *J Agric Res* 35:769–784

Longley AE (1961) *Breakage Points for Four Corn Translocation Series and Other Corn Chromosome Aberrations*. ARS 34–16. Agricultural Research Service, U.S. Department of Agriculture in cooperation with the California Institute of Technology, Washington.
Lough AN, Roark LM, Kato A, Ream TS, Lamb JC, Birchler JA, Newton KJ (2008) Mitochondrial DNA transfer to the nucleus generates extensive insertion site variation in maize. *Genetics* 178:47–55
Ma J, SanMiguel P, Lai J, Messing J, Bennetzen JL (2005) DNA rearrangement in orthologous *Orp* regions of the maize, rice and sorghum genomes. *Genetics* 170:1209–1220
Maheshwari P (1950) *An Introduction to the Embryology of Angiosperms*. McGraw-Hill, New York
Martínez-Férez IM, Dooner HK (1997) Sesqui-*Ds*, the chromosome-breaking insertion at *bz-m1*, links double *Ds* to the original *Ds* element. *Mol Gen Genet* 255:580–586
McClintock B (1931) Cytological observations of deficiencies involving known genes, translocations and an inversion in *Zea mays*. *Mo Agric Exp Stn Res Bull* 163:1–30
McClintock B (1932) Cytological observations in *Zea* on the intimate association of nonhomologous parts of chromosomes in mid-prophase of meiosis and its relationship to diakinesis configurations. *Proc VI Intl. Congr Genet* 2:126–138
McClintock B (1933) Association of non-homologous parts of chromosomes in mid-prophase of meiosis in *Zea mays*. *Z Zellforsch Mikrosk Anat* 21:293–328
McClintock B (1938a) A method for detecting potential mutations of a specific chromosome region. *Genetics* 23:159 (abstr)
McClintock B (1938b) The production of homozygous deficient tissues with mutant characteristic by means of the aberrant mitotic behavior of ring-shaped chromosomes. *Genetics* 23:315–376
McClintock B (1941) The association of mutants with homozygous deficiencies in *Zea mays*. *Genetics* 26:542–571
McClintock B (1944) The relation of homozygous deficiencies to mutations and allelic series in maize. *Genetics* 29:478–502
McClintock B (1950) The origin and behavior of mutable loci in maize. *Proc Natl Acad Sci USA* 36:344–355
Menzel MY, Dougherty BJ (1987) Transmission of duplication deficiencies from cotton translocations is unrelated to map lengths of the unbalanced segments. *Genetics* 116:321–330
Mickelson-Young L, Endo TR, Gill BS (1995) A cytogenetic ladder-map of the wheat homoeologous group-4 chromosomes. *Theor Appl Genet* 90:1007–1011
Moore DM (1976) *Plant Cytogenetics*. Chapman and Hall, London
Morell MK, Blennow A, Hashemi BK, Samuel MS (1997) Differential expression and properties of starch branching enzyme isoforms in developing wheat endosperm. *Plant Physiol* 113: 201–208
Morgan DT (1950) A cytogenetic study of inversions in *Zea mays*. Genetics 35:153–174
Mottinger JP (1970) The effects of X rays on the bronze and shrunken loci in maize. *Genetics* 64:259–271
Muller HJ (1940) An analysis of the process of structural changes in chromosomes of *Drosophila*. *J Genet* 40:1–66
Neuffer MG, England D (1995) Induced mutations with confirmed locations. *Maize Genet Coop Newslett* 69:43–46
Neuffer MG, Sheridan WF (1980) Defective kernel mutants of maize. I. Genetic and lethality studies. *Genetics* 95:929–944
Neuffer MG, Coe EH, Wessler SR (1997) *Mutants of Maize*. Cold Spring Harbor Laboratory, New York
Noda S (1974) Cytogenetics of *Scilla scilloides* complex. II. Evidence for homoeological relationship between the genomes. *Cytologia* 39:777–782
Nordenskjold H (1961) Tetrad analysis and the course of meiosis in three hybrids of *Luzula campestris*. *Hereditas* 47:203–238
Nuffer MG (1957) Additional evidence on the effect of X-ray and ultraviolet radiation on mutation in maize. *Genetics* 42:273–282

Paterson AH, Bowers JE, Chapman BA (2004) Ancient polyploidization predating divergence of the cereals, and its consequences for comparative genomics. *Proc Natl Acad Sci USA* 101:9903–9908

Patterson EB (1978) Properties and uses of duplicate-deficient chromosome complements in maize. In Walden DB (ed), *Maize Breeding and Genetics*. Wiley & Sons, New York, pp. 693–710

Patterson EB (1994) Translocations as genetic markers. In Freeling M, Walbot V (eds), *The Maize Handbook*. Springer-Verlag, New York, pp. 361–363

Rahman S, Regina A, Li Z, Mukai Y, Yamamoto M, Hashemi BK, Abrahams S, Morell MK (2001) Comparison of starch branching enzyme genes reveals evolutionary relationships among isoforms. Characterisation of a gene for starch branching enzyme IIa from the wheat D genome donor *Aegilops tauschii*. *Plant Physiol* 125:1314–1324

Rakha FA, Robertson DS (1970) A new technique for the production of A-B translocations and their use in genetic analysis. *Genetics* 65:223–240

Randolph LR (1941) Genetic characteristics of the B chromosome in maize. *Genetics* 26:608–631

Rees H, Thompson JB (1955) Localization of chromosome breakage at meiosis. *Heredity* 9:399–407

Reiger R (1957) Inhomologenhaarung und meiosenblauf bei haploiden formen von *Antirrhinum majus* L. *Chromosoma* 9:1–38

Rhoades MM (1941) Different rates of crossing over in male and female gametes of maize. *J Am Soc Agron* 33:603–615

Rhoades MM, Dempsey E (1953) Cytogenetic studies of deficient-duplicate chromosomes derived from inversion heterozygotes in maize. *Am J Bot* 40:405–424

Rick CM, Khush GS (1961) X-ray-induced deficiencies of chromosome 11 in the tomato. *Genetics* 46:1389–1393

Rickards GK (1983) Orientation behavior of chromosome multiples of interchange (reciprocal translocation) heterozygotes. *Annu Rev Genet* 17:443–498

Roberts LM (1942) The effects of translocation on growth in *Zea mays*. *Genetics* 27:584–603

Robertson DS (1975a) A new compound A-B translocation TB-5S,1L (8041). *Maize Genet Coop Newslett* 49:79–81

Robertson DS (1975b) An A-B translocation with segments from three different A chromosomes. *Maize Genet Coop Newslett* 49:81–82

Roman H, Ullstrup AJ (1951) The use of A-B translocations to locate genes in maize. *Agron J* 43:450–454

Roman H (1947) Mitotic nondisjunction in the case of interchanges involving the B-type chromosome in maize. *Genetics* 32:391–409

Russell WA, Burnham CR (1950) Cytogenetic studies of an inversion in maize. *Sci Agric* 30:93–111

Scanlon MJ, Stinard PS, James MG, Myers AM, Robertson DS (1994) Genetic analysis of sixty-three mutations affecting maize kernel development isolated from *Mutator* stocks. *Genetics* 136:281–294

Schubert I, Reiger R (1990) Alteration by centric fission of the diploid number in *Vicia faba* L. *Genetica* 81:67–69

Shadley JD, Weber DF (1984) Placement of sporophyte mutants within the long arm of chromosome 5. *Maize Genet Coop Newslett* 58:160–161

Sheridan WF, Auger DL (2006) Construction and uses of new compound B-A-A maize chromosome translocations. *Genetics* 174:1755–1765

Sheridan WF, Auger DL (2008) Chromosome segmental dosage analysis of maize morphogenesis using B–A–A translocations. *Genetics* 180:755–769

Sheridan WF, Neuffer MG (1980) Defective kernel mutants of maize II. Morphological and embryo culture studies. *Genetics* 95:945–960

Singh RJ, Kolb FL (1991) Chromosomal interchanges in six hexaploid oat genotypes. *Crop Sci* 31:726–729

Sjodin J (1971) Induced paracentric and pericentric inversions in *Vicia faba* L. *Hereditas* 67:39–54

Smith FH (1941) An inversion, a reciprocal translocation, trisomics, and tetraploids in barley. *J Agric Res* 63:741–750

Stadler LJ (1933) On the genetic nature of induced mutations in plants II. A haplo-viable deficiency in maize. *Mo Agric Exp Stn Res Bull* 204:3–29

Stadler LJ (1935) Genetic nature of a haplo-viable internal deficiency in maize. Am Nat 69:80–81 (abstr)

Stadler LJ, Roman H (1948) The effect of X-rays upon mutation of the gene A in maize. *Genetics* 33:273–303

Stephens SG (1961) A remote coincidence. *Am Nat* 95:279–293

Stupar RM, Lilly JW, Town CD, Cheng Z, Kaul S, Buell CR, Jiang J (2001) Complex mtDNA constitutes an approximate 620-kb insertion on *Arabidopsis thaliana* chromosome 2: implication of potential sequencing errors caused by large-unit repeats. *Proc Natl Acad Sci USA* 98:5099–5103

Sturtevant AH (1926) A crossover reducer in *Drosophila melanogaster* due to inversion of a section of the third chromosome. *Biol Zentralbl* 46:697–702

Sutka J, Galiba G, Vagujfalvi A, Gill BS, Snape JW (1999) Physical mapping of the *Vrn-A1* and *Fr1* genes on chromosome 5A of wheat using deletion lines. *Theor Appl Genet* 99:199–202

Thompson WP, Hutcheson I (1942) Chromosome behaviour and fertility in diploid wheat with translocation complexes of four and six chromosomes. *Can J Res Sect C Bot Sci* 20:267–281

Tsujimoto H, Yamada T, Hasegawa K, Usami N, Kojima T, Endo TR, Ogihara Y, Sasakuma T (2001) Large-scale selection of lines with deletions in chromosome 1B in wheat and applications for fine deletion mapping. *Genome* 44:501–508

Tuleen NA (1962) Progress on bigger rings Method 2, by X-rays. *Barley Newlett* 5:17

Vandepoele K, Simillion C, Van de Peer Y (2003) Evidence that rice and other cereals are ancient aneuploids. *Plant Cell* 15:2192–2202

Vollbrecht E, Hake S (1995) Deficiency analysis of female gametogenesis in maize. *Dev Genet* 16:44–63

Walbot V (1992) Strategies for mutagenesis and gene cloning using transposon tagging and T-DNA insertional mutagenesis. *Annu Rev Plant Physiol Plant Mol Biol* 43:49–82

Wang X, Shi X, Hao B, Ge S, Luo J (2005) Duplication and DNA segmental loss in the rice genome: implications for diploidization. *New Phytol* 165:937–946

Weber DF (1973) A test of distributive pairing in *Zea mays* utilizing doubly monosomic plants. *Theor Appl Genet* 43:167–173

Weber D, Chao L (1994) The *r-x1* deficiency system induces nondisjunction in the early embryo in maize. *Maydica* 39:29–33

Weil CF, Wessler SR (1993)Molecular evidence that chromosome breakage by *Ds* elements is caused by aberrant transposition. *Plant Cell* 5:515–522

Wright AD (1991) Parker's flint contains *orp1*. *Maize Genet Coop Newslett* 65:58

Wright AD, Neuffer MG (1989) Orange pericarp in maize: filial expression in maternal tissue. *J Hered* 80:229–233

Wright AD, Moehlencamp CA, Perrot GH, Neuffer MG, Cone KC (1992) The maize auxotrophic mutant *orange pericarp* is defective in duplicate genes for tryptophan synthase β. *Plant Cell* 4:711–719

Yamanouchi H, Nakamura Y (1992) Organ specificity of isoforms of starch branching enzyme (Q-enzyme) in rice. *Plant Cell Physiol* 33:985–991

Zhang J., Peterson T (1999) Genome rearrangements by nonlinear transposons in maize. *Genetics* 153:1403–1410

Zhang J, Yu C, Pulletikurti V, Lamb J, Danilova T, Weber DF, Birchler J, Peterson T (2009) Alternative *Ac*/*Ds* transposition induces major chromosomal rearrangements in maize. *Genes Dev* 23:755–765

Chapter 2
Genome Structure and Chromosome Function

Khwaja G. Hossain, Scott A. Jackson, and Shahryar F. Kianian

Abstract Aneuploidy refers to the loss or gain of individual chromosomes or loss of a portion of an individual chromosome from the normal chromosome set. The resulting gene-dosage imbalance may or may not noticeably affect phenotype. Although its phenotypic manifestations are usually apparent, information about the underlying alterations in structure, expression, and interphase organization of unbalanced chromosome sets is still sparse. Aneuploidy is the most common chromosomal aberration in plants, and aneuploids are valuable for the study of chromosome evolution, phenotypic manifestation of chromosome loss or gain, and mapping genes and genome. Breeding programs intended to transfer desirable genes from one species to another produce addition lines as intermediate crossing products. Such aneuploids can be used for further introgression, but their abnormal recombination and segregation interfere with production of stable introgression lines. They can have specific morphological characteristics, but more often additional confirmation is needed. Their genetic and cytogenetic properties make them powerful tools for fundamental research on regulation of homeologous recombination, distribution of chromosome-specific markers and repetitive DNA sequences, and regulation of heterologous gene expression. Recent advancements and availability of genomic resources have widened the scope for their use. They make possible assignment of individual linkage groups to specific chromosomes and can improve identification of quantitative trait loci (QTLs) and underlying DNA components/sequences.

K.G. Hossain (✉)
Division of Science and Mathematics, Mayville State University, Mayville, ND 58257, USA
e-mail: k.hossain@mayvillestate.edu

S.A. Jackson (✉)
Department of Agronomy, Purdue University, 915 West State Street, West Lafayette, IN 47907, USA
e-mail: sjackson@purdue.edu

S.F. Kianian (✉)
Department of Plant Sciences, North Dakota State University, 470G Loftsgard Hall,
Fargo, ND 58105, USA
e-mail: s.kianian@ndsu.edu

H.W. Bass and J.A. Birchler (eds.), *Plant Cytogenetics*, Plant Genetics and Genomics: Crops and Models 4, DOI 10.1007/978-0-387-70869-0_2,

Keywords Aneuploid · Gene dosage · Chromosomal abnormalities · Breeding · Homeologs · Introgressions

Abbreviations

CIMMYT	International Maize and Wheat Improvement Center
CSSLs	Chromosome segment substitution lines
DSB	Double-strand breakage
GISH	Genomic in situ hybridization
LDN	Langdon
NILs	Near isogenic lines
QTL	Quantitative trait locus
RCSLs	Recombinant chromosome substitution lines
RDA	Representation difference analysis
RH	Radiation hybrid

Contents

2.1 Plant Chromosome Addition

The normal or disomic condition of two gene doses per chromosome in a somatic cell is usually the basic state in an organism, but meiotic irregularities, chromosome aberrations, aging, or environmental stresses may result in deviation from the basic chromosome number in the genome. This deviation is termed aneuploidy and can occur in any eukaryotic organism. Aneuploids are represented symbolically by the somatic chromosome number because their gametic chromosome numbers vary. The deviation can consist of additions or subtractions of individual chromosomes, either of which has severe effects in mammals and is often lethal early in the life cycle. In plants, especially with higher ploidy levels, such changes in chromosome numbers are readily tolerated, but if the doses of several chromosomes are changed, the imbalance in gene interactions cannot be tolerated even in polyploid plants or their gametes.

2.2 Native Addition Lines

The addition of a single extra chromosome of a species to the normal somatic complement (2n) is termed trisomy, and in a diploid species it implies that one chromosome exists in three copies in each somatic cell, whereas all other

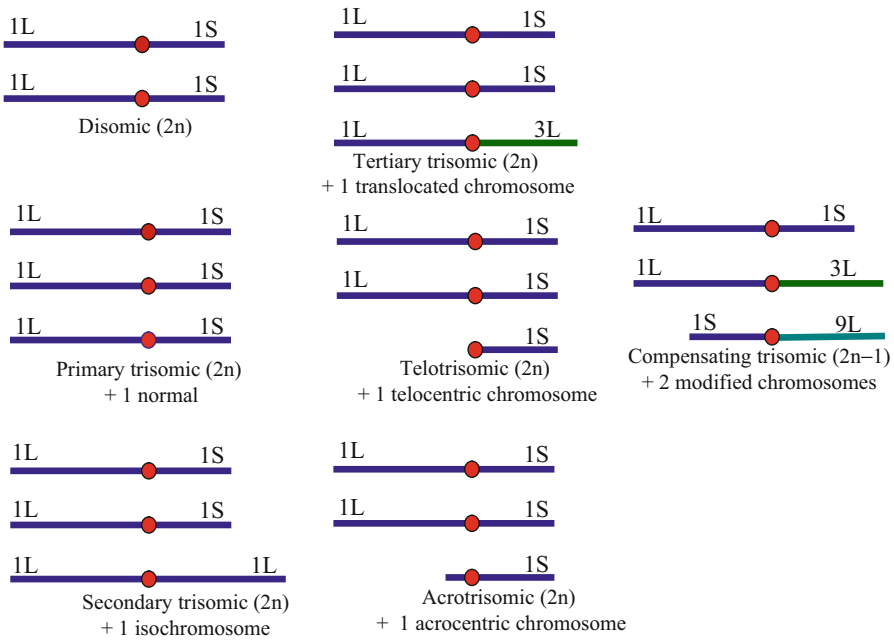

Fig. 2.1 Terms and diagrams illustrating the disomic and various trisomic states in diploid species

chromosomes exist in the normal two. In plants, depending on the composition of the extra chromosomes, trisomic states have been classified into different types that can be distinguished cytologically at meiosis (Fig. 2.1). Tetrasomy (2n + 2) is the state in which two extra copies of a chromosome is present, such that the cell has four doses of one chromosome but only two of other chromosomes. Double trisomics carry an extra copy of each of two nonhomologous chromosomes, i.e., three doses of each of two different chromosomes. The various terms and diagrams illustrating the disomic and other aneuploid states are presented in Fig. 2.1.

In the plant kingdom, trisomy is very common and was first discovered in jimsonweed, *Datura stramonium*, by Blakeslee (1921). Diploids usually tolerate the primary trisomic state, and depending on identity of the extra chromosome, vigor of the plant varies. Complete sets of primary trisomics exist in a number of diploid crop species, including barley (*Hordeum vulgare* L.; Tsuchiya 1958, 1961), maize (*Zea mays* L.; McClintock 1929; McClintock and Hill 1931), tomato (*Solanum lycopersicum* L.; Lesley 1932), and rye (*Secale cereale,* Kamanoi and Jenkins 1962). The modified trisomics (secondary, tertiary, etc.) are only viable in a few diploids, and extra effort is required to obtain them (Mattingly and Collins 1974).

The first detailed morphological description of a complete series of 12 primary trisomics was documented in *Datura* (Blakeslee 1934). Morphological distinctions of primary trisomy have now been described in *Avena* (oats; Azael 1973; Rajhathy 1975), *Pennisetum* (Manga 1976), and many other species (Khush 1973). In many species, the morphological distinctions are not large enough for identification of

primary trisomics, but the series of primary trisomics mentioned above and trisomics of many other species can be distinguished cytologically.

In plants, the phenotypic effects of trisomy are clearest in diploids; in polyploid species genome multiplication often masks the dosage effects of an extra chromosome. The trisomics of a series within a species are more easily differentiated from diploids and from each other when they are all in the same homozygous genetic background.

Trisomy affects many aspects of development and differentiation throughout the plant life cycle. In species with a range in chromosome length, extra copies of longer chromosomes can have more pronounced effects (including greater reduction in fertility, as was documented in rice (*Oryza sativa* L.) by Khush et al. 1984) than extras of shorter ones. Certain trisomic conditions modify different plant organs in the same direction. In tomato, for example, trisomies 3 and 4 increase the lengths of leaves, stems, inflorescences, fruits, and seeds; trisomies 7 and 10 decrease the lengths of most of these plant parts (Rick and Barton 1954). Trisomies are identified by key features, such as seedling traits in spinach, leaf traits in tomato, panicle types in sorghum, and seed-capsule size and shape in *Datura* (Weber 1983). In cases where chromosome morphology or phenotypic effects are not applicable, trisomies can be identified by chromosome banding and in situ hybridization, techniques applied to distinguish different primary trisomics in diploid wheat (*Triticum monococcum* L.) (Friebe et al. 1991).

Since the classical studies of *Datura* trisomics by Blakeslee (1921), primary trisomics have been used extensively to associate marker genes with a particular chromosome, to associate a genetic linkage group with the individual chromosome, and to test the independence of linkage groups (Singh 2003). The cytogenetic maps in maize (Rhoades and McClintock 1935), tomato (Rick and Barton 1954), barley (Tsuchiya 1967), and rice (Khush et al. 1984) have been established by the primary-trisomic method. A set of primary trisomics has been identified in soybean (*Glycine max* L. Merr.; Xu et al. 2000) and has been used to associate morphological mutants and SSR markers to their respective chromosomes (Zou et al. 2003).

2.3 Alien Addition Line

Addition of an alien chromosome (i.e., one from another species) to the somatic complement of a species is termed monosomic addition; it can arise in the progenies of interspecific hybrids and polyploids. Plant geneticists and breeders have gained interest in extending genetic variation of crop plants using germ plasm from related species. In a long-term crossing program, known as introgressive hybridization, economically or otherwise important genes are being incorporated into the recipient parent by sexual or somatic hybridization between related species or genera, followed by consecutive backcrossing with the recipient parent. In the offspring families, lines are selected in which only a single alien chromosomes has been added. Monosomic additions were first described by Leighty and Taylor (1924), but their use and potential were better demonstrated in a study by O'Mara (1940). Khush (1973) and Sybenga (1992) provide full overviews of alien additions in

Table 2.1 The complete sets of chromosome additions with their parental species, karyotype analysis, and references

Donor species	Recipient species	No. of alien addition sets	Cytogenetics	References
Aegilops speltoides	*Triticum aestivum* (wheat)	7	C-banding, FISH with repeat probes	Friebe et al. (2000)
Allium cepa (onion)	*Allium fistulosum*	8	Karyotype analysis	Shigyo et al. (1996)
Beta webbiana	*Beta vulgaris* (beet)	9	Karyotype analysis	Reamon-Ramos and Wricke (1992)
Beta patellaris	*Beta vulgaris* (beet)	9	Karyotype analysis	Mesbah et al. (1997)
Beta procumbens	*Beta vulgaris* (beet)	9	Karyotype analysis	Van Geyt et al. (1988)
Lycopersicon esculentum (tomato)	*Solanum tuberosum* (potato)	12	GISH	Ali et al. (2001)
Oryza officinalis	*Oryza sativa* (rice)	12	Karyotype analysis	Jena and Khush (1989)
Solanum lycopersicum	*Lycopersicon esculentum* (tomato)	12	Karyotype analysis	Chetelat et al. (1998)
Wheat	Various species	20	Karyotype analysis	Shepherd et al. (1988)
Zea mays (maize)	*Avena sativa* (oat)	10	Karyotype analysis	Kynast et al. (2001)
Barley	Wheat	7	karyotype analysis	Islam and Shepherd (2000)

relation to other aneuploids in plant genetics. Table 2.1 presents a list of monosomic addition lines in different plant species with their parental species, means of selection, and references.

Monosomic additions can be selected on the basis of specific alien traits, like disease resistance, aberrant plant phenotype, species-specific molecular markers, and karyotypic analysis. Morphological traits can be binary traits, like the *liguleless* leaves of the maize chromosome 3 monosomic addition in oat (Muehlbauer et al. 2000) and dominant resistance genes, or quantitative traits, such as plant size and spike morphology. The phenotypes of monosomic-addition-derived hybrids between genetically related parents often resemble those of the corresponding primary trisomic (Chetelat et al. 1998). Alien chromosomes are sometimes distinguished by karyotype analysis; examples are four monosomic additions to beet (*Beta* sp.) containing alien chromosomes from *Beta procumbens* C. Sm. or *B. patellaris* Moq. that confer nematode resistance (de Jong et al. 1986).

The most important tool for visualization of alien chromosome is genomic in situ hybridization (GISH). Reports establishing the number of alien chromosomes in intergeneric backcross families are numerous (Raina and Rani 2001); examples are tomato to potato (Jacobsen et al. 1995), maize to oat (Riera-Lizarazu et al. 1996),

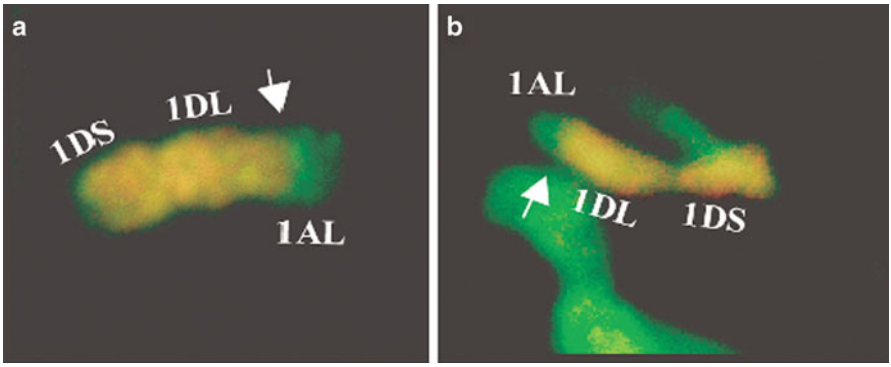

Fig. 2.2 GISH analysis of two putative 1DS. 1DL–1AL chromosomes in (**a**) (lo) durum *scs*^{ae}/LDN-dDt1A and (**b**) (lo) durum *scs*^{ae}/LDN 16. Fluorescein- (*yellow-green*) and rodamine-labeled (*red*) LDN-16 and *Aegilops tauschii* genomic DNA, respectively, were used in GISH analysis. The pattern of chromosome labeling suggests the presence of the short arm of chromosome 1D (1DS), the proximal region of the long arm of chromosome 1D (1DL), and a terminal segment that probably originated from a homoeologous distal region of chromosome 1A (1AL). *White arrows* mark the putative homoeologous recombination points (picture from Hossain et al. 2004b)

Beta corolliflora Zosimovic ex Buttler to beet (Gao et al. 2000), and S-genome chromosome to wheat (Belyayev et al. 2001).

The potential of alien chromosome addition for breeding programs depends largely on the genetic distance between the parental species, which is critical to the possibility of recombination between alien chromosomes and their homeologous counterparts in the recipient species. In parents that can be combined in sexual crosses, such as wheat and rye, maize and *Pennisetum*, and *Festuca* and *Lolium*, crossovers between homeologous chromosomes are not rare and may reveal recombinant chromosomes, even in the first backcross generations.

The extent of crossover recombination between the homeologs in monosomic additions depends primarily on the genetic relation between the parent species but is also influenced by difference in the alien chromosomes and their genetic background. In some cases, unequal crossovers between homeologs and alien chromosomes result in heteromorphic chromosome addition – for example, introgression and mapping of the species cytoplasm specific (*scs*) gene located on chromosome 1D in an alloplasmic durum wheat (*Triticum turgidum* L.; AABB) line to overcome incompatibility (Maan 1992, Hossain et al. 2004b). In this line, the portion of the *T. aestivum* L. chromosome 1D carrying the *scs* gene has been introgressed (Fig. 2.2). The lack of meiotic recombination of this 1D portion in the durum background made it suitable for physical mapping. By means of gamma-ray irradiation, the *scs* gene and the 1D chromosome have been physically mapped in wheat (Hossain et al. 2004b; Kalavacharla et al. 2006). The development of radiation hybrid (RH) lines from oat-maize somatic additions has allowed mapping of molecular markers on a subchromosome level of the maize genome (Riera-Lizarazu et al. 2000; Okagaki et al. 2001).

Monosomic alien addition lines have been used in genetic studies of genome organization and plant breeding in crops such as tomato, wheat, and sugi (*Cryptomeria* sp.; Kam-Morgan et al. 1989; Suyama et al. 1996; Chetelat et al. 1998). The series of individual *Allium cepa* L. chromosomes added to the diploid genome of *A. fistulosum* L. constitutes a unique resource for examining the genetic map of *A. cepa* and its genome organization (Barthes and Ricroch 2001). Complete sets of alien monosomic addition lines are valuable tools in genetic studies of plant genome organization (McGrath et al. 1990; Singh 1993). In wheat, tomato, and sugi, alien monosomic addition lines and other aneuploid lines have been used to assign linkage groups to chromosomes (Chetelat et al. 1998; Kam-Morgan et al. 1989; Suyama et al. 1996). Other uses of monosomic addition lines include deletion mapping (Werner et al. 1992b) and the transfer of important genes of wild species by means of translocation (Heijbroek et al. 1988; Jung et al. 1992). Alien-chromosome-addition lines are usually generated to transfer agronomically important gene(s) from wild relatives into cultivated crops, a cost-effective means of fostering germ-plasm use. In addition, these lines have been used for localization of genes for valuable traits on specific chromosomes (Kindiger et al. 1996; Yildirim et al. 1998; Ma et al. 1999), construction of DNA libraries for specific chromosomes after microdissection (Jung et al. 1992), isolation of chromosome-specific DNA sequences (Clarke et al. 1995; Delaney et al. 1995), selective isolation and/or chromosome mapping of cDNAs (Korzun et al. 1996; Li et al. 1996; Biyashev et al. 1997), research on genome composition and chromosome structure (Ananiev et al. 1998; Zhang et al. 1996), and assignment of DNA markers to specific chromosomes (Liu et al. 1996; Suen et al. 1997; Gallego et al. 1998; van Heusden et al. 2000). In recent years, disomic or monosomic addition lines have also been used to study nuclear architecture (Abranches et al. 1998), for analysis of meiotic chromosome behavior (Bass et al. 2000), and to clone specific DNA sequences with the help of representation difference analysis (RDA) techniques (Delaney et al. 1995; Chen et al. 1998). A set of seven disomic addition lines of wheat with *Thinopyrum bessarabicum* Savul. and Rayss chromosomes was produced at the International Maize and Wheat Improvement Center (CIMMYT).

Wheat (*Triticum aestivum* L.)–barley disomic chromosome addition lines have been developed through wide hybridization between the hexaploid ($2n = 6\times = 42$) wheat cultivar Chinese Spring and the diploid ($2n = 2\times = 14$) barley cultivar Betzes (Islam et al. 1975). Each addition line contains the full complement of wheat chromosomes and a single homeologous chromosome pair from barley. Wheat–barley disomic addition lines for six of the seven barley chromosomes, including 1(7H), 2(2H), 3(3H), 4(4H), 6(6H), and 7(5H), and ditelosomic addition lines harboring 13 of the 14 barley chromosome arms have been generated (Islam et al. 1981; Islam 1983; Islam and Shepherd 1990, 2000). Chromosome addition lines have been used often to map genes to donor chromosomes on the basis of the presence or absence of the genes on the chromosomes added to the recipient genome. By means of wheat–barley chromosome-addition lines, isozymes and DNA markers have been physically mapped to chromosomes and chromosome arms (Islam and Shepherd 1990; Garvin et al. 1998).

Wheat–barley chromosome addition lines are useful genetic resources for a variety of studies. Transcript accumulation patterns in Betzes barley, Chinese Spring wheat, and Chinese Spring–Betzes chromosome-addition lines were examined with the Barley1 Affymetrix GeneChip probe array. Of the 4,014 transcripts detected in Betzes but not in Chinese Spring, 365, 271, 265, 323, 194, and 369 were detected in wheat–barley disomic chromosome-addition lines 2(2H), 3(3H), 4(4H), 7(5H), 6(6H), and 1(7H), respectively. Thus, 1,787 barley transcripts were detected in a wheat genetic background and, by virtue of the addition line in which they were detected, were physically mapped to barley chromosomes.

Specific proteins/isozymes and GISH were used to detect the presence of *T. bessarabicum* chromosomes in the advanced backcross derivatives of *T. aestivum* and to establish tentatively the homeology of these added chromosomes (William and Mujeeb-Kazi 1995). Single chromosomes of wild species of *Beta* section IV (*B. procumbens*, *B. webbiana* Moq., *B. patellaris*) (Loptien 1984) were used to transfer resistance to beet cyst nematode into *B. vulgaris* (cultivated beet), and resistant diploids were obtained (Jung and Wricke 1987). Later, a full set of monosomic addition lines in *B. vulgaris* from *B. procumbens* was described morphologically (Lange et al. 1988) and characterized by isozyme markers (Van Geyt et al. 1988). Nine different monosomic addition lines carrying alien chromosomes from *B. webbiana* were differentiated by isozyme markers and morphological characters (Reamon-Ramos and Wricke 1992). A more refined method for identification of alien chromosome additions relies on sequences specific to wild beets that, when used as probes, yield characteristic banding patterns (DNA fingerprints).

2.4 Substitution Line

In aneuploids, replacement of a chromosome by its homeolog is called chromosome substitution and can be easily brought about in the backcross families of the interspecific hybrids and monosomic additions. The development of substitution lines involves the replacement of a pair of chromosomes in one variety or species, the recipient, by the homologous pair from another variety or species, the donor. The heteromorphic (homeologous) bivalents in such monosomic substitutions generally demonstrate higher levels of crossover recombination between the alien chromosome and its homeologous counterpart than those in the corresponding monosomic addition and are therefore more appropriate for producing recombinant chromosomes (Ji and Chetelat 2003). A set of monosomics (a monosomic, a $2n-1$ individual, has lost one chromosome from the 2n complement) and/or their derivatives such as nullisomics (which have lost both homologs and are $2n-2$) and monotelosomics (which are $2n-1$ pair $+1$ telosome) must be available to supply $n-1$ gametes for the crosses and backcrosses. Reciprocal substitutions, in which homologous chromosomes are exchanged, can also be established between two varieties with monosomic sets.

Some alien substitutions occur spontaneously after wide crosses and may not be noticed until some generations later, as happened in the development of some European wheat varieties. The wheat breeders unconsciously retained homeologous

a rye-wheat substitution (the wheat chromosome 1B pair replaced by rye chromosome 1R) during selection for several disease resistances from crosses between triticale (a hybrid of wheat and rye) and wheat (Zeller 1973). Another example of a spontaneous substitution occurred during transfer of a dominant gene for resistance to tobacco mosaic virus from a diploid species (*Nicotiana glutinosa* L.) to tetraploid tobacco (*N. tabacum* L.). The hexaploid amphiploid from the interspecific cross was backcrossed to *N. tabacum*. After a second backcross followed by selfing, a line was obtained with the same chromosome number of as *N. tabacum* that was homozygous for resistance (Gerstel 1943).

Substitution lines are available in many species, but their development may differ according to ploidy level. For example, in wheat the process of developing substitution lines in tetraploid wheat (*T. turgidum*) is different from that in hexaploid wheat (*T. aestivum*) because the vigor, fertility, and n – 1 gametic transmission rates of tetraploid monosomics are low (Sears 1966; Mochizuki 1968).

A considerable amount of genetic information can be obtained from substitution lines without further crosses. One-way or reciprocal substitutions, with duplicate lines, and their two parental varieties, can be grown in statistically designed arrangements, with several replications and preferably several environments over locations and years. The significant differences of quantitative traits in any of the substitution lines and the recipient variety can be attributed to the introgressed chromosome. If duplicates of a substitution line differ significantly in the same direction from the recipient variety, the interpretation is that one or more genes on the substituted chromosome have enough effect to be distinguished from their alleles on the recipient chromosome.

King et al. (2002) produced a large series of substitution lines from interspecific hybrids of *Festuca pratensis* Huds. and *Lolium perenne* L. The range of substitution lines, each with different recombinant chromosomes, provided excellent material for physical mapping of the introgressed *F. pratensis* chromosome segments and for comparing genetic and physical maps for the molecular markers on this chromosome.

In polyploids, some gametes with the euploid chromosome number are generated by unequal but numerically compensating divisions during meiosis, which in turn generate chromosomally unbalanced sporophytes. For example, in an autotetraploid species, the four homologs (or homeologs) of a chromosome may split 3–1 during anaphase I in a micro- or megaspore mother cell, whereas the homologs (homeologs) of another chromosome may split 1–3 (i.e., double-opposed nondisjunction). If other chromosomes separate equally, the resulting gametes will be monosomic for one chromosome and trisomic for another.

Chromosome substitution in allopolyploids can occur through nonhomologous/nonhomeologous substitution, as well as through homeologous substitution, i.e., replacement of a chromosome from one progenitor diploid species with a homeolog from another progenitor. Homeolog substitution can occur through compensating but unequal divisions of univalents and multivalents, and also through bivalent pairing of homeologs. Poole (1932) screened the progeny of a spontaneous cross between *Crepis rubra* L. and *C. foetida* L. for homeologous substitution of a single chromosome that was differentiated by a morphological marker.

An important advance in understanding of the genetics of polyploid wheat was the discovery that specific chromosomes in each of the genomes compensate for the

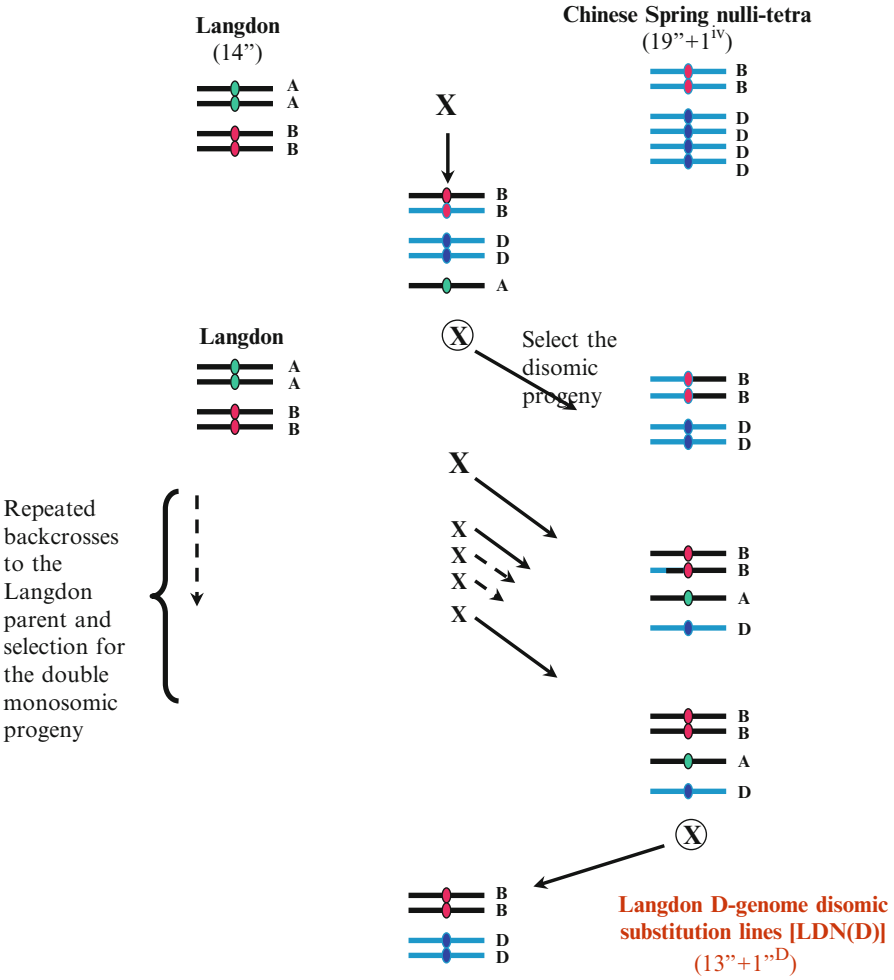

Fig. 2.3 Illustration of the process used by Joppa and Williams (1988) to generate the Langdon D-genome disomic substitution lines in tetraploid wheat. Only the critical chromosomes are shown in this illustration. The homoeologous chromosomes from different genomes do not pair with each other in the presence of *Ph* (pairing homoeologous) gene on 5BL. The hexaploid Chinese Spring chromosomes are represented in blue, the Langdon chromosomes in black, the recombined chromosomes in recombined colors, and the different genomes by colored centromeres

loss of other specific chromosomes in the other genomes. Sears's (1966) classic study of the compensating nullisomic-tetrasomic of Chinese Spring clearly demonstrated this principle. After that study, series of D-genome chromosome substitution lines in tetraploid durum wheat were developed by replacement of a chromosome from the A or B genome by its homeolog from the D-genome chromosome (e.g. see Fig. 2.3) (Joppa and Williams 1977). The procedures for localizing genes on chromosome are similar to those used in analysis of monosomics in hexaploid wheat, as

exemplified by the identification of chromosomal location of stem-rust resistance in Langdon (LDN) durum by means of monosomic substitution lines (Salazar and Joppa 1981). In the progeny of monosomic substitution, some plants disomic for the D-genome chromosome and nullisomic for the A- or B-genome chromosome were observed, and eventually Joppa and Williams (1988) developed complete sets of D-genome disomic substitution lines in tetraploid wheat (LDN-D substitutions). These substitution lines have been used to locate genes by simple observation of their presence or absence in the different aneuploids (du Cros et al. 1983; Joppa et al. 1983) or by crosses between aneuploids and a mutant line (Konzak and Joppa 1988). The LDN D-genome disomic-substitution lines have been used to produce sets of intervarietal chromosome substitution lines such as *Triticum dicoccoides* Koern. substitution lines (LDN-DIC) (Fig. 2.4). LDN-DIC substitutions have been analyzed for several important characters such as genes on the substituted chromosome that affect protein content of the grain (Joppa and Cantrell 1990) or confer higher yield (Cantrell and Joppa 1991). Joppa (1993) later used these LDN-DIC substitutions and the corresponding LDN D-genome disomic substitutions in an elegant crossing scheme to develop recombinant inbred chromosome lines in two generations. These lines have been extensively used to locate genes and quantitative trait loci to their chromosomes.

The availability of a set of *T. aestivum* Chinese Spring/*Aegilops tauschii* Coss. chromosomal substitution lines provided the opportunity to use the method of advanced backcross quantitative trait locus (QTL) analysis for the study of QTLs specific for individual chromosomes (Pestsova et al. 2001). New wheat introgression lines were developed by backcrossing of the chromosomal substitution lines with Chinese Spring wheat to produce different segments of individual chromosomes of *A. tauschii* in the common wheat background. The development of the lines was accompanied and confirmed by microsatellite-marker analysis (Pestsova et al. 2001).

In searching genetic variability in barley, Matus et al. (2003) developed a population of recombinant chromosome substitution lines (RCSLs) by crossing *H. spontaneum* (accession Caesarea 26–24, from Israel) and *H. vulgare* cultivar Harrington (North American malting quality standard). In a preliminary assessment of RCSLs, they noted that *H. spontaneum* ancestral genome introgression, in many cases, caused loss of acceptable phenotype in the cultivated progenitor, but in some cases that ancestral genome was a source of favorable alleles for some important agronomic traits and malting quality (Matus et al. 2003). RCSLs represent a useful source of genetic diversity that can be used as a model for physiological and genetic research. In rice, a relatively large segment of a particular chromosome from the donor parent is substituted in the recurrent parental background to form chromosome segment substitution lines (CSSLs), whereas a very small chromosomal segment containing the target QTLs or genes of a donor line is substituted (Yano 2001). Secondary mapping populations, such as CSSLs or near-isogenic lines, are required to facilitate a more comprehensive analysis of target QTLs. To facilitate the genetic analysis of quantitative traits and the use of marker-assisted breeding in rice, Ebitani et al. (2005) developed a novel mapping population consisting of 39 CSSLs.

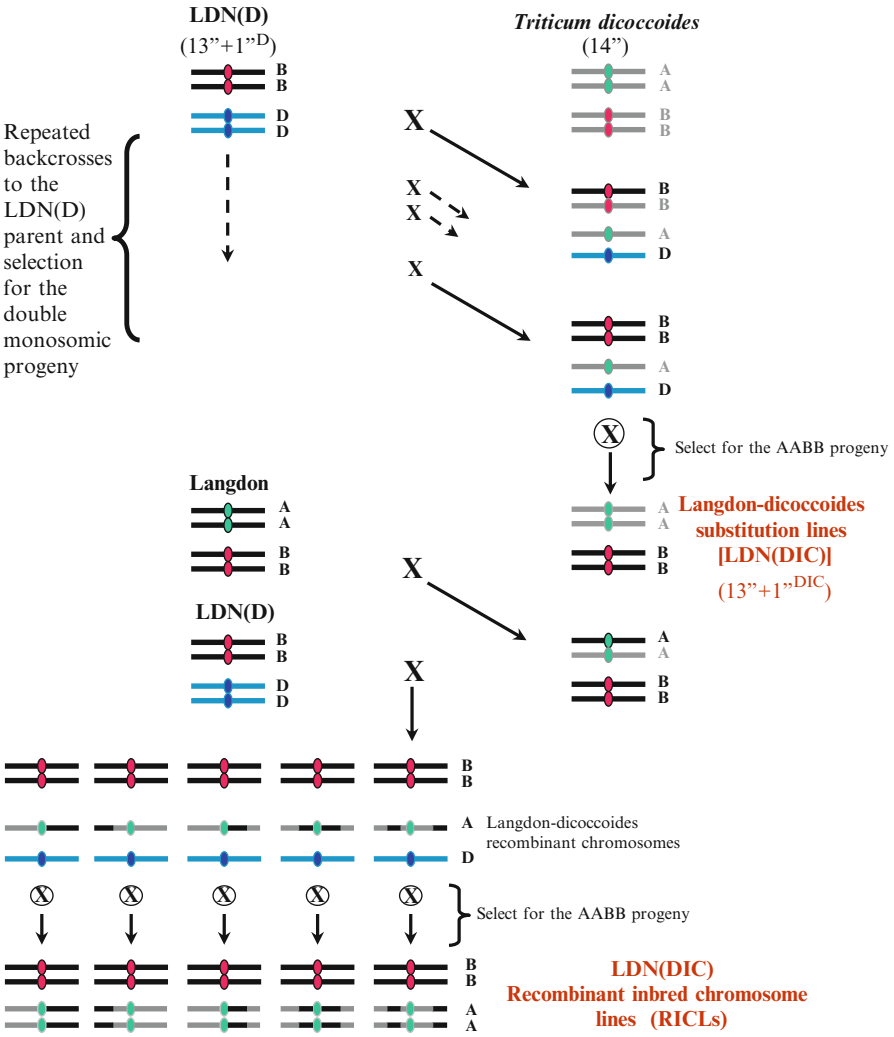

Fig. 2.4 Illustration of the process used by Joppa and Cantrell (1990) to generate the Langdon-*dicoccoides* substitution lines and that used by Joppa (1993) to develop homozygous recombinant inbred chromosome lines. Only the critical chromosomes are shown in this illustration. The homoeologous chromosomes from different genomes do not pair with each other in the presence of the *Ph* (pairing homoeologous) gene on 5BL. The *Triticum dicoccoides* chromosomes are represented in gray, the Langdon chromosomes in black, the D-genome chromosomes in blue, the recombined chromosomes in recombined colors, and the different genomes by colored centromeres

In each line, a different chromosomal segment of the *O. indica* cultivar Kasalath was substituted in the genetic background of the *O. japonica* cultivar Koshihikari (Japanese elite cultivar). The substituted chromosome segments in the 39 CSSLs covered most of the genome, except for small regions at the distal end of the short

arm of chromosome 8 and at the distal end of the long arm of chromosome 12. To verify the potential advantages of QTL detection in these CSSLs, they used the CSSLs to locate QTLs for heading date. Their results clearly demonstrated that the use of CSSLs permitted identification of a larger number of QTLs than did a BC_1F_3 population derived from the same cross combinations. Kubo et al. (1999) produced IR24 CSSLs with Asominori genetic background by repeated backcrossing and marker-assisted selections. The CSSLs carrying an IR24 homozygous segment at the middle region of chromosome 2 showed spotted, drooping, and somewhat yellowish green leaves at seedling stage under natural conditions.

2.5 Deletion Line

Chromosomal deletions are most commonly induced by ionizing radiation, which causes random breakages in double-stranded DNA. Depending on the type of break, repair of these breakages can occur through one of two general sets of mechanisms. The first, collectively called homologous recombination, occurs when the broken DNA strand uses a homologous template to prime repair DNA synthesis (van den Bosch et al. 2002; West 2003). In most cases of homologous recombination, the choice of an appropriate template results in conservation of the original DNA sequence at the break site. Alternatively, a double-strand breakage can be repaired by nonhomologous end joining, in which the broken chromosome is sealed without consultation of external homologies (Lieber et al. 2003) and results in the loss or addition of nucleotides. An alternative approach is to use transposons and site-specific recombination – an idea first proposed by van Harren and Ow (1993). According to this method, a T-DNA site is produced bearing a transposon and two copies of the target site for a site-specific recombinase. The transposon and one target site jump together and reinsert themselves into the chromosome at a location close to the T-DNA site. Recombination between the two specific sites, catalyzed by the recombinase, results in inversion or deletion of a large fragment of genome, depending on the alignment of the two specific sites.

Endo (1988) reported a unique genetic mechanism (gametocidal chromosomes) for the systematic production of even more powerful novel aneuploid stocks, namely, deletion stocks with terminal deletions of various sizes in individual chromosome arms, useful for subarm localization of genes. When a certain chromosome from *Aegilops cylindrica* is present in Chinese Spring in the monosomic condition, chromosomal breaks occur in the gametes that lack the *A. cylindrica* chromosome and generate various chromosome aberrations, including deletions. The broken chromosome ends, if not fused to other broken ends, are stabilized by the rapid gain of telomere structure (Werner et al. 1992a). Such deletions in plants without the *A. cylindrica* chromosome are transmitted regularly to the offspring. The breakpoints of deletion chromosomes carry telomere repetitive sequences (Werner et al. 1992a; Tsujimoto 1993), so deletion chromosomes are stable and transmitted to the offspring without further structural changes. This stability is also proved by the sequences of the breakpoints (Endo and Gill 1996; Tsujimoto et al. 1999). Thus, a

series of deletion lines on a chromosome can indicate specific chromosomal regions and can be used to isolate genes located in a specific chromosomal region (Kojima et al. 2000).

By this gametocidal technique, about 436 deletion lines have been developed in wheat. These stocks are immensely useful for localization of genes on chromosomes and chromosomes arms (Endo and Gill 1996; Lazo et al. 2004; McIntosh 1988). As the genome of common wheat is so large (2n = 6× = 42, AABBDD; 17,300 Mb), sequencing and mapping of the expressed portion is a logical first step for gene discovery. In a set of the deletion stocks, 7,104 expressed-sequence-tag unigenes have been localized on homeologous chromosomes of wheat (Conley et al. 2004; Hossain et al. 2004a; Lazo et al. 2004; Linkiewicz et al. 2004; Miftahudin et al. 2004; Munkvold et al. 2004; Peng et al. 2004; Qi et al. 2004; Randhawa et al. 2004).

In barley, a reliable, fast, and inexpensive approach has been developed by deletion mapping (Schubert et al. 1998). Diploid species like barley do not tolerate deletions, but deletion lines of barley can be obtained from wheat lines with single chromosomes 2C of *Aegilops cylindrica* and a pair of individual barley chromosome that have been developed (Shi and Endo 1997) in the genome background of Chinese Spring. Deletions and translocations of barley chromosomes in wheat lines have been identified that are monosomic for the *A. cylindrica* chromosome 2C (Schubert et al. 1998).

Chromosome deletions are useful tools for analyzing and manipulating plant genomes. Not only do they allow individual genes to be identified and mapped by classical and subtractive techniques, but also they can be used to eliminate a whole chromosome region, thus allowing analysis of chromatin structure and function (Gill et al. 1996; Cecchini et al. 1998; Visir and Mulligan 1999). In some plant species with large genomes and low gene density, genome deletion should provide the most efficient method for mutagenesis and gene mapping. The availability of detailed deletion libraries for plant species of agricultural and scientific importance is therefore highly desirable, but well-characterized deletions are difficult to generate.

RH mapping is based on radiation-induced chromosome breakage and analysis of chromosome-segment retention or loss with molecular markers. A high-resolution (100-kb) contiguous map of human chromosomes with 20,000 human genes has been constructed by means of the RH mapping approach and human-mouse cell hybrid lines (Hudson et al. 1995; Stewart et al. 1997; Deloukas et al. 1998). Since the success of RH mapping in human, this approach has been used in other animal genomes such as mouse (McCarthy et al. 1997), pig (Hawken et al. 1999), dog (Vignaux et al. 1999), zebrafish (Kwok et al. 1999), cat (Murphy et al. 2000), and rat (Watanabe et al. 1999). The duplicated and rearranged nature of plant genomes frequently complicates identification, chromosomal assignment, and eventual manipulation of DNA segments. Separating an individual chromosome or a portion of it from the full complement by its addition to an alien genetic background and subsequent mapping of radiation-induced deletions provide a powerful approach for analyses of these genomes. This potential has been realized in maize for mapping of duplicated sequences, gene families, and molecular markers to chromosome segments and for functional-genomics analyses using oat-maize chromosome-addition

lines (Riera-Lizarazu et al. 2000; Kynast et al. 2002). Extensive use of RH mapping in plant genomes is limited by the difficulty of identifying materials that contain different portions of the chromosome of interest. In durum wheat, an alloplasmic durum line, (lo) durum, has been identified with chromosome 1D of *T. aestivum* carrying the species-cytoplasm-specific (*scs*) gene. The chromosome 1D of this line segregates as a whole without recombination, precluding the use of conventional genome mapping. An RH mapping population was developed from a hemizygous (lo) *scs* line by means of 35-krad gamma rays. The analysis of 87 individuals of this population with 39 molecular markers mapped on chromosome 1D revealed 88 radiation-induced breaks in this chromosome. Analysis of molecular-marker retention allowed the localization of the *scs* gene and eight linked markers on the long arm of chromosome 1D (Hossain et al. 2004b). Physical mapping methods that do not rely on meiotic recombination are necessary for complex polyploid genomes such as wheat, because of the uneven distribution of recombination and significant variation in genetic-to-physical distance ratios, and RH mapping has proven valuable. A high-resolution RH map of wheat chromosome 1D (D genome) has been developed in a tetraploid durum-wheat (AB genomes) background that detected 2,312 chromosome breaks. The mapping resolution was estimated to be ~199 kb/break and provided the starting point for BAC contig alignment (Kalavacharla et al. 2006). To date, this resolution is the highest that has been obtained by plant RH mapping and serves as a first step for the development of RH resources in wheat. Analyzing 2,400 irradiated plants, Catanach et al. (2006) identified two major genomic regions in *Hieracium caespitosum* that collectively control apomixis, one at the level of the avoidance of meiosis and the other at the level of avoidance of fertilization. In conjunction with a BAC library, the deletion mapped is now being used to isolate sequences corresponding to the *LOA* and *LOP* loci. Radiation-induced deletion mapping has installed apomixis in target species and has therefore advanced us toward the goal of using this technology for the improvement of crop species to increase global welfare.

References

Abranches R, Beven AF, Aragón-Alcaide L, Shaw PJ (1998) Transcription sites are not correlated with chromosome territories in wheat nuclei. *J Cell Biol* 143:5–12

Ali SNH, Ramanna MS, Jacobsen E, Visser RGF (2001) Establishment of a complete series of a monosomic tomato chromosome addition lines in cultivated potato using RFLP and GISH analyses. *Theor Appl Genet* 103:687–697

Ananiev EV, Phillips RL, Rines HW (1998) Chromosome-specific molecular organization in maize (*Zea mays* L.) centromeric regions. *Proc Natl Acad Sci USA* 95:13073–13078

Azael A (1973) Beiträge zur Aufstellung eines Trisomen-Sortiments beim Hafer, *Avena sativa* L. *Z Pflanzenzücht* 70:289–305

Barthes L, Ricroch A (2001) Interspecific chromosomal rearrangements in monosomic addition lines of *Allium*. *Genome* 44:929–935

Bass HW, Riera-Lizarazu O, Ananiev EV, Bordoli SJ, Rines HW, Phillips RL, Sedat JW, Agard DA, Cande WZ (2000) Evidence for the coincident initiation of homolog pairing and synapsis during the telomere-clustering (bouquet) stage of meiotic prophase. *J Cell Sci* 113:1033–1042

Belyayev A, Raskina O, Nevo E (2001) Chromosomal distribution of reverse transcriptase-containing retroelements in two *Triticeae* species. *Chromosome Res* 9:129–136

Biyashev RM, Ragab RA, Maughan PJ, Maroof MAS (1997) Molecular mapping, chromosomal assignment, and genetic diversity analysis of phytochrome loci in barley (*Hordeum vulgare*). *J Hered* 88:21–26

Blakeslee AF (1921) Types of mutation and their possible significance in evolution. *Am Nat* 55:254–264

Blakeslee AF (1934) New jimson weeds from old chromosomes. *J Hered* 25:81–108

Cantrell RG, Joppa LR (1991) Genetic analysis of quantitative traits in wild emmer (*Triticum turgidum* L. var. *dicoccoides*). *Crop Sci* 31:645–649

Catanach AS, Erasmuson SK, Podivinsky E, Jordan BR, Bicknell R (2006) Deletion mapping of genetic regions associated with apomixis in *Hieracium. Proc Natl Acad Sci USA* 103:18650–18655

Cecchini E, Mulligan BJ, Covey SN, Milner JJ (1998) Characterization of gamma irradiation-induced deletion mutations at a selectable locus in *Arabidopsis. Mutat Res* 401:199–206

Chen Q, Conner RL, Laroche A, Thomas JB (1998) Genome analysis of *Thinopyrum intermedium* and *Thinopyrum ponticum* using genomic in situ hybridization. *Genome* 41:580–586

Chetelat RT, Rick CM, Cisneros P, Alpert KB, DeVerna JW (1998) Identification, transmission, and cytological behavior of *Solanum lycopersicoides* Dun. monosomic alien addition lines in tomato (*Lycopersicon esculentum* Mill.). *Genome* 41:40–50

Clarke JH, Mithen R, Brown JKM, Dean C (1995) QTL analysis of flowering time in *Arabidopsis thaliana*. *Mol Gen Genet* 248:278–286

Conley EJ, Nduati V, Gonzalez-Hernandez JL, Mesfin A, Trudeau-Spanjers M, Chao S, Lazo GR, Hummel DD, Anderson OD, Qi LL, Gill BS, Echalier B, Linkiewicz AM, Dubcovsky J, Akhunov ED, Dvorák J, Peng JH, Lapitan NLV, Pathan MS, Nguyen HT, Ma X-F, Miftahudin, Gustafson JP, Greene RA, Sorrells ME, Hossain KG, Kalavacharla V, Kianian SF, Sidhu D, Dilbirligi M, Gill KS, Choi DW, Fenton RD, Close TJ, McGuire PE, Qualset CO, Anderson JA (2004) A 2600-locus chromosome bin map of wheat homoeologous group 2 reveals interstitial gene-rich islands and colinearity with rice. *Genetics* 168: 625–637

de Jong JH, Speckmann GJ, de Bock SM, Lange W, Van Voorst A (1986) Alien chromosome fragments conditioning resistance to beet cyst nematode in diploid descendants from monosomic additions of *B. procumbens* to *B. vulgaris. Can J Genet Cytol* 28:439–443

Delaney DE, Nasuda S, Endo TR, Gill BS, Hulbert SH (1995) Cytologically based physical maps of the group 3 chromosomes of wheat. *Theor Appl Genet* 91:780–782

Deloukas P, Schuler GD, Gyapay G, Beasley EM, Soderlund C, Rodriguez-Tome P, Hui L, Matise TC, McKusick KB, Beckmann JS, Bentolila S, Bihoreau MT, Birren BB, Browne J, Butler A, Castle AB, Chiannilkulchai N, Clee C, Day PJR, Dehejia A, Dibling T, Drouot N, Duprat S, Fizames C, Fox S, Gelling S, Green L, Harrison P, Hocking R, Holloway E, Hunt S, Keil S, Lijnzaad P, Louis-Dit-Sully C, Ma J, Mendis A, Miller J, Morissette J, Muselet D, Nusbaum HC, Peck A, Rozen S, Simon D, Slonim DK, Staples R, Stein LD, Stewart EA, Suchard MA, Thangarajah T, Vega-Czarny N, Webber C, Wu X, Hudson J, Auffray C, Nomura N, Sikela JM, Polymeropoulos MH, James MR, Lander ES, Hudson TJ, Myers RM, Cox DR, Weissenbach J, Boguski MS, Bentley DR (1998) A physical map of 30,000 human genes. *Science* 282:744–746

du Cros DL, Joppa LR, Wrigley CW (1983) Two-dimensional analysis of gliadin proteins associated with quality in durum wheat: chromosomal location of genes for their synthesis. *Theor Appl Genet* 66:297–302

Ebitani T, Takeuchi Y, Nonoue Y, Yamamoto T, Takeuchi K, Yano M (2005) Construction and evaluation of chromosome segment substitution lines carrying overlapping chromosome segments of *indica* rice cultivar "Kasalath" in a genetic background of *japonica* elite cultivar "Koshihikari." *Breeding Sci* 55:65–73

Endo TR (1988) Induction of chromosomal structural changes by a chromosome from *Aegilops cylindrica* L. in common wheat. *J Hered* 79**:**366–370

Endo TR, Gill BS (1996) The deletion stocks of common wheat. *J Hered* 87:295–307

Friebe B, Mukai Y, Dhaliwal HS, Martin TJ, Gill BS (1991) Identification of alien chromatin specifying resistance to wheat streak mosaic virus and greenbug in wheat germplasm by C-banding and in-situ hybridization. *Theor Appl Genet* 81:381–389

Friebe B, Qi LL, Nasuda S, Zhang P, Tuleen NA, Gill BS (2000) Development of a complete set of *Triticum aestivum–Aegilops speltoides* chromosome addition lines. *Theor Appl Genet* 101:51–58

Gallego FJ, Lopez SE, Figueriras AM, Benito C (1998) Chromosome location of PCR fragment as a source of DNA markers linked to aluminum tolerance genes in rye. *Theor Appl Genet* 96:426–434

Gao D, Schmidt T, Jung C (2000) Molecular characterization and chromosomal distribution of species-specific repetitive DNA sequences from *Beta corolliflora*, a wild relative of sugar beet. *Genome* 43**:**1073–1080

Garvin C, Holdeman R, Strome S (1998) The phenotype of *mes-2*, *mes-3*, *mes-4*, and *mes-6*, maternal effect genes required for the survival of the germline in *C. elegans*, is sensitive to chromosome dosage. *Genetics* 148:167–185

Gerstel U (1943) Inheritance in *Nicotiana tabacum.* XVII. Cytogenetical analysis of glutinosa-type resistance to mosaic disease. *Genetics* 28:533–536

Gill KS, Gill BS, Endo TR, Taylor T (1996) Identification and high-density mapping of gene-rich regions in chromosome group 1 of wheat. *Genetics* 144:1883–1891

Hawken RJ, Murtaugh G, Flickinger H, Yerle M, Robic A, Milan D, Gellin J, Beattie CW, Schook LB, Alexander LJ (1999) A first-generation porcine whole-genome radiation hybrid map. *Mamm Genome* 10:824–830

Heijbroek W, Roelands AJ, de Jong JH, van Hulst C, Schoone AHL, Munning RG (1988) Sugar beets homozygous for resistance to beet cyst nematode (*Heterodera schachtii* Schm.) developed from monosomic additions of *Beta procumbens* to *B. vulgaris*. *Euphytica* 38:121–131

Hossain KG, Kalavacharla V, Lazo G, Hegstad J, Wentz MJ, Simons K, Gehlhar S, Rust JL, Syamala RR, Obeori K, Bhamidimarri S, Karunadharma P, Chao S, Anderson OD, Qi LL, Echalier B, Gill BS, Linkiewicz AM, Ratnasiri A, Dubcovsky J, Akhunov ED, Dvorák J, Miftahudin, Ross K, Gustafson JP, Radhawa HS, Dilbirligi M, Gill KS, Peng JH, Lapitan NLV, Greene RA, Bermudez-Kandianis CE, Sorrells ME, Feril O, Pathan MS, Nguyen HT, Gonzalez-Hernandez JL, Conley EJ, Anderson JA, Choi DW, Fenton D, Close TJ, McGuire PE, Qualset CO, Kianian SF (2004a) A chromosome bin map of 2148 EST loci of wheat homoeologous group 7. *Genetics* 168:687–699

Hossain KG, Riera-Lizarazu O, Kalavacharla V, Vales MI, Maan SS, Kianian SF (2004b) Radiation hybrid mapping of the species cytoplasm-specific (*scsae*) gene in wheat. *Genetics* 168:415–423

Hudson TJ, Stein LD, Gerety SS, Ma J, Castle AB, Silva J, Slonim DK, Baptista R, Kruglyak L, Xu SH, Hu XT, Colbert AME, Rosenberg C, Reeve-Daly MP, Rozen S, Hui L, Wu XY, Vestergaard C, Wilson KM, Bae JS, Maitra S, Ganiatsas S, Evans CA, DeAngelis MM, Ingalls KA, Nahf RW, Horton LT, Anderson MO, Collymore AJ, Ye WJ, Kouyoumjian V, Zemsteva IS, Tam J, Devine R, Courtney DF, Renaud MT, Nguyen H, O'Connor TJ, Fizames C, Fauré S, Gyapay G, Dib C, Morissette J, Orlin JB, Birren BW, Goodman N, Weissenbach J, Hawkins TL, Foote S, Page DC, Lander ES (1995) An STS-based map of the human genome. *Science* 270:1945–1954

Islam AKMR (1983) Ditelosomic additions of barley chromosomes to wheat. In: Sakamoto S (ed) *Proceedings of the 6th International Wheat Genetics Symposium.* Maruzen, Kyoto, Japan, pp. 233–238

Islam AKMR, Shepherd KW (1990) Incorporation of barley chromosomes into wheat. In: Bajaj YPS (ed), *Biotechnology in Agriculture and Forestry, Vol 13 Wheat.* Springer-Verlag, Berlin, pp. 128–151

Islam AKMR, Shepherd KW (2000) Isolation of a fertile wheat-barley addition line carrying the entire barley chromosome 1H. *Euphytica* 111:145–149

Islam AKMR, Shepherd KW, and Sparrow DHB (1975) Addition of individual barley chromosomes to wheat. In: Gaul H (ed), *Proceedings of the 3rd International Barley Genetics Symposium.* Verlag Karl Thiemig, Munchen, pp. 260–270

Islam AKMR, Shepherd KW, Sparrow DHB (1981) Isolation and characterization of euplasmic wheat-barley chromosome addition lines. *Heredity* 46:161–174

Jacobsen E, de Jong JH, Kamstra SA, van den Berg PM, Ramanna MS (1995) Genomic in situ hybridisation (GISH) and RFLP analysis for the identification of alien chromosomes in the backcross progeny of potato + tomato fusion hybrids. *Heredity* 74:250–257

Jena KK, Khush GS (1989) Monosomic alien addition lines of rice—production, morphology, cytology, and breeding behavior. *Genome* 32:449–455

Ji Y, Chetelat RT (2003) Homoeologous pairing and recombination in *Solanum lycopersicoides* monosomic addition and substitution lines of tomato. *Theor Appl Genet* 106:979–989

Joppa LR (1993) Chromosome engineering in tetraploid wheat. *Crop Sci* 33:908–913

Joppa LR, Cantrell RG (1990) Chromosomal location of genes for grain protein content of wild tetraploid wheat. *Crop Sci* 30:1059–1064

Joppa LR, Williams ND (1977) D-genome substitution monosomics of durum wheat. *Crop Sci* 17:772–776

Joppa LR, Williams ND (1988) Langdon durum disomic substitution lines and aneuploid analysis in tetraploid wheat. *Genome* 30:222–228

Joppa LR, Khan K, Williams ND (1983) Chromosomal location of genes for gliadin polypeptides in durum wheat *Triticum turgidum* L. *Theor Appl Genet* 64:289–293

Jung C, Wricke G (1987) Selection of diploid nematode resistant sugar beet from monosomic addition lines. *Plant Breed* 98:205–214

Jung C, Koch R, Fischer F, Brandes A, Wricke G, Herrmann RG (1992) DNA markers closely linked to nematode resistance genes in sugar beet (*Beta vulgaris* L.) using chromosome additions and translocations originating from wild beets of the *Procumbentes* species. *Mol Gen Genet* 232:271–278

Kalavacharla V, Hossain K, Gu Y, Riera-Lizarazu O, Vales MI, Bhamidimarri S, Gonzalez-Hernandez JL, Maan SS, Kianian SF (2006) High-resolution radiation hybrid map of wheat chromosome 1D. *Genetics* 173:1089–1099

Kamanoi M, Jenkins BC (1962) Trisomics in common rye, *Secale cereale* L. *Seiken Ziho* 13:118–123

Kam-Morgan LNW, Gill BS, Muthukrishnan S (1989) DNA restriction fragment length polymorphisms: a strategy for genetic mapping of D genome of wheat. *Genome* 32:724–732

Khush GS, Singh RJ, Sur SC, Librojo AL (1984) Primary trisomics of rice: origin, morphology, cytology and use in linkage mapping. *Genetics* 107:141–163

Khush GS (1973) *Cytogenetics of Aneuploids.* Academic Press, New York, London

Kindiger B, Sokolov V, Khatypova IV (1996) Evaluation of apomictic reproduction in a set of 39-chromosome maize-*Tripsacum* backcross hybrids. *Crop Sci* 36:1108–1113

King J, Roberts IA, Kearsey MJ, Thomas HM, Jones RN (2002) A demonstration of a 1:1 correspondence between chiasma frequency and recombination using a *Lolium perenne/Festuca pratensis* substitution. *Genetics* 161:307–314

Kojima T, Habu Y, Iida S, Ogihara Y (2000) Direct isolation of differentially expressed genes from a specific chromosome region of common wheat: application of the amplified fragment length polymorphism-based mRNA fingerprinting (AMF) method in combination with a deletion line of wheat. *Mol Gen Genet* 263:635–641

Konzak CF, Joppa LR (1988) The inheritance and chromosomal location of a gene for chocolate chaff in durum wheat. *Genome* 30:229–233

Korzun V, Melz G, Börner A (1996) RFLP mapping of the dwarfing (*Ddw1*) and hairy peduncle (*Hp*) genes on chromosome 5 of rye (*Secale cereale* L.). *Theor Appl Genet* 92:1073–1077

Kubo T, Nakamura K, Yoshimura A (1999). Development of a series of *Indica* chromosome segment substitution lines in *Japonica* background of rice. *Rice Genet Newslett* 16:104–106

Kwok C, Critcher R, Schmitt K (1999) Construction and characterization of zebrafish whole genome radiation hybrids. *Methods Cell Biol* 60:287–302

Kynast RG, Riera-Lizarazu O, Vales MI, Okagaki RJ, Maquieira SB, Chen G, Ananiev EV, Odland WE, Russell CD, Stec AO, Livingston SM, Zaia HA, Rines HW, Phillips RL (2001) A complete set of maize individual chromosome additions to the oat genome. *Plant Physiol* 125:1216–1227

Kynast RG, Okagaki RJ, Rines HW, Phillips RL (2002) Maize individualized chromosome and derived radiation hybrid lines and their use in functional genomics. *Funct Integr Genomics* 2:60–69

Lange W, De Bock TSM, Van Geyt JPC, Oleo M (1988) Monosomic additions in beet (*Beta vulgaris*) carrying extra chromosomes of *B. procumbens*. *Theor Appl Genet* 76:665–664

Lazo GR, Chao S, Hummel D, Edwards H, Crossman CC, Lui N, Matthews DE, Carollo VL, Hane DL, You FM, Butler GE, Miller RE, Close TJ, Peng JH, Lapitan NLV, Gustafson JP, Qi LL, Echalier B, Gill BS, Dilbirligi M, Randhawa HS, Gill KS, Greene RA, Sorrells ME, Akhunov ED, Dvorák J, Linkiewicz AM, Dubcovsky J, Hossain KG, Kalavacharla V, Kianian SF, Mahmoud AA, Miftahudin, Ma X-F, Conley EJ, Anderson JA, Pathan MS, Nguyen HT, McGuire PE, Qualset CO, Anderson OD (2004) Development of an expressed sequence tag (EST) resource for wheat (*Triticum aestivum* L.): EST generation, unigene analysis, probe selection and bioinformatics for a 16,000-locus bin-delineated map. *Genetics* 168: 585–593

Leighty CE, Taylor JW (1924) "Hairy neck" wheat segregates from wheat-rye hybrids. *J Agr Res* 28:567–576

Lesley JW (1932) Trisomic types of the tomato and their relations to the genes. *Genetics* 17:545–559

Li ZH, Matthews PD, Burr B, Wurtzel ET (1996) Cloning and characterization of a maize cDNA encoding phytoene desaturase, an enzyme of the carotenoid biosynthesis pathway. *Plant Mol Biol* 30:269–279

Lieber MR, Ma Y, Pannicke U, Schwarz K (2003) Mechanism and regulation of human non-homologous DNA end-joining. *Nat Rev Mol Cell Biol* 4:712–720

Linkiewicz AM, Qi LL, Gill BS, Ratnasiri A, Echalier B, Chao S, Lazo GR, Hummel DD, Anderson OD, Akhunov ED, Dvorák J, Pathan MS, Nguyen HT, Peng JH, Lapitan NLV, Miftahudin, Gustafson JP, La Rota CM, Sorrells ME, Hossain KG, Kalavacharla V, Kianian SF, Sandhu D, Bondareva SN, Gill KS, Conley EJ, Anderson JA, Fenton RD, Close TJ, McGuire PE, Qualset CO, Dubcovsky J (2004) A 2500-locus bin map of wheat homoeologous group 5 provides insights on gene distribution and colinearity with rice. *Genetics* 168:665–676

Liu ZW, Biyashev RM, Maroof MAS (1996) Development of simple sequence repeat DNA markers and their integration into a barley linkage map. *Theor Appl Genet* 93:869–876

Loptien H (1984) Breeding nematode-resistant beets. I. Development of resistant alien additions by crosses between *Beta vulgaris* L. and wild species of the section *Patellares*. *Z Pflanzenzücht* 92:208–220

Ma J, Zhou R, Dong Y, Jia J (1999) Chromosomal location of yellow rust resistance gene in *Triticum aestivum–Lophopyrum elongatum* substitution lines. *Chin Sci Bull* 44:65–69

Maan SS (1992) A gene for embryo endosperm compatibility and seed viability in alloplasmic *Triticum turgidum*. *Genome* 35:772–779

Manga V (1976) Chiasma frequencies in primary trisomics of pearl millet. *Can J Genet Cytol* 15:11–15

Mattingly CF, Collins GB (1974) The use of anther-derived haploids in *Nicotiana*. *Chromosoma* 46:29–36

Matus I, Corey A, Filichkin T, Hayes PM, Vales MI, Kling J, Riera-Lizarazu O, Sato K, Powell W, Waugh R (2003) Development and characterization of recombinant chromosome substitution lines (RCSLs) using *Hordeum vulgare* subsp. *spontaneum* as a source of donor alleles in a *Hordeum vulgare* subsp. *vulgare* background. *Genome* 46:1010–1023

McCarthy IC, Terrett J, Davis ME, Knight CJ, Smith AL, Critcher R, Schmitt K, Hudson J, Spurr NK, Goodfellow PN (1997) A first-generation whole genome–radiation hybrid map spanning the mouse genome. *Genome Res* 7:1153–1161

McClintock B (1929) A 2n–1 chromosomal chimera in maize. *J Hered* 20:218.

McClintock B, Hill HE (1931) The cytological identification of the chromosome associated with the R-G linkage group in *Zea mays*. *Genetics* 16:175–190

McGrath JM, Quiros CF, Harada JJ, Landry BS (1990) Identification of *Brassica oleracea* monosomic alien chromosome addition lines with molecular markers reveals extensive gene duplication. *Mol Gen Genet* 223:198–204

McIntosh RA (1988) Catalogue of gene symbols for wheat. In: Miller TE, Koebner, RMD (eds), *Proceedings of the 7th International Wheat Genetics Symposium.* Bath Press, Bath, UK, pp. 1225–1323

Mesbah M, De Block TSM, Sandbrink JM, Lankhorst KRM, Lang W (1997) Molecular and morphological characterization of monosomic additions in *Beta vulgaris*, carrying an extra chromosome of *B. procumbent* or *B. patellaris*. *Mol Breed* 3:147–157

Miftahudin, Ross K, Ma X-F, Mahmoud A, Layton J, Rodriguez Milla MA, Chikmawati T, Ramalingam J, Feril O, Pathan MS, Surlan Momirovic G, Kim S, Chema K, Fang P, Haule L, Struxness H, Birkes J, Yaghoubian C, Skinner R, McAllister J, Nguyen V, Qi LL, Echalier B, Gill BS, Linkiewicz AM, Dubcovsky J, Akhunov ED, Dvorák J, Dilbirligi M, Gill KS, Peng JH, Lapitan NLV, Bermudez-Kandianis CE, Sorrells ME, Hossain KG, Kalavacharla V, Kianian SF, Lazo GR, Chao X, Anderson OD, Gonzalez-Hernandez J, Conley EJ, Anderson JA, Choi D-W, Fenton RD, Close TJ, McGuire PE, Qualset CO, Nguyen HT, Gustafson JP (2004) Analysis of wheat expressed sequence tag loci on wheat chromosome group 4. *Genetics* 168:651–663

Mochizuki A (1968) The monosomics of durum wheat. In: Finlay KW, Shepherd KW (eds), *Proceedings of the 3rd International Wheat Genetics Symposium.* Butterworths, Sydney, pp. 310–315

Muehlbauer GJ, Riera-Lizarazu O, Kynast RG, Martin D, Phillips RL, Rines WH (2000) A maize-chromosome 3 addition line of oat exhibits expression of the maize homeobox gene liguleless3 and alterations of cell fates. *Genome* 43:1055–1064

Munkvold JD, Greene RA, Bermudez-Kandianis CE, La Rota CM, Edwards H, Sorrells SF, Dake T, Benscher D, Kantety R, Linkiewicz AM, Dubcovsky J, Akhunov ED, Dvorak J, Mifahudin, Gustafson JP, Pathan MS, Nguyen HT, Matthews DE, Chao S, Lazo GR, Hummel DD, Anderson OD, Anderson JA, Gonzalez-Hernandez JL, Peng JH, Lapitan N, Qi LL, Echalier B, Gill BS, Hossain KG, Kalavacharla V, Kianian SF, Sandhu D, Erayman M, Gill KS, McGuire PE, Qualset CO, Sorrells ME (2004) Group 3 chromosome bin maps of wheat and their relationship to rice chromosome 1. *Genetics* 168:639–650

Murphy WJ, Sun S, Chen Z, Yuhki N, Hirschmann D, Menotti-Raymond M, O'Brien SJ (2000) A radiation hybrid map of the cat genome: implications for comparative mapping. *Genome Res* 10**:**691–702

Okagaki RJ, Kynast RG, Livingston SM, Russell CD, Rines HW, Phillips RL (2001) Mapping maize sequences to chromosomes using oat-maize chromosome addition materials. *Plant Physiol* 125:1228–1235

O'Mara JG (1940) Cytogenetic studies on Triticinae. I. A method for determining the effect of individual *Secale* chromosomes on *Triticum*. *Genetics* 25:401–408

Peng JH, Zadeh H, Lazo GR, Gustafson JP, Chao S, Anderson OD, Qi LL, Echalier B, Gill BS, Dilbirligi M, Sandhu D, Gill KS, Greene RA, Sorrells AE, Akhunov ED, Dvorak J, Linkiewicz AM, Dubcovsky J, Hossain KG, Kalavacharla V, Kianian SF, Mahmoud AA, Miftahudin, Conley EJ, Anderson JA, Pathan MS, Nguyen HT, McGuire PE, Qualset CO, Lapitan NLV (2004) Chromosome bin map of expressed sequence tags in homoeologous group 1 of hexaploid wheat and homoeology with rice and *Arabidopsis. Genetics* 168:609–623

Pestsova EG, Börner A, Röder MS (2001) Development of a set of *Triticum aestivum-Aegilops tauschii* introgression lines. *Hereditas* 135:39–143

Poole CF (1932) The interspecific hybrid, *Crepis rubra* × *C. foetida*, and some of its derivatives. II. Two selfed generations from an amphidiploid hybrid. *Univ Calif Publ Agric Sci* 6:231–255

Qi LL, Echalier B, Chao S, Lazo GR, Butler GE, Anderson OD, Akhunov ED, Dvorak J, Linkiewicz AM, Ratnasiri A, Dubcovsky J, Bermudez-Kandianis CE, Greene RA, Kantety R, La Rota CM, Munkvold JD, Sorrells SF, Sorrells ME, Dilbirligi M, Sidhu D, Erayman M, Randhawa HS, Sandhu D, Bondareva SN, Gill KS, Mahmoud AA, Ma XF, Miftahudin, Gustafson JP, Conley EJ, Nduati V, Gonzalez-Hernandez JL, Anderson JA, Peng JH, Lapitan NLV, Hossain KG, Kalavacharla V, Kianian SF, Pathan MS, Zhang DS, Nguyen HT, Choi DW, Fenton RD, Close TJ, McGuire PE, Qualset CO, Gill BS (2004) A chromosome bin map of 16,000 expressed sequence tag loci and distribution of genes among the three genomes of polyploid wheat. *Genetics* 168:701–712

Raina SN, Rani V (2001) GISH technology in plant genome research. *Methods Cell Sci* 23:83–104

Rajhathy T (1975) Trisomics of *Avena strigosa*. *Can J Genet Cytol* 17:151–166

Randhawa HS, Dilbirligi M, Sidhu D, Erayman M, Sandhu D, Bondareva S, Chao S, Lazo GR, Anderson OD, Miftahudin, Gustafson JP, Echalier B, Qi LL, Gill BS, Akhunov ED, Dvorak J, Linkiewicz AM, Ratnasiri A, Dubcovsky J, Bermudez-Kandianis CE, Greene RA, Sorrells ME, Conley EJ, Anderson JA, Peng JH, Lapitan NLV, Hossain KG, Kalavacharla V, Kianian SF, Pathan MS, Nguyen HT, Endo TR, Close TJ, McGuire PE, Qualset CO, Gill KS (2004) Deletion mapping of homoeologous group *6*-specific wheat expressed sequence tags. *Genetics* 168:677–686

Reamon-Ramos SM, Wricke G (1992) A full set of monosomic addition lines in *Beta vulgaris* from *Beta webbiana*: morphology and isozyme markers. *Theor Appl Genet* 84:411–418

Rhoades MM, McClintock B (1935) The cytogenetics of maize. *Bot Rev* 1:292–325

Rick CM, Barton DW (1954) Cytological and genetical identification of the primary trisomics of the tomato. *Genetics* 39:640–666

Riera-Lizarazu O, Rines HW, Phillips RL (1996) Cytological and molecular characterization of oat × maize partial hybrids. *Theor Appl Genet* 93:123–135

Riera-Lizarazu O, Vales MI, Ananiev EV, Rines HW, Philips RL (2000) Production and characterization of maize chromosome 9 radiation hybrids derived from an oat-maize addition line. *Genetics* 156:327–339

Salazar GM, Joppa LR (1981) Use of substitution-monosomics to determine the chromosomal location of genes conditioning stem rust resistance in Langdon durum. *Crop Sci* 21: 681–685

Schubert I, Shi F, Fuchs J, Endo TR (1998) An efficient screening for terminal deletions and translocations of barley chromosomes added to common wheat. *Plant J* 14:489–495

Sears ER (1966) Nullisomic-tetrasomic combinations in hexaploid wheat. In: Lewis DR (ed), *Chromosome manipulation and plant genetics.* Oliver and Boyd, London, pp. 29–47

Shepherd KW, Islam KMR, Miller TE, Koebner RMD (1988) Fourth compendium of wheat-alien chromosome lines. In: Miller TE, Koebner RMD (eds) *Proceedings of the 7th International Wheat Genetics Symposium.* Bath Press, Bath, UK, pp. 1373–1393

Shi F, Endo TR (1997) Production of wheat-barley disomic addition lines possessing an *Aegilops cylindrica g*ametocidal chromosome. *Genes Genet Syst* 72:243–248

Shigyo M, Tashiro Y, Isshiki S, Miyazaki S (1996) Establishment of a series of alien monosomic addition lines of Japanese bunching onion (*Allium fistulosum* L.) with extra chromosomes from shallot (*A. cepa* L. Aggregatum group). *Genes Genet Syst* 71:363–371

Singh RP (1993) Genetic association of gene *Bdv1* for tolerance to Barley Yellow Dwarf Virus with genes *Lr34* and *Yr18* for adult plant resistance to rusts in bread wheat. *Plant Dis* 77:1103–1106.

Singh RJ (2003) *Plant Cytogenetics,* 2nd edition. CRC Press, Boca Raton, Florida.

Stewart E, Mckusick K, Aggarwal A, Bajorek E, Brady S, Chu A, Fang N, Hadley D, Harris M, Hussain S, Lee R, Maratukulam A, O'Connor K, Perkins S, Piercy M, Qin F, Reif T, Sanders C, She XH, Sun WL, Tabar P, Voyticky S, Cowles S, Fan JB, Mader C, Quackenbush J, Myers RM, Cox DR (1997) An STS-based radiation hybrid map of the human genome. *Genome Res* 7:422–433

Suen DF, Wang CK, Lin RF, Kao YY, Lee FM, Chen CC (1997) Assignment of DNA markers to *Nicotiana sylvestris* chromosomes using monosomic alien addition lines. *Theor Appl Genet* 94:331–337

Suyama Y, Kawamuro K, Kinoshita I, Yoshimura K, Tsumura Y, Takahara H (1996) DNA sequence from a fossil pollen of *Abies* spp. from Pleistocene peat. *Genes Genet Syst* 71:145–149

Sybenga J (1992) *Cytogenetics in Plant Breeding.* Monographs on Theoretical and Applied Genetics 17. Springer-Verlag, Berlin, Heidelberg, New York

Tsuchiya T (1958) Studies on the trisomics in barley. I. Origin and the characteristics of primary simple trisomics in *Hordeum spontaneum* C. Koch. *Seiken Ziho* 9:69–86

Tsuchiya T (1961) Studies on the trisomics in barley. II. Cytological identification of the extra chromosomes in crosses with Burnham's translocation testers. *Japan J Genet* 36:444–451

Tsuchiya T (1967) Establishment of a trisomic series in a two-rowed cultivated variety of barley. *Can J Genet Cytol* 9:667–682

Tsujimoto H (1993) Molecular cytological evidence for gradual telomere synthesis at the broken chromosome ends in wheat. *J Plant Res* 106:239–244

Tsujimoto S, Pelto-Huikko M, Aitola M, Meister B, Vik-Mo EO, Davanger S, Scheller RH, Bean AJ (1999) The cellular and developmental expression of Hrs-2 in rat. *Eur J Neurosci* 11:3047–3063

van den Bosch M, Lohman PH, Pastink A (2002) DNA double-strand break repair by homologous recombination. *Biol Chem* 383:783–892

Van Geyt JPC, Oleo M, Lange W, De Bock TSM (1988) Monosomic additions in beet (*Beta vulgaris*) carrying extra chromosomes of *Beta procumbens*. I. Identification of the alien chromosomes with the help of isozyme markers. *Theor Appl Genet* 76:577–586

van Haaren MJ, Ow DW (1993) Prospects of applying a combination of DNA transposition and site-specific recombination in plants: a strategy for gene identification and cloning. *Plant Mol Biol* 23:525–533

van Heusden AW, Shigyo M, Tashiro Y, Vrielink-van Ginkel R, Kik C (2000) AFLP linkage group assignment to the chromosomes of *Allium cepa* L. via monosomic addition lines. *Theor Appl Genet* 100:480–486

Vignaux F, Hitte C, Priat C, Chuat JC, Andre C, Galibert F (1999) Construction and optimization of a dog whole-genome radiation hybrid panel. *Mamm Genome* 10:888–894

Visir IY, Mulligan BJ (1999) Genetics of gamma-irradiation-induced mutations in *Arabidopsis thaliana:* large chromosomal deletions can be rescued through the fertilization of diploid eggs. *J Hered* 90:412–417

Watanabe TK, Bihoreau M-T, McCarthy LC, Kiguwa SL, Hishigaki H, Tsuji A, Browne J, Yamasaki Y, Mizoguchi-Miyakita A, Oga K, Ono T, Okuno S, Kanemoto N, Takahashi E, Tomita K, Hayashi H, Adachi M, Webber C, Davis M, Kiel S, Knights C, Smith A, Critcher R, Miller J, Thangarajah T, Day PJR, Hudson JR, Irie Y, Takagi T, Nakamura Y, Goodfellow PN, Lathrop GM, Tanigami A, James MR (1999) A radiation hybrid map of the rat genome containing 5,255 markers. *Nat Genet* 22:27–36

Weber DF (1983) Monosomic analysis in diploid crop plants. In: Swaminathan MS, Gupta PK, Sinha U (eds), *Cytogenetics of Crop Plants.* Macmillan, New Delhi, pp. 351–378

Werner JE, Endo TR, Gill BS (1992a) Toward a cytogenetically based physical map of the wheat genome. *Proc Natl Acad Sci USA* 89:11307–11311

Werner JE, Kota RS, Gill BS, Endo TR (1992b) Distribution of telomeric repeats and their role in the healing of broken chromosome ends in wheat. *Genome* 35:844–848

West SC (2003) Molecular views of recombination proteins and their control. *Nature Rev Mol Cell Biol* 4:435–445

William MDHM, Mujeeb-Kazi A (1995) Biochemical and molecular diagnostics of *Thinopyrum bessarabicum* chromosomes in *Triticum aestivum* germ plasm. *Theor Appl Genet* 90:952–956

Xu SJ, Singh RJ, Kollipara KP, Hymowitz T (2000) Primary trisomics in soybean: origin, identification, breeding behavior, and uses in gene mapping. *Crop Sci* 40:1543–1551

Yano M (2001) Genetic and molecular dissection of naturally occurring variation. *Curr Opin Plant Biol* 4:130–135

Yildirim A, Jones SS, Murray TD (1998) Mapping a gene conferring resistance to *Pseudocercosporella herpotrichoides* on chromosome 4V of *Dasypyrum villosum* in a wheat background. *Genome* 41:1–6

Zeller FJ (1973) 1B/1R wheat-rye chromosome substitutions and translocations. In: Sears ER, Sears LMS (eds), *Proceedings of the 4th International Wheat Genetics Symposium.* Columbia, Missouri, USA, pp. 209–221

Zhang XY, Dong YS, Wang RRC (1996) Characterization of genomes and chromosomes in partial amphidiploids of the hybrid *Triticum aestivum* x *Thinopyrum ponticum* by in situ hybridization, isozyme analysis, and RAPD. *Genome* 39:1062–1071

Zou JJ, Singh RJ, Lee J, Xu SJ, Cregan PB, Hymowitz T (2003) Assignment of molecular linkage groups to soybean chromosomes by primary trisomics. *Theor Appl Genet* 107:745–750

Chapter 3
Plant B Chromosomes: What Makes Them Different?

Andreas Houben and Mariana Carchilan

Abstract B chromosomes are dispensable elements that do not recombine with the A chromosomes of the regular complement and that follow their own evolutionary pathway. Here, we survey current knowledge on the DNA/chromatin composition, origin, and drive mechanisms of B chromosomes and discuss the potential research applications of supernumerary chromosomes.

Keywords Selfish element · Drive · Centromere · Genome · Evolution · Chromosome · Nondisjunction

Contents

A. Houben (✉) • M. Carchilan
Leibniz-Institute of Plant Genetics and Crop Plant Research (IPK), Chromosome Structure and Function Laboratory, Corrensstrasse 3 06466, Gatersleben, Germany
e-mail: houben@ipk-gatersleben.de

H.W. Bass and J.A. Birchler (eds.), *Plant Cytogenetics*, Plant Genetics and Genomics: Crops and Models 4, DOI 10.1007/978-0-387-70869-0_3,

3.1 Introduction

Many animal and plant species contain a variable number of supernumerary chromosomes, B chromosomes, in addition to the normal (A) chromosome complement. B chromosomes (Bs) differ from A chromosomes in three major aspects: they rarely carry active genes, they can distort Mendelian inheritance in their favor, and they neither pair nor recombine with chromosomes of the normal complement. As a result, B chromosomes follow their own species-specific evolutionary pathways. Because most Bs do not confer any advantages on the organisms that harbor them, they may be thought of as parasitic elements that persist in populations by making use of the cellular machinery required for the inheritance and maintenance of A chromosomes. Bs are one of the most cryptic components of the genome, and they have always attracted much attention. Nevertheless, their origin, structure, and evolution remain elusive.

Various aspects of B chromosome biology have been comprehensively reviewed; see for example, Jones and Rees (1982); Jones (1991); Jones and Puertas (1993); Beukeboom (1994); Jones (1995); Bougourd and Jones (1997); Covert (1998); Camacho et al. (2000); Puertas (2002); Jones and Houben (2003); Jones (2004); Camacho (2005); Burt and Trivers (2006); Jones et al. (2008a, b), and a special volume on Bs in the journal *Cytogenetic and Genome Research* edited by Camacho (2004). Here we discuss current insights into the molecular structure and evolution of Bs and point out new research developments of the last few years that pertain to these enigmatic chromosomes.

3.2 Occurrence of B Chromosomes Among Angiosperms

The distribution of Bs among angiosperms is not random. Among flowering plants, they are more likely to occur in outcrossing than in inbred species, and their presence is also positively correlated with genome size and negatively with chromosome number. They are not found any more frequently in polyploids than in diploids or in allopolyploid species (Palestis et al. 2004; Levin et al. 2005). In many plants, different morphological types of Bs exist within a single species. The relationship between genome size and B frequency may be explained on the grounds that species with large genomes can tolerate supernumerary chromosomes more readily (Puertas 2002) or that the greater amount of noncoding DNA, which is what largely constitutes large genomes, is itself a trigger for B formation (Levin et al. 2005). According to a survey of 23,652 angiosperm species (about 9% of the estimated 260,000 species), about 8% of monocots and 3% of eudicots have Bs, and of these by far the largest numbers of species belong to the Poaceae and Asteraceae (see examples in Fig. 3.1). Because these families are also highly speciose, however, several other families have a higher proportion of species with Bs. Among orders, the two B-chromosome "hot spots" are the Liliales and Commelinales (Palestis et al. 2004; Levin et al. 2005).

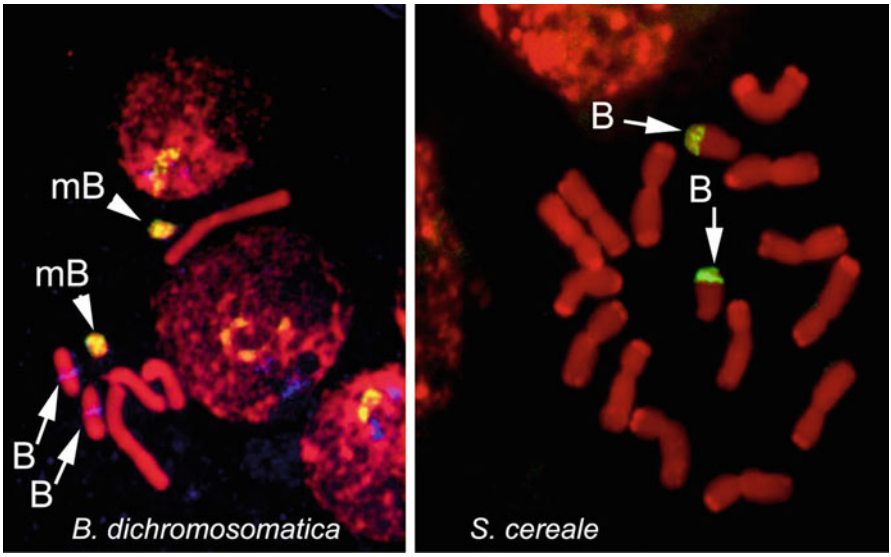

Fig. 3.1 B chromosomes of *Brachyscome dichromosomatica* (Asteraceae) and of rye (*Secale cereale* L.). *B. dichromosomatica* (2n = 4 + large Bs + micro Bs) occurs in four karyotypically distinct cytodemes. In some cases additional supernumerary A chromosome fragments are present, as well as different types of Bs within a single plant. The large Bs are somatically stable, and the dot-like micro Bs somatically unstable. The image shows a mitotic cell of *B. dichromosomatica* after FISH performed with a micro B-specific probe (Bdm29, Houben et al. 1997b), in *yellow* (*arrows*), and a standard B centromere-specific probe (Bd49, John et al. 1991), in *blue* (*arrows*). The rye (2n = 14 + Bs) image at mitotic metaphase shows two Bs (*arrows*) after FISH performed with the B-specific probe D1100 (in *red*), which marks the end of the long arm of each B (Sandery et al. 1990)

3.3 What Does DNA Analysis Tell Us About the Origin of Bs?

Several scenarios for the origin of Bs have been proposed, and they probably arose in different ways in different organisms (reviewed by Camacho et al. 2000; Jones and Houben 2003). The most widely accepted view is that they are derived from the As. Some evidence also suggests that Bs can be spontaneously generated in response to the new genomic conditions after interspecific hybridization. The involvement of sex chromosomes has also been argued for their origin in some animals (see e.g., Camacho et al. 2000). Despite the high number of species with Bs, their de novo formation is probably a rare event, because the occurrence of different B variants within species suggests a close relationship between the different variants (Jones and Puertas 1993; Houben et al. 1999).

The molecular processes that gave rise to Bs during evolution remain unclear, but the characterization of sequences residing on them sheds some light on their origin and evolution. In maize (*Zea mays* L.) and *Brachyscome* (*Brachycome*) *dichromosomatica* C. R. Carter, for example, the Bs contain sequences that originate from different As, so the Bs could represent an amalgamation of these diverse

A-derived sequences (Alfenito and Birchler 1993; Houben et al. 2001; Cheng and Lin 2003). In the progeny of a triploid rice plant, a newly formed B was recently identified, but on the basis of an analysis of B-positive plants that used 72 different chromosome arm-specific single-copy sequence markers, the B seems not to have been directly derived from a single A chromosome (Cheng et al. 2000). The actual process of sequence transfer from As to Bs is not clear, but recent results of Cheng and Lin (2004) and Lamb et al. (2007) indicate that transposition of mobile elements may have played an important role. Analysis of large DNA insert clones demonstrated that maize Bs are composed of B-specific sequences intermingled with those in common with the As. The 22-kb-long B-specific *StarkB* element, e.g., has been subject to frequent insertions by LTR-type retroelements (Lamb et al. 2007), in a fashion similar to the nested insertions seen in some intergenic A chromosome regions (SanMiguel et al. 1996). Using the LTR divergence of retroelements interrupting B-specific sequences, Lamb et al. (2007) have estimated the minimum age of the maize B to be at least two million years. Recently established oat-maize B chromosome addition lines (Kynast et al. 2007) should become an ideal material for the further characterization of the maize B sequence composition because of the low level of sequence similarity between oat and maize.

B chromosomes provide an ideal target for transposition of mobile elements (McAllister 1995), and insertion of such elements may therefore be responsible for the generation of structural variability in Bs (Camacho et al. 2000). Indeed, a B-specific accumulation of Ty3/gypsy retrotransposons has been reported for the fish *Alburnus alburnus* (L.) (Ziegler et al. 2003). In the same context, note that Bs contain types of coding and noncoding repeats similar to those found in extrachromosomal DNA of various organisms (Cohen et al. 2003). Extrachromosomal DNA with similarity to tandem repeat sequences shared by A and B chromosomes has recently been identified (Cohen et al. 2008), but whether an evolutionary link exists between extrachromosomal DNA and the evolution of Bs remains to be determined.

A preferential contribution of rDNA coding repeats to the evolution of B chromosomes has been proposed, because rDNA loci have been detected on Bs of many species, e.g., *Crepis capillaris* (L.) Wallr. (Maluszynska and Schweizer 1989), *Rattus rattus* (L.) (Stitou et al. 2000), *Trichogramma kaykai* Pinto & Stouthamer (van Vugt et al. 2005), and others (for review, see Green 1990; Jones 1995). In the herb *Plantago lagopus* L. the origin of a B chromosome seems to be associated with massive amplification of 5S rDNA sequences after fragmentation of an aneuploid A chromosome (Dhar et al. 2002). Alternatively, B chromosomal rDNA sites could be a consequence of the reported mobile nature of rDNA (Schubert and Wobus 1985); Bs may be the preferred "landing sites" because of B chromosome inactivity. Increasing evidence also indicates that ribosomal sequences can change position within the genome without corresponding changes in the surrounding sequences (Dubcovsky and Dvorak 1995; Shishido et al. 2000; Datson and Murray 2006). The sequence information of B-located rRNA genes has been used to study the likely origin of Bs by revealing the relatedness of the internal transcribed spacers (ITS) between the different chromosome types. Sequence analysis of A and B ITS

sequences of *C. capillaris* (Leach et al. 2005) and *B. dichromosomatica* (Donald et al. 1997; Marschner et al. 2007b), and comparisons with sequences of related species, indicates that the B chromosome rRNA genes are probably derived from those of the A chromosomes of the host species.

Some findings imply that B chromosomes may arise spontaneously in response to the genomic stress after interspecific hybridization, e.g., in *Coix aquatica* Roxb. and *C. gigantea* J. König ex Roxb. (Sapre and Deshpande 1987), *Poecilia latipinna* Lesueur, 1821) and *P. mexicana* Steindachner, 1863 (Schartl et al. 1995). After fertilization, the two different parental genomes are combined within a single nucleus, which in most cases is embedded within the maternal cytoplasm. Such a novel genomic constitution may result in conflicts, and as a consequence a genomic and epigenetic reorganization of the genomes can occur (Riddle and Birchler 2003). An incomplete loss of one parental genome during hybrid embryogenesis might play a role in the hybrid origin of Bs. Evidence exists that, during the uniparental chromosome elimination process, the centromeres of parental chromosomes undergoing elimination are the last to be lost (Gernand et al. 2005). If such a centric fragment is retained, rather than being eliminated, a subsequent spontaneous doubling could provide an ideal prerequisite for the de novo formation of a supernumerary chromosome. Indeed, a centric fragment was generated during the introgression of a chromosome region from the wasp *Nasonia giraulti* Darling into *N. vitripennis* (Walker). This neo B showed a lower than normal Mendelian segregation rate in meiosis, and some mitotic instability; but the transmission rate and mitotic stability then increased over successive generations (Perfectti and Werren 2001).

On the basis of new insights into the mechanisms of chromosome evolution (Hall et al. 2006; Lysak et al. 2006; Schubert 2007), we are tempted to ask, as did Patton (1977), whether the "by-product" of a Robertsonian translocation between two nonhomologous acrocentric chromosomes with breakpoints close to centromeres could evolve into a B-like chromosome (Fig. 3.2). Although the minichromosomes formed from Robertsonian translocation events are mainly composed of centromeric sequences, they are frequently lost because of the lack of essential genes and their failure to pair and to segregate properly during meiosis. Centromeric regions are also highly dynamic and display a low recombination frequency (Gaut et al. 2007), and recent findings by Hall et al. (2006) point to (peri)centromeres as genomic regions that may experience selective pressures distinct from those acting on euchromatin. They can tolerate rapid changes in structure and sequence content, such as large insertions of B chromosome–typical sequences, e.g., mobile elements, rDNA arrays, and satellite arrays. When a nonessential centromeric fragment survives, rapid sequence alteration may prevent meiotic pairing with the As, and the gain of a drive (by an unknown mechanism) may result in its finding its own evolutionary pathway as a proto-B.

In addition, tertiary trisomics, which appear in the progenies of translocation heterozygotes' chromosomes, have been hypothesized, under certain circumstances (e.g., suppressed crossing-over, rapid loss of genetic activity to overcome genetic imbalance, and positive selection for plants with an extra chromosome), to be suited for B chromosome formation (e.g., in the garden pea; Berdnikov et al. 2003).

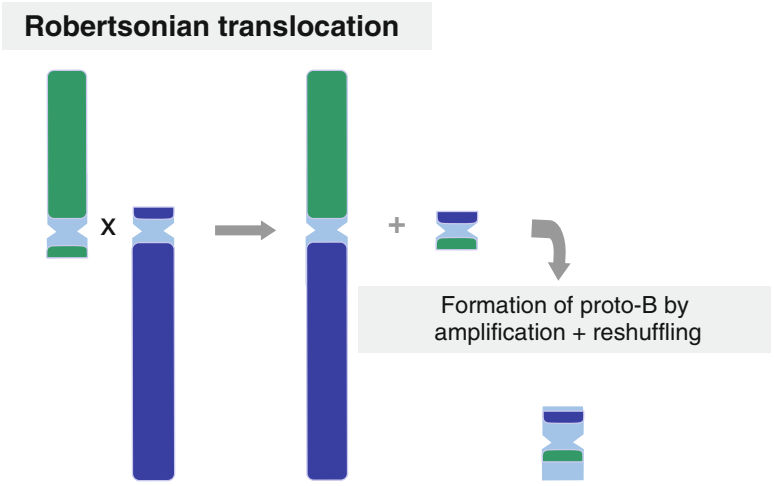

Fig. 3.2 Postulated mechanism of proto-B chromosome formation. A minichromosome, the "by-product" of a Robertsonian translocation between nonhomologous acrocentric chromosomes represents a nascent B. The nonrecombining minichromosome is composed of mainly (peri) centromeric sequences, which can undergo rapid structural changes (e.g., reshuffling, insertion, and amplification of noncoding sequences)

In the future, efficient and less costly sequencing tools should allow the analysis of megabase-long DNA fragments derived from A and B chromosomes. Comparative sequence analysis will then significantly improve our knowledge of the origin of Bs and hence of the evolution of genomes.

3.4 Do the Chromatin Compositions of As and Bs Differ?

Although chromatin structure is increasingly seen as having an essential role in different aspects of chromosome function, little information is available on the chromatin composition of Bs and whether it differs from that of the As. On the basis of classical cytological observations, an early survey suggested that the Bs in about half of the plant species that carry them are described as being heterochromatic (Jones 1975). Because no genes with specific phenotypic effects necessary for normal development are known for Bs, the finding that some of them are totally euchromatic is surprising.

Recent advances in chromatin characterization, in terms of epigenetic marks, have revealed the involvement of DNA methylation and posttranslational histone modifications in various aspects of chromosome biology (reviewed by Kouzarides 2007). The N-terminal tails of the nucleosomal core histones, extending from the nucleosome surface, are subjected to posttranslational modifications such as

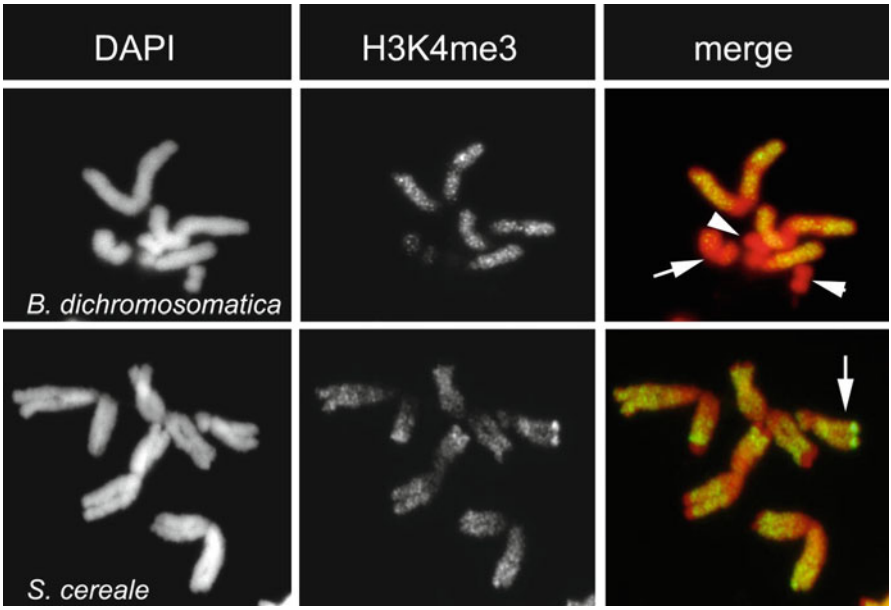

Fig. 3.3 Metaphase cell of *B. dichromosomatica* with two micro Bs (*arrowheads*) and one large B (*arrow*) and of rye (*S. cereale*) with a single B (*arrow*) after immunostaining with antibodies specific for histone H3K4me3. Note the strong immunolabeling of the rye B-terminal region and the weaker immunolabeling of the *B. dichromosomatica* Bs

acetylation, methylation, phosphorylation, ubiquitination, glycosylation, ADP-ribosylation, carbonylation, and sumoylation. Several studies have shown that modification of the histone H3 tail by methylation of lysine residues 9 and 27 negatively regulates transcription by mediating a compact chromatin structure. In contrast, euchromatin is marked by methylation of lysine residue 4 (reviewed by Martin and Zhang 2005). Although euchromatin-specific methylation of H3K4 is highly conserved among eukaryotes, heterochromatin indexing by methylation marks at H3K9/27 and H4K20 is more variable (reviewed by Fuchs et al. 2006).

In *B. dichromosomatica*, although C-banding and DAPI-staining results suggest similar eu- and heterochromatin compositions of large B and A chromosomes, the large Bs are characterized by a low level of euchromatic histone marks. Heteropycnotic, tandem repeat-enriched micro Bs revealed only traces of these histone modifications. No differences between A and B chromosomes were found for the heterochromatic marks H3K9me1/2 and H3K27me1, indicating that Bs are marked not by enrichment with heterochromatic histone marks but by a low level of euchromatin-associated histone modifications (Fig. 3.3; Marschner et al. 2007a). Although B and sex chromosomes differ in biology, in this context, sex-chromosome inactivation in mammals is, interestingly, associated with heterochromatin-specific histone modifications, for example, dimethylation of H3K9 and H3K27 (reviewed

by Heard 2005). Because of the general absence of functional genes on Bs, they probably have no need to be enriched with heterochromatin-specific histone modifications, which are involved in gene inactivation.

B chromosomes of *B. dichromosomatica* are also characterized by a low level of histone H4 acetylation at lysine positions 5 and 8 (Houben et al. 1997a), and no difference between A and Bs was found for the acetylated histone H4 at lysine positions 12 and 16. The association of histone acetylation with transcriptional activation of promoters, and of deacetylation with silencing of repetitive transgenes and rDNA, has been confirmed for plants (Tian et al. 2005). At the microscopic level, no correlation was observed between the distribution of immunosignals for acetylated H4 isoforms and transcriptional activity. At the chromosomal level, H4 acetylation is strongly associated with DNA replication, and this posttranslational modification may be required for postreplicational repair (reviewed by Fuchs et al. 2006).

In rye (*Secale cereale* L.), the subterminal heterochromatic domain of the B is characterized by a unique combination of histone methylation marks (Carchilan et al. 2007). Unlike the heterochromatic regions of A chromosomes, this domain is simultaneously marked by trimethylated histone H3K4 (Fig. 3.3) and by trimethylated H3K27. In addition this domain shows a dark Giemsa band at mitosis but undergoes decondensation during interphase (Morais-Cecilio et al. 1996; Langdon et al. 2000) and reveals transcription of B-specific high-copy-repeat families (Carchilan et al. 2007). The observed distribution patterns of the heterochromatin marks H3K9me1 along A and B chromosomes were mainly uniform, as reported for plants with large genomes (Houben et al. 2003). The terminal heterochromatic regions of As and Bs showed little H3K27me1 but were enriched in di- and trimethylated H3K27. Immunostaining against H4K20me1,2,3 resulted in a weak and dispersed labeling. The distribution pattern of 5-methylcytosine DNA residues showed a punctuated and uniform pattern along rye A and B chromosomes (Carchilan et al. 2007).

More comparative studies are needed before a general B-specific pattern of histone modifications can be affirmed, if such exists. The study of species in which the Bs are less or more heterochromatic than the A chromosomes might help to reveal possible relationships between posttranslational histone marks and the chromatin composition and unique behavior of Bs.

3.5 Segregation Behavior of B Chromosomes

Bs fail to pair with any members of the A chromosome set during meiosis, although they may pair and form chiasmata among themselves (Jones 1995). Because Bs appear to be devoid of essential genes and have no known adaptive advantage, their persistence in natural populations depends on the mechanisms of drive they have involved to ensure their survival. In many cases, maintenance is engendered by their transmission at higher than Mendelian frequencies, which allows their successful spread and accumulation in populations.

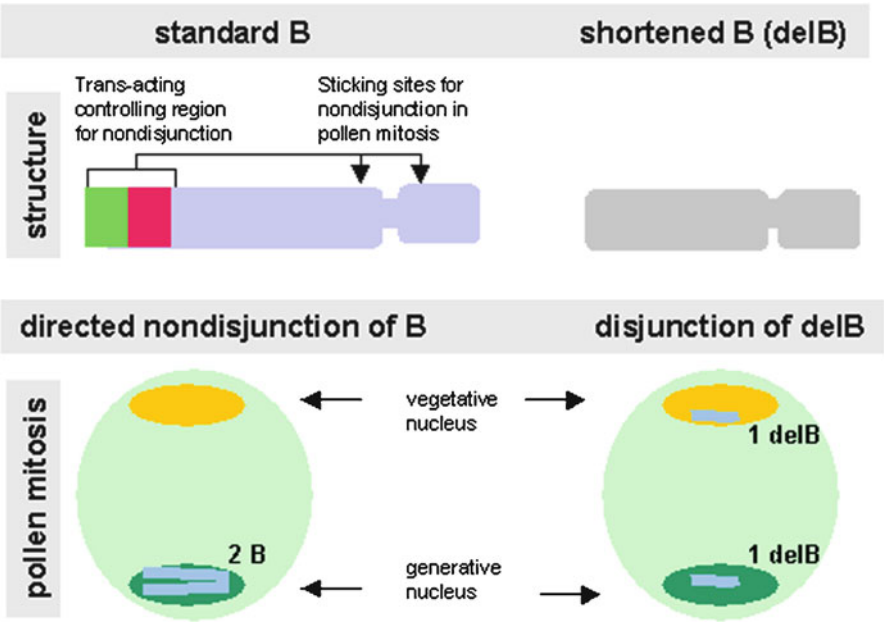

Fig. 3.4 Diagrammatic representation of the standard form of the B chromosome of rye and the form shortened by deletions. The B-specific repeats E3900 and D1100 are shown in green and red, respectively. Directed nondisjunction and normal disjunction of rye standard Bs and shortened Bs, respectively, at first pollen-grain mitosis. The shortened B does not undergo nondisjunction unless a normal B is present in the same nucleus, showing that the controlling element is trans-acting

The drive mechanisms of maize and rye Bs are well-studied examples that allow B chromosome accumulation. Bs of rye undergo a directed nondisjunction, into the generative nucleus, at the first mitosis of the pollen (Fig. 3.4). The generative nucleus then produces two sperm nuclei, each with an unreduced number of Bs. Essentially the B chromosome fails to separate its chromatids at this first division of the pollen, placing both chromatids of each B in the generative nucleus and thereby in the next generation. Notably, the B chromosome centromeres appear to divide normally, but on either side of the centromere are "sticking sites," which prevent normal anaphase separation of the chromatids and leading to nondisjunction at an average frequency of about 86% in rye (Matthews and Jones 1983). Nondisjunction works equally well when the rye B is introduced as an addition chromosome into hexaploid wheat (Müntzing 1970; Niwa et al. 1997; Endo et al. 2008) or *Secale vavilovii* Grossh. (Puertas et al. 1985). Therefore, the behavior of the B is autonomous and independent of the background genotype. The B itself controls the process of nondisjunction and B-transmission frequency (Romera et al. 1991). The accumulation mechanism of the rye B requires a factor located on the end of its long arm, which may also act in *trans*, Bs that lack this terminal region undergo normal disjunction (Müntzing 1948; Jones 1991; Endo et al. 2008), but if a standard B

(Lima-de-Faria 1962), or the terminal region of the long arm of the B (Endo et al. 2008) is also present in the same cell, the standard B mediates nondisjunction of both itself and the deficient B.

For analysis of the function of the terminal B-region in more detail, different rye B–wheat (*Triticum aestivum* L.) chromosome translocations and B deletions were generated using the wheat gametocidal system (Endo 2007; Endo et al. 2008). No whole-arm translocations were found between rye B and wheat A chromosomes, so the B centromere might have a unique structure that prevents centromeric fusion with the wheat centromere (Endo et al. 2008). Bs with deficiencies in the short arm retained the capacity for nondisjunction, albeit at lower frequencies than the standard B, so the size of the pericentromeric B-region might regulate the action of nondisjunction. Analysis of Bs with deficiencies in the long arm indicated that a critical nondisjunction element might be located within the region between the E3900- and D1100-positive chromosome region. Alternatively, the number of the repetitive sequences themselves could be the critical factor for nondisjunction. If the B-terminal region is translocated to a wheat chromosome, a balanced number of B centromeres and terminal regions seems to be required for the regulation of nondisjunction (Endo et al. 2008).

The nondisjunction process in maize differs from that in rye. At least three properties allow the maize B to increase in numbers: nondisjunction at the second pollen mitosis, preferential fertilization of the egg by the sperm containing the B (Roman 1948; Carlson 1969; Rusche et al. 1997), and suppression of meiotic loss when the Bs are unpaired (Carlson and Roseman 1992). The lack of meiotic loss of B univalents is a special feature of maize Bs. In rye, for example, the B univalents are lost in about 80% of 1B×0B crosses (Jimenez et al. 1997).

As in rye, the B-accumulation mechanism in maize requires a factor located on the end of the long arm of the B that may act in *trans* (Roman 1947; Carlson 1978; Lamb et al. 2006). In selected native maize accessions, nondisjunction occurs in nearly 100% of the gametes (Rosato et al. 1996; Chiavarino et al. 2001). In the TB-10L18 translocation line, nondisjunction also occurs at the first pollen mitosis (Rusche et al. 1997). Furthermore, B nondisjunction takes place in the endosperm and in binucleated tapetal cells, Bs mediate A chromosome instability (Chiavarino et al. 2000; Gonzalez-Sanchez et al. 2004). One A-located "gene" seems to codetermine maize B accumulation by preferential fertilization and another "gene(s)" determines the meiotic loss of Bs (Gonzalez-Sanchez et al. 2003). Sperm nuclei containing deletion derivatives of B-9 (translocations lines involving the B and chromosome 9), which lack the centric heterochromatin and possibly some adjacent euchromatin, no longer have the capacity for preferential fertilization (Carlson 2007).

So far no gene sequence, or nondisjunction element, on any B has been characterized that plays a role in B accumulation, and the speculate is therefore tempting that noncoding RNA acts on the process of B chromosome nondisjunction. In fission yeast, e.g., the repeats flanking the kinetochore are essential for sister chromatid cohesion and are maintained in a proper heterochromatic state by the RNAi machinery (Bernard et al. 2001; Volpe et al. 2003). Similarly, pericentromeric

heterochromatin is required for proper chromosome cohesion and disjunction in flies and also in other organisms (Pidoux and Allshire 2005; Vos et al. 2006). Notably, forced accumulation of human centromeric noncoding satellite transcripts leads to defects in separation of sister chromatids (Bouzinba-Segard et al. 2006). Also, for plants, RNA molecules have been shown to play a role in establishing centromeric heterochromatin domains (Topp et al. 2004). In *Arabidopsis,* double-stranded RNA molecules arising from centromeric repeats may direct the formation and maintenance of centromeric heterochromatin through RNA interference (May et al. 2005). In this context, the transcriptional activity of repeats located in the B chromosome-nondisjunction-controlling region of maize (Lamb et al. 2007) and of rye (Carchilan et al. 2007) is striking. The unique chromatin conformation and transcriptional activity of the B-terminal region could be involved in the trans-acting mechanism of directed nondisjunction characteristic of B transmission.

3.6 Centromeres of B Chromosomes

An understanding of the structure and regulation of A and B centromeres is a prerequisite for a better understanding of the unique segregation behavior of Bs. The B-specific repeat ZmBs has been used to describe extensively the centromere of maize Bs (Alfenito and Birchler 1993; Kaszas and Birchler 1996, 1998; Kaszas et al. 2002), which are among the best-characterized plant centromeres. The centromeres of the maize Bs contains several megabases of ZmBs, a 156-bp satellite repeat (CentC), and centromere-specific retrotransposons (CRM elements). Only a small fraction of the ZmBs repeats interacts with kinetochore protein CENH3, the histone H3 variant specific to functional centromeres. CentC, which marks the CENH3-associated chromatin in maize A centromeres, is restricted to a similar 700-kb domain within the larger context of the ZmBs repeats (Jin et al. 2005). Centromere specification must have an epigenetic component, as dicentric A-B translocation chromosomes are characterized by stable inheritance of an inactive state of one of the centromeres over several generations (Han et al. 2006).

A comparison of maize A and B chromosomes seems to show that Bs are enriched with DNA elements that are normally found at or near A centromeres (Lamb et al. 2005). A similar tendency has been described for the rye B, which is characterized by a higher copy number of the rye retrotransposon-like centromeric repeat pAWRC.1 (Wilkes et al. 1995; Francki 2001). In contrast to maize Bs (Lamb et al. 2005), the rye kinetochore protein CENH3 is present in equal amounts on both As and Bs (Houben, unpublished data).

The centromeric region of *B. dichromosomatica* standard Bs (cytodeme A1, A2, and A4) is enriched with a B-specific tandem repeat (Bd49) that is not microscopically detectable on A chromosomes (Leach et al. 1995; Franks et al. 1996). Initially the predominantly centromeric location of the Bd49 repeat suggested a possible role for this sequence in the drive process, but a noncentromeric Bd49 signal in *B. dichromosomatica* cytodeme A3 and differences in signal size among all the Bs of different cytodemes do not support this assumption (Leach et al. 2004).

3.7 Effects Associated with B Chromosomes and B Transcribed Sequences

Although Bs are not essential, some phenotypic effects have been reported, and these effects are usually cumulative, depending upon the number and not the presence or absence of Bs. In low number, Bs have little if any influence on the phenotype, but at high numbers they often have a negative influence on fitness and fertility of the organism (reviewed by Jones and Rees 1982; Jones 1995; Bougourd and Jones 1997).

Evidence exists that Bs directly or indirectly influence the behavior of A chromosomes. One of the most remarkable of such effects is the potential impact of Bs on diploidization in allopolyploid hybrids, e.g., *Lolium temulentum* × *L. perenne* + B (Evans and Davies 1985), where Bs prevent or suppress the homoeologous pairing of As. In wheat × *Aegilops* hybrids, Bs contributed by the *Aegilops* parent seem able to substitute for the *ph* locus of the hexaploid wheat (further examples are reviewed by Tanaka and Kawahara 1982; Jenkins and Jones 2004). The rDNA-negative B of rye seems to influence the interphase organization of rye and wheat A-chromosome ribosomal chromatin (Delgado et al. 1995, 2004; Morais-Cecilio et al. 2000). The authors proposed that the Bs are "genetically inert" but "chromosomally active."

Except for the B-located 45S rRNA gene of *C. capillaris*, however, in which one of two B-specific members of the rRNA gene family was weakly transcribed (Leach et al. 2005), no direct molecular evidence supports transcription of B chromosome genes in any plant species, whereas inactive ribosomal genes are found on Bs of several plants (e.g., *B. dichromosomatica,* Donald et al. 1997; Marschner et al. 2007b) and in mammals (e.g., *Rattus rattus,* Stitou et al. 2000).

Indirect evidence for weak transcriptional activity of Bs results from comparative analysis of esterase isozyme activity in plants with and without Bs in *Scilla autumnalis* L. (Ruiz Rejón et al. 1980) and rye (Bang and Choi 1990). In B-positive plants, additional bands were detected by protein electrophoresis, but in both cases whether the additional bands were caused by a B-located gene or whether Bs influenced the transcription behavior of an A-located gene remains unclear. For grasshoppers, Bs have been demonstrated to alter the expression of A chromosome genes (Cabrero et al. 1987).

Studies of the transcription behavior of animal Bs support the idea that Bs are genetically inert or weakly active. Autoradiographic studies of tritiated uridine incorporated into spermatocytes of the mouse *Apodemus peninsulae* (Thomas) (Ishak et al. 1991) and of the grasshoppers *Myrmeleotettix maculatus* (Thunberg) and *Chorthippus parallelus* (Zetterstedt) (Fox et al. 1974) indicated very little or no transcription of Bs.

Indirect evidence for transcription of Bs in the frog *Leiopelma hochstetteri* Fitzinger (Green 1988) and in the fly *Simulium juxtacrenobium* Bass & Brockhouse (Brockhouse et al. 1989) is based on the observation that meiotic Bs form lampbrush structures. Because transcribed coding and noncoding sequences (including highly repetitive sequences, Solovei et al. 1996) are organized as loops, the

lampbrush structure of the frog and the fly Bs may be caused by transcriptionally active coding or noncoding sequences. More recently, differential-display reverse transcription–polymerase chain reactions were performed for comparison of gene-expression profiles of mice (*Apodemus flavicollis* (Melchior)) with and without Bs (Tanic et al. 2005). Three cDNA fragments (chaperonin containing TCP-1, subunit 6b (zeta) (CCT6B), fragile histidine triad gene (FHIT), and hypothetical gene XP transcripts) were differentially expressed in mice with Bs, but not in animals without Bs, suggesting that the activity of some genes can be directly or indirectly associated with Bs. In canids the proto-oncogene C-KIT has been mapped to B chromosomes (Graphodatsky et al. 2005), and the observation that this gene is located on Bs of different canids raises questions about its functional significance and activity.

Besides some coding sequences, the transcriptional activity of B-specific repetitive sequences has been demonstrated. In maize, a retrotransposon-derived high-copy element is active (Lamb et al. 2007). In rye, two repeat families (E3900 and D1100), which are located at the subterminal region of the long B chromosome, are transcriptionally highly active, although with different tissue type-dependent activity (Carchilan et al. 2007). The function of these B-transcripts and the mechanism of transcription of B-repeats are unknown at present. It has been hypothesized that these transcripts could have a structural function in the organization and regulation of B chromosomes (Carchilan et al. 2007; Han et al. 2007).

3.8 Potential Uses of B Chromosomes

B chromosomes have been employed in mapping the A genome, modulating recombination, and exploring the structure of the centromere and the process of nondisjunction, as discussed by (Jones et al. 2008a, b). In the future, B chromosomes could become even important for the generation of chromosome-based vectors for gene transfer. Telomere-mediated chromosome truncation has recently been adapted for A and B chromosomes of maize (Yu et al. 2006, 2007; Birchler et al. 2008), work that raises the profile of this potential application. With respect to the possible use of Bs as a vector for transgenes, recall that Bs have little or no effect on an individual's phenotype, and this issue is only of concern where a high number Bs can reduce vigor (Puertas 2002). Constitutive transgene expression from B-derived minichromosomes suggests that inactivation of transgenes on B chromosomes (Yu et al. 2007), if it occurs, is at least not a rapid process. Because of the intrinsic post-meiotic drive of intact Bs, a B-chromosome-derived vector might potentially reveal an increase of transmission frequency above Mendelian expectation, and this feature would have to be silenced (Houben and Schubert 2007).

Acknowledgments The authors have been supported by the DAAD, DFG (1779/10-1), and the IPK (Germany). We thank Ingo Schubert and Neil Jones for discussions and helpful comments on the manuscript.

References

Alfenito MR, Birchler JA (1993) Molecular characterization of a maize B chromosome centric sequence. *Genetics* 135:589–597

Bang J-W, Choi HW (1990) Genetic analysis of esterase izozymes in rye (*Secale cereale* L.). *Korean J Genet* 12:87–94

Berdnikov VA, Gorel FL, Kosterin OE, Bogdanova VS (2003) Tertiary trisomics in the garden pea as a model of B chromosome evolution in plants. *Heredity* 91:577–583

Bernard P, Maure JF, Partridge JF, Genier S, Javerzat JP, Allshire RC (2001) Requirement of heterochromatin for cohesion at centromeres. *Science* 294:2539–2542

Beukeboom LW (1994) Bewildering Bs: an impression of the 1st B-chromosome conference. *Heredity* 73:328–336

Birchler J , Yu W, Han F (2008) Pant engineered minichromosomes and artificial chromosome platforms. *Cytogenet Genome Res* 120:228–232

Bougourd SM, Jones RN (1997) B chromosomes: a physiological enigma. *New Phytol* 137:43–54

Bouzinba-Segard H, Guais A, Francastel C (2006) Accumulation of small murine minor satellite transcripts leads to impaired centromeric architecture and function. Proc Natl Acad Sci USA 103:8709–8714

Brockhouse C, Bass JAB, Feraday RM, Straus NA (1989) Supernumerary chromosome evolution in the *Simulium vernum* Group (Diptera, Simuliidae). *Genome* 32:516–521

Burt A., Trivers R (2006) *Genes in Conflict: The Biology of Selfish Genetic Elements.* Belknap Press of Harvard University Press, Cambridge

Cabrero J, Alche JD, Camacho JPM (1987) Effects of B chromosomes on the activity of nucleolar organizer regions in the grasshopper *Eyprepocnemis plorans* – activation of a latent nucleolar organizer region on a B chromosome fused to an autosome. *Genome* 29:116–121

Camacho JPM (ed) (2004) B chromosomes in the eukaryote genome. *Cytogenet Genome Res* 106:147–410

Camacho JPM (2005) B chromosomes. In: Gregory TR (ed), *The Evolution of the Genome.* Elsevier, Burlington, pp 223–285

Camacho JPM, Sharbel TF, Beukeboom LW (2000) B-chromosome evolution. *Philos Trans R Soc B Biol Sci* 355:163–178

Carchilan M, Delgado M, Ribeiro T, Costa-Nunes P, Caperta A, Morais-Cecilio L, Jones RN, Viegas W, Houben A (2007) Transcriptionally active heterochromatin in rye B chromosomes. *Plant Cell* 19:1738–1749

Carlson WR (1969) Factors affecting preferential fertilization in maize. *Genetics* 62:543–554

Carlson WR (1978) B-chromosome of corn. *Annu Rev Genet* 12:5–23

Carlson WR (2007) Locating a site on the maize B chromosome that controls preferential fertilization. *Genome* 50:578–587.

Carlson WR, Roseman RR (1992) A new property of the maize B-chromosome. *Genetics* 131:211–223

Cheng YM, Lin BY (2003) Cloning and characterization of maize B chromosome sequences derived from microdissection. *Genetics* 164:299–310

Cheng YM, Lin BY (2004) Molecular organization of large fragments in the maize B chromosome: indication of a novel repeat. *Genetics* 166:1947–1961

Cheng ZK, Yu HX, Yan HH, Gu MH, Zhu LH (2000) B chromosome in a rice aneuploid variation. *Theor Appl Genet* 101:564–568

Chiavarino AM, Rosato M, Manzanero S, Jimenez G, Gonzalez-Sanchez M, Puertas MJ (2000) Chromosome nondisjunction and instabilities in tapetal cells are affected by B chromosomes in maize. *Genetics* 155:889–897

Chiavarino AM, Gonzalez-Sanchez M, Poggio L, Puertas MJ, Rosato M, Rosi P (2001) Is maize B chromosome preferential fertilization controlled by a single gene? *Heredity* 86:743–748

Cohen S, Yacobi K, Segal D (2003) Extrachromosomal circular DNA of tandemly repeated genomic sequences in *Drosophila. Genome Res* 13:1133–1145

Cohen S, Houben A, Segal D (2008) Extrachromosomal circular DNA derived from tandemly repeated genomic sequences in plants. *Plant J* 53, 1027–1034

Covert SF (1998) Supernumerary chromosomes in filamentous fungi. *Curr Genet* 33:311–319

Datson PM, Murray BG (2006) Ribosomal DNA locus evolution in *Nemesia:* transposition rather than structural rearrangement as the key mechanism? *Chromosome Res* 14:845–857

Delgado M, Morais-Cecilio L, Neves N, Jones RN, Viegas W (1995) The influence of B chromosomes on rDNA organization in rye interphase nuclei. *Chromosome Res* 3:487–491

Delgado M, Caperta A, Ribeiro T, Viegas W, Jones RN, Morais-Cecilio L (2004) Different numbers of rye B chromosomes induce identical compaction changes in distinct A chromosome domains. *Cytogenet Genome Res* 106:320–324

Dhar MK, Friebe B, Koul AK, Gill BS (2002) Origin of an apparent B chromosome by mutation, chromosome fragmentation and specific DNA sequence amplification. *Chromosoma* 111:332–340

Donald TM, Houben A, Leach CR, Timmis JN (1997) Ribosomal RNA genes specific to the B chromosomes in *Brachycome dichromosomatica* are not transcribed in leaf tissue. *Genome* 40:674–681

Dubcovsky J, Dvorak J (1995) Ribosomal RNA multigene loci: nomads of the Triticeae genomes. *Genetics* 140:1367–1377

Endo TR (2007) The gametocidal chromosome as a tool for chromosome manipulation in wheat. *Chromosome Res* 15:67–75

Endo TR, Nasuda S, Jones N, Dou QW, Akahori A, Wakimoto M, Tanka H, Niwa K, Tsujimoto H (2008) Dissection of rye B chromosomes and nondisjunction of the dissected segments in common wheat. *Genes Genet Syst* 83:23–30

Evans GM, Davies EW (1985) The genetics of meiotic chromosome pairing in *Lolium temulentum* × *Lolium perenne* tetraploids. *Theor Appl Genet* 71:185–192

Fox DP, Hewitt GM, Hall DJ (1974) DNA-replication and RNA transcription of euchromatic and heterochromatic chromosome regions during grasshopper meiosis. *Chromosoma* 45:43–62

Francki MG (2001) Identification of Bilby, a diverged centromeric Ty1-copia retrotransposon family from cereal rye (*Secale cereale* L.). *Genome* 44:266–274

Franks TK, Houben A, Leach CR, Timmis JN (1996) The molecular organisation of a B chromosome tandem repeat sequence from *Brachycome dichromosomatica. Chromosoma* 105:223–230

Fuchs J, Demidov D, Houben A, Schubert I (2006) Chromosomal histone modification patterns – from conservation to diversity. *Trends Plant Sci* 11:199–208

Gaut BS, Wright SI, Rizzon C, Dvorak J, Anderson LK (2007) Opinion – recombination: an underappreciated factor in the evolution of plant genomes. *Nat Rev Genet* 8:77–84

Gernand D, Rutten T, Varshney A, Rubtsova M, Prodanovic S, Bruss C, Kumlehn J, Matzk F, Houben A (2005) Uniparental chromosome elimination at mitosis and interphase in wheat and pearl millet crosses involves micronucleus formation, progressive heterochromatinization, and DNA fragmentation. *Plant Cell* 17:2431–2438

Gonzalez-Sanchez M, Gonzalez-Gonzalez E, Molina F., Chiavarino AM, Rosato M, Puertas MJ (2003) One gene determines maize B chromosome accumulation by preferential fertilisation; another gene(s) determines their meiotic loss. *Heredity* 90:122–129

Gonzalez-Sanchez M, Rosato M, Chiavarino M, Puertas MJ (2004) Chromosome instabilities and programmed cell death in tapetal cells of maize with B chromosomes and effects on pollen viability. *Genetics* 166:999–1009

Graphodatsky AS, Kukekova AV, Yudkin DV, Trifonov VA, Vorobieva NV, Beklemisheva VR, Perelman PL, Graphodatskaya DA, Trut LN, Yang FT, Ferguson-Smith MA, Acland GM, Aguirre GD (2005) The proto-oncogene C-KIT maps to canid B-chromosomes. *Chromosome Res* 13:113–122

Green DM (1988) Cytogenetics of the endemic New Zealand frog, *Leiopelma hochstetteri* – extraordinary supernumerary chromosome variation and a unique sex chromosome system. *Chromosoma* 97:55–70

Green DM (1990) Muller's rachet and the evolution of supernumerary chromosomes. *Genome* 33:818–824

Hall AE, Kettler GC, Preuss D (2006) Dynamic evolution at pericentromeres. *Genome Res* 16:355–364

Han F, Lamb JC, Birchler JA (2006) High frequency of centromere inactivation resulting in stable dicentric chromosomes of maize. *Proc Natl Acad Sci USA* 103:3238–3243

Han F, Lamb JC, Yu W, Gao Z, Birchler JA (2007). Centromere function and nondisjunction are independent components of the maize B chromosome accumulation mechanism. *Plant Cell* 19:524–533

Heard E (2005) Delving into the diversity of facultative heterochromatin: the epigenetics of the inactive X chromosome. *Curr Opin Genet Dev* 15:482–489

Houben A, Schubert I (2007) Engineered plant minichromosomes – a resurrection of B chromosomes? *Plant Cell* 19:2323–2327

Houben A, Belyaev ND, Leach CR, Timmis JN (1997a) Differences of histone H4 acetylation and replication timing between A and B chromosomes of *Brachycome dichromosomatica. Chromosome Res* 5:233–237

Houben A, Leach CR, Verlin D, Rofe R, Timmis JN (1997b) A repetitive DNA sequence common to the different B chromosomes of the genus *Brachycome. Chromosoma* 106:513–519

Houben A, Thompson N, Ahne R, Leach CR, Verlin D, Timmis JN (1999) A monophyletic origin of the B chromosomes of *Brachycome dichromosomatica* (Asteraceae). *Plant Syst Evol* 219:127–135

Houben A, Verlin D, Leach CR, Timmis JN (2001) The genomic complexity of micro B chromosomes of *Brachycome dichromosomatica. Chromosoma* 110:451–459

Houben A, Demidov D, Gernand D, Meister A, Leach CR, Schubert I (2003) Methylation of histone H3 in euchromatin of plant chromosomes depends on basic nuclear DNA content. *Plant J* 33:967–973

Ishak B, Jaafar H, Maetz JL, Rumpler Y (1991) Absence of transcriptional activity of the B chromosomes of *Apodemus peninsulae* during pachytene. *Chromosoma* 100:278–281

Jenkins G, Jones RN (2004) B chromosomes in hybrids of temperate cereals and grasses. *Cytogenet Genome Res* 106:314–319

Jimenez MM, Romera F, Gonzalez Sanchez M, Puertas MJ (1997) Genetic control of the rate of transmission of rye B chromosomes. 3. Male meiosis and gametogenesis. *Heredity* 78:636–644

Jin WW, Lamb JC, Vega JM, Dawe RK, Birchler JA, and Jiang J (2005) Molecular and functional dissection of the maize B chromosome centromere. *Plant Cell* 17:1412–1423

John UP, Leach CR, Timmis JN (1991) A sequence specific to B chromosomes of *Brachycome dichromosomatica. Genome* 34:739–744

Jones N, Houben A (2003) B chromosomes in plants: escapees from the A chromosome genome? *Trends Plant Sci* 8:417–423

Jones RN (1975) B chromosome systems in flowering plants and animal species. *Int Rev Cytol* 40:1–100

Jones RN (1991) B-chromosome drive. *Am Nat* 137:430–442

Jones RN (1995) Tansley Review No. 85: B chromosomes in plants. *New Phytol* 131:411–434

Jones RN (2004) B chromosomes. In: Goodman RM (ed), *Encyclopedia of Plant and Crop Science*. M. Dekker, New York, pp. 71–74

Jones RN, Rees H (1982) *B Chromosomes,* 1st edn. Academic, London.

Jones RN, Puertas MJ (1993). The B-chromosomes of rye (*Secale cereale* L.). In: Dhir KK, Sareen TS (eds), *Frontiers in Plant Science Research.* Bhagwati Enterprises, Dehli, pp. 81–112

Jones R N, Gonzalez-Sanchez M, Gonzalez-Garcia M, Vega JM, Puertas MJ (2008a) Chromosomes with a life of their own. *Cytogenet Genome Res* 120:265–280

Jones RN, Viegas W, Houben A (2008b) A century of B chromosomes in plants: so what? *Ann Bot (Lond)* 111:767–775

Kaszas E, Birchler JA (1996) Misdivision analysis of centromere structure in maize. *EMBO J* 15:5246–5255

Kaszas E, Birchler JA (1998) Meiotic transmission rates correlate with physical features of rearranged centromeres in maize. *Genetics* 150:1683–1692

Kaszas E, Kato A, Birchler JA (2002) Cytological and molecular analysis of centromere misdivision in maize. *Genome* 45:759–768

Kouzarides T (2007) Chromatin modifications and their function. *Cell* 128:693–705

Kynast RG, Galatowitsch MW, Huettl PA, Phillips RL, Rines, HW (2007) Adding B-chromosomes of *Zea mays* L. to the genome of *Avena sativa* L. *Maize Genet Coop Newslett* 81:17–19

Lamb J, Kato A, Birchler J (2005) Sequences associated with A chromosome centromeres are present throughout the maize B chromosome. *Chromosoma* 113:337–349

Lamb JC, Han F, Auger DL, Birchler J (2006) A trans-acting factor required for non-disjunction of the B chromosome is located distal to the TB-4Lb breakpoint on the B chromosome. *Maize Genet Coop Newslett* 80:51–54

Lamb JC, Riddle NC, Cheng YM, Theuri J, Birchler JA (2007) Localization and transcription of a retrotransposon-derived element on the maize B chromosome. *Chromosome Res* 15:383–398

Langdon T, Seago C, Jones RN, Ougham H, Thomas H, Forster JW, Jenkins G (2000) De novo evolution of satellite DNA on the rye B chromosome. *Genetics* 154:869–884

Leach CR, Donald TM, Franks TK, Spiniello SS, Hanrahan CF, Timmis JN (1995) Organization and origin of a B chromosome centromeric sequence from *Brachycome dichromosomatica. Chromosoma* 103:708–714

Leach CR, Houben A, Timmis JN (2004) The B chromosomes in *Brachycome. Cytogenet Genome Res* 106:199–209

Leach CR, Houben A, Field B, Pistrick K, Demidov D, Timmis JN (2005) Molecular evidence for transcription of genes on a B chromosome in *Crepis capillaris. Genetics* 171:269–278

Levin DA, Palestris BG, Jones RN, Trivers R (2005) Phyletic hot spots for B chromosomes in angiosperms. *Evolution* 59:962–969

Lima-de-Faria A (1962) Genetic interaction in rye expressed at the chromosome phenotype. *Genetics* 47:1455–1462

Lysak MA, Berr A, Pecinka A, Schmidt R, McBreen K, Schubert I (2006) Mechanisms of chromosome number reduction in *Arabidopsis thaliana* and related Brassicaceae species. *Proc Natl Acad Sci USA* 103:5224–5229

Maluszynska J, Schweizer D (1989) Ribosomal RNA genes in B chromosomes of *Crepis capillaris* detected by non-radioactive in situ hybridization. *Heredity* 62:59–65

Marschner S, Kumke K, Houben A (2007a) B chromosomes of *B. dichromosomatica* show a reduced level of euchromatic histone H3 methylation marks. *Chromosome Res* 15:215–222

Marschner S, Meister A, Blattner FR, Houben A (2007b) Evolution and function of B chromosomal 45S rDNA sequences in *Brachycome dichromosomatica. Genome* 50:638–644

Martin C, Zhang Y (2005) The diverse functions of histone lysine methylation. *Nat Rev Mol Cell Biol* 6:838–849

Matthews RB, Jones RN (1983) Dynamics of the B chromosome polymorphism in rye. II. Estimates of parameters. *Heredity* 50:119–137

May BP, Lippman ZB, Fang Y, Spector DL, Martienssen RA (2005) Differential regulation of strand-specific transcripts from *Arabidopsis* centromeric satellite repeats. *PLoS Genet* 1:e79

McAllister BF (1995) Isolation and characterization of a retroelement from B chromosome (PSR) in the parasitic wasp *Nasonia vitripennis. Insect Mol Biol* 4:253–262

Morais-Cecilio L, Delgado M, Jones RN, Viegas W (1996) Painting rye B chromosomes in wheat: interphase chromatin organization, nuclear disposition and association in plants with two, three or four Bs. *Chromosome Res* 4:195–200

Morais-Cecilio L, Delgado M, Jones RN, Viegas W (2000) Modification of wheat rDNA loci by rye B chromosomes: a chromatin organization model. *Chromosome Res* 8:341–351

Müntzing A (1948) Cytological studies of extra fragment chromosomes in rye. V. A new fragment type arisen by deletion. *Hereditas* 34:435–442

Müntzing A (1970) Chromosomal variation in the Lindström strain of wheat carrying accessory chromosomes in rye. *Hereditas* 66:279–286

Niwa K, Horiuchi G, Hirai Y (1997) Production and characterization of common wheat with B chromosomes of rye from Korea. *Hereditas* 126:139–146

Palestis BG, Trivers R, Burt A, Jones RN (2004) The distribution of B chromosomes across species. *Cytogenet Genome Res* 106:151–158

Patton JL (1977) B-chromosome systems in pocket mouse, *Perognathus baileyi*: meiosis and C-band studies. *Chromosoma* 60:1–14

Perfectti F, Werren JH (2001) The interspecific origin of B chromosomes: experimental evidence. *Evolution* 55:1069–1073

Pidoux AL, Allshire R (2005) The role of heterochromatin in centromere function. *Philos Trans R Soc Lond B Biol Sci* 360:569–579

Puertas MJ (2002) Nature and evolution of B chromosomes in plants: a non-coding but information-rich part of plant genomes. *Cytogenet Genome Res* 96:198–205

Puertas MJ, Romera F, Delapena A (1985) Comparison of B-chromosome effects on *Secale cereale* and *Secale vavilovii. Heredity* 55:229–234

Riddle NC, Birchler JA (2003) Effects of reunited diverged regulatory hierarchies in allopolyploids and species hybrids. *Trends Genet* 19:597–600

Roman H (1947) Mitotic nondisjunction in the case of interchanges involving the B-type chromosome in maize. *Genetics* 32:391–409

Roman H (1948) Directed fertilization in maize. *Proc Natl Acad Sci USA* 34:36–42

Romera F, Jimenez MM, Puertas MJ (1991) Genetic control of the rate of transmission of rye B chromosomes. 1. Effects in 2Bx0B crosses. *Heredity* 66:61–65

Rosato M, Chiavarino AM, Naranjo CA, Puertas MJ, Poggio L (1996) Genetic control of B chromosome transmission rate in *Zea mays* ssp. *mays* (Poaceae). *Am J Bot* 83:1107–1112

Ruiz Rejón M, Posse F, Oliver JL (1980) The B-chromosome system of *Scilla autumnalis* (Liliaceae) – effects at the isoenzyme level. *Chromosoma* 79:341–348

Rusche ML, Mogensen HL, Shi L, Keim P, Rougier M, Chaboud A, Dumas C (1997) B chromosome behavior in maize pollen as determined by a molecular probe. *Genetics* 147:1915–1921

Sandery MJ, Forster JW, Blunden R, Jones RN (1990) Identification of a family of repeated sequences on the rye B chromosome. *Genome* 33:908–913

SanMiguel P, Tikhonov A, Jin YK, Motchoulskaia N, Zakharov D, Melake-Berhan A, Springer PS, Edwards KJ, Lee M, Avramova Z, Bennetzen JL (1996) Nested retrotransposons in the intergenic regions of the maize genome. *Science* 274:765–768

Sapre B, Deshpande S (1987) Origin of B chromosomes in *Coix* L. through spontaneous interspecific hybridisation. *J Hered* 78:191–196

Schartl M, Nanda I, Schlupp I, Wilde B, Epplen JT, Schmid M, Parzefall J (1995) Incorporation of subgenomic amounts of DNA as compensation for mutational load in a gynogenetic fish. *Nature* 373:68–71

Schubert I (2007) Chromosome evolution. *Curr Opin Plant Biol* 10:109–115

Schubert I, Wobus U (1985). In situ hybridisation confirms jumping nucleolus organizing regions in *Allium. Chromosoma* 92:143–148

Shishido R, Sano Y, Fukui K (2000) Ribosomal DNAs: an exception to the conservation of gene order in rice genomes. *Mol Gen Genet* 263:586–591

Solovei IV, Joffe BI, Gaginskaya ER, Macgregor HC (1996) Transcription on lampbrush chromosomes of a centromerically localized highly repeated DNA in pigeon (*Columba*) relates to sequence arrangement. *Chromosome Res* 4:588–603

Stitou S, Diaz de La Guardia R, Jimenez R, Burgos M (2000) Inactive ribosomal cistrons are spread throughout the B chromosomes of *Rattus rattus* (Rodentia, Muridae). Implications for their origin and evolution. *Chromosome Res* 8:305–311

Tanaka M, Kawahara T (1982) Cytogenetical effects of B-chromosomes in plants – review. *Report of the Plant Germplasm Institute, Kyoto University*, 5:1–18

Tanic N, Vujosevic M, Dedovic-Tanic N, Dimitrijevic B (2005) Differential gene expression in yellow-necked mice *Apodemus flavicollis* (Rodentia, Mammalia) with and without B chromosomes. *Chromosoma* 113:418–427

Tian L, Fong MP, Wang JYJ, Wei NE, Jiang HM, Doerge RW, Chen ZJ (2005) Reversible histone acetylation and deacetylation mediate genome-wide, promoter-dependent and locus-specific changes in gene expression during plant development. *Genetics* 169:337–345

Topp CN, Zhong CX, Dawe RK (2004) Centromere-encoded RNAs are integral components of the maize kinetochore. *Proc Natl Acad Sci USA* 101:15986–15991

van Vugt J, de Nooijer S, Stouthamer R, de Jong H (2005) NOR activity and repeat sequences of the paternal sex ratio chromosome of the parasitoid wasp *Trichogramma kaykai. Chromosoma* 114:410–419

Volpe T, Schramke V, Hamilton GL, White SA, Teng G, Martienssen RA, Allshire RC (2003) RNA interference is required for normal centromere function in fission yeast. *Chromsome Res* 11:137–146

Vos LJ, Famulski JK, Chan GK (2006) How to build a centromere: from centromeric and pericentromeric chromatin to kinetochore assembly. *Biochem Cell Biol* 84:619–639

Wilkes TM, Francki MG, Langridge P, Karp A, Jones RN, Forster JW (1995) Analysis of rye B-chromosome structure using fluorescence in situ hybridization (FISH). *Chromosome Res* 3:466–472

Yu W, Lamb JC, Han F, Birchler JA (2006) Telomere-mediated chromosomal truncation in maize. *Proc Natl Acad Sci USA* 103:17331–17336

Yu W, Han F, Gao Z, Vega JM, Birchler JA (2007) Construction and behavior of engineered minichromosomes in maize. *Proc Natl Acad Sci USA* 104:8924–8929

Ziegler CG, Lamatsch DK, Steinlein C, Engel W, Schartl M, Schmid M (2003) The giant B chromosome of the cyprinid fish *Alburnus alburnus* harbours a retrotransposon-derived repetitive DNA sequence. *Chromosome Res* 11:23–35

Chapter 4
Cytogenetic Mapping in Plants

Debbie M. Figueroa, Ina E. Amarillo, and Hank W. Bass

Abstract The first cytological maps in plants were based on natural features such as centromeres, the nucleolus organizing regions, and euchromatin-heterochromatin boundaries. Subsequently, researchers identified and used stains such as quinacrine and Giemsa to stain types of chromatin, such as AT-rich regions, differentially. Cytology was instrumental in mapping various chromosomal rearrangements. Electron microscopy has also proven to be a powerful tool, permitting three-dimensional reconstruction of chromosomes from whole-nucleus preparations as well as providing a direct link between linkage and physical distance by localization of recombination nodules on synaptonemal-complex spreads. The application of in situ hybridization (ISH) greatly advanced plant cytogenetic mapping. The development of nonradioactive probe-labeling techniques, such as biotinylation and more recently fluorescence, has made ISH an accessible method for the localization of specific nucleic-acid sequences along the physical chromosomes of plants. A variety of DNA probes have been used in plant cytogenetic mapping, including genetic marker sequences, large DNA fragments, and repetitive sequences. Several tissues and techniques have been used to prepare target chromosomes for mapping, each affording different advantages and disadvantages with regard to resolution and availability. Recently, additional techniques have been developed that elongate chromosomes for even higher resolution. Cytogenetic mapping has proven useful for observing genome organization, and much research is currently focused on integration of plant cytological and linkage maps.

D.M. Figueroa
Department of Biological Science, Florida State University, Tallahassee, FL 32306-4295, USA

H.W. Bass (✉)
Institute of Molecular Biophysics, The Florida State University, Tallahassee, FL 32306-4370, USA

Department of Biological Science, The Florida State University,Tallahassee, FL 32306-4295, USA
e-mail: bass@bio.fsu.edu

I.E. Amarillo
Department of Pathology and Laboratory Medicine, David Geffen School of Medicine at UCLA, Los Angeles, CA 90024, USA

H.W. Bass and J.A. Birchler (eds.), *Plant Cytogenetics*, Plant Genetics and Genomics: Crops and Models 4, DOI 10.1007/978-0-387-70869-0_4,

Keywords Geimsa-banding · C-banding · Karyotype · Fluorescence in situ hybridization (FISH) · Probe detection and resolution

Abbreviations

3D	Three-dimensional
AFLP	Amplified fragment length polymorphism
BAC	Bacterial artificial chromosome
EM	Electron microscopy
FISH	Fluorescence in situ hybridization
FL	Fractional length
ISH	In situ hybridization
QD	Quantum dot
RFLP	Restriction fragment length polymorphism
RN	Recombination nodule
SC	Synaptonemal complex
SSR	Simple sequence-repeat

Contents

4.1 Cytological Maps of Chromosome Features

4.1.1 Mapping of Visible Cytological Features

The field of cytogenetic mapping in plants was initiated by the seminal work of Barbara McClintock, the first to identify unambiguously the ten pachytene bivalents of maize (*Zea mays* L., 2n = 20) and to narrow the position of a linkage group, involving genes for colored aleurone (*C*), shrunken endosperm (*Sh*), and waxy endosperm (*Wx1*), to the long arm of chromosome 9, as shown in Fig. 4.1 (McClintock 1929, 1931). She later identified the connection between physical exchanges between chromosomes (knobbed and knobless) and the recombination of inherited traits (colored aleurone and waxy endosperm) thereby establishing the physical basis of genetic recombination (McClintock 1930; Creighton and McClintock 1931). Pachytene chromosome maps were subsequently developed for rice (*Oryza sativa* L., Shastry and Misra 1961), sorghum (*Sorghum propinquum* (Kunth) Hitchc., Magoon and Shambulingappa 1961), tomato (*Solanum lycopersicum* L., Barton 1950; Ramanna and Prakken 1967), potato (*Solanum tuberosum* L., Yeh and Peloquin 1965), barley (*Hordeum vulgare* L., Singh and Tsuchiya 1975), *Solanum canasense* Hawkes (Haynes 1964), and other plant species. A carmine-based stain was used to visualize endogenous cytological features such as chromatic (darkly staining) regions, achromatic (lightly or nonstaining) regions, chromomeres (darkly staining granules), nucleolus organizing regions, and centromeres on these classical cytological maps.

Early studies of rice (2n = 24) chromosome morphology made use of somatic metaphase chromosomes; Nandi (1936) organized rice chromosomes into several "types" but could not differentiate a distinct set of diploid chromosomes. Subsequent efforts to organize the rice metaphase complement were also confounded by the small sizes and lack of cytological features of most of the chromosomes (reviewed by Misra and Shastry 1967). In 1960, Shastry et al. (as cited by Misra and Shastry 1967), published the first rice (var. *japonica*) pachytene karyotype. In these and subsequent studies, the greater resolution made possible by the longer meiotic chromosomes permitted organization of the rice genome into the 12 chromosomes of the haploid complement, on the basis of length, arm ratios, and presence of macrochromomeres (reviewed by Misra and Shastry 1967). A subsequent study by Misra and Shastry (1967) presented karyotypes for nine additional rice strains. The authors recognized that the small size of rice centromeres might cause their locations to be mistaken for gaps between chromomeres; they therefore emphasized the importance of making a large number of observations for karyotyping accuracy.

The first ideogram for the pachytene chromosomes of *Sorghum propinquum* (2n = 20) was developed by Magoon and Shambulingappa (1961), from the average arm lengths, total chromosome lengths, and arm ratios (ratios of long to short arm lengths). They also described centromere positions, chromomeres, and the relative lengths of "deeply staining" (chromatic) regions and were among the first to report chiasma frequency at diakinesis and metaphase I.

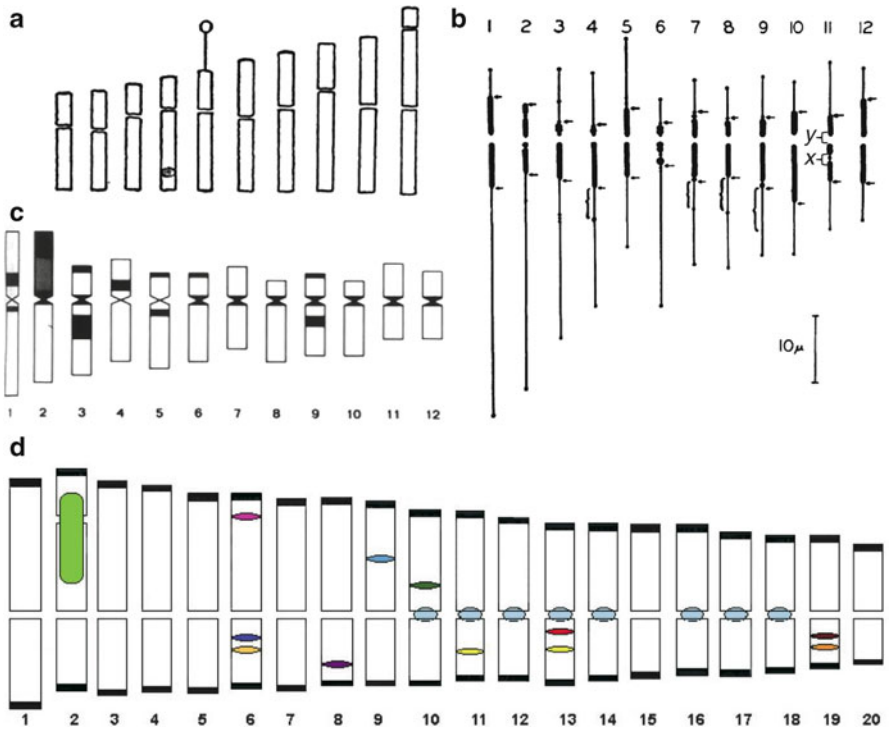

Fig. 4.1 Classical or initial ideograms produced for four plant species illustrate typical features derived from cytogenetic analysis. (**a**) The maize (*Zea mays* L.) genome (2n=2×=20) from pachytene-stage chromosomes as reported by McClintock (1929). Chromosomes are represented in order of increasing length (starting with chromosome number 10 at left), with short arm on top, and the positions of centromeres (gaps), a knob (*grey spot*) on chromosome 7, and the nucleolus organizing region (*circle*) on chromosome 6 are indicated. (**b**) The tomato (*Solanum lycopersicum* L.) genome (2n=2×=24) from pachytene-stage chromosomes as reported by Barton (1950). Chromosome numbers and the locations of heterochromatin (*thick lines*) and its boundaries (*arrows*) are indicated, as are zones of small chromomeres (brackets on chromosomes 4, 7, 8, and 9). Additional annotation marks regions (denoted here as X and Y) relevant to subsequent studies dealing with the location of centromere 11. (**c**) A haploid derivative (2n=2×=24) of a tetraploid (2n=4×=48) potato (*Solanum tuberosum* L., group Andigena) from somatic metaphase chromosomes as reported by Pijnacker and Ferwerda (1984). Chromosome numbers, centromere positions (constrictions), C-bands (*black bars*), and the nucleolus organizing region (*grey* area on chromosome 2) are indicated. (**d**) The narrow-leaf lupine (*Lupinus angustifolius* L.) genome (2n=40) from somatic metaphase chromosomes as reported by Kaczmarek et al. (2009). Chromosome number, centromere positions (gaps), telomere FISH signal locations (*black*), large rDNA gene cluster (*green* on chromosome 2), 5 S rDNA gene cluster (*red* on chromosome 13), and the Fok I repeat (*blue circles* on chromosomes 10–14, 16–18) are indicated, as are other loci derived from various FISH probes (see Kaczmarek et al. 2009 for additional details)

Although many researchers used McClintock's numbering system, designating the longest chromosome 1, the second longest 2, and so forth, many found identification and organization of the chromosomes of an entire pachytene complement

difficult, a problem frequently attributed to paucity of observations and indistinct morphological features, and could not agree on the centromere localization in some cases (Barton 1950; Yeh and Peloquin 1965; Ramanna and Prakken 1967; Khush and Rick 1968). For example, researchers had been trying since 1926 to identify cytological features that could be used to organize pachytene chromosomes of the tomato numerically, (Lesley 1926, as cited by Barton 1950). In 1950, Barton reported cytological features such as chromosome arm length and arm ratio to differentiate the 12 pachytene bivalents of tomato (2n = 24, Fig. 4.1b) and used McClintock's numbering method to organize them.

Even with Barton's findings, unambiguously identifying chromosomes 5, 7, 8, 9, and 12 of tomato remained difficult (Barton 1950; Gottschalk 1951; Ramanna and Prakken 1967). Cytogenetics recognized the importance of visualizing chromosomes to identification of any isolated bivalent (Gottschalk 1950, as cited by Ramanna and Prakken 1967). More than 10 years later, chromosomes 8 and 9 were described in sufficient detail to allow accurate and reproducible identification (Khush et al. 1964; Rick and Khush 1964; reviewed by Ramanna and Prakken 1967). In 1967, Ramanna and Prakken described the value of chromosomal "markers" such as centromeres, chromatic parts and achromatic parts, and telomeres for unequivocal differentiation of every tomato pachytene bivalent. Their research facilitated tomato chromosome identification in meiotic as well as somatic preparations.

Despite this new level of descriptive detail, resolving all discrepancies involving the location of functional features, such as centromeres, without use of additional molecular tools remained challenging. For example, chromosome 11 of tomato has three chromatic regions separated by achromatic regions, one of which was believed to contain the centromere (Fig. 4.1b). Gottschalk (1951) reported that the centromere was located between the second and third chromatic regions (near "x" in Fig. 4.1b), whereas Barton (1950) and later Ramanna and Prakken (1967) believed it was between the first and second (near "y" in Fig. 4.1b). Only use of tomato deficiencies by Khush and Rick (1968) resolved the question in favor of the Barton (1950) and Ramanna and Prakken (1967) view. They showed that a deficient chromosome 11 that was missing the entire portion of the long arm after the second chromatic region was still able to segregate normally during cell division and must therefore have retained a centromere.

Similar difficulties surrounded centromere localization and even the feasibility of reproducible chromosome identification in many *Solanum* species because of their large numbers of chromosomes (reviewed by Yeh and Peloquin 1965). To simplify cytogenetic karyotype development in potato (group Andigena, 2n = 48), Yeh and Peloquin (1965) examined pachytene chromosomes from haploid (2n = 24) plants (Fig. 4.1c). They were able to produce a 12-chromosome karyotype using features such as telochromomere (telomeric heterochromatin) morphology, relative lengths of chromatic segments, chromomeres, and centromere localization. This work also reinforced the importance of observing the relative features of the entire chromosomal complement from a single cell. In this regard, the work on plant cytogenetic karyotyping in potato was similar to that in tomato and barley in that no suitable procedure existed for the unambiguous identification of just one or a few

Table 4.1 Comparison of Giemsa and quinacrine staining methods in conjunction with cold treatment, summarized for several plant species, modified and updated from Vosa and Marchi (1972)

Species	Cold treatment	Quinacrine	Giemsa
Vicia faba L.	+	Intense	+
Allium carinatum L.	–	Intense	+
Scilla sibirica[a] Haw.	+	Less intense	+
Tulbaghia alliacea L.	+	Less intense	+
Tulbaghia verdoornia Vosa & Burb.	+	Less intense	+
Tulbaghia leucantha Baker	+	Less intense	+
Zea mays L.	–	No differentiation	+

[a]Positive only after at least 1 month of cold treatment

chromosomes (Barton 1950; Singh and Tsuchiya 1975). Differential chromosome staining techniques proved to be necessary for the advancement of chromosome identification and cytogenetic studies in plants.

4.1.2 Use of Staining to Visualize Additional Cytological Features

Caspersson et al. (1969, as cited by Lavania (1978) was the first to probe both animal and plant chromosomes with the fluorescent dye quinacrine; the result was called Q-banding. Pardue and Gall (1969) and Arrighi and Hsu (1971) were the first to use Giemsa in combination with DNA denaturation-renaturation, called Giemsa C-banding, for studies on animal chromosomes. In 1972, Vosa and Marchi compared the quinacrine Q-banding and the Giemsa C-banding techniques applied to chromosomes of various plant species to evaluate their efficacy (Table 4.1). Examples of quinacrine and C-banding in plant cytogenetics are shown in Fig. 4.2.

The results revealed that both quinacrine and Giemsa could be used for staining plant chromosomes and that each had both advantages and disadvantages (Vosa and Marchi 1972). Q-banding results from association of quinacrine with AT-rich regions in the chromatin (Vosa and Marchi 1972; Weisblum and de Haseth 1972). The C-banding technique stains constitutive heterochromatin, exploiting the rapid reassociation of repetitive DNA (reviewed by Gill and Kimber 1974). As a result, Q-banding results in a gradient from brightly stained regions (heterochromatin) to more lightly stained ones (euchromatin), whereas Giemsa C-banding produces a similar but more distinct pattern by only brightly staining the same regions brightly stained in Q-banding without producing a gradient (Vosa and Marchi 1972).

In their comparison, Vosa and Marchi (1972) included *Vicia faba* L. (field bean), *Allium carinatum* L. (ornamental onion), and maize (Fig. 4.2a). In general, effectiveness of Q-banding depended on the species studied; in some it produced poor or no differentiation, whereas Giemsa C-banding produced chromosomal differentiation

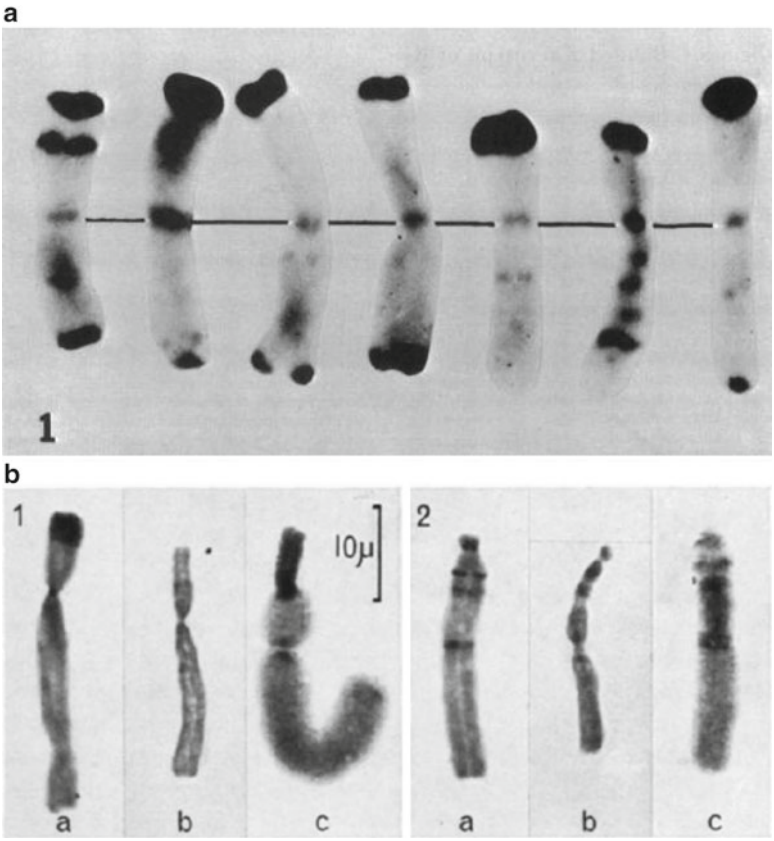

Fig. 4.2 (**a**) The Giemsa C-banded karyotype of rye somatic metaphase chromosomes, from Gill and Kimber (1974). (**b**) Direct comparison of two different *Trillium grandiflorum* chromosomes (insets 1 and 2) stained by three different techniques (*a* Giemsa stain; *b* Feulgen stain; *c* Giemsa stain after cold pretreatment), from Schweizer (1973)

in all of the species studied. Of particular interest, in maize, Q-banding produced no differentiation, whereas Giemsa C-banding produced more pronounced knob staining.

Since that study, investigators have found that pretreating chromosomes in various ways, for example with standard saline, trypsin, acid, and/or cold exposure, can cause Giemsa to stain various parts of chromosomes differentially (reviewed by Lavania 1978). Examples are Giemsa (G)-banding, the result of treatment with only a standard saline solution before Giemsa treatment, which causes staining of the AT-rich heterochromatin (reviewed by Lavania 1978; Harper and Cande 2000), and reverse Giemsa (R)-banding, produced when the chromosomes are denatured and then cooled only to 70°C immediately before Giemsa treatment (reviewed by Lavania 1978). Lavania (1978) published a thorough review of techniques that have been successfully used to stain the chromosomes of various plant species differentially.

Chromosomal differentiation by means of various dyes and stains provided researchers with additional tools that facilitated the organization of the chromosome complements in species where it had not previously been possible. For example, Giemsa staining techniques facilitated the differentiation of the prometaphase complement in common bean (*Phaseolus vulgaris* L., 2n = 22, Mok and Mok 1976) and rice (2n = 24, Kurata and Omura 1978), as well as the somatic metaphase chromosome complement in rye (*Secale cereale* L., Gill and Kimber 1974), potato (reviewed by Pijnacker and Ferwerda 1984), and *Sorghum* (Yu et al. 1991). In the case of bean, even with these advances, chromosome pairs could still be misidentified, especially chromosomes D–F, which have very similar banding patterns and sizes (Mok and Mok 1976). In all cases, ability to identify prometaphase chromosomes is advantageous because it removes the requirement of waiting for plants to mature and flower.

Gill and Kimber's (1974) C-banded karyotype for rye (var. Imperial, 2n = 14) is shown in Fig. 4.2b. It clearly differentiated the complement into seven distinct pairs of chromosomes and allowed for comparison of heterochromatin patterns of somatic and meiotic chromosome preparations (Lima-de-Faria 1952; Gill and Kimber 1974).

The potato cytogenetic map also initially posed a difficult problem because of the small chromosomes, high chromosome number (2n = 48), and polyploid genome (reviewed by Yeh and Peloquin 1965; Pijnacker and Ferwerda 1984). Pijnacker and Ferwerda (1984) used Giemsa C-banding together with $AgNO_3$-banding of the nucleolus organizing region on somatic metaphase chromosomes of a "haploid" derivative (2n = 2× = 24) of tetraploid (2n = 4× = 48) potato. They detected 12 different chromosome pairs (Fig. 4.1c). This study did improve researchers' ability to identify the somatic chromosomes of potato, but distinguishing chromosome 8 from 10 and 11 from 12 remained difficult with contemporary stains and dyes.

The case of *Sorghum bicolor* (2n = 20) was difficult because acetocarmine staining of somatic metaphase chromosomes did not clearly resolve several of the smallest (Gu et al. 1984). In all but the largest chromosome of *S. bicolor*, the centromere is near the middle, and the total arm lengths of the four smallest chromosomes overlapped by as much as a standard deviation (Gu et al. 1984). C-banding provided additional markers that allowed Yu et al. (1991) to distinguish most of the chromosomes.

Chromosome staining techniques, although an improvement over previous methods, are subject to experimental variability (Yu et al. 1991; Schweizer 1973). Schweizer (1973) found that cold treatment before Giemsa staining improved visualization in most of the species studied but not in *V. faba* and acknowledged that "different classes of heterochromatin may require different Giemsa techniques to react preferentially with the stain," establishing the need for species-specific optimization. Figure 4.2c shows the different appearances of chromosomes after different staining applications for two *Trillium grandiflorum* chromosomes. Despite the availability of several chromosome-staining techniques, the need remained for additional methods that would permit unambiguous chromosome differentiation. This need was met by the development of in situ hybridization (ISH), discussed later.

4.2 Mapping of Chromosomal Rearrangements

In the construction of the first cytological maps in maize (McClintock 1931; Anderson and Randolph 1945) and barley (Kasha and Burnham 1965), cytogenetic stocks with translocation breakpoints were used. McClintock's (1931) ordering of the C, *Sh*, and *Wx1* used a maize line that contained a segmental interchange between chromosomes 8 and 9, which facilitated the mapping efforts.

Translocation lines have also proven useful for physical mapping of the barley genome. In 2000, Künzel et al. created a cytologically integrated physical map of barley by mapping 429 restriction fragment length polymorphism (RFLP)-derived STS relative to 240 translocation breakpoints. They used these data to integrate the barley genetic and physical maps and found that the majority of recombination in barley (≤1 Mb/cM) is restricted to less than 5% of the entire genome. Such recombination hotspots or highly recombinogenic regions are a common feature of large-genome organisms, and mapping their locations is important for the development of efficient strategies for map-based cloning, genome assembly, and comparative genomics.

4.2.1 Use of Irradiation to Produce Additional Chromosomal Rearrangements

Use of irradiation to produce chromosomal rearrangements was described first in *Drosophila* (Muller 1927) and later in plants such as cotton, tobacco, maize, and wheat (reviewed by Parthasarathy 1938). These treatments produced gene mutations, duplications, chromosomal rearrangements, and deficiencies, all of which were valuable tools for genetic and cytogenetic analysis and mapping in plants (reviewed by Parthasarathy 1938). From 1935 through 1954, Anderson and coworkers cytologically localized over 90 translocations involving maize chromosomes 1, 3, 4, 6, 8, 9, and 10 resulting from X-ray irradiation (Anderson 1935, 1938, 1939, 1941; Anderson and Brink 1940; Anderson and Kramer 1954; Anderson et al. 1955a, b). In wheat, telocentric chromosomes where used to orient linkage maps and for cytogenetic localization of genes (Loegrin and Sears 1966). Similarly, in tomato, X-ray-induced deficiencies proved valuable in efforts to orient linkage groups as well as in localization of genes and centromeres (Khush and Rick 1968).

In 1968, Khush and Rick irradiated tomato var. Red Cherry pollen with X-rays or fast neutrons to produce 74 chromosomal deficiencies. These were used to localize centromere positions and 35 genes and to orient linkage groups and markers on most of the tomato chromosome arms. They observed that X-ray-induced deficiency distribution was nonrandom; 60% of breaks mapped to heterochomatin but only 15% to euchromatin. They also found that fast-neutron exposure was more effective than X-rays in inducing euchromatic breaks. For example, they irradiated pollen with fast neutrons to produce stocks that allowed them to localize new loci, identify the narrow chromosomal regions believed to contain various known tomato genes, and resolve discrepancies about the location of the centromere on chromosome 11.

4.2.2 Use of Gametocidal Genes to Produce Deletions for Mapping in Wheat

In wheat, gametocidal (*Gc*) genes have been used to induce stable chromosome deletion lines for creation of cytogenetically referenced physical maps. Such genes and chromosomes are found in some species of *Aegilops*. These *Gc* loci promote their own transmission by producing chromosome breakages in wheat gametes that lack *Gc* genes (Endo 1988; reviewed by Endo 2007). The *Gc* system was used in conjunction with C-banding to produce and characterize chromosome-deletion stocks of common wheat (*Triticum aestivum* L.) cv. Chinese Spring (2n = 6× = 42, AABBDD; Endo and Gill 1996). *Gc*-induced chromosome deletions have been used for physical and cytogenetic mapping of a plethora of RFLP, simple sequence-repeat (SSR), amplified fragment length polymorphism (AFLP), SSAP, and EST markers and phenotypic traits, including the β-amylase (*β-Amyf-A2*), pairing homeologous (*ph1*), and waxy (*Wx*) genes in wheat (reviewed by Endo 2007; Tsuchida et al. 2008).

The first known use of *Gc*-induced chromosome breaks in physical mapping of wheat was in 1988, when Endo and Mukai mapped a gene responsible for speltoid character of wheat spikes suppression (*q* gene) onto the distal 48% on the long arm of wheat chromosome 5A as shown in Fig. 4.3a. Fourteen *Gc* chromosomes, of differing degrees of lethality, have been discovered in wheat, including some with mild gametocidal activity (reviewed by Endo 2007). Analysis of the fate of the chromosomes with *Gc*-induced breaks revealed that the deletions were stabilized by rapid telomere formation at the breakpoints (reviewed by Endo 2007). Many of these chromosome aberrations could therefore be stably propagated in the homozygous or hemizygous condition and could be used in physical mapping as illustrated in Fig. 4.3 (Endo 1990; Endo and Gill 1996). C-band mapping of deletion derivatives is shown for wheat chromosomes 5A (Fig. 4.3a) and 5B (Fig. 4.3b).

Extending this approach, Werner et al. (1992) physically mapped RFLPs onto an entire homeologous group, chromosomes 7A, 7B, and 7D, of wheat chromosomes using *Gc*-induced deletion stocks. In their 1996 paper, Endo and Gill published chromosome-deletion stocks for every chromosome of common wheat. In all, 436 deletion lines have been identified and mapped by C-banding (reviewed by Endo 2007). Studies comparing the genetic and physical maps of wheat, made possible by these induced chromosome deletions, provided evidence that genes and recombination sites exhibit nonrandom distribution patterns, with preferential localization near the ends of the chromosomes (Werner et al. 1992; Gill et al. 1996a, b).

Although the *Gc* chromosomes of *Aegilops* can also induce chromosomal aberrations in diploid member of the Triticeae, such as barley and rye, the resulting deletions in these species are usually lethal (reviewed by Tsuchida et al. 2008). Researchers have found that they can alleviate the lethality of deletions in these diploid species by isolating and maintaining individual chromosomes as disomic additions in hexaploid wheat, thus taking advantage of the redundancy in the wheat genome to compensate for deletions in the alien chromosome (Endo et al. 1994; Endo and Gill 1996; Tsuchida et al. 2008). Approaches like this one extended the *Gc* system to permit mapping of barley, rye, and other diploid wheat relatives (Endo et al. 1994; Tsuchida et al. 2008).

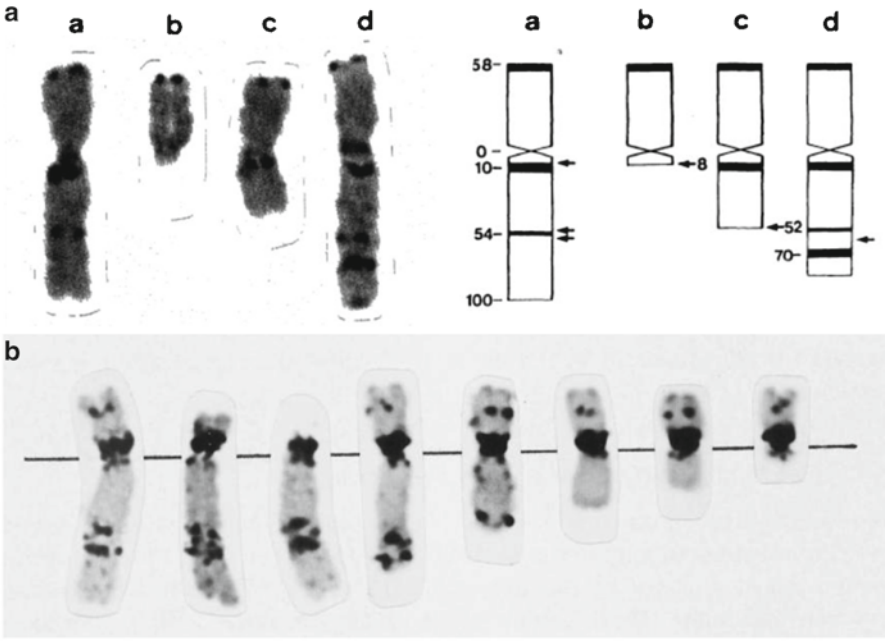

Fig. 4.3 Use of Giemsa C-banding to map and characterize chromosomal rearrangements and structural variants. (**a**) Photographs (*left*) and ideograms (*right*) from Endo and Mukai (1988) demonstrating the use of C-banding to define the structure of wheat (*Triticum aestivum* L.) chromosome 5A variants that were induced by the loss of the *Aegilops cylindrica* chromosome from a monosomic addition line. The normal chromosome 5A (*a*) is shown in comparison to two deletion derivatives (*b*, *c*) and one translocation derivative (*d*). Chromosome breakpoints (*arrows*) inferred from C-banding (*black lines*) and relative positions (*numbers*) of features are indicated. (**b**) The use of C-banding to map *Gc*-induced chromosome deletion points on wheat chromosome 5B, from Endo (1990). Wild-type chromosome 5B (at *left*) is shown along with seven different deletion chromosomes, all aligned at their centromeres (*lines*)

The strategy of deletion mapping of traits is limited by two main factors, the distance between any two deletion breakpoints and the ability to define deletions of chromosomal regions lacking chromomeres or C-bands. Genetically mapped markers can be physically localized to chromosome arms or segments on the basis of their presence or absence as indicated by Southern blot analysis of the deletion lines (Werner et al. 1992). Because this technique relies on the ability to identify the presences and locations of chromosome breakpoints by C-banding, it is hindered by a lack of terminal bands on some chromosome arms, such as 1AS (Endo and Gill 1996; Gill et al. 1996a, b). In general, researchers have found that chromosomal breakage preference seems to be correlated with recombination hotspots and therefore gene-rich regions (Gill et al. 1996a, b; Röder et al. 1998). *Gc* genes have been found in other plant species, such as rice, but until now the use of mild *Gc* genes to create deletion lines has been limited to wheat or alien chromosomes that can be successfully maintained as disomics in the wheat background (reviewed by Endo 2007).

4.2.3 B-A Translocations in Maize Physical Mapping

In maize, B-A translocations have been used to map recessive genes physically onto chromosome arms (reviewed by Beckett 1978, 1993). B chromosomes are supernumerary chromosomes found in some maize lines (Beckett 1978). When present, they frequently exhibit nondisjunction during the second division of the microspore, producing one hypoploid sperm without any B chromosomes and one hyperploid sperm with two, in the same pollen grain (Beckett 1978). Maize, like other flowering plants, exhibits a phenomenon known as double fertilization, in which one sperm cell fertilizes the egg cell to produce the embryo and the other from the same pollen grain merges with the two polar nuclei to produce triploid endosperm. About 40% of embryos fertilized by pollen carrying B-A translocated chromosomes are missing a portion of an A chromosome; these partial hypoploid embryos can be recognized by means of genetic markers (Beckett 1978). The use of B-A translocation can therefore be used to uncover recessive genes, allowing their assignment to specific chromosome arms or regions (Beckett 1993). B-A translocation lines have been used for physical mapping of many maize genes, including malate dehydrogenase structural genes (McMillin et al. 1979), alcohol dehydrogenase-1 (Birchler 1980), catalase structural genes (*cat1, cat2, cat3*; Roupakias et al. 1980), the sugary enhancer gene (Labonte and Juvik 1991), and the low phytic acid 1-2 and 2-1 genes (Raboy et al. 2000). Weber and Helentjaris (1989) also used B-A translocation lines to map maize RFLP loci.

Irradiation-induced chromosomal deficiencies, gametocidal factors, and B-A translocations have all been very useful, but each has its own distinct advantages, species specificities, and disadvantages. Irradiation and gametocidal factors seem more likely to induce deficiencies in certain regions of plant chromosomes, and detection of deficiencies induced by gametocidal factors can be challenging for certain parts of the genome without reference markers. B-A translocations in maize are a useful way to determine the location of recessive traits relative to chromosome arms or large regions. Despite the low resolution of these techniques, they have proven invaluable for mapping traits in maize.

4.3 Mapping by Electron Microscopy

4.3.1 Three-Dimensional Reconstructions of Chromosomes from Whole Nuclei

In 1973, Gillies produced a complete karyotype of maize using reconstructions of male meiotic prophase cells by three-dimensional (3D) electron microscopy (EM). In this approach, meiotic cells are fixed in aldehyde, stained with phosphotungstic acid, serially sectioned, and imaged, and the paths of individual chromosomes are then reconstructed from the image stack (Gillies 1972). Localization of the

centromeres on these chromosomes allowed Gillies (1973) to measure the arm lengths and determine the arm ratios for the entire complement of the maize line studied. He reported that the arm ratios were conserved within a given nucleus but that the total lengths were generally shorter than those derived from chromosome squash techniques, like those of Rhoades (1950). Importantly, the karyotype derived from the native chromosome structure as seen by Gillies (1973) confirmed the McClintock karyotype. This technique has also been used to localize the centromeres and three nucleolus organizing regions, to determine the arm lengths of *Lilium longiflorum* chromosomes, and to evaluate chromosome pairing during zygotene (Holm 1977).

3D EM reconstruction of pachytene-stage nuclei also provides information about sites of recombination, as marked by conspicuous recombination nodules (RNs), but this approach is not easily applied to a large number of observations. The advent of chromosome spreading techniques, which permitted the two-dimensional study of synaptonemal complexes (SCs), therefore greatly facilitated the study of large numbers of cells (reviewed by Sherman and Stack 1995).

4.3.2 Mapping of Recombination Nodules on SC Spreads

The application of EM to visualize SC spreads in plants was demonstrated by Gillies (1981) in maize, with well-spread complete nuclei. Subsequently SC karyotypes were produced for various plants, including *Allium* (Albini and Jones 1988), *Arabidopsis* (Albini 1994), and tomato (Sherman and Stack 1992). The frequency of distribution of RNs observed in SC spreads matched well those of genetic recombination sites, allowing cytogenetics to document and study crossovers without genetic markers or progeny analysis (reviewed by Sherman and Stack 1995). High-resolution RN maps from SC spreads for the entire genomes of tomato (Sherman and Stack 1995) and maize (Anderson et al. 2003) provide a unique method for integrating the cytological and linkage maps.

In 1992, Sherman et al. developed a technique to visualize the tomato (var. cherry) RNs clearly by means of a uranyl acetate–lead citrate stain as well as a silver staining technique. This approach was used by Sherman and Stack (1995) to produce a high-density RN map (physical/cytological map) spanning the entire tomato genome on which centiMorgan map (linkage map) units are indicated in Fig. 4.4 (Sherman et al. 1992).

Using the same approach, Anderson et al. (2003) created a high-resolution RN map for maize (var. KYS) and found evidence for line-specific variation in RN frequencies. They used this map to predict the location of markers on chromosome 9 (Anderson et al. 2004) and found that the RN-cM map is a reliable predictor of physical locations for markers ($r^2 = 0.996$). From this integrated information, a *Morgan2McClintock* translator has been produced, which can be used to predict the physical localization of either maize or tomato markers from their cM map position (Lawrence et al. 2006).

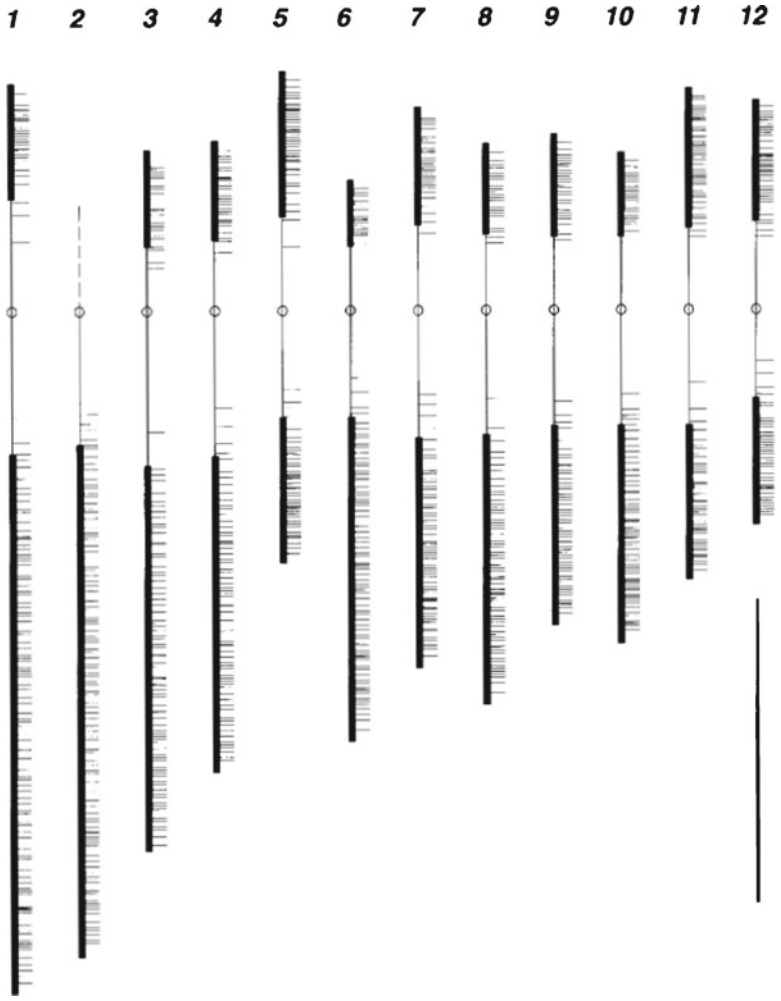

Fig. 4.4 Diagrammatic ideogram of tomato synaptonemal complexes showing the locations of centiMorgan map units. Recombination-nodule locations and frequencies were determined and used to extrapolate the locations of the linkage-map units on the physical/cytological pachytene-stage chromosomes (from Sherman and Stack 1995). The irregularity of cM/cytological distance ratio is clearly visible in this display, including the striking dearth of recombinations around the centromeres

Similarly, Chang et al. (2007) generated and used a RN-cM map of tomato to predict the locations of 17 genetically mapped markers that were then tested by FISH mapping of the corresponding bacterial artificial chromosomes (BACs) onto pachytene chromosome 1. Like Anderson et al. (2004), they found that the RN-cM map is a good predictor of the physical locations of markers, establishing the value of RN mapping as bridging information between linkage and physical maps in plants.

4.4 In Situ Hybridization (ISH)

The development of ISH marked the beginning of a major new phase of cytogenetics. The technique, also referred to as hybridization histochemistry, uses labeled DNA or RNA probes. These probes hybridize by sequence-specific base pairing to complementary sequences in the target DNA. They are subsequently visualized and provide sequence-specific stains for detection and characterization of relatively small segments of DNA.

4.4.1 Radioactive In Situ Hybridization

The use of radioactive nucleic acid probes for ISH (radio-ISH) was first developed and used in human HeLa cells and *Xenopus* oocytes (Gall and Pardue 1969; John et al. 1969; Pardue and Gall 1969, 1975). The probes were produced by in vitro synthesis of DNA or RNA incorporating nucleotides labeled with tritium (^{3}H) or iodine-125 (^{125}I). Notable applications of radio-ISH in plants involved the cytogenetic localization (or mapping) of abundant tandemly repeated sequences such as the knob repeats of maize (Peacock et al. 1981) and the ribosomal DNA genes of rice (Fukui et al. 1987). In these cases, preexisting visible features, such as the knobs and the nucleolus organizing regions, provided evidence for the specificity of the ISH signal locations. Radio-ISH was also used to map genes such as the *Waxy1* gene of maize (Shen et al. 1987) and the *rbcS* (Wu et al. 1986) and glutelin (Suzuki et al. 1991) genes of rice.

4.4.2 Biotinylated Probes for In Situ Hybridization

The radio-ISP procedure was powerful, but it was also hazardous and required a considerable amount of time for sufficient exposures to develop. In time, sensitive, rapid, and nonradioactive variations of ISH were developed, such as biotin labeling and fluorescence labeling (Langer-Safer et al. 1982). In 1985, Rayburn and Gill demonstrated the value of biotin-labeled probes for plants by combining them with ^{3}H-labeled probes to map wheat metaphase chromosomes. In 1986, Ambros et al. similarly localized a 17-kb T-DNA insertion in *Crepis capillaris* (L.) Wallr. using biotin-labeled probes and ^{3}H-labeled probes. The specificity and reliability of biotin-based ISH was thus well established by the late 1980s (Ambros et al. 1986).

Biotin-ISH relies on detection of probes labeled with biotin by means of a secondary reporter such as streptavidin or an antibody coupled to a horseradish peroxidase or a fluorescent molecule. The trade-offs between enzymatic and fluorescence detection systems have been reviewed by Jiang and Gill (1994). Nonradioactive ISH in plant cytogenetics was subsequently employed by many laboratories, as exemplified by the detection of the repeat sequences in wheat (Rayburn and Gill 1985) and

tomato (Lapitan et al. 1989), the secalin genes in rye (Gustafson et al. 1990), the rDNA in *Oryza indica* (Islam-Faridi et al. 1990), and RFLP probes in rice (Gustafson and Dillé 1992).

4.4.3 Fluorescence In Situ Hybridization

Fluorescence in situ hybridization (FISH) is currently the most common form of ISH used in plant cytogenetics. Its advances in imaging and sample preparation give rise to increasing sensitivity and resolution (reviewed by de Jong et al. 1999; Jiang and Gill 2006). FISH with multiple different fluorescent dyes allows for simultaneous detection of different sequences. Indirect FISH techniques made use of nonvisible labels, such biotin and digoxigenin, followed by a secondary labeling scheme (Griffor et al. 1991; reviewed by Jiang and Gill 1994). Methods for indirect FISH in plants were developed (Jiang et al. 1995; Zhong et al. 1996a, b; Jackson et al. 1998; Dong et al. 2000; Islam-Faridi et al. 2002) and found wide-spread use in many plant systems including tomato (Chang et al. 2007, 2008; Iovene et al. 2008; Koo et al. 2008; Szinay et al. 2008; Tang et al. 2009), potato (Iovene et al. 2008; Tang et al. 2009), maize (Sadder and Weber 2002; Koumbaris and Bass 2003; Ananiev et al. 2009), rice (Cheng et al. 2002a; Kim et al. 2005c; Kao et al. 2006), *Antirrhinum majus* L. (Zhang et al. 2005), *Brassica* species and *Arabidopsis* (Howell et al. 2002; Shibata and Murata 2004; Lysak et al. 2005), *Gossypium arboreum* (Wang et al. 2008), *Pinus* species (Hizume et al. 2002; Islam-Faridi et al. 2007), *Hydrangea* species (Van Laere et al. 2008), and *Medicago* (Schnabel et al. 2003).

Methods that further increase FISH signals have been developed. For example, the tyramide signal amplification system can boost signals by up to a hundredfold (Raap et al. 1995). This approach permits detection of small target sequences (Khrustaleva and Kik 2001; Stephens et al. 2004), but it can also be hampered in some cases by high background signal from naturally occurring biotin in plant cells (Stephens et al. 2004).

Direct FISH, on the contrary, uses fluorescently labeled nucleotides (Bass et al. 1997, 2000; Danilova and Birchler 2008; Szinay et al. 2008; Yan et al. 2006). Direct FISH has certain advantages over indirect FISH, mostly related to probe penetration, as reviewed by Kato et al. (2006). Both direct and indirect FISH are highly specific and widely used and are largely interchangeable. Numerous studies make use of a combination of the two (Koumbaris and Bass 2003; Ananiev et al. 2009; Tang et al. 2009). The choice between them depends on laboratory, physical form of the target sequences, and other factors such as cost of reagents and sensitivity of the microscopes or imaging equipment being used.

Recently, the use of semiconductor nanocrystals, called quantum dots (QDs), has been optimized for direct labeling of DNA in plant FISH (Ma et al. 2008b). QDs are inorganic fluorophores, brighter and more stable than organic fluorophores, and they have proven useful in mammalian FISH and live imaging and more recently in immunostaining and FISH in plants (Muller et al. 2006; Ma et al. 2008a, b). Ma et al. (2008b) used a metal-thiol bond technique developed by Wu et al. (2006) to demonstrate the use of QD FISH for localizing the TAG microsatellite of maize. The signal intensity

of direct-labeled QD FISH probes in this study was high, comparable to that of the best indirect FISH labeling method using biotin and streptavidin-Cy3 (Ma et al. 2008b). These findings are encouraging, as they suggest that QD-based FISH is also useful for detecting small, single-gene-sized targets without the need for signal amplification or other measures that can increase background signal.

FISH has proven ideal for rapid physical mapping of cloned DNA sequences onto individual chromosomes and subchromosomal regions (reviewed by Jiang and Gill 2006). This point is demonstrated by the vast literature on cytogenetic FISH mapping in various plant species, including *Arabidopsis* (Fransz et al. 1996, 1998; reviewed by Koornneef et al. 2003), *Beta vulgaris* (Desel et al. 2001), common bean (Pedrosa-Harand et al. 2009), tomato (Chang et al. 2007, 2008; Iovene et al. 2008; Szinay et al. 2008; Tang et al. 2009), *Medicago* (Kulikova et al. 2001), rice (Cheng et al. 2001a, b; Kao et al. 2006), potato (Iovene et al. 2008; Tang et al. 2009), *Petunia hybrida* (ten Hoopen et al. 1996, 1999), *S. bicolor* (Islam-Faridi et al. 2002; Kim et al. 2005a, c), maize (Chen et al. 2000; Sadder et al. 2000; Zhong et al. 2002; Jin et al. 2004; Kato et al. 2004; Amarillo and Bass 2007; Danilova and Birchler 2008; Zhang et al. 2008; Koo and Jiang 2009), and *Silene latifolia* Poir. (Lengerova et al. 2004). Maize chromosome 9 has been the focus of many FISH mapping studies using different probes and chromosome preparations, as illustrated in Fig. 4.5.

4.5 Types of DNA Probes

Various DNA probes are being used for cytogenetic FISH mapping. One essential factor, their detection during FISH analysis, relies heavily on the probe size and, in the case of genes, the presence of repeat-free sequences.

4.5.1 Genetically Mapped Probes

Among the first genetic markers to be FISH mapped were biotin-labeled RFLP markers of rice (Suzuki et al. 1991; Gustafson and Dillé 1992; Song and Gustafson 1995). This approach created valuable connections between the linkage and cytological maps and was widely adopted for use in many species for which molecular markers had been defined. AFLP markers have similarly been used for FISH mapping in plant species, helping to define the markers' order in asparagus (*Asparagus officinalis* L., Reamon-Buttner et al. 1999), chromosome assignment in wheat (Huang et al. 2000), and chromosome distribution in *Arabidopsis* (Peters et al. 2001).

The detection limit for Southern blot and PCR-based probes is typically about 3 kb for routine FISH applications. Probes smaller than 3 kb frequently require optimization, but the ability to detect these small probes can be very advantageous because they are comparable in size to most genes or other genetic elements such as individual transposons. This limitation can impede the conversion of any given RFLP, AFLP, or SSR probe into a FISH probe. The detection limit of genetic markers using

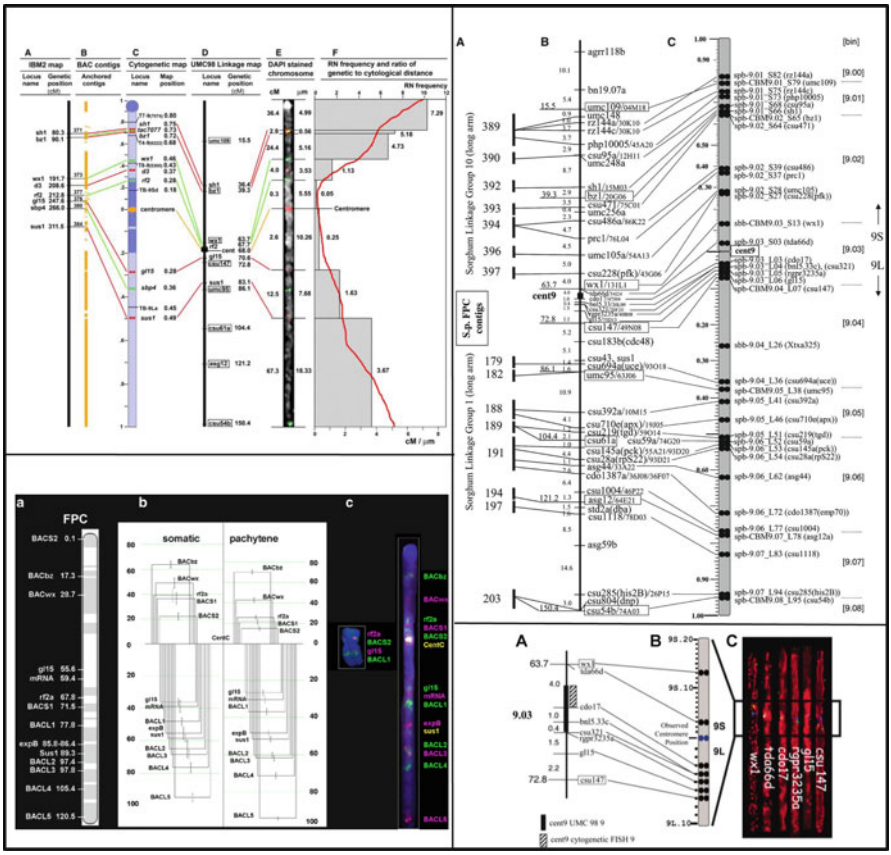

Fig. 4.5 Cytogenetic FISH maps of maize chromosome 9 from several different studies. *Upper left*: direct FISH mapping of 9 single-copy sequences onto pachytene-stage chromosome 9 of maize, from Wang et al. (2006). Colinearity of markers between the cytogenetic FISH map (D and E) and two linkage maps (A, IBM2 9 and D, UMC98 9) is diagrammed, as are recombination nodule frequency and genetic (cM)/cytological (μm) ratios. *Upper right*: high-density FISH mapping by means of sorghum BAC FISH probes on maize pachytene-stage chromosomes, from Amarillo and Bass (2007). Colinearity of markers between the cytogenetic FISH map (C) and a linkage map of maize (B, UMC98 9) and portions of the FPC BAC contig map of *S propinquum* (A) are diagrammed. *Lower left*: FISH mapping of 14 single-copy or single-BAC loci on maize chromosome 9 from Danilova and Birchler (2008). Single-copy sequences from genes or from informatically selected and PCR-amplified regions of individual maize BACs (Lamb et al. 2007a) were FISH mapped onto pachytene-stage and somatic metaphase chromosomes. The resulting cytogenetic loci were compared to each other (b) and to the FPC BAC map (A) of maize chromosome 9. *Lower right*: cytogenetic FISH mapping of genetic markers around the CentC cluster on maize chromosome 9 from Amarillo and Bass (2007). FISH-mapped loci (C) on the cytogenetic FISH map (B) and the linkage map (A) allowed for a refinement of the CentC-defined centromere of maize and assignment of markers *cdo17* and *bnl5.33c* to the long arm

FISH depends on factors like the labeling technique used and the plant species being studied. For example, the smallest FISH probes detected on whole-chromosome preparations were a 1.4-kb *chsA* cDNA in *P. hybrida* (Fransz et al. 1996), a 684-bp fragment of the *Hs1*$^{pro\text{-}1}$ gene in *B. vulgaris* (Desel et al. 2001), a 1.29-kb RFLP in rice (Ohmido et al. 1998), a 1.4-kb RFLP in *A. officinalis* (Guzzo et al. 2000), and the 3.1-kb *wx1* gene fragment in maize (Wang et al. 2006). These examples are impressive but technically difficult and thus not routine. Efforts to improve detection limits often include exposing chromosome preparations to various pepsin treatments before FISH is performed (Wang et al. 2006). These treatments were used in the development of a cytogenetic FISH map of chromosome 9 (Fig. 4.5, panel 1). In addition, signals can be amplified by enzymatic detection schemes or multiple layers of ligand-binding molecules. These signal amplifications are impressive but may also trade off with increased background, erroneous, or off-target signals.

4.5.2 Large DNA Fragment Probes

The small size of many of the molecular genetic markers used in linkage mapping prevents their use as FISH probes for cytogenetic mapping (Cheng et al. 2001b), but use of large-insert DNA clones that harbor these markers may overcome this technical challenge. For example, FISH mapping efficiency has been improved by the use of cosmids (Ohmido et al. 1998; Sadder et al. 2000; Sadder and Weber 2001, 2002), BACs (Jiang et al. 1995; Pedrosa-Harand et al. 2009), and yeast artificial chromosomes (Fuchs et al. 1996; Ohmido et al. 1998). These vectors accommodate large inserts of genomic DNA, which in turn provide more signal. These same clones are often integrated into the physical or linkage mapping projects, providing an additional connection to the cytological, physical, and linkage maps of any given plant species. FISH data from these large-insert clones can therefore make direct, primary, or confirmatory contributions to physical mapping and structural, functional, or comparative genomics.

In a well-known study, Sadder and Weber (2002) used a pair of cosmid clones as FISH probes to define the size of a chromosomal segment known to contain an insect-resistance quantitative trait locus. The cosmids, used on both mitotic and meiotic chromosomes, confirmed that the flanking markers were very far apart. Even larger clones, such as those from BAC libraries, can further boost the FISH signal but also increase the risk of unwanted repetitive sequences. BAC clones from plant genomes with high gene density can often be efficiently used as FISH probes. One of the first extensive BAC-based FISH cytogenetic maps in plants was made for sorghum (Islam-Faridi et al. 2002). It included images of 20 simultaneously mapped BAC clones hybridized to sites spanning an entire chromosome (Fig. 4.6). The order of the BAC loci was fully concordant with its corresponding genetic markers on the linkage map (Fig. 4.6c, d; Kim et al. 2005a, c). This technique was further extended and used to characterize all of the ten sorghum pachytene chromosomes and was used to compare the sorghum and rice genomes (Fig. 4.6d, Kim et al. 2005c). Subsequently, multi-BAC FISH mapping proved useful for establishing a correlation between the linkage maps and the physical chromosomes of sorghum, thus aiding in the establishment of a standard physical-linkage map nomenclature as demonstrated in Fig. 4.7 (Kim et al. 2005b).

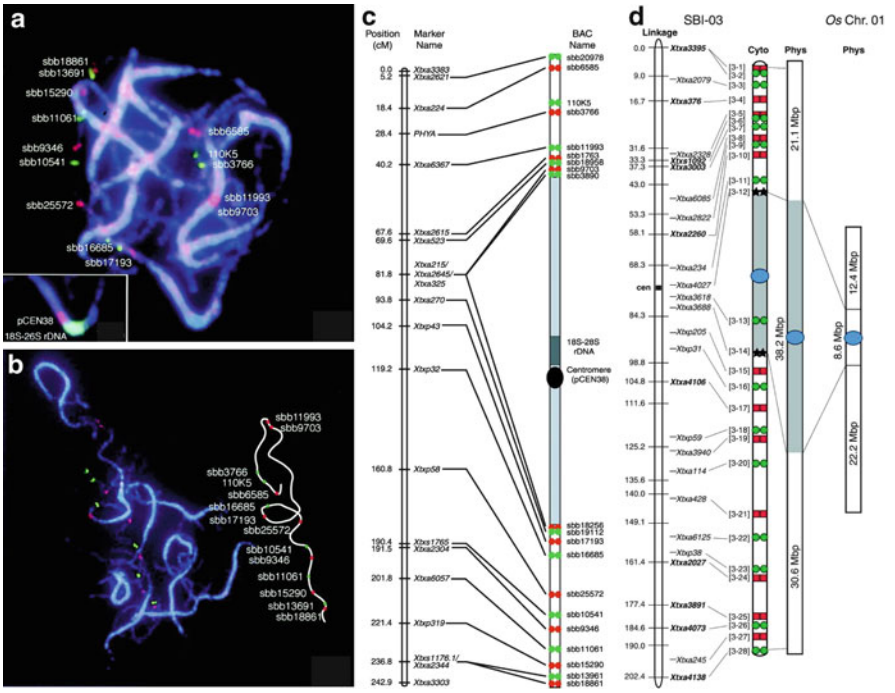

Fig. 4.6 Cytogenetic BAC FISH mapping of sorghum pachytene-stage chromosomes. Use of alternating BAC FISH fluorophores to illustrate use of up to 14 BAC FISH probes at once (**a**, **b**), from Islam-Faridi et al. (2002). This approach confirmed the colinearity of the markers on FISH, physical, and linkage maps, while illustrating the quality of axial resolution with BAC FISH. (**c**) Diagram of sorghum pachytene-stage chromosome 1 with the location of 20 FISH-mapped loci is shown in relation to their spacing on a sorghum linkage map, from Kim et al. (2005a). (**d**) Diagram of sorghum pachytene-stage chromosome 3 with the location of 28 FISH-mapped loci, from Kim et al. (2005c). Cytogenetic loci are shown in relation to their spacing on a sorghum linkage map and a physical map of sorghum and of rice chromosome 1

FISH mapping of BAC probes in tomato and potato also illustrates the use of FISH in genome-characterization projects. It has proven useful for determining the heterochromatin-euchromatin boundaries for many of the tomato chromosomes, resolving potential line-specific inversions, and subsequent selection of gene-rich

Fig. 4.7 Use of BAC FISH karyotyping to establish a standard chromosome nomenclature for *Sorghum bicolor* (BTx623), from Kim et al. (2005b). *Upper panel*: multi-BAC FISH cocktail was used to distinguish all 10 chromosomes pairs of *S. bicolor*. *Lower panel*: a proposed standardized nomenclature for the 10 *S. bicolor* chromosomes is shown in relation to previous linkage-group naming schemes, along with a summary of the cytological features from the FISH karyotype (Whitkus et al. 1992; Chittenden et al. 1994; Pereira et al. 1994; Dufour et al. 1997; Boivin et al. 1999; Crastra et al. 1999; Peng et al. 1999; Bhattramakki et al. 2000; Kong et al. 2000; Tao et al. 2000; Haussmann et al. 2002; Menz et al., 2002; Price et al. 2005, all as cited by Kim et al. 2005b)

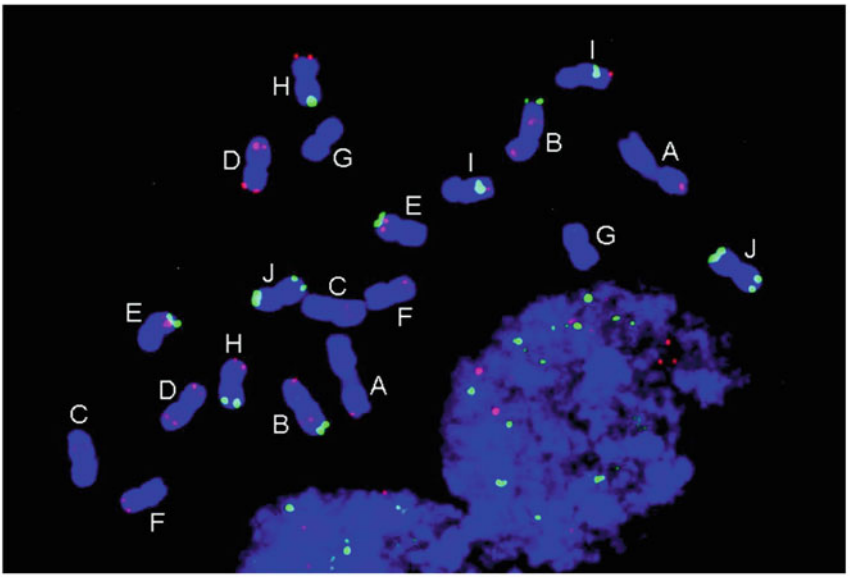

TABLE 1

Relationship of the FISH-based karyotype of sorghum and the linkage groups composing the various linkage maps of the sorghum genome

Chrom. no.[a]:	SBI-01	SBI-02	SBI-03	SBI-04	SBI-05	SBI-06	SBI-07	SBI-08	SBI-09	SBI-10
Linkage group (LG):	LG-01	LG-02	LG-03	LG-04	LG-05	LG-06	LG-07	LG-08	LG-09	LG-10
LG in Menz *et al.* (2002)[b]	A	B	C	D	J	I	E	H	F	G
LG in Pereira *et al.* (1994)	C	F	G	D	J	B	A	I	E	H
LG in Bowers *et al.* (2003)[c]	C	B	A	F	H	D	J	E	G	I
LG in Crastra *et al.* (1999)	G, K	D	A	C	J	F	E	H	I	B
LG in Boivin *et al.* (1999)[d]	C, K	F	G	D, L	J	B	A	I	E	H
LG in Whitkus *et al.* (1992)	B, C	D	F, M	H	G	E	A	K, L	I	J
FISH karyotype[e]										
Total length (μm)	5.11	3.87	3.85	3.5	3.44	3.15	3.13	3.07	2.98	2.94
Standard error[f]	0.047	0.035	0.038	0.032	0.037	0.029	0.028	0.026	0.029	0.023
Relative length[g]	14.59	11.06	10.98	9.99	9.82	9.00	8.92	8.75	8.51	8.39
Estimated DNA content[h]	119.3	90.5	89.8	81.7	80.3	73.6	73.0	71.6	69.6	68.6
Arm ratio[i]	1.32	1.16	1.13	1.14	1.02	1.42	1.06	1.10	1.02	1.04

[a] Chromosomes were ordered and numbered according to their rank of the total length at metaphase (full contraction).
[b] Linkage group designations are identical to those described in Peng *et al.* (1999), Kong *et al.* (2000), Bhattramakki *et al.* (2000), and Haussmann *et al.* (2002).
[c] Linkage group designations are identical to those described in Chittenden *et al.* (1994) and Tao *et al.* (2000).
[d] Linkage group designations are identical to those described in Dufour *et al.* (1997).
[e] The chromosomes are displayed according to cytogenetic convention with the short arm at the top of the vertical chromosome. The 17 BACs used for the karyotype are denoted in Figure 2 by an asterisk.
[f] The sample size for measurements was 40.
[g] Relative length = 100(chromosome length/genome length).
[h] Estimated DNA content = relative length × estimated genome size, *i.e.*, 818 Mbp (Price *et al.* 2005).
[i] Arm ratio = length of the long arm/the length of the short arm.

Fig. 4.7 (continued)

BACs (Peterson et al. 1999; Koo et al. 2008; Szinay et al. 2008; Stack et al. 2009). Similar cytogenetically based strategies have been employed for selection of BACs for the potato sequencing efforts (Visser et al. 2009). The use BAC FISH in structural genomics is facilitated by the genome structure of these species, relatively gene rich and with well-defined heterochromatin and euchromatin (reviewed by Stack et al. 2009). In contrast, BAC clones from maize or wheat are less useful as FISH probes because their genomes contain numerous dispersed repetitive sequences (Morgante et al. 2002; Koumbaris and Bass 2003; Lamb et al. 2007a). The extensive repetitive sequences in many plant species (Hake and Walbot 1980; SanMiguel et al. 1996; Bennetzen and Kellogg 1997; Kumar and Bennetzen 1999; Tikhonov et al. 1999; Meyers et al. 2001; Baucom et al. 2009) may result in erroneous cross-hybridization to multiple loci (Koumbaris and Bass 2003; Lamb et al. 2007a). Several strategies have been developed for addressing this problem.

One common approach is to produce an excess of unlabeled repetitive DNA to use as a "blocking" sequence along with the labeled probes. For example, the use of Cot1 DNA or even sheared total genomic DNA has been successful in both maize and common bean (Sadder et al. 2000; Pedrosa-Harand et al. 2009). In 2009, Pedrosa-Harand et al. successfully FISH mapped 19 direct-labeled BACs onto three common bean chromosomes. Despite the species' small genome (600 Mbp) six of these BACs required the use of blocking DNA to detect a single discrete signal. In addition, pericentromere-associated BACs were recalcitrant to FISH mapping in this species, despite the use of blocking DNA.

Another adaptation is selective amplification of the unique sequence portions of individual BAC clones and use of those PCR products as FISH probes. This technique requires that the BAC sequence be known so that primers can be designed and used to produce a collection of defined small segments from the same BAC (Lamb et al. 2007a). It has been used successfully in the detection of single genes on somatic chromosome 9 (Lamb et al. 2007a) and for the development of a somatic metaphase and pachytene cytogenetic map of maize chromosome 9 (Fig. 4.5, panel 3; Danilova and Birchler 2008).

Yet another adaptation involves the use of transgenomic BAC probes from related species with small genomes. In this case, one screens for BACs in silico or from a library and uses them as syntenic probes. These BAC probes do not contain the same collection of repetitive sequences as the target genome. This approach has been successfully used to map the liguleless genes in sorghum (Zwick et al. 1998) and to produce a FISH map of maize (Koumbaris and Bass 2003). The use of transgenomic FISH mapping is illustrated in Fig. 4.5 (panel 2) for maize chromosome 9 (Amarillo and Bass 2007). In this study, sorghum BACs selected by screening with maize RFLP probes were used to FISH map 32 loci on maize chromosome 9 (Amarillo and Bass 2007). Transgenomic FISH mapping is also valuable for comparative genomics and analysis of other pairs of closely related species, including sorghum and maize (Hulbert et al. 1990; Gomez et al. 1997), tomato and potato (Fuchs et al. 1996; Iovene et al. 2008; Tang et al. 2008, 2009), rice and sorghum (Zwick et al. 1998), and several *Brassica* species (Jackson et al. 2000; Mandakova and Lysak 2008). Multicolor

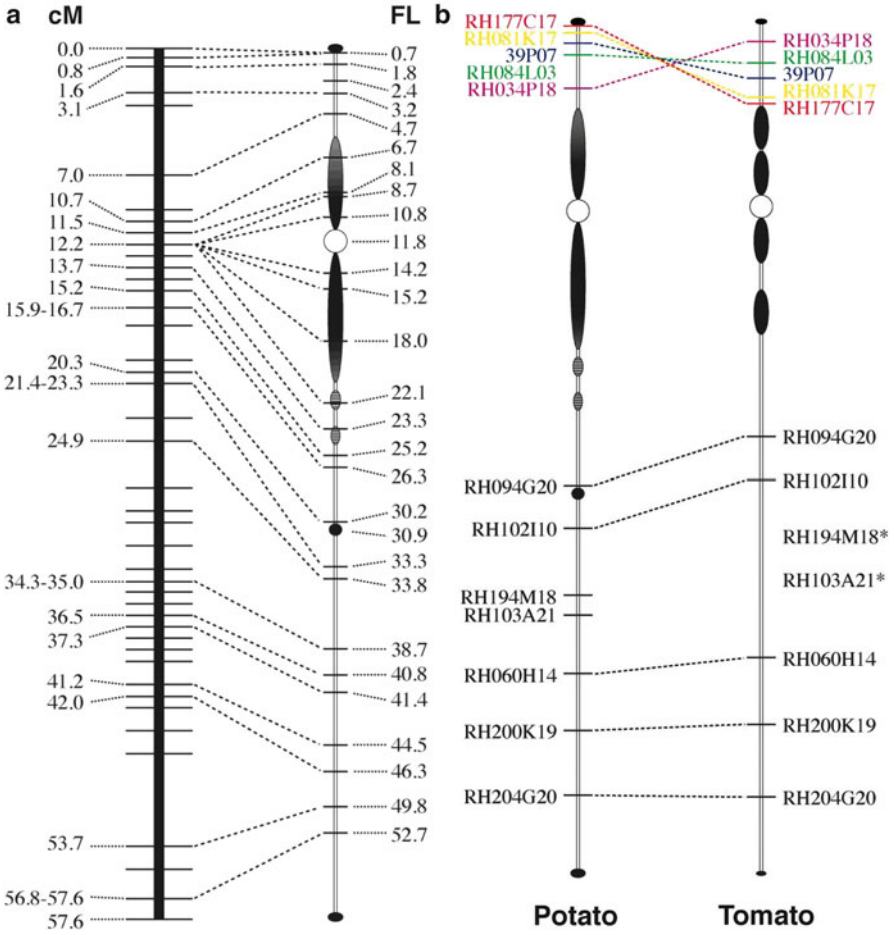

Fig. 4.8 High-density cytogenetic FISH map of pachytene-stage potato chromosome 6, from Iovene et al. (2008). (**a**) Distribution of loci on the linkage (cM) map in comparison to the pachytene-stage FISH locus map in fractional-length (FL) units. The pachytene-stage ideogram also shows the location of the centromere (*white circle*), heterochromatin (*solid/shaded black ovals*), and multiple small knobs (*hatched circles*). (**b**) Comparative ideograms of pachytene-stage orthologous chromosomes, potato six and tomato six. Variation in heterochromatin distribution and a large terminal inversion are evident

cross-species BAC-FISH mapping has been used efficiently in genome painting in *Arabidopsis* and was used to map chromosomal rearrangements between tomato and potato chromosomes 6 (Lysak et al. 2001, 2003; Iovene et al. 2008; Tang et al. 2008, 2009). In 2008, Iovene et al. created a high-density pachytene-stage cytogenetic map of potato chromosome 6 and compared it with tomato chromosome 6. Their results revealed a rearrangement along the short arms of the chromosomes that had not been definitively demonstrated previously, as shown in Fig. 4.8.

BAC probes have been successfully used for FISH cytogenetic mapping in many different plant species, including cotton (Hanson et al. 1995), tomato (Zhong et al. 1996b), barley (Lapitan et al. 1997), *Arabidopsis* (Fransz et al. 1996), rice (Jiang et al. 1995; Cheng et al. 2001a, b, 2002a), *Medicago* (Kulikova et al. 2001), sorghum (Islam-Faridi et al. 2002; Kim et al. 2002, 2005a, b), wheat (Zhang et al. 2004a, b), *Silene latifolia* (Lengerova et al. 2004), and maize (Koumbaris and Bass 2003; Wang et al. 2006; Amarillo and Bass 2007; Lamb et al. 2007a; Danilova and Birchler 2008). Biotin-labeled BAC probes were used in the development of a cytogenetic map for the somatic metaphase chromosomes of sorghum (Kim et al. 2002), whereas in tomato, the mapping of BACs relative to repeat sequences was used to identify gene-rich BACs located in the interstitial portions of chromosomes 2 and 6 (Koo et al. 2008; Szinay et al. 2008). These sorts of approaches for identification of gene-rich BACs can also provide useful information for ongoing genome-sequencing efforts.

4.5.3 Repetitive Sequences Probes

Repeat sequences are common in plant genomes (Hemleben et al. 2007; Baucom et al. 2009). Cytogenetic mapping of repetitive DNA sequences helps to define their overall genomic distribution and can, in some cases, be used to distinguish chromosomes that otherwise look the same. The abundant tandemly repeated rDNA gene clusters are by far the most widely used and a common starting point for FISH-based mapping or karyotyping efforts (Fransz et al. 1996; Hizume et al. 2002; Kaczmarek et al. 2009). For example, Xu and Earle (1996b) mapped the 45 S rDNA loci onto the tomato pachytene chromosomes, and Pedrosa et al. (2002) demonstrated the use of rDNA FISH for creating a karyotype of the model legume *Lotus japonicus* L. More recently Kaczmarek et al. (2009) FISH mapped telomeric, rDNA, and *FokI* repeat sequences along with several BAC probes to facilitate the identification of individual metaphase chromosomes of *Lupinus angustifolius* L. (Fig. 4.1d).

In addition, rDNA FISH in combination with other tandem repeats aids the generation of core cytogenetic maps, as has been demonstrated for maize (Peacock et al. 1981), wheat (Jiang and Gill 1994), cotton (Hanson et al. 1996), tomato (Xu and Earle 1996a, b), *Pinus* species (Hizume et al. 2002), and *Arabidopsis* (Koornneef et al. 2003). The rDNA sequences are conserved across most plant species, but other tandem repeats exhibit variable degrees of conservation, and their utility is often limited to single or closely related species (Hizume et al. 2002; Islam-Faridi et al. 2007; Kaczmarek et al. 2009).

Centromeric and telomeric sequences are also widely used in FISH mapping studies. Telomere repeats are highly conserved in plant species and occur in at least two major variants, (TTAGGG)n and (TTTAGGG)n (Lapitan et al. 1989; Adams et al. 2001; Fajkus et al. 2005). Although centromere and telomere FISH probes

stain structures that may already be evident from chromosome morphology, these probes can also be used as positive controls for optimizing FISH procedures. Furthermore, telomere FISH can also mark internal clusters of telomere repeats as distinct loci, usually indicative of ancestral chromosomal rearrangements such as inversions or fusions.

Probes that can detect centromere-associated sequences are typically primary and necessary reagents for cytogenetic FISH mapping, despite the high level of sequence variation in centromere repeat sequences within and among different species. Because the alpha satellite sequences have a tendency to accumulate at or very near centromere regions, these sequences can be ideal for FISH mapping of centromeres. They are typically AT rich, relatively short (150–200 bp repeat), and relatively fast evolving, so they exhibit considerable sequence divergence among species or even among chromosomes in the same species. The centromere-associated 156-bp tandem repeat of maize, CentC, was first discovered by Ananiev et al. (1998) and has become an invaluable cytogenetic reagent for maize and many related grass species. Similarly, CentO, a 155-bp centromere-specific satellite repeat sequence; the 180-bp satellite repeat; and CEN38, a 140-bp repeat sequence, have proven useful for labeling the primary constriction in rice, *Arabidopsis*, and sorghum, respectively (Heslop-Harrison et al. 1999; Zwick et al. 2000; Cheng et al. 2002b; Nagaki et al. 2003b; Kim et al. 2005c). Some retroelements are also preferentially colocalized with centromeres: the CRR of rice, the CRM and CentA of maize (Ananiev et al. 1998; Nagaki et al. 2003a; Wolfgruber et al. 2009), and the CentA1 and CentA2 of *Anthirhinum* (Zhang et al. 2005; Wang et al. 2009).

Combinatorial FISH with differentially labeled repetitive sequence probes (centromeric, rDNA, knobs, etc.) has proven extremely informative, as illustrated by Kato et al. (2004) in their analysis of the dynamic and diverse genomes of maize. Multicolor FISH probe cocktails produce distinct patterns on the 10 chromosomes of maize, making them useful for unambiguously identifying every individual chromosome. A comparison across 14 inbred maize lines demonstrated a remarkable degree of hybridization variation, as shown in Fig. 4.9 (Kato et al. 2004). Relatedly, FISH mapping and karyotyping with multicopy gene family clusters are also common (Fuchs and Schubert 1995; Stephens et al. 2004; Pedrosa-Harand et al. 2009). Even dispersed repetitive sequences are useful as FISH probes because they can differentially paint chromosomes or chromosomal regions and have therefore been used in comparative genomics (Bass et al. 2000; Riera-Lizarazu et al. 2000; Lysak et al. 2003; Lamb and Birchler 2006; Lamb et al. 2007b).

4.6 Target Chromosomes for Plant Cytogenetic Mapping

The nature of the target chromosome also influences the efficiency and resolution of FISH analysis. Chromosome material can be derived from different stages of cell division – mitotic prophase, prometaphase or metaphase, meiotic prophase (usually

Fig. 4.9 Somatic karyotype of 14 maize inbred lines with a 9-probe multicolor FISH-probe cocktail, from Kato et al. (2004). Ten individual maize chromosomes (listed across *top*) are identified by metaphase FISH. This probe mixture, which includes several repetitive sequence families, also demonstrates a highly variable pattern among different inbred lines (listed at *left*) of maize

the pachytene stage), or even interphase. A well-known trade-off in FISH mapping involves the choice between mitotic and meiotic chromosomes. Mitotic chromosomes are easily obtained from root-tip preparations within days of sprouting, whereas the pollen mother cells yield much longer chromosomes for more accurate mapping, along the chromosome axis, but are only available from reproductive organs that may take weeks or months to develop and last for only a few days of the life cycle.

4.6.1 Mitotic Metaphase and Prometaphase

Mitotic metaphase chromosomes are the most common cytological targets for FISH analysis in plants. Meristematic regions in root tips are excellent sources of cells for metaphase chromosome preparations, but highly condensed metaphase chromosomes have limited optical and axial resolution (see, e.g., Fig. 4.5, panel 3), as defined by the distance needed for determining their spatial arrangement (Ramanna and Prakken 1967; Jiang et al. 1995; Pedersen et al. 1995; Islam-Faridi et al. 2002; Zoller et al. 2004; Danilova and Birchler 2008). Axial resolution maxima for distinguishing or ordering closely spaced FISH signals are reported at 1–3 Mb for prometaphase chromosomes of rice (Cheng et al. 2002a) and 2–10 Mb for the more condensed metaphase chromosomes (Pedersen et al. 1995; Figueroa and Bass 2010). Axial resolution limits are estimates, as shown in Table 4.2, and can vary severalfold along even a single chromosome, depending on the location (Figueroa and Bass 2010).

Mitotic chromosomes can also be collected by flow-sorting of individual metaphase chromosomes, or flow karyotyping, as has been applied in physical mapping of mitotic chromosomes in many plant species (Dolezel et al. 2004, 2007). Unfortunately, most chromosomes for a given plant species give grouped peaks during flow karyotyping, creating technical limitations that prevent its more common use. Instead, flow-sorting is commonly used to obtain highly purified groups of chromosomes for various cytological or biochemical assays (Vlacilova et al. 2002; Kubalakova et al. 2003; Dolezel et al. 2004, 2007; Valarik et al. 2004; Jiang and Gill 2006; Rens et al. 2006; Gupta et al. 2008; Koo and Jiang 2009).

4.6.2 Meiotic Prophase

Pachytene-stage meiotic chromosomes are ideal for FISH mapping for several reasons. First, pachytene cytological maps serve as the most direct comparison with genetic maps because crossing over occurs at that stage (reviewed by Zickler and Kleckner 1998). Second, the extended synapsed bivalents appear as single fibers, revealing prominent cytological landmarks, such as knobs, nucleolus organizing regions, various chromomeres, and euchromatin-heterochromatin boundaries, that aid in chromosome identification and karyotyping (Wang et al. 2006; Lamb et al. 2007b) but are often concealed in the more highly condensed metaphase chromosomes (reviewed by Fransz et al. 1998; de Jong et al. 1999; Zhong et al. 1999; Chen et al. 2000; Adawy et al. 2004). Third, pachytene-stage chromosomes are typically several times longer than their mitotic counterparts and thus afford better axial resolution (Ramanna and Prakken 1967; de Jong et al. 1999; Zhong et al. 1999; Zoller et al. 2004; Kim et al. 2005c), as exemplified by FISH mapping in various plants (Zhong et al. 1996b, 1999; Fransz et al. 1998; Cheng et al. 2002a, b; Islam-Faridi et al. 2002; Sadder and Weber 2002; Danilova and Birchler 2008). The axial resolution for pairs of FISH probes on meiotic chromosomes has been reported to be 40–140 kb in euchromatic and 0.12–1.2 Mbps in heterochromatic regions (see Table 4.2;

Table 4.2 Axial resolution and probe size-detection limits in plant fluorescence in situ hybridization (FISH) (reproduced from Figueroa and Bass 2010)

Cell type	Cell stage	Target chromosome		Axial resolution limit[c] (kb)	Probe size detection limit[d] (kb)	References[e]
		Chromatin[a]	Preparation[b]			
Somatic	Metaphase			2,000–10,000	2.27–10	de Jong et al. (1999), Jiang and Gill (2006), Lamb et al. (2007a), Danilova and Birchler (2008)
		Euchromatin		4,000–5,000	>100	de Jong et al. (1999)
		Heterochromatin		5,000–10,000	50–100	de Jong et al. (1999), Danilova and Birchler (2008)
			Superstretched	70	1,000–2,000	Valarik et al. (2004)
	Prometaphase			2,000		Cheng et al. (2002a)
	Interphase			100	10	Jiang et al. (1996), Jiang and Gill (2006)
			Extended fiber	4.0	0.7	Fransz et al. (1996), Cheng et al. (2002a)
Meiotic	Pachytene			1–2,000	3.1	Jiang and Gill (2006), Wang et al. (2006), Danilova and Birchler (2008)
		Euchromatin		120	50.0	de Jong et al. (1999)
		Heterochromatin		1,200		de Jong et al. (1999)
			Superstretched	<50		Koo and Jiang (2009)

[a]The type of chromatin is indicated for studies where it was specified
[b]If other than conventional spread or squash technique
[c]The smallest reported probe size resulting in detection of a FISH signal in a given study
[d]The minimum reported distance between two FISH signals ordered and resolved along the chromosome axis
[e]Primary or review papers describing the resolution- or detection-limit value

Cheng et al. 2001a, b; Figueroa and Bass 2010). The increased resolution afforded by pachytene chromosomes was exploited for mapping the maize chromosome 9 CentC relative to the genetically mapped markers *wx1* and *cdo17* (Fig. 4.5, panel 4).

Despite the larger size and increased resolution, the pachytene chromosomes of some species are not amenable to cytological analysis, often perhaps because of the sheer number of similar-sized chromosomes with identical centromere placement, as seen in polyploids such as wheat (Gupta et al. 2008), or the inaccessibility of anthers or their small size, as seen in *Arabidopsis* (Koornneef et al. 2003). Strategies have therefore been developed for stretching metaphase chromosomes to the sizes of their pachytene counterparts as well as for spreading the readily available interphase chromatin into individual fibers for optimal resolving power.

4.7 High-Resolution Mapping

4.7.1 Extended or Superstretched Chromosomes

One procedure that gives excellent resolution involves stretching flow-sorted mitotic metaphase chromosomes and exposing them to a mild treatment with proteinase-K. It has been used successfully to stretch the chromosomes of wheat, barley, rye, and chickpea to more than 100 times their original lengths (Valarik et al. 2004), producing 70-kb resolution, similar to that of pachytene-stage chromosome preparations (Cheng et al. 2002a). This procedure is powerful for analysis of selected subregions of chromosomes as long as flow-sorting technology and amenable starting material are available (de Jong et al. 1999).

A related stretched-chromatin technique that involves a more gentle extension of the chromosome and retention of associated chromatin proteins has proven highly useful for observation of the interaction of maize and *A. thaliana* centromeric histone protein CENH3 with centromeric DNA sequences (Jin et al. 2004; Shibata and Murata 2004).

4.7.2 Interphase: Extended DNA Fibers

Extended DNA-fiber-based FISH mapping yields the highest resolution because the deproteinized DNA is deposited linearly on the slide before being subjected to FISH. In *A. thaliana*, DNA from interphase nuclei and BAC DNA sequences were spread as extended DNA fibers on glass slides for FISH analysis (Fransz et al. 1996; Jackson et al. 2000). This study extended the DNA fibers to 2.5–3.5 kb/μm, approximately the same size as native duplex B-DNA, 2.97 kb per/μm (Watson and Crick 1953; Wing et al. 1980). Ability to resolve probes only 8.2 kb apart was reported on extended DNA fibers of tomato (Fransz et al. 1996). This approach has proven useful for estimating the sizes of the physical gaps in the genome contig maps of *A. thaliana* (Jackson et al. 1998) and rice (Feng et al. 2002; Sasaki et al. 2002). This technique

was calibrated in rice with sequenced clones from a 1-Mb BAC DNA contig (Cheng et al. 2002a). The average fiber extension (3.21 kb/μm) among seven BAC clones matched the sequencing data, demonstrating the resolving power of this technique in cytogenetic mapping. This procedure has also been used to reveal the fine details of DNA structure in sorghum (Miller et al. 1998) and rice (Nagaki et al. 2004) and to confirm the order of BACs in contigs assembled by other methods.

4.8 Utility of Cytogenetic Maps

Genome structure can be described by cytogenetic maps revealing overall genome organization, particularly the ordering, spacing, and distribution of genes, the heterochromatin, and euchromatin regions within a genome (Islam-Faridi et al. 2002). These features are not revealed in genetic linkage maps or sequence maps. Integration of cytogenetic and genetic maps allows determination of the linear order and tests of preserved arrangements and distributions of genetic markers along target chromosomes (Gill et al. 1996a, b; Künzel et al. 2000; Cone et al. 2002). Cytogenetic and genetic maps have been successfully integrated in plant species such as potato (Dong et al. 2000; Tang et al. 2009), rice (Cheng et al. 2001a), *Medicago truncatula* Gaertn. (Kulikova et al. 2001), *Brassica oleracea* L. (Howell et al. 2002), sorghum (Kim et al. 2002, 2005b), *L. japonicus* (Pedrosa et al. 2002), and *A. majus* (Zhang et al. 2005). These integrated maps establish the relationship between linkage distance (cM) and physical distance (cMC) by providing visual clues to the relative spacing of flanking genetic markers on chromosomes. Significant discrepancies between genetic and physical distances have been reported in sorghum (Islam-Faridi et al. 2002), potato (Tang et al. 2009), and wheat and barley (Werner et al. 1992; Künzel et al. 2000). Chromosome studies of the large genomes and large chromosomes of wheat and barley revealed that recombination is concentrated along the distal halves of chromosomes and that suppression of recombination was observed in the centromeric regions, which constitute 50% of the chromosome. In the case of *A. thaliana*, the ratio of the genetic distance to the physical distance varies along the entire length of the chromosome. Relative hotspots and coldspots of recombination were distributed throughout the chromosome (Schmidt et al. 1995), but recombination suppression in the pericentromeric region was not evident, as it was in tomato, wheat, and barley chromosomes. Aside from discrepancies between genetic and cytogenetic distance, integrated maps can also reveal possible regions of hyperexpansion, as shown in Fig. 4.5 (panel 2).

References

Adams SP, Hartman TP, Lim KY, Chase MW, Bennett MD, Leitch IJ, Leitch AR (2001) Loss and recovery of *Arabidopsis*-type telomere repeat sequences 5'-(TTTAGGG)(n)-3' in the evolution of a major radiation of flowering plants. *Proc R Soc London B Biol Sci* 268:1541–1546.

Adawy SS, Stupar RM, Jiang J (2004) Fluorescence in situ hybridization analysis reveals multiple loci of knob-associated DNA elements in one-knob and knobless maize lines. *J Histochem Cytochem* 52:1113–1116.

Albini S (1994) A karyotype of the *Arabidopsis thaliana* genome derived from synaptonemal complex analysis at prophase I of meiosis. *Plant J* 5:665–672.

Albini SM, Jones GH (1988) Synaptonemal complex spreading in *Allium cepa* and *Allium fistulosum*. II. Pachytene observations: the SC karyotype and the correspondence of late recombination nodules and chiasmata. *Genome* 30:399–410.

Amarillo FI, Bass HW (2007) A transgenomic cytogenetic sorghum (*Sorghum propinquum*) bacterial artificial chromosome fluorescence in situ hybridization map of maize (*Zea mays* L.) pachytene chromosome 9, evidence for regions of genome hyperexpansion. *Genetics* 177:1509–1526.

Ambros PF, Matzke MA, Matzke AJ (1986) Detection of a 17 kb unique sequence (T-DNA) in plant chromosomes by in situ hybridization. *Chromosoma* 94:11–18.

Ananiev EV, Phillips RL, Rines HW (1998) Chromosome-specific molecular organization of maize (*Zea mays* L.) centromeric regions. *Proc Natl Acad Sci USA* 95:13073–13078.

Ananiev EV, Wu C, Chamberlin MA, Svitashev S, Schwartz C, Gordon-Kamm W, Tingey S (2009) Artificial chromosome formation in maize (*Zea mays* L.). *Chromosoma* 118:157–177.

Anderson EG (1935) Chromosomal interchanges in maize. *Genetics* 20:70–83.

Anderson EG (1938) Translocations in maize involving chromosome 9. *Genetics* 23:307–313.

Anderson EG (1939) Translocations in maize involving chromosome 8. *Genetics* 24:385–390.

Anderson EG (1941) Translocations in maize involving chromosome 1. *Genetics* 26:452–459.

Anderson EG, Brink RA (1940) Translocations in maize involving chromosome 3. *Genetics* 25:299–309.

Anderson EG, Kramer HH (1954) Translocations in maize involving chromosome 10. *Genetics* 39:506–512.

Anderson EG, Randolph LF (1945) Location of the centromeres on the linkage maps of maize. *Genetics* 30:518–526.

Anderson EG, Kramer HH, Longley AE (1955a) Translocations in maize involving chromosome 4. *Genetics* 40:500–510.

Anderson EG, Kramer HH, Longley AE (1955b) Translocations in maize involving chromosome 6. *Genetics* 40:531–538.

Anderson LK, Doyle GG, Brigham B, Carter J, Hooker KD, Lai A, Rice M, Stack SM (2003) High-resolution crossover maps for each bivalent of *Zea mays* using recombination nodules. *Genetics* 165:849–865.

Anderson LK, Salameh N, Bass HW, Harper LC, Cande WZ, Weber G, Stack SM (2004) Integrating genetic linkage maps with pachytene chromosome structure in maize. *Genetics* 166:1923–1933.

Arrighi FE, Hsu TC (1971) Localization of heterochromatin in human chromosomes. *Cytogenetics* 10:81–86.

Barton DW (1950) Pachytene morphology of the tomato chromosome complement. *Am J Bot* 37:639–643.

Bass HW, Marshall WF, Sedat JW, Agard DA, Cande WZ (1997) Telomeres cluster de novo before the initiation of synapsis: a three-dimensional spatial analysis of telomere positions before and during meiotic prophase. *J Cell Biol* 137:5–18.

Bass HW, Riera-Lizarazu O, Ananiev EV, Bordoli SJ, Rines HW, Phillips RL, Sedat JW, Agard DA, Cande WZ (2000) Evidence for the coincident initiation of homolog pairing and synapsis during the telomere-clustering (bouquet) stage of meiotic prophase. *J Cell Sci* 113: 1033–1042.

Baucom RS, Estill JC, Chaparro C, Upshaw N, Jogi A, Deragon JM, Westerman RP, SanMiguel PJ, Bennetzen JL (2009) Exceptional diversity, non-random distribution, and rapid evolution of retroelements in the B73 maize genome. *PLoS Genet* 5:e1000732.

Beckett JB (1978) B-A translocations in maize I. Use in locating genes by chromosome arms. *J Hered* 69:27–36.

Beckett JB (1993) Locating recessive genes to chromosome arm with B-A translocations. In: Freeling M, Walbot V (eds), *The Maize Handbook*. Springer, New York, pp. 315–327, 336–341.

Bennetzen JL, Kellogg EA (1997) Do plants have a one-way ticket to genomic obesity? *Plant Cell* 9:1509–1514.

Birchler JA (1980) The cytogenetic localization of the alcohol dehydrogenase-1 locus in maize. *Genetics* 94:687–700.

Chang SB, Anderson LK, Sherman JD, Royer SM, Stack SM (2007) Predicting and testing physical locations of genetically mapped loci on tomato pachytene chromosome 1. *Genetics* 176:2131–2138.

Chang SB, Yang TJ, Datema E, van Vugt J, Vosman B, Kuipers A, Meznikova M, Szinay D, Klein Lankhorst R, Jacobsen E, de Jong H (2008) FISH mapping and molecular organization of the major repetitive sequences of tomato. *Chromosome Res* 16:919–933.

Chen CC, Chen CM, Hsu FC, Wang CJ, Yang JT, Kao YY (2000) The pachytene chromosomes of maize as revealed by fluorescence in situ hybridization with repetitive DNA sequences. *Theor Appl Genet* 101:30–36.

Cheng Z, Buell CR, Wing RA, Gu M, Jiang J (2001a) Toward a cytological characterization of the rice genome. *Genome Res* 11:2133–2141.

Cheng Z, Presting GG, Buell CR, Wing RA, Jiang J (2001b) High-resolution pachytene chromosome mapping of bacterial artificial chromosomes anchored by genetic markers reveals the centromere location and the distribution of genetic recombination along chromosome 10 of rice. *Genetics* 157:1749–1757.

Cheng Z, Buell CR, Wing RA, Jiang J (2002a) Resolution of fluorescence in-situ hybridization mapping on rice mitotic prometaphase chromosomes, meiotic pachytene chromosomes and extended DNA fibers. *Chromosome Res* 10:379–387.

Cheng ZK, Dong FG, Langdon T, Shu OY, Buell CR, Gu MH, Blattner FR, Jiang JM (2002b) Functional rice centromeres are marked by a satellite repeat and a centromere-specific retrotransposon. *Plant Cell* 14:1691–1704.

Cone KC, McMullen MD, Bi IV, Davis GL, Yim YS, Gardiner JM, Polacco ML, Sanchez-Villeda H, Fang Z, Schroeder SG, Havermann SA, Bowers JE, Paterson AH, Soderlund CA, Engler FW, Wing RA, Coe EH Jr (2002) Genetic, physical, and informatics resources for maize. On the road to an integrated map. *Plant Physiol* 130:1598–1605.

Creighton HB, McClintock B (1931) A correlation of cytological and genetical crossing-over in *Zea mays. Proc Natl Acad Sci USA* 17:492–497.

Danilova TV, Birchler JA (2008) Integrated cytogenetic map of mitotic metaphase chromosome 9 of maize: resolution, sensitivity, and banding paint development. *Chromosoma* 117:345–356.

de Jong JH, Fransz P, Zabel P (1999) High resolution FISH in plants – techniques and applications. *Trends Plant Sci* 4:258–263.

Desel C, Jung C, Cai D, Kleine M, Schmidt T (2001) High-resolution mapping of YACs and the single-copy gene *Hs1pro-1* on *Beta vulgaris* chromosomes by multi-colour fluorescence in situ hybridization. *Plant Mol Biol* 45(1):113–122.

Dolezel J, Kubalakova M, Bartos J, Macas J (2004) Flow cytogenetics and plant genome mapping. *Chromosome Res* 12:77–91.

Dolezel J, Kubalakova M, Paux E, Bartos J, Feuillet C (2007) Chromosome-based genomics in the cereals. *Chromosome Res* 15:51–66.

Dong F, Song J, Naess SK, Helgeson JP, Gebhardt C, Jiang J (2000) Development and applications of a set of chromosome-specific cytogenetic DNA markers in potato. *Theor Appl Genet* 101: 1001–1007.

Endo TR (1988) Induction of chromosomal structural changes by a chromosome of *Aegilops cylindrica* L. in common wheat. *J Hered* 79:366–370.

Endo TR (1990) Gametocidal chromosomes and their induction of chromosome mutations in wheat. *Japan J Genet* 65:135–152.

Endo TR (2007) The gametocidal chromosome as a tool for chromosome manipulation in wheat. *Chromosome Res* 15:67–75.

Endo TR, Gill BS (1996) The deletion stocks of common wheat. *J Hered* 87:295–307.

Endo TR, Mukai Y (1988) Chromosome mapping of a speltoid suppressin gene of *Triticum aestivum* L. based on partial deletions in the long arm of chromosome 5A. *Japan J Genet* 63:501–505.

Endo TR, Yamamoto M, Mukai Y (1994) Structural changes of rye chromosome 1R induced by a gemetocidal chromosome. *Japan J Genet* 69:13–19.

Fajkus J, Sykorova E, Leitch AR (2005) Telomeres in evolution and evolution of telomeres. *Chromosome Res* 13:469–479.

Feng Q, Zhang Y, Hao P, Wang S, Fu G, Huang Y, Li Y, Zhu J, Liu Y, Hu X, Jia P, Zhao Q, Ying K, Yu S, Tang Y, Weng Q, Zhang L, Lu Y, Mu J, Zhang LS, Yu Z, Fan D, Liu X, Lu T, Li C, Wu Y, Sun T, Lei H, Li T, Hu H, Guan J, Wu M, Zhang R, Zhou B, Chen Z, Chen L, Jin Z, Wang R, Yin H, Cai Z, Ren S, Lv G, Gu W, Zhu G, Tu Y, Jia J, Chen J, Kang H, Chen X, Shao C, Sun Y, Hu Q, Zhang X, Zhang W, Wang L, Ding C, Sheng H, Gu J, Chen S, Ni L, Zhu F, Chen W, Lan L, Lai Y, Cheng Z, Gu M, Jiang J, Li J, Hong G, Xue Y, Han B (2002) Sequence and analysis of rice chromosome 4. *Nature* 420:316–320.

Figueroa DM, Bass HW (2010) A historical and modern perspective on plant cytogenetics. *Briefings Funct Genomics* 9:95–102.

Fransz PF, Alonso-Blanco C, Liharska TB, Peeters AJ, Zabel P, de Jones JH (1996) High-resolution physical mapping in *Arabidopsis thaliana* and tomato by fluorescence in situ hybridization to extended DNA fibres. *Plant J* 9:421–430.

Fransz P, Armstrong S, Alonso-Blanco C, Fischer TC, Torres-Ruiz RA, Jones G (1998) Cytogenetics for the model system *Arabidopsis thaliana. Plant J* 13:867–876.

Fuchs J, Schubert I (1995) Localization of seed protein genes on metaphase chromosomes of *Vicia faba* via fluorescence in situ hybridization. *Chromosome Res* 3:94–100.

Fuchs J, Kloos DU, Ganal MW, Schubert I (1996) In situ localization of yeast artificial chromosome sequences on tomato and potato metaphase chromosomes. *Chromosome Res* 4: 277–281.

Fukui K, Kakeda K, Hashimoto J, Matsuoka S (1987) In situ hybridization of ^{125}I labelled rRNA to rice chromosomes. *Rice Genet Newslett* 4:114–116.

Gall JG, Pardue ML (1969) Formation and detection of RNA-DNA hybrid molecules in cytological preparations. *Proc Natl Acad Sci USA* 63:378–383.

Gill BS, Kimber G (1974) The Giemsa C-banded karyotype of rye. *Proc Natl Acad Sci USA* 71:1247–1249.

Gill KS, Gill BS, Endo TR, Boyko EV (1996a) Identification and high-density mapping of gene-rich regions in chromosome group 5 of wheat. *Genetics* 143:1001–1012.

Gill KS, Gill BS, Endo TR, Taylor T (1996b) Identification and high-density mapping of gene-rich regions in chromosome group 1 of wheat. *Genetics* 144:1883–1891.

Gillies CB (1972) Reconstruction of the *Neurospora crassa* pachytene karyotype from serial sections of synaptonemal complexes. *Chromosoma* 36:119–130.

Gillies CB (1973) Ultrastructural analysis of maize pachytene karyotypes by three dimensional reconstruction of the synaptonemal complexes. *Chromosoma* 43:145–176.

Gillies CB (1981) Electron microscopy of spread maize pachytene synaptonemal complexes. *Chromosoma* 83:575–591.

Gomez MI, Islam-Faridi MN, Woo SS, Czeschin D Jr, Zwick MS, Stelly DM, Price HJ, Schertz KF, Wing RA (1997) FISH of a maize *sh2*-selected sorghum BAC to chromosomes of *Sorghum bicolor. Genome* 40:475–478.

Gottschalk W (1951) Untersuchungen am Pachytän normaler und röntgenbestrahlter Pollenmutterzellen von *Solanum lycopersicum*. *Chromosoma* 4:298–341.

Griffor MC, Vodkin LO, Singh RJ, Hymowitz T (1991) Fluorescent in situ hybridization to soybean metaphase chromosomes. *Plant Mol Biol* 17:101–109.

Gu M.-H., Ma H-T, Liang GH (1984) Karyotype analysis of seven species in the genus *Sorghum*. *J Hered* 75:196–202.

Gupta PK, Mir RR, Mohan A, Kumar J (2008) Wheat genomics: present status and future prospects. *Int J Plant Genomics* 2008:896451.

Gustafson JP, Dillé JE (1992) Chromosome location of *Oryza sativa* recombination linkage groups. *Proc Natl Acad Sci USA* 89:8646–8650.

Gustafson JP, Butler E, McIntyre CL (1990) Physical mapping of a low-copy DNA sequence in rye (*Secale cereale* L.). *Proc Natl Acad Sci USA* 87:1899–1902.

Guzzo F, Campagnari E, Levi M (2000) A new FISH protocol with increased sensitivity for physical mapping with short probes in plants. *J Exp Bot* 51:965–970.

Hake S, Walbot V (1980) The genome of *Zea mays*, its organization and homology to related grasses. *Chromosoma* 79:251–270.

Hanson RE, Zwick MS, Choi SD, Islam-Faridi MN, McKnight TD, Wing RA, Price HJ, Stelly DM (1995) Fluorescent in situ hybridization of a bacterial artificial chromosome. *Genome* 38:646–651.

Hanson RE, Islam-Faridi MN, Percival EA, Crane CF, Ji YF, McKnight TD, Stelly DM, Price HJ (1996) Distribution of 5 S and 18 S-28S rDNA loci in a tetraploid cotton (*Gossypium hirsutum* L.) and its putative diploid ancestors. *Chromosoma* 105:55–61.

Harper LC, Cande WZ (2000) Mapping a new frontier; development of integrated cytogenetic maps in plants. *Funct Integr Genomics* 1:89–98.

Haynes FL (1964) Pachytene chromosomes of *Solanum canasense*. *J Hered* 55:168–173.

Hemleben V, Kovarik A, Torres-Ruiz RA, Volkov RA, Beridze T (2007) Plant highly repeated satellite DNA: molecular evolution, distribution and use for identification of hybrids. Syst Biodiv 5:277–289.

Heslop-Harrison JS, Murata M, Ogura Y, Schwarzacher T, Motoyoshi F (1999) Polymorphisms and genomic organization of repetitive DNA from centromeric regions of *Arabidopsis* chromosomes. *Plant Cell* 11:31–42.

Hizume M, Shibata F, Matsusaki Y, Garajova Z (2002) Chromosome identification and comparative karyotypic analyses of four *Pinus* species. *Theor Appl Genet* 105:491–497.

Holm PB (1977) Three-dimensional reconstruction of chromosome pairing during the zygotene stage of meiosis in *Lilium longiflorum* (Thunb.). *Carlsberg Res Commun* 42:77–98.

Howell EC, Barker GC, Jones GH, Kearsey MJ, King GJ, Kop EP, Ryder CD, Teakle GR, Vicente JG, Armstrong SJ (2002) Integration of the cytogenetic and genetic linkage maps of *Brassica oleracea. Genetics* 161:1225–1234.

Huang XQ, Zeller FJ, Hsam SLK, Wenzel G, Mohler V (2000) Chromosomal location of AFLP markers in common wheat utilizing nulli-tetrasomic stocks. *Genome* 43:298–305.

Hulbert SH, Richter TE, Axtell JD, Bennetzen JL (1990) Genetic mapping and characterization of sorghum and related crops by means of maize DNA probes. *Proc Natl Acad Sci USA* 87: 4251–4255.

Iovene M, Wielgus SM, Wimon PW, Buell CR, Jiang J (2008) Chromatin structure and physical mapping of chromosome 6 of potato and comparative analyses with tomato. *Genetics* 180:1307–1317.

Islam-Faridi MN, Iscii T, Kumar L, Sitch A, Brar DS (1990) Chromosomal location of ribosomal RNA genes in rice by in situ hybridization. *Rice Genet Newslett* 7:144.

Islam-Faridi MN, Childs KL, Klein PE, Hodnett G, Menz MA, Klein RR, Rooney WL, Mullet JE, Stelly DM, Price HJ (2002) A molecular cytogenetic map of sorghum chromosome 1. Fluorescence in situ hybridization analysis with mapped bacterial artificial chromosomes. *Genetics* 161:345–353.

Islam-Faridi MN, Nelson CD, Kubisiak TL (2007) Reference karyotype and cytomolecular map for loblolly pine (*Pinus taeda* L.). *Genome* 50:241–251.

Jackson SA, Wang ML, Goodman HM, Jiang J (1998) Application of fiber-FISH in physical mapping of *Arabidopsis thaliana. Genome* 41:566–572.

Jackson SA, Cheng ZK, Wang ML, Goodman HM, Jiang JM (2000) Comparative fluorescence in situ hybridization mapping of a 431-kb *Arabidopsis thaliana* bacterial artificial chromosome contig reveals the role of chromosomal duplications in the expansion of the *Brassica rapa* genome. *Genetics* 156:833–838.

Jiang J, Gill BS (1994) Nonisotopic in situ hybridization and plant genome mapping: the first 10 years. *Genome* 37:717–725.

Jiang J, Gill BS (2006) Current status and the future of fluorescence in situ hybridization (FISH) in plant genome research. *Genome* 49:1057–1068.

Jiang J, Gill BS, Wang GL, Ronald PC, Ward DC (1995) Metaphase and interphase fluorescence in situ hybridization mapping of the rice genome with bacterial artificial chromosomes. *Proc Natl Acad Sci USA* 92:4487–4491.

Jiang J, Hulbert SH, Gill BS, Ward DC (1996) Interphase fluorescence in situ hybridization mapping: a physical mapping strategy for plant species with large complex genomes. *Mol Gen Genet* 252:497–502.

Jin WW, Melo JR, Nagaki K, Talbert PB, Henikoff S, Dawe RK, Jiang JM (2004) Maize centromeres: organization and functional adaptation in the genetic background of oat. *Plant Cell* 16: 571–581.

John HA, Birnstiel ML, Jones KW (1969) RNA-DNA hybrids at cytological level. *Nature* 223:582–587.

Kaczmarek A, Naganowska B, Wolko B (2009) Karyotyping of the narrow-leafed lupin (*Lupinus angustifolius* L.) by using FISH, PRINS and computer measurements of chromosomes. *J Appl Genet* 50:77–82.

Kao FI, Cheng YY, Chow TY, Chen HH, Liu SM, Cheng CH, Chung MC (2006) An integrated map of *Oryza sativa* L. chromosome 5. *Theor Appl Genet* 112:891–902.

Kasha KJ, Burnham CR (1965) The location of interchange breakpoints in barley. 1. Linkage studies and map orientation. *Can J Genet Cytol* 7:62–77.

Kato A, Lamb JC, Birchler JA (2004) Chromosome painting using repetitive DNA sequences as probes for somatic chromosome identification in maize. *Proc Natl Acad Sci USA* 101:13554–13559.

Kato A, Albert PS, Vega JM, Birchler JA (2006) Sensitive fluorescence in situ hybridization signal detection in maize using directly labeled probes produced by high concentration DNA polymerase nick translation. *Biotech Histochem* 81:71–78.

Khrustaleva LI, Kik C (2001) Localization of single-copy T-DNA insertion in transgenic shallots (*Allium cepa*) by using ultra-sensitive FISH with tyramide signal amplification. *Plant J* 25:699–707.

Khush GS, Rick CM (1968) Cytogenetic analysis of the tomato genome by means of induced deficiencies. *Chromosoma* 23:452–484.

Khush GS, Rick CM, Robinson RW (1964) Genetic activity in a heterochromatic chromosome segment of the tomato. *Science* 145:1432–1434.

Kim JS, Childs KL, Islam-Faridi MN, Menz MA, Klein RR, Klein PE, Price HJ, Mullet JE, Stelly DM (2002) Integrated karyotyping of sorghum by in situ hybridization of landed BACs. *Genome* 45:402–412.

Kim JS, Klein PE, Klein RR, Price HJ, Mullet JE, Stelly DM (2005a) Molecular cytogenetic maps of sorghum linkage groups 2 and 8. *Genetics* 169:955–965.

Kim JS, Klein PE, Klein RR, Price HJ, Mullet JE, Stelly DM (2005b) Chromosome identification and nomenclature of *Sorghum bicolor. Genetics* 169:1169–1173.

Kim JS, Islam-Faridi MN, Klein PE, Stelly DM, Price HJ, Klein RR, Mullet JE (2005c) Comprehensive molecular cytogenetic analysis of sorghum genome architecture: distribution of euchromatin, heterochromatin, genes and recombination in comparison to rice. *Genetics* 171:1963–1976.

Koo DH, Jiang J (2009) Super-stretched pachytene chromosomes for fluorescence in situ hybridization mapping and immunodetection of DNA methylation. *Plant J* 59:509–516.

Koo DH, Jo SH, Bang JW, Park HM, Lee S, Choi D (2008) Integration of cytogenetic and genetic linkage maps unveils the physical architecture of tomato chromosome 2. *Genetics* 179:1211–1220.

Koornneef M, Fransz P, de Jone H (2003) Cytogenetic tools for *Arabidopsis thaliana. Chromosome Res* 11:183–194.

Koumbaris GL, Bass HW (2003) A new single-locus cytogenetic mapping system for maize (*Zea mays* L.): overcoming FISH detection limits with marker-selected sorghum (*S. propinquum* L.) BAC clones. *Plant J* 35:647–659.

Kubalakova M, Valarik M, Bartos J, Vrana J, Cihalikova J, Molnar-Lang M, Dolezel J (2003) Analysis and sorting of rye (*Secale cereale* L.) chromosomes using flow cytometry. *Genome* 46:893–905.

Kulikova O, Gualtieri G, Geurts R, Kim DJ, Cook D, Huguet T, de Jong JH, Fransz PF, Bisseling T (2001) Integration of the FISH pachytene and genetic maps of *Medicago truncatula. Plant J* 27:49–58.

Kumar A, Bennetzen JL (1999) Plant retrotransposons. *Annu Rev Genet* 33:479–532.

Künzel G, Korzun L, Meister A (2000) Cytologically integrated physical restriction fragment length polymorphism maps for the barley genome based on translocation breakpoints. *Genetics* 154:397–412.

Kurata N, Omura T (1978) Karyotype analysis in rice I. A new method for identifying all chromosome pairs. *Japan J Genet* 54:251–255.
Labonte DR, Juvik JA (1991) Sugary-enhancer (SE) gene located on the long arm of chromosome 4 in maize (*Zea mays* L.). *J Hered* 82:176–178.
Lamb JC, Birchler JA (2006) Retroelement genome painting: cytological visualization of retroelement expansions in the genera *Zea* and *Tripsacum. Genetics* 173:1007–1021.
Lamb JC, Danilova T, Bauer MJ, Meyer JM, Holland JJ, Jensen MD, Birchler JA (2007a) Single-gene detection and karyotyping using small-target fluorescence in situ hybridization on maize somatic chromosomes. *Genetics* 175:1047–1058.
Lamb JC, Meyer JM, Corcoran B, Kato A, Han F, Birchler JA (2007b) Distinct chromosomal distributions of highly repetitive sequences in maize. *Chromosome Res* 15:33–49.
Langer-Safer PR, Levine M, Ward DC (1982) Immunological method for mapping genes on *Drosophila* polytene chromosomes. *Proc Natl Acad Sci USA* 79:4381–4385.
Lapitan NL, Ganal MW, Tanksley SD (1989) Somatic chromosome karyotype of tomato based on in situ hybridization of the TGRI satellite repeat. *Genome* 32:922–998.
Lapitan N, Brown S, Kennard W, Stephens JL, Knudson DL (1997) FISH physical mapping with barley BAC clones. *Plant J* 11:149–156.
Lavania UC (1978) Differential staining and plant chromosomes – progress in cytogenetics. *Curr Sci* 47:255–260.
Lawrence CJ, Seigfried TE, Bass HW, Anderson LK (2006) Predicting chromosomal locations of genetically mapped loci in maize using the *Morgan2McClintock* Translator. *Genetics* 172:2007–2009.
Lengerova M, Kejnovsky E, Hobza R, Macas J, Grant SR, Vyskot B (2004) Multicolor FISH mapping of the dioecious model plant, *Silene latifolia. Theor Appl Genet* 108:1193–1199.
Lima-de-Faria A (1952) Chromomere analysis of the chromosome complement of rye. *Chromosoma* 5:1–68.
Loegrin WQ, Sears ER (1966) Relationships among stem-rust genes on wheat chromosomes 2B, 4B and 6B. *Crop Sci* 6:157–160.
Lysak MA, Fransz PF, Ali HBM, Schubert I (2001) Chromosome painting in *Arabidopsis thaliana. Plant J* 28:689–697.
Lysak MA, Pecinka A, Schubert I (2003) Recent progress in chromosome painting of *Arabidopsis* and related species. *Chromosome Res* 11:195–204.
Lysak MA, Koch MA, Pecinka A, Schubert I (2005) Chromosome triplication found across the tribe Brassiceae. *Genome Res* 15:516–525.
Ma Q, Wang C, Su X (2008a) Synthesis and application of quantum dot-tagged fluorescent microbeads. *J Nanosci Nanotechnol* 8:1138–1149.
Ma L, Wu SM, Huang J, Ding Y, Pang DW, Li L (2008b) Fluorescence in situ hybridization (FISH) on maize metaphase chromosomes with quantum dot-labeled DNA conjugates. *Chromosoma* 117:181–187.
Magoon ML, Shambulingappa KG (1961) Karyomorphology of *Sorghum propinquum* and its bearing on the origin of 40-chromosome *Sorghum. Chromosoma* 12:460–465.
Mandakova T, Lysak MA (2008) Chromosomal phylogeny and karyotype evolution in x = 7 crucifer species (Brassicaceae). *Plant Cell* 20:2559–2570.
McClintock B (1929) Chromosome morphology in *Zea mays. Science* 69:629.
McClintock B (1930) A cytological demonstration of the location of an interchange between two non-homologous chromosomes of *Zea mays. Proc Natl Acad Sci USA* 16:791–796.
McClintock B (1931) The order of the genes *C*, *Sh* and *Wx* in *Zea mays* with reference to a cytologically known point in the chromosome. *Proc Natl Acad Sci USA* 17:485–491.
McMillin DE, Roupakias DG, Scandalios JG (1979) Chromosomal location of two mitochondrial malate dehydrogenase structural genes in *Zea mays* using trisomics and B-A translocations. *Genetics* 92:1241–1250.
Meyers BC, Tingey SV, Morgante M (2001) Abundance, distribution, and transcriptional activity of repetitive elements in the maize genome. *Genome Res* 11:1660–1676.

Miller JT, Jackson SA, Nasuda S, Gill BS, Wing RA, Jiang J (1998) Cloning and characterization of a centromere-specific repetitive DNA element from *Sorghum bicolor. Theor Appl Genet* 96:832–839.

Misra RN, Shastry SVS (1967) Pachytene analysis in *Oryza*. VIII. Chromosome morphology and karyotypic variation in *O. sativa*. *Indian J Genet Plant Breeding* 27:349–368.

Mok DWS, Mok MC (1976) A modified Giemsa technique for identifying bean chromosomes. *J Hered* 67:187–188.

Morgante M, Hanafey M, Powell W (2002) Microsatellites are preferentially associated with non-repetitive DNA in plant genomes. *Nat Genet* 30:194–200.

Muller F, Houben A, Barker PE, Xiao Y, Kas JA, Melzer M (2006) Quantum dots – a versatile tool in plant science? *J Nanobiotechnol* 4:5.

Muller HJ (1927) The effects of X-radiation on genes and chromosomes. *Science* 66:84–87.

Nagaki K, Song JQ, Stupar RM, Parokonny AS, Yuan QP, Ouyang S, Liu J, Hsiao J, Jones KM, Dawe RK, Buell CR, Jiang JM (2003a) Molecular and cytological analyses of large tracks of centromeric DNA reveal the structure and evolutionary dynamics of maize centromeres. *Genetics* 163:759–770.

Nagaki K, Talbert PB, Zhong CX, Dawe RK, Henikoff S, Jiang JM (2003b) Chromatin immunoprecipitation reveals that the 180-bp satellite repeat is the key functional DNA element of *Arabidopsis thaliana* centromeres. *Genetics* 163:1221–1225.

Nagaki K, Cheng Z, Ouyang S, Talbert PB, Kim M, Jones KM, Henikoff S, Buell CR, Jiang J (2004) Sequencing of a rice centromere uncovers active genes. *Nat Genet* 36:138–145.

Nandi HK (1936) The chromosome morphology, secondary association and origin of cultivated rice. *J Genet* 33:315–336.

Ohmido N, Akiyama Y, Fukui K (1998) Physical mapping of unique nucleotide sequences on identified rice chromosomes. *Plant Mol Biol* 38:1043–1052.

Pardue ML, Gall JG (1969) Molecular hybridization of radioactive DNA to DNA of cytological preparations. *Proc Natl Acad Sci USA* 64:600–604.

Pardue ML, Gall JG (1975) Nucleic acid hybridization to the DNA of cytological preparations. *Methods Cell Biol* 10:1–16.

Parthasarathy N (1938) Cytogenetical studies in Oryzeae and Phalarideae I. Cytogenetics of some X-ray derivatives in rice (*Oryza sativa* L.). *J Genet* 37:1–40.

Peacock WJ, Dennis ES, Rhoades MM, Pryor AJ (1981) Highly repeated DNA sequence limited to knob heterochromatin in maize. *Proc Natl Acad Sci USA* 78:4490–4494.

Pedersen C, Giese H, Linde-Laursen I (1995) Towards an integration of the physical and the genetic chromosome maps of barley by in situ hybridization. *Hereditas* 123:77–88.

Pedrosa A, Sandal N, Stougaard J, Schweizer D, Bachmair A (2002) Chromosomal map of the model legume *Lotus japonicus. Genetics* 161:1661–1672.

Pedrosa-Harand A, Kami J, Gepts P, Geffroy V, Schweizer D (2009) Cytogenetic mapping of common bean chromosomes reveals a less compartmentalized small-genome plant species. *Chromosome Res* 17:405–417.

Peters JL, Constandt H, Neyt P, Cnops G, Zethof J, Zabeau M, Gerats T (2001) A physical amplified fragment-length polymorphism map of *Arabidopsis. Plant Physiol* 127:1579–1589.

Peterson DG, Lapitan NL, Stack SM (1999) Localization of single- and low-copy sequences on tomato synaptonemal complex spreads using fluorescence in situ hybridization (FISH). *Genetics* 152:427–439.

Pijnacker LP, Ferwerda MA (1984) Giemsa C-banding of potato chromosomes. *Can J Genet Cytol* 26:415–419.

Raap AK, Vandecorput MPC, Vervenne RAW, Vangijlswijk RPM, Tanke HJ, Wiegant J (1995) Ultra-sensitive FISH using peroxidase-mediated deposition of biotin-tyramide or fluorochrome-tyramide. *Human Mol Genet* 4:529–534.

Raboy V, Gerbasi PF, Young KA, Stoneberg SD, Pickett SG, Bauman AT, Murthy PP, Sheridan WF, Ertl DS (2000) Origin and seed phenotype of maize low phytic acid 1-1 and low phytic acid 2-1. *Plant Physiol* 124:355–368.

Ramanna MS, Prakken P (1967) Structure of and homology between pachytene and somatic metaphase chromosomes of tomato. *Genetica* 38:115–133.

Rayburn AL, Gill BS (1985) Use of biotin-labeled probes to map specific DNA sequences on wheat chromosomes. *J Hered* 76:78–81.

Reamon-Buttner SM, Schmidt T, Jung C (1999) AFLPs represent highly repetitive sequences in *Asparagus officinalis* L. *Chromosome Res* 7:297–304.

Rens W, Moderegger K, Skelton H, Clarke O, Trifonov V, Ferguson-Smith MA (2006) A procedure for image enhancement in chromosome painting. *Chromosome Res* 14:497–503.

Rhoades MM (1950) Meiosis in maize. *J Hered* 41:58–67.

Rick CM, Khush GS (1964) Chromosome engineering in *Lycopersicon*. In: Riley R, Lewis KR (eds), *Chromosome Manipulations and Plant Genetics.* Oliver & Boyd, Edinburg, pp. 8–20.

Riera-Lizarazu O, Vales MI, Ananiev EV, Rines HW, Phillips RL (2000) Production and characterization of maize chromosome 9 radiation hybrids derived from an oat-maize addition line. *Genetics* 156:327–339.

Röder MS, Korzun V, Gill BS, Ganal MW (1998) The physical mapping of microsatellite markers in wheat. *Genome* 41:278–283.

Roupakias DG, McMillin DE, Scandalios JG (1980) Chromosomal location of the catalase structural genes in *Zea mays*, using B-A translocations. *Theor Appl Genet* 58:211–218.

Sadder MT, Weber G (2001) Karyotype of maize (*Zea mays* L.) mitotic metaphase chromosomes as revealed by fluorescence in situ hybridization (FISH) with cytogenetic DNA markers. *Plant Mol Biol Rep* 19:117–123.

Sadder T, Weber G (2002) Comparison between genetic and physical maps in *Zea mays* L. of molecular markers linked to resistance against *Diatraea* spp. *Theor Appl Genet* 104:908–915.

Sadder MT, Ponelies N, Born U, Weber G (2000) Physical localization of single-copy sequences on pachytene chromosomes in maize (*Zea mays* L.) by chromosome in situ suppression hybridization. *Genome* 43:1081–1083.

SanMiguel P, Tikhonov A, Jin YK, Motchoulskaia N, Zakharov D, Melake-Berhan A, Springer PS, Edwards KJ, Lee M, Avramova Z, Bennetzen JL (1996) Nested retrotransposons in the intergenic regions of the maize genome. *Science* 274:765–768.

Sasaki T, Matsumoto T, Yamamoto K, Sakata K, Baba T, Katayose Y, Wu J, Niimura Y, Cheng Z, Nagamura Y, Antonio BA, Kanamori H, Hosokawa S, Masukawa M, Arikawa K, Chiden Y, Hayashi M, Okamoto M, Ando T, Aoki H, Arita K, Hamada M, Harada C, Hijishita S, Honda M, Ichikawa Y, Idonuma A, Iijima M, Ikeda M, Ikeno M, Ito S, Ito T, Ito Y, Iwabuchi A, Kamiya K, Karasawa W, Katagiri S, Kikuta A, Kobayashi N, Kono I, Machita K, Maehara T, Mizuno H, Mizubayashi T, Mukai Y, Nagasaki H, Nakashima M, Nakama Y, Nakamichi Y, Nakamura M, Namiki N, Negishi M, Ohta I, Ono N, Saji S, Sakai K, Shibata M, Shimokawa T, Shomura A, Song J, Takazaki Y, Terasawa K, Tsuji K, Waki K, Yamagata H, Yamane H, Yoshiki S, Yoshihara R, Yukawa K, Zhong H, Iwama H, Endo T, Ito H, Hahn JH, Kim HI, Eun MY, Yano M, Jiang J, Gojobori T (2002) The genome sequence and structure of rice chromosome 1. *Nature* 420:312–316.

Schmidt R, West J, Love K, Lenehan Z, Lister C, Thompson H, Bouchez D, Dean C (1995) Physical map and organization of *Arabidopsis thaliana* chromosome 4. *Science* 270:480–483.

Schnabel E, Kulikova O, Penmetsa RV, Bisseling T, Cook DR, Frugoli J (2003) An integrated physical, genetic and cytogenetic map around the *sunn* locus of *Medicago truncatula. Genome* 46:665–672.

Schweizer D (1973) Differential staining of plant chromosomes. *Chromosoma* 40:307–320.

Shastry SV, Misra RN (1961) Pachytene analysis in *Oryza*. 2. Sterility in *japonica-indica* rice hybrids. *Chromosoma* 12:248–271.

Shen DL, Wang ZF, Wu M (1987) Gene mapping on maize pachytene chromosomes by in situ hybridization. *Chromosoma* 95:311–314.

Sherman, JD, Stack SM (1992) Two-dimensional spreads of synaptonemal complexes from solanaceous plants. 5. Tomato (*Lycopersicon esculentum*) karyotype and idiogram. *Genome* 35:354–359.

Sherman JD, Stack SM (1995) Two-dimensional spreads of synaptonemal complexes from solanaceous plants. VI. High-resolution recombination nodule map for tomato (*Lycopersicon esculentum*). *Genetics* 141:683–708.

Sherman JD, Herickhoff LA, Stack SM (1992) Silver staining two types of meiotic nodules. *Genome* 35:907–915.

Shibata F, Murata M (2004) Differential localization of the centromere-specific proteins in the major centromeric satellite of *Arabidopsis thaliana. J Cell Sci* 117:2963–2970.

Singh RJ, Tsuchiya T (1975) Pachytene chromosomes of barley. *J Hered* 66:165–167.

Song YC, Gustafson JP (1995) The physical location of 14 RFLP markers in rice (*Oryza sativa* L). *Theor Appl Genet* 90:113–119.

Stack SM, Royer SM, Shearer LA, Chang SB, Giovannoni JJ, Westfall DH, White RA, Anderson LK (2009) Role of fluorescence in situ hybridization in sequencing the tomato genome. *Cytogenet Genome Res* 124:339–350.

Stephens JL, Brown SE, Lapitan NL, Knudson DL (2004) Physical mapping of barley genes using an ultrasensitive fluorescence in situ hybridization technique. *Genome* 47:179–189.

Suzuki HY, Futsuhara F, Takaiwa F, Kurata N (1991) Localization of glutelin gene in rice chromosome by in situ hybridization. *Japan J Genet* 66:305–312.

Szinay D, Chang SB, Khrustaleva L, Peters S, Schijlen E, Bai Y, Stiekema WJ, van Ham RC, de Jong H, Klein Lankhorst RM (2008) High-resolution chromosome mapping of BACs using multi-colour FISH and pooled-BAC FISH as a backbone for sequencing tomato chromosome 6. *Plant J* 56:627–637.

Tang X, Szinay D, Lang C, Ramanna MS, van der Vossen EA, Datema E, Klein Lankhorst R, deBoer J, Peters SA, Bachem C, Stiekema W, Visser RG, de Jone H, Bai Y (2008) Cross-species bacterial artificial chromosome-fluorescence in situ hybridization painting of the tomato and potato chromosome 6 reveals undescribed chromosomal rearrangements. *Genetics* 180:1319–1328.

Tang X, de Boer JM, van Eck HJ, Bachem C, Visser RG, deJong H (2009) Assignment of genetic linkage maps to diploid *Solanum tuberosum* pachytene chromosomes by BAC-FISH technology. *Chromosome Res* 17:899–915.

ten Hoopen R, Robbins T, Fransz PF, Montijn BM, Oud O, Gerats AGM, Nanninga N (1996) Localization of T-DNA insertions in petunia by fluorescence in situ hybridization: physical evidence for suppression of recombination. *Plant Cell* 8:823–830.

ten Hoopen R, Montijn BM, Veuskens JT, Oud OJ, Nanninga N (1999) The spatial localization of T-DNA insertions in petunia interphase nuclei: consequences for chromosome organization and transgene insertion sites. *Chromosome Res* 7:611–623.

Tikhonov AP, SanMiguel PJ, Nakajima Y, Gorenstein NM, Bennetzen JL, Avramova Z (1999) Colinearity and its exceptions in orthologous adh regions of maize and sorghum. *Proc Natl Acad Sci USA* 96:7409–7414.

Tsuchida M, Fukushima T, Nasuda S, Masoudi-Nejad A, Ishikawa G, Nakamura T, Endo TR (2008) Dissection of rye chromosome 1R in common wheat. *Genes Genet Syst* 83:43–53.

Valarik M, Bartos J, Kovarova P, Kubalakova M, de Jong JH, Dolezel J (2004) High-resolution FISH on super-stretched flow-sorted plant chromosomes. *Plant J* 37:940–950.

Van Laere K, Van Huylenbroeck J, Van Bockstaele E (2008) Karyotype analysis and physical mapping of 45 S rRNA genes in *Hydrangea* species by fluorescence in situ hybridization. *Plant Breeding* 127:301–307.

Visser RGF, Bachem CWB, de Boer JM, Bryan GJ, Chakrabati SK, Feingold S, Gromadka R, van Ham RCHJ, Huang S, Jacobs JME, Kuznetsov B, de Melo PE, Milbourne D, Orjeda G, Sagredo B, Tang XM (2009) Sequencing the potato genome: outline and first results to come from the elucidation of the sequence of the world's third most important food crop. *Am J Potato Res* 86:417–429.

Vlacilova K, Ohri D, Vrana J, Cihalikova J, Kubalakova M, Kahl G, Dolezel J (2002) Development of flow cytogenetics and physical genome mapping in chickpea (*Cicer arietinum* L.). *Chromosome Res* 10:695–706.

Vosa CG, Marchi P (1972) Quinacrine fluorescence and Giemsa staining in plants. *Nat New Biol* 237:191–192.

Wang CJ, Harper L, Cande WZ (2006) High-resolution single-copy gene fluorescence in situ hybridization and its use in the construction of a cytogenetic map of maize chromosome 9. *Plant Cell* 18:529–544.

Wang G, Zhang X, Jin W (2009) An overview of plant centromeres. *J Genet Genomics* 36:529–537.

Wang, K, Guan B, Guo W, Zhou B, Hu Y, Zhu Y, Zhang T (2008) Completely distinguishing individual A-genome chromosomes and their karyotyping analysis by multiple bacterial artificial chromosome – fluorescence in situ hybridization. *Genetics* 178:1117–1122.

Watson JD, Crick FH (1953) The structure of DNA. *Cold Spring Harb Symp Quant Biol* 18:123–131.

Weber D, Helentjaris T (1989) Mapping RFLP loci in maize using B-A translocations. *Genetics* 121:583–590.

Weisblum B, de Haseth PL (1972) Quinacrine, a chromosome stain specific for deoxyadenylate-deoxythymidylate-rich regions in DNA. *Proc Natl Acad Sci USA* 69:629–632.

Werner JE, Endo TR, Gill BS (1992) Toward a cytogenetically based physical map of the wheat genome. *Proc Natl Acad Sci USA* 89:11307–11311.

Wing R, Drew H, Takano T, Broka C, Tanaka S, Itakura K, Dickerson RE (1980) Crystal structure analysis of a complete turn of B-DNA. *Nature* 287:755–758.

Wolfgruber TK, Sharma A, Schneider KL, Albert PS, Koo D-H, Shi J, Gao Z, Han F, Lee H, Xu R, Allison J, Birchler JA, Jiang J, Dawe RK, Presting GG (2009) Maize centromere structure and evolution: sequence analysis of centromeres 2 and 5 reveals dynamic loci shaped primarily by retrotransposons. *PLoS Genet* 5:e1000743.

Wu HK, Chung MC, Xie Y, Wu R (1986) Chromosomal localization of rice *rbcS* genes. *Rice Genet Newslett* 3:58.

Wu SM, Zhao X, Zhang ZL, Xie HY, Tian ZQ, Peng J, Lu ZX, Pang DW, Xie ZX (2006) Quantum-dot-labeled DNA probes for fluorescence in situ hybridization (FISH) in the microorganism *Escherichia coli. Chemphyschem* 7:1062–1067.

Xu J, Earle ED (1996a) Direct FISH of 5 S rDNA on tomato pachytene chromosomes places the gene at the heterochromatic knob immediately adjacent to the centromere of chromosome 1. *Genome* 39:216–221.

Xu J, Earle ED (1996b) High resolution physical mapping of 45 S (5.8 S, 18 S and 25 S) rDNA gene loci in the tomato genome using a combination of karyotyping and FISH of pachytene chromosomes. *Chromosoma* 104:545–550.

Yan H, Ito H, Nobuta K, Ouyang S, Jin W, Tian S, Lu C, Venu RC, Wang GL, Green PJ, Wing RA, Buell CR, Meyers GC, Jiang J (2006) Genomic and genetic characterization of rice *Cen3* reveals extensive transcription and evolutionary implications of a complex centromere. *Plant Cell* 18:2123–2133.

Yeh BP, Peloquin SJ (1965) Pachytene chromosomes of the potato (*Solanum tuberosum*, group Andigena). *Am J Bot* 52:1014–1020.

Yu H, Liang GH, Kofoid KD (1991) Analysis of C-banding chromosome patterns of *Sorghum. Crop Sci* 31:1524–1527.

Zhang DF, Yang QY, Bao WD, Zhang Y, Han B, Xue YB, Cheng ZK (2005) Molecular cytogenetic characterization of the *Antirrhinum majus* genome. *Genetics* 169:325–335.

Zhang P, Li W, Fellers J, Friebe B, Gill BS (2004a) BAC-FISH in wheat identifies chromosome landmarks consisting of different types of transposable elements. *Chromosoma* 112:288–299.

Zhang P, Li W, Friebe B, Gill BS (2004b) Simultaneous painting of three genomes in hexaploid wheat by BAC-FISH. *Genome* 47:979–987.

Zhang W, Lee HR, Koo DH, Jiang J (2008) Epigenetic modification of centromeric chromatin: hypomethylation of DNA sequences in the CENH3-associated chromatin in *Arabidopsis thaliana* and maize. *Plant Cell* 20:25–34.

Zhong CX, Marshall JB, Topp C, Mroczek R, Kato A, Nagaki K, Birchler JA, Jiang J, Dawe RK (2002) Centromeric retroelements and satellites interact with maize kinetochore protein CENH3. *Plant Cell* 14:2825–2836.

Zhong X-B, Fransz PF, Wennekes-van Eden J, Zabel P, van Kammen A, de Jong JH (1996a) High-resolution mapping on pachytene chromosomes and extended DNA fibres by fluorescence in-situ hybridisation. *Plant Mol Biol Rep* 14:232–242.

Zhong X-B, de Jong JH, Zabel P (1996b) Preparation of tomato meiotic pachytene and mitotic metaphase chromosomes suitable for fluorescence in situ hybridization (FISH). *Chromosome Res* 4:24–28.

Zhong XB, Bodeau J, Fransz PF, Williamson VM, van Kammen A, de Jong JH, Zabel P (1999) FISH to meiotic pachytene chromosomes of tomato locates the root knot nematode resistance gene *Mi-1* and the acid phosphatase gene *Aps-1* near the junction of euchromatin and pericentromeric heterochromatin of chromosome arms 6 S and 6 L, respectively. *Theor Appl Genet* 98:365–370.

Zickler D, Kleckner N (1998) The leptotene-zygotene transition of meiosis. *Annu Rev Genet* 32:619–697.

Zoller JF, Herrmann RG, Wanner G (2004) Chromosome condensation in mitosis and meiosis of rye (*Secale cereale* L.). *Cytogenet Genome Res* 105:134–144.

Zwick MS, Islam-Faridi MN, Dzeschin DG Jr, Wing RA, Hart GE, Stelly DM, Price HJ (1998) Physical mapping of the liguleless linkage group in *Sorghum bicolor* using rice RFLP-selected sorghum BACs. *Genetics* 148:1983–1992.

Zwick MS, Islam-Faridi MN, Zhang HB, Hodnett GL, Gomez MI, Kim JS, Price HJ, Stelly DM (2000) Distribution and sequence analysis of the centromere-associated repetitive element CEN38 of *Sorghum bicolor* (Poaceae). *Am J Bot* 87:1757–1764.

Chapter 5
DNA and Chromatin Fiber-Based Plant Cytogenetics

Jason G. Walling and Jiming Jiang

Abstract Development of the fluorescence in situ hybridization (FISH) technique revolutionized cytogenetic research. FISH on prepared chromosomes has become the most commonly used technique in plant molecular cytogenetics, especially as a physical mapping tool in plant genome research. Despite its popularity, chromosome-based FISH analysis is limited in its capacity to distinguish DNA probes that separated by less than a few megabases. Development of FISH methods based on extended DNA fibers has dramatically increased the resolving power of this technique to the point where one can identify clones separated by only a few kilobases. In addition to the conventional fiber-FISH analysis, specialized techniques have been developed to prepare DNA or chromatin fibers that are suitable for restriction mapping (optical mapping) or immunofluorescence assays. Fiber-FISH and its derivatives are now used extensively in various mapping and genome research projects.

Keywords DNA fibers · Fiber-FISH protocol · Plant nuclei isolation · DNA probe · Antibody detection · Fluorescence

Abbreviations

BAC	Bacterial artificial chromosome
FISH	Fluorescence in situ hybridization
mtDNA	Mitochondrial DNA

J.G. Walling (✉) • J. Jiang
Department of Horticulture, University of Wisconsin, 1575 Linden Drive, Madison, WI 53706, USA
e-mail: walling@wisc.edu

H.W. Bass and J.A. Birchler (eds.), *Plant Cytogenetics*, Plant Genetics and Genomics: Crops and Models 4, DOI 10.1007/978-0-387-70869-0_5,

Contents

5.1 Fiber-FISH Mapping of Repetitive DNA Sequences

Significant portions of most plant genomes consist of highly repetitive DNA sequences. The composition and organization of these sequences, especially the long arrays of satellite repeat sequences, is difficult to study. Chromosomal domains containing satellite repeats, such as the centromeres in most eukaryotes, provide significant challenges to genome sequencing projects. Fiber-fluorescence in situ hybridization (FISH) of satellite repeats generates contiguous and measurable signals and provides important information about the structure and organization of the repeat families (Fransz et al. 1996; Jackson et al. 1998; Jiang and Gill 2006), which cannot be readily addressed by traditional gel-blot-based methods.

If a specific satellite repeat family exists as a single locus in a plant species, the organization of such a repeat can be directly visualized by fiber-FISH. For example, many plant species contain a single 5S ribosomal RNA gene cluster (Ohmido et al. 2000). One can estimate the size of such a DNA locus by averaging the measurements of a large number of individual fiber-FISH signals (Ohmido et al. 2000; Adawy et al. 2004; Tek and Jiang 2004), but if the satellite repeat family exists as multiple loci in the genome, then identification of a specific locus can be problematic. A reference DNA probe adjacent to a specific satellite repeat locus may become necessary for unambiguous identification. Satellite repeats are often interrupted by other DNA elements, such as retrotransposons. Interruptions like these can be identified as either gaps that are consistantly present in the fiber-FISH signal patterns or by comapping of the satellite repeat with other repeats (Pich and Schubert 1998; Cheng et al. 2002; Jin et al. 2004). A single satellite repeat array as long as 3.7 Mb can be visualized by means of fiber-FISH (Jin et al. 2004) (Fig. 5.1).

Telomeric and centromeric regions often contain satellite repeats. Fiber-FISH has been proven to be a valuable approach for characterizing the telomeric and centromeric satellite sequences. Zhong et al. (1998) first sought to characterize telomere-specific sequences in tomato (*Solanum lycopersicum* L.). By using DNA probes specific to the telomeric and subtelomeric regions, the authors found 27 different combinations of these two repeats that differed not only in the size of the array but also in the patterning of the repeats. The results demonstrated that all chromosome ends have their own unique telomere organizations (Zhong et al. 1998).

Centromeres in most plant species contain long arrays of satellite repeats (Jiang et al. 2003). Measuring the sizes of the centromeric satellite repeat arrays is usually complicated by the cross-hybridization of the probe to all centromeres in the same

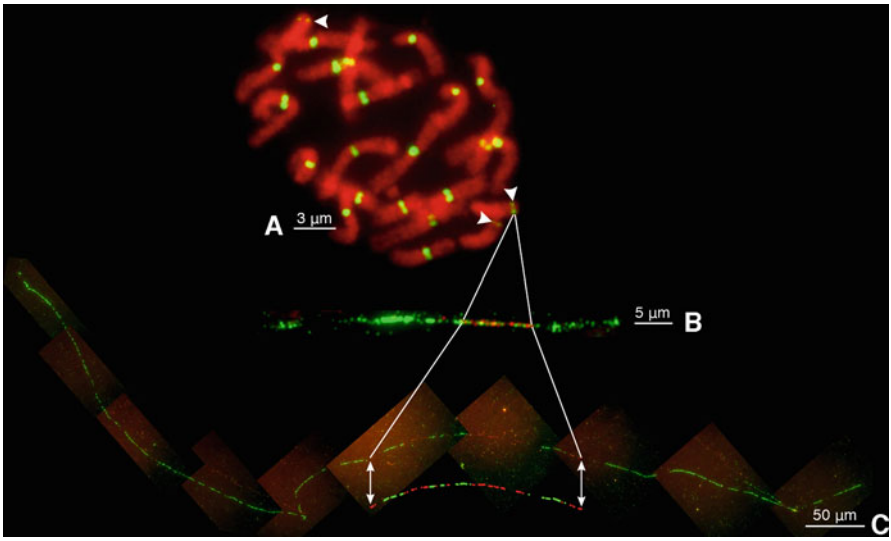

Fig. 5.1 Mapping of DNA and proteins associated with the centromere of maize B chromosome. (**a**) Immunodetection of the centromere-specific histone CENH3 on somatic metaphase chromosomes of a maize line containing three B chromosomes. *Arrowheads* point to the signals on the three B chromosomes. (**b**) Detection of CENH3 (*red*) and a B chromosome-specific centromeric satellite repeat ZmBs (*green*) on an extended chromatin fiber. (**c**) Fiber-FISH mapping of the ZmBs repeat (*green*) and CentC (*red*), a satellite repeat located in the centromeres of both A and B chromosomes of maize. This fiber-FISH signal is approximately 3.7 Mb long. The CENH3-binding domain contains both ZmBs and CentC repeats. The fiber-FISH signal pattern within this domain is illustrated in a diagram. Details of these mapping experiments were described by Jin et al. (2005). Image copyright American Society of Plant Biologists

species, but cytogenetic stocks, such as chromosome-addition lines, can be used to study individual centromeres of one species in the background of another species (Jin et al. 2004). A chromosome-specific centromeric satellite repeat array can also be identified by use of DNA probes adjacent to the array (Jin et al. 2005; Yan et al. 2006). By means of these approaches, the sizes of the centromeric satellite repeat arrays have been determined in several rice (*Oryza sativa* L.) and maize (*Zea mays* L.) chromosomes (Fig. 5.1).

5.2 Fiber-FISH Mapping of Large and Complex Genomic Loci

The ability of fiber-FISH to visualize directly DNA molecules as long as several megabases makes it an excellent tool for the analysis of large and complex genomic DNA loci. The first demonstration of this application was the characterization of a ~620-kb mitochondrial DNA (mtDNA) insertion in chromosome 2 of *Arabidopsis thaliana* (L.) Heynh. (Stupar et al. 2001). This insertion was originally estimated to

be ~270-kb on the basis of bacterial artificial chromosome (BAC) fingerprinting and DNA sequencing (Lin et al. 1999). Fingerprinting of BACs associated with this insertion was complicated by the duplicated nature of the inserted mtDNA fragment and presence of BAC clones derived from true mtDNA in the BAC library. In displaying the putative mtDNA insertion-related BAC contig on extended DNA fibers, the authors detected large gaps in the contig that were otherwise not detected or described in the sequencing data (Stupar et al. 2001). By using different combinations of probes derived from both genomic DNA and mtDNA, the authors showed that this mtDNA insertion included a complete copy and a significant portion of another copy of the mitochondrial genome.

Complex DNA loci can be generated during plant transformation, especially by means of biolistic transformation approaches. Fiber-FISH in combination with metaphase FISH is an effective method for characterizing the size and organization of such complex transgenic sites. Multicopy integration and structural rearrangements of the transgene constructs can be visualized by fiber-FISH (Wolters et al. 1998; Jackson et al. 2001; Svitashev and Somers 2001). Such complex DNA structures would be difficult to characterize by the traditional gel-blot-based methods. Transgenic sites are more prone to structural rearrangements when large DNA constructs are used in transformation. Fiber-FISH is especially valuable for analyzing the transgenic sites derived from such large constructs (Nakano et al. 2005; Phan et al. 2007). We also expect fiber-FISH to be a powerful approach to studying the structure of the recently reported plant artificial chromosomes (Yu et al. 2007).

BAC contig-based physical maps have been constructed in many plant species. Complete genome sequencing based on BAC physical maps has been accomplished in *A. thaliana* and rice and is also underway in maize and potato. BAC contig development is often an essential step in map-based cloning projects. Physical gaps are inevitable in BAC contig-based physical mapping because of the presence satellite repeats or unclonable sequences in the plant genomes. Fiber-FISH analysis of BACs spanning the physical gaps provides a robust method of estimating the size of such gaps (Jackson et al. 1998). This approach was used to measure most of the remaining physical gaps in the rice sequence maps (Feng et al. 2002; Sasaki et al. 2002; Yu et al. 2003).

5.3 Fiber-FISH Mapping on Cloned and Organelle DNA Molecules

Perhaps one of the most visually striking examples of applying fiber-FISH-based analyses is the mapping of single individual DNA molecules from BAC clones and chloroplasts. Because the average DNA extension in fiber-FISH experiments is approximately 3 kb/μm, a 7.8-kb BAC vector consistently generates a detectable fiber-FISH signal that consists of two to three consecutive fluorescence dots (Jackson et al. 1999). Most BAC molecules (>100 kb) produce sufficiently long fiber-FISH

signals to allow mapping of different subregions within the BAC inserts. Mapping individual BAC molecules can reveal the organization of different subclones or repeats within the BAC inserts (Jackson et al. 1999; Nagaki et al. 2003; Lin et al. 2005). Comparative fiber-FISH mapping of a specific BAC clone and the corresponding genomic region of the BAC insert reveals the integrity of the cloned DNA fragment and whether the BAC inserts have been rearranged during the propagation (Yuan et al. 2002; Nagaki et al. 2003).

The dynamics of many endogenous molecules such as the chloroplast genome, with its circular structure and canonical inverted repeats, had been well documented (Backert et al. 1995), but the advent of fiber-FISH technology now allows us to visualize these molecules physically with unprecedented clarity and resolution (Lilly et al. 2001). A fiber-FISH based analysis of chloroplast molecules from several plant species, including *Arabidopsis,* tobacco (*Nicotiana tabacum* L.), and pea (*Pisum sativum* L.), revealed a remarkable amount of structural heterogeneity that had previously gone unreported from any DNA-sequence-based analysis. Even within species, Lilly et al. (2001) observed several unreported higher-level multimers of the chloroplast DNA molecule as well as incomplete chloroplast genome equivalents. The fiber-FISH images provided a direct visualization of the highly dynamic nature of the chloroplast genome (Lilly et al. 2001).

5.4 Optical Mapping of Extended DNA Molecules

A single DNA molecule-based platform that is somewhat tangential to previously described hybridization-based fiber approaches, but nevertheless can still be considered a form of DNA fiber analysis, is optical mapping. Optical mapping was developed in the laboratory of David C. Schwartz as a fully integrated system for genome analysis based on the construction of restriction maps spanning entire genomes (Schwartz et al. 1993). In short, millions of individual DNA molecules (~500 kb) are stretched and immobilized on charged glass surfaces by means of microfluidic devices and digested with a restriction endonuclease. Restriction digestion produces double stranded “cuts” at specific recognition sequences, and these cleavage events are visualized by fluorescence microscopy as gaps as a result of coil relaxation occurring at nascent ends (Fig. 5.2); consecutive restriction fragments remain in register, producing an ordered restriction map (barcode) after sizing operations (Dimalanta et al. 2004; Li et al. 2007). This system is now fully automated and can quickly generate genome-wide ordered restriction maps that can be used to resolve sequence misassemblies, to characterize sequence gaps, and to reveal structural variation and mutations (Aston et al. 1999; Zhou et al. 2007). Although optical mapping was initially focused mainly within the realm of microbial genomics, recent developments now allow the construction of optical maps spanning large genomes such as those of humans (Kidd et al. 2008) and rice (Zhou et al. 2007). The rice genome has been fully sequenced, and the in silico digestion of its genome sequence

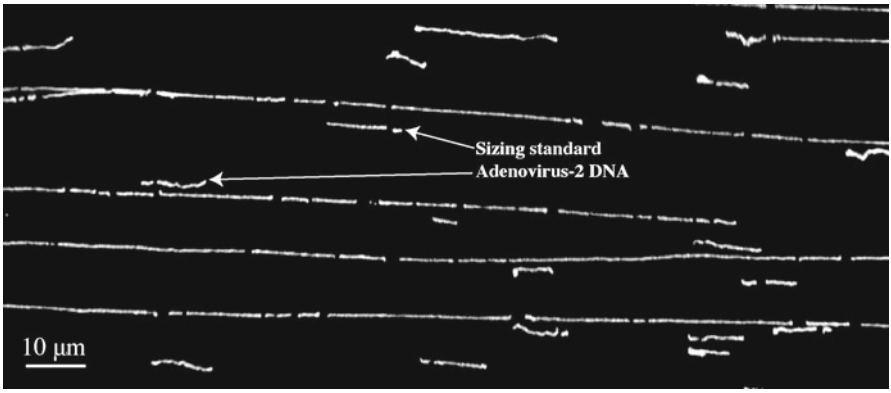

Fig. 5.2 Optical mapping of genomic DNA of maize digested with *Swa*I with Adenovirus-2 DNA as fragment-sizing standard. Image provided by Drs. David C. Schwartz and Shiguo Zhou

therefore provides means to validate sequence builds in a complex plant genome by optical mapping. Zhou et al. (2007) demonstrated that the optical mapping analysis of the entire rice genome physically spanned sequence gaps, characterized centromeric regions, and pinpointed regions of misassembly.

5.5 Immunoassays on Extended Chromatin Fibers

The explosive interest in epigenetic modifications of chromatin, specifically modifications to histones, has sparked a demand for reliable techniques for experimentally examining such a phenomenon. Immunostaining, or the identification of proteins by means of fluorescently labeled antibodies, is one method of tracking down chromosomal locations of specific proteins and visualizing protein–DNA associations. Although most modified histones can be readily detected on chromosomes, metaphase chromosome mapping provides only limited resolution of the association of histones with specific chromosomal domains.

Haaf and Ward (1994) were the first to use extended chromatin fibers in immunoassays. Extended chromatin fibers were prepared by mild lysis of the cells with both detergent and salt (Haaf and Ward 1994). Combining FISH and immunoassay on extended chromatin fibers allowed the authors to map human centromeric proteins to chromosomal domains containing a specific subfamily of the centromeric alpha satellite repeat (Haaf and Ward 1994). The technical challenge is in controlling the degree of lysis and extension, both of which can affect the protein binding to the chromatin fibers. Improved techniques for fiber preparation now allow mapping of various modified histones on extended chromatin fibers. Application of this method was paramount in revealing the unique characteristics associated with centromeric chromatin in animal species (Blower et al. 2002; Sullivan and Karpen 2004).

Preparation of chromatin fibers for immunoassays is technically more challenging in plants than in animal species. Isolating clean nuclei from plant tissues is difficult because of the presence of cell walls. Nevertheless, several plant labs have been successful in applying immunodetection on chromatin fibers (Jin et al. 2004; Shibata and Murata 2004; Jin et al. 2005; Houben et al. 2007) (Fig. 5.1). These reports demonstrated the physical interaction between the centromeric satellite repeats and the centromere-specific histone CENH3. Zhang et al. (2008) recently detected both CENH3 and methylcytosine on extended chromatin fibers. The authors were able to conclude that the DNA sequences in the centromeric domain containing CENH3 are hypomethylated (Zhang et al. 2008). Future refinements of chromatin-fiber preparation will make this technique more widely applicable in plant cytogenetic research.

Acknowledgments We are grateful to Drs. David C. Schwartz and Shiguo Zhou for their input on our summary of optical mapping and for providing the image in Fig. 5.2. The most recent cytogenetic mapping research in the authors' laboratory has been supported by grants DBI-0421671 and DBI-0603927 from the National Science Foundation.

References

Adawy SSM, Stupar RM, Jiang J (2004) Fluorescence in situ hybridization of knob-associated DNA elements analysis reveals multiple loci in one-knob and knobless maize lines. *J Histochem Cytochem* 52:1113–1116

Aston C, Mishra B, Schwartz DC (1999) Optical mapping and its potential for large-scale sequencing projects. *Trends Biotech* 17:297–302

Backert S, Dorfel P, Borner T (1995) Investigation of plant organellar DNAs by pulsed-field gel electrophoresis. *Curr Genet* 28:390–399

Blower MD, Sullivan BA, Karpen GH (2002) Conserved organization of centromeric chromatin in flies and humans. *Dev Cell* 2:319–330

Cheng ZK, Dong F, Langdon T, Ouyang S, Buell CB, Gu MH, Blattner FR, Jiang J (2002) Functional rice centromeres are marked by a satellite repeat and a centromere-specific retrotransposon. *Plant Cell* 14:1691–1704

Dimalanta ET, Lim A, Runnheim R, Lamers C, Churas C, Forrest DK, de Pablo JJ, Graham MD, Coppersmith SN, Goldstein S, Schwartz DC (2004) A microfluidic system for large DNA molecule arrays. *Anal Chem* 76:5293–5301

Feng Q, Zhang YJ, Hao P, Wang SY, Fu G, Huang YC, Li Y, Zhu JJ, Liu YL, Hu X, Jia PX, Zhang Y, Zhao Q, Ying K, Yu SL, Tang YS, Weng QJ, Zhang L, Lu Y, Mu J, Lu YQ, Zhang LS, Yu Z, Fan DL, Liu XH, Lu TT, Li C, Wu YR, Sun TG, Lei HY, Li T, Hu H, Guan JP, Wu M, Zhang RQ, Zhou B, Chen ZH, Chen L, Jin ZQ, Wang R, Yin HF, Cai Z, Ren SX, Lv G, Gu WY, Zhu GF, Tu YF, Jia J, Zhang Y, Chen J, Kang H, Cen XY, Shao CY, Sun Y, Hu QP, Zhang XL, Zhang W, Wang LJ, Ding CW, Sheng HH, Gu JL, Chen ST, Ni L, Zhu FH, Chen W, Lan LF, Lai Y, Cheng ZK, Gu MH, Jiang, JM, Li, JY, Hong GF, Xue YB, Han B (2002) Sequence and analysis of rice chromosome 4. *Nature* 420:316–320

Fransz PF, Alonso-Blanco C, Liharska TB, Peeters AJM, Zabel P, de Jong JH (1996) High-resolution physical mapping in *Arabidopsis thaliana* and tomato by fluorescence in situ hybridization to extended DNA fibres. *Plant J* 9:421–430

Haaf T, Ward DC (1994) Structural analysis of alpha satellite DNA and centromere proteins using extended chromatin and chromosomes. *Hum Mol Genet* 3:697–709

Houben A, Schroeder-Reiter E, Nagaki K, Nasuda S, Wanner G, Murata M, and Endo TR (2007) CENH3 interacts with the centromeric retrotransposon cereba and GC-rich satellites and locates to centromeric substructures in barley. *Chromosoma* 116:275–283

Jackson SA, Wang ML, Goodman HM, Jiang J (1998) Application of fiber-FISH in physical mapping of *Arabidopsis thaliana*. *Genome* 41:566–572

Jackson SA, Dong FG, Jiang JM (1999) Digital mapping of bacterial artificial chromosomes by fluorescence in situ hybridization. *Plant J* 17:581–587

Jackson SA, Zhang P, Chen WP, Phillips RL, Friebe B, Muthukrishnan S, Gill BS (2001) High-resolution structural analysis of biolistic transgene integration into the genome of wheat. *Theor Appl Genet* 103:56–62

Jiang JM, Gill BS (2006) Current status and the future of fluorescence in situ hybridization (FISH) in plant genome research. *Genome* 49:1057–1068

Jiang J, Birchler JA, Parrott WA, Dawe RK (2003) A molecular view of plant centromeres. *Trends Plant Sci* 8:570–575

Jin WW, Melo JR, Nagaki K, Talbert PB, Henikoff S, Dawe RK, Jiang J (2004) Maize centromeres: organization and functional adaptation in the genetic background of oat. *Plant Cell* 16:571–581

Jin WW, Lamb JC, Vega JM, Dawe RK, Birchler JA, Jiang J (2005) Molecular and functional dissection of the maize B centromere. *Plant Cell* 17:1412–1423

Kidd JM, Cooper GM, Donahue WF, Hayden HS, Sampas N, Graves T, Hansen N, Teague B, Alkan C, Antonacci F, Haugen E, Zerr T, Yamada NA, Tsang P, Newman TL, Tuzun E, Cheng Z, Ebling HM, Tusneem N, David R, Gillett W, Phelps KA, Weaver M, Saranga D, Brand A, Tao W, Gustafson E, McKernan K, Chen L, Malig M, Smith JD, Korn JM, McCarroll SA, Altshuler DA, Peiffer DA, Dorschner M, Stamatoyannopoulos J, Schwartz D, Nickerson DA, Mullikin JC, Wilson RK, Bruhn L, Olson MV, Kaul R, Smith DR, Eichler EE (2008) Fine-scale mapping and sequencing of structural variation from eight human genomes. *Nature* 453:56–64

Li HF, Valouev A, Schwartz DC, Waterman MS, Li LM (2007) A quantile method for sizing optical maps. *J Comput Biol* 14:255–266

Lilly JW, Havey MJ, Jackson SA, Jiang J (2001) Cytogenomic analyses reveal the structural plasticity of the chloroplast genome in higher plants. *Plant Cell* 13:245–254

Lin JY, Jacobus BH, SanMiguel P, Walling JG, Yuan Y, Shoemaker RC, Young ND, Jackson SA (2005) Pericentromeric regions of soybean (*Glycine max* L. Merr.) chromosomes consist of retroelements and tandemly repeated DNA and are structurally and evolutionarily labile. *Genetics* 170:1221–1230

Lin XY, Kaul SS, Rounsley S, Shea TP, Benito MI, Town CD, Fujii CY, Mason T, Bowman CL, Barnstead M, Feldblyum TV, Buell CR, Ketchum KA, Lee J, Ronning CM, Koo HL, Moffat KS, Cronin LA, Shen M, Pai G, Van Aken S, Umayam L, Tallon LJ, Gill JE, Adams MD, Carrera AJ, Creasy TH, Goodman HM, Somerville CR, Copenhaver GP, Preuss D, Nierman WC, White O, Eisen JA, Salzberg SL, Fraser CM, Venter JC (1999) Sequence and analysis of chromosome 2 of the plant *Arabidopsis thaliana*. *Nature* 402:761–768

Nagaki K, Song J, Stupar SM, Parokonny AS, Yuan Q, Ouyang S, Liu J, Hsiao J, Jones KM, Dawe RK, Buell CR, Jiang J (2003) Molecular and cytological analyses of large tracks of centromeric DNA reveal the structure and evolutionary dynamics of maize centromeres. *Genetics* 163:759–770

Nakano A, Suzuki G, Yamamoto M, Turnbull K, Rahman S, Mukai Y (2005) Rearrangements of large-insert T-DNAs in transgenic rice. *Mol Genet Genomics* 273:123–129

Ohmido N, Kijima K, Akiyama Y**,** de Jong JH, Fukui K (2000) Quantification of total genomic DNA and selected repetitive sequences reveals concurrent changes in different DNA families in indica and japonica rice. *Mol Gen Genet* 263:388–394

Phan BH, Jin WW, Topp CN, Zhong CX, Jiang JM, Dawe RK, Parrott WA (2007) Transformation of rice with long DNA-segments consisting of random genomic DNA or centromere-specific DNA. *Transgenic Res* 16:341–351

Pich U, Schubert I (1998) Terminal heterochromatin and alternative telomeric sequences in *Allium cepa*. *Chromosome Res* 6:315–321

Sasaki T, Matsumoto T, Yamamoto K, Sakata K, Baba T, Katayose Y, Wu JZ, Niimura Y, Cheng ZK, Nagamura Y, Antonio BA, Kanamori H, Hosokawa S, Msukawa M, Arikawa K, Chiden Y, Hayashi M, Okamoto M, Ando T, Aoki H, Arita K, Hamada M, Harada C, Hijishita S, Honda M, Ichikawa Y, Idonuma A, Iijima M, Ikeno M, Ito S, Ito T, Ito Y, Ito Y, Iwabuchi A, Kamiya K, Karasawa W, Katagiri S, Kikuta A, Kobayashi N, Kono I, Machita K, Maehara T, Mizuno H, Mizubayashi T, Mukae Y, Nagasaki H, Nakashima M, Nakama Y, Nakamichi Y, Nakamura M, Namiki N, Negishi M, Ohta I, Ono N, Saji S, Sakai K, Shibata M, Shimokawa T, Shomura A, Song JY, Takazaki Y, Terasawa K, Tsuji, K, Waki K, Yamagata H, Yamane H, Yoshiki S, Yoshihara R, Yukawa K, Zhong HS, Iwama H, Endo T, Ito H, Hahn JH, Kim HI, Eun MY, Yano M, Jiang JM, Gojohori T (2002) The genome sequence and structure of rice chromosome 1. *Nature* 420:312–316

Schwartz DC, Li XJ, Hernandez LI, Ramnarain SP, Huff EJ, Wang YK (1993) Ordered restriction maps of *Saccharomyces cerevisiae* chromosomes constructed by optical mapping. *Science* 262:110–114

Shibata F, Murata M (2004) Differential localization of the centromere-specific proteins in the major centromeric satellite of *Arabidopsis thaliana*. *J Cell Sci* 117:2963–2970

Stupar RM, Lilly JW, Town CD, Cheng Z, Kaul S, Buell CR, Jiang J (2001) Complex mtDNA constitutes an approximate 620-kb insertion on *Arabidopsis thaliana* chromosome 2: implication of potential sequencing errors caused by large-unit repeats. *Proc Natl Acad Sci USA* 98:5099–5103

Sullivan BA, Karpen GH (2004) Centromeric chromatin exhibits a histone modification pattern that is distinct from both euchromatin and heterochromatin. *Nat Struct Mol* Biol 11: 1076–1083

Svitashev SK, Somers DA (2001) Genomic interspersions determine the size and complexity of transgene loci in transgenic plants produced by microprojectile bombardment. *Genome* 44:691–697

Tek AL, Jiang J (2004) The centromeric regions of potato chromosomes contain megabase-sized tandem arrays of telomere-similiar sequence. *Chromosoma* 113:77–83

Wolters A-MA, Trindade LM, Jacobsen E, Visser RGF (1998) Fluorescence in situ hybridization on extended DNA fibers as a tool to analyze complex T-DNA loci in potato. *Plant J* 13:837–847

Yan HH, Ito H, Nobuta K, Ouyang S, Jin WW, Tian SL, Lu C, Venu RC, Wang G-L, Green PJ, Wing RA, Buell CR, Meyers BC, Jiang J (2006) Genomic and genetic characterization of rice *Cen3* reveals extensive transcription and evolutionary implications of a complex centromere. *Plant Cell* 18:2123–2133

Yu WC, Han FP, Gao Z, Vega JM, Birchler JA (2007) Construction and behavior of engineered minichromosomes in maize. *Proc Natl Acad Sci USA* 104:8924–8929

Yu YS, Rambo T, Currie J, Saski C, Kim HR, Collura K, Thompson S, Simmons J, Yang TJ, Nah G, Patel AJ, Thurmond S, Henry D, Oates R, Palmer M, Pries G, Gibson J, Anderson H, Paradkar M, Crane L, Dale J, Carver MB, Wood T, Frisch D, Engler F, Soderlund C, Palmer LE, Tetylman L, Nascimento L, de la Bastide M, Spiegel L, Ware D, O'Shaughnessy A, Dike S, Dedhia N, Preston R, Huang E, Ferraro K, Kuit K, Miller B, Zutavern T, Katzenberger F, Muller S, Balija V, Martienssen RA, Stein L, Minx P, Johnson D, Cordum H, Mardis E, Cheng ZK, Jiang JM, Wilson R, McCombie Wr, Wing RA, Yuan QP, Su OY, Liu J, Jones KM, Gansberger K, Moffat K, Hill J, Tsitrin T, Overton L, Bera J, Kim M, Jin SH, Tallon L, Ciecko A, Pai G, Van Aken S, Utterback T, Reidmuller S, Bormann J, Feldblyum T, Hsiao J, Zismann V, Blunt S, de Vazeilles A, Shaffer T, Koo H, Suh B, YangQ, Haas B, Peterson J, Pertea M, Volfovsky N, Wortman J, White O, Salzberg SL, Fraser CM, Buell CR, Messing J, Song RT, Fuks G, Llaca V, Kovchak S, Young S, Bowers JE, Paterson AH, Johns MA, Mao L, Pan HW, Dean RA (2003) In-depth view of structure, activity, and evolution of rice chromosome 10. *Science* 300:1566–1569

Yuan Q, Hill J, Hsiao J, Moffat K, Ouyang S, Cheng Z, Jiang J, Buell CR (2002) Genome sequencing of a 239-kb region of rice chromosome 10 L reveals a high frequency of gene duplication and a large chloroplast DNA insertion. *Mol Genet Genomics* 267:713–720

Zhang WL, Lee H-R, Koo D-H, Jiang JM (2008) Epigenetic modification of centromeric chromatin: hypomethylation of DNA sequences in the CENH3-associated chromatin in *Arabidopsis thaliana* and maize. *Plant Cell* 20:25–34

Zhong XB, Fransz PF, Wennekes-van Eden J, Ramanna MS, van Kammen A, Zabel P, de Jong JH (1998) FISH studies reveal the molecular and chromosomal organization of individual telomere domains in tomato. *Plant J* 13:507–517

Zhou S, Bechner MC, Place M, Churas CP, Pape L, Leong SA, Runnheim R, Forrest DK, Goldstein S, Livny M, Schwartz DC (2007) Validation of rice genome sequence by optical mapping. *BMC Genomics* 8: Art. No. 278

Part II
Function, Organization, and Dynamics in Plant Cytogenetics

Chapter 6
Plant Centromeres

James A. Birchler, Zhi Gao, and Fangpu Han

Abstract The centromeres of maize, *Arabidopsis*, and rice are compared. Plant centromeres are quite diverse on the DNA sequence level but possess similar structural features across taxa, namely megabase-sized arrays of small repeats interspersed with a specific retrotransposon family. On the contrary, the protein components of the kinetochore that functions in chromosome movement and forms over the site of the centromere is highly conserved. Plant centromeres exhibit epigenetic properties of specification as evidenced by the frequent finding of inactive centromeres that contain a full spectrum of DNA elements but are inherited over generations without forming a kinetochore. Plant centromeres have been demonstrated to be divisible by the process of misdivision, but the smaller centromeres produced show impaired function when their size falls below a threshold of a few hundred kilobases.

Keywords Centromere · Kinetochore · CenH3 · B chromosome · Meiosis · Retrotransposon · Cohesion

J.A. Birchler (✉) • Z. Gao
Division of Biological Sciences, University of Missouri-Columbia, 117 Tucker Hall, Columbia, MO 65211, USA
e-mail: birchlerj@missouri.edu

F. Han
Division of Biological Sciences, University of Missouri, 117 Tucker Hall, Columbia, MO 65211, USA

Department of Molecular Agrobiology, Institute of Genetics and Developmental Biology, Chinese Academy of Sciences, Beijing, China

H.W. Bass and J.A. Birchler (eds.), *Plant Cytogenetics*, Plant Genetics and Genomics: Crops and Models 4, DOI 10.1007/978-0-387-70869-0_6,

Contents

6.1 Introduction

The centromere is the part of the chromosome that organizes the spindle attachment site, otherwise known as the kinetochore. In plants, the DNA sequences that underlie the centromere are typically small repeats together with specific retrotransposons. The sequence of the centromere-specific repeat evolves rapidly, so although the proteins involved with the kinetochore are strongly conserved, the repeat sequences of distantly related plants show little to no resemblance. Here, the focus will be centered on the three model systems that have contributed the most knowledge about plant centromeres: maize, *Arabidopsis*, and rice.

6.2 Maize Centromeres

Maize centromeres are composed of a repeated element referred to as CentC that is present in tandem arrays at all centromeres (Ananiev et al. 1998). Interspersed with CentC are copies of various forms of a retrotransposon collectively referred to as CRM (centromere retrotransposon maize) (Ananiev et al. 1998; Nagaki et al. 2003a; Fig. 6.1). The span of this conglomerate ranges for different centromeres from about 800 kb up to 2.7 Mb (Nagaki et al. 2003a), although variation is extensive among maize varieties in the extent of CentC arrays at the centromeres of each member of the karyotype (Kato et al. 2004).

The inner kinetochore protein is a variant of histone H3 called CenH3 because it is present only in nucleosomes present at active centromeres (see Henikoff et al. 2001; Zhong et al. 2002). Its presence across multicellular eukaryotes is consistently correlated with active centromeres, in contrast with the presence of the centromeric DNA sequences. Sequences alone do not always organize a kinetochore, and neocentromeres can form over unique sequences (Henikoff et al. 2001). CenH3 is therefore generally considered to be the appropriate molecular correlate of active centromeres and has been identified in maize (Zhong et al. 2002).

Maize possesses a supernumerary B chromosome whose centromere has been subjected to extensive analysis (Alfenito and Birchler 1993; Kaszas and Birchler 1996, 1998; Jin et al. 2005). This chromosome possesses a specific repeat element, present within and surrounding the B centromere, that has allowed the study of this

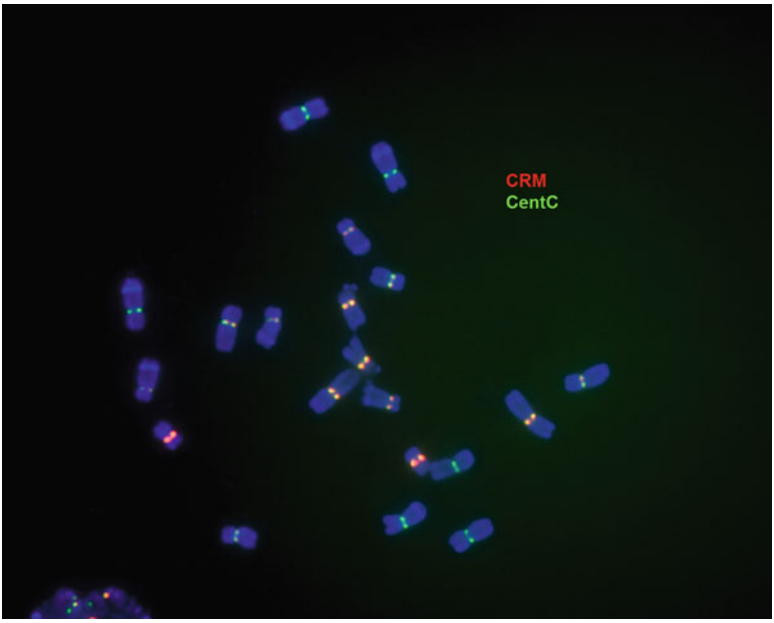

Fig. 6.1 Fluorescence in situ hybridization of satellite, CentC, and retrotransposon, CRM, to maize somatic chromosomes. Root-tip chromosome preparations were probed with CentC with a *green* fluorescent tag and CRM with a *red*-labeled probe. The differential representation of CentC and CRM in different chromosomes is illustrated by the varying amounts of *red* and *green* at the primary constrictions. The chromosomes were stained with DAPI. The *deep blue* regions are knob heterochromatin. Photo by Zhi Gao

centromere separately from all others in the maize genome (Alfenito and Birchler 1993; Lamb et al. 2005; Jin et al. 2005), which otherwise cannot be distinguished from each other.

The maize B centromere was found to undergo misdivision in the translocation chromosome, TB-9Sb, by Carlson (1970). Centromere misdivision had been documented in several species previously and suggests that centromeres could be divided and that each part could still function. With the isolation of the B-specific repeat, the misdivision derivatives were analyzed, and each rearrangement was found to change the restriction pattern of the specific repeat (Kaszas and Birchler 1996, 1998), a result that confirmed both that the repeat was part of the centromere and that the fragments of a subdivided centromere could still function. Subsequent studies of continued misdivisions resulted in the recovery of increasingly reduced numbers of the specific repeat (Kaszas and Birchler 1998; Phelps-Durr and Birchler 2004). The smallest derivatives contained a few hundred kilobases of specific repeats and show stability problems in meiosis and mitosis. These studies suggested that the smallest recoverable centromeres in maize are in the range of a few hundred kilobases in size.

Analyses of the B centromere with FiberFISH established that it is composed of an intersection of CentC, CRM, and the B-specific repeat (Jin et al. 2005; Lamb et al. 2005). The size of this intersection is approximately 700 kb. When a selection of B-centromere misdivision derivatives was examined, all of them were found to have breakpoints within this "core" region. With the decreasing size of the B centromere, the amount of detectable CenH3 associated with the B-specific repeat was correspondingly reduced (Jin et al. 2005).

Although all known maize centromeres contain the CentC and CRM elements, the mere presence of CentC and CRM does not necessarily indicate an active centromere. From a collection of minichromosomes derived from the chromosome type breakage-fusion-bridge cycle, several stabilized chromosomes were found, which included two sets of centromere repeats (Kato et al. 2005; Han et al. 2006), but examination revealed that only one of the two sets of repeats was associated with the inner kinetochore protein CenH3 (Han et al. 2006). This observation revealed that centromeres could become inactive in maize and provided evidence for an epigenetic component to their specification together with the discovery of a neocentromere with canonical repeats in barley (Nasuda et al. 2005). One B centromere was recovered on the tip of chromosome arm 9S and found to be inactive. Subsequently, an inversion on chromosome 8 was found in which the A centromere sequences were divided and part of the sequences had activity and the remainder did not (Lamb et al. 2007). Furthermore, the B chromosome was found to contain many sites of CentC localization along the length of the chromosome but no evidence of centromere activity was found in either mitosis or meiosis (Lamb et al. 2005). The centromeres of maize contain an RNA moiety derived from the repeats, but whether the epigenetic component of centromeres relies on this process is not known (Topp et al. 2004). Clearly, therefore, DNA sequence alone does not ensure centromere activity.

The B chromosome is basically inert and confers no advantage or disadvantage at low copy numbers. It is a "selfish" entity that persists in maize populations by an accumulation mechanism composed of two aspects. First, the B centromere undergoes nondisjunction at the second pollen mitosis, which produces the two sperm (Roman 1947), and then the sperm with the B chromosomes preferentially fertilizes the egg, rather than the polar nuclei, in the process of double fertilization (Roman 1948). At least two sites along the long arm of the B chromosome are required in trans for the centromere to undergo this nondisjunction (Ward 1973; Lin 1978). When either of them is deleted, the B centromere behaves as does any other centromere in maize.

The presence of an inactive centromere at the tip of chromosome arm 9S (Han et al. 2006) presented the opportunity to determine whether the nondisjunction property relies on an active centromere. The inactive centromere line does not contain the long arm of the B chromosome and is therefore stable, but when normal B chromosomes are introduced into the line, the inactive B centromere at the tip of 9S causes nondisjunction of the whole of chromosome 9 or, more often, breakage of chromosome 9S (Han et al. 2007a). This result indicated that the nondisjunction property is independent of centromere function.

A number of minichromosomes have been recovered that consist basically of the centromere of the B chromosome (Zheng et al. 1999; Kato et al. 2005; Han et al. 2007b). These small chromosomes do not undergo nondisjunction alone (Han et al. 2007b), but when full-sized B chromosomes are combined with the small chromosomes, they are induced to do so (Han et al. 2007b). The B-specific repeat may therefore be the target of the trans-acting factors because it is the only major repeat represented that is correlated with the nondisjunction property. The CentC and CRM elements are also present in A chromosomes but do not confer nondisjunction in the presence of B chromosomes.

The collection of small chromosomes derived from the B chromosome allowed an examination of the pairing properties and sister chromatid behavior (Han et al. 2007b). Previous work in maize had revealed that small chromosomes tend to lack sister chromatid cohesion at anaphase I of meiosis (McClintock 1938; Maguire 1987; Zheng et al. 1999). The small chromosomes were seldom found to exhibit homologue pairing. In other words, a sufficient size appears to be necessary for homologues to be successful in finding their pairing partners in prophase of meiosis. Nevertheless, some examples did in fact show high fidelity of pairing, but regardless of whether homologue pairing took place, all small chromosomes did indeed show a lack of sister chromatid cohesion in meiosis I. In meiosis II, distribution of chromosomes is random. Such behavior is also found for small chromosomes with A centromeres (McClintock 1938; Rhoades 1940; Maguire 1987; Brock and Pryor 1996).

Investigators of plant centromeres have long been interested in the development of artificial chromosome vectors. Two approaches have been taken. One is to transform centromere sequences in an attempt to make them function, and the other is to truncate the chromosome arm so that only the centromere remains but at the same time to provide a means for future engineering and additions. Centromere sequences have been transformed into plants, but they are integrated into the chromosomes without function (Phan et al. 2006), illustrating again the epigenetic nature of centromere sequences. De novo function could occur, but it has yet to be convincingly demonstrated. The second approach, telomere truncation, has been successful (Yu et al. 2006). Introduction of transformation plasmids with telomere repeats asymmetrically placed at one end into maize cells by either *Agrobacterium* or biolistic transformation resulted in the truncation of chromosomes. The truncated chromosomes could be recognized between the time of transformation and any subsequent haploid gametophyte generation that would eliminate them. The truncating plasmids carried with them site-specific recombination modules that were demonstrated to take part in recombination in these terminal positions (Yu et al. 2007). In the case of the B chromosome truncations, examples were recovered that consisted basically of the centromeric region. These engineered minichromosomes provide a proof of concept for the development of artificial chromosome vectors in plants. Because the technique relies on the introduction of telomere sequences for truncations, and the telomere sequence is the same in most plants, the technique can readily be applied to other species.

6.3 *Arabidopsis*

The centromere regions of *Arabidopsis* are composed of a common repeat present on all five chromosomes (Murata et al. 1994; Thompson et al. 1996). The repeat unit is 180 bp and is present at the primary constriction of all chromosomes. The diversity of these repeats has been studied, and the regions around the clusters show reduced recombination, as is typical of centromeres (Round et al. 1997; Copenhaver et al. 1999; Heslop-Harrison et al. 1999). The evolution of the 180-bp satellite is rapid, as revealed by comparison of sequences from related *Arabidopsis* species (Hall et al. 2003, 2005; Heslop-Harrison et al. 2003; Kawabe and Nasuda 2005, 2006). The centromeric histone CenH3 has been identified (Talbert et al. 2002) and shown to associate with the 180-bp satellite arrays (Nagaki et al. 2003b), although not with all copies (Shibata and Murata 2004). The deposition of CenH3 is during G2 of the cell cycle (Lermontova et al. 2006). Transposons, referred to as 106B, are also present within the arrays and might be responsible for initiating transcripts into the repeats (May et al. 2005). Small interfering RNAs have been documented for the centromere repeats in *Arabidopsis*, but their role in determining centromere function, if any, is not yet known.

6.4 Rice

The rice centromeres are composed of a satellite repeat, CentO, together with a centromere-specific retrotransposon, CRR (Dong et al. 1998; Miller et al. 1998; Nagaki et al. 2005). The complete sequence of the centromere of chromosome 8 in rice is known (Nagaki et al. 2004; Wu et al. 2004), as is that of centromere 4 (Zhang et al. 2004). They are composed primarily of CentO repeats, which are related to CentC in maize, and CRR elements, which are related to CRM (Sharma and Presting 2008), although multiple families are present in each lineage. The CRR elements are transcribed, and the RNAs enter into the RNAi pathway (Neuman et al. 2007). There are also a few active genes in rice centromeres (Nagaki et al. 2004; Yan et al. 2006). Some relatives of rice have other novel centromere repeats as well (Lee et al. 2005; Zhang et al. 2005; Bao et al. 2006). The sequencing of rice centromere 8 has allowed a determination of the association of CenH3 with the repeated elements present and the recombination-free region typical of centromeres (Yan et al. 2005). The CenH3 sites of deposition are interspersed with those containing the canonical H3. Recombination is reduced around centromeres as a general rule in all plants, and the molecular determinants of this effect have been documented for rice centromere 8. The reduced recombination is not associated with any particular sequence features and must have an epigenetic component (Yan et al. 2005).

The evolution of centromere repeats has been studied in rice (Lee et al. 2005). Interestingly, one of the major modes of change involves significant duplications and rearrangements rather than apparent new insertions into the centromere arrays

(Ma and Bennetzen 2006; Ma and Jackson 2006; Ma et al. 2007a, b). These findings are interesting in the context of homogenization of the centromere repeats among different centromeres.

6.5 Concluding Remarks

Although significant progress has been made in the past decade in understanding of the structural features of plant centromeres, much remains to be learned. A central unresolved issue concerns the balance between epigenetic and genetic components in kinetochore specification. Another important problem is the mechanism of rapid evolution of centromere repeat units and retrotransposons. A related question is how both types of sequences become homogenized across nonhomologous chromosomes. Future research promises many new discoveries about plant centromeres.

Acknowledgments Research on this topic in our laboratory is supported by grants DBI 0423898, DBI 0421671, and DBI 0701297 from the National Science Foundation.

References

Alfenito MR, Birchler JA (1993) Molecular characterization of a maize B-chromosome centric sequence. *Genetics* 135:589–597

Ananiev E, Phillips RL, Rines H (1998) Chromosome-specific molecular organization of maize (*Zea mays* L.) centromeric regions. *Proc Natl Acad Sci* USA 95:13073–13078

Bao W, Zhang W, Yang Q, Zhang Y, Han B, Gu M, Xue Y, Cheng Z (2006) Diversity of centromeric repeats in two closely related wild rice species, *Oryza officinalis* and *Oryza rhizomatis*. *Mol Genet Genomics* 275:421–430

Brock RD, Pryor AJ (1996) An unstable minichromosome generates variegated *oil yellow* maize seedlings. *Chromosoma* 104:575–584

Carlson WR (1970) Nondisjunction and isochromosome formation in the B chromosome of maize. *Chromosoma* 30:356–365

Copenhaver GP, Nickel K, Kuromori T, Benito M, Kaul S, Lin X, Bevan M, Murphy G, Harris B, Parnell LD, McCombie WR, Martienssen RA, Marra M, Preuss D (1999) Genetic definition and sequence analysis of *Arabidopsis* centromeres. *Science* 286:2468–2474

Dong F, Miller JT, Jackson SA, Wang G-L., Ronald PC, Jiang J (1998) Rice (*Ozyza sativa*) centromeric regions consist of complex DNA. *Proc Natl Acad Sci USA* 95:8135–8140

Hall SE, Kettler G, Preuss D (2003) Centromere satellites from *Arabidopsis* populations: maintenance of conserved and variable domains. *Genome Res* 13:195–205

Hall SE, Luo S, Hall AE, Preuss D (2005) Differential rates of local and global homogenization in centromere satellites from *Arabidopsis* relatives. *Genetics* 170:1913–1927

Han F, Lamb JC, Birchler JA (2006) High frequency of centromere inactivation resulting in stable dicentric chromosomes of maize. *Proc Natl Acad Sci USA* 103:3238–3243

Han F, Lamb JC, Yu W, Gao Z, Birchler JA (2007a) Centromere function and nondisjunction are independent components of the maize B chromosome accumulation mechanism. *Plant Cell* 19:524–533

Han F, Gao Z, Yu W, Birchler JA (2007b) Minichromosome analysis of chromosome pairing, disjunction, and sister chromatid cohesion. *Plant Cell* 19:3853–3863

Henikoff S, Ahmad K, Malik HS (2001) The centromere paradox: stable inheritance with rapidly evolving DNA. *Science* 293:1098–1102

Heslop-Harrison JS, Murata M, Ogura Y, Schwarzacher T, Motoyoshi F (1999) Polymorphisms and genomic organization of repetitive DNA from the centromeric regions of *Arabidopsis* chromosomes. *Plant Cell* 11:31–42

Heslop-Harrison JS, Brandes A, Schwarzacher T (2003) Tandemly repeated DNA sequences and centromeric chromosomal regions of *Arabidopsis* species. *Chromosome Res* 11: 241–253

Jin W, Lamb JC, Vega JM, Dawe RK, Birchler JA and Jiang J (2005) Molecular and functional dissection of the maize B chromosome centromere. *Plant Cell* 17:1412–1423

Kaszas E, Birchler J (1996) Misdivision analysis of centromere structure in maize. *EMBO J* 15:5246–5255

Kaszas E, Birchler J (1998) Meiotic transmission rates correlate with physical features of rearranged centromeres in maize. *Genetics* 150:1683–1692

Kato A, Lamb, JC, Birchler JA (2004) Chromosome painting in maize using repetitive DNA sequences as probes for somatic chromosome identification. *Proc Natl Acad Sci USA* 101:13554–13559

Kato A, Zheng Y-Z, Auger DL, Phelps-Durr T, Bauer MJ, Lamb JC, Birchler JA (2005) Minichromosomes derived from the B chromosome of maize. *Cytogenet Genome Res* 109: 156–165

Kawabe A, Nasuda S (2005) Structure and genomic organization of centromeric repeats in *Arabidopsis* species. *Mol Genet Genomics* 272:593–602

Kawabe A, Nasuda S (2006) Polymorphic chromosomal specificity of centromere satellite families in *Arabidopsis halleri* ssp. *gemmifera*. *Genetica* 126:335–342

Lamb JC, Kato A, Birchler JA (2005) Centromere associated sequences are present throughout the maize B chromosome. *Chromosoma* 113:337–349

Lamb JC, Meyer JM, Birchler JA (2007) A hemicentric inversion in the maize line knobless Tama flint created two sites of centromeric elements and moved the kinetochore-forming region. *Chromosoma* 116:237–247

Lee HR, Zhang W, Langdon T, Jin W, Yan H, Cheng Z, Jiang J (2005) Chromatin immunoprecipitation cloning reveals rapid evolutionary patterns of centromeric DNA in *Oryza* species. *Proc Natl Acad Sci USA* 102:11793–11798

Lermontova I, Schubert V, Fuchs J, Klatte S, Macas J, Schubert I (2006) Loading of *Arabidopsis* centromeric histone CENH3 occurs mainly during G2 and requires the presence of the histone fold domain. *Plant Cell* 18:2443–2451

Lin B-Y (1978) Regional control of nondisjunction of the B chromosome in maize. *Genetics* 90:613–627

Ma J, Bennetzen JL (2006) Recombination, rearrangement, reshuffling, and divergence in a centromeric region of rice. *Proc Natl Acad Sci USA* 103:383–388

Ma J, Jackson SA (2006) Retrotransposon accumulation and satellite amplification mediated by segmental duplication facilitate centromere expansion in rice. *Genome Res* 16:251–259

Ma J, Wing RA, Bennetzen JL, Jackson SA (2007a) Evolutionary history and positional shift of a rice centromere. *Genetics* 177:1217–1220

Ma J, Wing RA, Bennetzen JL, Jackson SA (2007b) Plant centromere organization: a dynamic structure with conserved functions. *Trends Genet* 23:134–139

Maguire MP (1987) Meiotic behavior of a tiny fragment chromosome that carries a transposed centromere. *Genome* 29:744–747

May BP, Lippman ZB, Fang Y, Spector DL, Martienssen RA (2005) Differential regulation of strand-specific transcripts from *Arabidopsis* centromeric satellite repeats. *PLoS Genet* 1:e79

McClintock B (1938) The production of homozygous deficient tissues with mutant characteristics by means of the aberrant mitotic behavior of ring-shaped chromosomes. *Genetics* 23:315–376

Miller JT, Cong FG, Jackson SA, Song J, Jiang JM (1998) Retrotransposon-related DNA sequences in the centromeres of grass chromosomes. *Genetics* 150:1615–1623

Murata M, Ogura Y, Motoyoshi F (1994) Centromeric repetitive sequences in *Arabidopsis thaliana*. *Japan J Genet* 69:361–370

Nagaki K, Song J, Stupar RM, Parokonny AS, Yuan Q, Ouyang S, Liu J, Hsiao J, Jones KM, Dawe RK, Buell CR, Jiang J (2003a) Molecular and cytological analyses of large tracks of centromeric DNA reveal the structure and evolutionary dynamics of maize centromeres. *Genetics* 163:759–770

Nagaki K, Talbert PB, Zhong CX, Dawe RK, Henikoff S, Jiang J (2003b) Chromatin immunoprecipitation reveals that the 180 bp satellite repeat is the key functional DNA element of *Arabidopsis thaliana* centromeres. *Genetics* 163:1221–1225

Nagaki K, Cheng Z, Ouyang S, Talbert PB, Kim M, Jones KM, Henikoff S, Buell CR, Jiang J (2004) Sequencing of a rice centromere uncovers active genes. *Nat Genet* 36:138–145

Nagaki K, Neumann P, Zhang D, Ouyang S, Buell CR, Cheng Z, Jiang J (2005) Structure, divergence, and distribution of the CRR centromeric retrotransposon family in rice. *Mol Biol Evol* 22:845–855

Nasuda S, Hudakova S, Schubert I, Houben A, Endo TR (2005) Stable barley chromosomes without centromeric repeats. *Proc Natl Acad Sci USA* 102:9842–9847

Neuman P, Yan H, Jiang J (2007) The centromeric retrotransposons of rice are transcribed and differentially processed by RNA interference. *Genetics* 176:749–761

Phan BH, Jin W, Topp CN, Zhong CX, Jiang J, Dawe RK, Parrott WA (2006) Transformation of rice with long DNA-segments consisting of random genomic DNA or centromere-specific DNA. *Transgenic Res* 16:341–351

Phelps-Durr TL, Birchler JA (2004) An asymptotic determination of minimum centromere size for the maize B chromosome. *Cytogenet Genome Res* 106:309–313

Rhoades MM (1940) Studies of a telocentric chromosome in maize with reference to the stability of its centromere. *Genetics* 25:483–521

Roman HL (1947) Mitotic nondisjunction in the case of interchanges involving the B-type chromosome in maize. *Genetics* 32:391–409

Roman HL (1948) Directed fertilization in maize. *Proc Natl Acad Sci USA* 34:36–42

Round EK, Flowers SK, Richards EJ (1997) *Arabidopsis thaliana* centromere regions: genetic map positions and repetitive DNA structure. *Genome Res* 7:1045–1053

Sharma A, Presting GG (2008) Centromeric retrotransposon lineages predate the maize/rice divergence and differ in abundance and activity. *Mol Genet Genomics* 279:133–147

Shibata F, Murata M (2004) Differential localization of the centromere-specific proteins in the major satellite of *Arabidopsis thaliana. J Cell Sci* 117:2963–2970

Talbert PB, Masuelli R, Tyagi AP, Comai L, Henikoff S (2002) Centromeric localization and adaptive evolution of an *Arabidopsis* histone H3 variant. *Plant Cell* 14:1053–1066

Thompson H, Schmidt R, Brandes A, Heslop-Harrison JS, Dean C (1996) A novel repetitive sequence associated with the centromeric regions of *Arabidopsis thaliana* chromosomes. *Mol Gen Genet* 253:247–252

Topp CN, Zhong CX, Dawe RK (2004) Centromere-encoded RNAs are integral components of the maize kinetochore. *Proc Natl Acad Sci USA* 101:15986–15991

Ward E (1973) Nondisjunction: localization of the controlling site in the maize B chromosome. *Genetics* 73:387–391

Wu J, Yamagata H, Hayashi-Tsugane M, Hijishita S, Fujisawa M, Shibata M, Ito Y, Nakamura M, Sakaguchi M, Yoshihara R, Kobayashi H, Ito K, Karasawa W, Yamamoto M, Saji S, Katagiri S, Kanamori H, Namiki N, Katayose Y, Matsumoto T, Sasaki T (2004) Composition and structure of the centromeric region of rice chromosome 8. *Plant Cell* 16:967–976

Yan H, Jin W, Nagaki K, Tian S, Ouyang S, Buell CR, Talbert PB, Henikoff S, Jiang J (2005) Transcription and histone modifications in the recombination-free region spanning a rice centromere. *Plant Cell* 17:3227–3238

Yan H, Ito H, Nobuta K, Ouyang S, Jin W, Tian S, Lu C, Venu RC, Wang GL, Green PJ, Wing RA, Buell CR, Meyers BC, Jiang J (2006) Genomic and genetic characterization of rice Cen3 reveals extensive transcription and evolutionary implications of a complex centromere. *Plant Cell* 18:2123–2133

Yu W, Lamb JC, Han F, Birchler JA (2006) Telomere-mediated chromosomal truncation in maize. *Proc Natl Acad Sci USA* 103:17331–17336

Yu W, Han F, Gao Z, Vega JM, Birchler JA (2007) Construction and behavior of engineered minichromosomes in maize. *Proc Natl Acad Sci USA* 104:8924–8929

Zhang W, Yi C, Bao W, Liu B, Cui J, Yu H, Cao X, Gu M, Liu M, Cheng Z (2005) The transcribed 165-bp CentO satellite is the major functional centromeric element in the wild rice species *Oryza punctata*. *Plant Physiol* 139:306–315

Zhang Y, Huang Y, Zhang L, Li Y, Lu T, Lu Y, Feng Q, Zhao Q, Cheng Z, Xue Y, Wing RA, Han B (2004) Structural features of the rice chromosome 4 centromere. *Nucleic Acids Res* 32:2023–2030

Zheng Y-Z, Roseman RR, Carlson WR (1999) Time course study of the chromosome-type breakage-fusion-bridge cycle in maize. *Genetics* 153:1435–1444

Zhong CX, Marshall JB, Topp C, Mroczek R, Kato A, Nagaki K, Birchler JA, Jiang J, Dawe RK (2002) Centromeric retroelements and satellites interact with maize kinetochore protein CENH3. *Plant Cell* 14:2825–2836

Chapter 7
Plant Telomeres

Jonathan C. Lamb, Eugene V. Shakirov, and Dorothy E. Shippen

Abstract Most plant chromosomes terminate in an array of 7-bp DNA repeats (TTTAGGG). DNA-binding proteins associate with this repeat to form a protective nucleoprotein cap termed the telomere, an essential role of which is to prevent chromosome ends from being joined by double-strand break-repair mechanisms. The telomere repeat array (TRA) is highly dynamic. It is extended by telomerase, an enzyme that synthesizes additional telomere repeats, and it is shortened by incomplete replication during S phase, recombination, and other factors. From the starting point of the mammalian model of telomere structure, several proteins that may interact with telomeric DNA and that are important for forming a functional telomere have been identified in plants. Also, additional components of the *Arabidopsis* telomerase holoenzyme have been found. In many species, arrays of longer satellite sequences are located adjacent to the TRAs, and such arrays have been used as cytological tools to identify chromosomes in several grass species. Transgenic introduction of TRAs can lead to formation of a functional telomere and loss of the distal chromosomal segment. This technology has the potential to allow manipulation of plant chromosomes.

Keywords Telomerase · Anaphase bridges · T-loop · Shelterin · Arabidopsis · De novo telomere formation · OB-fold · Telomere dysfunction

J.C. Lamb
Department of Biochemistry and Biophysics, Texas A&M University, 2128 TAMU, College Station, TX 77843-2128, USA

Monsanto Corporation, St. Louis, MO, USA

E.V. Shakirov • D.E. Shippen (✉)
Department of Biochemistry and Biophysics, Texas A&M University, 2128 TAMU, College Station, TX 77843-2128, USA
e-mail: dshippen@tamu.edu

H.W. Bass and J.A. Birchler (eds.), *Plant Cytogenetics*, Plant Genetics and Genomics: Crops and Models 4, DOI 10.1007/978-0-387-70869-0_7,

Abbreviations

ALT	Alternative lengthening of telomeres
ChIP	Chromatin immunoprecipitation
co-FISH	Chromosome orientation FISH
DBD	DNA-binding domain
EMSAs	Electrophoretic mobility-shift assays
FISH	Fluorescence in situ hybridization
NHEJ	Nonhomologous end joining
OB-folds	Oligonucleotide/oligosaccharide folds
SS	Single-strand
TAS	Telomere-associated sequence
TERT	Telomerase reverse transcriptase
TRAP	Telomere repeat amplification protocol
TRAs	Telomere repeat arrays
TRD	Telomere rapid deletion

Contents

7.1 Introduction

The specialized structures at the ends of chromosomes, termed telomeres, were, in large part, introduced to the world by the pioneering work of Barbara McClintock almost 70 years ago. Using an elegant genetic strategy, McClintock induced the

formation of dicentric chromosomes in maize (*Zea mays* L.). During anaphase, the two centromeres could be pulled to opposite poles, creating an "anaphase bridge" as the two complements of chromosomes segregated. Eventually, chromosomes in the bridges fractured, only to fuse again later and then be torn apart. This "breakage-fusion-bridge" cycle continued in the endosperm, creating kernels with mosaic color patterns as marker genes were lost, but in the embryo, the defective chromosomes were "healed" as a consequence of new telomere formation, underscoring the critical function of this structure.

Linear chromosomes face two major challenges not encountered by circular chromosomes. The first is to distinguish the ends from breaks in DNA strands that need repair, a function accomplished by the unique architecture of the telomeric tract and its interactions with a suite of specialized proteins, termed shelterin (de Lange 2005) in mammals. Shelterin forms a nucleoprotein complex that "caps" the chromosome terminus to prevent inappropriate processing of the terminus by nucleases and by DNA repair and recombination activities. Shelterin also regulates access of the telomerase ribonucleoprotein reverse transcriptase that synthesizes telomeric DNA.

The second challenge faced by linear chromosomes is the end replication problem, first described by James Watson and Russian theoretician Alexander Olovnikov (Olovnikov 1971, 1973; Watson 1972). In the absence of a compensatory mechanism, telomeric DNA tracts shorten each time the DNA is replicated, ultimately preventing the terminus from assuming its protective cap. Without a protective telomere structure, chromosome ends elicit a DNA damage response that causes cell-cycle arrest. Chromosomes can then be joined end-to-end, a process that leads to genome instability, senescence, and apoptosis. Telomerase solves the end-replication problem by continually replenishing telomeric DNA that is lost to incomplete replication.

Although many of the key insights in telomere research in recent years have derived from studies in yeast and mammals, interest is now being renewed in plant telomere composition and function as our understanding of the intimate relationship between cellular proliferation and telomere maintenance evolves. Here, we discuss fundamental properties of telomeres and their synthesis by telomerase, focusing on recent advances in deciphering the structure, organization, and dynamics of plant telomeres and their role in promoting stability of the plant genome.

7.2 Plant Telomeric DNA

7.2.1 Telomere DNA Structure

7.2.1.1 The Telomere Contains an Array of Telomere Repeats and a Single-Strand Overhang

In the majority of eukaryotes, telomeres comprise short G-C-rich tandem repeat arrays in which the G residues are clustered on the strand that runs from 5′ to 3′ toward the chromosome terminus. Plant telomeres consist of the seven-base repeat

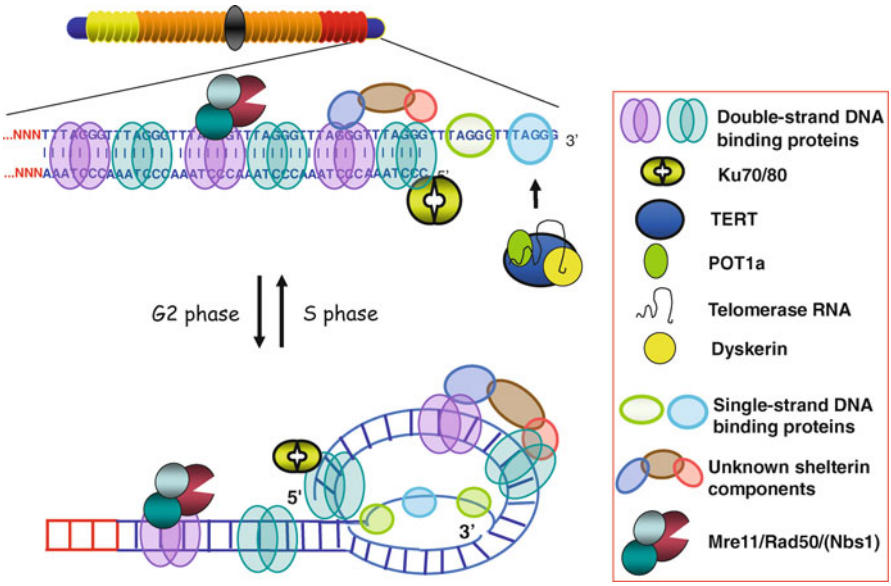

Fig. 7.1 Diagram of an *Arabidopsis* telomere. Telomeres are composed of a double-strand G-rich repeat (TTTAGGG in most plants) and a single-strand (SS) overhang. Telomeric DNA is bound by specific proteins, and collectively the protein-DNA complex is termed shelterin. Shelterin includes double-strand binding proteins (*purple*), SS binding proteins (*green*), and proteins (*blue*, *brown*, *pink*) that are at telomeres through association with the DNA-binding proteins. Shelterin helps the SS overhang invade the duplex DNA to form a circular structure called a T-loop. The telomere is thought to be highly dynamic, unfolding in S-phase to allow access for telomerase and replication machinery and then refolding in G2 to provide chromosome end protection

TTTAGGG, whereas human telomeres consist of the related six-base repeat TTAGGG. At the extreme terminus of the chromosome, the G-rich strand forms a 3′ single-strand (SS) protrusion, which is the substrate for telomere repeat addition by telomerase (Fig. 7.1). In most organisms, subtelomeric DNA repeats containing degenerate copies of the terminal repeat sequence lie just internal to the canonical telomere repeats.

7.2.1.2 The T-Loop

The telomere repeat arrays (TRAs) at chromosome ends can fold back onto themselves to form a looped structure called a T-loop (Fig. 7.1). This structure was first seen among purified human telomeres. Electron micrographs showed circles of various sizes, each with a protruding tail (Griffith et al. 1999). These loops are stabilized by cross-linking reagents that link pyrimidines of opposite strands in duplexed DNA, suggesting that T-loops form when the SS G overhang invades the double-strand region to form base-pairs with the C strand of the duplex DNA. The structure formed by the displaced C strand is called the D-loop.

Because T-loops are dissimilar to simple double-strand breaks (DSBs), they probably function in chromosome end protection by masking the telomere from DNA repair machinery. T-loops have been detected in many different species, including trypanosomes, ciliates, nonhuman vertebrates, and plants (Murti and Prescott 1999; Munoz-Jordan et al. 2001; Cesare et al. 2003). An exception to the T-loop telomere structure is found in *Saccharomyces cerevisiae* Meyen ex E.C. Hansen, where telomere repeats form a simple fold-back structure (without strand invasion), perhaps because the repeat arrays are too short or too irregular to form a loop (De Bruin et al. 2000, 2001). Thus, the arrangement of telomeric DNA repeats into a higher-order structure is generally conserved among eukaryotes.

In plants, T-loops have only been studied in pea, *Pisum sativum* L. (Cesare et al. 2003). Southern blots of restriction digests of genomic DNA from *P. sativum* hybridized with telomere probes produce a broad smear centered at 23 kb but extending to over 100 kb and below 6 kb. The size of pea T-loops ranges from 2 to 75 kb (mean 22 kb), and the length of looped molecules including the stem shows a distribution similar to that of the telomere signal. T-loops observed in *P. sativum* are larger than those in any previously examined organism. Previous models of T-loop formation assumed that the site of invasion of the duplex telomeric DNA by the G overhang was unbiased, but because average T-loop size in *P. sativum* is more than half that of the total telomere length, the data imply that loops involving a large amount of the telomere are favored. Although large T-loops are frequent in *P. sativum* preparations, loops as small as 2 kb were also observed. Because 2 kb is apparently sufficient to allow T-loop formation, even plants with telomeres in the lower end of the size range, such as *Arabidopsis* (2–5 kb), are likely to harbor these structures, and T-loop formation can reasonably be predicted to be a conserved feature of plant telomeres.

T-loops probably do not persist throughout the cell cycle. At a minimum, the T-loop must open to allow passage of the DNA replication machinery during S phase and extension of the single strand by telomerase. T-loop formation is therefore a dynamic process. In humans, various shelterin components have been shown to have properties that facilitate T-loop formation. In particular, TRF2, a double-strand telomere repeat binding (TRB) protein, can promote formation of T-loops from naked telomere DNA substrates in vitro (Griffith et al. 1999), possibly because of its ability to bind the chicken-foot conformation formed at the site of invasion of the duplex DNA by the G overhang (Khan et al. 2007). As discussed later, the shelterin complex also recruits proteins to the telomere that are involved in DNA repair and could help form a T-loop. Thus, the shelterin complex, either directly or through recruitment of additional components, appears to control T-loop formation.

7.2.1.3 Telomeric Chromatin

Like the rest of the genome, the TRA is wrapped around nucleosomes. At telomeres in species with the *Arabidopsis* repeat (TTTAGGG), nucleosomes are regularly positioned once every ~157 (±5) base pairs of DNA (Fajkus et al. 1995; Vershinin et al. 1995). This periodicity is different from that of the rest of the genome, where

the amount of DNA, including the space between nucleosomes, varies quite a bit but averages 180 bp (Fajkus et al. 1995). Despite being arranged more compactly, telomeric DNA is more accessible to nuclease than DNA at other satellite repeats in the genome (Fajkus et al. 1995). The tighter spacing of telomeric nucleosomes may reflect a higher-order chromatin structure that is conducive to telomere function (see e.g., Fajkus and Trifonov 2001). Nucleosome position along DNA is not influenced by the nucleotide sequence of TRAs (Fajkus and Trifonov 2001). Perhaps the regular periodicity of nucleosome position at telomeres is influenced by the shelterin complex. In *Silene latifolia* Poir., a species with short telomeres, the short nucleosome periodicity extends into the subtelomeric region as well (Sykorova et al. 2001). In rye (*Secale cereale* L.) as well, repetitive DNA in the subtelomeric regions, pSc250, has an expected nucleosomal periodicity similar to that of telomeric chromatin (Vershinin and Heslop-Harrison 1998), so the telomeric chromatin structure may extend beyond the TRA.

In mammals, the histone modifications at telomeres resemble those of heterochromatic regions (Blasco 2007). Perturbations to those modifications are correlated with changes in telomere length and frequency of recombination at telomeres. In addition, several proteins with chromatin-remodeling properties have a role in regulating telomere length. These new findings in mammals indicate that the chromatin state is an important feature of the telomere structure and will be a topic of interest to plant biologists.

7.2.2 Plant Telomere Repeat Variants

The telomere repeat sequence identified in *Arabidopsis*, TTTAGGG, is evolutionarily ancient in plants (Fig. 7.2). The *Arabidopsis*-type repeat is found at chromosome ends in the green alga *Chlorella vulgaris* Beijerinck (Higashiyama et al. 1995), mosses and ferns (Suzuki 2004), and pine, as well as most monocot and dicot lineages (Cox et al. 1993; Fuchs et al. 1995). A second green-algal lineage has a similar repeat (TTTTAGGG) (Petracek et al. 1990). Although a single mutation in the telomerase RNA (TER) template could theoretically lead to an altered telomere repeat sequence, any changes may diminish the ability of the shelterin complex to recognize the resulting telomere array and lead to genome instability and a massive decrease in fitness. Despite this danger, variant telomere repeat sequences have been discovered in several plant lineages. These cases provide an opportunity to study the genome's response to altered telomere repeats and thus may provide insight into telomere function.

7.2.2.1 Asparagales, a Monocot Order with Noncanonical Telomere Repeats

The first indication that the *Arabidopsis*-type repeat was not uniformly present in higher plants came from a cytological survey of 44 species belonging to 14 plant

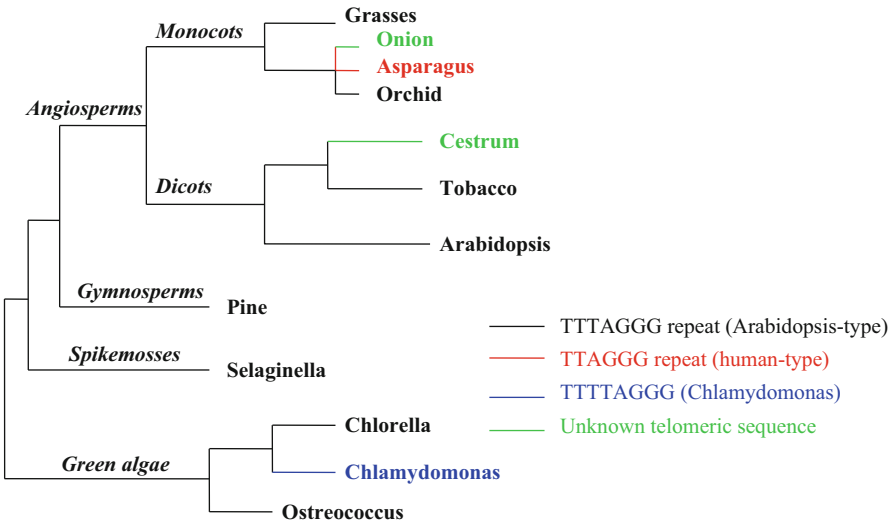

Fig. 7.2 Phylogenetic tree showing telomere-repeat variants

families including angiosperms, gymnosperms, and bryophytes. When fluorescence in situ hybridization (FISH) was performed with the *Arabidopsis*-type repeat, terminal signals were detected in all species examined except those in the family Alliaceae (Fuchs et al. 1995). The absence of this repeat from several of the Alliaceae was confirmed with additional molecular techniques including Southern blotting followed by hybridization with the *Arabidopsis* repeat (Pich et al. 1996). When *Aloe* species (family Asphodelaceae) were also found to lack it (Adams et al. 2000), the search was expanded to additional members of the order Asparagales, where several families, all grouped in a single clade with a common ancestor 80–90 million years ago, lacked it (Adams et al. 2001). This phylogenetic grouping indicates that the loss of the *Arabidopsis* telomere repeat occurred once in this lineage.

7.2.2.2 The Asparagales Telomerase Encodes the Vertebrate-Type Telomere Repeat

FISH with a labeled oligonucleotide probe corresponding to the vertebrate telomere repeat, TTAGGG, was attempted for several Asparagales species, including *Othocallis siberica* (Haw. ex Andr.), *Speta* (Hyacinthaceae), and *Aloe* species (Weiss et al. 2001; Weiss and Scherthan 2002). Surprisingly, signal was detected at chromosome ends, suggesting that the *Arabidopsis* repeat had been replaced by the vertebrate repeat. This discovery prompted a search among additional Asparagales (Puizina et al. 2003; Sykorova et al. 2003d), and indeed, with the exception of a subset of species in the family Alliaceae, discussed later, all plants lacking the *Arabidopsis*-type repeat were shown to have the vertebrate type at their telomeres (Sykorova et al. 2003d).

Telomere synthesis by an altered telomerase enzyme that generated a six-nucleotide vertebrate repeat instead of the seven nucleotide *Arabidopsis* repeat was confirmed by an in vitro assay for telomerase activity, the telomere repeat amplification protocol (TRAP). TRAP uses a nuclear protein extract containing telomerase activity to extend a synthetic oligonucleotide primer that mimics the G-rich 3′ overhang. Once telomere repeats are added, the products are amplified with a primer corresponding to the telomere repeat. Strikingly, TRAP products with a six-base periodicity were generated (Sykorova et al. 2003d). Although the bulk of the repeats synthesized in vitro were perfect copies of the vertebrate telomere repeat, variant repeats were also produced at a low but significant level, especially those that differed from the vertebrate repeat by incorporation of an additional G to produce the *Arabidopsis* type or replacement of A with G to produce the *Tetrahymena*-type repeat, TTGGGG (Sykorova et al. 2003d).

7.2.2.3 Some Asparagales Species Have Additional Microsatellites at Their Telomeres

In addition to the vertebrate-type repeat, several Asparagales species have other repeats near the chromosome ends, usually the *Arabidopsis* and/or the *Tetrahymena* type. For example, the family Hyacinthaceae contains several members with and without the *Arabidopsis*-type repeat signal at the ends of chromosomes as detected by FISH on mitotic chromosome preparations (Adams et al. 2001), but the vertebrate repeat is also present at chromosome ends, and examination of TRAP results showed that all Hyacinthaceae give rise to telomerase extension products with a six-base-pair periodicity (Sykorova et al. 2003d).

One explanation is that telomere repeat variants are produced at a high frequency by a low fidelity telomerase. Indeed, TRAP products often do contain repeat variants, including the *Arabidopsis*-type (Sykorova et al. 2003d), but the variants are not distributed uniformly throughout the telomere as expected from stochastic production by telomerase. Instead, the *Arabidopsis* and *Tetrahymena* signals appear as distinct spots near the ends of metaphase FISH preparations and overlap only a portion of the signal from the vertebrate-type repeat (Sykorova et al. 2003d). Also, on stretched DNA preparations from *Ornithogalum virens* L. labeled with FISH probes, the *Arabidopsis*- and *Tetrahymen*a-type repeats are present as discrete spots in the middles or at the bases of vertebrate repeat arrays, away from the chromosome end (Rotkova et al. 2004).

A similar phenomenon is seen in species with the *Arabidopsis*-type repeat. Cloned telomere arrays in *Arabidopsis* contain frequent repeat variations that tend to be clustered together and are more common near the base of TRA (Richards et al. 1992). Therefore, in addition to low-fidelity telomerase, other mechanisms, such as unequal recombination or gene conversion, probably affect the organization and frequency of repeat variants.

7.2.2.4 Cloning and Characterization of Asparagales Telomerases

The most likely explanation for the change from *Arabidopsis*- to vertebrate-type repeats in the order Asparagales is a mutation in the TER template domain, but because the TER subunit has yet to be identified in plants, Sykorova et al. (2006b) compared six telomerase reverse transcriptase (TERT) genes from different Asparagales species, including examples with both types of telomere repeats, that could contribute to the production of variant repeats. In species that synthesize the human-type repeat, a small number of amino-acid changes were present in and around known functional motifs (Sykorova et al. 2006b). Sykorova et al. proposed that changes to the Asparagales TERT protein are related to the evolutionary switch from *Arabidopsis*-type to vertebrate-type telomere repeats, but whether these changes actually alter telomerase function is unclear.

7.2.2.5 *Allium* Telomeres Consist of Unknown Sequences

For several species in the family Alliaceae, neither the vertebrate nor the *Arabidopsis*-type telomere repeats were detectable at chromosome ends, so a second change to telomeres had occurred in this lineage. Cytological observations were confirmed by failure of asymmetric PCR and the lack of hybridization signal in Southern blots for several Alliaceae (Pich et al. 1996). Also, onion, *Allium cepa* L., nuclear extracts fail to extend any permutations of the vertebrate or *Arabidopsis* telomere repeats in vitro but do not inhibit TRAP reactions carried out with extracts from other Asparagales (Sykorova et al. 2003d). An examination of many different Alliaceae species using slot blots and FISH revealed that the loss of the vertebrate telomere repeat was limited to species in the genus *Allium* (Sykorova et al. 2006a). *Allium* species were tested for the presence of telomere repeats from several different eukaryotes, including *Bombyx* (TTAGG), *Chlamydomonas* (TTTTAGGG), and *Oxytricha* (TTTTGGGG). Although several of these repeats were found in one or more *Allium* species, none was located at the chromosome ends.

If the ends of *Allium* chromosomes are not composed of any known microsatellite repeats, what are they made from? They may be produced and maintained by a telomerase that synthesizes a yet unidentified repeat. Currently, only a relatively small number of all possible short microsatellite sequences have been tested, so many candidate sequences remain.

An intriguing alternative to the typical short telomere repeat has been proposed for *Allium* on the basis of the discovery of a highly abundant ~375-bp satellite in *A. cepa* that labels chromosome ends in cytological preparations (Barnes et al. 1985; Pich et al. 1996). The satellite is present in long arrays of repeats, an arrangement similar to that of chromosome ends in the insect genus *Chironomus*, where chromosomes terminate with arrays of larger satellites, either ~340 or ~180 bp in length, which serve to maintain and protect chromosome ends (Lopez et al. 1996; Kamnert et al. 1997). Relatively little is known about how the longer satellites are produced and how they form a protective cap in *Chironomus*. The possibility of a plant model with a similar telomere style that would allow intrakingdom comparisons is exciting.

Examination of cytological preparations has not, however, provided definitive evidence that the satellites are the most terminal sequences on onion chromosomes. In fact, the signal on pachytene chromosomes is most similar to that of known subtelomeric satellites such as those of maize, tomato (*Solanum lycopersicum* L.), and rice (*Oryza sativa* L.) (Zhong et al. 1998; Cheng et al. 2001; Lamb et al. 2007).

7.2.2.6 A Dicot Lineage Without *Arabidopsis*-Type Telomere Repeats

In addition to the monocot order Asparagales, a second group of plants, the *Cestrum* clade in the family Solanaceae, has telomeres that do not consist of the *Arabidopsis*-type telomere repeat (Sykorova et al. 2003b). This clade includes the three closely related genera *Cestrum*, *Vestia*, and *Sessea.* Several known telomere repeats, including the vertebrate type, were checked for a telomeric location, but none was present at chromosome ends (Sykorova et al. 2003c).

7.2.3 Subtelomeric Regions

7.2.3.1 Subtelomeric Satellites

With only a few exceptions (described earlier), the telomere repeat is conserved in nearly all plant lineages. In many species, the region proximal to the telomere, the subtelomere, is also composed of tandem arrays of particular DNA elements, called satellites (Fig. 7.3). Like the TRA, the number of satellite copies can differ in different individuals of the same species. Unlike those of the telomere itself, however, the primary sequences of subtelomeric satellites are not conserved beyond close relatives. Not all plants have subtelomeric satellite arrays or heterochromatin blocks. For example, *Arabidopsis* lacks these features, and rice has satellite arrays at only some of the chromosome ends. Nevertheless, satellites and heterochromatin are found at chromosome ends in numerous species, including many plants as well as diverse eukaryotes. Also, the unrelated satellites found at various species' chromosome ends have some common features, so although not absolutely required, these sequences may serve some purpose at chromosome ends or be caused by similar processes.

Most satellites are the correct size to associate with a discreet number of nucleosomes (~165 bp or about twice that number, 340 bp; Macas et al. 2002; Sharma and Raina 2005). Because satellites are organized in arrays, a one-to-one (or two-to-one) ratio of nucleosomes to DNA repeats could cause a uniform distribution of nucleosomes throughout the array and thereby facilitate folding of chromatin into higher-order structures. Consistent with this hypothesis, satellites often contain A-T-rich stretches and the motif CAAAA (Macas et al. 2002), features that may allow the satellites to bend in a manner that positions nucleosomes or that is favorable to a tighter chromatin arrangement. In addition, tandem arrays may foster heterochromatin formation through the RNAi machinery (May et al. 2005). Indeed,

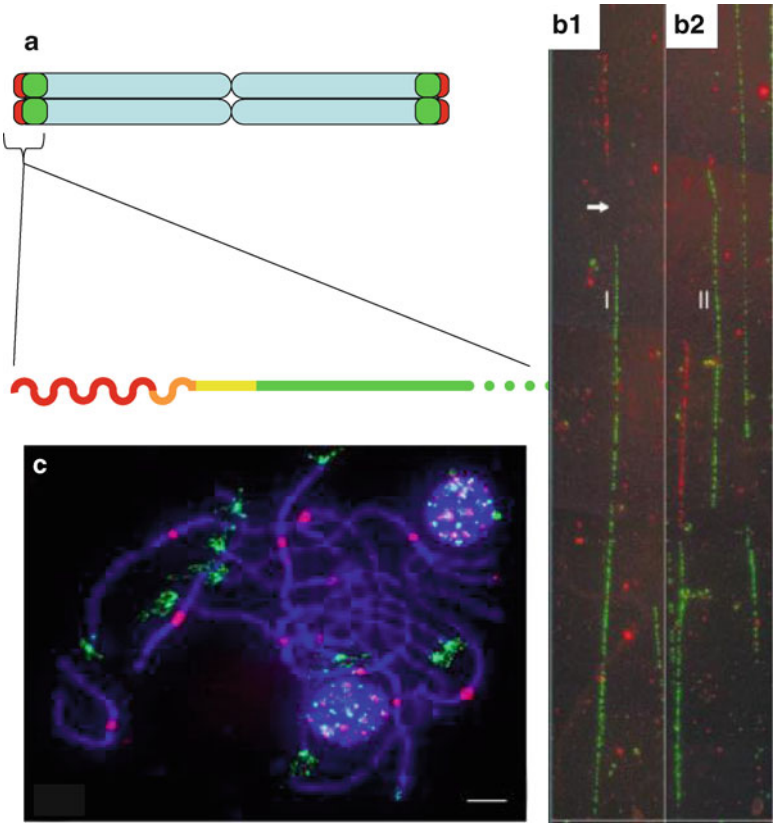

Fig. 7.3 Typical plant chromosomes have repetitive DNA elements next to the telomere repeat array (TRA). (**a**) A typical chromosome has a terminal block of perfect telomere repeats (*red*) preceded by a heterochromatic block of subtelomeric repeats (*green*). This section of the chromosome is enlarged to show a short telomere-associated sequence (TAS) (*yellow*) and degenerate telomere repeats (*orange*) at the base of the perfect TRA (*red*). (**b1** and **b2**) Two different stretched DNA fibers from tomato hybridized with the telomere repeat (*red*) and a tomato subtelomeric repeat (*green*) (images from Zhong et al. 1998). The *arrow* in (**b1**) indicates the TAS, which lacks signal. In other cases (**b2**), the telomere repeat abuts the subtelomere repeat array. (**c**) A subtelomere repeat (TrsC in *green*) in *Oryza officinalis* (rice) hybridizes in a cloud-like pattern at the end of pachytene chromosomes (image from Bao et al. 2006). The *red* signal is from a centromere probe

histone modifications such as Me2K9H3 and Me2K27H3 and extensive DNA methylation mark satellite arrays as heterochromatic (Blasco 2007), and subtelomeric satellite arrays often form heterochromatin blocks that are cytologically detectable. The purpose of satellite arrays may therefore be to foster a specific chromatin state in the subtelomeric region.

Examples of Subtelomeric Satellites from Plants

Numerous plant satellites have been identified in a wide selection of different plant lineages. Much of the impetus for their discovery has been the possibility of using them to determine phylogenetic relationships or to distinguish genomes of related species. In particular, satellites can differentiate homeologous chromosomes in allopolyploid species because they evolve rapidly and closely related species may have very different satellites, especially in the agronomically important Triticeae tribe, which includes wheat (*Triticum aestivum* L.), rye, and oats (*Avena sativa* L.). Also, because of their abundance, satellites make excellent FISH probes. A comprehensive listing or description of all characterized satellites is beyond the scope of this article, but a few examples of subtelomeric satellites are given below. Several reviews of satellite distribution, function, and evolution are available (Macas et al. 2002; Ugarkovic and Plohl 2002; Sharma and Raina 2005).

Triticeae

The subtelomeric regions of rye form prominent blocks of heterochromatin, which are readily discernable by any of a variety of staining techniques. They account for ~12–18% of the total genome and contain a number of different satellite repeats and other repetitive DNA (Sharma and Raina 2005). The satellites include a 340-bp satellite similar to pAs1, which was initially cloned from *Aegilops tauschii* Coss., and to a 118-bp satellite, pSc119.2. Both of these satellites are present in various forms throughout the Triticeae, including the genera *Triticum*, *Hordeum*, and *Secale*, and probably in other closely related species. pSc119.2 is found in the genus *Avena.* Additional satellite families present at the terminal heterochromatic blocks of rye include a ~380-bp repeat, pSc200, and a ~550-bp repeat, pSc250. Species- or genus-specific variations of these repeats can be used to distinguish the different contributing genomes of allopolyploids in this tribe. Generally, one or more variants are present at high copy numbers at subtelomeric and interstitial positions on both arms of most chromosomes in a genome (Sharma and Raina 2005).

Oryza

In relatives of rice, two subtelomeric repeats have been identified in searches for centromeric sequences (Lee et al. 2005; Bao et al. 2006). In *Oryza rhizomatis* Vaughan, a 366-bp satellite, CentO-C2, physically associates with the histone H3 variant, CenH3, that defines the centromere region, but on FISH preparations, the majority of the CentO-C2 signal is present at large subtelomeric blocks present at several chromosome arms (Lee et al. 2005). In another study, a 366-bp satellite, TrsC, was found through sequencing of BACs located at centromeric positions in *O. rhizomatis* (Bao et al. 2006). TrsC is also found at several centromeres as well as subtelomeric positions but is only found at subtelomeric locations in a close relative, *Oryza officinalis* Wall ex Watt (Bao et al. 2006). The locations of TrsC and

CentO-C2 imply that they have moved from subtelomeric positions to the centromere, so the same repeat is present at the functional centromere as well as the subtelomeric heterochromatin.

Organization of Chromosome Ends with Satellite Repeats

DNA Sequence Organization

Although satellite arrays can be found immediately adjacent to the TRAs, they are often separated by a short linker sequence called the telomere-associated sequence (TAS). Use of FISH on stretched DNA fibers (fiber-FISH) permits visualization of the arrangement of satellites, TASs, and TRAs (Fig. 7.3). In tomato, signals from the subtelomeric satellite, TGR1, directly abut the telomere repeat signal or are separated by a small gap with no signal ranging from 13 to 98 kb (Zhong et al. 1998). Similarly, in *S. latifolia* as well as several tobacco species, cloning of the base of the TRA identified cases in which the telomere array is connected directly to the subtelomeric satellite array as well as cases in which the two are separated by a short linker sequence (Horakova and Fajkus 2000; Sykorova et al. 2003a). In contrast, the rice TrsA repeat always appears immediately adjacent to the TRA in fiber-FISH preparations in *indica* rice (Ohmido et al. 2001).

In the case of *S. latifolia*, the linker TASs are composed of sequence without similarity to the telomere repeats, the subtelomeric repeat, X43.1, or other known sequences (Sykorova et al. 2003a). Instead, the cloned TAS sequences include degenerate telomere repeats adjacent to the TRA, as well as short arrays of novel satellites, satellites previously identified from nontelomeric locations, and novel sequences found at multiple chromosome ends (Sykorova et al. 2003a). The authors noted that some features of the TAS DNA could allow it to serve as a transition between chromatin states at the telomere and the subtelomere.

Cytological Observations of Telomere-Subtelomere Macrostructure

Although telomeres are at the terminal DNA sequences of chromosomes, telomere FISH signals do not usually appear at the extreme ends of chromosomes on fully condensed mitotic chromosome preparations. This finding suggests that telomeric DNA is tightly condensed, whereas subtelomeric DNA sequences are held in less condensed loops. In pachytene spreads labeled with subtelomeric satellites and telomere repeats, the respective signals are typically found in an inverted orientation, with the subtelomeric signal at the chromosome end. This pattern has been noted in several plants, first tomato (Zhong et al. 1998) and later rice and maize (Ohmido et al. 2001; Lamb et al. 2007), as well as nonplant species (Moens and Pearlman 1990b). In several other reports, images are presented that show a cloud-like subtelomeric satellite signal at the ends of meiotic chromosomes (Fig. 7.3). When a technique is used that spreads out the DNA in mouse chromosomes at the pachytene stage, some repeats, such as an abundant LINE element, appear as diffuse

signals in DNA looping out from the synaptonemal complex. In contrast, telomere signals appear as tight spots of hybridization at the ends of these complexes (Moens and Pearlman 1990a). Therefore, the inverted orientation of telomere and subtelomere signals may be caused by diffusion of the subtelomeric repeats, but Zhong et al. noted that the telomere and subtelomere repeat signals of tomato pachytene chromosomes do not overlap as would be expected if diffusion were the complete explanation (Zhong et al. 1998). The inverted orientation of telomere and subtelomeric signals may reflect an organized structure involving both the telomere and subtelomeric regions during pachytene.

Subtelomeric Sequence Variation in *Arabidopsis* and Other Plants Without Large Satellite Arrays

Satellites may not be the only sequences at subtelomeric positions shared by nonhomologous chromosomes. The subtelomeric regions in humans consist of a "patchwork" of shared sequences that arose through repeated translocations (Mefford and Trask 2002). Recombination in the subtelomeric regions of nonhomologous chromosomes occurs at shared sequences. As a result, the subtelomeric regions change rapidly, sections are shuffled, and sequences are gained and lost during primate evolution (Linardopoulou et al. 2005). Recombination between nonhomologous chromosomes has also contributed to the evolution of subtelomeric regions in several other species, as has DSB repair by nonhomologous end joining (NHEJ).

In plants, most subtelomeric sequences that have been characterized are from species with subtelomeric satellite arrays. Direct observation of recombination breakpoints in satellite repeat arrays would be technically challenging because of the difficulties in cloning, sequencing, and analyzing tracts of repetitive DNA. A number of recent studies focusing on the subtelomeric regions in rice and *Arabidopsis*, two species lacking satellite arrays at some or all chromosome ends, allow the organization of subtelomeric regions of plants to be compared with those in other model systems.

The rice satellite TrsA is present at 12 of the 48 chromosome ends in *japonica* rice and at only four ends in *indica* (Ohmido et al. 2000). The remaining ends lack cytologically detectable satellite sequence. Although the rice draft genome has been published, gaps remain in the sequence coverage, including the subtelomeric regions, so comprehensive comparisons among the chromosome ends are not currently possible. Analysis has been conducted for several chromosome ends that have been sequenced and for most of the sequenced arms; no sequences are unique to, or even enriched at, chromosome ends (Yang et al. 2005; Mizuno et al. 2006). The gene density near the chromosome end is higher than the genomic average, and repetitive elements are distributed similarly to the rest of the genome. Except for chromosome 10S, the DNA at the characterized chromosome ends lacks features that distinguish it from other genomic locations. 10S ended with a pair of inverted sequences composed of four units of 100 bp and a single 42-bp sequence. This arrangement could be an early step in the generation of new satellite sequences.

All chromosome arms in *Arabidopsis* have been sequenced to the telomere tract, allowing a thorough search for evidence of movement of subtelomeric sequence among chromosomes. Although nonhomologous subtelomeric regions (e.g., 2R and 4R) share some sequences (Heacock et al. 2004), the extent of similarity is less than that in humans or other model systems. *Arabidopsis*, like rice, has an unusually small genome, consistent with the loss of many noncoding DNA sequences over an evolutionarily short period, so subtelomeric sequences may frequently be lost in these two species, eliminating the features typical of subtelomeric regions. As a consequence, evidence for interchromosomal recombination would be lost.

An alternative approach to comparing the sequences of the different chromosome ends in a single genome is to look at changes accumulated over evolutionary time. Kuo and coworkers examined 3.5 kb of sequence, including the base of the TRA from chromosome 1 (north) in 35 different *Arabidopsis* ecotypes from different geographic locations (Kuo et al. 2006). The distal 1.4-kb portions from different ecotypes differed in numerous small insertions, deletions, and base-pair substitutions and were shown to be much more variable than the more proximal portion. In addition, several larger rearrangements were evident in some lines, including larger deletions, a 1.4-kb inversion, and a deletion filled in by a retrotransposon sequence. Some of the larger deletions were flanked by short direct repeats, a signature of DSB repair by NHEJ. Indeed, many of the mutations appeared to have been caused by imperfect double-strand DNA break repair as seen in other eukaryotes, but without a comparison of changes in the subtelomeric region to those in other noncoding portions of the genomes, one cannot conclude that something special is occurring in the subtelomeric region.

The base of the TRA consists of degenerate telomere repeats, and the degenerate region extends either ~85 or ~221 bp in most lines. The length of the degenerate region is correlated with two specific patterns of rearrangement in the subtelomeric region (Kuo et al. 2006). The subtelomere and the base of the telomeres remain associated while alterations accumulate in both regions. This pattern of mutation accumulation indicates that meiotic crossovers or other forms of recombination are infrequent in this region. Therefore, insertions into and deletions from both the telomere repeat and the subtelomeric region, including those from NHEJ-type DNA repair, but not homologous recombination, contributed to the evolution of this region. This profile contrasts with evidence of frequent recombination in other eukaryotes and may reflect the greater role of NHEJ in plants.

7.3 The Shelterin Complex

7.3.1 Shelterin at Human Telomeres

Shelterin components in humans are well studied and provide the basic model for telomere structure and function. The human shelterin complex consists of a core group of six proteins that are associated with telomeres and that can be biochemically

purified as a single group. They include two double-strand telomere-binding proteins, TRF1 and TRF2; a SS binding protein, POT1; and three additional proteins, Rap1, TPP1, and TIN2, that attach to the DNA-binding proteins and link them together. Because TRF1, TRF2, and POT1 have specific sequence requirements for binding, they confer specificity on the shelterin complex and limit its capping abilities to stretches of telomeric repeats. Although all components can associate in a single complex, various combinations of the shelterin components may be present along the TRA.

Shelterin confers telomere function (end protection and telomere maintenance) in three ways. First, shelterin formation shapes telomeric DNA, thereby controlling access of replication and repair proteins, including telomerase. Second, individual components of the shelterin complex have specific abilities that are required at the telomere. For example, POT1 and TRF2 prevent signaling by the central DNA damage regulators ATR and ATM, respectively (Denchi and de Lange 2007). In vitro, TRF2 and Rap1 prevent NHEJ of linear DNA molecules ending with properly oriented telomere repeats (Bae and Baumann 2007). Third, shelterin recruits proteins to the telomeres that have additional roles in the genome. For example, the KU heterodimer, an essential component of the NHEJ DSB repair pathway, is recruited to telomeres through interactions with TRF1 and TRF2 (Hsu et al. 2000; Song et al. 2000). Once recruited, KU functions in telomere length regulation and end protection. Several additional proteins involved in DNA repair and replication are enriched at telomeres through interactions with shelterin, where they may help the T-loop form or ensure efficient replication during S-phase of the G-rich telomere repeats.

Orthologs of human shelterin components have been identified in other organisms, so a universal model for eukaryotic telomere structure can be proposed. The first layer of telomere structure is the repeat array. One or more sequence-specific double-strand and one or more SS DNA-binding proteins with specificity for the telomere repeat sequence form the next layer. These DNA-binding proteins are joined by linking proteins and components that prevent detection of the telomere by DSB repair machinery. Together, these proteins assemble the telomere into a T-loop configuration that further distinguishes the chromosome end from a DSB and also promotes DNA replication and telomerase regulation.

7.3.2 Shelterin Components in Plants

Identification of putative shelterin components in plants has thus far heavily relied on database searches for genes with similarity to components in other species. This approach has identified several putative homologs for DNA-binding proteins, but the other shelterin components (Rap1, TPP1, and TIN2) cannot be discerned in the rice or *Arabidopsis* genomes. These proteins may have diverged too much for successful identification by current search strategies. Alternatively, new proteins may have evolved to assume their roles at plant telomeres. In vitro screens have identified several additional proteins that bind telomeric DNA, but these do not have

Table 7.1 *Arabidopsis* proteins with roles in telomere biology

Function	Protein (gene)	Role
Double-strand telomere binding proteins (putative)		
	TBP1 (At5g13820)	Negative
	TRP1 (At5g59430)	Unknown
	TRFL1 (At3g46590)	Unknown
	TRFL2 (At1g07540)	Unknown
	TRFL4 (At3g53790)	Unknown
	TRFL9 (At3g12560)	Unknown
	AtPURalpha (At2g32080)	Unknown
	TRB1 (At1g49950)	Unknown
	TRB2 (At5g67580)	Unknown
	TRB3 (At3g49850)	Unknown
Single-strand telomere binding proteins		
	POT1b (At5g06310)	Positive
	WHY1 (At1g14410)	Negative
	STEP1 (At4g24770)	Negative
DNA repair		
	KU70 (At1g16970)	Negative, regulation of TRD
	KU80 (At1g48050)	Negative, regulation of TRD
	ATM (At3g48190)	Positive,[a] regulation of TRD
	ATR (At5g40820)	Positive,[a] regulation of TRD
Telomerase RNP		
	RAD50 (At2g31970)	Positive
	MRE11 (At5g54260)	Negative[b]
	TERT (At5g16850)	Positive
	POT1a (At2g05210)	Positive
	Dyskerin (At3g57150)	Positive

[a]Mutant phenotypes are observed only in telomerase-negative background
[b]Mutant lines differ in phenotype

homology to shelterin components in other eukaryotes, and their function at telomeres is uncertain. Figure 7.1 shows a general model of shelterin at *Arabidopsis* telomeres, and Table 7.1 lists *Arabidopsis* genes that are thought to function at telomeres.

A common feature of double-strand telomere-binding proteins in diverse eukaryotes is the presence of a conserved myb-type DNA-binding domain, but many myb-containing genes are present in plant genomes, ~185 in *Arabidopsis* (Yanhui et al. 2006), so efforts to study telomeres have focused on those with the greatest similarity to the human double-strand telomere proteins. Two major classes of myb-containing proteins bind plant telomere sequences: proteins with the myb domain at their C-termini, typified by rice telomere binding protein 1 (RTBP1), and proteins with the myb domain at their N-termini, the TRB family.

Vertebrate TRF1 and TRF2 contain a C-terminal Myb domain and a central dimerization domain. Candidate plant homologs with a similar structure were identified by

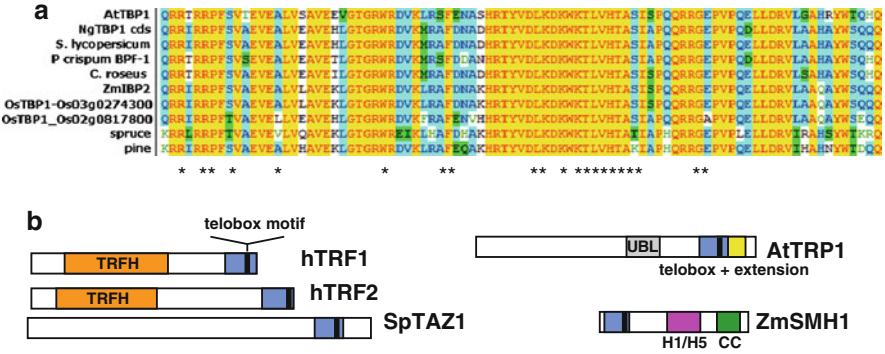

Fig. 7.4 Double-strand telomere-binding proteins. (**a**) A multiple alignment of the telomere-binding myb and extension domain of RTBP1 homologs. *Asterisks* indicate amino acids that are conserved with the human telomere binding domain. (**b**) The human and yeast double-strand telomere binding proteins contain a myb domain (*blue*) with a "telobox" motif (*vertical black line*). The plant RTBP1 homologs (represented here by AtTRP1) have the myb domain as well as a plant-specific extension (*yellow*) that is required for binding telomere sequences. RTBP1 proteins also have a ubiquitin-like domain (*gray*). The TRBs (represented here by ZmSMH1) have a myb domain at the N-terminus as well as a histone-like domain (H1/H5) and a coiled-coil motif. (**b**) Adapted from Zellinger and Riha (2007)

searching of plant sequence databases (Bilaud et al. 1996; Yu et al. 2000). A rice homolog, RTBP1, was cloned and translated in vitro, and the protein was shown, by electrophoretic mobility-shift assay (EMSA), to bind specifically to the plant telomere repeat (Yu et al. 2000). Additional genes encoding RTBP1 homologs have been identified by molecular approaches or by searches of the growing database of plant DNA sequences. These include the maize initiator binding proteins ZmIBP1 and ZmIBP2; the parsley (*Petroselinum crispum* L.) BoxP binding factor, BPF1; tomato LeTBP1; and tobacco TBP1 (Yu et al. 2000; Chen et al. 2001; Hwang et al. 2001, 2005; Yang et al. 2003; Karamysheva et al. 2004; Moriguchi et al. 2006). Several of these homologs, including those from tobacco (*Nicotiana tabacum* L.), tomato, and *Arabidopsis* have been shown to bind telomeric DNA in vitro. A search of several public databases reveals additional putative RTBP1 homologs in plants. An amino-acid alignment of the telomere-binding domain of several of these proteins is presented in Fig. 7.4.

The RTBP1 homologs from flowering plants are about 666 amino acids and display several conserved motifs. The C-terminus contains the Myb-like motif as well as an additional plant-specific motif, called the myb extension (Karamysheva et al. 2004). Together, these motifs are necessary and sufficient for binding telomeric DNA in vitro. This DNA-binding domain (DBD) is remarkably well conserved in all flowering plants; most of the residues show little or no amino-acid variation. The DBD forms three helices with a helix-turn-helix motif, similar to double-strand telomere-binding proteins from nonplant species. The plant-specific Myb extension forms a fourth helix that probably helps stabilize the structure (Sue et al. 2006).

Comparison of the domain bound and unbound to DNA suggests that the third helix confers DNA specificity.

The DBD is able to bind to double-strand oligonucleotides containing as few as two telomere repeats (5′ TTTAGGGTTTAGGG 3′) in vitro. Binding of this oligonucleotide involves the central six base pairs (GGGTTT) (Yu et al. 2000; Yang et al. 2003). The RTBP1 homologs form dimers (Karamysheva et al. 2004), and when more copies of the telomere repeat are present, the full-length RTBP1 homologs form higher-molecular-weight complexes (Yu et al. 2000; Yang et al. 2003; Karamysheva et al. 2004; Moriguchi et al. 2006). In this way, they are similar to nonplant telomere-binding proteins, which typically bind DNA as dimers. Also, like human TRF1 and TRF2, plant RTBP1 homologs can bend DNA (Hwang et al. 2005), probably by binding repeats at different locations along the telomere tract.

Several plant-specific regions are present in all plant RTBP1 homologs. Putative nuclear localization signals have been identified (Karamysheva et al. 2004), as have ubiquitination and phosphorylation sites (Yang et al. 2003) and a region with similarity to the H1 histone protein. Also, a region has been defined that is required for in vitro interaction with the Ku70 protein (Kuchar and Fajkus 2004), a negative regulator of telomere length in *Arabidopsis* (discussed later). Another region is similar to the H1 histone protein; this dimerization domain remains to be identified.

The RTBP1 homologs are implicated both in negative regulation of telomere length and in chromosome end protection. T-DNA insertions in rice RTBP1 and AtTBP1 (from *Arabidopsis*) lead to increased telomere length (Hong et al. 2007; Hwang and Cho 2007). Telomeres in the rice mutant increased dramatically in the first generation but did not continue to elongate in subsequent generations (Hong et al. 2007). Plants with mutations in RTBP1 also have morphological defects indicative of meristem problems. The morphological defects are best explained by genome instability resulting from chromosome fusions at unprotected telomeres. Indeed, evidence for fused chromosomes was detected as anaphase bridges in pollen mother cells. Telomere FISH signal was detected on the DNA stretched between the two separating groups of chromosomes (Hong et al. 2007). Interestingly, morphological abnormalities became progressively more severe in each generation, although the telomere length did not increase further. In tobacco-cell culture, antisense-mediated knock-down of the tobacco RTBP1 homolog, NgTRF1, also causes telomere elongation accompanied by reduced cell viability and activation of an apoptosis-like mechanism (Yang et al. 2004). Likewise, overexpression of NgTRF1 causes shorter telomeres and also decreases cell viability. Overexpression of the tomato homolog in tobacco-cell culture results in a phenotype similar to that caused by overexpression of the endogenous protein (Moriguchi et al. 2006).

Unlike the rice TBP1 mutant, the AtTBP1 mutant produced no phenotypic abnormalities beyond elongated telomeres, but *Arabidopsis* has six RTBP1 paralogs (Karamysheva et al. 2004). All six bind telomeric DNA in vitro and can form dimers with each other. Because the proteins are very similar to each other, they may be functionally redundant, such that elimination of only AtTBP1 does not cause the loss of chromosome end protection. Alternatively, the telomere-length-regulation

and end-protection functions of RTBP1 may be fulfilled by different proteins in *Arabidopsis.*

Whether *Arabidopsis* is unusual in possessing six homologs remains unclear. In rice, tobacco, and tomato, the RTBP1 homologs appear, from Southern blot analysis, to be single-copy, but such analysis would not detect more divergent RTBP1 homologs. Indeed, when we examined the rice genome database, a second candidate gene was detected (see Fig. 7.4). Alignment of the tobacco and tomato RTBP1 homologs with those from *Arabidopsis* shows that they group with AtTBP1 and its closest homolog, AtTRFL9 (Moriguchi et al. 2006). In poplar, a species closer to *Arabidopsis* than to tobacco and tomato, five RTBP1 homologs are detected (E. Shakirov, unpublished results). Occurrence of multiple RTBP1 homologs in plants would not be surprising, as many eukaryotes have two Myb-domain-containing double-strand telomere-binding proteins with different roles at the telomere.

The second family of myb-domain containing plant proteins, the TRBs, contains a myb-like domain with similarity to human TRF1 at their N-termini (Marian et al. 2003). TRB homologs were identified in maize (Smh1), rice, parsley, and *Arabidopsis* (AtTRB1, AtTRB2, and AtTRB3). As the RTBP1 homologs, the maize TRB protein, Smh1, and the *Arabidopsis* proteins, AtTRB2 and AtTRB3, bind double-strand telomere repeats in vitro (Marian et al. 2003). The TRB proteins are about 300 amino acids in length and contain a conserved globular domain in the middle of the protein similar to that found in the linker histones H1 and H5. At the C-terminus is a coiled-coil domain that may mediate protein–protein interactions.

EMSA indicates that TRB proteins bind duplex plant telomere sequences containing at least two repeats (Marian et al. 2003; Schrumpfova et al. 2004). The TRB proteins also bind the SS G-rich telomere repeat with high affinity (Schrumpfova et al. 2004). Interestingly, the *Arabidopsis* TRB's low level of binding to nonspecific SS oligonucleotides is increased by the addition of a small amount of the G-rich telomere repeat (Schrumpfova et al. 2004). *Arabidopsis* TRBs can form homodimers and heterodimers (Kuchar and Fajkus 2004; Schrumpfova et al. 2004). An in vitro interaction was detected between AtTRB1 and AtPOT1b (Kuchar and Fajkus 2004), a protein with some structural similarities to the human POT1.

Myb-domain-containing double-strand binding proteins in other eukaryotes do not contain linker histone domains or coiled-coil domains. Also, binding of both double-strand and SS telomere sequences by shelterin components is novel. Therefore, if the TRB proteins are bona fide telomere proteins, they represent a divergence in shelterin composition between plants and mammals. No direct evidence currently indicates that TRB proteins function at plant telomeres.

7.3.3 Shelterin Components as Transcription Factors

Shelterin components have been implicated as regulator elements in many eukaryotes. In fact, one of the first telomere proteins to be described is the yeast RAP1 protein, which was originally defined as a transcription factor (Shore and Nasmyth

1987). In plants, approximately one and a half copies of the telomere repeat, called a telobox in this context, function as regulatory elements in the promoter regions of many plant genes (Bilaud et al. 1996; Tremousaygue et al. 1999; Manevski et al. 2000). The maize RTBP1 homolog, ZmIBP1, was originally identified through an in vitro screen of proteins that bound the shrunken gene promoter (Lugert and Werr 1994), which also contains a telobox motif. Because it bound the promoter, had nuclear localization sequences, and had an N-terminal domain with some similarity to bacterial RNA polymerase binding domains, the primary role of ZmIBP1 was assumed to be that of transcription factor, but ZmIBP1 or other RTBP1 homologs have not been shown to affect transcription of any genes. Nevertheless, the ability of bona fide telomere proteins to bind to gene regulatory elements in vitro raises the possibility that properties required for telomere function could be coopted into gene-regulation networks.

The converse may also be true: the properties of proteins required for gene activation may also be of value for telomere functions. For example, the AtPURalpha gene was identified by screening of a phage library for proteins that bind to the telobox (Tremousaygue et al. 1999). AtPURalpha interacts with other transcription factors and transactivators. The DNA-binding domain of human PURalpha has been shown to open chromatin by locally destabilizing the double helix. Notably, this motif is well conserved between human and *Arabidopsis.* Given that AtPURalpha is capable of binding telomeric DNA in vitro, AtPURalpha could associate with telomeric DNA directing the chromatin remodeling associated with gene transcription to TRAs and affect telomere length and stability. Because many plant promoters contain teloboxes, including many controlled in a cell-cycle dependent fashion, further consideration of dual roles for telomere/transcription factors is warranted.

7.3.3.1 Single-Strand Binding Proteins

Oligonucleotide/Oligosaccharide-Fold-Containing Proteins

SS telomere binding proteins are critical components of shelterin complexes. The first was identified in ciliates, and subsequently additional members of this protein family were identified by sequence homology in other eukaryotes, including mammals and plants (Baumann et al. 2002). Members of this family of proteins share signature N-terminal oligonucleotide/oligosaccharide folds (OB-folds) and have been shown to regulate telomere length and protect chromosome ends. Because loss of the *Schizosaccharomyces pombe* SS telomere binding protein results in massive chromosome-end degradation and end-to-end chromosome fusions, these proteins were dubbed the protection-of-telomeres (POT1) proteins (Baumann and Cech 2001).

Like those of humans and *S. pombe*, most plant genomes encode only a single POT1 protein (E. Shakirov and D. Shippen, unpublished). *Arabidopsis* and other members of the Brassicaceae are unusual in that they encode two proteins with N-terminal POT-like OB-fold domains (Shakirov et al. 2005). Although POT1a and

POT1b clearly evolved from a common ancestor, they have greatly diverged and are now only ~50% similar at the amino-acid level. Both proteins have been implicated in telomere biology.

Overexpression of the C-terminus (non-OB-fold portion) of AtPOT1b leads to a drastic reduction in telomere length and frequent chromosome fusions manifested cytogenetically as anaphase bridges (Shakirov et al. 2005). Although this finding suggests a role in chromosome-end protection, complete removal of AtPOT1b by means of a T-DNA knockout has only a slight effect on G overhangs (E. Shakirov and D. Shippen, unpublished). Overexpression of a fragment of POT1b therefore probably has a dominant negative effect. Dominant negative proteins can have deleterious effects by associating with the normal binding partners, inhibiting their activity or titrating them out of functional associations. AtPOT1b, although dispensable for end-protection, may therefore interact with a key component of the shelterin complex.

The OB-fold of the AtPOT1a is less similar to the plant consensus sequence than the corresponding region of AtPOT1b. Furthermore, AtPOT1a is a physical component of the telomerase RNP complex rather than a shelterin component (Surovtseva et al. 2007 and discussion below). *Arabidopsis* also encodes a third POT1-like gene, *AtPOT1c*, which is a recent duplication of just the OB-fold of AtPOT1a. This gene's functional significance for telomere biology in *Arabidopsis* remains unknown.

Other Single-Strand Telomere Binding Proteins

POT1 proteins may not be the only group of SS-DNA-binding proteins present at telomeres. Through DNA affinity chromatography, an approach that, unlike computational searches, does not presuppose that plant SS-binding proteins will be similar to other eukaryotic proteins, several candidate SS telomere-binding proteins have been identified (Kwon and Chung 2004).

One protein to be identified in this fashion was the *Arabidopsis single-stranded telomere protein*, AtSTEP1 (Kwon and Chung 2004). AtSTEP1 binds telomeric DNA by means of a pair of RNA-binding motifs that are highly similar to those of the mammalian protein hnRNP A1/UP1. The mammalian protein has well-established roles in RNA shuttling but it has also been shown to function at telomeres. hnRNP A1/UP1 binds SS telomere repeats of both RNA and DNA with high affinity (LaBranche et al. 1998). It positively regulates telomere length (LaBranche et al. 1998), associates with telomerase, stimulates telomerase activity (Fiset and Chabot 2001), and localizes to chromosome ends (Zhang et al. 2006). It can simultaneously bind the TER template and SS telomere DNA, suggesting that it might function by directing telomerase to the G overhang (Fiset and Chabot 2001). Proteins such as AtSTEP1 and hnRNP A1/UP1 may not be part of the core shelterin complex, but like numerous other proteins with functions elsewhere in the cell, they may be coopted by shelterin to assist in telomere replication or stability.

A second SS telomere binding protein identified by DNA affinity chromatography is a transcription factor called *Arabidopsis* Whirly 1 (AtWHY1) (Yoo et al. 2007).

AtWHY1 has been shown to be involved in disease response and is part of a family of transcription factors with a pinwheel-shaped DNA-binding domain (Desveaux et al. 2004). Although the reasons why a telomere protein would function as a disease-resistance gene, or vice versa, is not clear, the in vitro assay clearly shows that AtWHY1 can bind SS telomere repeats. Furthermore, an AtWHY1 knock-out line has increased telomere length, and overexpression of AtWHY1 causes shorter telomeres (Yoo et al. 2007). Also, addition of either the full-length AtWHY1 protein or the WHY DBD increases telomerase activity in vitro.

7.4 Telomerase RNP in Plants

Telomerase is a multisubunit ribonucleoprotein complex. Although its catalytic core includes TERT and TER, a number of accessory factors have been identified that promote RNP biogenesis and telomere functions in vivo (Fig. 7.5).

7.4.1 TERT

TERT was the first protein identified in plants that is essential for telomerase activity. It was identified in a search of the *Arabidopsis* DNA databases with the protein sequence of the human telomerase reverse-transcriptase (Fitzgerald et al. 1999). Disruption of the *Arabidopsis* TERT gene leads to progressive telomere shortening, at a rate of ~200–500 bp per plant generation. In later generations, the telomere tract becomes too short to provide end protection and chromosomes are fused at the ends (Riha et al. 2001). Chromosome fusions can be observed as anaphase bridges or detected by PCR techniques beginning in the fourth generation of telomerase deficiency (G4), although plants still appear phenotypically normal. In subsequent generations, more and more cells contain fused chromosomes, and plants display defects in growth and development that are consistent with cell-proliferation failure.

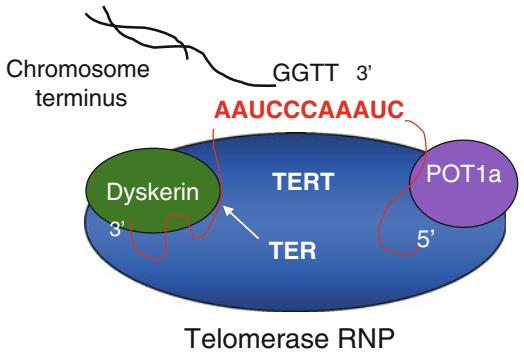

Fig. 7.5 Diagram of the *Arabidopsis* telomerase RNP. Shown are the known components of the enzyme, including the predicted RNA templating domain of TER, which is aligned with the 3′ G overhang on the chromosome terminus

By the tenth generation, all plants arrest in a miniature dedifferentiated state and do not produce seeds (Riha et al. 2001).

AtTERT is strongly expressed in highly proliferative tissues, such as flowers, and its expression is down-regulated in vegetative tissues (Fitzgerald et al. 1999). In contrast, the rice TERT is expressed in all tissues studied, although telomerase activity is low in vegetative tissue (Oguchi et al. 2004). The difference between expression and activity could be explained by the phosphorylation status of TERT. Telomerase activity in rice protein extracts, including leaf extracts, is stimulated by certain protein kinases and inhibited by phosphatases. Similarly, phosphorylation appears to modulate telomerase activity in tobacco (Tamura et al. 1999; Yang et al. 2002). In contrast, *Arabidopsis* telomerase activity is not affected by these treatments (Oguchi et al. 2004). Transcriptional regulation of TERT may therefore play a more prominent role in controlling telomerase in *Arabidopsis.*

In addition to developmental regulation of gene in expression, TERT levels may also be subject to control by cell-cycle and plant hormones (Tamura et al. 1999; Yang et al. 2002). Alternative splicing also appears to be a common feature of *TERT* gene expression from rice and *Arabidopsis* (Oguchi et al. 2004; Rossignol et al. 2007), but whether splicing plays a role in plant telomerase regulation as proposed in humans (Aisner et al. 2002) is not known.

7.4.1.1 Telomerase RNA Template

Telomerases use an internal RNA molecule to guide synthesis of the telomere repeats. The TER typically contains at least one and a half copies of the C-rich strand of the telomere repeat sequence. The SS G overhang on the telomere array end is complementary to the template region of TER. TER forms Watson-Crick base pairs with the G overhang, and TERT catalyzes addition of nucleotides by its reverse-transcriptase activity. After the 5′ end of the template is copied, the enzyme translocates, realigning the telomeric G-strand bases at the beginning of the template for another round of synthesis.

Characterization of TER in other species has established models for TER structure, function, and evolution. The TER sequences from several vertebrates have been determined and compared. The primary sequence of TER varies dramatically in length and composition, but computer modeling and phylogenetic analysis suggest similar secondary and tertiary structures (Chen et al. 2000). Comparison of TER sequences from more distantly related eukaryotes reveals several structural elements that are shared across kingdoms (Chen and Greider 2004a). Importantly, the template region is always single-stranded, reflecting its role in pairing with the telomeric overhang and guiding base-pair addition.

Although the genomes of two model plant species, rice and *Arabidopsis*, have been nearly completely sequenced, and extensive sequence information is available for many more, no examples of a plant TER have yet been reported. Computational methods for seeking TER sequences are complicated by several factors. First, the primary sequence of the TER gene is not expected to be well conserved, so searches based on similarities to known TER genes from other organisms are ruled out. Second, the telomere repeat sequence is present at many locations throughout plant

genomes, including many promoters. Therefore, searches for the expected template sequence, one and a half copies of the telomere repeat, find too many sequences for a candidate approach to be useful. Identification of plant TER genes will require biochemical approaches.

7.4.1.2 Dyskerin

Biochemically purified human telomerase complex includes TERT, TER, and dyserkin, a pseudouridyl synthase also implicated in processing of small nucleolar RNAs and rRNAs. Mutations in dyskerin lead to defects in telomere maintenance and give rise to the human disease dyskeratosis congenita. Human dyskerin stabilizes TER and helps it fold properly (Mitchell et al. 1999; Chen and Greider 2004b). Dyskerin has recently been shown to associate with the *Arabidopsis* telomerase RNP and to be required for maximum telomerase activity in vitro and in vivo (Kannan et al. 2008). Telomerase RNP composition and biogenesis therefore appear to be conserved among higher eukaryotes. Both dyskerin and *Arabidopsis* TERT are localized to the nucleolus (Rossignol et al. 2007; Kannan et al. 2008), suggesting that RNP assembly occurs in that cell compartment.

7.4.1.3 POT1a

Arabidopsis POT1a was identified as a telomere-related protein because it contains two predicted OB-folds with similarity to the *S. pombe* and human POT1 proteins. In contrast to POT1 from these other organisms, *Arabidopsis* POT1a does not have a direct role in chromosome end protection. Instead, it is required for telomere length maintenance (Shakirov et al. 2005; Surovtseva et al. 2007). Its disruption causes telomeres to shorten progressively, a phenotype indistinguishable from that of plants without functional TERT (Surovtseva et al. 2007). TRAP assays show that telomerase activity is reduced by about tenfold in POT1a-deficient plants.

Biochemical analysis indicates that *Arabidopsis* POT1a is physically associated with the telomerase RNP (Rossignol et al. 2007; Surovtseva et al. 2007). Chromatin immunoprecipitation (ChIP) of synchronized cell cultures revealed that AtPOT1a associates with telomeres during S-phase but not at other points in the cell cycle (Surovtseva et al. 2007). Furthermore, AtPOT1 and TERT association peaks during S-phase. Because AtPOT1a-deficient plants still retain a low level of telomerase, AtPOT1a is not an essential catalytic component of the telomerase enzyme. Instead, it may recruit or stabilize telomerase at chromosome ends.

A yeast-two-hybrid screen with AtPOT1a identified five putative interacting proteins, including TERT and a protein kinase (Rossignol et al. 2007). As shown for human telomerase, many different proteins may transiently associate with one or more telomerase RNP components to regulate its activity, either developmentally, through the cell-cycle, or in response to environmental stimuli.

7.5 Telomere Dynamics

7.5.1 Introduction

Maintenance of the telomere tract is essential for genome integrity. In all organisms, a species-specific telomere-length set point is achieved by a balance of forces that promote telomere elongation and those that result in telomere shortening. Here we review the major mechanisms involved in establishing and maintaining telomere length.

7.5.1.1 Telomere Length Is Highly Variable

Eukaryotic taxa differ widely in telomere length. At one extreme, some unicellular ciliates have telomeres of less than 50 bp, whereas human telomeres range from 6 to 10 kb and mouse telomeres from ~10 to 60 kb (McEachern et al. 2000). Plants also display dramatic variation in telomere lengths, from 2 to 5 kb in *Arabidopsis* to >150 kb in tobacco (Table 7.2). In addition, even different populations of the same species can differ in telomere length. Different *Arabidopsis* ecotypes and differ in telomere length by up to twofold (Shakirov and Shippen 2004; Maillet et al. 2006). Rice can vary similarly (Mizuno et al. 2006), and in maize the differences can be as great as 25-fold (Burr et al. 1992).

In *Arabidopsis*, eight out of ten chromosome arms harbor unique subtelomere sequences that allow these chromosome ends, including the length of the specific telomere tract, to be tracked individually (Heacock et al. 2004). The size of individual telomere tracts fluctuates within a size range defined for the plant, not specific chromosomes arms (Shakirov and Shippen 2004). The telomere length range is therefore set globally. Telomeres of progeny appear to be longer or shorter than those of the parents, moving toward an optimal species- or population-specific size. For the Columbia accession of *Arabidopsis*, this optimum appears to be 3.5 kb, and telomeres longer than this size gradually shorten in subsequent generations, whereas shorter ones are gradually extended. Differences in the ranges of telomere length among species or varieties probably reflect differences in the optimal set point.

7.5.1.2 Telomere Length Is Under Genetic Control

Although different plants have different telomere length ranges, the set point is under genetic control and is faithfully maintained across multiple generations (Shakirov and Shippen 2004; Maillet et al. 2006). In crosses between *Arabidopsis* accessions with different telomere lengths, the size range of F1 progeny is usually intermediate between those of the parents. In subsequent generations, the intermediate range is maintained, suggesting that more than one genetic factor contributes to telomere-length regulation (Shakirov and Shippen 2004; Maillet et al. 2006).

Table 7.2 Telomere lengths and sequences of plant species

Species	Telomere sequence	Telomere sequence (kb)	References
Green algae			
Chlamydomonas reinhardtii	TTTTAGGG	~0.3	Petracek et al. (1990)
Chlorella vulgaris	TTTAGGG	~0.5	Higashiyama et al. (1995)
Spikemosses			
Selaginella moellendorffii	TTTAGGG	0.5–5.5	Shakirov and Shippen (unpublished)
Gymnosperms			
Ginkgo biloba	TTTAGGG	3.6–5.2	Liu et al. (2007)
Pine	TTTAGGG	0.6–28	Flanary and Kletetschka (2005)
Angiosperms, dicotyledonous			
Tomato	TTTAGGG	20–60	Broun et al. (1992) and Ganal et al. (1991)
Tobacco	TTTAGGG	60–150	Fajkus et al. (1995)
Silene latifolia	TTTAGGG	2.5–4.5	Riha et al. (1998)
Arabidopsis thaliana	TTTAGGG	2–9[a]	Richards and Ausubel (1988) and Shakirov and Shippen (2004)
Carica papaya	TTTAGGG	10–60	Shakirov and Shippen (unpublished)
Angiosperms, monocotyledonous			
Hyacinthella dalmatica	TTAGGG	5–15	Puizina et al. (2003)
Othocallis siberica	TTAGGG	0.10	Weiss-Schneeweiss et al. (2004)
Maize	TTTAGGG	2–40[a]	Burr et al. (1992)
Barley	TTTAGGG	5–150	Kilian et al. (1995)
Rice	TTTAGGG	5–10	Mizuno et al. (2006)

[a]Individual plant accessions differ in telomere length

Quantitative-trait-locus analysis of telomere length indicates that three genetic loci control at least 50% of telomere length polymorphism in maize (Burr et al. 1992).

Although the major regulators of telomere length appear to be shelterin components and factors involved in forming or controlling telomerase, many additional classes of proteins have been found to influence telomere length, including DNA damage-response factors, DNA replication proteins, histone-modifying enzymes, transcription factors, and many others. A deletion screen of all nonessential yeast genes identified ~200 candidates whose absence resulted in deregulated telomeres (Askree et al. 2004). Although most of these genes probably affect telomere length indirectly, this study underscores the dynamic and complex nature of telomere length regulation.

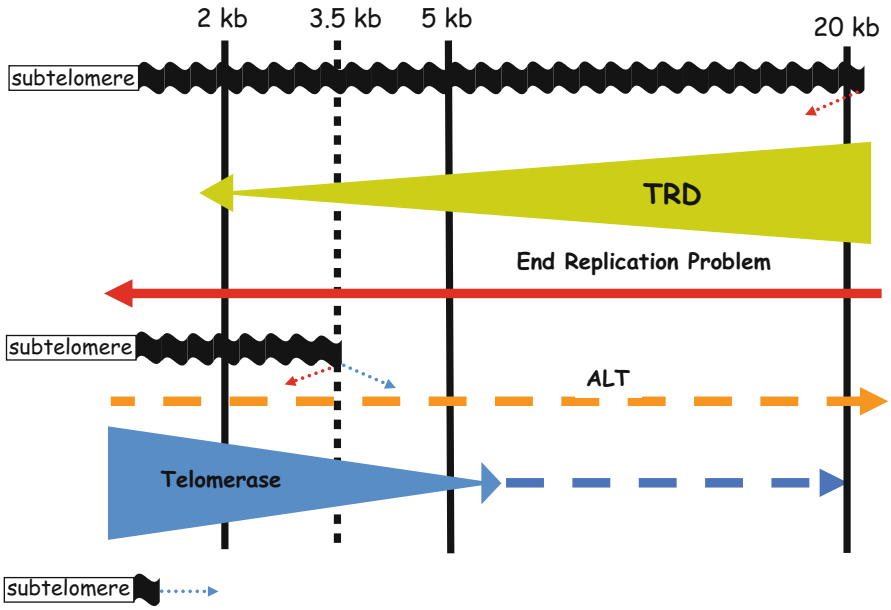

Fig. 7.6 Multiple forces contribute to the telomere length set point. Telomerase is the primary mechanism for lengthening telomeres and acts preferentially on short telomeres. Problems with end replication cause a constant decay of telomere length in dividing cells. Abrupt decreases in telomere length, called telomere rapid deletion (TRD), result from recombination-based mechanisms. Recombination can also lead to telomere length increase, called alternative lengthening of telomere (ALT). In the Columbia ecotype of *Arabidopsis*, the telomere-length set point is 3.5 kb. Telomeres longer than 3.5 kb tend to be shortened and shorter ones to be lengthened

7.5.2 Model of Telomere Length Homeostasis

To make sense of the bewildering array of factors that influence telomere length, we present a conceptual model in Fig. 7.6 that includes several general processes that either increase or decrease telomere length, including the forces that act in opposition to maintain the optimal set point. The major process that shortens telomeres is the end-replication problem, which stems from the inability of conventional DNA replication to replicate chromosome ends fully. Shortening can also arise from a recombination mechanism termed telomere rapid deletion (TRD) and by nuclease attack at chromosome ends. The main factor promoting telomere lengthening is telomerase, but additional means include a recombination mechanism termed alternative lengthening of telomeres (ALT). The model shown in Fig. 7.6 takes into account the observation that telomere length influences the degree to which these processes act, represented by tapered arrows in the diagram. For example, telomerase increases telomere length but is ineffective at long telomeres. How the length of the telomere is able to influence these processes is not known, but it probably involves the double-strand-binding components of shelterin as discussed later.

7.5.2.1 End-Replication Problem and End Processing

At every cell division, a small amount of telomere tract is lost on each chromosome because the DNA-replication machinery cannot copy the lagging strand. The amount lost is at least equal to the length of the RNA primer laid down by primase (Olovnikov 1971, 1973; Watson 1972). The resulting amount of erosion can be approximated by examination of telomeres in successive generations of a telomerase-deficient background. In *Arabidopsis* mutants with a disruption in TERT, approximately 200 bp are lost per generation (Fitzgerald et al. 1999; Shakirov and Shippen 2004). This relatively small loss suggests that the lagging-strand replication process is able to synthesize most of the telomere tract effectively. On the basis of an estimate of the number of cell divisions per plant generation (~1,000), this rate of telomere loss has been suggested to be too low for the end-replication problem so a lengthening process other than telomerase, perhaps the ALT process described below, may be acting (Fajkus et al. 2005).

Unlike telomerase and recombination, the loss of DNA to the end-replication problem is steady and not affected by telomere length (illustrated by a leftward facing arrow in the diagram). In contrast, perturbations in shelterin components can make the end sensitive to nuclease attack, as can perturbations to DNA repair and replication machinery. For example, loss of the *Arabidopsis* ATR, a key kinase involved in sensing accumulation of SS DNA at replication forks, combined with a telomerase deficiency causes telomeres to decay markedly faster (Vespa et al. 2005).

7.5.2.2 Addition of Telomere Repeats by Telomerase

Telomerase action is the primary mechanism for telomere extension and is regulated by a number of factors, including the production of telomerase RNP components, enzyme activity, and accessibility of individual chromosome ends.

Telomerase activity is low or undetectable in most differentiated human and vertebrate cells and is limited to reproductive organs, stem cells, and highly proliferative tissues (see e.g., Harley et al. 1990). As a result, telomeres shorten in somatic cells. In plants as well, telomerase activity is developmentally regulated and has been shown to be low or absent in leaves and other differentiated tissue (Fitzgerald et al. 1996; Kilian et al. 1998). In contrast, rapidly dividing cells, in plants or in cell culture, have elevated levels of telomerase activity (Fitzgerald et al. 1996), but unlike those of vertebrates, telomeres do not shorten in differentiated tissues for several plant species, including tomato (Broun et al. 1992), *Arabidopsis* (Riha et al. 1998), and *S. latifolia* (Riha et al. 1998). Although telomerase activity is low in differentiating tissues, fewer cell divisions take place there, so little telomere extension may be required to counteract the end-replication problem. Lack of telomere shortening in differentiated tissues is not universal among plants. For example, telomeres in barley shorten several folds during growth and aging (Kilian et al. 1995).

Even when telomerase is active in cells, it does not extend all telomeres equally. In mammals, the number of telomerase RNP complexes is rate limiting, and their activity is directed to the shortest telomeres (Liu et al. 2002). Although none of the

known *Arabidopsis* telomerase components is limiting (Kannan et al. 2008), the enzyme does preferentially extend short telomeres (Shakirov and Shippen 2004). The Ku70/Ku80 heterodimer in plants negatively regulates telomerase (Riha et al. 2002), and *Arabidopsis* plants null for *KU70* or *KU80* display dramatic telomere elongation; telomeres are extended by as much as 15 kb per generation (Riha et al. 2002; Gallego et al. 2003; Watson and Shippen 2007). In a single generation, the bulk telomere length becomes twice that of the wild type (Riha et al. 2002). The extension depends on the presence of telomerase (Gallego et al. 2003; Riha and Shippen 2003), and by the third mutant generation, a new set point is achieved. In both mammals and yeast, KU physically associates with the telomerase RNP and is involved in telomerase regulation (Stellwagen et al. 2003; Ting et al. 2005), but in contrast to the situation in plants, it is a positive regulator of telomerase extension.

The recruitment of telomerase to short telomeres is regulated by shelterin. In yeast, Marcand et al. (1997) have proposed that a certain number of telomere double-strand-binding proteins (Rap1) must coat the telomere tract to make it inaccessible to telomerase. When the number of telomere protein-binding sites drops below optimal, the telomeres undergo a shift to the more open state, allowing telomerase to engage. Telomerase will add enough telomeric repeats to restore the optimal number of telomere protein-binding sites, and the telomere will resume a closed state, inaccessible by telomerase.

7.5.2.3 Recombination Pathways for Telomere Length Maintenance

Telomere Rapid Deletion

TRD is the abrupt shortening of individual telomere tracts (Li and Lustig 1996), as opposed to the gradual telomere decay caused by the end-replication problem. In mammals and yeast, it can result when the Holiday junction-like structure at the base of the T-loop is "resolved," releasing the T-loop as an extrachromosomal circle. Recombination between two telomeres, usually sister chromatids, can also cause abrupt shortening. Telomeric interchromatid exchange is rare under most circumstances but is frequent in cells employing ALT to maintain their telomeres (see later). Because all repeats in the telomere are oriented in the same direction, interchromatid exchange at telomeres is detected cytologically by strand-specific FISH (explained in Fig. 7.7). Although this technique has been used in plants to examine the orientation of subtelomeric repeats (Navratilova et al. 2005), it has only been used to detect sister-chromatid exchanges at telomeres in mammalian cells (Bailey et al. 2004). The first evidence for TRD in *Arabidopsis* was obtained by tracking of individual telomere lengths (Shakirov and Shippen 2004). Occasional drops in telomere length from one generation to the next, or within an individual plant, were observed that were greater than the loss expected from the end-replication problem (Shakirov and Shippen 2004; Watson and Shippen 2007). Moreover, in plants lacking KU, extrachromosomal telomere circles accumulate that presumably arise from TRD (Zellinger et al. 2007).

Because TRD involves the removal of the T-loop, it is predicted to cause larger deletions when the telomere is long enough to form large T-loops. Several proteins

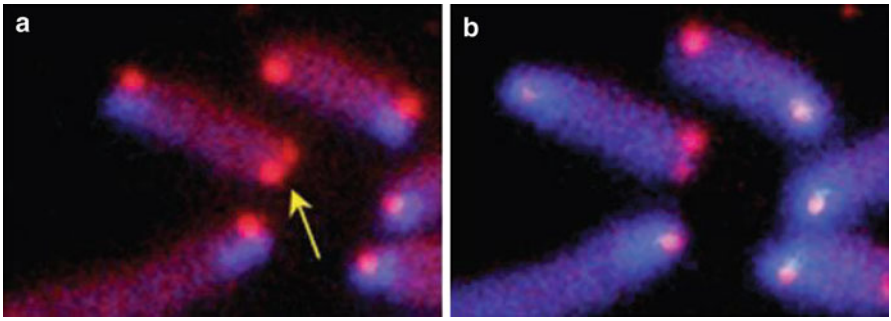

Fig. 7.7 Chromosome orientation FISH (co-FISH) allows detection of mitotic recombination. The co-FISH technique allows a single DNA strand to be detected in each sister chromatid. Cells are incubated with bromosubstituted nucleotides, which are incorporated into the newly synthesized strand. After fixation and chromosome spreading, the substituted strand is nicked by exposure to UV and removed with exonuclease III. A single-stranded probe is used for FISH to label only one chromatid of each chromosome arm. (**a**) Chromosomes are probed with the C-rich telomere probe and (**b**) are stripped and reprobed with the G-rich probe. The opposite chromatids are labeled in (**a**) and (**b**). The *arrow* in (**a**) indicates a chromosome end that has signal on both chromatids, indicating a mitotic recombination event. Probing with the G-rich strand also produces signal on both chromatids; signal on the opposite chromatid is more intense. This image of human chromosomes is from Bailey et al. (2004)

with primary roles in DNA repair are implicated in limiting TRD in *Arabidopsis* mutants deficient in Ku70/Ku80, AtATM, and AtRad50 (Vannier et al. 2006; Vespa et al. 2007; Zellinger et al. 2007). The increase in frequency and size of TRD events prevents unlimited telomere-length increase in the absence of KU, and a new set point is achieved that balances the rapid extension of telomeres by telomerase and increased telomere loss by TRD (Watson and Shippen 2007).

Although TRD appears to play a minor role in telomere-length homeostasis in the short telomere of Columbia ecotype *Arabidopsis*, it may be more important in plants with longer telomeres. For example, telomeres in barley are both longer (5–150 kb) and more variable than those in *Arabidopsis* (2–5 kb in Columbia ecotype), and they rapidly shorten in differentiating tissues as telomerase activity is reduced (Kilian et al. 1995). In resting wheat embryos, extra-chromosomal telomere circles are abundant, but then lost upon germination when cell division resumes (Bucholc and Buchowicz 1995), suggesting that TRD acts to limit telomere length in this case.

Alternative Lengthening of Telomeres

After multiple cell divisions, telomeres in mammalian and yeast cells deficient for telomerase become critically shortened and cause cells to stop dividing. A small portion of the cells that can use a recombination-based strategy to increase and maintain telomere length then begin to grow again. The extrachromosomal circles

released by resolution of the Holiday junction at the base of the T-loop can be copied by a rolling-circle mechanism and generates long TRAs that are added to chromosomes by recombination (Cesare and Griffith 2004). The frequent interchromatid exchanges observed at telomeres in cells using ALT could also lead to telomere length increases in a portion of cells (Bailey et al. 2004).

Like telomerase-deficient human and yeast cells, cells in liquid cell culture derived from eighth-generation (G8) telomerase-negative *Arabidopsis* plants go through a crisis that includes genome instability followed by reconstitution of the cell population by a small number of cells that begin dividing again (Watson et al. 2005). In contrast to other "survivor" cell populations, the plant cells showed no ALT-like mechanism, and telomeres were not reextended. Instead, the telomere sequence is largely lost from the cells, but the genome is somehow stabilized, and cells continue to divide. The underlying mechanism for survival of these cells is unknown.

In two subsequent studies, evidence for telomere extension by ALT was observed in telomerase-negative *Arabidopsis* plants (Watson and Shippen 2007; Zellinger et al. 2007). Although the bulk telomere length decreases, individual telomeres are occasionally extended. ALT frequencies are greater in KU-deficient plants, and cell-culture lines derived from plants lacking both KU and telomerase can be established that maintain their telomeres by ALT (Zellinger et al. 2007). Because they are mechanistically related, repression of both TRD and ALT by KU is not surprising.

7.6 Consequences of Telomere Dysfunction

When telomeres lose their ability to protect the chromosome termini, the chromosomes fuse with one another to form dicentric chromosomes and enter the breakage-fusion-bridge cycle first described by McClintock (1939, 1941), which results in genome instability, loss or duplication of genetic material, and usually cell death. Telomere failure can occur when the TRA becomes too small to accommodate shelterin formation or when critical components of shelterin become compromised. One of the most spectacular examples of telomere failure is found in human cells that are induced to express a dominant negative form of the double-strand telomere binding protein TRF2. In this case, the bulk telomeres do not shorten. Instead, chromosomes immediately become uncapped, and chromosome ends join to create a long chain of chromosomes (Van Steensel et al. 1998). In plants, knocking out the rice TRF-like protein RTBP1 also produces chromosome fusions (Hong et al. 2007), but the effect is not immediate or as devastating as that of the dominant negative human TRF2. Other shelterin components can therefore partially compensate for RTBP1 loss.

Because telomerase deficiency is not immediately lethal in *Arabidopsis*, this plant has served as a model for study of the process of chromosome uncapping that occurs as telomeres become critically shortened (Fig. 7.8). Plants with a T-DNA insert in TERT survive for up to ten homozygous generations, although telomeres shorten each generation. When a critical size threshold for telomeres is reached,

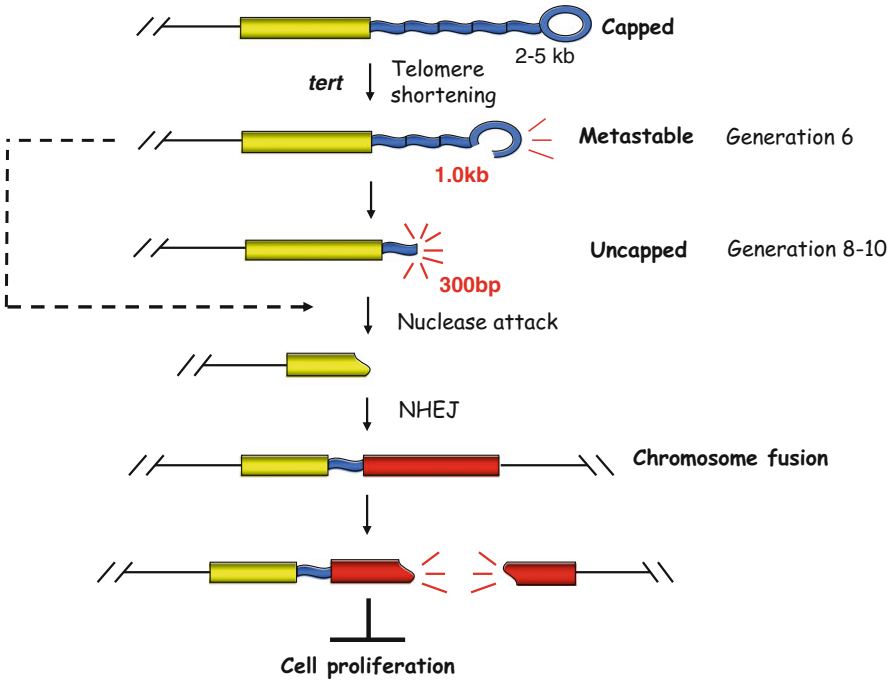

Fig. 7.8 Model for telomere dynamics in telomerase-deficient *Arabidopsis*. In wild-type plants, telomeres range in length from 2 to 5 kb and can readily form T-loops. In the absence of telomerase, telomeres shorten progressively through successive plant generations. By the sixth generation of a telomerase deficiency, when the shortest telomeres reach a length of ~1 kb, end-to-end chromosome fusion is initiated; 1 kb is termed the metastable length and represents a critical size threshold. Telomeres below this threshold may be too short to assume a stable T-loop conformation. Not all telomeres fuse when they reach 1 kb, however, and bulk telomere tracts continue to shorten. The terminal plant generation is reached in generations 8–10, when the shortest telomeres are ~300 bp. All the telomeres become completely uncapped at this point and are subject to extensive nuclease digestion and then nonhomologous end joining (NHEJ). Chromosome fusions result from NHEJ, and the chromosomes enter the bridge-breakage fusion cycle ultimately leading to cessation of cell proliferation

~1,000 bp in *Arabidopsis*, chromosome arms begin to fuse (Heacock et al. 2004). Examination of fusions reveals that the minimal functional telomere length, i.e., telomere tracts that retain a G overhang and are not joined by NHEJ, is only ~300 bp (Heacock et al. 2004), so 1,000 bp may be a "metastable" length at which the protective properties of the telomere are partially compromised and allow rapid telomere erosion. This threshold may reflect the minimal length needed for stable T-loop formation. Telomeres continue to shorten below 1,000 bp and ultimately end-joining occurs on all chromosome ends when telomere tracts reach 300 bp. Starting from the fifth generation, morphological and reproductive defects appear, and plants became increasingly sick and sterile (Fig. 7.9).

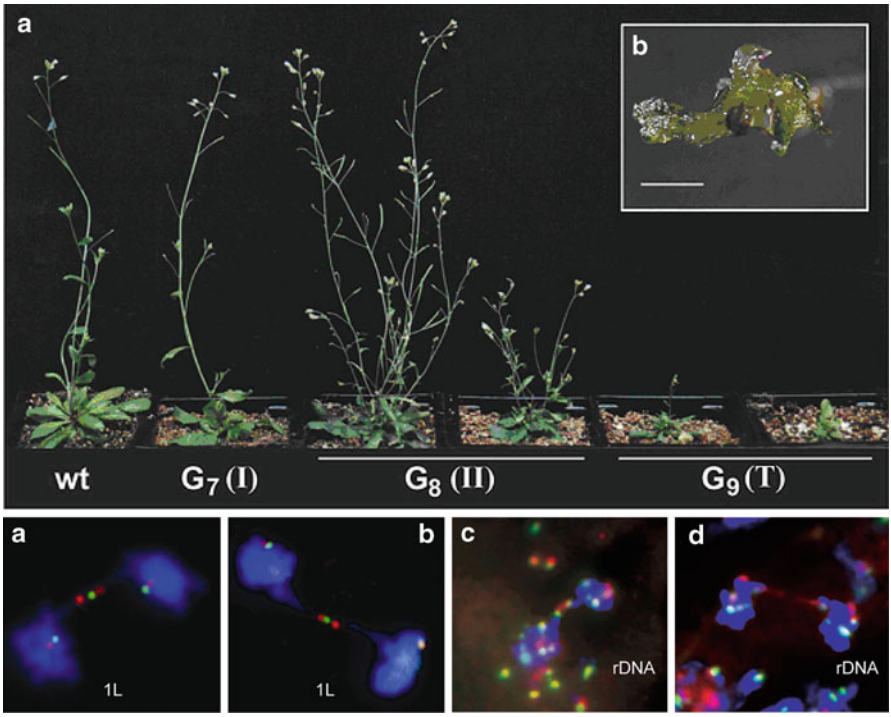

Fig. 7.9 Telomerase-deficient plants have developmental abnormalities and fused chromosomes in later generations. (**1a** and **1b**) Wild-type plants and *tert* mutants lacking telomerase activity. In generations one through six (G1–G6) most mutants resemble the wild type. Starting in G6–G7, some plants display mild mutant phenotypes (I), including smaller, asymmetric leaves. In subsequent generations, mutant plants show more pronounced mutant phenotypes (II) that include multiple stems, curled leaves, and partial sterility. The terminal phenotype (T) of late-generation mutant plants is developmental arrest in a vegetative state (**1b**). Concurrent with the onset of developmental irregularities, chromosome fusions are observed (**2a–d**). Fusions are detected cytologically as bridged chromosomes at mitotic anaphase. (**2a** and **2b**) FISH was performed on chromosome preparations containing anaphase bridges with a subtelomeric BAC on chromosome 1L (*red*) and the telomere repeat (*green*). These images show sister-chromatid fusions. (**2c** and **2d**) FISH was performed with the 25S (*red*) and 5S (*green*) ribosomal gene clusters. The 25S ribosomal gene cluster is adjacent to the telomere on chromosomes 2L and 4L. Images in **1** from Riha et al. (2001), those in **2** from Vespa et al. (2007)

Terminal-generation plants remain metabolically active but are unable to reproduce and display a highly dedifferentiated callus-like shoot apical meristem (Riha et al. 2001). The onset of morphological defects is correlated with the accumulation of critically shortened telomeres and an increased number of chromosome aberrations, as manifested by anaphase bridges. Anaphase bridges are evident in at the fifth generation and increase from 0.7% to over 40% in terminal plant generations. In addition, late-generation plants often display multiple chromosomes stretched between the segregating chromosomes (Fig. 7.9).

By means of subtelomere-specific FISH probes, the chromosomes involved in end fusions can be identified cytologically (Fig. 7.9). Typically, only one or a few arms account for most of the fusions, and in many cases fusion involves sister-chromatid fusions (Siroky et al. 2003; Mokros et al. 2006; Vespa et al. 2007). The arm or arms that fuse have the shortest telomeres in the genome (Vespa et al. 2007). Examination of the fusion junctions reveals that uncapped chromosome ends are joined by a hierarchy of conventional NHEJ mechanisms (Heacock et al. 2004, 2007).

7.7 Role of Telomeres in Chromosome Movement and Positioning

7.7.1 The Rabl Structure

During mitotic anaphase, sister chromatids are pulled to the newly forming daughter cells by the centromeres, and the chromosome arms trail behind. After the daughter cells reform, the organization of the chromosomes in the nuclei reflects the segregation process. The centromeres and telomeres are located on opposite sides of the nucleus, and telomeres are clustered adjacent to the plane of cell division (see Fig. 7.10). This pattern was first reported in 1885 by Rabl (1885) and is known as the Rabl configuration. Although the forces exerted on chromosomes during anaphase are clearly sufficient to organize them into the Rabl configuration, unconstrained diffusion within the nucleus would lead to a random distribution of centromeres and telomeres. In many species, however, the nucleus remains polarized during interphase after chromosomes have decondensed.

The mechanism that maintains this arrangement is not known, nor is its functional significance. Few experiments have been reported that directly address this phenomenon in any organism apart from yeast. In yeast, telomeres are tethered to the nuclear envelope by multiple mechanisms. Telomere positioning and the silent state of chromatin in regions adjacent to telomeres are mutually reinforcing (reviewed by Pandita et al. 2007), but the strong silencing near yeast telomeres is not a general feature of chromosome ends, the degree to which the yeast model is applicable to other organisms is not clear. In human and mouse, the telomeric DNA is attached to the nuclear matrix, not the nuclear envelope, and a binding site occurs at least every 1 kb (Luderus et al. 1996). Although the composition and function of the nuclear matrix are uncertain, association with structural components of the nucleus could limit or direct telomere movement and thereby contribute to retention of the Rabl conformation.

Nuclear positioning of chromosomes would facilitate compartmentalization of the nucleus and local enrichment of the various complexes required for nuclear processes. For example, heterochromatin-determining components could be located in one portion of the nucleus together with the heterochromatic portions of the Rabl-oriented chromosomes (Cowan et al. 2001). A nuclear compartmentalization model

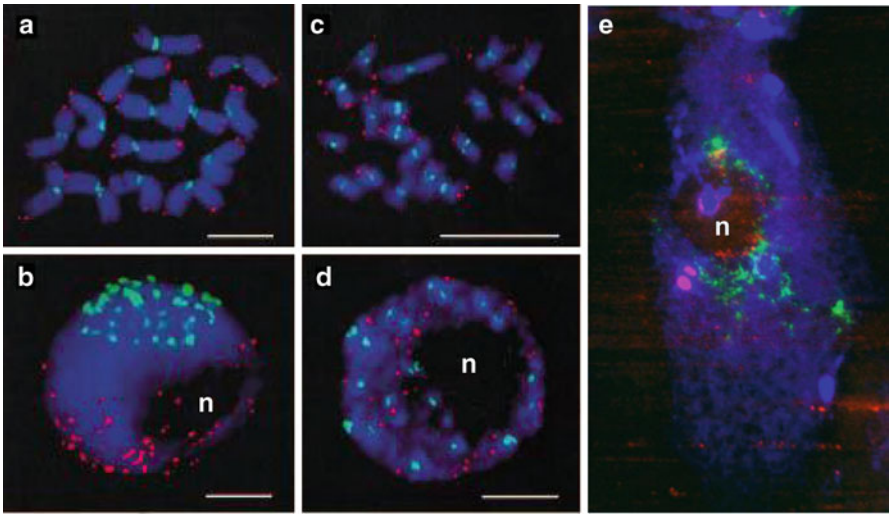

Fig. 7.10 Patterns of telomere distribution in the interphase plant nuclei. (**a**) Rye metaphase chromosome spread and (**b**) interphase nucleus from wheat, labeled by FISH with centromeric (*green*) and telomere (*red*) DNA probes. The chromosomes and nuclei were counterstained with DAPI (*blue*). (**c**) Metaphase chromosome spread and (**d**) interphase nucleus from sorghum (*Sorghum bicolor* (L.) Moench.) root tips hybridized to centromere (*green*) and telomere (*red*) probes. The chromosomes and nuclei were counterstained with DAPI. (**e**) Endoreduplicated *Arabidopsis* cell labeled with a mixture of eight subtelomeric BACs (*green*) and the telomere repeat (*red*). "n" denotes the location of the nucleolus. The Rabl arrangement of chromosomes is evident in wheat nuclei but is absent from sorghum. In *Arabidopsis*, telomeres cluster in and around the nucleolus. All bars are 10 μm. Images (**a**–**d**) from Dong and Jiang (1998), (**e**) provided by JCL

is especially attractive as an explanation for telomere positioning. Sequestering telomeres into a nuclear region that excludes some DNA-repair mechanisms could complement the protective role of the shelterin complex in shielding telomeres from DSB repair. In yeast, repair of DSBs near telomeres is less efficient when telomere localization is perturbed (Therizols et al. 2006), so DNA repair at telomeres differs from that of the rest of the genome and is related to nuclear position.

Species with larger genomes tend to have more pronounced Rabl organization (Cowan et al. 2001). Interestingly, the Rabl conformation is not observed in diploid cells in rice, but it is present in endoreduplicated xylem vessel cells (Prieto et al. 2004). As discussed earlier, the presence of large arrays of satellites adjacent to telomeres is common. These heterochromatic blocks may well affect the nuclear position of telomeres. Indeed, among plant species surveyed, a correlation between the presence of distal heterochromatic blocks and the persistence of the Rabl conformation in interphase was observed (Dong and Jiang 1998).

Telomere position in *Arabidopsis* is unusual in that the Rabl configuration does not persist after mitosis. Instead, telomeres are clustered around the nucleolus (Fig. 7.10). This arrangement has not been noted in other plants and may be a recent adaptation. Given the relatively small genome of *Arabidopsis*, some of the hypothesized benefits

of a Rabl nucleus may not be important. Because the *Arabidopsis* telomerase RNP is located in the nucleolus, this organization could allow telomeres to be extended without placing telomerase in contact with the rest of the genome, an arrangement that might decrease the likelihood of inadvertent telomere addition to a DSB.

7.7.2 Bouquet Formation During Meiosis

During meiotic prophase, a telomere clustering called the meiotic bouquet is observed in all plant species and nearly all eukaryotes. The formation and function of the bouquet has been reviewed (Cowan et al. 2001; Harper et al. 2004; Scherthan 2006, 2007; de La Roche Saint-André 2007) and is covered extensively in the chapter on meiosis in the present volume, so it will be only briefly discussed here.

Because bouquet formation typically occurs just before homologous chromosome alignment, the bouquet is commonly thought to be involved in this process as well as in chromosome synapsis. The arrangement formed by the meiotic bouquet brings all the chromosome ends to one location and orients them in roughly the same direction, reducing the effective volume of homology search. This explanation for bouquet formation is very attractive, as it explains the general conservation of the bouquet by connecting it to another conserved process, chromosome pairing, but several lines of evidence suggest that bouquet formation is not essential for chromosome alignment but rather serves to make the process more efficient (Harper et al. 2004).

Although telomere clustering occurs in both Rabl and bouquet formation, the mechanisms responsible are likely to be different (Cowan et al. 2001). Like the Rabl conformation, the degree of telomere clustering in the bouquet differs with plant species; some (e.g., rye and wheat) show tight clustering and others (e.g., maize and lily) a looser arrangement (Cowan et al. 2001). Unlike the Rabl conformation, however, this arrangement does not involve centromeres. In some species, the Rabl conformation does not persist into interphase in somatic cells, but the bouquet is still formed, albeit loosely, in meiosis. In others, hexaploid wheat for example, telomeres are clustered into the Rabl conformation and are brought together even more tightly during meiotic prophase (Cowan et al. 2001). Yet another pattern is observed in maize; the loose Rabl conformation seen in somatic cells dissolves in early meiosis, and the bouquet is formed subsequently (Carlton and Cande 2002). Bouquet formation therefore does not require telomeres to be preoriented in the Rabl conformation.

Recent work in mice, yeast, and plants, especially maize, has provided some information about the process and mechanisms that form the meiotic bouquet (reviewed by Harper et al. 2004; Scherthan 2006, 2007). Briefly, after cells enter meiosis, telomeres associate with the nuclear envelope at random and then move along the inner surface of the nuclear envelope. This movement is directed in such a way that the telomeres are brought together in plants at the nuclear cortex or region of low microtubule abundance (Cowan et al. 2002). At this stage, nuclear pores are concentrated on the opposite side of the nucleus from the bouquet. In other

organisms, the bouquet is located next to the microtubule organizing center (Scherthan 2007). As telomeres move toward the site of bouquet formation, they can come into contact with other telomeres and form associations. Bouquet dissolution depends on cohesin and may be delayed until completion of recombinational repair of DNA breaks induced early in meiosis.

The TRAs themselves are critical for bouquet formation. Centromere misdivision creates a broken end at a centromere that can be healed by de novo telomere addition to the broken end. The telomeres of maize chromosomes created by this process participate in bouquet formation despite being located next to active centromeres (Carlton and Cande 2002). In addition, the meiotic behavior of TRAs contained in circular chromosomes has been characterized (Carlton and Cande 2002). Because these arrays are not at the physical end of the chromosome, they cannot be considered true telomeres. Nevertheless, they cluster with true telomeres, demonstrating that the telomere repeat tract itself causes participation in the meiotic bouquet. In contrast, small ring chromosomes lacking telomere repeats do not localize to the bouquet in mice meiocytes, yet they still pair correctly (Voet et al. 2003).

In yeast, telomere-binding proteins are required for proper bouquet formation (Scherthan 2007). Meiosis-specific proteins have been identified in yeast that attach telomeres to the nuclear envelope by binding to a telomere-associated protein and an inner-nuclear-envelope-bound protein (a protein with a SUN domain) (de La Roche Saint-André 2007). The SUN-domain protein associates with an outer-nuclear-membrane-protein that links the cytoplasmic cytoskeleton (especially actin) to telomeres, causing telomere movement (de La Roche Saint-André 2007). The mechanism by which telomeres stick together is not known, but attachment to the microtubule organizing center appears to involve cohesin and/or other components. In mammals as well, proteins containing SUN domains have been identified and shown to be involved in anchoring telomeres to the nuclear envelope and attaching telomeres to structures in the cytoplasm (Ding et al. 2007; Schmitt et al. 2007). The mechanism for telomere movement during meiosis is therefore at least partly conserved from yeast to mammals, but a meiotic linker protein has neither been identified in mammals nor have the telomere proteins required for bouquet formation. Proteins with the SUN domain are also present in plants, although their role in bouquet formation is untested.

Identification of factors required for the bouquet in other eukaryotes has not been easy. Because TRAs are sufficient in *cis* to direct chromosomal loci to participate in the bouquet, shelterin components are likely to be involved, perhaps through associations with nuclear-envelope-bound proteins. In addition, the chromatin state of the telomere or subtelomere may play a role in nuclear envelope attachment and bouquet formation.

Although the meiotic bouquet is nearly ubiquitous in eukaryotes, *Arabidopsis thaliana* may be an exception. During meiotic interphase and early prophase, telomeres cluster around the nucleolus, in a localization pattern similar to that in somatic interphase cells (Armstrong et al. 2001). Telomere signals range from 10 to 20 ($2n = 10$), and the number decreases to ten by mid- to late leptotene, suggestive of pairing at the chromosome termini. By late leptotene, telomeres have dispersed

from around the nucleolus to become widely distributed in the nucleus. A modest telomere clustering that resembles a meiotic bouquet appears briefly in zygotene (Armstrong et al. 2001). The perinucleolar pattern of telomere distribution in *Arabidopsis*, although different from a classical bouquet, could nevertheless function similarly to foster chromosome alignment. Alternatively, the brief appearance of the loose bouquet during zygotene may in fact be the canonical bouquet, whereas the perinucleolar localization at earlier stages may be caused by the unusual somatic organization of *Arabidopsis* telomeres.

7.8 De Novo Telomere Formation

DSBs can be repaired by several distinct pathways in eukaryotic cells, including homologous recombination, NHEJ, and the de novo formation of telomeres at the broken ends. Telomere formation at breaks away from the extreme chromosome termini lead to the production of chromosome fragments without centromeres that would be lost in subsequent cell divisions. Accordingly, broken ends are processed predominantly by other DNA-repair mechanisms; spontaneous de novo telomere formation (DNTF) is a rare event. It has been studied mostly in *S. cerevisiae*, and a few studies have addressed it in human cells, but two recent papers describing applications of DNTF to engineering of plant chromosomes have been published, and additional work on this topic is probably forthcoming.

7.8.1 Telomere Formation from a Nontelomeric Substrate

Functional telomeres require both the array of telomere repeats and the proteins associated with them, so for DNTF to occur, a TRA must be generated at the broken end and be bound by the shelterin complex. When it is present, telomerase can generate the repeats needed to form a telomere. In vitro, telomerase efficiently extends substrates that terminate with sequences containing less than a single telomere repeat (Fitzgerald et al. 1996). Because only a few base pairs of homology are required, DSBs at many locations in the genome would expose potential telomerase extension sites, but because DNTF is rare, most broken ends appear to be refractory to telomerase, or alternatively, the enzyme may be inhibited or sequestered after DNA damage.

In yeast, DNTF is prevented by a helicase, Pif1, that disrupts telomerase template annealing to overhangs (Schulz and Zakian 1994; Zhou et al. 2000). Spontaneous DNTF can be detected by the loss of nonessential marker genes placed at the ends of chromosomes. In the absence of Pif1, spontaneous DNTF is much more frequent. Telomere addition occurs mostly at sequences that could serve as telomerase template-annealing sites. When Pif1 elimination is combined with mutations that reduce the efficiency of DNA repair, the frequency of spontaneous DNTF events increases synergistically (Myung et al. 2001).

In human cells, telomerase access to broken ends may be limited by sequestering of the telomerase enzyme in the nucleolus. In normal human fibroblasts, GFP-tagged telomerase accumulates in the nucleolus (Wong et al. 2002), where it associates with nucleolin (Khurts et al. 2004). Nucleolar localization is less pronounced or abolished during DNA replication when telomerase acts to extend telomeres. In some cell lines, transgenic telomerase can accumulate throughout the nucleus, but inducing DNA damage with ionizing radiation causes telomerase to be rapidly relocated to the nucleolus (Wong et al. 2002). Sequestration in the nucleolus during most of the cell cycle or upon DNA damage spatially separates telomerase from DSBs.

7.8.2 Telomere Formation at Telomere Repeat Arrays

In yeast, induction of a DNA break near a TRA at interstitial locations can lead to telomere formation and chromosome truncation (Pennaneach et al. 2006). Recent work in mammals showing that the shelterin complex can repress DNA repair in vitro (Bae and Baumann 2007) provides a likely explanation for this phenomenon. Shelterin can assemble at the interstitial TRA (Mignon-Ravix et al. 2002), predisposing it to telomere formation. When a break is introduced adjacent to the TRA, the shelterin complex inhibits DNA repair, recruits telomerase, and folds the TRA into a T-loop.

In mammalian cells, transgenically introduced TRAs can acquire telomere function and cause truncation of the chromosome at the site of transgene integration. As little as 250 bp of telomere sequence is sufficient to generate de novo telomeres in mammalian cells, although the percentage of total transformation events that result in DNTF is greater when longer arrays are used (Okabe et al. 2000). Cellular levels of human TRF1 are correlated with the efficiency of transgenic-TRA-seeded DNTF events (Okabe et al. 2000), so the availability of shelterin components may be rate limiting for the conversion of telomere sequences into a bona fide telomeres with protective and replicative functions.

DNTF using transgenic TRAs has recently been demonstrated in plant cells (Fig. 7.11). Use of either *Agrobacterium* (Yu et al. 2006) or biolistics (Yu et al. 2007) to deliver transgene constructs containing a selectable marker and a 2.6-kb TRA into maize cells resulted in recovery of plants in which the TRA acquired telomere function, resulting in chromosome truncation. DNTF events were detected cytologically by use of FISH to visualize the transgene position and confirmed by molecular approaches.

Chromosome truncation efficiencies were modest (8.7% when *Agrobacterium* was used) compared to frequencies observed in mammalian cells, but the actual frequency may be higher, as some events may not have been recovered if loss of genetic material prevented regeneration of whole plants. Consistent with this hypothesis, truncation frequencies were higher for a dispensable B chromosome than for the standard complement (Yu et al. 2007).

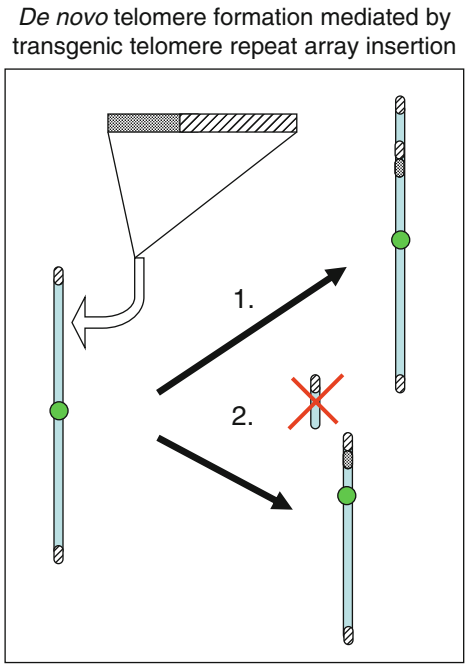

Fig. 7.11 Model for de novo telomere formation mediated by transgenic TRA insertion. Upon integration of a transgene containing a TRA (*slanted lines*), the transgene can be inserted at an internal position in the chromosome (*1*), or the TRA can become a functional telomere (*2*). If the TRA forms a telomere, the chromosome is truncated at the site of insertion

7.8.3 Application of DNTF for Chromosome Engineering

The primary goal of the DNTF studies in maize was the generation of artificial chromosome vectors. Such chromosomes could be used to carry multiple transgenes, allowing whole gene pathways to be transformed into a single plant and segregated as a single genetic unit. This process would offer a number of important advantages over inserting transgenes at random. For example, movement of the transgene complex could be accomplished by a simple backcross scheme without concern for genetic drag. Also, expression levels from a given promoter would be more predictable, as the "artificial" chromosome vector would provide a known chromatin environment into which additional transgenes could be placed.

Yu and coworkers used DNTF to truncate naturally occurring supernumerary B chromosomes and add sequence-specific recombination sites (Yu et al. 2007). Because they are stably maintained in the maize genome and have almost no effect on plant phenotype, maize B chromosomes should make ideal vectors for transgene expression. The minichromosomes that were generated segregate independently from other chromosomes in the complement and could be stably maintained over sexual generations. Minichromosomes were generated in maize by removal of the arms of chromosome 7, leaving just the region near the centromere (Yu et al. 2007). Surprisingly, the minichromosome did not pair with its progenitor chromosome during meiosis and instead segregated independently, despite retaining a substantial amount

of centromere-proximal sequence (Yu et al. 2007). This procedure demonstrated the feasibility of generating artificial chromosome vectors by whittling down regular chromosomes by TRA-mediated chromosome truncation.

Acknowledgments Research in the Shippen laboratory is funded by grants from the National Institutes of Health (GM065383) and the National Science Foundation (MCB-0349993 and MCB-0615928). Dr. Jonathan Lamb is supported by a Ruth L. Kirchstein National Research Service postdoctoral fellowship award from the National Institutes of Health (F32GM080005). Because of the nature and scope of this chapter, we were unable to cite all relevant publications in this field, and apologize to our colleagues whose work was not discussed here.

References

Adams SP, Leitch IJ, Bennett MD, Leitch AR (2000) *Aloe* L.—a second plant family without $(TTTAGGG)_n$ telomeres. *Chromosoma* 109:201–205

Adams SP, Hartman TP, Lim KY, Chase MW, Bennett MD, Leitch IJ, Leitch AR (2001) Loss and recovery of *Arabidopsis*-type telomere repeat sequences 5′-(TTTAGGG)(n)-3′ in the evolution of a major radiation of flowering plants. *Proc R Soc Lond B Biol Sci* 268:1541–1546

Aisner, DL, Wright WE, Shay JW (2002) Telomerase regulation: not just flipping the switch. *Curr Opin Genet Dev* 12:80–85

Armstrong SJ, Franklin FC, Jones GH (2001) Nucleolus-associated telomere clustering and pairing precede meiotic chromosome synapsis in *Arabidopsis thaliana. J Cell Sci* 114:4207–4217

Askree SH, Yehuda T, Smolikov S, Gurevich R, Hawk J, Coker C, Krauskopf A, Kupiec M, McEachern MJ (2004) A genome-wide screen for *Saccharomyces cerevisiae* deletion mutants that affect telomere length. *Proc Natl Acad Sci USA* 101:8658–8663

Bae NS, Baumann P (2007) A RAP1/TRF2 complex inhibits nonhomologous end-joining at human telomeric DNA ends. *Mol Cell* 26:323–334

Bailey SM, Brenneman MA, Goodwin EH (2004) Frequent recombination in telomeric DNA may extend the proliferative life of telomerase-negative cells. *Nucleic Acids Res* 32:3743–3751

Bao W, Zhang W, Yang Q, Zhang Y, Han B, Gu M, Xue Y, Cheng Z (2006) Diversity of centromeric repeats in two closely related wild rice species, *Oryza officinalis* and *Oryza rhizomatis. Mol Genet Genomic*s 275:421–430

Barnes SR, James AM, Jamieson G (1985) The organisation, nucleotide sequence, and chromosomal distribution of a satellite DNA from *Allium cepa. Chromosoma* 92:185–192

Baumann P, Cech TR (2001) Pot1, the putative telomere end-binding protein in fission yeast and humans. *Science* 292:1171–1175

Baumann P, Podell E, Cech TR (2002) Human Pot1 (protection of telomeres) protein: cytolocalization, gene structure, and alternative splicing. *Mol Cell Biol* 22:8079–8087

Bilaud T, Koering CE, Binet-Brasselet E, Ancelin K, Pollice A, Gasser SM, Gilson E (1996) The telobox, a Myb-related telomeric DNA binding motif found in proteins from yeast, plants and human. *Nucleic Acids Res* 24:1294–1303

Blasco MA (2007) The epigenetic regulation of mammalian telomeres. *Nat Rev Genet* 8:299–309

Broun P, Ganal MW, Tanksley SD (1992) Telomeric arrays display high levels of heritable polymorphism among closely related plant varieties. *Proc Natl Acad Sci USA* 89:1354–1357

Bucholc M, Buchowicz J (1995) An extrachromosomal fragment of telomeric DNA in wheat. *Plant Mol Biol* 27:435–439

Burr B, Burr FA, Matz EC, Romero-Severson J (1992) Pinning down loose ends: mapping telomeres and factors affecting their length. *Plant Cell* 4:953–960

Carlton PM, Cande WZ (2002) Telomeres act autonomously in maize to organize the meiotic bouquet from a semipolarized chromosome orientation. *J Cell Biol* 157:231–242

Cesare AJ, Griffith JD (2004) Telomeric DNA in ALT cells is characterized by free telomeric circles and heterogeneous t-loops. *Mol Cell Biol* 24:9948–9957
Cesare AJ, Quinney N, Willcox S, Subramanian D, Griffith JD (2003) Telomere looping in *P. sativum* (common garden pea). *Plant J* 36: 271–279
Chen CM, Wang CT, Ho CH (2001) A plant gene encoding a Myb-like protein that binds telomeric GGTTAG repeats in vitro. *J Biol Chem* 276:16511–16519
Chen JL, Greider CW (2004a) An emerging consensus for telomerase RNA structure. *Proc Natl Acad Sci USA* 101:14683–14684
Chen JL, Greider CW (2004b) Telomerase RNA structure and function: implications for dyskeratosis congenita. *Trends Biochem Sci* 29:183–192
Chen JL, Blasco MA, Greider CW (2000) Secondary structure of vertebrate telomerase RNA. *Cell* 100:503–514
Cheng Z, Stupar RM, Gu M, Jiang J (2001) A tandemly repeated DNA sequence is associated with both knob-like heterochromatin and a highly decondensed structure in the meiotic pachytene chromosomes of rice. *Chromosoma* 110:24–31
Cowan CR, Carlton PM, Cande WZ (2001) The polar arrangement of telomeres in interphase and meiosis. Rabl organization and the bouquet. *Plant Physiol* 125:532–538
Cowan CR, Carlton PM, Cande WZ (2002) Reorganization and polarization of the meiotic bouquet-stage cell can be uncoupled from telomere clustering. *J Cell Sci* 115:3757–3766
Cox AV, Bennett ST, Parokonny AS, Kenton A, Callimassia MA, Bennett MD (1993) Comparison of plant telomere locations using a PCR-generated synthetic probe. *Ann Bot (Lond)* 72: 239–247
de Bruin D, Kantrow SM, Liberatore RA, Zakian VA (2000) Telomere folding is required for the stable maintenance of telomere position effects in yeast. *Mol Cell Biol* 20:7991–8000
de Bruin D, Zaman Z, Liberatore RA, Ptashne M (2001) Telomere looping permits gene activation by a downstream UAS in yeast. *Nature* 409:109–113
de Lange T (2005) Shelterin: the protein complex that shapes and safeguards human telomeres. *Genes Dev* 19:2100–2110
de La Roche Saint-André C (2007) Alternative ends: telomeres and meiosis. *Biochimie* 90:181–189
Denchi EL, de Lange T (2007) Protection of telomeres through independent control of ATM and ATR by TRF2 and POT1. *Nature* 448:1068–1071
Desveaux D, Subramaniam R, Despres C, Mess JN, Levesque C, Fobert PR, Dangl JL, Brisson N (2004) A "Whirly" transcription factor is required for salicylic acid-dependent disease resistance in *Arabidopsis. Dev Cell* 6:229–240
Ding X, Xu R, Yu J, Xu T, Zhuang Y, Han M (2007) SUN1 is required for telomere attachment to nuclear envelope and gametogenesis in mice. *Dev Cell* 12:863–872
Dong F, Jiang J (1998) Non-Rabl patterns of centromere and telomere distribution in the interphase nuclei of plant cells. *Chromosome Res* 6:551–558
Fajkus J, Trifonov EN (2001) Columnar packing of telomeric nucleosomes. *Biochem Biophys Res Commun* 280:961–963
Fajkus J, Kovarik A, Kralovics R, Bezdek M (1995) Organization of telomeric and subtelomeric chromatin in the higher plant *Nicotiana tabacum. Mol Gen Genet* 247: 633–638
Fajkus J, Sykorova E, Leitch AR (2005) Telomeres in evolution and evolution of telomeres. *Chromosome Res* 13:469–479
Fiset S, Chabot B (2001) hnRNP A1 may interact simultaneously with telomeric DNA and the human telomerase RNA in vitro. *Nucleic Acids Res* 29:2268–2275
Fitzgerald MS, McKnight TD, Shippen DE (1996) Characterization and developmental patterns of telomerase expression in plants. *Proc Natl Acad Sci USA* 93:14422–14427
Fitzgerald MS, Riha K, Gao F, Ren S, McKnight TD, Shippen DE (1999) Disruption of the telomerase catalytic subunit gene from *Arabidopsis* inactivates telomerase and leads to a slow loss of telomeric DNA. *Proc Natl Acad Sci USA* 96:14813–14818
Flanary BE, Kletetschka G (2005) Analysis of telomere length and telomerase activity in tree species of various life-spans, and with age in the bristlecone pine *Pinus longaeva. Biogerontology* 6:101–111

Fuchs J, Brandes A, Schubert I (1995) Telomere sequence localization and karyotype evolution in higher plants. *Plant Syst Evol* 196:227–241

Gallego ME, Jalut N, White CI (2003) Telomerase dependence of telomere lengthening in Ku80 mutant *Arabidopsis. Plant Cell* 15:782–789

Ganal MW, Lapitan NLV, Tanksley SD (1991) Macrostructure of the tomato telomeres. *Plant Cell* 3:87–94

Griffith JD, Comeau L, Rosenfield S, Stansel RM, Bianchi A, Moss H, de Lange T (1999) Mammalian telomeres end in a large duplex loop. *Cell* 97:503–514

Harley CB, Futcher AB, Greider CW (1990) Telomeres shorten during aging of human fibroblasts. *Nature* 345:458–460

Harper L, Golubovskaya I, Cande WZ (2004) A bouquet of chromosomes. *J Cell Sci* 117: 4025–4032

Heacock M, Spangler E, Riha K, Puizina J, Shippen DE (2004) Molecular analysis of telomere fusions in *Arabidopsis:* multiple pathways for chromosome end-joining. *EMBO J* 23:2304–2313

Heacock ML, Idol RA, Friesner JD, Britt AB, Shippen DE (2007) Telomere dynamics and fusion of critically shortened telomeres in plants lacking DNA ligase IV. *Nucleic Acids Res* 35:6490–6500

Higashiyama T, Maki S, Yamada T (1995) Molecular organization of *Chlorella vulgaris* chromosome I: presence of telomeric repeats that are conserved in higher plants. *Mol Gen Genet* 246:29–36

Hong JP, Byun MY, Koo DH, An K, Bang JW, Chung IK, An G, Kim WT (2007) Suppression of RICE TELOMERE BINDING PROTEIN1 results in severe and gradual developmental defects accompanied by genome instability in rice. *Plant Cell* 19:1770–1781

Horakova M, Fajkus J (2000) TAS49—a dispersed repetitive sequence isolated from subtelomeric regions of *Nicotiana tomentosiformis* chromosomes. *Genome* 43:273–284

Hsu HL, Gilley D, Galande SA, Hande MP, Allen B, Kim SH, Li GC, Campisi J, Kohwi-Shigematsu T, Chen DJ (2000) Ku acts in a unique way at the mammalian telomere to prevent end joining. *Genes Dev* 14:2807–2812

Hwang MG, Cho MH (2007) *Arabidopsis thaliana* telomeric DNA-binding protein 1 is required for telomere length homeostasis and its Myb-extension domain stabilizes plant telomeric DNA binding. *Nucleic Acids Res* 35:1333–1342

Hwang MG, Chung IK, Kang BG, Cho MH (2001) Sequence-specific binding property of *Arabidopsis thaliana* telomeric DNA binding protein 1 (AtTBP1). *FEBS Lett* 503:35–40

Hwang MG, Kim K, Lee WK, Cho MH (2005) AtTBP2 and AtTRP2 in *Arabidopsis* encode proteins that bind plant telomeric DNA and induce DNA bending in vitro. *Mol Genet Genomics* 273:66–75

Kamnert I, Lopez CC, Rosen M, Edstrom JE (1997) Telomeres terminating with long complex tandem repeats. *Hereditas* 127:175–180

Kannan K, Nelson AD, Shippen DE (2008) Dyskerin is a component of the *Arabidopsis* telomerase RNP required for telomere maintenance. *Mol Cell Biol* 28:23332–2341

Karamysheva ZN, Surovtseva YV, Vespa L, Shakirov EV, Shippen DE (2004) A C-terminal Myb extension domain defines a novel family of double-strand telomeric DNA-binding proteins in *Arabidopsis. J Biol Chem* 279:47799–47807

Khan SJ, Yanez G, Seldeen K, Wang H, Lindsay SM, Fletcher TM (2007) Interactions of TRF2 with model telomeric ends. *Biochem Biophys Res Commun* 363:44–50

Khurts S, Masutomi K, Delgermaa L, Arai K, Oishi N, Mizuno H, Hayashi N, Hahn WC, Murakami S (2004) Nucleolin interacts with telomerase. *J Biol Chem* 279:51508–51515

Kilian A, Stiff C, Kleinhofs A (1995) Barley telomeres shorten during differentiation but grow in callus culture. *Proc Natl Acad Sci USA* 92:9555–9559

Kilian A, Heller K, Kleinhofs A (1998) Developmental patterns of telomerase activity in barley and maize. *Plant Mol Biol* 37:621–628

Kuchar M, Fajkus J (2004) Interactions of putative telomere-binding proteins in *Arabidopsis thaliana:* identification of functional TRF2 homolog in plants. *FEBS Lett* 578:311–315

Kuo HF, Olsen KM, Richards EJ (2006) Natural variation in a subtelomeric region of *Arabidopsis:* implications for the genomic dynamics of a chromosome end. *Genetics* 173:401–417

Kwon C, Chung IK (2004) Interaction of an *Arabidopsis* RNA-binding protein with plant single-stranded telomeric DNA modulates telomerase activity. *J Biol Chem* 279:12812–12818

LaBranche H, Dupuis S, Ben-David Y, Bani M-R, Wellinger RJ, Chabot B (1998) Telomere elongation by hnRNP A1 and a derivative that interacts with telomeric repeats and telomerase. *Nat Genet* 19:199–202

Lamb JC, Meyer JM, Corcoran B, Kato A, Han F, Birchler JA (2007) Distinct chromosomal distributions of highly repetitive sequences in maize. *Chromosome Res* 15:33–49

Lee HR, Zhang W, Langdon T, Jin W, Yan H, Cheng Z, Jiang J (2005) Chromatin immunoprecipitation cloning reveals rapid evolutionary patterns of centromeric DNA in *Oryza* species. *Proc Natl Acad Sci USA* 102:11793–11798

Linardopoulou EV, Williams EM, Fan Y, Friedman C, Young JM, Trask BJ (2005) Human subtelomeres are hot spots of interchromosomal recombination and segmental duplication. *Nature* 437:94–100

Liu Y, Kha H, Ungrin M, Robinson MO, Harrington L (2002) Preferential maintenance of critically short telomeres in mammalian cells heterozygous for mTert. *Proc Natl Acad Sci USA* 99:3597–3602

Liu D, Qiao N, Song H, Hua X, Du J, Lu H, Li F (2007) Comparative analysis of telomeric restriction fragment lengths in different tissues of Ginkgo biloba trees of different age. *J Plant Res* 120:523–528

Lopez CC, Nielsen L, Edstrom JE (1996) Terminal long tandem repeats in chromosomes form *Chironomus pallidivittatus. Mol Cell Biol* 16:3285–3290

Luderus ME, van Steensel B, Chong L, Sibon OC, Cremers FF, de Lange T (1996) Structure, subnuclear distribution, and nuclear matrix association of the mammalian telomeric complex. *J Cell Biol* 135:867–881

Lugert T, Werr W (1994) A novel DNA-binding domain in the Shrunken initiator-binding protein (IBP1). *Plant Mol Biol* 25:493–506

Li B, Lustig AJ (1996) A novel mechanism for telomere size control in *Saccharomyces cerevisiae*. *Genes Dev* 10:1310–1326

Macas J, Meszaros T, Nouzova M (2002) PlantSat: a specialized database for plant satellite repeats. *Bioinformatics* 18:28–35

Maillet G, White CI, Gallego ME (2006) Telomere-length regulation in inter-ecotype crosses of *Arabidopsis. Plant Mol Biol* 62:859–866

Manevski A, Bertoni G, Bardet C, Tremousaygue D, Lescure B (2000) In synergy with various cis-acting elements, plant interstitial telomere motifs regulate gene expression in *Arabidopsis* root meristems. *FEBS Lett* 483:43–46

Marcand S, Gilson E, Shore D (1997) A protein-counting mechanism for telomere length regulation in yeast. *Science* 275:986–990

Marian CO, Bordoli SJ, Goltz M, Santarella RA, Jackson LP, Danilevskaya O, Beckstette M, Meeley R, Bass HW (2003) The maize Single myb histone 1 gene, Smh1, belongs to a novel gene family and encodes a protein that binds telomere DNA repeats in vitro. *Plant Physiol* 133:1336–1350

May BP, Lippman ZB, Fang Y, Spector DL, Martienssen RA (2005) Differential regulation of strand-specific transcripts from *Arabidopsis* centromeric satellite repeats. *PLoS Genet* 1:e79

McClintock B (1939) The behavior in successive nuclear divisions of a chromosome broken at meiosis. *Proc Natl Acad Sci USA* 25:405–416

McClintock B (1941) The stability of broken ends of chromosomes in *Zea mays. Genetics* 26:234–282

McEachern MJ, Krauskopf A, Blackburn EH (2000) Telomeres and their control. *Annu Rev Genet* 34:331–358

Mefford HC, Trask BJ (2002) The complex structure and dynamic evolution of human subtelomeres. *Nat Rev Genet* 3: 91–102

Mignon-Ravix C, Depetris D, Delobel B, Croquette MF, Mattei MG (2002) A human interstitial telomere associates in vivo with specific TRF2 and TIN2 proteins. *Eur J Hum Genet* 10: 107–112

Mitchell JR, Wood E, Collins K (1999) A telomerase component is defective in the human disease dyskeratosis congenita. *Nature* 402:551–555

Mizuno H, Wu J, Kanamori H, Fujisawa M, Namiki N, Saji S, Katagiri S, Katayose Y, Sasaki T, Matsumoto T (2006) Sequencing and characterization of telomere and subtelomere regions on rice chromosomes 1S, 2S, 2L, 6L, 7S, 7L and 8S. *Plant J* 46:206–217

Moens PB, Pearlman RE (1990a) Telomere and centromere DNA are associated with the cores of meiotic prophase chromosomes. *Chromosoma* 100:8–14

Moens PB, Pearlman RE (1990b) In situ DNA sequence mapping with surface-spread mouse pachytene chromosomes. *Cytogenet Cell Genet* 53:219–220

Mokros P, Vrbsky J, Siroky J (2006) Identification of chromosomal fusion sites in *Arabidopsis* mutants using sequential bicolour BAC-FISH. *Genome* 49:1036–1042

Moriguchi R, Kanahama K, Kanayama Y (2006) Characterization and expression analysis of the tomato telomere-binding protein LeTBP1. *Plant Sci* 171:166–174

Munoz-Jordan JL, Cross GA, de Lange T, Griffith JD (2001) t-loops at trypanosome telomeres. *EMBO J* 20:579–588

Murti KG, Prescott DM (1999) Telomeres of polytene chromosomes in a ciliated protozoan terminate in duplex DNA loops. *Proc Natl Acad Sci USA* 96:14436–14439

Myung K, Chen C, Kolodner RD (2001) Multiple pathways cooperate in the suppression of genome instability in *Saccharomyces cerevisiae. Nature* 411:1073–1076

Navratilova A, Neumann P, Macas J (2005) Long-range organization of plant satellite repeats investigated using strand-specific FISH. *Cytogenet Genome Res* 109:58–62

Oguchi K, Tamura K, Takahashi H (2004) Characterization of *Oryza sativa* telomerase reverse transcriptase and possible role of its phosphorylation in the control of telomerase activity. *Gene* 342:57–66

Ohmido N, Kijima K, Akiyama Y, de Jong JH, Fukui K (2000) Quantification of total genomic DNA and selected repetitive sequences reveals concurrent changes in different DNA families in *indica* and *japonica* rice. *Mol Gen Genet* 263:388–394

Ohmido N, Kijima K, Ashikawa I, de Jong JH, Fukui K (2001) Visualization of the terminal structure of rice chromosomes 6 and 12 with multicolor FISH to chromosomes and extended DNA fibers. *Plant Mol Biol* 47:413–421

Okabe J, Eguchi A, Masago A, Hayakawa T, Nakanishi M (2000) TRF1 is a critical trans-acting factor required for de novo telomere formation in human cells. *Hum Mol Genet* 9:2639–2650

Olovnikov AM (1971) Principle of marginotomy in template synthesis of polynucleotides. *Dokl Akad Nauk SSSR* 201:1496–1499

Olovnikov AM (1973) A theory of marginotomy. The incomplete copying of template margin in enzymic synthesis of polynucleotides and biological significance of the phenomenon. *J Theor Biol* 41:181–190

Pandita TK, Hunt CR, Sharma GG, Yang Q (2007) Regulation of telomere movement by telomere chromatin structure. *Cell Mol Life Sci* 64:131–138

Pennaneach V, Putnam CD, Kolodner RD (2006) Chromosome healing by de novo telomere addition in *Saccharomyces cerevisiae*. *Mol Microbiol* 59:1357–1368

Petracek ME, Lefebvre PA, Silflow CD, Berman J (1990) *Chlamydomonas* telomere sequences are A+T-rich but contain three consecutive G-C base pairs. *Proc Natl Acad Sci USA* 87:8222–8226

Pich U, Fuchs J, Schubert I (1996) How do Alliaceae stabilize their chromosome ends in the absence of TTTAGGG sequences? *Chromosome Res* 4:207–213

Prieto P, Santos AP, Moore G, Shaw P (2004) Chromosomes associate premeiotically and in xylem vessel cells via their telomeres and centromeres in diploid rice (*Oryza sativa*). *Chromosoma* 112:300–307

Puizina J, Weiss-Schneeweiss H, Pedrosa-Harand A, Kamenjarin J, Trinajstic I, Riha K, Schweizer D (2003) Karyotype analysis in *Hyacinthella dalmatica* (Hyacinthaceae) reveals vertebrate-type telomere repeats at the chromosome ends. *Genome* 46:1070–1076

Rabl C (1885) Uber Zelltheilung. *Morphol Jahrb* 10:214–330

Richards EJ, Ausubel FM (1988) Isolation of a higher eukaryotic telomere from *Arabidopsis thaliana. Cell* 53:127–136

Richards EJ, Chao S, Vongs A, Yang J (1992) Characterization of *Arabidopsis thaliana* telomeres isolated in yeast. *Nucleic Acids Res* 20:4039–4046

Riha K, Shippen DE (2003) Ku is required for telomeric C-rich strand maintenance but not for end-to-end chromosome fusions in *Arabidopsis. Proc Natl Acad Sci USA* 100:611–615

Riha K, Fajkus J, Siroky J, Vyskot B (1998) Developmental control of telomere lengths and telomerase activity in plants. *Plant Cell* 10:1691–1698

Riha K, McKnight TD, Griffing LR, Shippen DE (2001) Living with genome instability: plant responses to telomere dysfunction. *Science* 291:1797–1800

Riha K, Watson JM, Parkey J, Shippen DE (2002) Telomere length deregulation and enhanced sensitivity to genotoxic stress in *Arabidopsis* mutants deficient in Ku70. *EMBO J* 21:2819–2826

Rossignol P, Collier S, Bush M, Shaw P, Doonan JH (2007) *Arabidopsis* POT1A interacts with TERT-V(I8), an N-terminal splicing variant of telomerase. *J Cell Sci* 120:3678–3687

Rotkova G, Sklenickova M, Dvorackova M, Sykorova E, Leitch AR, Fajkus J (2004) An evolutionary change in telomere sequence motif within the plant section Asparagales had significance for telomere nucleoprotein complexes. *Cytogenet Genome Res* 107:132–138

Scherthan H (2006) Factors directing telomere dynamics in synaptic meiosis. *Biochem Soc Trans* 34:550–553

Scherthan H (2007) Telomere attachment and clustering during meiosis. *Cell Mol Life Sci* 64: 117–124

Schmitt J, Benavente R, Hodzic D, Hoog C, Stewart CL, Alsheimer M (2007) Transmembrane protein Sun2 is involved in tethering mammalian meiotic telomeres to the nuclear envelope. *Proc Natl Acad Sci USA* 104:7426–7431

Schrumpfova P, Kuchar M, Mikova G, Skrisovska L, Kubicarova T, Fajkus J (2004) Characterization of two *Arabidopsis thaliana* myb-like proteins showing affinity to telomeric DNA sequence. *Genome* 47:316–324

Schulz VP, Zakian VA (1994) The *Saccharomyces* PIF1 DNA helicase inhibits telomere elongation and de novo telomere formation. *Cell* 76:145–155

Shakirov EV, Shippen DE (2004) Length regulation and dynamics of individual telomere tracts in wild-type *Arabidopsis. Plant Cell* 16:1959–1967

Shakirov EV, Surovtseva YV, Osbun N, Shippen DE (2005) The *Arabidopsis* Pot1 and Pot2 proteins function in telomere length homeostasis and chromosome end protection. *Mol Cell Biol* 25:7725–7733

Sharma S, Raina SN (2005) Organization and evolution of highly repeated satellite DNA sequences in plant chromosomes. *Cytogenet Genome Res* 109:15–26

Shore D, Nasmyth K (1987) Purification and cloning of a DNA binding protein from yeast that binds to both silencer and activator elements. *Cell* 51:721–732

Siroky J, Zluvova J, Riha K, Shippen DE, Vyskot B (2003) Rearrangements of ribosomal DNA clusters in late generation telomerase-deficient *Arabidopsis. Chromosoma* 112:116–123

Song K, Jung D, Jung Y, Lee SG, Lee I (2000) Interaction of human Ku70 with TRF2. *FEBS Lett* 481:81–85

Stellwagen AE, Haimberger ZW, Veatch JR, Gottschling DE (2003) Ku interacts with telomerase RNA to promote telomere addition at native and broken chromosome ends. *Genes Dev* 17:2384–2395

Sue SC, Hsiao HH, Chung BC, Cheng YH, Hsueh KL, Chen CM, Ho CH, Huang TH (2006) Solution structure of the *Arabidopsis thaliana* telomeric repeat-binding protein DNA binding domain: a new fold with an additional C-terminal helix. *J Mol Biol* 356:72–85

Surovtseva YV, Shakirov EV, Vespa L, Osbun N, Song X, Shippen DE (2007) *Arabidopsis* POT1 associates with the telomerase RNP and is required for telomere maintenance. *EMBO J* 26:3653–3661

Suzuki K (2004) Characterization of telomere DNA among five species of pteridophytes and bryophytes. *J Bryol* 26:175–180

Sykorova E, Fajkus J, Ito M, Fukui K (2001) Transition between two forms of heterochromatin at plant subtelomeres. *Chromosome Res* 9:309–323

Sykorova E, Cartagena J, Horakova M, Fukui K, Fajkus J (2003a) Characterization of telomere-subtelomere junctions in *Silene latifolia. Mol Genet Genomics* 269:13–20

Sykorova E, Lim KY, Chase MW, Knapp S, Leitch IJ, Leitch AR, Fajkus J (2003b) The absence of *Arabidopsis*-type telomeres in *Cestrum* and closely related genera *Vestia* and *Sessea* (Solanaceae): first evidence from eudicots. *Plant J* 34:283–291

Sykorova E, Lim KY, Fajkus J, Leitch AR (2003c) The signature of the *Cestrum* genome suggests an evolutionary response to the loss of (TTTAGGG)n telomeres. *Chromosoma* 112:164–172

Sykorova E, Lim KY, Kunicka Z, Chase MW, Bennett MD, Fajkus J, Leitch AR (2003d) Telomere variability in the monocotyledonous plant order Asparagales. *Proc R Soc Lond B Biol Sci* 270:1893–1904

Sykorova E, Fajkus J, Meznikova M, Lim KY, Neplechova K, Blattner FR, Chase MW, Leitch AR (2006a) Minisatellite telomeres occur in the family Alliaceae but are lost in *Allium. Am J Bot* 93:814–823

Sykorova E, Leitch AR, Fajkus J (2006b) Asparagales telomerases which synthesize the human type of telomeres. *Plant Mol Biol* 60:633–646

Tamura K, Liu H, Takahashi H (1999) Auxin induction of cell cycle regulated activity of tobacco telomerase. *J Biol Chem* 274:20997–21002

Therizols P, Fairhead C, Cabal GG, Genovesio A, Olivo-Marin JC, Dujon B, Fabre E (2006) Telomere tethering at the nuclear periphery is essential for efficient DNA double strand break repair in subtelomeric region. *J Cell Biol* 172:189–199

Ting NS, Yu Y, Pohorelic B, Lees-Miller SP, Beattie TL (2005) Human Ku70/80 interacts directly with hTR, the RNA component of human telomerase. *Nucleic Acids Res* 33:2090–2098

Tremousaygue D, Manevski A, Bardet C, Lescure N, Lescure B (1999) Plant interstitial telomere motifs participate in the control of gene expression in root meristems. *Plant J* 20:553–561

Ugarkovic D, Plohl M (2002) Variation in satellite DNA profiles—causes and effects. *EMBO J* 21:5955–5959

van Steensel B, Smogorzewska A, de Lange T (1998) TRF2 protects human telomeres from end-to-end fusions. *Cell* 92:401–413

Vannier JB, Depeiges A, White C, Gallego ME (2006) Two roles for Rad50 in telomere maintenance. *EMBO J* 25:4577–4585

Vershinin AV, Schwarzacher T, Heslop-Harrison JS (1995) The large-scale genomic organization of repetitive DNA families at the telomeres of rye chromosomes. *Plant Cell* 7:1823–1833

Vershinin AV, Heslop-Harrison JS (1998) Comparative analysis of the nucleosomal structure of rye, wheat and their relatives. *Plant Mol Biol* 36:149–161

Vespa L, Couvillion M, Spangler E, Shippen DE (2005) ATM and ATR make distinct contributions to chromosome end protection and the maintenance of telomeric DNA in *Arabidopsis. Genes Dev* 19:2111–2115

Vespa L, Warrington RT, Mokros P, Siroky J, Shippen DE (2007) ATM regulates the length of individual telomere tracts in *Arabidopsis. Proc Natl Acad Sci USA* 104:18145–18150

Voet T, Liebe B, Labaere C, Marynen P, Scherthan H (2003) Telomere-independent homologue pairing and checkpoint escape of accessory ring chromosomes in male mouse meiosis. *J Cell Biol* 162:795–807

Watson JD (1972) Origin of concatemeric T7 DNA. Nat New Biol 239:197–201

Watson JM, Shippen DE (2007) Telomere rapid deletion regulates telomere length in *Arabidopsis thaliana. Mol Cell Biol* 27:1706–1715

Watson JM, Bulankova P, Riha K, Shippen DE, Vyskot B (2005) Telomerase-independent cell survival in *Arabidopsis thaliana. Plant J* 43:662–674

Weiss H, Scherthan H (2002) *Aloe* spp.—plants with vertebrate-like telomeric sequences. *Chromosome Res* 10:155–164

Weiss H, Scherthan H, Pfosser M, Schweizer D (2001) Telomeric sequences in chromosomes of *Aloe* and *Othocallis*—abundance and localization. *Chromosome Res* 9(Suppl):L118

Weiss-Schneeweiss H, Riha K, Jang CG, Puizina J, Scherthan H, Schweizer D (2004) Chromosome termini of the monocot plant *Othocallis siberica* are maintained by telomerase, which specifically synthesises vertebrate-type telomere sequences. *Plant J* 37:484–493

Wong JM, Kusdra L, Collins K (2002) Subnuclear shuttling of human telomerase induced by transformation and DNA damage. *Nat Cell Biol* 4:731–736

Yang SW, Jin E, Chung IK, Kim WT (2002) Cell cycle-dependent regulation of telomerase activity by auxin, abscisic acid and protein phosphorylation in tobacco BY-2 suspension culture cells. *Plant J* 29:617–626

Yang SW, Kim DH, Lee JJ, Chun YJ, Lee JH, Kim YJ, Chung IK, Kim WT (2003) Expression of the telomeric repeat binding factor gene NgTRF1 is closely coordinated with the cell division program in tobacco BY-2 suspension culture cells. *J Biol Chem* 278:21395–21407

Yang SW, Kim SK, Kim WT (2004) Perturbation of NgTRF1 expression induces apoptosis-like cell death in tobacco BY-2 cells and implicates NgTRF1 in the control of telomere length and stability. *Plant Cell* 16:3370–3385

Yang TJ, Yu Y, Chang SB, de Jong H, Oh CS, Ahn SN, Fang E, Wing RA (2005) Toward closing rice telomere gaps: mapping and sequence characterization of rice subtelomere regions. *Theor Appl Genet* 111:467–478

Yanhui C, Xiaoyuan Y, Kun H, Meihua L, Jigang L, Zhaofeng G, Zhiqiang L, Yunfei Z, Xiaoxiao W, Xiaoming Q, Yunping S, Li Z, Xiaohui D, Jingchu L, Xing-Wang D, Zhangliang C, Hongya G, Li-Jia Q (2006) The MYB transcription factor superfamily of *Arabidopsis:* expression analysis and phylogenetic comparison with the rice MYB family. *Plant Mol Biol* 60:107–124

Yoo HH, Kwon C, Lee MM, Chung IK (2007) Single-stranded DNA binding factor AtWHY1 modulates telomere length homeostasis in *Arabidopsis. Plant J* 49:442–451

Yu EY, Kim SE, Kim JH, Ko JH, Cho MH, Chung IK (2000) Sequence-specific DNA recognition by the Myb-like domain of plant telomeric protein RTBP1. *J Biol Chem* 275:24208–24214

Yu W, Lamb JC, Han F, Birchler JA (2006) Telomere-mediated chromosomal truncation in maize. *Proc Natl Acad Sci USA* 103:17331–17336

Yu W, Han F, Gao Z, Vega JM, Birchler JA (2007) Construction and behavior of engineered minichromosomes in maize. *Proc Natl Acad Sci USA* 104:8924–8929

Zellinger B, Riha K (2007) Composition of plant telomeres. *Biochim Biophys Acta—Gene Struct Exp* 1769:399–409

Zellinger B, Akimcheva S, Puizina J, Schirato M, Riha K (2007) Ku suppresses formation of telomeric circles and alternative telomere lengthening in *Arabidopsis. Mol Cell* 27:163–169

Zhang QS, Manche L, Xu RM, Krainer AR (2006) hnRNP A1 associates with telomere ends and stimulates telomerase activity. *RNA* 12:1116–1128

Zhong XB, Fransz PF, Wennekes-Eden J, Ramanna MS, van Kammen A, Zabel P, Hans de Jong J (1998) FISH studies reveal the molecular and chromosomal organization of individual telomere domains in tomato. *Plant J* 13:507–517

Zhou J, Monson EK, Teng SC, Schulz VP, Zakian VA (2000) Pif1p helicase, a catalytic inhibitor of telomerase in yeast. *Science* 289:771–774

Chapter 8
Genetics and Cytology of Meiotic Chromosome Behavior in Plants

Shaun P. Murphy and Hank W. Bass

Abstract Meiosis is the process by which sexually reproducing organisms reduce their genomes from diploid (2n) to haploid (n) during the formation of gametes. It requires that homologous chromosomes pair, synapse, recombine, and finally segregate. These widely conserved processes are under genetic control, yet the exact details of many of the underlying molecular mechanisms remain under active investigation. The initial pairing and subsequent synapsis events are immediately preceded by the clustering of telomeres on the nuclear envelope in a widely conserved structure referred to as the bouquet arrangement of meiotic chromosomes. In animals and plants, genes required for genome reduction at meiosis I have been characterized and show a high degree of conservation between kingdoms and species within them. Plants have provided an excellent large-genome model system for the study of the cytology of homologous chromosome behavior and therefore have allowed an in depth dissection of the meiotic process in eukaryotes.

Keywords Meiotic prophase · Pachytene · Synapsis · Bouquet · Synaptonemal complex · Homolog · Chromosome pairing

S.P. Murphy (✉)
Institute of Molecular Biophysics, The Florida State University, Tallahassee, FL 32306-4370, USA

H.W. Bass
Institute of Molecular Biophysics, The Florida State University, Tallahassee, FL 32306-4370, USA

Department of Biological Science, The Florida State University, Tallahassee, FL 32306-4295, USA

H.W. Bass and J.A. Birchler (eds.), *Plant Cytogenetics*, Plant Genetics and Genomics: Crops and Models 4, DOI 10.1007/978-0-387-70869-0_8,

Abbreviations

CE	Central element
DAPI	4′,6-Diamidino-2-phenylindole
DSB	Double-stranded break
EM	Electron microscopy
FISH	Fluorescence in situ hybridization
LE	Lateral element
MAR	Matrix attachment region
NE	Nuclear envelope
NMD	Nonsense-mediated mRNA decay
NPC	Nuclear pore complex
PHD	Plant homeodomain
PI	Propidium iodide
RN	Recombination nodule
SAR	Scaffold attachment region
SC	Synaptonemal complex
SI	Structured illumination

Contents

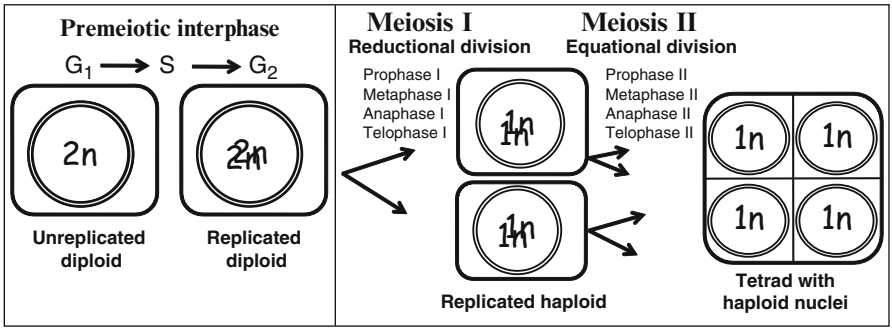

Fig. 8.1 Overview of typical male plant meiosis illustrating change in ploidy. Cells (*squares*) and the nucleus (*double-lined circles*) are indicated. The interphase subdivisions (G1, S, and G2) are shown along with the ploidy (diploid, 2n) and replication status of the genome. The first meiotic division (meiosis I) results in genome reduction (replicated haploid, 1n, state), and the second (meiosis II) in the production of four haploid cells that subsequently divide by mitosis (not indicated) to produce pollen

8.1 Introduction

The mechanism of meiosis is highly conserved among sexually reproducing species (Darlington 1931a, 1977; John and Lewis 1965; Anderson 1972; Moens 1987; John 1990). Although its molecular mechanisms differ considerably in different kingdoms and different species within them, plant meiosis does not differ from that of nonplant species, exhibiting cellular, nuclear, and chromosomal events typical of eukaryotes. These events involve commitment to and initiation of meiosis, homologous chromosome synapsis and synaptonemal complex (SC) formation, interhomolog reciprocal recombination, disjunctive segregation, and haploid gamete or gametophyte formation. Meiosis consists of two distinct and specialized cell divisions, meiosis I and meiosis II, diagrammed in Fig. 8.1. The first occurs only once per reproductive life cycle and has long fascinated plant cytologists because of its prolonged prophase I. During this stage, the chromosomes become organized as replicated synapsed fibers revealing the full haploid genome content. The five substages of meiotic prophase I, named for their chromatin-fiber appearance, are in order of occurrence the leptotene (thin thread), zygotene (coupled thread), pachytene (thick thread), diplotene (paired thread), and diakinesis (moving apart) stages. Homologous recombination between parental chromosomes during meiotic prophase I encompasses major genetic events: the establishment of physical connections for bipolar spindle attachment between the homologs and the generation of novel allelic combinations. This genetically controlled progression of chromosome breaking, homology searching, and reciprocal recombination is required to reduce the genome from the diploid to the haploid state (Darlington 1931a, b). Throughout prophase I, dramatic changes in meiotic nuclear architecture and chromosome morphology accompany the remarkable events that take place (Naranjo and Corredor 2008). The cellular behavior of the genetic material has fascinated biochemists, cell biologists, and geneticists for many decades, and observations of plant chromosomes at meiosis

have contributed fundamental principles to our understanding of inheritance while providing a mechanistic basis for the general rules of Mendelian genetics.

Here we review the cytology of meiotic chromosome behavior, particularly prophase I meiotic chromosome behavior – those programmed changes in nuclear architecture, chromatin structure, and homolog interactions that are necessary to achieve accurate genome reduction and chromosome segregation. The genetic control of meiosis in higher plants has been the subject of several recent and thorough reviews (Ma 2005; Pawlowski and Cande 2005; Hamant et al. 2006; Mezard et al. 2007; Jenkins et al. 2008; Mercier and Grelon 2008), so we emphasize the cytology and cytogenetic aspects of plant chromosome behavior during meiosis.

8.2 The Plant Life Cycle

Plants reproduce both asexually and sexually. Sexual reproduction involves two major events, meiosis and fertilization, which, respectively, accomplish the two ploidy-change events of the life cycle – from diploidy to haploidy and back again to diploidy. Unlike fertilization (represented by "Nuclear fusion" in Fig. 8.2),

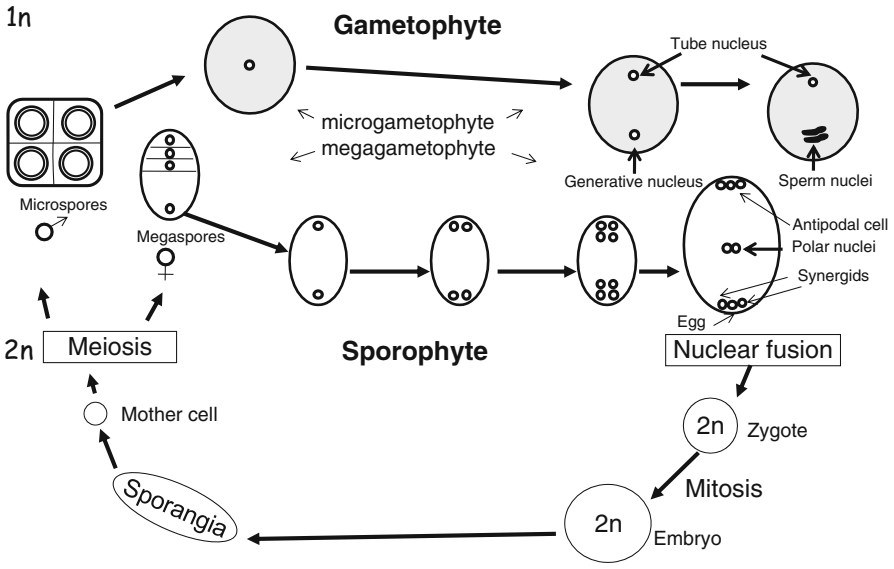

Fig. 8.2 A generalized plant life cycle, showing the haploid stage (1n, gametophyte) at the *top* and the diploid stage (2n, sporophyte) at the *bottom.* Meiosis and fertilization are the events that define the beginnings of the gametophyte and sporophyte stages, respectively. Cell reproduction at all other stages is accomplished by mitosis. The gametophytes typically represent small proportions of both the life cycle duration and overall plant body mass in flowering plants (angiosperms). Meiosis is initiated within mircosporangia and megasporangia. Subsequent development of the microgrametophye and megagametophyte are diagrammed. Double fertilization produces the embryo zygote (2n) and associated endosperm (3n), marking the beginning of the diploid sporophyte phase of the plant life cycle

meiosis requires elaborate mechanisms for pairing, crossover formation, and disjunction of all pairs of homologous chromosomes. Plants differ widely in the proportions of the life cycle that are haploid and diploid, but the vast majority of higher plants spend most of the life cycle in the diploid state. In flowering plants, spore-forming structures (anthers and gynoecium) produce four haploid microspores for each meiosis in the male flower and one haploid megaspore for each meiosis in the female flower (Drews et al. 1998; Grossniklaus and Schneitz 1998; Yadegari and Drews 2004; Ma 2005). The male gametophyte gives rise to the pollen grain, and the female gametophyte produces the egg. Diploidy is restored at fertilization, and the diploid sporophyte stage continues until reproduction.

8.3 Cytological Approaches Used to Study the Behavior of Plant Meiotic Chromosomes

The study of plant meiosis revealed long ago the value of combining genetic and biochemical approaches with cytology to visualize and characterize an organism's genome. The cytology and behavior of meiotic chromosomes in plants have been dissected for more than a century by a combination of cytological, genetic, and biochemical approaches (Wilson 1925; McClintock 1929a, b; Darlington 1932; Stern and Hotta 1974; Golubovskaya 1979; Golubovskaya and Khristolyubova 1985; Ross et al. 1996; Dawe 1998; Armstrong and Jones 2003; de Jong 2003; Jenkins et al. 2005; Ma 2005; Pawlowski and Cande 2005; Hamant et al. 2006; Jiang and Gill 2006). More recently, live-cell imaging with cultured anthers has been used to elucidate the cell biology of meiosis in higher plants (Chan and Cande 2000; Shaw 2006; Sheehan and Pawlowski 2009). Cytological techniques that facilitate direct (or indirect) visualization of meiotic chromosomes in situ have traditionally relied on a combination of tools including bright-field microscopy, electron microscopy (EM), fluorescence in situ hybridization (FISH), and protein immunolocalization to probe the architecture and behavior of meiotic chromosomes in plants and animals. More recently, new ultrahigh-resolution light microscopic techniques, such as structured illumination (SI) microscopy, have been used to obtain exceptional images of chromatin and chromosome structure during meiosis in a variety of organisms including plants (Carlton 2008; Gustafsson et al. 2008; Shao et al. 2008; Fig. 8.3e).

8.3.1 Light Microscopy

Bright-field microscopy with chromosome-staining dyes has permitted a detailed description of the genetics and cytology of meiotic chromosome behavior in plants (Belling 1921; McClintock 1929a, b; Buck 1935; McGoldrick et al. 1954; Jongedijk 1987; Chang and Neuffer 1989; Fig. 8.3a). Carmine is a widely used basic

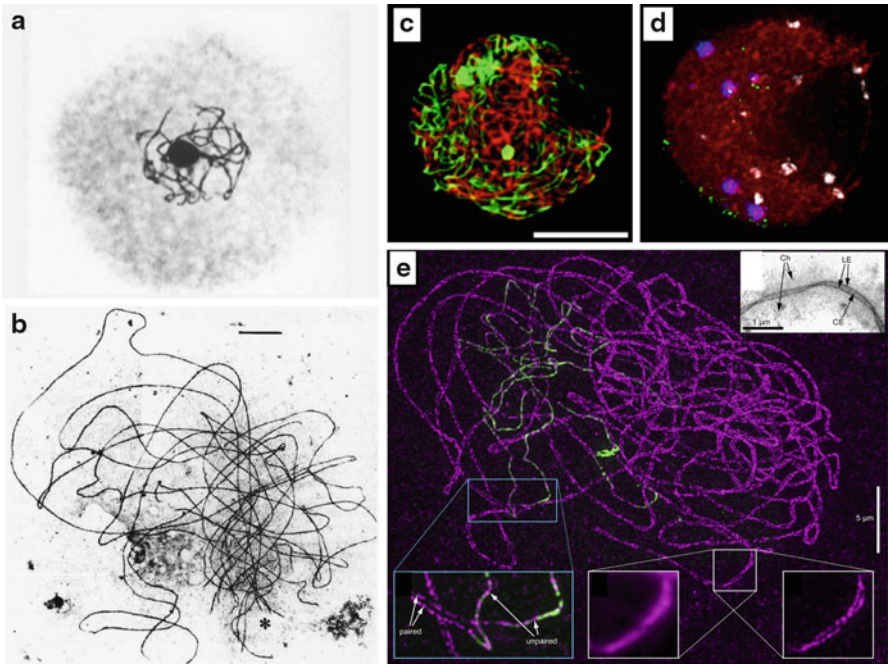

Fig. 8.3 Cytological techniques used to visualize meiotic prophase chromosomes. (**a**) Acetocarmine-stained pachytene-staged cell prepared by smear (from Fig. 1, plate 4, of Chang and Neuffer 1989). The position of the nucleus organizing region on chromosome 6 is indicted (*arrow*). (**b**) Surface-spread silver-stained whole-mount leptotene nucleus from haploid rye (from Santos et al. 1994). This technique shows chromosome axes in high contrast. Scale bar is 5 µm; *asterisk* marks the telomere cluster bouquet. (**c**) Projection of immunofluorescence images of a midprophase pollen mother cell from rye (from Mikhailova et al. 2006). Anti-ASY1 (*red*) and anti-ZYP1C (*green*) show colocalization of the axial elements and an SC component, respectively. Scale bar is 10 µm. (**d**) Projection of multicolor fluorescence in situ hybridization (FISH) image of early prophase nucleus of maize near the onset of the telomere bouquet stage. FISH probes are specific to telomeres (*green*) and centromeres (CentC probe, *white*). Knobs (*blue*) are shown along with the DAPI (*red*) image according to the 3D acrylamide FISH technique of Bass et al. (1997). Scale bar 5 µm. (**e**) Example of high-resolution (structured illumination microscopy, SIM) immunofluorescence projection of a midprophase pollen cell from maize (Gustafsson et al. 2008). Anti-AFD1 (*magenta*) image showing the location of an SC-associated rec8 homolog overlaid with anti-ASY1 (*green*) image revealing unsynapsed regions of the genome. Standard TEM image of synapsed chromosomes (*inset*, *upper right*) is shown for comparison. Close-up views of partially synapsed region (*bottom left*), synapsed region lacking clear resolution of lateral elements (LEs) by conventional microscopy (*bottom middle*), and LE resolution by SIM (*bottom right*) are shown. Scale bar is 5 µm

chromosome-staining dye prepared from the insect *Coccus cacti* L. Acetocarmine images represent a familiar view of chromosome morphology as shown in Fig. 8.3a. Carmine and derivative dyes, used in conjunction with coagulative or dehydrating fixatives, provide high-contrast images that capture snapshots of the meiotic nuclei.

General chromosome morphology can also be viewed by means of any of a variety of fluorescent dyes, including DAPI (4′,6-diamidino-2-phenylindole), propidium iodide (PI), and Hoechst. DAPI binds to dsDNA and can be detected by epifluorescence microscopy. In vitro studies have shown that DAPI forms a fluorescent complex when it is bound to the minor groove of AT-rich DNA sequences. It can also form intercalative complexes with DNA in other regions, such as GC sequences, ssDNA, and dsRNA, but these complexes are generally nonfluorescent or less fluorescent (Manzini et al. 1985; Kapuscinski 1995; Banerjee and Pal 2008). Repetitive DNA sequences such as those found in pericentromeric heterochromatin, nucleolus organizing regions, and heterochromatic knob sequences tend to be relatively rich in AT and to stain brightly with DAPI (Kubista et al. 1987; Lam et al. 2004). Hoechst 33258 preferentially binds to AT-rich regions and has spectral properties similar to those of DAPI (Latt and Stetten 1976; Cesarone et al. 1979). PI binds preferentially to dsDNA, but its fluorescence is red. The spectral properties of DAPI, PI, and Hoechst make them useful as general chromatin stains to be visualized separately from fluorescein with standard fluorescent-microscopy filter sets.

FISH has provided a wealth of insight into the structural organization and behavior of meiotic chromosome domains in plants and animals (Arndt-Jovin and Jovin 1989; de Jong 2003; Jiang and Gill 2006). This technology is based on sequence-specific hybridization of fluorescent DNA or RNA probes with their respective chromosomal or nuclear targets, allowing for the visual detection of specific DNA sequences in situ (Figs. 8.3d and 8.6). Capturing FISH images with CCD cameras and analyzing them with computerized tools has characterized major recent advances in the cytology of meiotic chromosomes (Dawe et al. 1994; Bass et al. 1997; Fransz et al. 2002; Jones et al. 2003; Jiang and Gill 2006). In particular, 3D FISH has proven to be an excellent approach to understanding the spatial and temporal control of meiotic chromosomes when they are visualized at previously intractable, yet biologically important, stages of meiosis. For example, 3D telomere FISH was used to establish the timing of telomere bouquet formation and dissolution during meiotic prophase I in maize as well as the timing of homolog pairing in diploid and polyploid species (Bass et al. 1997, 2000; Moore 2002; Schubert et al. 2007).

8.3.2 Electron Microscopy

For suboptical, nanometer-scale resolution, an ultrastructural approach such as EM provides great insight into the architecture of meiotic chromosomes and chromatin substructure. Cells are typically prepared for EM with a glutaraldehyde fixative and an electron-dense chromatin stain such as osmium tetroxide. Fixed, stained cells are then embedded in resin for fine sectioning and imaging by transmission or scanning EM. Serial sectioning of meiotic nuclei followed by reconstruction by EM analysis has provided an extraordinary level of detail, particularly in chromosome pairing and SC analyses in haploid and hexaploid wheat, lily, and maize (Fig. 8.3b; Holm

1977a, 1986; Hobolth 1981; Wang 1988). Alternatively, spread nuclei can be stained and imaged as high-contrast SC spreads, revealing the morphology of synapsis, intermediates, and recombination nodules (RNs) in situ (Stack 1982; Albini and Jones 1984; Anderson et al. 1988; Zickler and Kleckner 1999). EM analyses with surface-spread meiotic chromosomes yield tremendous detail, including the spatial orientation and behavior of SC components, nucleolus organizing regions, telomere-nuclear envelope (NE) interaction, and RN distribution.

8.4 The Commitment to and Initiation of Meiosis

The initiation of meiosis in mitotically dividing cells is usually triggered by a change in photoperiod or temperature or by developmental progression. During the initiation of flowering, a genetic control mechanism ensures that vegetative meristematic tissues become reproductive before the meiotic commitment of a subset of these cells in the developing floral meristems (Simpson et al. 1999; Bhatt et al. 2001). Forward and reverse genetic studies have begun to identify key genes that participate in the initial transition from vegetative to reproductive growth (Simpson et al. 1999; Ma 2005; Dennis and Peacock 2007). Unlike those in animals, some of which are primordial germ-line cells, plant meiotic cells arise from somatic subepidermal cells within the anthers and ovules (Yang and Sundaresan 2000; Bhatt et al. 2001; Lavania et al. 2002; Ma 2005; Hamant et al. 2006). In maize, the *Mac1* (*Multiple archesporial cells* 1) gene is required for cell-fate determination and in the initial commitment of hypodermal cells to the meiotic pathway in female ovules (Sheridan et al. 1996) and in male anthers (Sheridan et al. 1999). In *Arabidopsis thaliana* (L.) Heynh. plants with mutations in the *SPL/NZZ* (*SPOROCYTELESS/NOZZLE*) locus are phenotypically male sterile because they cause a genetic block in anther wall formation and meiotic cell differentiation. This gene is suspected to play a role as an essential MADS box–related transcriptional regulator required for early sporophyte development and differentiation (Schiefthaler et al. 1999; Yang and Sundaresan 2000; Ma 2005). In addition, mutations in the *Arabidopsis EMS1* (*EXCESS MALE SPOROCYTES1*) and *TPD1* (*TAPETUM DETERMINANT1*) genes have been revealed to play a prominent role in a signaling pathway that is required for tapetum differentiation and meiocyte formation in these plants (Ma 2005).

Two additional meiotic initiation genes, the *Am1* (*Ameiotic1*) gene of maize (Palmer 1971; Staiger and Cande 1992; Golubovskaya et al. 1993, 1997; Pawlowski et al. 2009) and the *SWI1/DYAD* (*SWITCH1/DYAD*) gene of *Arabidopsis* (Mercier et al. 2001; Agashe et al. 2002) are required for the initiation of meiosis (Bhatt et al. 2001; Hamant et al. 2006). Mutations in *Am1* result in a mitosis-like division phenotype in male meiotic cells (Staiger and Cande 1992; Hamant et al. 2006). A unique allele of *Am1*, *am1-pra1* (*Ameiotic 1 prophase arrest 1*), is unique in that cells bearing it appear to enter meiotic prophase showing a characteristic leptotene chromosome morphology but lack downstream bouquet formation, recombination initiation, and synapsis mediated by the SC (Golubovskaya et al. 1993, 1997; Pawlowski et al.

2009). In a related case, four *swi* mutant alleles (*swi1-1*, *swi1-2*, *ms4*, and *dyad*) have been isolated and found to confer defects in meiosis initiation (Mercier et al. 2001; Hamant et al. 2006). The *swi1/dyad* mutants also display defects in meiotic chromosome morphology and progression through meiosis in both males and females (Mercier et al. 2003). The molecular, genomic, and cytological analyses of genes such as *Mac1*, *SPL/NZZ*, *SWI1/DYAD*, *Am1*, *EMS1*, and *TPD1* are beginning to reveal a molecular cascade of events required for plant reproductive organogenesis and for the commitment of selected cells to the meiosis pathway.

Once committed to meiosis, cells irreversibly enter a pathway where major structural changes in the genetic information and nuclear architecture lead to accurate chromosome segregation. Relatively little is known of molecular processes that monitor and coordinate progression through the meiotic cell cycle in higher plants, but just as in animals and fungi, cyclins and associated cyclin-dependent kinases appear to play a major role. In *Arabidopsis*, the *TAM1* (*TARDY ASYNCHRONOUS MEIOSIS*) gene was found to encode an A-type cyclin (Cyca1;2), detectable in male meiotic cells at meiotic prophase I (Magnard et al. 2001; Wang et al. 2004). The *tam1* mutants display asynchronous cell division during male meiosis I and II, indicative of a role for this gene in the control of meiotic progression (Wang et al. 2004). The *SDS* (*SOLO DANCERS*) gene is expressed specifically in meiotic tissues in *Arabidopsis*, and *sds* mutants are defective in synapsis, recombination, and bivalent formation (Azumi et al. 2002). In addition, *sds* mutants differ significantly from wild-type cells in the frequency and distribution of cells at prophase I; the number of cells in leptotene and zygotene stages is drastically lower. The significant sequence similarity between the SDS protein and the C-termini of several well-known cyclins, together with evidence for protein-protein interaction with two CDKs, Cdc2a and Cdc2b, suggests that the SDS protein functions in the control of meiotic progression and chromosome behavior (Wang et al. 2004; Azumi et al. 2002).

The *DUET* gene of *A. thaliana* encodes a putative plant homeodomain (PHD) finger protein that is expressed in meiotic tissues (Reddy et al. 2003). The *duet* mutants are defective in meiotic chromosome organization and display an arrest at metaphase I, and genetic analysis reveals an interaction with *SWI1/DYAD*, a gene required for chromosome cohesion and meiotic progression (Agashe et al. 2002; Reddy et al. 2003). More recently, a member of the rice *ARGONAUT* gene family, *Mel1* (*Meiosis Arrested at Leptotene 1*), was shown to be expressed specifically within the germ cells and is required not only for the regulation of cell division in premeiotic germ cells but also for proper meiotic chromosome structure and overall progression through meiosis (Nonomura et al. 2007). The *Mel1* gene is the first identified *ARGONAUT* family member shown to play a role in sexual reproduction in plants, probably through a small RNA pathway. Together, the behaviors of these mutants begin to clarify aspects of meiotic checkpoints specific to plants.

Angiosperm species appear to vary widely in the overall timing and duration of meiosis (Bennett 1977). The duration of meiosis in plants has been measured in several ways, including pulse labeling and direct observation. The duration of the meiotic cycle is correlated with several factors, including the nuclear DNA content (c-value), the ploidy level of the organism, environmental conditions, and to a great

extent, the genetic background (Bennett 1971, 1977; Singh 1993). For example, it is inversely proportional to temperature in bread wheat, *Triticum aestivum* L., and several other higher plant species (Bennett 1971). The prophase I stage occupies the majority of the meiotic cycle, and males and females of the same species, or even individual plants, can differ in the cycle's duration, despite genomes of identical size. Surprisingly some polyploid plants exhibit shorter cycle times than their related diploids, despite their higher DNA content (Bennett 1971, 1977; Bennett et al. 1971, 1973, 1974; John 1990; Singh 1993). A few studies in higher plants have revealed an important biochemical distinction between mitotic and premeiotic S-phase with regard to the length of time required to replicate the genome. Tritium labeling and autoradiographic studies with *Lilium* (Stern and Hotta 1974; Holm 1977b) and *Trillium* (Yoshioka et al. 1981) have shown that the premeiotic S-phase can last ~3 times longer than that of a typical somatic S-phase in the same plants (Stern and Hotta 1974). This lengthening may reflect a general reduction in origin of replication site firing rather than a lower rate of replication itself. Alternatively, cell-cycle checkpoints, more extensive "proofreading," or installation of meiotic chromatin and cohesion complex proteins may contribute.

The *SMG7* gene in *A. thaliana* has been found to be required for the successful passage of meiotic nuclei through anaphase II and eventual exit from meiosis. The *smg7* mutants are characterized by delays in chromosome decondensation and dephosphorylation of histone H3 (at Ser10) and by aberrant meiotic spindle organization (Riehs et al. 2008). SMG7 regulates CDK activity through an evolutionarily conserved nonsense-mediated mRNA decay (NMD) mechanism, and knowledge of this gene and its mode of action will probably reveal new regulatory pathways that govern cell-cycle progression and exit in plants.

8.5 Meiotic Prophase I

An elaborate sequence of specialized mechanisms is required during meiotic prophase I to ensure that homologous chromosomes reorganize spatially and temporally, pair, synapse, and recombine with high fidelity, as illustrated in Fig. 8.4a. Unlike mitosis, in which replicated sister chromatids segregate to opposite poles, equally dividing the nucleus, at the end of meiosis I, maternal and paternal homologous chromosome pairs segregate from each other as centromere-joined pairs of sister chromatids to accomplish the reductional nuclear division (Churchill 1970). Aside from an evolutionary role in generating novel alleles, meiotic recombination and successful crossover formation are required for the mechanics of homolog disjunction on the meiosis I spindle. Homologous chromosome pairing and synapsis are two distinct and cytologically distinguishable events within meiotic prophase I, but the terms are often used interchangeably to describe physical interactions or associations between the maternal and paternal homologs. We refer to the colocalization of homologous chromosomes as pairing and to physical fusion of paired homologs connected along their lengths by the structurally conserved SC (a highly conserved tripartite proteinaceous structure) as synapsis (Gillies et al.

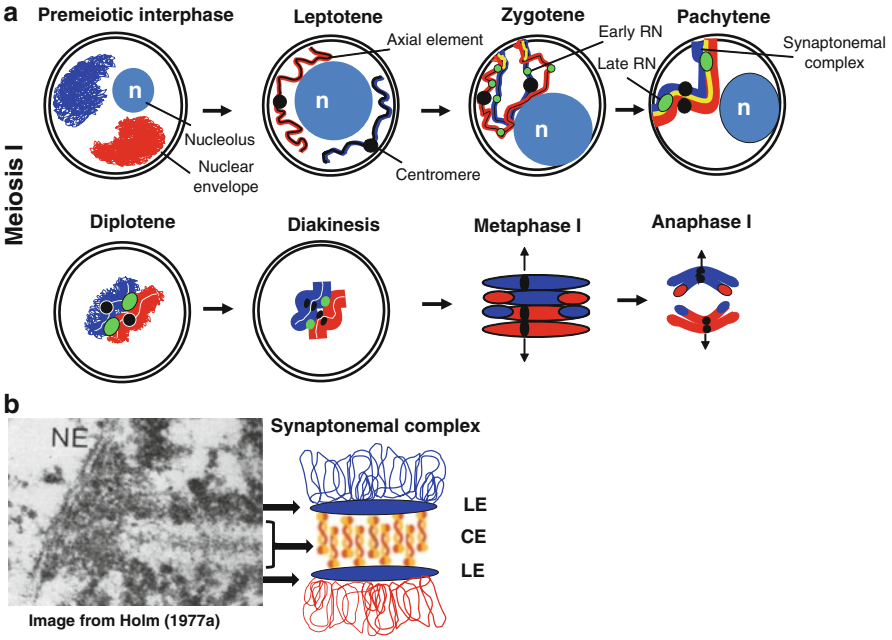

Fig. 8.4 Overview of the changes in chromosomes throughout meiosis I for a typical plant cell nucleus. (**a**) Homologs (indicted by one *red* chromosome and one *blue* chromosome) are spatially separated before meiotic prophase. The nuclear envelope (NE) and nucleolus are labeled. At the onset of meiotic prophase, in the leptotene stage, replicated chromosomes appear as elongated fibers, and the large centralized nucleolus is conspicuous. Centromeres (*black circles*) are indicated as single structures for each homolog. At the zygotene stage, telomeres attach to the NE to form the bouquet, early recombination nodules (RN, *green circles*) are evident, and the installation of the synaptonemal complex (SC, *yellow*) commences at subtelomeric sites. At the pachytene stage, homologs are synapsed along their entire length, and late RNs (*green ovals*) are evident. (**b**) A close-up EM image of a telomeric attachment (from Holm 1977a) is shown along with an interpretive diagram showing the substructure of the SC as consisting of two LEs connected by a central element (CE). At the diplotene and diakinesis stages, paired bivalents continue to condense and remain adjoined at sites of crossovers (late RNs, *green ovals*)

1974; von Wettstein et al. 1984; Moens 1994; Page and Hawley 2004; Zickler 2006). Homolog pairing is normally a prerequisite for synapsis, but the two processes can occur simultaneously or independently (Zickler and Kleckner 1999).

8.5.1 Sister Chromatid Cohesion and Condensin

The role of chromatin structure in meiotic chromosome behavior is not easily tested and therefore not fully understood. Studies of it are confounded by concurrent DNA metabolism and progressive chromosome compaction. Unique meiotic chromosome arrangements occur at least as early as premeiotic S-phase. Chromatin

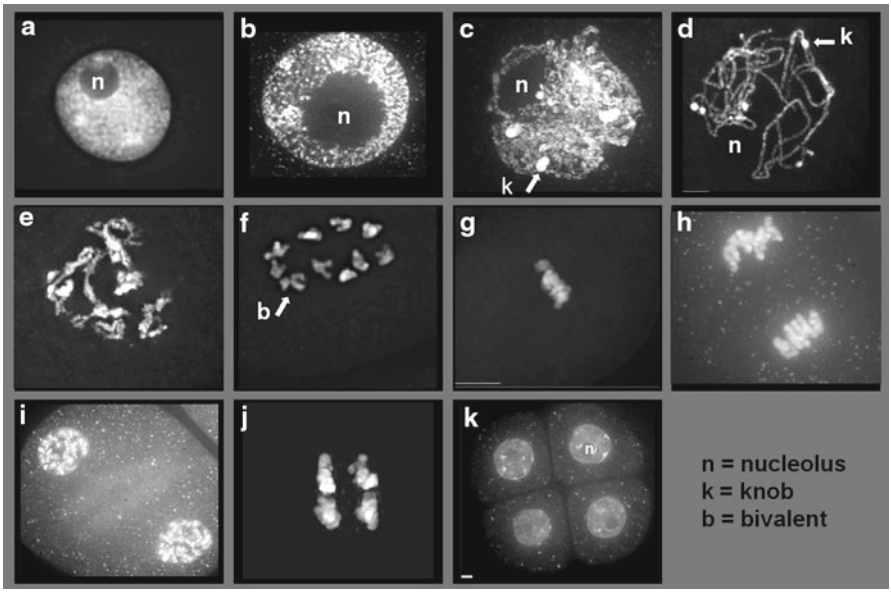

Fig. 8.5 Cytology of meiotic chromosome behavior in pollen mother cells of maize. Formaldehyde-fixed, DAPI-stained pollen mother cells, imaged by 3D deconvolution microscopy and shown as maximum-intensity through-focus projections. (**a**) Premeiotic interphase, (**b**) leptotene, (**c**) mid to late zygotene, (**d**) pachytene, (**e**) diplotene, (**f**) diakinesis, (**g**) metaphase I, (**h**) late anaphase I, (**i**) telophase I/prophase II, (**j**) anaphase II, (**k**) tetrad

in plants and animals appears rather diffuse during the premeiotic interphase, but in some species brightly staining foci such as heterochromatic regions are observed (Fig. 8.5). During the premeiotic S-phase, chromosomes are replicated, and the resulting sister chromatids remain connected to each other by the cohesion complex. This complex consists of the meiosis-specific Rec8, a heterodimer containing proteins for the structural maintenance of chromosomes (SMCs, Smc1 and Smc3) as well as other associated non-SMC proteins like Scc1 and Scc3 (Nasmyth 2002; Page and Hawley 2004; Chelysheva et al. 2005; Hamant et al. 2006; Revenkova and Jessberger 2006). Some plant homologs of animal or fungal cohesin-complex proteins have been identified. Genes for these include a *Rec8*/*Rad21* homolog in maize; *Afd1* (*Absence of First Division1*; Fig. 8.3e; Golubovskaya et al. 2006), *REC8*, and *SYN1*/*DIF1*, as well as those encoding the SCC3 proteins in *Arabidopsis* (Bhatt et al. 1999; Cai et al. 2003; Chelysheva et al. 2005) and rice (Zhang et al. 2006). In addition to sister-chromatid cohesion, the *Arabidopsis* Rec8/Scc3-containing complex is necessary for meiotic chromosome-axis formation (like the maize Afd1) but also for metaphase I monopolar attachment and orientation of the sister kinetochores. Also in *Arabidopsis*, genes *ASK-1* (*ARABIDOPSIS SKP1-LIKE*) and *SWI1*/*DYAD* play a key role in chromosome dynamics and function (Mercier et al. 2001, 2003).

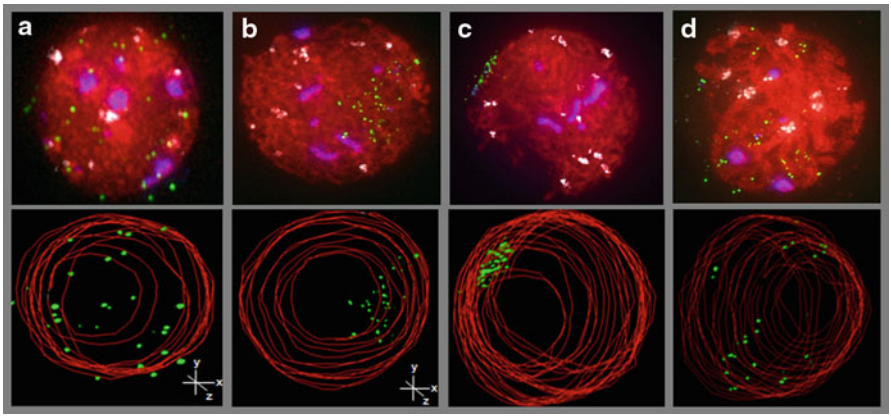

Fig. 8.6 3D acrylamide FISH of telomeres, centromeres, and knobs in meiotic prophase nuclei. Maize (inbred line A344) meiotic cells were stained by multicolor 3D FISH as described by Bass et al. (1997). Changes in telomere distribution are evident as cells progress from premeiotic interphase though midprophase. Images show FISH signals for oligonucleotide probes designed to detect telomeres (*green*), knobs (*blue*), and centromeres (*white*). Total DNA is stained with DAPI (*red*). Pollen mother cells are shown at the following stages: (**a**) premeiotic interphase, (**b**) late leptotene/prezygotene, (**c**) zygotene, (**d**) mid–late pachytene. Computer modeling of 3D image is shown below each projection. The boundary of the nucleus (*red wire*) and position of telomere FISH signals (*green dots*) are shown

8.5.2 Cytology and Behavior of Leptotene Chromosomes

Meiotic chromosomes are cytologically discernable as individual fibers at prophase I at the onset of the leptotene stage (Figs. 8.4a, 8.5b, and 8.6b). The chromosomes during this stage appear thin and thread-like, and the sister chromatids are not cytologically resolved because of their intimate cohesion along their entire length. At the same time, the nuclear and nucleolar volume has increased significantly (Figs. 8.4a and 8.5b). The leptotene fiber contains a proteinaceous axial element along the length of each sister chromatid (Sen 1970; Moens and Pearlman 1988). In *Arabidopsis*, a screen for T-DNA–disrupted alleles of meiotic genes led to the discovery of the mutant *as1* (*asynaptic1*), which conferred a complete asynaptic phenotype (Ross et al. 1997). The gene was later cloned and shown to contain HORMA (Hop1p, Rev7p, MAD2; Aravind and Koonin 1998) and SWIRM (Swi3p, Rsc8p, Moira; Aravind and Iyer 2002) domains, which are found in a large variety of chromosome-remodeling proteins (Caryl et al. 2000; Qian et al. 2005; Sanchez-Moran et al. 2008) and have partial sequence similarity to the N-terminal region of the yeast axial-element protein HOP1 (Caryl et al. 2000).

The *ASY1* gene appears to be widely conserved within plants; homologs have been cloned and characterized in rice (*Pair2*; Nonomura et al. 2006), *Brassica* (*BoAsy1*; Armstrong et al. 2002), and wheat (*TaAsy1*; Boden et al. 2007). Antibodies raised against *Arabidopsis* ASY1 have proven useful in immunocytochemistry in maize

(Fig. 8.3c, e; Golubovskaya et al. 2006), rye (Mikhailova et al. 2006), and several other plant species (Sanchez-Moran et al. 2008). In *Arabidopsis*, ASY1 can be immunodetected just before the onset of leptotene as punctuate foci distributed on the chromatin and later remains intimately associated with the chromosome axes until the homologs begin to desynapse at diplotene (Armstrong et al. 2002), but in maize, localization of ASY1 becomes undetectable when the homologs are fully synapsed at pachytene (Golubovskaya et al. 2006; Murphy and Bass, unpublished data). Not only is ASY1 required for axial-element formation and eventual SC establishment, but it is also necessary for maintaining and stabilizing the meiosis-specific recombinase DMC1 on *Arabidopsis* leptotene chromosomes (Sanchez-Moran et al. 2007).

8.5.3 Meiotic Chromosome Loop Domains

The axial element of the chromosomes appears to be organized into looped domains, with regularly spaced attachments to the chromosome axis (Fig. 8.4b; Zickler and Kleckner 1999; Page and Hawley 2004). Reported meiotic loop sizes vary considerably, from 20 kb in yeast to 2,500 kb in the grasshopper; they are estimated, for somatic interphase, at ~45 kb in maize and ~25 kb in *Arabidopsis* (Moens and Pearlman 1988; Paul and Ferl 1998). Within species, the meiotic chromatin loops associated with the SC are highly uniform along the length of the SC axes (Zickler and Kleckner 1999). In addition, studies in tomato have revealed regions of the genome termed matrix and scaffold attachment regions (MARs and SARs) that serve not only to anchor chromatin loop domains on the nuclear matrix (or chromosome scaffold) but also to facilitate the packaging and organization of the chromatin within the nucleus during interphase and mitosis. Molecular details of the numerous chromosome-topology and chromatin-fiber models remain highly speculative, and their resolution remains a major focus of contemporary meiosis research (Zickler and Kleckner 1999).

8.5.4 Initiation of Meiotic Chromosome Pairing

The pairing of chromosomes is a hallmark of meiosis. Chromosome pairing and synapsis occurs while chromosome morphology and nuclear architecture are undergoing dramatic changes (Zickler and Kleckner 1998, 1999; Naranjo and Corredor 2008). The complete pairing of all homolog pairs for any given species represents a complex and delicate task probably requiring the ability to move chromosomes and to reorganize the architecture of the nucleus to facilitate those processes. In plant species, evidence for presynaptic or premeiotic alignment of homologous chromosomes before meiosis is scarce (Dawe 1998; Naranjo and Corredor 2008), despite the observation of homologous associations during premeiotic interphase in *Arabidopsis* and grass taxa including wheat, rye, *Triticale*, maize, and rice (Maguire 1967; Fransz et al. 2002; Prieto et al. 2004; Schubert et al. 2007). Furthermore, maize leptotene nuclei

display a semipolarized arrangement of centromeres, but this polarization is only brief and dissipates in zygotene (Carlton and Cande 2002). A 3D chromosome-painting study showed that homologs exhibited no evidence of premeiotic alignment or juxtaposition, even at the onset of the bouquet stage at the leptotene-to-zygotene transition (Bass et al. 2000).

8.5.5 The Leptotene-to-Zygotene Transition

A unique transitional stage can be observed in plant nuclei between the leptotene and zygotene stages. This transition, termed the prezygotene, includes a brief spatial separation of sister chromatids and a conspicuous elongation of normally spherical heterochromatic knobs (Dawe et al. 1994). These unique changes in chromosome morphology are part of a series of structural changes both within the nucleus and within the chromosomes themselves as seen in Figs. 8.4 and 8.5. The physical association and synapsis of coaligned homologs defines the beginning of zygotene stage of prophase I. During this stage, the chromosomes continue to shorten and thicken, and the nucleolus often occupies an eccentric location within the nucleus in many higher plant species (see Figs. 8.4a and 8.5c; Holm 1977a; Ross et al. 1996; Bass et al. 1997; Boden et al. 2007). The NE also plays a major role in chromosome behavior and segregation at meiotic prophase I. NE proteins mediate a variety of fundamental activities and are increasingly recognized for their roles in meiotic chromosome behavior (Conrad et al. 2007; Scherthan 2007; Phillips et al. 2009).

8.5.6 The Telomere Bouquet Arrangement of Meiotic Chromosomes

The clustering of telomeres on the NE during meiotic prophase I defines bouquet stage (Fig. 8.6c; Loidl 1990; Zickler and Kleckner 1998; Scherthan 2001, 2007; Bass 2003; Harper et al. 2004; Ma 2005; Hamant et al. 2006; Hiraoka 2007; Bozza and Pawlowski 2008; de La Roche Saint-Andre 2008). The bouquet forms de novo in early prophase and typically lasts from late leptotene to the middle pachytene stages (Bass et al. 1997; Zickler and Kleckner 1998). EM has revealed electron-dense structures (a conical thickening) at the point of end-on chromosome-NE attachments. These attachments are unique to meiosis and are a conserved aspect of meiotic telomere architecture (Fig. 8.4b; Esponda and Giménez-Martín 1972; Loidl 1994). The telomere bouquet stage was cytologically characterized over a century ago, although its functional significance in the meiotic telomere cluster was the subject of speculation for many subsequent decades (Bass 2003; Scherthan 2001). In maize, the early pachytene telomere cluster disperses as the NE-attached telomeres disassociate and spread out over the NE (Bass et al. 1997). Several views on the role and functional significance of the bouquet

arrangement have been put forth. Loidl (1990) argued that the complex 3D task of homolog recognition and pairing within the nucleus could be made more efficient if the homology search was essentially limited to two dimensions in a limited region of the NE. Loidl (1990) also argued that formation of the bouquet arrangement on the NE can bring spatially separated chromosomes into proximity, catalyzing productive contacts between the homologs.

8.5.7 The Mechanism of Bouquet Formation in Plants

The cytological details of the timing of the bouquet formation have been well documented and seem to follow a maize-like pattern in most plant species, but interesting exceptions do exist. For example, in *Arabidopsis*, telomeres cluster on the nucleolus, whereas in wheat, the telomere clustering stage begins before meiotic prophase (Martínez-Pérez et al. 1999; Armstrong et al. 2001). In yeast, meiotic telomere clustering on the NE requires actin, and cohesin is necessary for exit from this actin-based telomere clustering and dispersal of telomeres on the NE after the bouquet stage (Trelles-Sticken et al. 2005). The current models for plants also include cytoskeletal involvement in the organized movements of the telomeres along the NE (Schmit et al. 1994, 1996; Cowan and Cande 2002). Interestingly, the plant equivalent of the animal centrosome (the microtubule organizing center) is distributed over the NE itself (Rose et al. 2004; Meier 2007), so plausibly, microtubules interact with NE-associated proteins to direct telomere movements that typify meiotic prophase I. With a monoclonal antibody raised against calf centrosomes, studies have shown that this antiserum cross-reacts with a variety of nuclear structures throughout prophase I, including the entire NE; reacts with the chromosome termini at zygotene; and is eventually completely redistributed from the NE to the SC of the chromosomes (Schmit et al. 1994, 1996). This redistribution of this epitope from the NE to the chromosome termini at zygotene could provide the necessary reagents for telomere redistribution during meiotic prophase I (Dawe 1998).

In plants such as rye and wheat, colchicine, a microtubule-specific inhibitor, is known to disrupt crossover formation, presumably by interfering with the telomere bouquet (Loidl 1990; Cowan and Cande 2002). In a lily, meiotic cells exposed early to colchicine arrest in pachytene, whereas cells treated later, in prophase I, were able to proceed through metaphase I, albeit with defective chiasmata (Shepard et al. 1974). When rye anther cultures were used, meiotic telomere clustering was inhibited by colchicine treatment, but it did not affect the dispersal of telomeres along the NE during postbouquet stages (Cowan and Cande 2002). Coincident with the telomere bouquet in rye nuclei is the rearrangement of microtubules within the cytoskeleton as well as a change in the distribution of nuclear pore complexes (NPCs) opposite of the telomere bouquet. Changes in these pore complexes and cytostolic microtubules appear to occur independently of bouquet formation (Cowan et al. 2002). In a lily, these pore complexes also rearrange themselves in zygotene nuclei into two nuclear pore "fields," and the telomeres are localized at the NE in an area

between the two (Holm 1977a). Interestingly, depolymerization of cytoplasmic microtubules does not affect telomere clustering, suggesting that the mechanism of bouquet formation is independent of cytoplasmic microtubule organization (Cowan and Cande 2002) and is actually intrinsic within the nucleus itself. In a lily, a trypsin-sensitive, NE-associated colchicine binding activity has been characterized as distinct from the cytoplasmic colchicine-binding protein (Stern and Hotta 1974). Despite the clues from numerous descriptive analyses, the underlying molecular details of bouquet formation remain unknown.

8.5.8 Telomere Bouquet Proteins

In yeast, meiotic proteins are required to tether the telomeres to the spindle pole body (the fungal equivalent of the centrosome; Martin-Castellanos et al. 2005; Chikashige et al. 2006; Jaspersen et al. 2006; Tomita and Cooper 2006; Bupp et al. 2007; Conrad et al. 2007; Hiraoka 2007). In fission yeast, the inner nuclear membrane protein Bqt3 and associated Bqt4/Taz1-enriched telomeres are anchored to the NE during mitotic interphase, during which the centromeres are attached to the spindle pole body (Chikashige et al. 2009). The most recent models depict two unique steps during bouquet formation in this organism. First, upon induction of meiosis, Bqt1 and Bqt2 are expressed and function to connect SUN (Sad1/Unc-84) domain–containing protein Sad1 to the telomeres (Chikashige et al. 2006, 2009). Once the centromeres detach from the spindle pole body, Sad1-enriched telomeres are brought to the NE and are guided to the site of the spindle pole body, probably by an actin- or microtubule-based motility mechanism. In mammals (humans and mice), SUN domain–containing proteins have been identified, and elegant genetic and cytological studies in the mouse system have demonstrated their direct role in tethering meiotic telomeres on the inner surface of the NE as well as a role in homologous chromosome pairing, synapsis, and recombination (Ding et al. 2007; Schmitt et al. 2007).

SUN-domain proteins are widely conserved across eukaryotes, form a functional and mechanical link from the NE to the cytoskeleton, and are probably responsible for directed telomere movement throughout meiotic prophase I (Tomita and Cooper 2006; Starr 2007). So far, relatively little is known about the NE-associated proteins of meiosis, but SUN-domain proteins are beginning to be identified and characterized in several plant species including *Arabidopsis* and rice (Moriguchi et al. 2005; Tzur et al. 2006; Graumann et al. 2009).

Genetic analysis of bouquet function in plants has focused on the asynaptic (*as1* and *Asb*) mutants in tomato and the *dy* (*desynaptic*), *dsy1*, *phs1*, *afd1*, *ms25*, and *dsyCS* mutants of maize (Havekes et al. 1994; Bass 2003; Hamant et al. 2006). None of these mutants is completely unable to form a telomere bouquet as a primary defect. For example, the maize *dsy1* mutation exhibits a partial telomere bouquet configuration (Bass et al. 2003) and incomplete synapsis as the primary cytological lesions, indicating a requirement for the bouquet in efficient chromosome pairing

and synapsis in maize. Additional bouquet-related mutants, *sy1* and *sy9* in rye, form axial elements but no or incomplete SCs. Their defects are ultimately manifest as sterility because of extensive univalent accumulation at metaphase I (Sosnikhina et al. 2005).

Although the majority of eukaryotic organisms possess a telomere bouquet stage, *A. thaliana* is among the small minority of species that lack an NE-associated bouquet. FISH analyses revealed that it has instead a persistent association of the telomeres with the nucleolus throughout meiotic interphase, but during leptotene they lose this association and disperse throughout the nucleus (Armstrong et al. 2001; Armstrong and Jones 2003). Once the chromosomes begin to pair and synapse at zygotene, the telomeres become loosely polarized in one hemisphere of the nucleus, and their attachment to the outer edge of the nucleolus at zygotene might facilitate the same meiotic telomere functions that typically involve telomere-NE associations.

8.5.9 Chromosome Synapsis and the Synaptonemal Complex in Plants

Homologous chromosome synapsis includes the assembly of the SC, which bridges the axial elements of coaligned chromosomes (Gillies et al. 1974; von Wettstein et al. 1984; Moens 1994; Maguire 1995; Page and Hawley 2004; Zickler 2006). The initial installation of the SC in plants is similar to that of other eukaryotes in that initiation of synapsis typically occurs near the telomeric regions of the chromosomes but is not limited to these regions (Holm 1977a; Albini and Jones 1987). Ultrastructural approaches involving serial sectioning followed by 3D reconstruction and SC spreading techniques in plants have contributed to our understanding of this structure, especially in rye, lily, wheat, *Arabidopsis*, maize, onion, and barley (Holm 1977a, 1986; Mogensen 1977; Hobolth 1981; Albini and Jones 1984; Anderson et al. 1988; Wang 1988; Santos et al. 1994; Sherman and Stack 1995; Zhang et al. 2002; Lopez et al. 2008). Comparative analyses of the results from these and other plant SC studies established that plants have a canonical SC substructure consisting of two lateral elements (LEs) (derived from and presumably similar in composition to the leptotene-stage axial elements) connected by a central element (CE) (Fig. 8.4b) that is directed longitudinally and equidistant from the two LEs (Zickler and Kleckner 1999). The SC central region spans nearly 100 nm and contains a complex substructure of interdigitated transverse filaments (Zickler and Kleckner 1999; Page and Hawley 2004). Other dense structures termed RNs are also cytologically observable within the central region from zygotene through the disassembly of the SC in late pachytene and early diplotene.

Synapsis occurs preferentially between homologous chromosomes, but even nonhomologous synapsis can lead to the formation of a normal-appearing SC. If homologous synapsis is inhibited or rendered impossible by haploidy, partial haploidy, or chromosomal rearrangements, then nonhomologous synapsis can occur (McClintock 1933; Ting 1973; Gillies et al. 1974; Santos 1994; von Wettstein et al.

1984; Zickler and Kleckner 1999; Pawlowski et al. 2004). One issue caused by synapsis of long chromosomes and multiple points of initiation is interlocking and tangling of the chromosomes (John 1990; Zickler and Kleckner 1999). These configurations form during zygotene and appear to be resolved by pachytene. Evidence of unusual but regular right-handed twisting of the SC is known for *Rhoeo discolor* (L'Hér.) Hance ex Walp. and presumably reflects some aspect of SC assembly or subunit geometry (Moens 1972), but the hypothesis underlying mechanics of SC assembly and interlock resolution remain challenging to test with conventional cytology of fixed cells.

Abundant descriptive cytological analyses of the plant SC are now being investigated through the identification, cloning, and characterization of genes that encode proteins to make, regulate, or form the SC. Particularly informative are the *asynaptic* and *desynaptic* mutants from maize, rye, tomato, and *Arabidopsis* (Osman et al. 2006). Poor sequence homology within SC components hampers in silico approaches used for gene discovery. Nevertheless, the rice *Pair2* gene was initially cloned and characterized, revealed a similar sequence similarity, and was identified as the ortholog of the *Arabidopsis* axial element protein ASY1 (Nonomura et al. 2004a, b, 2006). Immunolocalization experiments revealed a localization pattern similar to that of ASY1, but PAIR2 is not detected on the bulk of the chromatin axes at pachytene, except for persistent localization at the centromeres through diplotene (Nonomura et al. 2006). Pair2 is not essential for axial-element formation or elongation but is probably required for recruiting the transverse filaments of the CE. In *Arabidopsis*, the first plant SC transverse-filament protein, ZYP1, was discovered by means of modified bioinformatics approaches that overcome the limitation of poor sequence homology (Higgins et al. 2005). The epitope used to generate an antibody cross reacts with wheat SCs, suggesting conservation of at least that part of the protein. These approaches, along with fluorescent protein tagging, hold great promise for further dissecting the dynamics of the SC in plants.

8.5.10 Early Recombination Pathway in Plants

In recent years, many genes involved in meiotic recombination have been cloned and characterized (Schwarzacher 2003; Hamant et al. 2006; Mezard et al. 2007; Mercier and Grelon 2008). The field is expected to expand and progress rapidly, and only a few selected genes will be discussed here to illustrate aspects of the plant recombination pathway. The initial steps of meiotic recombination begin during early prophase I with the induction of genome-wide double-stranded breaks (DSBs) by the highly conserved meiosis-specific yeast protein Spo11 (Esposito and Esposito 1969). Spo11 is homologous to the catalytic subunit of archeal type-VIA topoisomerase (Keeney et al. 1997). *Arabidopsis* has three Spo11 homologues, SPO11-1, SPO11-2, and SPO11-3, the first two of which interact, probably as a heterodimer, and contribute essential functions for the initiation of meiotic recombination (Grelon et al. 2001; Stacey et al. 2006). Loss of *SPO11* function

results in an asynaptic cytological phenotype and a severe reduction in meiotic recombination. The *Arabidopsis* SPO11-1 protein interacts with the N-terminal region of PRD1 (PUTATUVE RECOMBINATION INITIATION DEFECT 1), a protein that is required for meiotic DSB formation (De Muyt et al. 2007). SPO11-mediated DSBs are processed by the highly conserved MRN (Mre11, Rad50, Nbs1) complex characterized mainly in *Arabidopsis* but presumed to be conserved (Bleuyard et al. 2004; Puizina et al. 2004; Waterworth et al. 2007).

After production of DSBs, homologs of the yeast Rad51, a RecA family protein, mediate the strand-invasion step required for the homology search and the conversion of DSBs into hybrid joint molecules (Krogh and Symington 2004). In *Arabidopsis*, rice, lily, maize, and barley, genes encoding homologs of the yeast Rad51 protein have been identified and well characterized (*AtDMC1*, *OsDmc1*, *Lim15*, *ZmRad51a* and *ZmRad51b*, and *HvDmc1*, respectively; Schwarzacher 2003; Mezard et al. 2007; Mercier and Grelon 2008). Other *At*RAD51-interacting proteins, *At*RAD51C and *At*XRCC3, are thought to cooperate with RAD51 in the repair of DSBs in plants.

Immunocytochemistry has also revealed aspects of meiotic recombination in plants. The RAD51 and LIM15 proteins in a lily were immunolocalized in spread nuclei with anti-human RAD51 and anti-LIM15 antibodies. RAD51 foci were visualized as discrete in meiotic prophase I. Foci were abundant in leptotene and early zygotene, but their abundance showed stage-specific decreases as cells progressed into pachytene (Terasawa et al. 1995). In maize leptotene nuclei, RAD51 signals were quite diffuse, but as chromosomes began to pair, nearly 500 foci were visualized coincident with the bouquet stage. In the same study, only several foci remained at pachytene (Pawlowski et al. 2003). The dynamic localization of RAD51 and LIM15 proteins in maize and lily in meiotic nuclei are therefore consistent with their roles in the homology search during the early to mid stages of recombination. In the maize *dsy2* (*desynaptic*2) mutant, reduced pairing, abnormal chromosome synapsis, and a decrease in recombination are associated with elongated RAD51 foci, suggesting a role for DSY2 in proper RAD51 behavior at meiotic prophase (Franklin et al. 2003).

Other key genes within *Arabidopsis* that are likely to be involved in the strand-invasion step are *MND1*, *AHP2*, and *BRCA2* (Siaud et al. 2004). An interaction between BRCA2 and DMC1 was found in two-hybrid analyses. Silencing of the *BRCA2* gene in *Arabidopsis* by means of RNAi leads to unrepaired DSBs (Siaud et al. 2004). The MND1 protein is localized to the chromatin during meiosis, and its distribution along the chromosomes depends on AHP2 but not on recombination initiation by SPO11 (Vignard et al. 2007). Furthermore, the accumulation of DMC1 foci on the chromosomes depended on RAD51 but not XRCC3. Taken together, these findings indicate that in *Arabidopsis* MND1 and AHP2 interact with both RAD51 and DMC1 in a dynamic fashion to catalyze the DNA strand-exchange events during the homology search in meiotic recombination. In *Arabidopsis*, the homolog to the human ATM protein kinase has been identified and characterized (Garcia et al. 2003), although its precise role in meiosis (and in particular in DNA repair during recombination) is still not clear. Finally, *Arabidopsis* has at least

six different RecQ-like helicases within its genome (Hartung et al. 2000). RecQ helicases in fungi and animals are involved in DNA repair and recombination. Although the precise roles of these helicases are still under investigation, some of them may act in the branch-migration step at the Holliday junction and may be required for RAD51 removal.

8.5.11 Cytology of Early Recombination Nodules

RNs are electron-dense spherical or ellipsoidal structures (~50–200 nm) associated with the SC (Carpenter 1975; Dawe 1998; Zickler and Kleckner 1999; Mezard et al. 2007) that have fascinated cell biologists and cytologists for many decades. Those that are abundant in early zygotene through the middle of pachytene are referred to as early RNs and are typically associated with euchromatic regions in plants (Anderson et al. 2001; Anderson and Stack 2005). Late RNs are less abundant, are prevalent in pachytene, and probably mark the actual sites of chiasmata. The cumulative distribution of late RNs on pachytene chromosomes has been used to generate a cytological recombination map that inherently relates genetic and physical distances along the chromosomes (Sherman and Stack 1995; Anderson et al. 2003).

8.5.12 Late Recombination Nodules and Crossover Interference in Plants

At least one mature crossover event must be installed between homologous chromosomes to ensure segregation at anaphase I. Meiotic DSBs can be resolved into crossover or noncrossover products. A gene unique to the plant kingdom, *PTD* (*PARTING DANCERS*), has been studied in *Arabidopsis* and shown to play a role in crossover formation, mainly promoting interference-sensitive crossovers (Wijeratne et al. 2006). The amino acid sequence of PTD reveals some homology to the yeast Ercc1 and may be involved in resolving meiotic double Holliday junctions. Still other genes involved in the later steps of meiotic recombination have been thoroughly studied in *Arabidopsis*; these include *MLH1*, *MLH3*, *ZIP4*, *MPA1*, and *RCK*, all of which are required for successful crossover formation (Sanchez-Moran et al. 2004; Mercier and Grelon 2008).

During the zygotene-to-pachytene transition, most of the early RNs are removed, disintegrate, or simply disassociate from the SC altogether. The late RNs appear de novo or are derived from a subset of early RNs (Dawe 1998; Zickler and Kleckner 1999). Late RNs have not been observed with unsynapsed regions of chromosomes and are usually associated with the CE of the SC, consistent with the evidence that late RNs mark crossover sites (von Wettstein et al. 1984; Sherman and Stack 1995). Ultrastructural studies in a variety of plant species show that synapsis generally proceeds from the sites of axial-element interaction that tend to load early RNs (Albini and Jones 1984, 1987). Some evidence in plants indicates that late RNs actually arise

from early RNs, and the two types of nodules may or may not be present at the same time (Albini and Jones 1988). Nevertheless, the early RNs visualized in plant nuclei far outnumber the late RNs seen in pachytene preparations.

In plants, chiasmata can be found at points along the chromosome fibers but show a preference for the terminal regions (von Wettstein et al. 1984; Zickler and Kleckner 1999). Analysis of chiasma formation in the maize *dy* mutant revealed that recombination alone is insufficient for stabilizing chiasma positions, suggesting that additional factors mediate chiasma maintenance (Maguire et al. 1991, 1993).

RN research in plants remains an active area of genetic and cytogenetic studies (La Cour and Wells 1970; Albini and Jones 1984, 1988; Maguire et al. 1991, 1993; Dawe 1998; Ji et al. 1999; Zickler and Kleckner 1999; Caryl et al. 2003; Higgins et al. 2005).

8.5.13 Recombination and Chiasma Distribution in Plants

Crossover control is no doubt under selective pressure to generate diverse allelic combinations. Crossover distribution is shaped by crossover events in the genome (Mezard 2006; Mezard et al. 2007). Regions of the genome with high frequencies of recombination are referred to as "hot spots." In *Arabidopsis*, recombination hot spots were examined and proved to be correlated with gene-rich regions of the genome, whereas relatively gene-poor centromeric and pericentromeric regions were recombinationally less active (Fransz et al. 2000). This pattern is typical among plant species that have been studied in the past (Stack 1984; Stephan and Langley 1998; Mezard 2006; Mezard et al. 2007).

8.5.14 Cytology and Behavior of Chromosomes in Middle and Late Meiotic Prophase

In the transition from the zygotene to the pachytene stage of meiotic prophase, chromosomes continue to shorten and thicken, and the installation of the SC is completed. The intimate synapsis of homologs along the entire bivalent results in a single thick fiber. This structure, when viewed as a pachytene chromosome spread, provides cytologists with a unique view of an entire genome, organized into the haploid number of chromosome fibers as shown in Figs. 8.5d and 8.6d. For these reasons, the pachytene stage of meiotic prophase is among the most thoroughly characterized stages of meiosis. The elongated, synapsed fibers are ideal for karyotyping, mapping translocations, and pachytene FISH mapping in many plant species (Zhong et al. 1996; Cheng et al. 2001; Kim et al. 2005; Wang and Chen 2005). Although the pachytene stage marks the completion of synapsis and the end of the homology search, the chromosomes are far from static at this stage. In maize, telomeres remain attached to the NE as the bouquet disperses, after which the telomere-NE connection is dissolved at some point later in the pachytene stage

(Bass et al. 1997; Bass 2003). Live imaging further reveals dramatic chromosome and nuclear movements during the pachytene stage and shows that these movements require functional cytoskeletal motility systems (Sheehan and Pawlowski 2009).

By the late pachytene and early diplotene stages, the chromosomes undergo a marked transformation from somewhat knobby, tubular fibers to less regular and somewhat scraggly-looking bivalent fiber configurations (Fig. 8.5e). In particular, a transient decondensation that occurs during the pachytene-to-diplotene transition has been referred to as "the diffuse stage" (Moens 1968; Zickler and Kleckner 1999; Stronghill and Hasenkampf 2007). At this transition, the chromosomes appear fuzzy and undercondensed. This diffuse stage has not been reported for many plant species, but in *Arabidopsis* it has been observed and found to coincide with overcondensation of centromeres (Stronghill and Hasenkampf 2007). This intriguing change may reflect the initial stages of chromatin restructuring required for the subsequent axial compaction and further condensation that is characteristic of diakinesis.

A hallmark of diplotene is the desynapsis of the homologs (Fig. 8.5e). Bivalents begin to separate at one or more places along their length until they are completely detached except for the connections at sites of crossover. Centromere FISH analyses in *Arabidopsis* showed that the centromeric regions of the bivalents are among the last regions to desynapse (Armstrong and Jones 2003). The crossovers, also known as chiasmata, serve to hold homologous chromosome pairs together until they disjoin to accomplish a defining event of meiosis, genome reduction from diploid to haploid at anaphase of the first meiotic division.

As meiocytes enter diakinesis, further chromosome compaction and shortening occur, the bivalents take on a dispersed arrangement within the nucleus, the nucleolus becomes much smaller, and the SC disappears by mechanisms that remain largely unknown.

In diakinesis, the sister chromatids remain tightly associated, yet homologous chromosomes appear to move away from one another in a phenomenon referred to as repulsion, a bowing out of the homolog that may result from structural features of chiasmata together with chromosome compaction (Zickler and Kleckner 1999). Diakinesis bivalents often take on one of several shapes, depending on the number and locations of the chiasmata. A single crossover in a bivalent will result in a cross-shaped bivalent if the chiasma is in the middle but a rod-shaped bivalent if it is at one end or the other. A common configuration is the ring-shaped bivalent, which results from two chiasmata located at opposite ends of the chromosomes.

8.6 Bivalent-Spindle Interactions in Meiosis I

Chiasma and bivalency may also have a role in the formation of a functional bipolar meiotic spindle apparatus. Genetic studies of meiosis- and synapsis-impaired mutants revealed defects in both bivalent and spindle formation (Staiger and Cande 1990; Chan and Cande 1998; Dawe 1998; Shamina 2005). In meiosis, as opposed to mitosis, the bivalents themselves appear to nucleate microtubule arrays, which later converge and are incorporated into the metaphase I spindle.

At the onset of anaphase I, interzonal microtubules coalesce into discrete bundles, and homologous chromosomes disjoin as the chiasmata finally fall apart. The *SGO* (*SHUGOSHIN*) gene is necessary for the protection of sister centromeric cohesion at meiosis I, and unlike that of its animal counterpart, the loading of plant SGO apparently requires presence of AFD1/REC8 on the chromosomes (Hamant et al. 2005). In addition, the enzyme separase (AESP in *Arabidopsis*) also mediates the release of cohesion from the chromosome arms, except at the centromeres (Liu and Makaroff 2006). At the onset of telophase I, the phragmoplast forms briefly, then disintegrates as radial microtubule arrays and the NE reform (Van Damme et al. 2004). The *dv* (*divergent spindle*) meiotic mutant of maize (Clark 1940) inhibits the convergence of microtubule spindle fibers at the poles at metaphase I and shows persistent microtubule organization defects during meiosis II (Staiger and Cande 1990); it is also found to disrupt NE breakdown during vesiculation (Shamina et al. 2000). Ultimately, this mutation results in chromosome missegregation, aneuploidy, and sterility and may shed light on factors that connect NE disassembly with spindle assembly in meiosis. Taken together, molecular-genetic and cytological analyses in *Arabidopsis*, maize, and other plant species support the self-assembly model for meiotic spindle formation in which microtubules initially grow from a number of sites around the condensed chromosomes before their organization into bipolar arrays (Hyman and Karsenti 1996; Shamina 2005).

The *ATK1* (*Arabidopsis thaliana KINESIN 1*) gene was identified as a male-specific Ds-tagged gene that affected meiotic spindle organization (Chen et al. 2002). Cloning of this gene revealed its similarity to kinesin motor domain families found in yeast, which are responsible for generating a motive force along microtubules by hydrolyzing ATP (Goldstein 2001). Mutants are defective in chromosome segregation at meiosis, failing to align chromosomes in parallel at metaphase I and II and subsequently producing aberrant disjunctive segregation events at anaphase I and II. Furthermore, meiotic spindles were broad and multiaxial at the poles at metaphase I, suggesting a clear role for a putative kinesin-like microtubule motor protein in meiotic spindle morphogenesis in plants (Chen et al. 2002).

8.7 Meiosis II

The cytology and morphological characteristics of chromosomes during meiosis II superficially resemble those of mitotic nuclear divisions. At the beginning of prophase II, the chromatids appear partially separated and typically surround the nucleolus. During metaphase II, associated sister chromatids are greatly contracted and align at the equatorial plate, the NE breaks down, and the nucleolus disappears. During anaphase II, sister centromeres finally separate as the enzyme separase/AESP cleaves the remaining SYN1/REC8, which served to hold the centromeres together (Liu and Makaroff 2006). The chromatids, most of which are recombinant, move to opposite poles, resulting in the equational nuclear division of meiosis. Completion of the second division and the subsequent cell division mark the beginning of the gametophyte phase, the haploid generation of the plant life cycle.

8.8 Meiotic Centromeres

Most plants have regional centromeres that consist of large arrays of rapidly evolving satellite DNA sequences, in which species-specific retrotransposons are prevalent, and nucleosomes with a specialized centromeric histone H3 variant, CENH3 (Ma et al. 2007; Wang et al. 2009). CENH3-containing nucleosomes may be a primary structural element in centromeres, because they are required for kinetochore formation and therefore represent an epigenetic determinant for centromere specification (Wang et al. 2009). How the meiotic kinetochore regulates chromosome movements and its molecular components are still being elucidated in higher plants (Dawe 1998; Yu et al. 2000; Shi et al. 2010). Light and electron microscopic analysis of meiotic kinetochores revealed the presence of two domains. The inner domain contains structural proteins, including CENP-C (Dawe et al. 1999) and NDC80 (Du and Dawe 2007), and the outer contains various motility and cell-cycle checkpoint proteins, including MAD2, which ensures the proper completion of metaphase before progress into anaphase (Yu et al. 1999; Dawe et al. 2005).

Many plant species can also exhibit neocentromeres. Maize neocentromeres orchestrate non-kinetochore-based chromosome movements toward the spindle poles (Rhoades and Vilkomerson 1942; Dawe and Hiatt 2004). The knob-based neocentromeres are heterochromatic domains that can make lateral attachments to spindle microtubules, moving chromosomes to the spindle poles and, under certain conditions, effecting meiotic drive (Yu et al. 1997; Hiatt et al. 2002). The evolutionary origin, role in meiotic drive, and molecular mechanisms of plant neocentromeres remain intriguing areas of research (Dawe and Hiatt 2004).

8.9 Meiotic Chromatin

Primary chromatin proteins include the core nucleosomal histones, H2A, H2B, H3, and H4, plus the nonnucleosomal linker histone H1. Of these, the linker histones show the most variation from one cell type to another. Sheridan and Stern (1967) extracted and analyzed histones from the male meiotic cells of a lily and found the histones mostly to resemble those of somatic cells, with the exception of the striking appearance of a meiosis-specific variant they called “the meiotic histone” (Sheridan and Stern 1967). Later cloned and referred to as *Meiotin-1*, this meiotic H1 histone variant, which lacks a charged N-terminal region, was found to be present together with but at a lower concentration than histone H1 (Riggs and Hasenkampf 1991; Riggs 1994, 1997). The meiotic histone/meiotin-1 protein appears to be primarily associated with chromatin in early prophase, where it is thought to help maintain chromatin and chromosomal structures conducive to synapsis and homologous chromosome recombination (Hasenkampf et al. 1998).

In addition to changes in the composition of chromatin proteins, plants exhibit meiosis-specific patterns of histone modification. For example, the phosphorylation of serine 10 of histone H3 (H3-Ser10) shows interesting spatial and temporal patterns on meiotic chromosomes (Kaszas and Cande 2000; Hamant et al. 2006;

Houben et al. 2007). Changes in the phosphorylation status of H3-Ser10 are correlated with changes in the cohesion status of the sister chromatids, and phosphorylation of H3-Thr3/11 is correlated with condensed mitotic and meiotic chromatin and occurs along the entire length of the chromosomes in a variety of plant species (Kaszas and Cande 2000; Houben et al. 2005). Future studies of the significance of the occurrence, location, and dynamics of these and other histone modifications during meiosis will provide much-needed information about the role of chromatin structure in plant meiosis (Loidl 2004).

8.10 Ploidy Level and Meiotic Challenges

The majority of angiosperm species exhibit polyploidy, the condition in which nuclear genomes have more than one set of homologous pairs of chromosomes (Masterson 1994; Moore 2002). Allopolyploidy can result when hybridization combines genomes from related species, whereas autopolyploidy can result from various mechanisms that cause chromosome doubling. These changes in genome constitution pose additional challenges for the ability of meiosis to maintain balanced genomes. In plants, polyploidy can result from spontaneous doubling or from genetic mutations that result in aberrant meiosis (Sears 1976; Ramsey and Schemske 1998). Regardless of cause, polyploidy confounds meiosis because the cells must pair and segregate homologous and homeologous chromosomes in a normal disomic fashion (Nicolas et al. 2008). Polyploid organisms exploit different genetic, structural, and mechanical mechanisms to ensure that chromosome pairing and segregation at meiosis proceed with high efficiency (Chapman and Kimber 1992a, b; Otto and Whitton 2000; Moore 2002; Griffiths et al. 2006; Otto 2007). Among the best-characterized polyploid systems is the allohexaploid bread wheat, in which three different sets of chromosomes are present, called A, B, and D. The dominant *Ph1* locus is known to increase the fidelity of subgenome synapsis while reducing homeologous interactions (Martínez-Pérez et al. 2000; Moore 2002). Efforts to map and characterize the *Ph1* locus have focused on a small region of chromosome 5B (Griffiths et al. 2006; Sidhu et al. 2008). Multiple candidate genes reflect the complexity of this locus, which has intrigued and puzzled plant cytogeneticists for decades (Sidhu et al. 2008; Martínez-Pérez et al. 2001).

8.11 Future Directions for Cytogenetics of Plant Meiosis

Plants have clearly been at the forefront of cytological observations of meiotic chromosome behavior for over a century (Figueroa and Bass 2010). Recently, the genetic control of meiosis and chromosome behavior in higher plants has been well characterized by means of forward and reverse genetics approaches, primarily in *Arabidopsis* but also in rice, maize, tomato, wheat, and other plant species (Mercier

and Grelon 2008). Although more than 50 meiotic genes have been cloned and characterized from plant species, significant gaps remain in our knowledge of their specific molecular mechanisms and the pathways in which they interact. Classic genetics, functional genomics, and cytogenetics offer a powerful combination for exploring unanswered questions about plant meiotic chromosomes, including the regulation of progression through the stages of meiosis, the functional significance of changes in chromosome structure, the mechanisms that govern specificity and fidelity in homolog pairing, the molecular control of crossover initiation and distribution, and the role of small RNAs or epigenetic regulation in meiosis. Finally, comparative analyses across the plant kingdom promise to reveal aspects of meiosis that are conserved across all eukaryotes while highlighting evolutionary innovations unique to plants or specific groups of plants as defined by their phylogenetic relationships.

Acknowledgments We thank A.B. Thistle and members of the Bass laboratory for critical reading of the chapter and insightful comments. This work was supported by an American Heart Association predoctoral fellowship to SPM (# 0715487B, AHA, Greater Southeast Affiliate) and by the National Science Foundation (HWB, DBI-0321639).

References

Agashe B, Prasad CK, Siddiqi I (2002) Identification and analysis of DYAD: a gene required for meiotic chromosome organisation and female meiotic progression in *Arabidopsis. Development* 129:3935–3943.

Albini SM, Jones GH (1984) Synaptonemal complex–associated centromeres and recombination nodules in plant meiocytes prepared by an improved surface-spreading technique. *Exp Cell Res* 155:588–592.

Albini SM, Jones GH (1987) Synaptonemal complex spreading in *Allium cepa* and *Allium fistulosum*. I. The initiation and sequence of pairing. *Chromosoma* 95:324–338.

Albini SM, Jones GH (1988) Synaptonemal complex spreading in *Allium cepa* and *Allium fistulosum.* II. Pachytene observations: the SC karyotype and the correspondence of late recombination nodules and chiasmata. *Genome* 30:399–410.

Anderson E (1972) *The Meiotic Process: Pairing, Recombination, and Chromosome Movements; Papers.* MSS Information, New York.

Anderson LK, Stack SM (2005) Recombination nodules in plants. *Cytogenet Genome Res* 109:198–204.

Anderson LK, Stack SM, Sherman JD (1988) Spreading synaptonemal complexes from *Zea mays*. I. No synaptic adjustment of inversion loops during pachytene. *Chromosoma* 96:295–305.

Anderson LK, Hooker KD, Stack SM (2001) The distribution of early recombination nodules on zygotene bivalents from plants. *Genetics* 159:1259–1269.

Anderson LK, Doyle GG, Brigham B, Carter J, Hooker KD, Lai A, Rice M, Stack SM (2003) High-resolution crossover maps for each bivalent of *Zea mays* using recombination nodules. *Genetics* 165:849–865.

Aravind L, Iyer LM (2002) The SWIRM domain: a conserved module found in chromosomal proteins points to novel chromatin-modifying activities. *Genome Biol* 3(8):0039.1.

Aravind L, Koonin EV (1998) The HORMA domain: a common structural denominator in mitotic checkpoints, chromosome synapsis and DNA repair. *Trends Biochem Sci* 23:284–286.

Armstrong SJ, Jones GH (2003) Meiotic cytology and chromosome behaviour in wild-type *Arabidopsis thaliana. J Exp Bot* 54:1–10.

Armstrong SJ, Franklin FC, Jones GH (2001) Nucleolus-associated telomere clustering and pairing precede meiotic chromosome synapsis in *Arabidopsis thaliana. J Cell Sci* 114: 4207–4217.

Armstrong SJ, Caryl, AP, Jones GH, Franklin FC (2002) Asy1, a protein required for meiotic chromosome synapsis, localizes to axis-associated chromatin in *Arabidopsis* and *Brassica. J Cell Sci* 115:3645–3655.

Arndt-Jovin DJ, Jovin TM (1989) Fluorescence labeling and microscopy of DNA. *Methods Cell Biol* 30:417–448.

Azumi Y, Liu D, Zhao D, Li W, Wang G, Hu Y, Ma H (2002) Homolog interaction during meiotic prophase I in *Arabidopsis* requires the SOLO DANCERS gene encoding a novel cyclin-like protein. *EMBO J* 21:3081–3095.

Banerjee D, Pal SK (2008) Dynamics in the DNA recognition by DAPI: exploration of the various binding modes. *J Phys Chem B* 112:1016–1021.

Bass HW (2003) Telomere dynamics unique to meiotic prophase: formation and significance of the bouquet. *Cell Mol Life Sci* 60:2319–2324.

Bass HW, Marshall WF, Sedat JW, Agard DA, Cande WZ (1997) Telomeres cluster de novo before the initiation of synapsis: a three-dimensional spatial analysis of telomere positions before and during meiotic prophase. *J Cell Biol* 137:5–18.

Bass HW, Riera-Lizarazu O, Ananiev EV, Bordoli SJ, Rines HW, Phillips RL, Sedat JW, Agard DA, Cande WZ (2000) Evidence for the coincident initiation of homolog pairing and synapsis during the telomere-clustering (bouquet) stage of meiotic prophase. *J Cell Sci* 113: 1033–1042.

Bass HW, Bordoli SJ, Foss EM (2003) The *desynaptic* (*dy*) and *desynaptic1* (*dsy1*) mutations in maize (*Zea mays* L.) cause distinct telomere-misplacement phenotypes during meiotic prophase. *J Exp Bot* 54:39–46.

Belling J (1921) On counting chromosomes in pollen-mother cells. *Am Nat* 66:573–574.

Bennett MD (1971) The duration of meiosis. *Proc R Soc Lond B Biol Sci* 178:277–299.

Bennett MD (1977) The time and duration of meiosis. *Phil Trans R Soc Lond B Biol Sci* 277:201–226.

Bennett MD, Chapman V, Riley R (1971) The duration of meiosis in pollen mother cells of wheat, rye, and *Triticale*. *Proc R Soc Lond B Biol Sci* 178:259–275.

Bennett MD, Finch RA, Smith JB, Rao MK (1973) The time and duration of female meiosis in wheat, rye, and barley. *Proc R Soc Lond B Biol Sci* 183:301–319.

Bennett MD, Dover GA, Riley R (1974) Meiotic duration in wheat genotypes with or without homoeologous meiotic chromosome pairing. *Proc R Soc Lond B Biol Sci* 187:191–207.

Bhatt AM, Lister C, Page T, Fransz P, Findlay K, Jones GH, Dickson HG, Dean C (1999) The *DIF1* gene of *Arabidopsis* is required for meiotic chromosome segregation and belongs to the *REC8/RAD21* cohesin gene family. *Plant J* 19:463–472.

Bhatt AM, Canales C, Dickinson HG (2001) Plant meiosis: the means to 1N. *Trends Plant Sci* 6:114–121.

Bleuyard J-Y, Gallego ME, White CI (2004) Meiotic defects in the *Arabidopsis rad50* mutant point to conservation of the MRX complex function in early stages of meiotic recombination. *Chromosoma* 113:197–203.

Boden SA, Shadiac N, Tucker EJ, Langridge P, Able JA (2007) Expression and functional analysis of *TaASY1* during meiosis of bread wheat (*Triticum aestivum*). *BMC Mol Biol* 8:65.

Bozza CG, Pawlowski WP (2008) The cytogenetics of homologous chromosome pairing in meiosis in plants. *Cytogenet Genome Res* 120:313–319.

Buck JB (1935) Permanent aceto-carmine preparations. *Science* 81:75.

Bupp JM, Martin AE, Stensrud ES, Jaspersen SL (2007) Telomere anchoring at the nuclear periphery requires the budding yeast Sad1-UNC-84 domain protein Mps3. *J Cell Biol* 179:845–854.

Cai X, Dong F, Edelmann RE, Makaroff CA (2003) The *Arabidopsis* SYN1 cohesin protein is required for sister chromatid arm cohesion and homologous chromosome pairing. *J Cell Sci* 116:2999–3007.

Carlton PM (2008) Three-dimensional structured illumination microscopy and its application to chromosome structure. *Chromosome Res* 16:351–365.
Carlton PM, Cande WZ (2002) Telomeres act autonomously in maize to organize the meiotic bouquet from a semipolarized chromosome orientation. *J Cell Biol* 157:231–242.
Carpenter AT (1975) Electron microscopy of meiosis in *Drosophila melanogaster* females: II. The recombination nodule—a recombination-associated structure at pachytene? *Proc Natl Acad Sci USA* 72:3186–3189.
Caryl AP, Armstrong SJ, Jones GH, Franklin FC (2000) A homologue of the yeast *HOP1* gene is inactivated in the *Arabidopsis* meiotic mutant *asy1*. *Chromosoma* 109:62–71.
Caryl AP, Jones GH, Franklin FC (2003) Dissecting plant meiosis using *Arabidopsis thaliana* mutants. *J Exp Bot* 54:25–38.
Cesarone CF, Bolognesi C, Santi L (1979) Improved microfluorometric DNA determination in biological material using 33258 Hoechst. *Anal Biochem* 100:188–197.
Chan A, Cande WZ (1998) Maize meiotic spindles assemble around chromatin and do not require paired chromosomes. *J Cell Sci* 111:3507–3515.
Chan A, Cande WZ (2000) Maize meiocytes in culture. *Plant Cell* 60:187–195.
Chang MT, Neuffer MG (1989) Maize microsporogenesis. Genome 32:232–244.
Chapman CG, Kimber G (1992a) Developments in the meiotic analysis of hybrids. I. Review of theory and optimization in triploids. *Heredity* 68:97–103.
Chapman CG, Kimber G (1992b) Developments in the meiotic analysis of hybrids. II. Amended models for tetraploids. *Heredity* 68:105–113.
Chelysheva L, Diallo S, Vezon D, Gendrot G, Vrielynck N, Belcram K, Rocques N, Marquez-Lema A, Bhatt AM, Horlow C, Mercier R, Mezard C, Grelon M (2005) AtREC8 and AtSCC3 are essential to the monopolar orientation of the kinetochores during meiosis. *J Cell Sci* 118:4621–4632.
Chen C, Marcus A, Li W, Hu Y, Calzada JP, Grossniklaus U, Cyr RJ, Ma H (2002) The *Arabidopsis ATK1* gene is required for spindle morphogenesis in male meiosis. *Development* 129:2401–2409.
Cheng Z, Buell CR, Wing RA, Gu M, Jiang J (2001) Toward a cytological characterization of the rice genome. *Genome Res* 11:2133–2141.
Chikashige Y, Tsutsumi C, Yamane M, Okamasa K, Haraguchi T, Hiraoka Y (2006) Meiotic proteins bqt1 and bqt2 tether telomeres to form the bouquet arrangement of chromosomes. Cell 125:59–69.
Chikashige Y, Yamane M, Okamasa K, Tsutsumi C, Kojidani T, Sato M, Haraguchi T, Hiraoka Y (2009) Membrane proteins Bqt3 and −4 anchor telomeres to the nuclear envelope to ensure chromosomal bouquet formation. *J Cell Biol* 187:413–427.
Churchill FB (1970) Hertwig, Weismann, and the meaning of reduction division circa 1890. *Isis* 61:429–457.
Clark FJ (1940) Cytogenetic studies of divergent meiotic spindle formation in *Zea mays*. *Am J Bot* 27:547–559.
Conrad MN, Lee CY, Wilkerson JL, Dresser ME (2007) MPS3 mediates meiotic bouquet formation in *Saccharomyces cerevisiae. Proc Natl Acad Sci USA* 104:8863–8868.
Cowan CR, Cande WZ (2002) Meiotic telomere clustering is inhibited by colchicine but does not require cytoplasmic microtubules. *J Cell Sci* 115:3747–3756.
Cowan CR, Carlton PM, Cande WZ (2002) Reorganization and polarization of the meiotic bouquet-stage cell can be uncoupled from telomere clustering. *J Cell Sci* 115:3757–3766.
Darlington CD (1931a) The mechanism of crossing-over. *Science* 73:561–562.
Darlington CD (1931b) Meiosis. *Biol Rev* 6:221–252.
Darlington CD (1932) *Recent Advances in Cytology.* Churchill, London.
Darlington CD (1977) Meiosis in perspective. *Phil Trans R Soc Lond B Biol Sci* 277:185–189.
Dawe RK (1998) Meiotic chromosome organization and segregation in plants. *Annu Rev Plant Physiol Plant Mol Biol* 49:371–395.
Dawe RK, Hiatt EN (2004) Plant neocentromeres: fast, focused, and driven. *Chromosome Res* 12:655–669.

Dawe RK, Sedat JW, Agard DA, Cande WZ (1994) Meiotic chromosome pairing in maize is associated with a novel chromatin organization. Cell 76:901–912.
Dawe RK, Reed LM, Yu HG, Muszynski MG, Hiatt EN (1999) A maize homolog of mammalian CENPC is a constitutive component of the inner kinetochore. *Plant Cell* 11:1227–1238.
Dawe RK, Richardson EA, Zhang X (2005) The simple ultrastructure of the maize kinetochore fits a two-domain model. *Cytogenet Genome Res* 109:128–133.
de Jong H (2003) Visualizing DNA domains and sequences by microscopy: a fifty-year history of molecular cytogenetics. *Genome* 46:943–946.
de La Roche Saint-André C (2008) Alternative ends: telomeres and meiosis. *Biochimie* 90:181–189.
De Muyt A, Vezon D, Gendrot G, Gallois JL, Stevens R, Grelon M (2007) AtPRD1 is required for meiotic double strand break formation in *Arabidopsis thaliana. EMBO J* 26:4126–4137.
Dennis ES, Peacock WJ (2007) Epigenetic regulation of flowering. *Curr Opin Plant Biol* 10:520–527.
Ding X, Xu R, Yu J, Xu T, Zhuang Y, Han M (2007) SUN1 is required for telomere attachment to nuclear envelope and gametogenesis in mice. *Dev Cell* 12:863–872.
Drews GN, Lee D, Christensen CA (1998) Genetic analysis of female gametophyte development and function. Plant Cell 10:5–17.
Du Y, Dawe RK (2007) Maize NDC80 is a constitutive feature of the central kinetochore. *Chromosome Res* 15:767–775.
Esponda P, Giménez-Martín G (1972) The attachment of the synaptonemal complex to the nuclear envelope. An ultrastructural and cytochemical analysis. *Chromosoma* 38:405–417.
Esposito MS, Esposito RE (1969) The genetic control of sporulation in *Saccharomyces.* I. The isolation of temperature-sensitive sporulation-deficient mutants. *Genetics* 61:79–89.
Figueroa DM, Bass HW (2010) A historical and modern perspective on plant cytogenetics. *Briefings Funct Genomics* 9:95–102.
Franklin AE, Golubovskaya IN, Bass HW, Cande WZ (2003) Improper chromosome synapsis is associated with elongated RAD51 structures in the maize *desynaptic2* mutant. *Chromosoma* 112:17–25.
Fransz PF, Armstrong S, de Jong JH, Parnell LD, van Drunen C, Dean C, Zabel P, Bisseling T, Jones GH (2000) Integrated cytogenetic map of chromosome arm 4S of *A. thaliana:* structural organization of heterochromatic knob and centromere region. *Cell* 100:367–376.
Fransz P, de Jong JH, Lysak M, Castiglione MR, Schubert I (2002) Interphase chromosomes in *Arabidopsis* are organized as well defined chromocenters from which euchromatin loops emanate. *Proc Natl Acad Sci USA* 99:14584–14589.
Garcia V, Bruchet H, Camescasse D, Granier F, Bouchez D, Tissier A (2003) *AtATM* is essential for meiosis and the somatic response to DNA damage in plants. *Plant Cell* 15:119–132.
Gillies CB, Rasmussen SW, von Wettstein D (1974) The synaptinemal complex in homologous and nonhomologous pairing of chromosomes. *Cold Spring Harbor Symp Quant Biol* 38:117–122.
Goldstein LS (2001) Molecular motors: from one motor many tails to one motor many tales. *Trends Cell Biol* 11:477–482.
Golubovskaya IN (1979) Genetic control of meiosis. *Int Rev Cytol* 58:247–290.
Golubovskaya IN, Khristolyubova NB (1985) The cytogenetic evidence of the gene control of meiosis: maize meiosis and mei-genes. In: Freeling M (ed), *Plant Genetics*. Alan R. Liss, New York, pp. 723–738.
Golubovskaya I, Grebennikova ZK, Avalkina NA, Sheridan WF (1993) The role of the *ameiotic1* gene in the initiation of meiosis and in subsequent meiotic events in maize. *Genetics* 135:1151–1166.
Golubovskaya I, Avalkina N, Sheridan WF (1997) New insights into the role of the maize *ameiotic1* locus. *Genetics* 147:1339–1350.
Golubovskaya IN, Hamant O, Timofejeva L, Wang CJ, Brand D, Meeley R, Cande WZ (2006) Alleles of *afd1* dissect REC8 functions during meiotic prophase I. *J Cell Sci* 119:3306–3315.
Graumann K, Runions J, Evans DE (2009) Characterization of SUN-domain proteins at the higher plant nuclear envelope. *Plant J* 61:134–144.

Grelon M, Vezon D, Gendrot G, Pelletier G (2001) AtSPO11-1 is necessary for efficient meiotic recombination in plants. *EMBO J* 20:589–600.

Griffiths S, Sharp R, Foote TN, Bertin I, Wanous M, Reader S, Colas I, Moore G (2006) Molecular characterization of *Ph1* as a major chromosome pairing locus in polyploid wheat. *Nature* 439:749–752.

Grossniklaus U, Schneitz K (1998) The molecular and genetic basis of ovule and megagametophyte development. *Semin Cell Dev Biol* 9:227–238.

Gustafsson MG, Shao L, Carlton PM, Wang CJ, Golubovskaya IN, Cande WZ, Agard DA, Sedat JW (2008) Three-dimensional resolution doubling in wide-field fluorescence microscopy by structured illumination. *Biophys J* 94:4957–4970.

Hamant O, Golubovskaya I, Meeley R, Fiume E, Timofejeva L, Schleiffer A, Nasmyth K, Cande WZ (2005) A REC8-dependent plant Shugoshin is required for maintenance of centromeric cohesion during meiosis and has no mitotic functions. *Curr Biol* 15:948–954.

Hamant O, Ma H, Cande WZ (2006) Genetics of meiotic prophase I in plants. Annu Rev Plant Biol 57:267–302.

Harper L, Golubovskaya I, Cande WZ (2004) A bouquet of chromosomes. *J Cell Sci* 117: 4025–4032.

Hartung F, Plchova H, Puchta H (2000) Molecular characterisation of RecQ homologues in *Arabidopsis thaliana. Nucleic Acids Res* 28:4275–4282.

Hasenkampf CA, Qureshi M, Rzepczyk A (1998) Meiotin-1, a meiosis-enriched protein present in normal leptotene chromosomes and lacking in precociously condensed leptotene chromosomes. *Chromosome Res* 6:277–283.

Havekes FW, de Jong JH, Heyting C, Remanna MS (1994) Synapsis and chiasma formation in four meiotic mutants of tomato (*Lycopersicon esculentum*). *Chromosome Res* 2:315–325.

Hiatt EN, Kentner EK, Dawe RK (2002) Independently regulated neocentromere activity of two classes of tandem repeat arrays. *Plant Cell* 14:407–420.

Higgins JD, Sanchez-Moran E, Armstrong SJ, Jones GH, Franklin FC (2005) The *Arabidopsis* synaptonemal complex protein ZYP1 is required for chromosome synapsis and normal fidelity of crossing over. *Genes Dev* 19:2488–2500.

Hobolth P (1981) Chromosome pairing in allohexaploid wheat var. Chinese Spring. Transformation of multivalents into bivalents, a mechanism for exclusive bivalent formation. *Carlsberg Res Commun* 46:129–173.

Holm PB (1977a) Three-dimensional reconstruction of chromosome pairing during the zygotene stage of meiosis in *Lillium longiflorum* (Thunb). *Carlsberg Res Commun* 42:103–151.

Holm PB (1977b) The premeiotic DNA replication of euchromatin and heterochromatin in *Lilium longiflorum* (Thunb). *Carlsberg Res Commun* 42:249–281.

Holm PB (1986) Chromosome pairing and chiasma formation in allohexaploid wheat, *Triticum aestivum* analyzed by spreading of meiotic nuclei. *Carlsberg Res Commun* 51:239–294.

Houben A, Demidov D, Rutten T, Scheidtmann KH (2005) Novel phosphorylation of histone H3 at threonine 11 that temporally correlates with condensation of mitotic and meiotic chromosomes in plant cells. *Cytogenet Genome Res* 109:148–155.

Houben A, Demidov D, Caperta AD, Karimi R, Agueci F, Vlasenko L (2007) Phosphorylation of histone H3 in plants—a dynamic affair. *Biochim Biophys Acta* 1769:308–315.

Hyman AA, Karsenti E (1996) Morphogenic properties of microtubules and mitotic spindle assembly. *Cell* 84:401–410.

Jaspersen SL, Martin AE, Glazko G, Giddings TH Jr, Morgan G, Mushegian A, Winey M (2006) The Sad1-UNC-84 homology domain in Mps3 interacts with Mps2 to connect the spindle pole body with the nuclear envelope. *J Cell Biol* 174:665–675.

Jenkins G, Mikhailova EI, Langdon T, Tikholiz OA, Sosnikhina SP, Jones RN (2005) Strategies for the study of meiosis in rye. *Cytogenet Genome Res* 109:221–227.

Jenkins G, Phillips D, Mikhailova EI, Timofejeva L, Jones RN (2008) Meiotic genes and proteins in cereals. *Cytogenet Genome Res* 120:291–301.

Ji Y, Stelly DM, De Donato M, Goodman MM, Williams CG (1999) A candidate recombination modifier gene for *Zea mays* L. *Genetics* 151:821–830.

Jiang J, Gill BS (2006) Current status and the future of fluorescence in situ hybridization (FISH) in plant genome research. *Genome* 49:1057–1068.
John B (1990) *Meiosis.* Cambridge University Press, Cambridge, UK, New York.
John B, Lewis KR (1965) *The Meiotic System.* Springer-Verlag, Wien, New York.
Jones GH, Armstrong SJ, Caryl AP, Franklin FC (2003) Meiotic chromosome synapsis and recombination in *Arabidopsis thaliana;* an integration of cytological and molecular approaches. *Chromosome Res* 11:205–215.
Jongedijk E (1987) A quick enzyme squash technique for detailed studies on female meiosis in *Solanum. Stain Technol* 62:135–141.
Kapuscinski J (1995) DAPI: a DNA-specific fluorescent probe. *Biotech Histochem* 70:220–233.
Kaszas E, Cande WZ (2000) Phosphorylation of histone H3 is correlated with changes in the maintenance of sister chromatid cohesion during meiosis in maize, rather than the condensation of the chromatin. *J Cell Sci* 113:3217–3226.
Keeney S, Giroux CN, Kleckner N (1997) Meiosis-specific DNA double-strand breaks are catalyzed by Spo11, a member of a widely conserved protein family. *Cell* 88:375–384.
Kim JS, Islam-Faridi MN, Klein PE, Stelly DM, Price HJ, Klein RR, Mullet JE. (2005) Comprehensive molecular cytogenetic analysis of sorghum genome architecture: distribution of euchromatin, heterochromatin, genes and recombination in comparison to rice. *Genetics* 171:1963–1976.
Krogh BO, Symington LS (2004) Recombination proteins in yeast. *Annu Rev Genet* 38:233–271.
Kubista M, Ackerman B, Norden B (1987) Characterization of interaction between DNA and 4′,6-diamidino-2-phenylindole by optical spectroscopy. *Biochemistry* 26:4545–4553.
La Cour LF, Wells B (1970) Meiotic prophase in anthers of asynaptic wheat. *Chromosoma* 29:419–427.
Lam E, Kato N, Watanabe K (2004) Visualizing chromosome structure/organization. *Annu Rev Plant Biol* 55:537–554.
Latt SA, Stetten G (1976) Spectral studies on 33258 Hoechst and related bisbenzimidazole dyes useful for fluorescent detection of deoxyribonucleic acid synthesis. *J Histochem Cytochem* 24:24–33.
Lavania UC, Lavania S, Vimala Y (2002) Mitosis-meiosis transition, the regulation of the means to sexual reproduction. *Curr Sci* 82:15–16.
Liu Z, Makaroff CA (2006) *Arabidopsis* separase AESP is essential for embryo development and the release of cohesin during meiosis. *Plant Cell* 18:1213–1225.
Loidl J (1990) The initiation of meiotic chromosome pairing: the cytological view. *Genome* 33:759–778.
Loidl J (1994) Cytological aspects of meiotic recombination. *Experientia* 50:285–294.
Loidl P (2004) A plant dialect of the histone language. *Trends Plant Sci* 9:84–90.
Lopez E, Pradillo M, Romero C, Santos JL, Cnado N (2008) Pairing and synapsis in wild type *Arabidopsis thaliana. Chromosome Res* 16:701–708.
Ma H (2005) Molecular genetic analyses of microsporogenesis and microgametogenesis in flowering plants. *Annu Rev Plant Biol* 56:393–434.
Ma J, Wing RA, Bennetzen JL, Jackson SA (2007) Plant centromere organization: a dynamic structure with conserved functions. *Trends Genet* 23:134–139.
Magnard JL, Yang M, Chen YC, Leary M, McCormick S (2001) The *Arabidopsis* gene *tardy asynchronous meiosis* is required for the normal pace and synchrony of cell division during male meiosis. *Plant Physiol* 127:1157–1166.
Maguire M (1967) Evidence for homologous pairing of chromosomes prior to meiotic prophase in maize. *Chromosoma* 21:221–231.
Maguire MP (1995) Is the synaptonemal complex a disjunction machine? *J Hered* 86:330–340.
Maguire MP, Paredes AM, Riess RW (1991) The desynaptic mutant of maize as a combined defect of synaptonemal complex and chiasma maintenance. *Genome* 34:879–887.
Maguire MP, Riess RW, Paredes AM (1993) Evidence from a maize desynaptic mutant points to a probable role of synaptonemal complex central region components in provision for subsequent chiasma maintenance. *Genome* 36:797–807.

Manzini, G, Xodo L, Barcellona ML, Quadrifoglio F (1985) Interaction of DAPI with double-stranded ribonucleic acids. *Nucleic Acids Res* 13:8955–8967.
Martin-Castellanos C, Blanco M, Rozalén AE, Pérez-Hidalgo L, García AI, Conde F, Mata J, Elermeier C, Davis L. San-Degundo P, Smith GR, Moreno S (2005) A large-scale screen in *S. pombe* identifies seven novel genes required for critical meiotic events. *Curr Biol* 15:2056–2062.
Martínez-Pérez E, Shaw P, Reader S, Aragon-Alcaide L, Miller T, Moore G (1999) Homologous chromosome pairing in wheat. *J Cell Sci* 112:1761–1769.
Martínez-Pérez E, Shaw PJ, Moore G (2000) Polyploidy induces centromere association. *J Cell Biol* 148:233–238.
Martínez-Pérez E, Shaw PJ, Moore G (2001) The *Ph1* locus is needed to ensure specific somatic and meiotic centromere association. *Nature* 411:204–207.
Masterson J (1994) Stomatal size in fossil plants: evidence for polyploidy in majority of angiosperms. *Science* 264:421–424.
McClintock B (1929a) A cytological and genetical study of triploid maize. *Genetics* 14:180–222.
McClintock B (1929b) Chromosome morphology in *Zea mays. Science* 69:629.
McClintock B (1933) The association of non-homologous parts of chromosomes at mid-prophase of meiosis in *Zea mays*. *Z Zellforsch Mikrosk Anat* 19:191–237.
McGoldrick PT, Bohn GW, Whitaker TW (1954) An acetocarmine technic for *Cucurbita. Stain Technol* 29:127–130.
Meier I (2007) Composition of the plant nuclear envelope: theme and variations. *J Exp Bot* 58:27–34.
Mercier R, Grelon M (2008) Meiosis in plants: ten years of gene discovery. *Cytogenet Genome Res* 120:281–290.
Mercier R, Vezon D, Bullier E, Motamayor JC, Sellier A, Lefèvre F, Pelletier G, Horlow C (2001) SWITCH1 (SWI1): a novel protein required for the establishment of sister chromatid cohesion and for bivalent formation at meiosis. *Genes Dev* 15:1859–1871.
Mercier R, Armstrong SJ, Horlow C, Jackson NP, Makaroff CA, Vezon D, Pelletier G, Jones GH, Franklin FC (2003) The meiotic protein SWI1 is required for axial element formation and recombination initiation in *Arabidopsis. Development* 130:3309–3318.
Mezard C (2006) Meiotic recombination hotspots in plants. *Biochem Soc Trans* 34:531–534.
Mezard C, Vignard J, Drouaud J, Mercier R (2007) The road to crossovers: plants have their say. *Trends Genet* 23:91–99.
Mikhailova EI, Phillips D, Sosnikhina SP, Lovtsyus AV, Jones RN, Jenkins G (2006) Molecular assembly of meiotic proteins Asy1 and Zyp1 and pairing promiscuity in rye (*Secale cereale* L.) and its synaptic mutant *sy10. Genetics* 174:1247–1258.
Moens PB (1968) The structure and function of the synaptinemal complexes in *Lilium longiflorum* sporocytes. *Chromosoma* 23:418–451.
Moens P (1972) Fine structure of chromosome coiling at meiotic prophase in *Rhoeo discolor. Can J Genet Cytol* 14:801–808.
Moens PB (1987) *Meiosis.* Academic Press, Orlando.
Moens PB (1994) Molecular perspectives of chromosome pairing at meiosis. *Bioessays* 16:101–106.
Moens P, Pearlman R (1988) Chromatin organization at meiosis. *BioEssays* 9:151–153.
Mogensen HL (1977) Ultrastructural analysis of female pachynema and the relationship between synaptonemal complex length and crossing-over in *Zea mays*. *Carlsberg Res Commun* 42:475–497.
Moore G (2002) Meiosis in allopolyploids—the importance of "Teflon" chromosomes. *Trends Genet* 18:456–463.
Moriguchi K, Suzuki T, Ito Y, Yamazaki Y, Niwa Y, Kurata N (2005) Functional isolation of novel nuclear proteins showing a variety of subnuclear localizations. *Plant Cell* 17:389–403.
Naranjo T, Corredor E (2008) Nuclear architecture and chromosome dynamics in the search of the pairing partner in meiosis in plants. *Cytogenet Genome Res* 120:320–330.

Nasmyth K (2002) Segregating sister genomes: the molecular biology of chromosome separation. *Science* 297:559–565.

Nicolas SD, Leflon M, Liu Z, Eber F, Chelysheva L., Coriton O, Chèvre AM, Jenczewski E (2008) Chromosome "speed dating" during meiosis of polyploid *Brassica* hybrids and haploids. *Cytogenet Genome Res* 120:331–338.

Nonomura K, Nakano M, Fukuda T, Eiguchi M, Miyao A, Hirochika H, Kurata N (2004a) The novel gene *HOMOLOGOUS PAIRING ABERRATION IN RICE MEIOSIS1* of rice encodes a putative coiled-coil protein required for homologous chromosome pairing in meiosis. *Plant Cell* 16:1008–1020.

Nonomura KI, Nakano M, Murata K, Miyoshi K, Eiguchi M., Miyao A., Hirochika H, Kurata N (2004b) An insertional mutation in the rice *PAIR2* gene, the ortholog of *Arabidopsis ASY1,* results in a defect in homologous chromosome pairing during meiosis. *Mol Genet Genomics* 271:121–129.

Nonomura K, Nakano M, Eiguchi M, Suzuki T, Kurata N (2006) PAIR2 is essential for homologous chromosome synapsis in rice meiosis I. *J Cell Sci* 119:217–225.

Nonomura K, Morohoshi A, Nakano M, Eiguchi M, Miyao A, Hirochika H, Kurata N (2007) A germ cell specific gene of the *ARGONAUTE* family is essential for the progression of premeiotic mitosis and meiosis during sporogenesis in rice. *Plant Cell* 19:2583–2594.

Osman K, Sanchez-Moran E, Higgins JD, Jones GH, Franklin FC (2006) Chromosome synapsis in *Arabidopsis:* analysis of the transverse filament protein ZYP1 reveals novel functions for the synaptonemal complex. Chromosoma 115:212–219.

Otto SP (2007) The evolutionary consequences of polyploidy. *Cell* 131:452–462.

Otto SP, Whitton J (2000) Polyploid incidence and evolution. *Annu Rev Genet* 34:401–437.

Page SL, Hawley RS (2004) The genetics and molecular biology of the synaptonemal complex. *Annu Rev Cell Dev Biol* 20:525–558.

Palmer RG (1971) Cytological studies of ameiotic and normal maize with reference to premeiotic pairing. *Chromosoma* 35:233–246.

Paul AL, Ferl RJ (1998) Higher order chromatin structures in maize and *Arabidopsis. Plant Cell* 10:1349–1359.

Pawlowski WP, Cande WZ (2005) Coordinating the events of the meiotic prophase. *Trends Cell Biol* 15:674–681.

Pawlowski WP, Golubovskaya IN, Cande WZ (2003) Altered nuclear distribution of recombination protein RAD51 in maize mutants suggests the involvement of RAD51 in meiotic homology recognition. *Plant Cell* 15:1807–1816.

Pawlowski WP, Golubovskaya IN, Timofejeva L, Meeley RB, Sheridan WF, Cande WZ (2004) Coordination of meiotic recombination, pairing, and synapsis by PHS1. *Science* 303:89–92.

Pawlowski WP, Wang CJ, Golubovskaya IN, Szymaniak JM, Shi L, Hamant O, Zhu T, Harper L, Sheridan WF, Cande WZ (2009) Maize AMEIOTIC1 is essential for multiple early meiotic processes and likely required for the initiation of meiosis. *Proc Natl Acad Sci USA* 106:3603–3608.

Phillips CM, McDonald KL, Dernburg AF (2009) Cytological analysis of meiosis in *Caenorhabditis elegans. Methods Mol Biol* 558:171–195.

Prieto P, Santos AP, Moore G, Shaw P (2004) Chromosomes associate premeiotically and in xylem vessel cells via their telomeres and centromeres in diploid rice (*Oryza sativa*). *Chromosoma* 112:300–307.

Puizina J, Siroky J, Mokros P, Schweizer D, Riha K (2004) Mre11 deficiency in *Arabidopsis* is associated with chromosomal instability in somatic cells and Spo11-dependent genome fragmentation during meiosis. *Plant Cell* 16:1968–1978.

Qian C, Zhang Q, Li S, Zeng L, Walsh MJ, Zhou MM (2005) Structure and chromosomal DNA binding of the SWIRM domain. *Nat Struct Mol Biol* 12:1078–1085.

Ramsey J, Schemske DW (1998) Pathways, mechanisms, and rates of polyploid formation in flowering plants. *Annu Rev Ecol Syst* 29:467–501.

Reddy TV, Kaur J, Agashe B, Sundaresan V, Siddiqi I (2003) The DUET gene is necessary for chromosome organization and progression during male meiosis in *Arabidopsis* and encodes a PHD finger protein. *Development* 130:5975–5987.

Revenkova E, Jessberger R (2006) Shaping meiotic prophase chromosomes: cohesins and synaptonemal complex proteins. Chromosoma 115:235–240.

Rhoades MM, Vilkomerson H (1942) On the anaphase movement of chromosomes. *Proc Natl Acad Sci USA* 28:433–436.

Riehs N, Akimcheva S, Puizina J, Bulankova P, Idol RA, Siroky J, Schleiffer A, Schweizer D, Shippen DE, Riha K (2008) *Arabidopsis* SMG7 protein is required for exit from meiosis. *J Cell Sci* 121:2208–2216.

Riggs CD (1994) Molecular cloning of cDNAs encoding variants of meiotin-1. A meiotic protein associated with strings of nucleosomes. *Chromosoma* 103:251–261.

Riggs CD (1997) Meiotin-1: the meiosis readiness factor? *Bioessays* 19:925–931.

Riggs CD, Hasenkampf CA (1991) Antibodies directed against a meiosis-specific, chromatin-associated protein identify conserved meiotic epitopes. *Chromosoma* 101:92–98.

Rose A, Patel S, Meier I (2004) Plant nuclear envelope proteins. *Symp Soc Exp Biol* 56:69–88.

Ross KJ, Fransz P, Jones GH (1996) A light microscopic atlas of meiosis in *Arabidopsis thaliana. Chromosome Res* 4:507–516.

Ross KJ, Fransz P, Armstrong SJ, Vizir I, Mulligan B, Franklin FC, Jones GH (1997) Cytological characterization of four meiotic mutants of *Arabidopsis* isolated from T-DNA-transformed lines. *Chromosome Res* 5:551–559.

Sanchez-Moran E, Jones GH, Franklin FC, Santos JL (2004) A puromycin-sensitive aminopeptidase is essential for meiosis in *Arabidopsis thaliana. Plant Cell* 16:2895–2909.

Sanchez-Moran E, Santos JL, Jones GH, Franklin FC (2007) ASY1 mediates AtDMC1-dependent interhomolog recombination during meiosis in *Arabidopsis. Genes Dev* 21:2220–2233.

Sanchez-Moran E, Osman K, Higgins JD, Pradillo M, Cunado N, Jones GH, Franklin FC (2008) ASY1 coordinates early events in the plant meiotic recombination pathway. *Cytogenet Genome Res* 120:302–312.

Santos JL, Jimenez MM, Diez M (1994) Meiosis in haploid rye: extensive synapsis and low chiasma frequency. *Heredity* 73:580–588.

Scherthan H (2001) A bouquet makes ends meet. *Nat Rev Mol Cell Biol* 2:621–627.

Scherthan H (2007) Telomere attachment and clustering during meiosis. *Cell Mol Life Sci* 64:117–124.

Schiefthaler U, Balasubramanian S, Sieber P, Chevalier D, Wisman E, Schneitz K (1999) Molecular analysis of *NOZZLE,* a gene involved in pattern formation and early sporogenesis during sex organ development in *Arabidopsis thaliana. Proc Natl Acad Sci USA* 96:11664–11669.

Schmit AC, Stoppin V, Chevrier V, Job D, Lambert AM (1994) Cell cycle dependent distribution of a centrosomal antigen at the perinuclear MTOC or at the kinetochores of higher plant cells. *Chromosoma* 103:343–351.

Schmit AC, Endle MC, Lambert AM (1996) The perinuclear microtubule-organizing center and the synaptonemal complex of higher plants share a common antigen: its putative transfer and role in meiotic chromosomal ordering. *Chromosoma* 104:405–413.

Schmitt J, Benavente R, Hodzic D, Hoog C, Stewart CL, Alsheimer M (2007) Transmembrane protein Sun2 is involved in tethering mammalian meiotic telomeres to the nuclear envelope. *Proc Natl Acad Sci USA* 104:7426–7631.

Schubert V, Kim YM, Berr A, Fuchs J, Meister A, Marschner S, Schubert I (2007) Random homologous pairing and incomplete sister chromatid alignment are common in angiosperm interphase nuclei. *Mol Genet Genomics* 278:167–176.

Schwarzacher T. (2003) Meiosis, recombination and chromosomes: a review of gene isolation and fluorescent in situ hybridization data in plants. *J Exp Bot* 54:11–23.

Sears ER (1976) Genetic control of chromosome pairing in wheat. *Annu Rev Genet* 10:31–51.

Sen SK (1970) Axial elements in plant meiotic chromosomes. *Nature* 228:79–80.

Shamina NV (2005) Formation of division spindles in higher plant meiosis. *Cell Biol Int* 29:307–318.

Shamina N, Dorogova N, Trunova S (2000) Radial spindle and the phenotype of the maize meiotic mutant *dv*. *Cell Biol Int* 24:729–736.

Shao L, Isaac B, Uzawa S, Agard DA, Sedat JW, Gustafsson MGL (2008) I^{5}S: widefield light microscopy with 100-nm-scale resolution in three dimensions. *Biophys J* 94:4971–4983.

Shaw SL (2006) Imaging the live plant cell. *Plant J* 45:573–598.

Sheehan MJ, Pawlowski WP (2009) Live imaging of rapid chromosome movements in meiotic prophase I in maize. *Proc Natl Acad Sci USA* 106:20989–20994.

Shepard J, Boothroyd ER, Stern H (1974) The effect of colchicine on synapsis and chiasma formation in microsporocytes of *Lilium. Chromosoma* 44:423–437.

Sheridan WF, Stern H (1967) Histones of meiosis. *Exp Cell Res* 45:323–335.

Sheridan WF, Avalkina NA, Shamrov II, Batygina TB, Golubovskaya IN (1996) The mac1 gene: controlling the commitment to the meiotic pathway in maize. *Genetics* 142:1009–1020.

Sheridan WF, Golubeva EA, Abrhamova LI, Golubovskaya IN (1999) The mac1 mutation alters the developmental fate of the hypodermal cells and their cellular progeny in the maize anther. *Genetics* 153:933–941.

Sherman JD, Stack SM (1995) Two-dimensional spreads of synaptonemal complexes from solanaceous plants. VI. High-resolution recombination nodule map for tomato (*Lycopersicon esculentum*). *Genetics* 141:683–708.

Shi J, Wolf SE, Burke JM, Presting GG, Ross-Ibarra J, Dawe RK (2010) Widespread gene conversion in centromere cores. *PLoS Biol* 9:e1000327.

Siaud N, Dray E, Gy I, Gérard E, Takvorian N, Doutriaux MP (2004) Brca2 is involved in meiosis in *Arabidopsis thaliana* as suggested by its interaction with Dmc1. *EMBO J* 23:1392–1401.

Sidhu GK, Rustgi S, Shafqat MN, von Wettstein D, Gill KS (2008) Fine structure mapping of a gene-rich region of wheat carrying *Ph1,* a supressor of crossing over between homoeologous chromosomes. *Proc Natl Acad Sci USA* 15:5815–5820.

Simpson GG, Gendall AR, Dean C (1999) When to switch to flowering. *Annu Rev Cell Dev Biol* 15:519–550.

Singh RJ (1993) *Plant Cytogenetics.* CRC Press, Boca Raton.

Sosnikhina SP, Mikhailova EI, Tikholiz OA, Priyatkina SN, Smimov VG, Dadashev SY, Kolomiets OL, Bogdanov YF (2005) Meiotic mutations in rye *Secale cereale* L. *Cytogenet Genome Res* 109:215–220.

Stacey NJ, Kuromori T, Azumi Y, Roberts G, Breuer C, Wada T, Maxwell A, Roberts K, Sugimoto-Shirasu K (2006) *Arabidopsis* SPO11-2 functions with SPO11-1 in meiotic recombination. *Plant J* 48:206–216.

Stack S (1982) Two-dimensional spreads of synaptonemal complexes from solanaceous plants. I. The technique. *Stain Technol* 57:265–272.

Stack SM (1984) Heterochromatin, the synaptonemal complex and crossing over. *J Cell Sci* 71:159–176.

Staiger CJ, Cande WZ (1990) Microtubule distribution in *dv,* a maize meiotic mutant defective in the prophase to metaphase transition. *Dev Biol* 138:231–242.

Staiger CJ, Cande WZ (1992) *Ameiotic,* a gene that controls meiotic chromosome and cytoskeletal behavior in maize. *Dev Biol* 154:226–230.

Starr DA (2007) Communication between the cytoskeleton and the nuclear envelope to position the nucleus. *Mol Biosyst* 3:583–589.

Stephan W, Langley CH (1998) DNA polymorphism in *Lycopersicon* and crossing-over per physical length. *Genetics* 150:1585–1593.

Stern H, Hotta Y (1974) Biochemical controls of meiosis. *Annu Rev Genet* 7:37–66.

Stronghill PE, Hasenkampf CA (2007) Analysis of substage associations in prophase I of meiosis in floral buds of wild-type *Arabidopsis thaliana* (Brassicaceae). *Am J Bot* 94:2063–2067.

Terasawa M, Shinohara A, Hotta Y, Ogawa H, Ogawa T (1995) Localization of RecA-like recombination proteins on chromosomes of the lily at various meiotic stages. *Genes Dev* 9:925–934.

Ting YC (1973) Synaptonemal complex of haploid maize. *Cytologia* 38:497–500.

Tomita K, Cooper JP (2006) The meiotic chromosomal bouquet: SUN collects flowers. *Cell* 125:19–21.

Trelles-Sticken E, Adelfalk C, Loidl J, Scherthan H (2005) Meiotic telomere clustering requires actin for its formation and cohesin for its resolution. *J Cell Biol* 170:213–223.

Tzur YB, Wilson KL, Gruenbaum Y (2006) SUN-domain proteins: "Velcro" that links the nucleoskeleton to the cytoskeleton. *Nat Rev Mol Cell Biol* 7:782–788.

Van Damme D, Bouget FY, Van Poucke K, Inzé D, Geelen D (2004) Molecular dissection of plant cytokinesis and phragmoplast structure: a survey of GFP-tagged proteins. *Plant J* 40:386–398.

Vignard J, Siwiec T, Chelysheva L, Vrielynck N, Gonord F, Armstrong SJ, Schlögelhofer P, Mercier R (2007) The interplay of RecA-related proteins and the MND1-HOP2 complex during meiosis in *Arabidopsis thaliana. PLoS Genet* 3:1894–1906.

von Wettstein D, Rasmussen SW, Holm PB (1984) The synaptonemal complex in genetic segregation. *Annu Rev Genet* 18:331–413.

Wang CJ, Chen CC (2005) Cytogenetic mapping in maize. *Cytogenet Genome Res* 109:63–69.

Wang G, Zhang X, Jin WW (2009) An overview of plant centromeres. *J Genet Genomics* 36:529–537.

Wang X (1988) Chromosome pairing analysis in haploid wheat by spreading of meiotic nuclei. *Carlsberg Res Commun* 53:135–166.

Wang Y, Magnard JL, McCormick S, Yang M (2004) Progression through meiosis I and meiosis II in *Arabidopsis* anthers is regulated by an A-type cyclin predominately expressed in prophase I. *Plant Physiol* 136:4127–4135.

Waterworth WM, Altun C, Armstrong SJ, Roberts N, Dean PJ, Young K, Weil CF, Bray CM, West CE (2007) NBS1 is involved in DNA repair and plays a synergistic role with ATM in mediating meiotic homologous recombination in plants. *Plant J* 52:41–52.

Wijeratne AJ, Chen C, Zhang W, Timofejeva L, Ma H (2006) The *Arabidopsis thaliana PARTING DANCERS* gene encoding a novel protein is required for normal meiotic homologous recombination. *Mol Biol Cell* 17:1331–1343.

Wilson EB (1925) *The Cell in Development and Heredity.* Macmillan, New York.

Yadegari R, Drews GN (2004) Female gametophyte development. *Plant Cell* 16:S133–S141.

Yang WC, Sundaresan V (2000) Genetics of gametophyte biogenesis in *Arabidopsis. Curr Opin Plant Biol* 3:53–57.

Yoshioka M, Maeda M, Ito M (1981) The time and duration of premeiotic interphase in microsporocytes of *Trillium kamtschaticum*. *Bot Mag Tokyo* 94:371–378.

Yu HG, Hiatt EN, Chan A, Sweeney M, Dawe RK (1997) Neocentromere-mediated chromosome movement in maize. *J Cell Biol* 139:831–840.

Yu HG, Muszynski MG, Dawe, RK (1999) The maize homologue of the cell cycle checkpoint protein MAD2 reveals kinetochore substructure and contrasting mitotic and meiotic localization patterns. *J Cell Biol* 145:425–435.

Yu HG, Hiatt EN, Dawe RK (2000) The plant kinetochore. *Trends Plant Sci* 5:543–547.

Zhang L, Murray BG, Pickering RA (2002) Variable patterns of chromosome synapsis at pachytene in *Hordeum vulgare* × *H. bulbosum* hybrids and their parents. *Hereditas* 137:90–95.

Zhang L, Tao J, Wang SX, Chong K, Wang T (2006) The rice OsRad21-4, an orthologue of yeast Rec8 protein, is required for efficient meiosis. *Plant Mol Biol* 60:533–554.

Zhong XB, de Jong JH, Zabel P (1996) Preparation of tomato meiotic pachytene and mitotic metaphase chromosomes suitable for fluorescence in situ hybridization (FISH). *Chromosome Res* 4:24–28.

Zickler D (2006) From early homologue recognition to synaptonemal complex formation. *Chromosoma* 115:158–174.

Zickler D, Kleckner N (1998) The leptotene-zygotene transition of meiosis. *Annu Rev Genet* 32:619–697.

Zickler D, Kleckner N (1999) Meiotic chromosomes: integrating structure and function. *Annu Rev Genet* 33:603–754.

Chapter 9
Chromosomal Distribution and Functional Interpretation of Epigenetic Histone Marks in Plants

Jörg Fuchs and Ingo Schubert

Abstract Histones, the main protein component of the chromatin, are subjected to several different posttranslational modifications that control the structure and/or function of the chromatin fiber. Together with DNA methylation, these modifications constitute the "epigenetic code." Here, we survey current knowledge on the nuclear and chromosomal distribution of histone acetylation, phosphorylation, and methylation marks in plants, discuss functional consequences, and point out similarities and differences between nonplant eukaryotes and plants.

Keywords Chromatin organization · Histone modification · Methylation · Acetylation · Phosphorylation · Euchromatin · Heterochromatin · Immunostaining

Abbreviations

NORs Nucleolar organizing regions

Contents

J. Fuchs (✉) • I. Schubert
Leibniz-Institute of Plant Genetics and Crop Plant Research, Chromosome Structure and Function Laboratory, Corrensstrasse 3 06466, Gatersleben, Germany
e-mail: fuchs@ipk-gatersleben.de; schubert@ipk-gatersleben.de

H.W. Bass and J.A. Birchler (eds.), *Plant Cytogenetics*, Plant Genetics and Genomics: Crops and Models 4, DOI 10.1007/978-0-387-70869-0_9,

9.1 Introduction

The organization of DNA into a hierarchy of chromatin fibers facilitates the packaging within the nucleus and regulates expression and maintenance of nuclear genetic information. The basic units of chromatin, the nucleosomes, are each composed of ~147 bp of DNA wrapped around a histone octamer (Kornberg 1974). These octamers consist of two molecules of each core histone H2A, H2B, H3, and H4. The core histones are relatively small and highly basic and possess amino-terminal tails that extend from the surfaces of the nucleosomes (for review see Kornberg and Lorch 1999). Since Allfrey and coworkers described acetylation and methylation as the first modifications of core histones with an influence on transcriptional activity (Allfrey et al. 1964), many types of covalent histone modifications have been described, including phosphorylation, ubiquitination, sumoylation, and ADP-ribosylation (Loidl 2004). These posttranslational modifications, mainly at the N-terminal tails, constitute the "histone code" or, together with DNA methylation, the "epigenetic code" (Strahl and Allis 2000; Turner 2000; Jenuwein and Allis 2001). They control the folding of nucleosome arrays into higher-order structures and mediate signaling for developmental processes. Although the histones and their modifications are conserved among eukaryotes, plants and nonplant eukaryotes and, to a lesser degree, even phylogenetic groups of plant may differ in chromosomal distribution and/or the biological meaning of the individual modifications.

Although molecular analyses of chromatin modifications characterize either the total chromatin or regions of individual DNA sequences, the cytological approach, i.e., immunostaining with antibodies specific for individual modifications, detects at the microscopic level the subnuclear and chromosomal distribution of these marks.

Here we provide a survey of histone acetylation, phosphorylation, and methylation as well as of DNA methylation and their functional meaning in higher plants.

9.2 Histone Acetylation

More than 40 years ago, Allfrey and coworkers proposed a general correlation between histone acetylation and transcriptional activity (Allfrey et al. 1964). Because of their high content of lysine and arginine residues, the amino-terminal tails of the histones are highly basic (Luger and Richmond 1998). Acetylation of conserved lysine residues neutralizes the positive charge of the histone tails, decreases their affinity for negatively charged DNA, and thus promotes the accessibility to chromatin of, for example, the transcriptional machinery (Wade et al. 1997). Alternatively, combinations of different covalent modifications of lysines and/or arginines on histone tails, such as acetylation and methylation, may provide signals for the recruitment of specific chromatin-associated proteins, which in turn alter the chromatin structure and affect the regulation of transcription, as proposed by the "histone code" hypothesis (Strahl and Allis 2000; Turner 2000; Jenuwein and Allis 2001).

The lysine residues K4, K9, K14, K18, K23, K27, and K36 of histone H3 as well as K5, K8, K12, K16, and K20 of histone H4 can be acetylated by histone

acetyltransferases and deacetylated by deacetylases (Lusser et al. 2001; Loidl 2004; Hizume et al. 2007; Morris et al. 2007). High levels of acetylation have been found to be connected with decondensation of the nucleosome structure mediating transcription and DNA replication, repair, and recombination (Lee et al. 1993; Grunstein 1997; Ikura et al. 2000; McBlane and Boyes 2000; McMurry and Krangel 2000; Bird et al. 2002).

In mammals, all acetylatable N-terminal lysines of H3 and H4 show the lowest level of acetylation at the pericentric heterochromatin (Jeppesen et al. 1992; Belyaev et al. 1996). A similar low level is found at the inactive X chromosome, whereas the early-replicating euchromatin (R bands) displays the highest acetylation level (Jeppesen and Turner 1993; Belyaev et al. 1996). In polytene chromosomes of *Drosophila*, the euchromatic chromosome arms are enriched in H3K9ac, H3K14ac, H4K5ac, and H4K8ac, whereas the heterochromatic chromocenter is depleted of these isoforms and instead strongly acetylated at lysine 12 (Turner et al. 1992; Nowak and Corces 2000; Ebert et al. 2006). H4K16ac is only found in the transcriptionally hyperactive X chromosome of male larvae and is absent from autosomes of male and from all chromosomes of female larvae (Turner et al. 1992).

Plant chromosomes display, depending on the acetylated isoform tested, either a more or less uniform distribution or, more often, a lower abundance of acetylated histones at heterochromatin and often a clustering at nucleolar organizing regions (NORs). Contrary to the situation in mammals, the patterns of acetylated H3 and H4 isoforms often do not coincide in plants.

In field bean (*Vicia faba* L.), antibodies directed against H4 acetylated at lysine 5, 8, and 12 label the entire chromosome complement except for the large blocks of heterochromatin, mainly or exclusively composed of Fok-I (Fig. 9.2a; Fuchs et al. 1994) or other tandem repetitive elements (Fig. 9.2b; Houben et al. 1996). H4K16ac is uniformly distributed along the chromosomes (Fig. 9.2b). The NOR was most strongly acetylated for all investigated lysine residues (Fig. 9.2b; Houben et al. 1996). As in animals, highly acetylated H4 isoforms are associated with potentially transcriptionally active regions and less so with heterochromatic regions (except for H4K16ac). Histone H3 was found to be weakly acetylated at lysine residues 9/18 and 14 within the Fok-I element–containing heterochromatin, whereas NORs and heterochromatic regions not composed of Fok-I elements were more acetylated at these residues (Fig. 9.2b; Belyaev et al. 1998). Acetylation of H3K23 was uniform, except for the NOR that showed no fluorescence (Fig. 9.2b; Belyaev et al. 1998). H3K27ac showed a distribution similar to those of H4K5ac, H4K8ac, and H4K12ac (Fig. 9.2b). Treatment with trichostatin A, a specific inhibitor of histone deacetylase, several hours before mitosis mediated a switch to extensive acetylation of H4 (at K5, 12, and 16) within heterochromatin, whereas H3 acetylation remained unchanged (Belyaev et al. 1997, 1998). This result suggested that histone H4 acetylation of specific chromosomal domains varies during interphase. Indeed, Jasencakova et al. (2000) found a strong correlation between the extent of H4 acetylation and replication of eu- and heterochromatic domains. The acetylation intensity at euchromatin and heterochromatin increases during replication for H4K5, H4K12, and H4K16. Nearer to mitosis, heterochromatin becomes deacetylated mostly to a level below that of euchromatin. Compared with euchromatin, NORs were more

strongly acetylated at H4 during mitosis, but nucleoli were less acetylated during S phase. H3 acetylation, in contrast, remained fairly constant throughout the cell cycle (Jasencakova et al. 2000). In barley (*Hordeum vulgare* L.), acetylation of H4 is altered during the cell cycle in a similar way, whereas H3 acetylation is not, but the apparently deposition-related acetylation in barley is restricted to H4K5 and H4K12. The same is true for the stronger acetylation of NORs in mitosis (Jasencakova et al. 2001). Comparable to the situation in field bean, acetylation of H4 and transcriptional activity showed no clear correlation at the level of large chromatin domains.

In contrast to the situation in field bean and barley, in *Arabidopsis thaliana* (L.) Heynh., a replication-linked increase of acetylation occurred only at H4K16 and surprisingly also at H3K18, which showed no replication-related acetylation in other plants (Fig. 9.1b, c; Jasencakova et al. 2003). Strong H4 acetylation within nucleoli as well as at the rDNA-containing chromocenters was consistently lacking in *Arabidopsis*.

Surprisingly, no difference in the acetylation level of H4 could be found between the two X chromosomes of female *Silene latifolia* Poir. (Vyskot et al. 1999), although one X chromosome is supposed to be inactive as a consequence of dosage compensation, heavy DNA methylation, and late replication (Vyskot et al. 1993; Siroky et al. 1998).

Obviously, the chromosomal distribution of histone acetylation marks in plants shows some conserved features as well as plant- or even species-specific peculiarities.

In contrast to the well-established correlation between histone acetylation and ongoing transcription at the level of individual genes (Cheung et al. 2000), at the level of large chromatin domains, cell cycle-dependent modulation of histone acetylation is correlated with the replication, as in mammals (Taddei et al. 1999). Contrary to acetylation of H4, the nuclear patterns of H3 acetylation did not change significantly during the cell cycle in field bean or barley (Jasencakova et al. 2000, 2001).

9.3 Histone Phosphorylation

One of the most thoroughly analyzed modifications is the phosphorylation of histone H3. It seems to be crucial for cell cycle-dependent chromosome condensation, for centromeric sister chromatid cohesion, activation of transcription, initiation of

Fig. 9.1 Chromatin modifications in *Arabidopsis thaliana* nuclei. (**a**) Heterochromatin organized as highly condensed chromocenters. (**b**) Distribution of acetylated histones on leaf nuclei. H3K9ac, H4K5ac, H4K8ac, and H4K12ac are located within euchromatin, whereas H4K16ac shows three different patterns (from *left* to *right*): chromocenters unlabeled, labeled as strongly as euchromatin, or labeled more strongly than euchromatin. (**c**) Cell cycle-correlated acetylation of H3K18 and H4K16. No cell cycle dependence was found for H3K9, H3K14, H4K5, H4K8, and H4K12. (**d**) Histone methylation: H3K9me1,2, H3K27me1,2, and H4K20me1 are heterochromatin-specific marks, whereas H3K4me1,2,3, H3K36me1,2,3, H3K9me3, and H3K27me3 label euchromatin. (**e**) DNA methylation occurs preferentially at chromocenters. (**b**, **c**) are reproduced from Jasencakova et al. (2003) and Fuchs et al. (2006), respectively

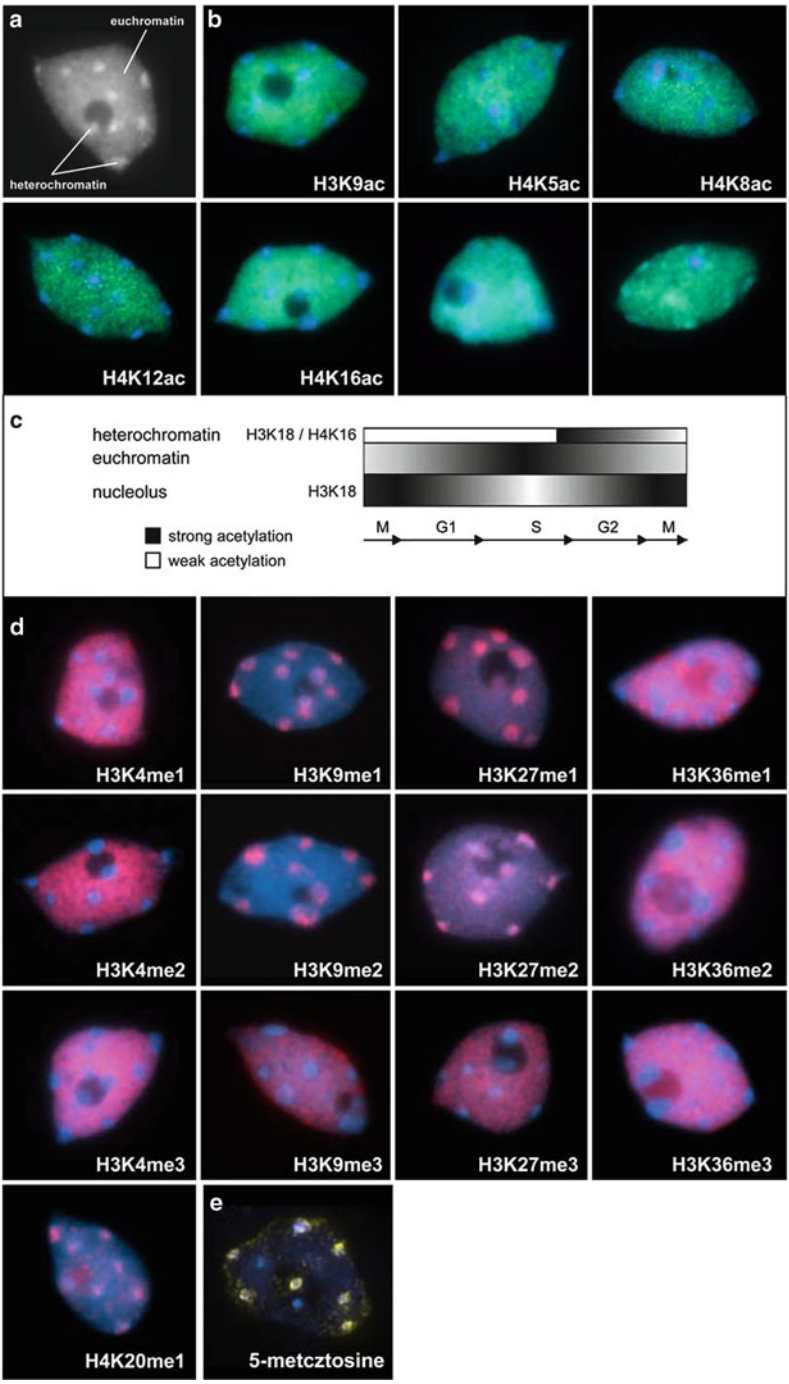

Fig. 9.1 (continued)

apoptosis, and DNA repair (Prigent and Dimitrov 2003; Loury and Sassone-Corsi 2004). Phosphorylation occurs at four different sites, at serines 10 and 28 as well as at threonines 3 and 11. Early investigations on Chinese hamster (*Cricetulus griseus* Milne-Edwards) cells demonstrated that the level of H3 phosphorylation at serine 10 is associated with chromosome condensation during mitosis and meiosis (Gurtley et al. 1975). Using antibodies specific for histone H3S10ph, Hendzel and coworkers showed that the phosphorylation of H3 begins in late G2 within pericentromeric heterochromatin and spreads throughout the chromatin as it undergoes condensation up to the end of mitosis in mammalian cells (Hendzel et al. 1997). A similar mitosis-specific phosphorylation of histone H3 was found for serine 28 (Goto et al. 1999). Immunostaining with antibodies against phosphorylated H3T11 revealed labeling from prophase to early anaphase, particularly around centromeres (Preuss et al. 2003).

In *Drosophila*, mitotic chromosomes show a distribution of H3S10ph similar to that in mammals (Adams et al. 2001), but the *borr* mutant, which lacks high levels of H3S10 phosphorylation, did not show any effect on chromosome condensation (Hanson et al. 2005). H3S10ph therefore does not drive chromosome condensation in *Drosophila*.

In plants, however, H3S10ph and H3S28ph are restricted to the pericentromeres during mitosis (Fig. 9.2c; Houben et al. 1999; Kaszás and Cande 2000; Gernand et al. 2003; Zhang et al. 2005). At meiosis, the chromosomes are phosphorylated along their entire length during the first division, whereas phosphorylation is restricted to the pericentromeric regions during the second division (Kaszás and Cande 2000; Manzanero et al. 2000). In contrast to bivalents, single chromatids resulting from equational divisions of univalents at anaphase I showed no phosphorylation (Manzanero et al. 2000). Nevertheless, these chromatids were normally condensed, and their kinetochores interacted with the spindle microtubules. Univalents of the maize (*Zea mays* L.) mutant afd1, which is defective in sister chromatid cohesion, showed strong phosphorylation of H3S10 only at the pericentromeric regions during metaphase I (Kaszás and Cande 2000). Although a dicentric chromosome of barley revealed strong phosphorylation only at the functional centromere (Houben et al. 1999), polycentric chromosomes of *Luzula luzuloides* (de Lamarck) Dandy & Wilmott and *Rhynchospora tenuis* Baldw. ex Gray were labeled along the entire lengths of their chromosomes during mitosis (Gernand et al. 2003; Guerra et al. 2006). Taken together, these findings indicate that in plants H3S10ph and H3S28ph are required for sister (peri)centromere cohesion during mitosis and meiotic metaphase II and for cohesion of sister chromatids during metaphase I (Manzanero et al. 2000; Gernand et al. 2003).

Phosphorylation at threonine 3 and 11 occurs in plants along the entire chromosome arms during mitosis and meiosis and is correlated with chromosome condensation (Fig. 9.2c; Houben et al. 2005, 2007). This situation is the opposite of that in mammals, where H3T3ph and H3T11ph are found at centromeres (Preuss et al. 2003; Polioudaki et al. 2004).

Although the cell cycle-dependent phosphorylation of H3S10, H3S28, H3T3, and H3T11 is present in both plants and animals, phosphorylated threonine and

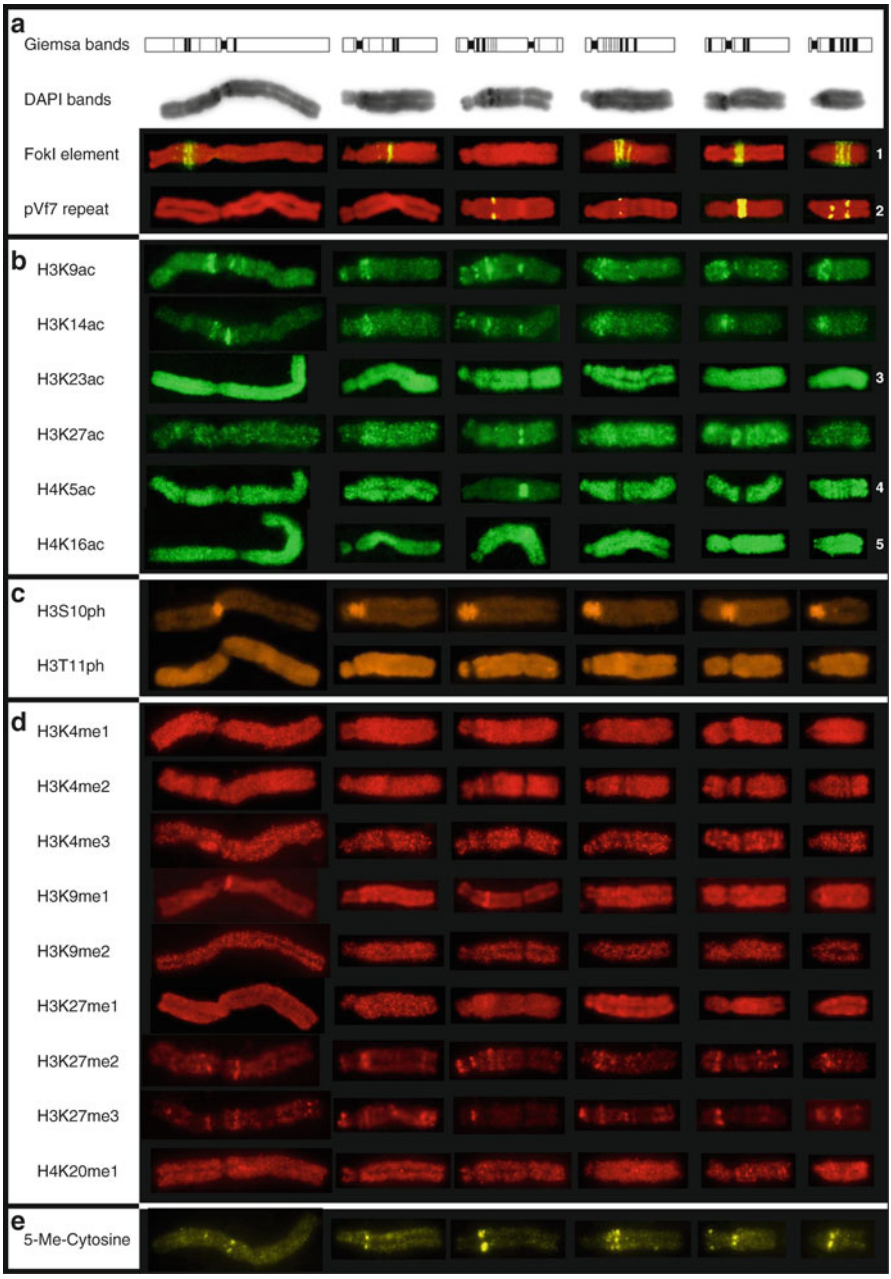

Fig. 9.2 Chromatin modifications on metaphase chromosomes of the translocation karyotype ACB of *Vicia faba*. (**a**) Characterization of distinct heterochromatic chromatin fractions by means of Giemsa banding (Döbel et al. 1978), DAPI staining, and FISH with the FokI-element (Fuchs et al. 1994) and with pVf7 (Fuchs et al. 1998). (**b**) Histone acetylation. (**c**) Histone phosphorylation. (**d**) Histone methylation. (**e**) DNA methylation detected with an antibody against 5-methylcytosine. 1–5 are reproduced from Fuchs et al. (1994), Fuchs et al. (1998), Belyaev et al. (1998), Belyaev et al. (1997), and Houben et al. (1996), respectively

serine residues apparently switched functions during evolution. In mammals, H3S10ph and H3S28ph along the entire chromosome arms are linked to chromosome condensation, and H3T3ph and H3T11ph at the centromeres might be involved in sister centromere cohesion. The opposite seems true for plants, where H3S10ph and H3S28ph are restricted to the pericentromeric regions during mitosis and metaphase I, apparently connected with (peri)centromere cohesion, and H3T3ph and H3T11ph label the entire chromosome arms and are probably involved in condensation processes.

The most direct relationship between a posttranslational modification and the response of a cell to DNA damage is the phosphorylation of a subfraction of histone H2A. In yeast and metazoa, H2AX becomes phosphorylated at S139 of its C-terminal tail within ~50 kb on either site of a double-strand break (for review see Thiriet and Hayes 2005). In plants, phosphorylation of H2AX in response to gamma-irradiation occurs only at one third of the rate observed in yeast and mammals (Friesner et al. 2005). Plants either form fewer breaks in response to irradiation or have greater capacity for DNA repair and/or damage tolerance than do mammals (Friesner et al. 2005). Data on possible phosphorylation of the histone-tail threonines T6, T22, T32, and T80 are not available so far.

9.4 Histone Methylation

Histone methylation, in particular the mono-, di-, and trimethylation of lysines 4, 9, 27, and 36 of histone H3 and lysine 20 of histone H4 along with cytosine methylation of DNA, are considered either euchromatic or heterochromatic marks. Despite their widespread occurrence, yeast, *Neurospora*, *Drosophila*, mammals, and plants differ in their subnuclear distribution (Table 9.1).

Whereas the euchromatin-specific methylation of H3K4 and H3K36 seems to be highly conserved among eukaryotes, organisms differ in the indexing of heterochromatin by methylation of H3K9, H3K27, and H4K20. In *Schizosaccharomyces pombe* (fission yeast), the small amount of repressed chromatin at centromeres, telomeres, and mating-type loci is characterized by H3K9me2 and H3K9me3 (Nakayama et al. 2001; Noma et al. 2001; Yamada et al. 2005). H3K27 methylation is not detectable in fission yeast (Lachner et al. 2004). H4K20me1,2,3 are prominent marks in the *S. pombe* genome and are probably involved in the DNA damage response, but not in gene regulation or heterochromatin formation (Lachner et al. 2004; Sanders et al. 2004). In contrast to *Neurospora crassa* (bread mold) and higher eukaryotes, *S. pombe* lacks any detectable DNA methylation (Wilkinson et al. 1995).

In *Neurospora*, the only repressive methylation mark, H3K9me3, controls all types of DNA methylation (Tamaru and Selker 2001; Tamaru et al. 2003). The *Neurospora* homolog of *Heterochromatin Protein 1* (*HP1*) is essential for DNA methylation (Freitag et al. 2004). Because its localization to heterochromatic foci is lost in mutants defective in the H3 methyltransferase that specifically trimethylates lysine 9 (*DIM-5*), *HP1* is probably recruited by H3K9me3 (Allshire and Selker 2007).

Table 9.1 Heterochromatin specificity of histone methylation marks in different organisms (modified from Fuchs et al. 2006)

Species	Genome size	H3K4			H3K9			H3K27			H3K36			H4K20			References
	Mbp	me1	me2	me3	me1	me2	me3	me1	me2	me3	me1	me2	me3	me1	me2	me3	
Schizosaccharomyces pombe[a]	14	–	–	–	?	++	++	nd	nd	nd	?	–	–	+	+	+	Nakayama et al. (2001); Morris et al. (2005); Sanders et al. (2004); Lachner et al. (2004)
Neurospora crassa[a]	40	?	–	?	?	–	++	?	?	?	–	–	–	?	?	?	Tamaru et al. (2003); Adhvaryu et al. (2005)
Drosophila melanogaster	180	?	–	–	++	++	++[b]	++	++	++[b]	–	–	–	+	+	++	Ebert et al. (2004); Schotta et al. (2004); Ebert et al. (2006)
Mus musculus	3,200	–	–	–	–	+/++	++	++	–	–/++[c]	?	?	?	–++[c]	–	++	Schotta et al. (2004); Peters et al. (2003); Heard (2005)
Arabidopsis thaliana (L.) Heynh.	160	–	–	–	++	++	–	++	++	–	–	–	–	++	–	–	Soppe et al. (2002); Jackson et al. (2004); Lindroth et al. (2004); Naumann et al. (2005)
Raphanus sativus L.	540	–	–	–	++	++	–	++	++	–	?	?	?	?	?	?	
Glycine max L. Merr.	1,000	–	–	–	++	++	–	++	–	–	?	?	?	?	?	?	
Brachyscome dichromosomatica C. R. Carter	1,510	–	–	–	+	+	–	+	–	–	?	?	?	?	?	?	Houben et al. (2003); Marschner et al. (2007)
Vicia faba L.	12,740	+	–	–	++[d]	+	?	+	++[d]	++[d]	?	?	?	+	?	?	Houben et al. (2003); Fuchs et al. (2006)

(continued)

Table 9.1 (continued)

Species	Genome size	H3K4			H3K9			H3K27			H3K36			H4K20			References
	Mbp	me1	me2	me3	me1	me2	me3	me1	me2	me3	me1	me2	me3	me1	me2	me3	
Zea mays L.	2,670	?	–	?	+	–[e]	–	+	++	–	?	?	?	nd	nd	nd	Houben et al. (2003); Shi and Dawe (2006)
Hordeum vulgare L.	5,100	–	–	–	+	+	–	+	–	–	?	?	?	+	?	?	Houben et al. (2003); Fuchs et al. (2006)
Secale cereale L.	8,110	–	–	–	+	+	–	+	++	++	?	?	?	nd	nd	nd	Houben et al. (2003); Carchilan et al. (2007)
Picea abies (L.) Karst.	19,600	?	–	?	–	+	+	+	++	++	?	?	?	nd	?	?	Fuchs et al. (2008)
Pinus sylvestris L.	22,500	?	–	?	–	+	++	+	++	++	?	?	?	nd	?	?	Fuchs et al. (2008)

++, higher than in euchromatin; +, equal to euchromatin; –, lower than euchromatin; ?, nuclear distribution not yet investigated; *nd,* not detectable

[a]Data about nuclear distribution of the methylation marks in these species are mainly based on ChIP analysis of active genes and inactive chromosomal regions

[b]Only chromocenter core labeled

[c]Prominent mark of facultative heterochromatin

[d]Local enrichment in various individual (but not all) heterochromatic regions

[e]In contrast, Rossi et al. (2007) reported a uniform distribution along the chromatin, including the heterochromatin

H3K9me1,2,3, H3K27me1,2,3, and H4K20me3 are considered predominant marks of pericentric heterochromatin in *Drosophila* (Ebert et al. 2004; Schotta et al. 2004), although none of these marks is restricted to pericentric heterochromatin (Ebert et al. 2006). H3K9me2 and 3, in *Drosophila* mediated mainly but not exclusively by the methyltransferase SU(VAR)3-9, establish binding sites for HP1 (Bannister et al. 2001; Lachner et al. 2001). Together with SU(VAR)3-7, another heterochromatin-associated protein, methylated H3K9 and HP1 result in a multimeric protein complex responsible for heterochromatin assembly (Delattre et al. 2000). Trimethylation of H4K20 in heterochromatic regions by SUV4-20 strongly depends on the presence of H3K9me2 and HP1 (Schotta et al. 2004). Independent of H3K9 methylation, *Enhancer of zeste* [*E*(*z*)] mediates all three H3K27 methylation states in *Drosophila* (Ebert et al. 2004).

In mouse (*Mus musculus* L.) nuclei, constitutive heterochromatin is preferentially marked by H3K9me3, H3K27me1, and H4K20me3 (Peters et al. 2003; Rice et al. 2003; Schotta et al. 2004). As in *Drosophila*, methylation of H3K9 provides binding sites for HP1.

The facultative heterochromatin, however, represented by the inactive X chromosome is marked by H3K9me2, H3K27me3, and H4K20me1 (Plath et al. 2003; Silva et al. 2003; Lachner et al. 2004; Heard 2005).

In plants, most data on the distribution of methylation marks are available for *A. thaliana.* In that species, H3K9me1,2, H3K27me1,2, and H4K20me1 were found to be enriched at the heterochromatic chromocenters (Fig. 9.1d; Soppe et al. 2002; Jasencakova et al. 2003; Tariq et al. 2003; Lindroth et al. 2004; Naumann et al. 2005), but the restriction of these marks to microscopically detectable heterochromatin is not conserved among plants. In 24 plant species with different genome sizes, H3K4me2 was found exclusively in euchromatic regions, whereas H3K9me2 displayed two different distribution patterns. In plant species with a genome size below 500 Mbp/1C, the labeling was confined to the heterochromatic chromocenters (as in *Arabidopsis*), but in species with larger genomes, H3K9me2 was distributed all over the nuclei (Houben et al. 2003). Apparently, increasing numbers of mobile elements are interspersed in the euchromatin of larger genomes and must be silenced by "heterochromatinization" involving heterochromatin-specific methylation marks.

A distribution similar to that in *Arabidopsis* was also found in *Raphanus sativus* L. (radish), whereas in *Glycine max* L. Merr. (soybean) and *Brachyscome dichromosomatica* C. R. Carter, only H3K9me1,2 and H3K27me1 could be identified as heterochromatin-specific (Marschner et al. 2007; Fuchs unpublished).

In *V. faba*, H3K9me1,2, H3K27me1,2,3, and H4K20me1 are uniformly distributed over the entire chromatin (Fig. 9.2d; Fuchs et al. 2006), as described for the heterochromatin-specific mark H3K9me2 in plants with large genomes (Houben et al. 2003). In addition, H3K9me1 and H3K27me2 are locally enriched in various individual heterochromatic regions, mainly characterized as weaker Giemsa bands (Fig. 9.2a, d; Fuchs et al. 1998), and H3K27me3 is locally enriched even in regions not defined as Giemsa-banded heterochromatin (Fig. 9.2d, Fuchs et al. 2006). Heterochromatin indexing in *V. faba* therefore seems to display sequence-specific

peculiarities. The DNA methylation pattern, examined by means of an antibody directed against 5-methylcytosine, coincided to some extent with the distribution of H3K27me2 (Fig. 9.2e). Whether the accumulation of 5-methylcytosine, H3K9me1, and H3K27me2,3 at distinct chromosomal regions is correlated with particular DNA sequences and the functional meaning of any such accumulation remains to be resolved.

In maize, H3K9me1, H3K27me1, and H3K27me2 are enriched in heterochromatin, but only H3K27me2 marks heterochromatin specifically (Shi and Dawe 2006). Surprisingly, H3K9me2, a mark strongly labeling the heterochromatin in all other investigated angiosperms, was classified as a euchromatic mark because of its low abundance at intensely DAPI-stained chromomeres and its distribution, which is positively correlated with that of H3K4me2 and negatively with that of H3K27me2 (Shi and Dawe 2006). Rossi et al. (2007), however, reported a uniform distribution of H3K9me2 along maize chromatin, including the densely DAPI-stained regions.

In *H. vulgare*, H3K9me1,2, H3K27me1, and H4K20me1 are more or less uniformly distributed over the interphase chromatin and metaphase chromosomes (Fuchs et al. 2006), again as described for H3K9me2 in plants with large genomes. Surprisingly, H3K27me2, a heterochromatin-specific mark in *Arabidopsis*, has been found exclusively in euchromatic nuclear domains and at the distal regions of metaphase chromosomes where euchromatin-specific marks are located as well (Fuchs et al. 2006).

In *Secale cereale* L. (rye), the heterochromatic marks H3K9me1 and 2 show a dispersed distribution over the entire metaphase chromosomes. H3K9me3 and H4K20me1,2,3 are only scarcely detectable on the chromosomes and show no clear preference for either eu- or heterochromatin (Carchilan et al. 2007). Whereas H3K27me1 was found to be enriched in proximal chromosomal regions including the pericentromeres, H3K27me2,3 were exclusively found at the terminal heterochromatin blocks (Carchilan et al. 2007).

In the gymnosperm species *Picea abies* (L.) Karst. and *Pinus sylvestris* L., five marks were considered typical for heterochromatin because they either showed a homogeneous distribution over the entire chromatin within these large genomes (H3K9me2 and H3K27me1 in both species; H3K9me3 only in *P. abies*) or because of an additional enrichment in regions known or assumed to contain tandem repetitive sequences (H3K27me2,3 in both species; H3K9me3 only in *P. sylvestris*). Surprisingly, H3K9me1, a mark typical of heterochromatin in all investigated angiosperms, did not show a heterochromatin-specific, but instead a euchromatin-specific distribution, like H3K4me2 (Fuchs et al. 2008).

From the available data we conclude that methylation of H3K4 is restricted to euchromatin in plants; H3K9me1, H3K9me2, and H3K27me1 mark heterochromatin in angiosperms, although they may spread into euchromatin in species with genomes larger than 500 Mb/1C; and H3K27me2 and H3K27me3 show species-specific chromosomal distribution. Heterochromatin in gymnosperms is characterized by H3K9me2,3 and H3K27me1,2,3.

Histone methylation marks are therefore conserved in plants, whereas distributions and functional meanings of individual marks might have diverged during evolution.

In general, H3K9 methylation seems to be a hallmark of constitutive heterochromatin from fission yeast to mammals and plants. In angiosperms and *Drosophila*, H3K9me1 and 2 are enriched at heterochromatin, whereas in gymnosperms H3K9me2 and 3 and in *Neurospora* and mice, H3K9me3 is enriched at silent loci. Methylation of H3K27 is restricted to metazoa and plants. Although only H3K27me1 occurs at centromeric heterochromatin in mice, in a number of plant species, H3K27me2, and in *V. faba*, *S. cereale*, gymnosperms and *Drosophila*, even H3K27me3 are also characteristic of heterochromatin. H4K20me3 is heterochromatin-specific in *Drosophila* and mice, as is H4K20me1 in at least a few plant species. Except for H3K27me3 in rye, none of the trimethylated lysines seems to be typical of heterochromatic regions in plants (Table 9.1).

Previously, histone methylation was considered stable and irreversible, but more recent identifications of several mammalian enzymes that remove methyl groups, especially the discovery of the *Lysine-Specific Demethylase 1* (*LSD1*) and the JmjC-domain-containing histone demethylases, disproved this view. *LSD1* specifically demethylates H3K4me1 and H3K4me2 by amine oxidation (Shi et al. 2004, 2005) and, in complex with an androgen receptor, also H3K9me2 (Metzger et al. 2005). *JHDM1A* demethylates H3K36me1 and H3K36me2 (Tsukada et al. 2006); *JHDM2A* demethylates H3K9me1 and H3K9me2 (Yamane et al. 2006); *JHDM3/JMJD2* demethylate H3K9me3 and H3K36me3 (Cloos et al. 2006; Fodor et al. 2006; Klose et al. 2006; Whetstine et al. 2006); *UTX/JmJD3* demethylates H3K27me3 and H3K27me2 (De Santa et al. 2007; Lan et al. 2007; Lee et al. 2007a; Xiang et al. 2007); and *JARID1* demethlates H3K4me3 and H3K4me2 (Klose et al. 2007). Meanwhile, homologs of *LSD1* and of JmjC-domain-containing histone demethylases with the corresponding demethylating activity could be identified also in *Drosophila* (Di Stefano et al. 2007; Eissenberg et al. 2007; Lee et al. 2007b; Rudolph et al. 2007; Secombe et al. 2007).

Recently, three of the four *Arabidopsis LSD1* homologs, *LDL1*, *LDL2*, and *FLD*, have been shown to be involved in controlling H3K4 methylation at *FWA* and *FLC* loci and to act to repress these genes (Jiang et al. 2007).

9.5 Interplay Between Histone Methylation and DNA Methylation in *Arabidopsis*

The combination of DNA and histone modification has long been assumed to specify chromatin structure and subsequently to determine its transcriptional competence (Richards and Elgin 2002). In this respect, functional links between DNA and histone methylation, as the most stable covalent modifications, have received particular attention.

In contrast to DNA methylation in mammals, which is mainly restricted to symmetrical CG sequences (Bird 2002), plant DNA methylation occurs at CG, CNG (N = any nucleotide), and CHH (H = A, C, or T) sequences (Finnegan and Kovac 2000). The *A. thaliana* genome contains three classes of DNA methyltransferases.

METHYLTRANSFERASE 1 (*MET1*), the homolog of the mammalian *DNMT1*, is considered to be a maintenance DNA methyltransferase. Null allele mutants of *MET1* resulted in a complete loss of CG methylation (Saze et al. 2003). The maintenance of the plant-specific CNG methylation is catalyzed by *CHROMOMETHYLASE 3* (*CMT3*) (Bartee et al. 2001; Lindroth et al. 2001). In addition, *CMT3* also controls asymmetric CHH methylation in a locus-specific manner and is probably redundant with *DOMAINS REARRANGED METHYLTRANSFERASES* (*DRM*) *1* and *DRM2* (Cao and Jacobsen 2002). *DRM1* and *DRM2* were found to be responsible for de novo methylation of cytosines in all sequence contexts (for review see Chan et al. 2005).

Loss of DNA methylation in *met1* and *ddm1* (*DECREASE IN DNA METYLATION 1*, Vongs et al. 1993) mutants is associated with reduced levels of H3K9me2 and a relaxation of the heterochromatic chromocenters (Soppe et al. 2002; Tariq et al. 2003), but the distribution of mono- and dimethylated H3K27 was not influenced by DNA methylation at CG sites (Mathieu et al. 2005). Because, in nuclei of the first backcross generation of *ddm1* to wild-type, half of the chromocenters restored neither CG methylation nor H3K9me2, DNA methylation at CG sequences was suggested to direct specifically the dimethylation of H3K9 at the chromocenters (Soppe et al. 2002). Recently, Johnson et al. (2007) showed that the SRA domain of the H3K9me2-specific histone methyltransferase *KRYPTONITE* (*KYP*, also named *SUVH4*) interacts directly with methylated DNA. In contrast to the methylation at CG sites, methylation outside CG has no effect on histone methylation (Johnson et al. 2002), but histone methylation in turn directs DNA methylation at CNG sites (Jackson et al. 2002). Mutants of the histone methyltransferase *KYP* resulted in a loss of methylation at non-CG sites, but not at CG sites, suggesting that non-CG methylation depends on KYP activity (Jackson et al. 2002; Malagnac et al. 2002). *CMT3*, responsible for this non-CG DNA methylation, binds in vitro directly to H3K9me3 and H3K27me3 (Lindroth et al. 2004). Recently, Mathieu et al. (2007) demonstrated that loss of CG methylation in successive generations of *met1* triggers a transgenerationally progressive genome-wide aberrant de novo non-CG methylation, even at previously unmarked locations. This alternative "backup" mechanism, which also leads to redirection of H3K9me2 to the chromocenters, acts in a random and uncoordinated manner (Mathieu et al. 2007).

Although KYP is a major H3K9me2 methyltransferase, other homologs of the *Drosophila SU*(*VAR*)*3-9* methyltransferase have been shown to be involved in the maintenance of H3K9 methylation in vivo as well (Ebbs et al. 2005; Naumann et al. 2005; Ebbs and Bender 2006). Strikingly, the relative contributions of *KYP*/*SUVH4*, *SUVH5*, and *SUVH6* seem to be locus-specific. *SUVH4*, *SUVH5*, and with only minor contribution, *SUVH6* control transposon sequences, whereas mainly *SUVH4* and *SUVH6* act together at transcribed inverted repeats. The *suvh4 suvh5 suvh6* triple mutant shows a complete loss of H3K9me1 and H3K9me2 and a loss of non-CG methylation, similar to a *cmt3* mutant, at the target loci (Ebbs et al. 2005; Ebbs and Bender 2006). Mutation of *SUVH2* is reported to reduce the levels of all heterochromatin-specific marks, in particular those of H4K20me1 (Naumann et al. 2005).

The *Heterochromatin Protein 1* (*HP1*) and its homologues have been shown to be key components of heterochromatin in fission yeast, *Neurospora*, *Drosophila*, and mammals (James and Elgin 1986; Aagaard et al. 1999; Grewal and Moazed 2003; Freitag et al. 2004). The only homolog of *HP1* in *Arabidopsis* (*TFL2*/*LHP1*) apparently does not contribute to heterochromatin formation in vivo. Instead, it localizes preferentially to euchromatic regions for suppression of development-specific genes (Lindroth et al. 2004; Libault et al. 2005; Nakahigashi et al. 2005). *TFL2*/*LHP1* associates almost exclusively with chromatin marked by H3K27me3, but is not itself involved in the deposition of this mark (Turck et al. 2007; Zhang et al. 2007b). Instead, it recognizes specifically H3K27me3 and is involved in the repression machinery of euchromatic genes.

9.6 Summary and Outlook

Although the components of the "histone code" are conserved throughout eukaryotes, evidence is growing that the functional meanings of the individual marks in different phyla have diverged. For example, H3S10ph and H3S28ph seem to be involved in sister centromere cohesion and H3T3ph and H3T11ph in chromosome condensation in plants, whereas inverse functions are postulated for mammals. Of the three known heterochromatin-specific methylation marks in mammals (H3K9me3, H3K27me1, and H4K20me3), only one (H3K27me1) is regularly found to be associated with heterochromatin in plants. The other heterochromatin-specific marks of plants are associated with euchromatin or with facultative heterochromatin in mammals. In addition, the chromosomal distribution of histone marks may also vary among plants, in particular that of H3K27me2. A species-specific cell cycle-dependent modulation of acetylation at individual lysine residues was found at the chromosomal level in plants.

So far, most of the investigations on plant histone H3 modification have been performed without consideration of the individual isoforms of H3, although *Arabidopsis* is known to encode 15 histone H3 genes, including five H3.1, three H3.3, and five H3.3-like paralogs (Okada et al. 2005). Variability between individual H3 variants in occurrence of distinct modifications cannot be excluded.

Although evidence is growing that methylation of histone arginines is involved in regulating chromatin remodeling and transcription (Bedford and Richard 2005; Dacwag et al. 2007), little is known about this modification in plants (Wang et al. 2007). Analyzing posttranslational modifications of histone H2B variants of *A. thaliana* by a combination of reversed-phase chromatography and tandem mass spectrometry identified new acetylation, methylation, and ubiquitination sites (Bergmüller et al. 2007).

More and more clearly, individual modifications may "cross talk" to each other during or after their establishment. For example, H3 methylation of lysine K4 and gene silencing are regulated by H2BK123 ubiquitination in budding yeast (Sun and

Allis 2002), a ubiquitin ligase is required for histone methyltransferase localization and silencing at heterochromatic loci in fission yeast (Jia et al. 2005) deubiquitination of H2A regulates transcription by coordinating histone acetylation and dissociation of the linker histone H1 in humans (Zhu et al. 2007), deubiquitination of H2B controls H3K9me2 and DNA methylation in *A. thaliana* (Sridhar et al. 2007), H3K18ac stimulates methylation of H3R17 in humans (Daujat et al. 2002), arginine methylation at H3R2 controls deposition of H3K4me3 in budding yeast (Kirmizis et al. 2007), H3S10ph and H3K14ac together lead to transcriptional activation of mammalian genes during ovary differentiation (Salvador et al. 2001), and the combinatorial readout of H3K9me3 and H3S10ph regulates HP1 binding to pericentric heterochromatin in mammals (Fischle et al. 2005). Meanwhile, the increasing number of described individual cross-regulations of histone modifications has allowed the discovery of complex functional networks (for review see Latham and Dent 2007).

Chromosomal distribution patterns of chromatin modifications in combination with mass spectroscopy data (Johnson et al. 2004) and genome-wide mapping of DNA and/or histone methylation by high-density tiling microarrays (Zhang et al. 2007a; Zilberman et al. 2007) will provide further insights into epigenetic complexity.

Acknowledgments This work was supported by a grant of the Land Sachsen-Anhalt to J.F. and I.S.

References

Aagaard L, Laible G, Selenko P, Schmid M, Dorn R, Schotta G, Kuhfittig S, Wolf A, Lebersorger A, Singh PB, Reuter G, Jenuwein T (1999) Functional mammalian homologues of the *Drosophila* PEV-modifier *Su(var)3-9* encode centromere-associated proteins which complex with the heterochromatin component M31. *EMBO J* 18:1923–1938

Adams RR, Maiato H, Earnshaw WC, Carmena M (2001) Essential roles of *Drosophila* inner centromere protein (INCENP) and aurora B in histone H3 phosphorylation, metaphase chromosome alignment, kinetochore disjunction, and chromosome segregation. *J Cell Biol* 153:865–880

Adhvaryu KK, Morris SA, Strahl BD, Selker EU (2005) Methylation of histone H3 lysine 36 is required for normal development in *Neurospora crassa*. *Eukaryot Cell* 4:1455–1464

Allfrey VG, Faulkner R, Mirsky AE (1964) Acetylation and methylation of histones and their possible role in the regulation of RNA synthesis. *Proc Natl Acad Sci USA* 51:786–794

Allshire RC, Selker EU (2007) Fungal models for epigenetic research: *Schizosaccharomyces pombe* and *Neurospora crassa*. In: Allis CD, Jenuwein T, Reinberg D, Caparros M-L (eds) *Epigenetics.* Cold Spring Harbor Laboratory Press, Cold Spring Harbor, pp 101–125

Bannister AJ, Zegerman P, Partridge JF, Miska EA, Thomas JO, Allshire RC, Kouzarides T (2001) Selective recognition of methylated lysine 9 on histone H3 by the HP1 chromo domain. *Nature* 410:120–124

Bartee L, Malagnac F, Bender J (2001) *Arabidopsis cmt3* chromomethylase mutations block non-CG methylation and silencing of an endogenous gene. *Genes Dev* 15:1753–1758

Bedford MT, Richard S (2005) Arginine methylation an emerging regulator of protein function. *Mol Cell* 18:263–272

Belyaev N, Keohane AM, Turner BM (1996) Differential underacetylation of histones H2A, H3 and H4 on the inactive X chromosome in human female cells. *Hum. Genet* 97:573–578

Belyaev ND, Houben A, Baranczewski P, Schubert I (1997) Histone H4 acetylation in plant heterochromatin is altered during the cell cycle. *Chromosoma* 106:193–197

Belyaev ND, Houben A, Baranczewski P, Schubert I (1998) The acetylation patterns of histones H3 and H4 along *Vicia faba* chromosomes are different. *Chromosome Res* 6:59–63

Bergmüller E, Gehrig PM, Gruissem W (2007) Characterization of post-translational modifications of histone H2B-variants isolated from *Arabidopsis thaliana*. *J Proteome Res* 6:3655–3668

Bird A (2002) DNA methylation patterns and epigenetic memory. *Genes Dev* 16:6–21

Bird AW, Yu DY, Pray-Grant MG, Qiu Q, Harmon KE, Megee PC, Grant PA, Smith MM, Christman MF (2002) Acetylation of histone H4 by Esa1 is required for DNA double-strand break repair. *Nature* 419:411–415

Cao X, Jacobsen SE (2002) Locus-specific control of asymmetric and CpNpG methylation by the *DRM* and *CMT3* methyltransferase genes. *Proc Natl Acad Sci USA* 99 Suppl 4:16491–16498

Carchilan M, Delgado M, Ribeiro T, Costa-Nunes P, Caperta A, Morais-Cecílio L, Jones RN, Viegas W, Houben A (2007) Transcriptionally active heterochromatin in rye B chromosomes. *Plant Cell* 19:1738–1749

Chan SW-L, Henderson IR, Jacobsen SE (2005) Gardening the genome: DNA methylation in *Arabidopsis thaliana*. *Nat Rev Genet* 6:351–360

Cheung WL, Briggs SD, Allis CD (2000) Acetylation and chromosomal functions. *Curr Opin Cell Biol* 12:326–333

Cloos PAC, Christensen J, Agger K, Maiolica A, Rappsilber J, Antal T, Hansen KH, Helin K (2006) The putative oncogene GASC1 demethylates tri- and dimethylated lysine 9 on histone H3. *Nature* 442:307–311

Dacwag CS, Ohkawa Y, Pal S, Sif S, Imbalzano AN (2007) The protein arginine methyltransferase Prmt5 is required for myogenesis because it facilitates ATP-dependent chromatin remodeling. *Mol Cell Biol* 27:384–394

Daujat S, Bauer UM, Shah V, Turner B, Berger S, Kouzarides T (2002) Crosstalk between CARM1 methylation and CBP acetylation on histone H3. *Curr Biol* 12:2090–2097

De Santa F, Totaro MG, Prosperini E, Notarbartolo S, Testa G, Natoli G (2007) The histone H3 lysine-27 demethylase Jmjd3 links inflammation to inhibition of polycomb-mediated gene silencing. *Cell* 130:1083–1094

Delattre M, Spierer A, Tonka C-H, Spierer P (2000) The genomic silencing of position-effect variegation in *Drosophila melanogaster*: interaction between the heterochromatin-associated proteins Su(var)3-7 and HP1. *J Cell Sci* 113 Pt 23:4253–4261

Di Stefano L, Ji J-Y, Moon N-S, Herr A, Dyson N (2007) Mutation of *Drosophila Lsd1* disrupts H3-K4 methylation, resulting in tissue-specific defects during development. *Curr Biol* 17:808–812

Döbel P, Schubert I, Rieger R (1978) Distribution of heterochromatin in a reconstructed karyotype of *Vicia faba* as identified by banding- and DNA-late replication patterns. *Chromosoma* 69:193–209

Ebbs ML, Bartee L, Bender J (2005) H3 lysine 9 methylation is maintained on a transcribed inverted repeat by combined action of SUVH6 and SUVH4 methyltransferases. *Mol Cell Biol* 25:10507–10515

Ebbs ML, Bender J (2006) Locus-specific control of DNA methylation by the *Arabidopsis* SUVH5 histone methyltransferase. *Plant Cell* 18:1166–1176

Ebert A, Schotta G, Lein S, Kubicek S, Krauss V, Jenuwein T, Reuter G (2004) Su(var) genes regulate the balance between euchromatin and heterochromatin in *Drosophila*. *Genes Dev* 18: 2973–2983

Ebert A, Lein S, Schotta G, Reuter G (2006) Histone modification and the control of heterochromatic gene silencing in *Drosophila*. *Chromosome Res* 14:377–392

Eissenberg JC, Lee MG, Schneider J, Ilvarsonn A, Shiekhattar R, Shilatifard A (2007) The trithorax-group gene in *Drosophila little imaginal discs* encodes a trimethylated histone H3 Lys4 demethylase. *Nat Struct Mol Biol* 14:344–346

Finnegan EJ, Kovac KA (2000) Plant DNA methyltransferases. *Plant Mol Biol* 43:189–201

Fischle W, Tseng BS, Dormann HL, Ueberheide BM, Garcia BA, Shabanowitz J, Hunt DF, Funabiki H, Allis CD (2005) Regulation of HP1-chromatin binding by histone H3 methylation and phosphorylation. *Nature* 438:1116–1122

Fodor BD, Kubicek S, Yonezawa M, O'Sullivan RJ, Sengupta R, Perez-Burgos L, Opravil S, Mechtler K, Schotta G, Jenuwein T (2006) Jmjd2b antagonizes H3K9 trimethylation at pericentric heterochromatin in mammalian cells. *Genes Dev* 20:1557–1562

Freitag M, Hickey PC, Khlafallah TK, Read ND, Selker EU (2004) HP1 is essential for DNA methylation in *Neurospora*. *Mol Cell* 13:427–434

Friesner JD, Liu B, Culligan K, Britt AB (2005) Ionizing radiation-dependent gamma-H2AX focus formation requires ataxia telangiectasia mutated and ataxia telangiectasia mutated and Rad3-related. *Mol Biol Cell* 16:2566–2576

Fuchs J, Jovtchev G, Schubert I (2008) The chromosomal distribution of histone methylation marks in gymnosperms differs from that of angiosperms. *Chromosome Res* 16:891–898

Fuchs J, Pich U, Meister A, Schubert I (1994) Differentiation of field bean heterochromatin by *in situ* hybridization with a repeated *FokI* sequence. *Chromosome Res* 2:25–28

Fuchs J, Strehl S, Brandes A, Schweizer D, Schubert I (1998) Molecular-cytogenetic characterization of the *Vicia faba* genome-heterochromatin differentiation, replication patterns and sequence localization. *Chromosome Res* 6:219–230

Fuchs J, Demidov D, Houben A, Schubert I (2006) Chromosomal histone modification patterns-from conservation to diversity. *Trends Plant Sci* 11:199–208

Gernand D, Demidov D, Houben A (2003) The temporal and spatial pattern of histone H3 phosphorylation at serine 28 and serine 10 is similar in plants but differs between mono- and polycentric chromosomes. *Cytogenet Genome Res* 101:172–176

Goto H, Tomono Y, Ajiro K, Kosako H, Fujita M, Sakurai M, Okawa K, Iwamatsu A, Okigaki T, Takahashi T, Inagaki M (1999) Identification of a novel phosphorylation site on histone H3 coupled with mitotic chromosome condensation. *J Biol Chem* 274:25543–25549

Grewal SIS, Moazed D (2003) Heterochromatin and epigenetic control of gene expression. *Science* 301:798–802

Grunstein M (1997) Histone acetylation in chromatin structure and transcription. *Nature* 389: 349–352

Guerra M, Brasileiro-Vidal AC, Arana P, Puertas MJ (2006) Mitotic microtubule development and histone H3 phosphorylation in the holocentric chromosomes of *Rhynchospora tenuis* (Cyperaceae). *Genetica* 126:33–41

Gurtley LR, Walters RA, Tobey RA (1975) Sequential phosphorylation of histone subfraction in the Chinese hamster cell cycle. *J Biol Chem* 250:3936–3944

Hanson KK, Kelley AC, Bienz M (2005) Loss of *Drosophila borealin* causes polyploidy, delayed apoptosis and abnormal tissue development. *Development* 132:4777–4787

Heard E (2005) Delving into the diversity of facultative heterochromatin: the epigenetics of the inactive X chromosome. *Curr Opin Genet Dev* 15:482–489

Hendzel MJ, Wei Y, Mancini MA, Van Hooser A, Ranalli T, Brinkley BR, Bazett-Jones DP, Allis CD (1997) Mitosis-specific phosphorylation of histone H3 initiates primarily within pericentromeric heterochromatin during G2 and spreads in an ordered fashion coincident with mitotic chromosome condensation. *Chromosoma* 106:348–360

Hizume K, Yoshimura SH, Kumeta M, Takeyasu K (2007) Structural organization of dynamic chromatin. *Subcell Biochem* 41:3–28

Houben A, Belyaev ND, Turner BM, Schubert I (1996) Differential immunostaining of plant chromosomes by antibodies recognizing acetylated histone H4 variants. *Chromosome Res* 4:191–194

Houben A, Wako T, Furushima-Shimogawara R, Presting G, Künzel G, Schubert I, Fukui K (1999) Short communication: the cell cycle dependent phosphorylation of histone H3 is correlated with the condensation of plant mitotic chromosomes. *Plant J* 18:675–679

Houben A, Demidov D, Gernand D, Meister A, Leach CR, Schubert I (2003) Methylation of histone H3 in euchromatin of plant chromosomes depends on basic nuclear DNA content. *Plant J* 33:967–973

Houben A, Demidov D, Rutten T, Scheidtmann KH (2005) Novel phosphorylation of histone H3 at threonine 11 that temporally correlates with condensation of mitotic and meiotic chromosomes in plant cells. *Cytogenet Genome Res* 109:148–155

Houben A, Demidov D, Caperta AD, Karimi R, Agueci F, Vlasenko L (2007) Phosphorylation of histone H3 in plants-a dynamic affair. *Biochim Biophys Acta* 1769:308–315

Ikura T, Ogryzko VV, Grigoriev M, Groisman R, Wang J, Horikoshi M, Scully R, Qin J, Nakatani Y (2000) Involvement of the TIP60 histone acetylase complex in DNA repair and apoptosis. *Cell* 102:463–473

Jackson JP, Lindroth AM, Cao X, Jacobsen SE (2002) Control of CpNpG DNA methylation by the KRYPTONITE histone H3 methyltransferase. *Nature* 416:556–560

Jackson JP, Johnson L, Jasencakova Z, Zhang X, Perez-Burgos L, Singh PB, Cheng X, Schubert I, Jenuwein T, Jacobsen SE (2004) Dimethylation of histone H3 lysine 9 is a critical mark for DNA methylation and gene silencing in *Arabidopsis thaliana*. *Chromosoma* 112:308–315

James TC, Elgin SCR (1986) Identification of a nonhistone chromosomal protein associated with heterochromatin in *Drosophila melanogaster* and its gene. *Mol Cell Biol* 6:3862–3872

Jasencakova Z, Meister A, Walter J, Turner BM, Schubert I (2000) Histone H4 acetylation of euchromatin and heterochromatin is cell cycle dependent and correlated with replication rather than with transcription. *Plant Cell* 12:2087–2100

Jasencakova Z, Meister A, Schubert I (2001) Chromatin organization and its relation to replication and histone acetylation during the cell cycle in barley. *Chromosoma* 110:83–92

Jasencakova Z, Soppe WJJ, Meister A, Gernand D, Turner BM, Schubert I (2003) Histone modifications in *Arabidopsis*-high methylation of H3 lysine 9 is dispensable for constitutive heterochromatin. *Plant J* 33:471–480

Jenuwein T, Allis CD (2001) Translating the histone code. *Science* 293:1074–1080

Jeppesen P, Mitchell A, Turner B, Perry P (1992) Antibodies to defined histone epitopes reveal variations in chromatin conformation and underacetylation of centric heterochromatin in human metaphase chromosomes. *Chromosoma* 101:322–332

Jeppesen P, Turner BM (1993) The inactive X chromosome in female mammals is distinguished by a lack of histone H4 acetylation, a cytogenetic marker for gene expression. *Cell* 74: 281–289

Jia S, Kobayashi R, Grewal SIS (2005) Ubiquitin ligase component Cul4 associates with Clr4 histone methyltransferase to assemble heterochromatin. *Nat Cell Biol* 7:1007–1013

Jiang D, Yang W, He Y, Amasino RM (2007) *Arabidopsis* relatives of the human lysine specific demethylase1 repress the expression of *FWA* and *FLOWERING LOCUS C* and thus promote the floral transition. *Plant Cell* 19:2975–2987

Johnson LM, Cao X, Jacobsen SE (2002) Interplay between two epigenetic marks. DNA methylation and histone H3 lysine 9 methylation. *Curr Biol* 12:1360–1367

Johnson LM, Mollah S, Garcia BA, Muratore TL, Shabanowitz J, Hunt DF, Jacobsen SE (2004) Mass spectrometry analysis of *Arabidopsis* histone H3 reveals distinct combinations of post-translational modifications. *Nucleic Acids Res* 32:6511–6518

Johnson LM, Bostick M, Zhang X, Kraft E, Henderson I, Callis J, Jacobsen SE (2007) The SRA methyl-cytosine-binding domain links DNA and histone methylation. *Curr Biol* 17:379–384

Kaszás É, Cande WZ (2000) Phosphorylation of histone H3 is correlated with changes in the maintenance of sister chromatid cohesion during meiosis in maize, rather than the condensation of the chromatin. *J Cell Sci* 113 (Pt 18):3217–3226

Kirmizis A, Santos-Rosa H, Penkett CJ, Singer MA, Vermeulen M, Mann M, Bähler J, Green RD, Kouzarides T (2007) Arginine methylation at histone H3R2 controls deposition of H3K4 trimethylation. *Nature* 449:928–932

Klose RJ, Yamane K, Bae Y, Zhang D, Erdjument-Bromage H, Tempst P, Wong J, Zhang Y (2006) The transcriptional repressor JHDM3A demethylates trimethyl histone H3 lysine 9 and lysine 36. *Nature* 442:312–316

Klose RJ, Yan Q, Tothova Z, Yamane K, Erdjument-Bromage H, Tempst P, Gilliland DG, Zhang Y, Kaelin WG, Jr (2007) The retinoblastoma binding protein RBP2 is an H3K4 demethylase. *Cell* 128:889–900

Kornberg RD (1974) Chromatin structure: a repeating unit of histones and DNA. *Science* 184:868–871

Kornberg RD, Lorch Y (1999) Twenty-five years of the nucleosome, fundamental particle of the eukaryote chromosome. *Cell* 98:285–294

Lachner M, O'Carroll D, Rea S, Mechtler K, Jenuwein T (2001) Methylation of histone H3 lysine 9 creates a binding site for HP1 proteins. *Nature* 410:116–120

Lachner M, Sengupta R, Schotta G, Jenuwein T (2004) Trilogies of histone lysine methylation as epigenetic landmarks of the eukaryotic genome. *Cold Spring Harb Symp Quant Biol* 69: 209–218

Lan F, Bayliss PE, Rinn JL, Whetstine JR, Wang JK, Chen S, Iwase S, Alpatov R, Issaeva I, Canaani E, Roberts TM, Chang HY, Shi Y (2007) A histone H3 lysine 27 demethylase regulates animal posterior development. *Nature* 449:689–694

Latham JA, Dent SY (2007) Cross-regulation of histone modifications. *Nat Struct Mol Biol* 14:1017–1024

Lee DY, Hayes JJ, Pruss D, Wolffe AP (1993) A positive role for histone acetylation in transcription factor access to nucleosomal DNA. *Cell* 72:73–84

Lee MG, Villa R, Trojer P, Norman J, Yan K-P, Reinberg D, Croce LD, Shiekhattar R (2007a) Demethylation of H3K27 regulates polycomb recruitment and H2A ubiquitination. *Science* 318:447–450

Lee N, Zhang J, Klose RJ, Erdjument-Bromage H, Tempst P, Jones RS, Zhang Y (2007b) The trithorax-group protein Lid is a histone H3 trimethyl-Lys4 demethylase. *Nat Struct Mol Biol* 14:341–343

Libault M, Tessadori F, Germann S, Snijder B, Fransz P, Gaudin V (2005) The *Arabidopsis* LHP1 protein is a component of euchromatin. *Planta* 222:910–925

Lindroth AM, Cao X, Jackson JP, Zilberman D, McCallum CM, Henikoff S, Jacobsen SE (2001) Requirement of *CHROMOMETHYLASE3* for maintenance of CpXpG methylation. *Science* 292:2077–2080

Lindroth AM, Shultis D, Jasencakova Z, Fuchs J, Johnson L, Schubert D, Patnaik D, Pradhan S, Goodrich J, Schubert I, Jenuwein T, Khorasanizadeh S, Jacobsen SE (2004) Dual histone H3 methylation marks at lysines 9 and 27 required for interaction with *CHROMOMETHYLASE3*. *EMBO J* 23:4286–4296

Loidl P (2004) A plant dialect of the histone language. *Trends Plant Sci* 9:84–90

Loury R, Sassone-Corsi P (2004) Analysis of histone phosphorylation: coupling intracellular signaling to chromatin remodeling. *Methods Enzymol* 377:197–212

Luger K, Richmond TJ (1998) The histone tails of the nucleosome. *Curr Opin Genet Dev* 8:140–146

Lusser A, Kölle D, Loidl P (2001) Histone acetylation: lessons from the plant kingdom. *Trends Plant Sci* 6:59–65

Malagnac F, Bartee L, Bender J (2002) An *Arabidopsis* SET domain protein required for maintenance but not establishment of DNA methylation. *EMBO J* 21:6842–6852

Manzanero S, Arana P, Puertas MJ, Houben A (2000) The chromosomal distribution of phosphorylated histone H3 differs between plants and animals at meiosis. *Chromosoma* 109:308–317

Marschner S, Meister A, Blattner FR, Houben A (2007) Evolution and function of B chromosome 45 S rDNA sequences in *Brachycome dichromosomatica*. *Genome* 50:638–644

Mathieu O, Probst AV, Paszkowski J (2005) Distinct regulation of histone H3 methylation at lysines 27 and 9 by CpG methylation in *Arabidopsis*. *EMBO J* 24:2783–2791

Mathieu O, Reinders J, aikovski M, Smathajitt C, Paszkowski J (2007) Transgenerational stability of the *Arabidopsis* epigenome is coordinated by CG methylation. *Cell* 130:851–862

McBlane F, Boyes J (2000) Stimulation of V(D)J recombination by histone acetylation. *Curr Biol* 10:483–486

McMurry MT, Krangel MS (2000) A role for histone acetylation in the developmental regulation of VDJ recombination. *Science* 287:495–458

Metzger E, Wissmann M, Yin N, Müller JM, Schneider R, Peters AHFM, Günther T, Buettner R, Schüle R (2005) LSD1 demethylates repressive histone marks to promote androgen-receptor-dependent transcription. *Nature* 437:436–439

Morris SA, Shibata Y, Noma K, Tsukamoto Y, Warren E, Temple B, Grewal SIS, Strahl BD (2005) Histone H3 K36 methylation is associated with transcription elongation in *Schizosaccharomyces pombe*. *Eukaryot Cell* 4:1446–1454

Morris SA, Rao B, Garcia BA, Hake SB, Diaz RL, Shabanowitz J, Hunt DF, Allis CD, Lieb JD, Strahl BD (2007) Identification of histone H3 lysine 36 acetylation as a highly conserved histone modification. *J Biol Chem* 282:7632–7640

Nakahigashi K, Jasencakova Z, Schubert I, Goto K (2005) The *Arabidopsis* heterochromatin protein1 homolog (TERMINAL FLOWER2) silences genes within the euchromatic region but not genes positioned in heterochromatin. *Plant Cell Physiol* 46:1747–1756

Nakayama J, Rice JC, Strahl BD, Allis CD, Grewal SIS (2001) Role of histone H3 lysine 9 methylation in epigenetic control of heterochromatin assembly. *Science* 292:110–113

Naumann K, Fischer A, Hofmann I, Krauss V, Phalke S, Irmler K, Hause G, Aurich A-C, Dorn R, Jenuwein T, Reuter G (2005) Pivotal role of AtSUVH2 in heterochromatic histone methylation and gene silencing in *Arabidopsis*. *EMBO J* 24:1418–1429

Noma K, Allis CD, Grewal SIS (2001) Transitions in distinct histone H3 methylation patterns at the heterochromatin domain boundaries. *Science* 293:1150–1155

Nowak SJ, Corces VG (2000) Phosphorylation of histone H3 correlates with transcriptionally active loci. *Genes Dev* 14:3003–3013

Okada T, Endo M, Singh MB, Bhalla PL (2005) Analysis of the histone H3 gene family in *Arabidopsis* and identification of the male-gamete-specific variant *AtMGH3*. *Plant J* 44:557–568

Peters AHFM, Kubicek S, Mechtler K, O'Sullivan RJ, Derijck AAHA, Perez-Burgos L, Kohlmaier A, Opravil S, Tachibana M, Shinkai Y, Martens JHA, Jenuwein T (2003) Partitioning and plasticity of repressive histone methylation states in mammalian chromatin. *Mol Cell* 12:1577–1589

Plath K, Fang J, Mlynarczyk-Evans SK, Cao R, Worringer KA, Wang H, de la Cruz CC, Otte AP, Panning B, Zhang Y (2003) Role of histone H3 lysine 27 methylation in X inactivation. *Science* 300:131–135

Polioudaki H, Markaki Y, Kourmouli N, Dialynas G, Theodoropoulos PA, Singh PB, Georgatos SD (2004) Mitotic phosphorylation of histone H3 at threonine 3. *FEBS Lett* 560:39–44

Preuss U, Landsberg G, Scheidtmann KH (2003) Novel mitosis-specific phosphorylation of histone H3 at Thr11 mediated by Dlk/ZIP kinase. *Nucleic Acids Res* 31:878–885

Prigent C, Dimitrov S (2003) Phosphorylation of serine 10 in histone H3, what for? *J Cell Sci* 116:3677–3685

Rice JC, Briggs SD, Ueberheide B, Barber CM, Shabanowitz J, Hunt DF, Shinkai Y, Allis CD (2003) Histone methyltransferases direct different degrees of methylation to define distinct chromatin domains. *Mol Cell* 12:1591–1598

Richards EJ, Elgin SCR (2002) Epigenetic codes for heterochromatin formation and silencing: rounding up the usual suspects. *Cell* 108:489–500

Rossi V, Locatelli S, Varotto S, Donn G, Pirona R, Henderson DA, Hartings H, Motto M (2007) Maize histone deacetylase *hda101* is involved in plant development, gene transcription, and sequence-specific modulation of histone modification of genes and repeats. *Plant Cell* 19:1145–1162

Rudolph T, Yonezawa M, Lein S, Heidrich K, Kubicek S, Schäfer C, Phalke S, Walther M, Schmidt A, Jenuwein T, Reuter G (2007) Heterochromatin formation in *Drosophila* is initiated through active removal of H3K4 methylation by the LSD1 homolog SU(VAR)3-3. *Mol Cell* 26: 103–115

Salvador LM, Park Y, Cottom J, Maizels ET, Jones JCR, Schillace RV, Carr DW, Cheung P, Allis CD, Jameson JL, Hunzicker-Dunn M (2001) Follicle-stimulating hormone stimulates protein kinase A-mediated histone H3 phosphorylation and acetylation leading to select gene activation in ovarian granulosa cells. *J Biol Chem* 276:40146–40155

Sanders SL, Portoso M, Mata J, Bähler J, Allshire RC, Kouzarides T (2004) Methylation of histone H4 lysine 20 controls recruitment of Crb2 to sites of DNA damage. *Cell* 119:603–614

Saze H, Mittelsten Scheid O, Paszkowski J (2003) Maintenance of CpG methylation is essential for epigenetic inheritance during plant gametogenesis. *Nat Genet* 34:65–69

Schotta G, Lachner M, Sarma K, Ebert A, Sengupta R, Reuter G, Reinberg D, Jenuwein T (2004) A silencing pathway to induce H3-K9 and H4-K20 trimethylation at constitutive heterochromatin. *Genes Dev* 18:1251–1262

Secombe J, Li L, Carlos L, Eisenman RN (2007) The Trithorax group protein Lid is a trimethyl histone H3K4 demethylase required for dMyc-induced cell growth. *Genes Dev* 21:537–551

Shi J, Dawe RK (2006) Partitioning of the maize epigenome by the number of methyl groups on histone H3 lysines 9 and 27. *Genetics* 173:1571–1583

Shi Y-J, Matson C, Lan F, Iwase S, Baba T, Shi Y (2005) Regulation of LSD1 histone demethylase activity by its associated factors. *Mol Cell* 19:857–864

Shi Y, Lan F, Matson C, Mulligan P, Whetstine JR, Cole PA, Casero RA, Shi Y (2004) Histone demethylation mediated by the nuclear amine oxidase homolog LSD1. *Cell* 119:941–953

Silva J, Mak W, Zvetkova I, Appanah R, Nesterova TB, Webster Z, Peters AHFM, Jenuwein T, Otte AP, Brockdorff N (2003) Establishment of histone h3 methylation on the inactive X chromosome requires transient recruitment of Eed-Enx1 polycomb group complexes. *Dev Cell* 4:481–495

Siroky J, Castiglione MR, Vyskot B (1998) DNA methylation patterns of *Melandrium album* chromosomes. *Chromosome Res* 6:441–446

Soppe WJJ, Jasencakova Z, Houben A, Kakutani T, Meister A, Huang MS, Jacobsen SE, Schubert I, Fransz PF (2002) DNA methylation controls histone H3 lysine 9 methylation and heterochromatin assembly in *Arabidopsis*. *EMBO J* 21:6549–6559

Sridhar VV, Kapoor A, Zhang K, Zhu J, Zhou T, Hasegawa PM, Bressan RA, Zhu J-K (2007) Control of DNA methylation and heterochromatic silencing by histone H2B deubiquitination. *Nature* 447:735–738

Strahl BD, Allis CD (2000) The language of covalent histone modifications. *Nature* 403:41–45

Sun Z-W, Allis CD (2002) Ubiquitination of histone H2B regulates H3 methylation and gene silencing in yeast. *Nature* 418:104–108

Taddei A, Roche D, Sibarita J-B, Turner BM, Almouzni G (1999) Duplication and maintenance of heterochromatin domains. *J Cell Biol* 147:1153–1166

Tamaru H, Selker EU (2001) A histone H3 methyltransferase controls DNA methylation in *Neurospora crassa*. *Nature* 414:277–283

Tamaru H, Zhang X, McMillen D, Singh PB, Nakayama J, Grewal SI, Allis CD, Cheng X, Selker EU (2003) Trimethylated lysine 9 of histone H3 is a mark for DNA methylation in *Neurospora crassa*. *Nat Genet* 34:75–79

Tariq M, Saze H, Probst AV, Lichota J, Habu Y, Paszkowski J (2003) Erasure of CpG methylation in *Arabidopsis* alters patterns of histone H3 methylation in heterochromatin. *Proc Natl Acad Sci USA* 100:8823–8827

Thiriet C, Hayes JJ (2005) Chromatin in need of a fix: phosphorylation of H2AX connects chromatin to DNA repair. *Mol Cell* 18:617–622

Tsukada Y, Fang J, Erdjument-Bromage H, Warren ME, Borchers CH, Tempst P, Zhang Y (2006) Histone demethylation by a family of JmjC domain-containing proteins. *Nature* 439:811–816

Turck F, Roudier F, Farrona S, Martin-Magniette M-L, Guillaume E, Buisine N, Gagnot S, Martienssen RA, Coupland G, Colot V (2007) *Arabidopsis* TFL2/LHP1 specifically associates with genes marked by trimethylation of histone H3 lysine 27. *PLoS Genet* 3:e86

Turner BM, Birley AJ, Lavender J (1992) Histone H4 isoforms acetylated at specific lysine residues define individual chromosomes and chromatin domains in *Drosophila* polytene nuclei. *Cell* 69:375–384

Turner BM (2000) Histone acetylation and an epigenetic code. *BioEssays* 22:836–845

Vongs A, Kakutani T, Martienssen RA, Richards EJ (1993) *Arabidopsis thaliana* DNA methylation mutants. *Science* 260:1926–1928

Vyskot B, Araya A, Veuskens J, Negrutiu I, Mouras A (1993) DNA methylation of sex chromosomes in a dioecious plant, *Melandrium album*. *Mol Gen Genet* 239:219–224

Vyskot B, Siroky J, Hladilova R, Belyaev ND, Turner BM (1999) Euchromatic domains in plant chromosomes as revealed by H4 histone acetylation and early DNA replication. *Genome* 42:343–350

Wade PA, Pruss D, Wolffe AP (1997) Histone acetylation: chromatin in action. *Trends Biochem Sci* 22:128–132

Wang X, Zhang Y, Ma Q, Zhang Z, Xue Y, Bao S, Chong K (2007) SKB1-mediated symmetric dimethylation of histone H4R3 controls flowering time in *Arabidopsis*. *EMBO J* 26:1934–1941

Whetstine JR, Nottke A, Lan F, Huarte M, Smolikov S, Chen Z, Spooner E, Li E, Zhang G, Colaiacovo M, Shi Y (2006) Reversal of histone lysine trimethylation by the JMJD2 family of histone demethylases. *Cell* 125:467–481

Wilkinson CRM, Bartlett R, Nurse P, Bird AP (1995) The fission yeast gene *pmt1+* encodes a DNA methyltransferase homologue. *Nucleic Acids Res* 23:203–210

Xiang Y, Zhu Z, Han G, Lin H, Xu L, Chen CD (2007) JMJD3 is a histone H3K27 demethylase. *Cell Res* 17:850–857

Yamada T, Fischle W, Sugiyama T, Allis CD, Grewal SIS (2005) The nucleation and maintenance of heterochromatin by a histone deacetylase in fission yeast. *Mol Cell* 20:173–185

Yamane K, Toumazou C, Tsukada Y, Erdjument-Bromage H, Tempst P, Wong J, Zhang Y (2006) JHDM2A, a JmjC-containing H3K9 demethylase, facilitates transcription activation by androgen receptor. *Cell* 125:483–495

Zhang X, Li X, Marshall JB, Zhong CX, Dawe RK (2005) Phosphoserines on maize CENTROMERIC HISTONE H3 and histone H3 demarcate the centromere and pericentromere during chromosome segregation. *Plant Cell* 17:572–583

Zhang X, Clarenz O, Cokus S, Bernatavichute YV, Pellegrini M, Goodrich J, Jacobsen SE (2007a) Whole-genome analysis of histone H3 lysine 27 trimethylation in *Arabidopsis*. *PLoS Biol* 5:e129

Zhang X, Germann S, Blus BJ, Khorasanizadeh S, Gaudin V, Jacobsen SE (2007b) The *Arabidopsis* LHP1 protein colocalizes with histone H3 Lys27 trimethylation. *Nat Struct Mol Biol* 14:869–871

Zhu P, Zhou W, Wang J, Puc J, Ohgi KA, Erdjument-Bromage H, Tempst P, Glass CK, Rosenfeld MG (2007) A histone H2A deubiquitinase complex coordinating histone acetylation and H1 dissociation in transcriptional regulation. *Mol Cell* 27:609–621

Zilberman D, Gehring M, Tran RK, Ballinger T, Henikoff S (2007) Genome-wide analysis of *Arabidopsis thaliana* DNA methylation uncovers an interdependence between methylation and transcription. *Nat Genet* 39:61–69

Part III
Methods, Informatics, and Instruction in Plant Cytogenetics

Chapter 10
Chromosome Microdissection and Utilization of Microisolated DNA

Andreas Houben

Abstract Plant chromosome microdissection techniques, together with the isolation and amplification methods of microisolated DNA, are described; and a number of applications (e.g., generation of chromosome-specific markers, physical mapping, cloning of chromosome-specific genes) of microisolated chromosomes are discussed.

Keywords DOP-PCR · Microcloning · Library · Micromanipulation · Chromosome painting · FISH · Marker

Abbreviations

BAC	Bacterial artificial chromosomes
DOP-PCR	Degenerate oligonucleotide-primed PCR
LA-PCR	Linker adapter PCR
MDA	Multiple-displacement amplification
rDNA	Ribosomal DNA
YAC	Yeast artificial chromosomes

A. Houben (✉)
Leibniz-Institute of Plant Genetics and Crop Plant Research (IPK), Chromosome Structure and Function Laboratory, Corrensstrasse 3, 06466 Gatersleben, Saxony-Anhalt, Germany
e-mail: houben@ipk-gatersleben.de

H.W. Bass and J.A. Birchler (eds.), *Plant Cytogenetics*, Plant Genetics and Genomics: Crops and Models 4, DOI 10.1007/978-0-387-70869-0_10,

Contents

10.1 Chromosome Recognition and Microdissection Equipment

The isolation of individual chromosomes is probably the most direct approach to obtaining chromosome-specific DNA. Specific chromosomes can be isolated from the rest of the genome by flow sorting, microdissection, or other means. In contrast to flow sorting (reviewed by Dolezel et al. 2004), microdissection allows for the isolation of small chromosome fragments, and the preparation of chromosome specimens suitable for microdissection is relatively simple. The disadvantage of microdissection is that only a small number of chromosomes can be isolated and therefore a DNA amplification step which results in short DNA fragments (less than 1 kb) is necessary. Nonetheless, DNA isolated by either microdissection or flow sorting can be used for genomic research, including the generation of chromosome-specific libraries/markers, physical mapping, and cloning of chromosome-specific expressed sequences/genes.

One method for identification of specific chromosomes for microdissection is to choose karyotypes with chromosomes bearing prominent morphological features – for example, relatively large and distinguishable somatic A chromosomes (Fukui et al. 1992; Pich et al. 1994), reconstructed translocation chromosomes (Macas et al. 1993; Sorokin et al. 1994), telochromosomes (Busch et al. 1995), B chromosomes (Jamilena et al. 1995), or sex chromosomes (Grant et al. 1994). Another is to select genotypes with distinct pairing behavior at meiosis, e.g., monosomic addition lines (Jung et al. 1992). For isolation of defined subchromosome regions of species with relatively small metaphase chromosomes, the more extended pachytene chromosomes can be used (Stein et al. 1998). Successful isolation of DNA from microisolated fragments of Giemsa-banded chromosomes, as demonstrated for humans (Ludecke et al. 1989), has not yet been reported in plants.

In species with a low degree of mitotic cell synchronization, meiotic anther tissue is more favorable for microdissection experiments. Meiotic cell division within and between anthers at the same stage of development is highly synchronized in many species and provides an easily accessible chromosome source.

The smallest size of chromosome fragments that can be obtained is determined by the physical constraints of the dissecting and microscope equipment. Different micromanipulation systems fitted on upright or, more commonly, inverted light

microscopes are commercially available. Three-dimensional hydraulic, pneumatic, or stepping-motor-driven manipulators are suitable for this application. Fine glass needles are commonly used for the mechanical dissection of chromosomes. Alternatively, a laser microbeam has also been successfully used for the dissection of plant chromosomes, e.g., those of barley (*Hordeum vulgare*; Fukui et al. 1992), rye (*Secale cereale*; Houben et al. 1996b), and *Silene* (Hobza et al. 2004; Kejnovsky et al. 2007; Matsunaga et al. 1999). Laser microdissection works because, at high photon density, light can liquefy, evaporate, or break down biological material. Avoiding the use of laser wavelengths close to the absorption maximum of DNA (250 nm) preserves the DNA of laser-dissected chromosome segments. Usually, the movement of the laser beam is controlled manually or semiautomatically (Houben et al. 1996a).

The less costly micromanipulation system, in which a glass microneedle is used as a dissection tool, is sufficient for most chromosome microdissection experiments, however. Vibration must be kept to an absolute minimum during the procedure; the micromanipulation system should therefore be placed on a vibration-free table. The room in which the experiments are being performed should also be free of movement.

10.2 Handling and Amplification of Microdissected Chromosomal DNA

Only minute quantities of chromosomal DNA are available after microdissection. The quality of this DNA depends critically on the pretreatment, e.g., chromosome fixation and staining, which should be performed as carefully as possible. The microdissected DNA must be assumed to be only a partial representation of the chromosome region being investigated. The first successful microcloning of DNA from microdissected plant chromosomes involved the microchemical manipulation and direct cloning of dissected chromosomal DNA into a lambda phage vector (Sandery et al. 1991). For this approach, a very large number of dissected chromosomes were required, but only very few recombinant clones were obtained. The addition of PCR technology to the microcloning procedure has brought a substantial improvement in cloning efficiency. In two different approaches, the microdissected DNA was micromanipulated as usual and then ligated to a modified plasmid vector (Jung et al. 1992) or to specific adaptors/linkers (Grant et al. 1994). The adaptor provided the primer-binding sites necessary for PCR amplification. This technique requires an experienced operator, however, and the microchemical manipulations can be avoided if this method is scaled up and performed as a "single tube" reaction (Albani et al. 1993; Chen and Armstrong 1995). The other method described is called degenerate oligonucleotide-primed PCR (DOP-PCR) and was developed by Telenius et al. (1992). It is very rapid, is less difficult to handle, and involves direct PCR amplification of DNA contained in dissected fragments, with a universal primer composed of a mixture of oligonucleotide sequences that lack absolute complementarity to the target template sequences. The mixture contains multiple degenerated bases. When these primers are used in PCR amplification, and lower

Table 10.1 Examples for the generation of chromosome-specific libraries by chromosome microdissection and cloning

Species	Target	Method	References
Brachyscome (*Brachycome*) *dichromosomatica* C. R. Carter	B chromosome	DOP-PCR	Houben et al. (1997)
Beta patellaris Moq.	Additional chromosome	LA-PCR	Jung et al. (1992)
Hordeum vulgare L.	Chromosome 1Hs	LA-PCR	Schondelmaier et al. (1993)
	Chromosome 7H	LA-PCR	Wang et al. (1998)
	Chromosome 3Hl	LA-PCR	Busch et al. (1995)
Zea mays L.	Chromosome 6s	LA-PCR	Stein et al. (1998)
	B chromosome	DOP-PCR	Cheng and Lin (2003)
Aegilops markgrafii (Greuter) K. Hammer	Additional chromosome B	DOP-PCR	Potz et al. (1996)
Pinus densiflora Sieb. et Zucc.	Centromeric regions	DOP-PCR	Hizume et al. (2001)
Rumex acetosa L.	Sex chromosome	DOP-PCR	Mariotti et al. (2006)
Citrus grandis (L.) Osbeck	Chromosome 1	Linker PCR	Huang et al. (2004)
Glycine max L. Merr.	Unidentified single chromosome	Linker-PCR	Zhou et al. (2001)
Silene latifolia Poir.	Sex chromosome	LA-PCR, DOP-PCR	Grant et al. (1994), Matsunaga et al. (1999), Hobza and Vyskot (2007)
Secale cereale L.	B chromosome	Phage cloning, DOP-PCR	Sandery et al. (1991), Houben et al. (1996b)
	Chromosome 1R	LA-PCR	Zhou et al. (1999)
Triticum aestivum L.	Unidentified chromosome arms	LA-PCR	Hu et al. (2004)
	Chromosome 6B	LA-PCR	Liu et al. (1997)
	Chromosome 5Bl	DOP-PCR	Albani et al. (1993)
Thinopyrum intermedium (Host) Barkworth and D.R. Dewey	Additional chromosome	DOP-PCR	Dong et al. (2002)
Lilium regale Wilson	Single chromosome	LA-PCR	Dang et al. (1998)

LA-PCR Linker adapter PCR; *DOP-PCR* degenerate oligonucleotide-primed PCR

PCR annealing temperatures are selected, complementary sequences that contain significant homologies can be amplified. A DOP-PCR protocol adapted for plants by Pich et al. (1994) has been successfully used for a number of plant species (see Table 10.1).

The efficient generation of probes has also been achieved with OmniPlex TM library technology (Rubiscon Genomics, Ann Arbor), from human (Gribble et al. 2004) and plant (Houben, unpublished) chromosomes. This method involves the random fragmentation of microdissected DNA before application of adaptors at either end of the DNA. Universal primer sites on the adaptors allow amplification of the DNA fragments. The commercial GenomePlex® Single Cell Whole Genome Amplification kit (Sigma-Aldrich) gives satisfactory results with picogram quantities of chromosomal DNA (Note that, throughout, the mention of trademarks does not imply approval to the exclusion of other products that may also be suitable).

Recently, multiple-displacement amplification (MDA) has been employed for successful amplification of small amounts of DNA (Hellani et al. 2004). In MDA, DNA is amplified isothermally by means of phage Φ29 polymerase. The MDA product was found to be an improvement over other PCR-based whole-genome amplification techniques in amplification bias, size, reproducibility, and diagnosis (Hosono et al. 2003). MDA products are large, averaging 70 kb in length. Progress in amplifying very small amounts of DNA has been difficult because of the background synthesis that occurs in the MDA reaction, even without added template, but Zhang et al. (2006) recently established "single cell genomics," after almost complete sequencing of microorganism genomes on the basis of MDA performed on DNA obtained from single cells. In the future, MDA in combination with microdissection could become a tool for overcoming the limited size of DNA clones derived from chromosome microdissection/PCR experiments (Zhou and Hu 2007). Further protocols and references are supplied by practical guides to microdissection/cloning (e.g., Hagag and Viola 1993; Hobza and Vyskot 2007).

The procedures described below for the isolation and PCR amplification of DNA from microisolated chromosomes are reproducible, and no problems will occur if they are performed carefully. If possible, the fixation should be performed in 70% ethanol, which does not affect the quality of the chromosomal DNA. Strict precautions, described below, must also be taken to avoid the PCR amplification of contaminant DNA. So that the quality of the solution can be monitored, a controlled PCR reaction without template DNA should be performed in parallel.

10.3 Use of Microdissected Chromosomes

The main application of microdissection in nonplant cytogenetics is the generation of chromosome-specific, or chromosome-fragment-specific, fluorescence in situ hybridization probes suitable for chromosome painting experiments (Meltzer et al. 1992), but although chromosome painting would also be extremely useful for plant evolutionary studies, it has been problematical in large-genome species, because of their tremendous number of repetitive sequences (Fuchs et al. 1996a). Successful painting of plant chromosomes with DNA obtained from microdissected sex (Hobza et al. 2004; Shibata et al. 1999) or B chromosomes (Houben et al. 1997) was only possible because of the enrichment for chromosome-specific repetitive sequences,

rather than the chromosome-specific low- and single-copy sequences that are responsible for the painting of mammalian chromosomes. No repetitive sequences that uniquely label entire chromosomes are known for plant A chromosomes, however. In plants with relatively small genomes, and with a small proportion of repetitive DNA (e.g., *Sorghum bicolor* (L.) Moench., 2C = 1.6 pg; rice, *Oryza sativa* L., 2C = 1 pg; tomato, *Solanum lycopersicum* L., 2C = 1.72 pg, *Arabidopsis thaliana* (L.) Heynh., 2C = 0.3 pg), genomic DNA fragments cloned in bacterial (BAC) or yeast artificial chromosomes (YAC) have been successfully used as probes to color chromosome regions (e.g., by Fuchs et al. 1996b; Jiang et al. 1995; Lysak et al. 2001). Microdissection of plant chromosomes has been successfully used for the generation of chromosome-specific markers for a number of species (see Table 10.1).

A direct approach to integrating genetic and physical chromosome maps is to hybridize genetically mapped DNA probes to chromosomes in situ. This technique is more difficult in plants than in human chromosomes. Physical localization of specific sequences to microscopically defined chromosome segments can also be attained by microisolation of morphologically distinct chromosomes and the use of their DNA as template for PCR with sequence-specific primers (Macas et al. 1993). Kunzel et al. (2000) used this PCR-mediated technique for integrating translocation breakpoints into barley genetic maps. Microisolated translocation chromosomes for PCR with primers derived from genetically mapped RFLP probes were used to integrate the regions of 240 translocation breakpoints as physical landmarks into linkage maps of the seven barley chromosomes, with an accuracy comparable to that of the deletion-based ladder maps of wheat (Gill et al. 1996).

Chromosome microdissection in combination with PCR has been also used for evolutionary studies on retroelements of sex chromosomes in *Silene latifolia* (Kejnovsky et al. 2007), for ribosomal DNA (rDNA) of the A chromosomes of *Allium cepa* L. and *A. schoenoprasum* L. (Shibata and Hizume 2002), and for B chromosomes of *Brachyscome dichromosomatica* (Donald et al. 1997; Marschner et al. 2007) and *Crepis capillaris* (Leach et al. 2005). Genes-encoding rRNA are the most evolutionarily conserved genomic sequences, whereas the transcribed and untranscribed spacers show high levels of sequence variation and have consequently been used extensively in studies of close phylogenetic groups.

When a chromosome is microdissected, the DNA recovered from the microdissected fragment will include, to some degree, a representation of the transcribed regions present in the original chromosome. This observation has stimulated the development of strategies for isolating genes by chromosome microdissection (Meltzer et al. 1997). The isolation of plant chromosome-specific genes/expressed sequence tags by microdissection was undertaken by Delichère et al. (1999), Hernould et al. (1997), and Zhou et al. (2008), who used it for the isolation of chromosome-specific transcripts. For isolation of genes involved in restoring male fertility in alloplasmic male-sterile tobacco, chromosomes carrying these genes were microdissected and their DNA DOP-PCR amplified and cloned (Hernould et al. 1997). Coding sequences were selected by differential hybridization of the resulting chromosome-specific plasmid library with labeled cDNA derived from floral buds of the cytoplasmic male-sterile and restored lines.

For the successful isolation of an active Y-linked gene of *S. latifolia,* DOP-PCR-amplified Y-chromosome DNA was used as a probe to screen a male flower-bud cDNA library (Delichère et al. 1999).

10.4 Materials and Methods

10.4.1 Materials

Glass petri dishes for seed germination on filter paper
Chemical glassware
Coverslips, 24×60 mm, 22×22 mm
Microscope slides
Borosilicate capillary tubes with 1 mm outer diameter and 0.65 mm inner diameter (e.g., Hilgenberg, BRD)

10.4.2 Equipment

Inverted microscope, with phase-contrast objectives
Micromanipulator, e.g., model ECET 5170 (Eppendorf)
Needle puller, e.g., model Livingstone (Bachhofer)
Microforge, e.g., model MF-9 (Nurashige)
PCR machine
Centrifuge, bench top
Adjustable-volume pipettes

10.4.3 Solutions

1. Root-tip enzyme solution: Dissolve in 1 mL buffer (75 mM KCl, 7.5 mM EDTA, pH 4.0) 25 mg pectolyase Y-23 and 25 mg cellulase "Onozuka R-10." Store at −20°C in 0.05 mL aliquots.
2. 3:1 Fixative: Mix 3 volumes of 96% ethanol with 1 volume of glacial acetic acid. Prepare the fixative just before use.
3. Water-saturated paraffin oil: Mix 5 volumes of paraffin oil (Merck, Cat. No. 7161) with 1 volume of distilled, sterile water. Prepare the solution at least 1 day in advance.
4. Chromosome-collection-drop solution: Dissolve 0.5 mg DNA-free proteinase K (PCR grade, Roche Cat No. 85025022) in 1 mL buffer (10 mM Tris–HCl, 10 mM NaCl, 0.1% sodium dodecyl sulfate). Store at −20°C in 0.05-mL aliquots.
5. DOP-PCR kit: Ready-to-use reaction (Roche Cat. No. 11644963001).

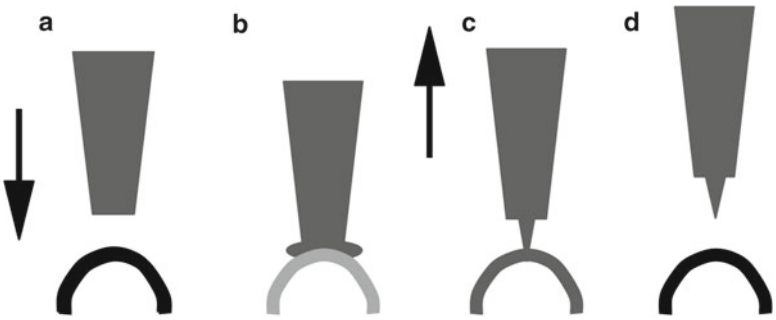

Fig. 10.1 Microneedle preparation by microforge. (**a**) Lower glass capillary until tip (~1 mm) rests on the platinum wire. (**b**) Heat platinum wire so that the glass tip becomes molten. (**c**) Decrease heat. Raise needle, forge a short, fine, closed needle tip (**d**) of less than 3 μm, depending on the size of chromosomes to be microdissected

10.4.4 Procedures

10.4.4.1 Preparation of Microdissection Needles

Pull a borosilicate capillary tube with a needle puller to obtain a microdissection needle with a tip diameter of less than 0.2 mm. Alternatively, pull capillaries manually over a gas burner. Depending on the size of the target chromosome region, prepare the needle tip with a microforge, according to Fig. 10.1. The tip of the finished needle must be closed.

10.4.4.2 Preventive Measures Against DNA Contamination of PCR

Strict precautions must be taken against contaminant DNA, which could be PCR-amplified. Prepare all solutions and glass- and plasticware under sterile conditions, and if possible, keep the micromanipulation system used for the isolation of chromosomes in a sterile hood. Irradiate plastic and glassware, buffers, and stock solutions (except nucleotides, primers, and enzymes) with UV light (260 nm wavelength) for 12 h. To remove UV-light-induced radicals, keep the treated material for several days before use.

10.4.4.3 Preparation of Chromosomes for Microdissection

Preparation of Mitotic Chromosomes

1. Fix root tips for less than 20 min in 45% acetic acid. The fixation period should be as short as possible, because acetic acid damages DNA by depurination; longer exposure can result in relatively short (50–100 bp long) chromosomal DNA fragments.
2. Remove the fixative by several washes in 70% ethanol, and store the tissue in 70% ethanol at 4°C for up to several months.

3. Wash the root tips in several changes of deionized H_2O, and macerate the meristems in root-tip enzyme solution at 37°C for up to 30 min.
4. Carefully wash the root tips in several changes of deionized H_2O.
5. Squash the macerated meristems between two different-sized sterile coverslips in a drop of 45% acetic acid; use the larger coverslip (24×60 mm) as the base and the smaller (22×22 mm) as the cover. A microscope slide should be used as a carrier to stabilize the coverslips.
6. Examine the preparation under a phase-contrast microscope.
7. Transfer the coverslips to dry ice or liquid nitrogen and separate them.
8. Air dry and dehydrate the larger coverslip in a series of 70 and 100% (v/v) ethanol.

Preparation of Meiotic Chromosomes

1. Squash unfixed anthers at metaphase I in a drop of 45% acetic acid between two coverslips.
2. Proceed as described above for mitotic chromosomes.

Chromosome preparations can be maintained for several months in 70% ethanol at −20°C or in 100% glycerol at 4°C. Before microdissection, chromosome preparations stored in glycerol must be washed in several changes of deionized H_2O.

10.4.4.4 Chromosome Microdissection Procedure

If a phase-contrast microscope is not available, stain the chromosomes briefly with 0.05% methylene blue, rinse coverslips in water, and air dry them.

1. Place a 1-μL collection drop on a sterile siliconized coverslip. To avoid evaporation, introduce the collection drop into a small volume of water-saturated paraffin oil.
2. Secure the coverslip bearing the chromosomes, spread side up, next to the sterile siliconized coverslip carrying the collection drop in the coverslip-holding petri dish under the microscope (see Fig. 10.2).
3. Alternatively, transfer microisolated chromosomes directly into PCR tubes.
4. Position the dissection needle approximately above the target chromosome, such that the needle is visible but not in focus.
5. Move the dissection needle to within a few micrometers of the chromosome. Use a high-magnification lens (40×, 63×, or 100×).
6. Perform microdissection by moving the needle tip across the chromosome or chromosome region (Fig. 10.3).
7. Transfer the isolated chromosome into the collection drop. After a sufficient number of chromosome fragments are collected, transfer the collection drop, together with the surrounding paraffin oil, into a PCR tube.

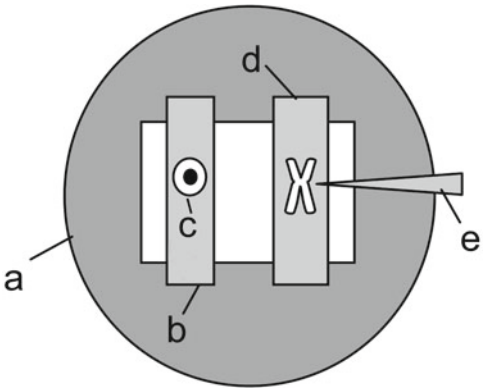

Fig. 10.2 Microdissection setup. (**a**) Microscope stage. (**b**) Siliconized carrier coverslip. (**c**) Collection drop with paraffin oil overlay. (**d**) Specimen coverslip. (**e**) Microneedle

The precision of the dissection is limited by the degree of magnification and the tip size of the dissection needle. Only isolate chromosomes when the one of interest is located at the periphery of the metaphase spread and separated sufficiently from other chromosomes. The time required to dissect a specific chromosome depends on the quality and number of chromosome spreads on the coverslip.

10.4.4.5 PCR Amplification of Microdissected Chromosomal DNA by DOP-PCR

Proteinase K Treatment

After a 3-h incubation at 55°C, inactivate proteinase K by exposing the sample to 90°C for 10 min.

DOP-PCR

1. Add the PCR components to the PCR tube containing the 1-μL collection drop. The components are 0.7 μM degenerate primer (5′-CCGACTCGAGNNN-NNNATGTGG-3′, Telenius et al. 1992), 0.2 mM dNTPs, 2.5 mM $MgCl_2$, 1× *Taq* DNA Polymerase buffer. Adjust the sample volume, with water, to yield a total reaction volume of 49 μL.
2. Alternatively, use a ready-to-use DOP-PCR kit (Roche Cat. No. 11644963001).
3. Perform PCR amplification according to the following steps:

   (a) Denature the DNA template at 94°C for 5 min, cool it to 85°C for 2 min, and add 1 μL (2.5 U) *Taq* polymerase.
   (b) Run five cycles at 94°C for 1 min, 30°C for 1.5 min, and 72°C for 3 min with a transition time of 3 min to 72°C.
   (c) Subsequently run 30 cycles at 94°C for 1 min, 55°C for 1 min, 72°C for 1.5 min, with an autoextension step of 1 s/cycle and a final extension at 72°C for 10 min.

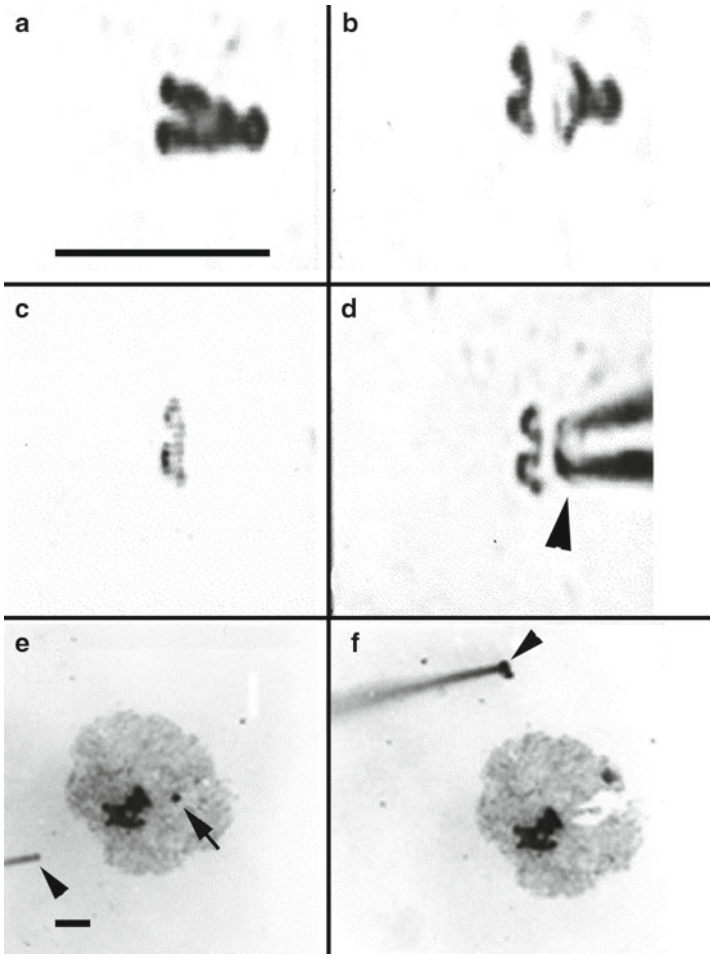

Fig. 10.3 Microdissection of mitotic and meiotic chromosomes. (**a**–**d**) Laser microdissection of the subterminal region of the mitotic rye B chromosome. (**a**) Before, (**b**) during, and (**c**) after the ablation of the remaining portion of the B chromosome by the UV-microlaser beam and (**d**) the isolation of the remaining segment with a microneedle (*arrowhead*). (**e**, **f**) Microdissection of a meiotic rye B chromosome at first metaphase with a glass microneedle. (**e**) Before (the unpaired B chromosome is indicated by an *arrow*, the needle by an *arrowhead*) and (**f**) after microdissection. The isolated chromosome sits on the tip of the needle (*arrowhead*). Size *bars* in (**a**) and (**e**) represent 10 μm

4. Analyze 15 μL of the amplified DNA by agarose gel electrophoresis to check for PCR success. If necessary, perform a second round of PCR using 5 μL of the first product as described above, without the PCR section (b).
5. Purify the PCR product.

References

Albani D, Cote MJ, Armstrong KC, Chen QF, Segal A, Robert LS (1993) PCR amplification of microdissected wheat chromosome arms in a simple single tube reaction. *Plant J* 4:899–903

Busch W, Martin R, Herrmann RG, Hohmann U (1995) Repeated DNA sequences isolated by microdissection. I. Karyotyping of barley (*Hordeum vulgare* L.). *Genome* 38:1082–1090

Chen QF, Armstrong K (1995) Characterization of a library from single microdissected oat (*Avena sativa* L.) chromosome. *Genome* 38:706–714

Cheng YM, Lin BY (2003) Cloning and characterization of maize B chromosome sequences derived from microdissection. *Genetics* 164:299–310

Dang BY, Hu ZM, Zhou YH, Cui LH, Wang LL, Li LC, Chen ZH (1998) Construction of single-chromosome DNA library from *Lilium regale* Wilson. *Chin Sci Bull* 43:434–439

Delichère C, Veuskens J, Hernould M, Barbacar N, Mouras A, Negrutiu I, Monéger F (1999) SIY1, the first active gene cloned from a plant Y chromosome, encodes a WD-repeat protein. *EMBO J* 18:4169–4179

Dolezel J, Kubalakova M, Bartos J, Macas J (2004) Flow cytogenetics and plant genome mapping. *Chromosome Res* 12:77–91

Donald TM, Houben A, Leach CR, Timmis JN (1997) Ribosomal RNA genes specific to the B chromosomes in *Brachycome dichromosomatica* are not transcribed in leaf tissue. *Genome* 40:674–681

Dong YZ, Liu ZL, Liu B, Bu XL, He MY, Huang BQ, Hao S (2002) Microdissection of individual chromosomes of *Thinopyrum intermedium* and isolation of molecular markers that are useful in detecting *Th. intermedium* chromatin introgressed into wheat. *Cereal Res Commun* 30:253–260

Fuchs J, Houben A, Brandes A, Schubert I (1996a) Chromosome "painting" in plants – a feasible technique? *Chromosoma* 104:315–320

Fuchs J, Kloos DU, Ganal MW, Schubert I (1996b) In situ localization of yeast artificial chromosome sequences on tomato and potato metaphase chromosomes. *Chromosome Res* 4:277–281

Fukui K, Minezawa M, Kamisugi Y, Ishikawa M, Ohmido N, Yanagisawa T, Fujishita M, Sakai F (1992) Microdissection of plant chromosomes by argon-ion laser beam. *Theor Appl Genet* 84:787–791

Gill KS, Gill BS, Endo TR, Boyko EV (1996) Identification and high-density mapping of gene-rich regions in chromosome group 5 of wheat. *Genetics* 143:1001–1012

Grant S, Houben A, Vyskot B, Siroky J, Pan WH, Macas J, Saedler H (1994) Genetics of sex determination in flowering plants. *Dev Genet* 15:214–230

Gribble S, Ng BL, Prigmore E, Burford DC, Carter NP (2004) Chromosome paints from single copies of chromosomes. *Chromosome Res* 12:143–151

Hagag NG, Viola MV (1993) *Chromosome Microdissection and Cloning: A Practical Guide.* Academic Press, San Diego

Hellani A, Coskun S, Benkhalifa M, Tbakhi A, Sakati N, Al-Odaib A, Ozand P (2004) Multiple displacement amplification on single cell and possible PGD applications. *Mol Hum Reprod* 10:847–852

Hernould M, Glimelius K, Veuskens J, Bergman P, Mouras A (1997) Microdissection and amplification of coding sequences from a chromosome fragment restoring male fertility in alloplasmic male-sterile tobacco. *Plant J* 12:703–709

Hizume M, Shibata F, Maruyama Y, Kondo T (2001) Cloning of DNA sequences localized on proximal fluorescent chromosome bands by microdissection in *Pinus densiflora* Sieb. & Zucc. *Chromosoma* 110:345–351

Hobza R, Vyskot B (2007) Laser micro dissection-based analysis of plant sex chromosomes. *Laser Manip Cells Tissues* 82:433–453

Hobza R, Lengerova M, Cernohorska H, Rubes J, Vyskot B (2004) FAST-FISH with laser beam microdissected DOP-PCR probe distinguishes the sex chromosomes of *Silene latifolia. Chromosome Res* 12:245–250

Hosono S, Faruqi AF, Dean FB, Du Y, Sun Z, Wu X, Du J, Kingsmore SF, Egholm M, Lasken RS (2003) Unbiased whole-genome amplification directly from clinical samples. *Genome Res* 13:954–964

Houben A, Franke J, Leclerc N, Ahne R (1996a) Computer-assisted system combining image analysis and chromosome dissection. *Microsc Res Tech* 34:474–477

Houben A, Kynast RG, Heim U, Hermann H, Jones RN, Forster JW (1996b) Molecular cytogenetic characterisation of the terminal heterochromatic segment of the B-chromosome of rye (*Secale cereale*). *Chromosoma* 105:97–103

Houben A, Leach CR, Verlin D, Rofe R, Timmis JN (1997) A repetitive DNA sequence common to the different B chromosomes of the genus *Brachycome. Chromosoma* 106:513–519

Hu ZM, Wang H, Shi R, Dang BY, Hu J, Yin WB, Chen YH, Jung SM, Chen ZH (2004) Microdissection and construction of region-specific DNA libraries of wheat chromosome 6B. *Acta Bot Sin* 46:1357–1365

Huang D, Wu W, Zhou Y, Hu Z, Lu L (2004) Microdissection and molecular manipulation of single chromosomes in woody fruit trees with small chromosomes using pomelo (*Citrus grandis*) as a model. I. Construction of single chromosomal DNA libraries. *Theor Appl Genet* 108:1366–1370

Jamilena M, Garrido-Ramos M, Ruiz Rejón M, Ruiz Rejón C, Parker JS (1995) Characterisation of repeated sequences from microdissected B chromosomes of *Crepis capillaris. Chromosoma* 104:113–120

Jiang JM, Gill BS, Wang GL, Ronald PC, Ward DC (1995) Metaphase and interphase fluorescence in situ hybridization mapping of the rice genome with bacterial artificial chromosomes. *Proc NatlAcad Sci USA* 92:4487–4491

Jung C, Claussen U, Horsthemke B, Fischer F, Herrmann RG (1992) A DNA library from an individual *Beta patellaris* chromosome conferring nematode resistance obtained by microdissection of meiotic metaphase chromosomes. *Plant Mol Biol* 20:503–511

Kejnovsky E, Hobza R, Kubat Z, Widmer A, Marais GAB, Vyskot B (2007) High intrachromosomal similarity of retrotransposon long terminal repeats: evidence for homogenization by gene conversion on plant sex chromosomes? *Gene* 390:92–97

Kunzel G, Korzun L, Meister A (2000) Cytologically integrated physical restriction fragment length polymorphism maps for the barley genome based on translocation breakpoints. *Genetics* 154:397–412

Leach CR, Houben A, Field B, Pistrick K, Demidov D, Timmis JN (2005) Molecular evidence for transcription of genes on a B chromosome in *Crepis capillaris. Genetics* 171:269–278

Liu B, Segal G, Vega JM, Feldman M, Abbo S (1997) Isolation and characterization of chromosome-specific DNA sequences from a chromosome arm genomic library of common wheat. *Plant J* 11:959–965

Ludecke HJ, Senger G, Claussen U, Horsthemke B (1989) Cloning defined regions of the human genome by microdissection of banded chromosomes and enzymatic amplification. *Nature* 338:348–350

Lysak MA, Fransz PF, Ali HBM, Schubert I (2001) Chromosome painting in *Arabidopsis thaliana. Plant J* 28:689–697

Macas J, Weschke W, Bumlein H, Pich U, Houben A, Wobus U, Schubert I (1993) Localization of vicilin genes via polymerase chain reaction on microisolated field bean chromosomes. *Plant J* 3:883–886

Mariotti B, Navajas-Perez R, Lozano R, Parker JS, de la Herran R, Ruiz Rejón C, Ruiz Rejón M, Garrido-Ramos M, Jamilena M (2006) Cloning and characterization of dispersed repetitive DNA derived from microdissected sex chromosomes of *Rumex acetosa. Genome* 49:114–121

Marschner S, Meister A, Blattner FR, Houben A (2007) Evolution and function of B chromosome 45S rDNA sequences in *Brachycome dichromosomatica. Genome* 50:638–644

Matsunaga S, Kawano S, Michimoto T, Higashiyama T, Nakao S, Sakai A, Kuroiwa T (1999) Semi-automatic laser beam microdissection of the Y chromosome and analysis of Y chromosome DNA in a dioecious plant, *Silene latifolia. Plant Cell Physiol* 40:60–68

Meltzer PS, Guan XY, Burgess A, Trent JM (1992) Rapid generation of region specific probes by chromosome microdissection and their application. *Nat Genet* 1:24–28

Meltzer PS, Guan XY, Su YA, Gracia E, Trent JM (1997) Identification of region specific genes by chromosome microdissection. *Cancer Genet Cytogenet* 93:29–32

Pich U, Houben A, Fuchs J, Meister A, Schubert I (1994) Utility of DNA amplified by degenerate oligonucleotide-primed PCR (DOP-PCR) from the total genome and defined chromosomal regions of field bean. *Mol Gen Genet* 243:173–177

Potz H, Schubert V, Houben A, Schubert I, Weber WE (1996) Aneuploids as a key for new molecular cloning strategies: development of DNA markers by microdissection using *Triticum aestivum–Aegilops markgrafii* chromosome addition line B. *Euphytica* 89:41–47

Sandery MJ, Forster JW, Macadam SR, Blunden R, Jones RN, Brown DM (1991) Isolation of a sequence common to A- and B-chromosomes of rye (*Secale cereale*) by microcloning. *Plant Mol Biol Rep* 9:21–30

Schondelmaier J, Martin R, Jahoor A, Houben A, Graner A, Koop HU, Herrmann RG, Jung C (1993) Microdissection and microcloning of the barley (*Hordeum vulgare* L.) chromosome 1Hs. *Theor Appl Genet* 86:629–636

Shibata F, Hizume M (2002) Evolution of 5S rDNA units and their chromosomal localization in *Allium cepa* and *Allium schoenoprasum* revealed by microdissection and FISH. *Theor Appl Genet* 105:167–172

Shibata F, Hizume M, Kuroki Y (1999) Chromosome painting of Y chromosomes and isolation of a Y chromosome-specific repetitive sequence in the dioecious plant *Rumex acetosa. Chromosoma* 108:266–270

Sorokin A, Marthe F, Houben A, Pich U, Graner A, Kunzel G (1994) Polymerase chain reaction mediated localization of RFLP clones to microisolated translocation chromosomes of barley. *Genome* 37:550–555

Stein N, Ponelies N, Musket T, McMullen M, Weber G (1998) Chromosome micro-dissection and region-specific libraries from pachytene chromosomes of maize (*Zea mays* L.). *Plant J* 13:281–289

Telenius H, Carter NP, Bebb CE, Nordenskjold M, Ponder BAJ, Tunnacliffe A. (1992) Degenerate oligonucleotide-primed PCR – general amplification of target DNA by a single degenerate primer. *Genomics* 13:718–725

Wang H, Zhou YH, Dang BY, Hu ZM, Wang LL, Li LC, Chen ZH (1998) Chromosome microdissection by laser microbeam, chromosomal fragment isolation and amplification in vitro in barley (*Hordeum vulgare* L.). *Chin Sci Bull* 43:851–855

Zhang K, Martiny AC, Reppas NB, Barry KW, Malek J, Chisholm SW, Church GM (2006) Sequencing genomes from single cells by polymerase cloning. *Nat Biotechnol* 24:680–686

Zhou RN, Hu ZM (2007) The development of chromosome microdissection and microcloning technique and its applications in genomic research. *Curr Genomics* 8:67–72

Zhou RN, Shi R, Jiang SM, Yin WB, Wang HH, Chen YH, Hu J, Wang RR, Zhang XQ, Hu ZM (2008) Rapid EST isolation from chromosome 1R of rye. *BMC Plant Biol* 8:28

Zhou YH, Hu ZM, Dang BY, Wang HA, Deng XD, Wang LL, Chen ZH (1999) Microdissection and microcloning of rye (*Secale cereale* L.) chromosome 1R. *Chromosoma* 108:250–255

Zhou YH, Dang BY, Wang H, Hu ZM, Wang LL, Chen ZH (2001) Microdissection of a single chromosome and construction of the microclone library from soybean. *Euphytica* 121:129–135

Chapter 11
Maize Antibody Procedures: Immunolocalization and Chromatin Immunoprecipitation

X. Li, C.N. Topp, and R.K. Dawe

Abstract Antibodies are powerful tools for studying protein localization and function. Here we describe methods for two of the more challenging applications: immunolocalization and chromatin immunoprecipitation (ChIP). Immunolocalization can be carried out on nearly any maize tissue, but we focus here on localizing proteins to male meiocytes, which are large cells with relatively porous cell walls that make them ideal for this purpose. ChIP is a biochemical technique for identifying DNA sequences that interact with chromatin proteins such as histones. We describe a thoroughly tested method for native ChIP (useful for histones) and one method for crosslinking ChIP, which can be used for proteins that bind to the surface of DNA.

Keywords Maize · Meiosis · Mitosis · Centromeric histone H3 · Kinetochore · Spindle · Immunolocalization · Chromatin immunoprecipitation · Nucleosome

Abbreviations

ChIP	Chromatin immunoprecipitation
LN_2	Liquid nitrogen
ME	2-Mercaptoethanol
nChIP	Native ChIP
PAS	Protein A sepharose
PBS	Phosphate-buffered saline
PI	Protease inhibitor tablet
PMSF	Phenylmethanesulphonylfluoride
SDS	Sodium dodecyl sulfate
xChIP	Crosslinking ChIP

X. Li • C.N. Topp • R.K. Dawe (✉)
Department of Plant Biology, University of Georgia, Athens, GA 30602, USA
e-mail: kelly@plantbio.uga.edu

H.W. Bass and J.A. Birchler (eds.), *Plant Cytogenetics*, Plant Genetics and Genomics: Crops and Models 4, DOI 10.1007/978-0-387-70869-0_11,

Contents

The era of maize functional genomics is approaching with the recent release and annotation of the genome sequence by the Maize Genome Sequencing Project. As we move to characterizing gene products and their functions, protein localization will play a large role. Characterization can be done very generally, by identification of the tissues in which a protein is found, specifically by demonstration of where a protein is found within the cell, or in a very detailed way by identification of the molecules and substructures a protein interacts with. Here we will focus on the latter two approaches by describing immunolocalization and chromatin immunoprecipitation (ChIP).

Protein labeling is usually carried out with fluorescent tags. A fusion tag can be added to the coding sequence (for example, green fluorescent protein derivatives), or the protein can be labeled with antibodies (a process called immunolocalization). A drawback of using fusion proteins in maize is that fusion tags require transforming the plant, which is labor-intensive. Consequently, few fusion-tag lines are available for maize. In contrast, antibodies can be prepared faster (for about the same cost) and are often viewed as superior because immunolocalization does not involve changing the sequence of the protein under study. The development of standard protocols for raising antibodies in a variety of animals also makes this an appealing method.

In many cases, localizing a protein precisely is important. A variety of protocols are available that make use of antibodies – often the same antibodies used in immunolocalization. Among these is ChIP, a biochemical method for partially purifying and characterizing chromatin–DNA complexes. The use of ChIP in various forms has revealed precise molecular interactions in a wide array of species. ChIP has been used to identify regions of the genome associated with transcription, with epigenetic switching, and with centromeres. In maize, these studies are in their infancy, but reliable methods are now available for identifying the regions associated with particular histone modifications (native ChIP, nChIP) as well as for identifying loci that interact with nonhistone chromatin proteins (crosslinked ChIP, xChIP). Both ChIP methods will be reviewed here, after a description of our methods for preparing and analyzing maize chromosomes by immunolocalization.

11.1 Immunofluorescence with Maize Male Meiotic Cells

Maize is renowned for its use in chromosome studies. The basic methods for preparing and identifying chromosomes have therefore been extensively reviewed, including current methods for fluorescent in situ hybridization (Kato et al. 2006), but immunolocalization methods have not been summarized in detail.

The tassel is the male inflorescence. It has long lower branches and shorter upper branches that carry spikelets (flowers). Each spikelet contains a primary and a secondary floret, and each floret contains three anthers. Within each anther are hundreds of meiocytes that go through meiosis in synchrony with each other. Because of the gradient of maturation along the tassel, nearly every stage of meiosis is available over a 2- to 3-day period. These attributes of maize – separation of male and female flowers, large accessible inflorescences, numerous meiocytes, and large chromosomes – make it an ideal species for chromosome studies.

In the basic method for meiotic immunolocalization (Dawe et al. 1999; Hiatt et al. 2002; Shi and Dawe 2006), tassels are pulled from the plant and the anthers dissected into dishes. Anthers are then fixed in formaldehyde and the meiocytes extruded onto coverslips. Once on coverslips, the cells are incubated with the antibodies of choice. Generally, two antigenic sera produced in different animals are used simultaneously; one serves as an internal control.

1. Harvest tassels. Identify plants with about eight fully developed leaf sheaths and locate the thickened stem that indicates tassel growth. Hold the maize stem in one hand and incise gently along the flat side of the stem with a gardening knife. Pull out several branches and wrap them with wet paper towels. The remaining portion of the tassel can be pushed back into the plant and will usually mature normally. The upper branches of the tassel flower earlier than lower branches, so good meiotic cells may be available on lower tassel branches if the upper branches are too old. If the primary florets are too old, the smaller secondary florets can be used, but they often lack synchrony or produce poor specimens.
2. Dissect out the anthers. Add 2 mL 1× buffer A to a cell-culture dish (35 × 10 mm, Corning) and place it under a dissecting microscope. Remove a floret from the middle of a tassel and put it in the buffer A. Hold the floret base and cut the floret open longitudinally with #55 forceps to release the anthers. The anthers will float in the dish. Discard the glumes and other leafy tissue.
3. Stage the anthers. Check the fresh anthers to make sure all stages of meiosis are represented on the tassel that was harvested. Hold one end of an anther, cut off the other end with a scalpel, and extrude the enclosed cells gently with the side of the blade. The tetrads come out in fours, whereas spores, which are too old, fall out singly (you will need a high-powered dissecting microscope to tell these apart). Note the size of the anthers that contain tetrads and where they were on the tassel. Now continue collecting fresh anthers in the dish. Start at tetrad-containing florets and move down, taking every floret until the anthers become very small (~1.0 mm). Dissect about 50 anthers per dish.
4. Fix the anthers. Remove buffer A with a transfer pipet and fix the anthers with buffer B for 2–3 h with gentle shaking at room temperature. The fixative must penetrate several layers of outer tissue before the meiocytes are fixed. Reducing the time will reduce the number of usable cells.

Table 11.1 Appearance of meiocytes extruded from anthers after being fixed in formaldehyde

Stage of meiosis	Appearance of extruded cells under dissecting microscope
Premeiosis	Cells difficult to extrude
Leptotene–early pachytene	Cells in tight column
Late pachytene	Cells in loose column
Diakinesis	Large single cells that tend to dissociate, and each cell seems to have a "hole" in the middle
Telophase I–prophase II	A faint line appears to run down the middle of each cell
Metaphase II–telophase II	Half-moon-shaped cells next to each other
End of meiosis	Four cells, usually stuck together
Spores/pollen grains	Single, shiny cells; often confused with diakinesis!

5. Rinse the fixed anthers in phosphate-buffered saline (PBS) 3 times, 5 min each, at room temperature. At this point, the process can be halted. Fixed anthers/cells remain usable for up to 2 weeks in PBS at 4°C, but freshly fixed cells always produce better labeling than old ones.
6. Extrude cells from the fixed anthers in PBS under the dissecting microscope. The stage of meiosis can be accurately determined from their appearance under a dissecting microscope (Table 11.1).
7. Spin onto coverslips. Transfer ~40 μL of solution containing meiotic cells onto a poly-L-lysine-coated coverslip (not the slide; microscopes are optimized to focus just below the coverslip). Spin the coverslips at 100×*g* in a swinging-bucket centrifuge for 1 min. A rubber stopper is a good surface on which to set the coverslips. To prepare poly-L-lysine coverslips, coat them with poly-L-lysine (1 mg/mL in water) with a Q-tip and let them dry at room temperature.
8. Block the cells with 100 μL animal serum (1:50 dilution in PBS) in blocking buffer for 90 min at room temperature. Choose the serum on the basis of the animal in which the primary antibody was prepared. For example, if the primary antibody was made in rabbit, use rabbit serum for blocking.
9. Incubate with primary antibodies. Apply 75–100 μL primary antibody dilution (in blocking buffer) and put the coverslips in a moist chamber at room temperature for 6–12 h. The usable dilutions of antibodies vary widely with quality of the antibody, maize line, and user. Begin with a 1:50 dilution and use the lowest amount of antibody you can (1:500 is usually the limit). A high background is the reason for many failures, and background goes up as more antibodies are applied. Some antibodies work well for meiotic cells, but not for mitotic cells; some work well for western blots but not for cells; and some work for cells, but not for ChIP.
10. Rinse the cells in PBS 3 times, 5 min each, at room temperature.
11. Incubate with secondary antibodies conjugated to the fluorescent or alternative tag of your choice. Apply 100 μL secondary antibody dilution in PBS or blocking buffer. Generally, a 1:200 dilution will work well, but as much as 1:50 may be necessary. Incubate in a moist chamber at room temperature, in the dark, for ~2–3 h or as determined empirically.
12. Rinse the cells in PBS 3 times, 5 min each, at room temperature.
13. Mound the coverslip with 8 μL Vectashield with DAPI (Vector Laboratories).

14. Seal the slides. Absorb extra Vectashield with bibulous paper by gently pushing down, then seal the coverslip edges with nail polish. Dry the nail polish in the dark and store the slides at 4°C. Slides will usually retain their staining for 3–6 months, but the quality will decline over time.

Buffers:

Buffer A: 80 mM KCl, 20 mM NaCl, 2 mM EDTA, 0.5 mM EGTA, 15 mM PIPES buffer, pH 7.0.

Buffer B: 1 mL 1× buffer A, 0.5 mL 2× buffer A, 0.5 mL paraformaldehyde, 20 μL 10% Triton X-100 solution.

PBS: 53.6 mM KCl, 274 mM NaCl, 29.4 mM KH_2PO_4, 17.5 mM Na_2HPO_4, pH 7.2.

Blocking buffer: 3% BSA, 0.02% sodium azide in PBS.

11.2 Chromatin Immunoprecipitation Procedures

Chromatin immunoprecipitation is a powerful technique designed for partial purification of chromatin fragments associated with a known chromatin protein or modification. It falls into two types: native ChIP and crosslinked ChIP. Antibodies against a protein within the nucleosome itself can be used on native, unfixed chromatin (Zhong et al. 2002), because nucleosomes are very stable. In contrast, proteins on the "outside" of the nucleosome are generally associated by weaker interactions that must be stabilized by physical crosslinking (Gendrel et al. 2005). Crosslinked ChIP can also be used to purify proteins within nucleosomes, although native ChIP is the simpler procedure. Histone antibodies are used here as examples, but recent experiments have shown that antibodies to maize transcription factors can also be used in ChIP (Hernandez et al. 2007). Hundreds of antihistone antibodies are available from sources such as Upstate and Abcam. A summary of antibodies known to identify maize histones is given by Shi and Dawe (2006), although only a subset of these are likely to work well in ChIP applications.

11.2.1 Native Chromatin Immunoprecipitation

11.2.1.1 Preparation of Chromatin

Be certain to read the "Notes" section before performing this protocol for the first time.

1. Grind rapidly growing young maize tissue to a fine powder in liquid nitrogen (LN_2) using a prechilled mortar and pestle. Do not allow tissue to thaw (see Notes 1 and 2).
2. Scrape ground tissue into four volumes of cold grinding buffer with a cold metal spatula and mix until no tissue clusters are visible; then incubate on ice for 10 min (see Note 3).

3. Remove debris by filtering through miracloth (Calbiochem). Repeat (see Note 4).
4. Pellet nuclei at 3,000×*g* for 30 min at 4°C.

   Hints: Inspect the pellet – a white layer should appear at the very bottom, occasionally with a thin black line in the middle; these fractions are the desired intact nuclei. If the tissue is from ears or root tips, this layer may be surrounded by yellow-brown mucosal material: starch and other debris, most of which should be gently scraped off with a glass Pasteur pipet. If the tissue is from seedlings, the pellet will be surrounded by a loose layer of dark green material (chlorophyll and other debris), which will be removed in step 6.

5. Resuspend the pellet in a volume of wash buffer 1 equal to that used in step 2, and spin at 10,000×*g* for 15 min at 4°C (see Note 5).

   Hints: Gently pipet to resuspend the pellet. Avoid foaming – excess air in contact with chromatin will denature it. This is a convenient time to prepare a 1% agarose gel in preparation for step 10.

6. Wash the pellet with wash buffer 2, leaving the white pellet intact. Repeat until the debris surrounding the white pellet is removed.
7. Resuspend the pellet in 1 mL digestion buffer, and take A_{260} on a spectrophotometer. Extra chromatin can be kept at −20 or −80°C for future use.
8. Dilute chromatin to 2.5 μg/μL with digestion buffer and save 10 μL as your "undigested chromatin" sample for gel analysis in step 10 (see Note 6).
9. Add 10 U DNase I or 50 U micrococcal nuclease (MNase) to 1 mL chromatin solution [2.5 μg/μL] and incubate for 10 min in a 37°C water bath (see Note 7).
10. Put the sample on ice to arrest the digestion. Run 5 μL of undigested sample, 5 μL of digested sample, and a 1-kb marker on a 1% agarose gel at low power (2–3 V/cm) for 30–45 min. A smear of EtBr stain between 150 and 1,200 bp (fragments roughly 1–8 nucleosomes long) is a common range to use as ChIP input. Larger fragments generally result in high background and poor-quality immunoprecipitation. Continue the digestion until the desired size range is achieved (see Note 8).

    Hint: This is a good time to wash the protein A sepharose beads used in step 16 and step 2, Sect. 11.2.1.2 (see Note 9).

11. Halt the reaction completely by adding 1/100 volume of 0.5 M EDTA.
12. Centrifuge at 11,600×*g* for 10 min at 4°C and save the supernatant containing soluble chromatin fragments in a fresh tube.
13. Resuspend the pellet with 1 mL lysis buffer and incubate on ice for 10 min. This step solubilizes remaining insoluble chromatin.
14. Centrifuge at 11,600×*g* for 10 min at 4°C and combine the supernatant with the supernatant from step 12. If you are processing the same tissue in several tubes, combine them before preclearing in step 16.
15. Measure the combined supernatants and add 1.25 volume of incubation buffer to form the input.
16. Add 50 μL 50% Protein A sepharose (PAS) slurry per 1 mL of input and incubate

on a tube mixer for at least 1 h at 4°C to "preclear" the input. The preclearing step removes nonspecific associations between the chromatin sample and the PAS matrix and is used in lieu of a "no antibody" negative control (see Note 10).

17. Centrifuge at maximum speed for 2 min at 4°C to pellet the PAS and retain the supernatant as precleared input. Discard the PAS pellet.

11.2.1.2 Immunocomplex Formation and Capture

18. Divide the precleared input as desired, reserving 2–5% as a precleared-input control, then add the requisite antibodies. Incubate on a tube mixer overnight at 4°C to form antibody-chromatin immunocomplexes (see Note 11).
19. Add 50 μL 50% PAS per 1 mL of sample and incubate on a tube mixer 4 h at 4°C to capture the immunocomplexes.
20. Centrifuge at 3,800 × *g* for 2 min at 4°C and discard the supernatant.

    Hint: The supernatant (depleted fraction) may be desired for further analyses, for example, for calculation of the percentage of a particular DNA sequence that was immunoprecipitated.

11.2.1.3 Washing the Captured Immunocomplexes

21. Incubate the PAS pellet (containing immunoprecipitated chromatin) with 10 volumes of wash buffer 3 for 15 min on a tube mixer at 4°C.
22. Centrifuge at 3,800 × *g* for 2 min at 4°C and discard wash buffer.
23. Wash the PAS pellet sequentially with 10 volumes of wash buffer 4, wash buffer 5, and TE buffer.

    Hint: The TE-buffer wash is included to remove any salt remaining in the sample. These washes can be modulated to suit individual experiments; we also commonly use a 100-, 150-, 300-mM NaCl series (see Note 12).

24. Incubate the PAS pellet with room temperature elution buffer at a volume 10× that of the PAS pellet for 30 min at room temperature on a tube mixer (see Note 13).
25. Centrifuge at 3,800 × *g* for 2 min at room temperature to pellet the PAS, and save the supernatant, containing the eluted sample, in a fresh tube.
26. Repeat steps 4 and 5, then pool the two supernatants as the immunoprecipitated fraction (IP). The IP sample can be stored at −20 or −80°C indefinitely.

11.2.1.4 Nucleic Acid Purification

See Notes 14 and 15.

27. To the precleared input control (step 1, Sect. 11.2.1.2) and IP fraction, add 1 volume of phenol:chloroform:isoamyl alcohol (25:24:1), pH ≥6.7, and then vortex 15 s (see Note 16).

28. Centrifuge at 10,000 × *g* for 5 min at room temperature, then transfer the aqueous supernatant into a fresh tube – do not disturb the interface. Hint: If the speed of centrifugation is lower, then increase the centrifugation time (e.g., centrifuge at 5,000 × *g* for 10 min). The two phases should be fully separated.
29. Add 1 volume of chloroform to the aqueous supernatant and vortex 15 s. This step and step 4 can be omitted to preserve more sample, but residual phenol may contaminate it.
30. Centrifuge at 10,000 × *g* for 5 min at room temperature and transfer the aqueous supernatant into a fresh tube. If the samples being processed are large, they can be partitioned temporarily into 1.5-mL microfuge tubes, ≤400 μL per tube, for the centrifugation step.
31. Add 1/10 volume of 3 M NaOAc (pH 5.2), vortex, then add 2 volumes of EtOH. Vortex and incubate at −20°C overnight. Hint: We routinely use glycogen at 10 μg per sample (0.5 μL of 20 μg/μL stock from Invitrogen) as a carrier to ensure the recovery of nucleic acids, but glycogen may interfere with some downstream applications (according to Invitrogen product information).
32. Pellet the precipitated DNA at maximum speed in a high-speed microcentrifuge (e.g., 20,800 × *g*) for ≥30 min at 4°C.
33. Carefully remove the supernatant without disturbing the pellet – leave a small amount of liquid in the tube. If glycogen or another carrier is used, the pellet will be visible as a thin white stripe; if not, take extra care not to disturb the very bottom of the tube.
34. Wash the pellet with 500 μL 70% EtOH by vortexing briefly and centrifuging at maximum speed for ≥10 min at 4°C.
35. Carefully remove the supernatant without disturbing the pellet – leave a small amount of liquid in the tube.
36. Leave the tubes open to air dry for 30 min at room temperature (see Note 17).
37. Resuspend the pellet in a suitable amount of nuclease-free double-distilled H_2O or TE buffer (e.g., 20 μL). If a fixed-angle microcentrifuge is used, much of the nucleic acid will be stuck to the back wall of the tube.

Buffers: Tris–HCl buffer at pH 8.0, and see Note 18.

Grinding buffer: 250 mM sucrose, 50 mM Tris–HCl, 10 mM 2-mercaptoethanol (ME), 1 mM $MgCl_2$, 1× protease inhibitor tablet (PI), EDTA-free.

Wash buffer 1: 250 mM sucrose, 50 mM Tris–HCl, 10 mM ME.

Wash buffer 2: 50 mM Tris–HCl, 10 mM ME.

Digestion buffer: 320 mM sucrose, 50 mM Tris–HCl, 4 mM $MgCl_2$, 1 mM $CaCl_2$, 0.1 mM phenylmethanesulphonylfluoride (PMSF).

Lysis buffer: 1 mM Tris–HCl, 0.2 mM EDTA, 0.2 mM PMSF, and 1× PI.

Incubation buffer: 50 mM NaCl, 20 mM Tris–HCl, 5 mM EDTA, 1× PI.

Wash buffer 3: 50 mM Tris–HCl, 10 mM EDTA, 150 mM NaCl.

Wash buffer 4: 50 mM Tris–HCl, 10 mM EDTA, 300 mM NaCl.

Wash buffer 5: 50 mM Tris–HCl, 10 mM EDTA, 500 mM NaCl.

TE buffer: 10 mM Tris–HCl, 1 mM EDTA.

Elution buffer: 20 mM Tris–HCl, 5 mM EDTA, 50 mM NaCl, 1% sodium dodecyl sulfate (SDS).

11.2.2 Crosslinked Chromatin Immunoprecipitation

Be certain to read the "Notes" section before performing this protocol for the first time (see Note 19).

11.2.2.1 Crosslinking of Protein and DNA Interactions

1. Prepare 37 mL of 1% formaldehyde, 0.02% silwet-77 solution in a beaker, per 2 g of tissue. Two grams of tissue is equivalent to about two young ears 5 cm long (see Notes 2 and 20).
2. Place the fresh tissue directly in the beaker, mix well with a magnetic stir bar, and place under vacuum for 15 min. Most of the tissue will have sunk to the bottom of the beaker, and all of it should appear water-soaked, indicating infiltration of the formaldehyde through the tissue (see Note 21).
3. Add 2.5 mL 2 M glycine per 37 mL formaldehyde solution, mix with the stir bar, and continue vacuum for 5 min.
4. Line a large plastic funnel with miracloth and pour the crosslinked tissue through. Rinse several times with deionized H_2O.
5. Scrape the tissue off the miracloth and blot it dry. Dried, crosslinked tissue can now be placed in a 50-mL tube, flash-frozen in LN_2, and stored indefinitely at −80°C.

11.2.2.2 Isolation and Fragmentation of Chromatin

6. Grind dried, crosslinked tissue to a fine powder in LN_2 – do not allow tissue to thaw (see Note 1).
7. Scrape frozen powder into 40 mL extraction buffer 1 and mix with a cold spatula or stir bar (use 40 mL buffer per 2 g tissue) until homogenized (see Note 3).
8. Filter homogenized tissue through miracloth; repeat (see Note 4).
9. Centrifuge samples in 50-mL tubes at 2,500 × *g* for 30 min at 4°C in a swinging-bucket centrifuge.
10. Gently pour off the supernatant and scrape off the top, sticky layer with a Pasteur pipet, taking care not to disturb the nuclei underneath. At this point, a white pellet consisting of intact nuclei and an overlayer of sticky brown starch should be apparent. Removing the starch allows more efficient sonication of the sample (step 13).

11. Resuspend the pellet in 1.5 mL extraction buffer 2 and transfer it to a microcentrifuge tube. Centrifuge at 12,000 × *g* for 10 min at 4°C.
12. Remove the supernatant and resuspend the pellet in 600 μL extraction buffer 3 by pipetting, keeping foam to a minimum.
13. Slowly pipet the resuspended pellet from step 7 on top of 600 μL extraction buffer 3 in a fresh microcentrifuge tube; avoid mixing the layers.
14. Centrifuge at 16,000 × *g* for 1 h at 4°C.
15. Meanwhile, prepare fresh nucleus lysis buffer (add SDS just before use), dilution buffer, and a 1% agarose gel for step 16.
16. Discard the supernatant and any remaining brown material still on top of the white pellet.
17. Resuspend the pellet in 400 μL nucleus lysis buffer by pipetting, keeping foam to a minimum. Remove 10 μL as your "unsonicated control" to compare with the sonicated samples in step 14 (see Note 5).
18. Sonicate the sample 5 times, 5 min each, at ~45 W in a cup horn (6.4 cm inner diameter) filled with a small amount of crushed ice (1 cm thick) and water. Place on ice for 2 min after each bout of sonication while replacing the ice water in the cup horn. Reserve 10 μL samples from sonications 1, 3, and 5 for step 16. The solution should become less and less viscous as the chromatin solubilizes (see Note 22).
19. Centrifuge the sample at 12,000 × *g* for 5 min at 4°C to pellet nonsoluble debris.
20. Transfer the supernatant to a fresh tube and store on ice while checking the chromatin size on an agarose gel in step 16. If the same tissue is being processed in several tubes, combine them before preclearing in step 18.
21. Run 5 μL each of the unsonicated control, the three samples reserved in step 13, and a 1-kb marker on a 1% agarose gel at low power (2–3 V/cm) for 30–45 min. A smear of EtBr stain between 150 and 1,200 bp (roughly 1–8 nucleosome fragments) is a common range to use as ChIP input (see Fig. 11.1). Continue sonicating until a desirable size range is reached (see Notes 8 and 22). Hint: This is a good time to prepare the PAS used in step 18 and step 2, Sect. 11.2.2.3 (see Note 9).
22. Dilute sonicated chromatin 10× in dilution buffer to reduce SDS concentration to ≤0.1% (see Note 23).
23. Add 50 μL 50% Protein A sepharose slurry per 1 mL of diluted sample from step 17. Incubate on a tube mixer for at least 1 h at 4°C to preclear the input.

    Hints: The preclearing step removes nonspecific associations between the chromatin sample and the PAS matrix and is used in lieu of a "no antibody" negative control.

24. Centrifuge at maximum speed for 2 min at 4°C to pellet the PAS. Retain the supernatant as "precleared input" and discard the PAS pellet.

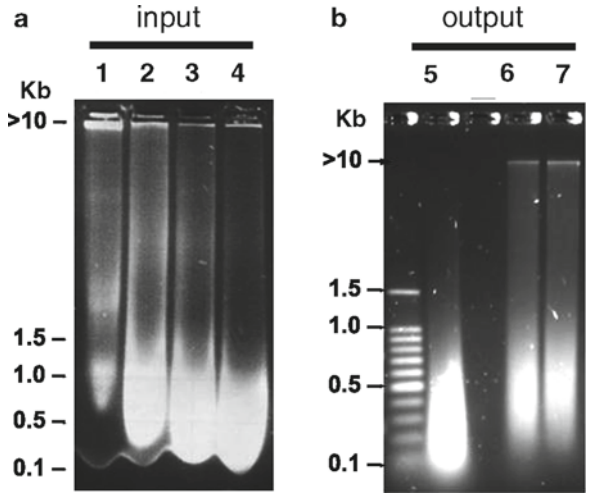

Fig. 11.1 (**a**) Input samples. Lane 1 is untreated chromatin, mostly insoluble or too large to migrate out of the well. Lanes 2, 3, and 4 are the same sample as in lane 1, sheared by sonication (xChIP protocol) for totals of 5, 15, and 25 min, respectively, with a final size range of approximately 150–1,200 nt (1–8 nucleosomes). A time course of enzymatically digested chromatin (nChIP protocol) looks nearly identical. (**b**) Output samples. Lanes 5, 6, and 7 are purified DNA from an xChIP procedure. Lane 5 is 1 μg of precleared input, and lanes 6 and 7 are 500 ng of the immunoprecipitated fractions from two separate antibody treatments. Note that the immunoprecipitation procedure favors recovering larger chromatin fragments

11.2.2.3 Immunocomplex Formation and Capture

25. Divide the precleared input as desired, reserving 2–5% as a "precleared input" control, and add the requisite antibodies (see Note 11). Incubate on a tube mixer overnight at 4°C to form antibody-chromatin immunocomplexes.
26. Add 50 μL 50% PAS per 1 mL sample and continue incubation 4 h.
27. Pellet the PAS-antibody complex by centrifugation at 3,800 × *g* for 2 min. The supernatant (depleted fraction) may be desired for further analyses, for example, for calculation of the percentage of a particular DNA sequence that was immunoprecipitated.
28. Wash the pellet consecutively with a 5× volume of each of the following buffers, first rinsing the pellet with each buffer, then incubating it 5 min in that buffer before going on to the next.

    i. Low-salt wash
    ii. High-salt wash
    iii. LiCl wash
    iv. TE Incubate at 4°C on a rotator/shaker, and centrifuge at 3,800 × *g* for 2 min after each wash.

29. Add elution buffer at 5× the pellet volume. Mix by vortexing and incubate at 65°C for 15 min, vortexing every 2 min. Alternatively, the samples can be left on a tube mixer for 45 min at room temperature.
30. Centrifuge at 3,800×*g* for 2 min to pellet the PAS; transfer the supernatant containing your sample to a fresh tube.
31. Repeat steps 5 and 6, then pool the two supernatants as the IP. Leave the IP at room temperature; otherwise the SDS will precipitate.

11.2.2.4 Nucleic Acid Purification

32. Remove the formaldehyde crosslinks by adding 20 μL 5 M NaCl per 500 μL sample (200 mM final) and incubating overnight at 65°C.

    Hints: Do not forget to uncrosslink the input and/or depleted fractions (your controls). At this point, the samples can be stored at −20 to −80°C indefinitely.

33. Purify the nucleic acid as described in the native ChIP section.

Buffers: Tris–HCl buffer at pH 7.8, and see Note 18.

Extraction buffer 1: 400 mM sucrose, 10 mM Tris–HCl, 10 mM $MgCl_2$, 5 mM ME, 0.1 mM PMSF, 1× PI (protease inhibitor, see Note 18).

Extraction buffer 2: 250 mM sucrose, 10 mM Tris–HCl, 10 mM $MgCl_2$, 1% Triton X-100, 5 mM ME, 0.1 mM PMSF, 1× PI.

Extraction buffer 3: 1.7 M sucrose, 10 mM Tris–HCl, 2 mM $MgCl_2$, 0.15% Triton X-100, 5 mM ME, 0.1 mM PMSF, 1× PI.

Nucleus lysis buffer: 50 mM Tris–HCl, 10 mM EDTA, 1% SDS, 1× PI.

Dilution buffer: 16.7 mM Tris–HCl, 1.2 mM EDTA, 167 mM NaCl, 1.1% Triton X-100, 1× PI.

Elution buffer: 1% SDS, 0.168 g $NaHCO_3$ in a 20-mL volume.

Low-salt wash buffer: 20 mM Tris–HCl, 2 mM EDTA, 150 mM NaCl, 1% Triton X-100, 0.1% SDS.

High-salt wash buffer: 20 mM Tris–HCl, 2 mM EDTA, 500 mM NaCl, 1% Triton X-100, 0.1% SDS.

LiCl wash buffer: 10 mM Tris–HCl, 1 mM EDTA, 250 mM LiCl, 1% Nonidet P-40, 1% deoxycholate (if Nonidet P-40 is unavailable, use IGEPAL CA-360 as a substitute).

TE wash buffer: 10 mM Tris–HCl, 1 mM EDTA.

11.3 Notes

1. Any step during which the sample is likely to warm past 4°C (for example, nucleus/chromatin isolation) should be carried out in the cold room. All buffers except elution buffer should be at 4°C or ice-cold.

2. Young ears 5–10 cm in length after husks and silks are removed are the best source of tissue, but root tips and seedlings also work. With a fresh razor blade, shave off the soft developing kernels directly into LN_2 (nChIP), formaldehyde solution (xChIP), or a weighing boat. More developed kernels contain more starch and fewer nuclei per gram. One young ear, 5 cm long, will provide ~2 mL (1 g) of ground tissue, which is plenty for downstream analyses with PCR.
3. Wait until the LN_2 evaporates and scrape the frozen powder directly into 50-mL tubes containing buffer. Mix in the cold room using a tube mixer or a beaker and a stir bar.
4. Fold a square of miracloth into quarters and open one side to form a conical funnel. Place it in a plastic funnel over a 50-mL tube or a beaker. The first filtration will be viscous; gently squeeze the cloth funnel to extract the buffer, then discard the miracloth.
5. The nuclei lyse because of swelling of the chromatin that results from removal of the divalent cation Mg^{2+} from the buffer.
6. The A_{260} reading should be around 2.5 μg/μL to ensure sufficient input chromatin. If the reading is between 1.0 and 2.5 μg/μL, use proportionally less DNAse I in step 9, Sect. 11.2.1.1. If the A_{260} is below 1.0 μg/μL, the sample is probably poor and can be discarded.
7. (i) We use RQ1 RNase-free DNase (Promega), supplied at 1 U/μL, or lyophilized MNase from Worthington Biochemical. MNase is susceptible to degradation and should be frozen in aliquots at the working concentration of 10 U/μL. Titrate each freshly made batch of working stocks initially to determine the optimal concentration of that batch for ChIP (start with 50 U/mL of chromatin solution [2.5 μg/μL]); aliquots stored at −20°C for single use are stable. (ii) DNase vs. MNase: Micrococcal nuclease is a commonly used enzyme for chromatin digestion, but it is also a weak RNase. The RNase activity may disrupt chromatin complexes stabilized by RNA and/or degrade RNA of interest. Furthermore, MNase specifically degrades the linker DNA between nucleosomes and may therefore bias the sample. Conversely, DNase, in the presence of Mg^{2+}, digests DNA both on and between nucleosomes and has no reported RNase activity, but its use in ChIP assays has not, so far as we know, been widely tested outside our lab and may have unknown disadvantages.
8. Although the samples at this point are DNA–protein complexes, 1% agarose gel electrophoresis predicts their sizes remarkably well and is a good diagnostic of the quality of the input chromatin. The expected results are shown in Fig. 11.1.
9. Protein A Sepharose (GE Healthsciences) comes in a 20% ethanol slurry and requires washing before use. Centrifuge the desired amount at 3,800 × *g* for 2 min and discard the supernatant – note the volume of the PAS bed. Add 5 volumes of incubation buffer (nChIP) or ChIP dilution buffer (xChIP) (protease inhibitors are unnecessary for washing steps), mix, and repeat centrifugation. Wash twice more and resuspend the PAS bed in incubation or dilution buffer to a 50% slurry.

10. Protein A is a bacterial protein that binds the Fc portion of all IgG antibody molecules. PAS is protein A bound to a sepharose matrix so that it can be easily sedimented. This reagent is used to pull down ("precipitate") the immunocomplexes.
11. (i) Antibodies should be titrated individually because every antibody is different. A good starting place is 1:200 dilution of an antibody at 1 mg/mL. (ii) A useful control is a purified IgG against an unrelated or nonchromatin protein, for monitoring background associations (noise).
12. Wash buffers 3, 4, and 5 have increasingly higher amounts of NaCl, thereby increasing the ionic stringency of the wash and decreasing the background of nonspecific epitope binding. Washing parameters can be altered to tighten or relax the stringency.
13. The elution buffer contains 1% SDS, which denatures proteins and disrupts the chromatin-antibody and antibody–protein A interaction, thereby releasing the immunoprecipitated material from the PAS. An alternative, SDS-free, method for elution is detailed in the PAS instructions.
14. This entire section can be omitted in favor of a commercially available PCR or gel cleanup column (e.g., Qiagen PCR cleanup columns), but when scaling up, we have obtained reduced yields with such columns. One reason may be that most of the columns retain only nucleic acids ≥200 nucleotides and would theoretically eliminate any mononucleosome-sized fragments (~150 nucleotides) from the IP sample.
15. Although ChIP is most often used to analyze the DNA sequences associated with particular chromatin modifications, it can be very useful for looking at the proteins associated with these same antigens, particularly in crosslinked chromatin where weaker in vivo molecular interactions are maintained. Here we present a protocol for recovering acid-soluble proteins (such as chromatin proteins) from the organic/interphase of a standard nucleic acid purification (nChIP protocol, section D):

    (a) To each sample, add 1/3 volume of phenol:chloroform:isoamyl alcohol (25:24:1), pH ≥ 6.7, and vortex for 15 s.
    (b) Centrifuge at 10,000 × *g* for 5 min at room temperature:

        (i) Transfer the aqueous supernatant into a fresh tube; proceed to nChIP step 27.
        (ii) Transfer the organic (phenolic) phase and interphase (containing most of the protein) to a 15-mL conical tube.

    (c) To organic/interphase, add:

        1/100 volume of [10 M] H_2SO_4 (sulphuric acid)
        1/80 volume [1 mg/mL] BSA (bovine serum albumin)
        12 Volumes acetone

    (d) Vortex and store at −20°C for several hours to overnight.

        Hint: the protein precipitate should be white and flaky.

    (e) Centrifuge at ~2,000 × *g* in a swinging-bucket rotor for 2 min at 4°C.

(f) Add 6 volumes cold acidified acetone (100 mM H_2SO_4 in acetone), vortex, and spin as in step e.
(g) Add 6 volumes acetone, vortex, and spin as in step e. Repeat twice.
(h) Remove all residual acetone from the pellet by placing it briefly (1–5 min) in a vacuum or by leaving the tubes open on the bench.
(i) Resuspend each pellet in solubilization buffer.
100 mM Na2CO3 (sodium carbonate)
100 mM DTT (dithiothreitol)

Hint: Use the smallest volume of solubilization buffer that will resuspend the pellet; it should go into suspension immediately. Start with 50 mL.

(j) Once the protein is recovered, separate it by SDS-PAGE and analyze by protein staining or western blotting.

Another method for protein recovery is to boil the PAS pellet in SDS-containing sample buffer after the washing steps. Boil for 5 min (nChIP) or 30 min (xChIP; boil longer to reverse crosslinks), then centrifuge at maximum speed for ~5 min. The supernatant will contain immunoprecipitated proteins and DNA.

The major drawback of recovering proteins from immunoprecipitated samples is that a large fraction of the sample will consist of the antibody used in the ChIP. Antibody will run at ~70 and ~55 kDa on an SDS gel and will contaminate western blots at the same locations. One way to avoid this problem is to crosslink the antibody covalently to the PAS matrix before immunoprecipitation, thereby combining the immunocomplex formation and capture.

16. Phenol:chloroform denatures chromatin proteins and separates them from DNA and RNA by partitioning proteins to the organic (lower) phase and nucleic acids to the aqueous (upper) phase. If primarily RNA is to be analyzed, use acidic phenol:chloroform (5:1), pH ~4.3. In this case, the RNA is partitioned to the aqueous phase, whereas much of the DNA remains with proteins in the organic phase.
17. A speedvac can also be used, but do not overdry the samples. A properly processed sample should have trace amounts of water, which remain after the EtOH has evaporated. Small DNAs may denature when completely lyophilized and be difficult to resuspend. RNAs are even more sensitive to overdrying.
18. (i) Make a PMSF stock in EtOH at 100 mM and store it indefinitely at −20°C. Add it just before the use of any buffer because it has an aqueous half-life of ~30 min.
(ii) Prepare a protease inhibitor cocktail (Roche) stock by dissolving one PI tablet in ddH_2O to 25×. Use the EDTA-free version, because EDTA will chelate necessary cations (Mg^{2+} and Ca^{2+}). The stock solution can be kept on ice for a few days or at −20°C for several weeks.
19. This xChIP protocol is adapted from Gendrel et al. (2005).
20. Formaldehyde solutions vary in quality; we use 37%, ACS grade (Sigma). Commercial, aqueous preparations contain some methanol, which inhibits their

polymerization to insoluble paraformaldehyde, but polymerization still occurs, so the effective concentration of a solution of formaldehyde is reduced over time. This problem is avoided if the stock solution is replaced once a year.

21. The silwet-77 and vacuum ensure that the formaldehyde infiltrates the cell walls.
22. Sonication (ultrasound treatment) creates small, rapidly moving bubbles (microcavitation) that shear chromatin mechanically. Sonication is therefore ideal for solubilizing crosslinked chromatin, which is refractory to enzymatic digestion. One major drawback is that a lot of heat is released in the process that can disrupt protein complexes. Another drawback is that sonication forces can be uneven within a sample and vary depending on the amount of crosslinking, the sample concentration, and the overall viscosity of the solution. Therefore, members of each laboratory must explore the optimal conditions for their equipment and samples. It is best to avoid the microtips that come with many sonicators. Microtips tend to cause sample loss by foaming and are particularly prone to overheating. Two options for avoiding the microtip are a water-bath-style sonicator and a cup horn attached to a standard sonicator. In a water-bath sonicator, the energy is distributed evenly throughout a large volume of liquid (we have used a "Bioruptor" by Diagenode). A cup-horn adapter is similar in that it allows the tubes to be immersed in water, but when a cup horn is used, each microfuge tube must contain the same volume and each sample must be sonicated at the same distance from the ultrasonic probe (for example, a fill line can be marked on the cup horn). Also note that sonication has limits: If repeated sonications do not seem to change the EtBr smear on an agarose gel, the sample is overcrosslinked.
23. SDS at high concentrations denatures most proteins, including antibodies.

References

Dawe RK, Reed L, Yu H-G, Muszynski MG, Hiatt EN (1999) A maize homolog of mammalian CENPC is a constitutive component of the inner kinetochore. *Plant Cell* 11:1227–1238

Gendrel AV, Lippman Z, Martienssen R, Colot V (2005) Profiling histone modification patterns in plants using genomic tiling microarrays. *Nat Methods* 2:213–218

Hernandez JM, Feller A, Morohashi K, Frame K, Grotewold E (2007) The basic helix loop helix domain of maize R links transcriptional regulation and histone modifications by recruitment of an EMSY-related factor. *Proc Natl Acad Sci USA* 104:17222–17227

Hiatt EN, Kentner EK, Dawe RK (2002) Independently-regulated neocentromere activity of two classes of satellite sequences in maize. *Plant Cell* 14:407–420

Kato A, Albert PS, Vega JM, Birchler JA (2006) Sensitive fluorescence in situ hybridization signal detection in maize using directly labeled probes produced by high concentration DNA polymerase nick translation. *Biotech Histochem* 81:71–78

Shi JH, Dawe RK (2006) Partitioning of the maize epigenome by the number of methyl groups on histone H3 lysines 9 and 27. Genetics 1173:1571–1583

Zhong CX, Marshall JB, Topp C, Mroczek R, Kato A, Nagaki K, Birchler JA, Jiang JM, Dawe RK (2002) Centromeric retroelements and satellites interact with maize kinetochore protein CENH3. *Plant Cell* 14:2825–2836

Chapter 12
Methods of Fluorescence In Situ Hybridization on Extended DNA Fibers (Fiber-FISH)

Jason G. Walling, Robert M. Stupar, and Jiming Jiang

Abstract Fiber-fluorescence in situ hybridization (fiber-FISH) is a cytogenetic technique that can be used to visualize DNA probes on extended DNA fibers. Fiber-FISH provides a significantly higher mapping resolution than do the chromosome- or chromatin-based cytogenetic mapping techniques. Here we report a simple procedure for performing fiber-FISH. In general, we consider the overall protocol to comprise four distinct steps, each of which is critical to the success of the experiment: the isolation of nuclei from plant tissue, the extension of fibers on glass slides, the hybridization of labeled DNA probes to denatured DNA fibers, and the immunodetection of the probes. We end the protocol discussion by addressing some of the more frequently asked questions with regard to common problems encountered and the technical limitations of the procedure.

Keywords Fiber fluorescent in situ hybridization · Fiber-FISH · Optical mapping · Immunostaining · Organelle DNA mapping · Repetitive DNA mapping

Abbreviations

Fiber-FISH	Fluorescence in situ hybridization procedure on extended DNA fibers
NIB	Nucleus isolation buffer

J.G. Walling (✉) • J. Jiang
Department of Horticulture, University of Wisconsin, 1575 Linden Drive, Madison, WI 53706, USA
e-mail: walling@wisc.edu

R.M. Stupar
Department of Agronomy and Plant Genetics, University of Minnesota, St. Paul, MN 55108, USA

H.W. Bass and J.A. Birchler (eds.), *Plant Cytogenetics*, Plant Genetics and Genomics: Crops and Models 4, DOI 10.1007/978-0-387-70869-0_12,

Contents

The fluorescence in situ hybridization (FISH) procedure on extended DNA fibers (fiber-FISH) can be divided into three relatively independent steps, which can be completed in two consecutive days: isolation of plant nuclei (morning of day 1), DNA fiber preparation and FISH (afternoon of day 1), and fiber-FISH signal detection and analysis (day 2).

12.1 Isolation of Plant Nuclei

1. Freeze 5–10 g of fresh leaf material in liquid nitrogen and grind to a fine powder with a precooled (−20°C) mortar and pestle.
2. Transfer powder to a 50-mL centrifuge tube, add 20 mL chilled "nucleus isolation buffer" (NIB) and mix *gently* (be sure to break up clumps using gentle agitation; if necessary a scoopula, dowel, or forceps can be used to break up the clumps). Incubate on ice for no more than 5 min (in an ice bucket on a shaker). (NIB: 10 mM Tris–HCl pH 9.5, 10 mM EDTA, 100 mM KCl, 0.5 M sucrose, 4.0 mM spermidine, 1.0 mM spermine, 0.1% 2-mercaptoethanol.) NIB can be prepared in larger quantities and stored as a stock solution at 4°C. 2-Mercaptoethanol should not be included in the stock, but should instead be added just before use.
3. Before nylon mesh filtration, the solution can be filtered through a large-pore Sigma screen, MiraCloth, or four layers of cheesecloth. Filter through nylon mesh: 50 and 30 μm, sequentially, into ice-cold 50-mL centrifuge tubes (nylon filters obtained from Tetko Inc.) using a cooled funnel.

   Some published protocols suggest filtrations of cell suspensions with nylon mesh filters of 50-, 30-, and 20-μm mesh sizes. Although in some cases the 20-μm filtration better removes unwanted debris, it frequently reduces the final concentration of nuclei significantly and is therefore usually omitted for most plant materials.
4. Add 1 mL NIB containing 10% (v/v) Triton X-100 (0.9 mL NIB + 0.1 mL Triton X-100; mix) and *gently* mix the filtrate. Triton X-100 (final concentration of 0.5%) is used to remove any chloroplast contamination. Centrifuge at 2,000 × *g* for 10 min at 4°C. Decant the supernatant. If your pellet is very small, you may wish to skip the subsequent cleaning steps and move directly to step 7. If your pellet is large enough, however, you should resuspend it in 20 mL NIB (with 2-mercaptoethanol added).
5. Filter through nylon mesh again: 50 and 30 μm sequentially, into ice-cold 50-mL centrifuge tubes using a cooled funnel.

6. Add 1 mL NIB containing 10% (v/v) Triton X-100 (premixed) and *gently* mix the filtrate, as in step 4. Centrifuge at 2,000 × *g* for 10 min at 4°C.
7. Decant the supernatant and resuspend the pellet in 1 mL of 1:1 NIB:100% glycerol (neither 2-mercaptoethanol nor Triton X-100 added). Store at −20°C for at least 24 h. The debris and nuclei will settle at the bottom of the tube. Typically, the cellular debris will settle a little faster than the nuclei, which will therefore settle as a layer on top of the debris.

Important notes: The quality of fiber-FISH signals depends largely on the quality of the nuclei. The youngest and most succulent tissues available from a particular plant usually provide the best yields. Most often, this tissue is the newest growth found on the plant; actively growing leaf meristems and cotyledons or early leaves from newly germinated plants provide the best material. Older plants whose leaves have hardened and in which active growth has almost ceased, should be avoided. In many species, that hold up to pruning (such as grasses), a successful strategy is to cut the plant back and to sample the leaf material that emerges the next week. Some plants have very fine or fibrous leaves, and larger amounts of tissue will be needed to yield sufficient numbers of nuclei.

The harvested plant tissue should be used immediately for extraction of nuclei. If it cannot be used immediately, it should be flash frozen in liquid nitrogen (immediately after harvest), stored at −80°C, and not allowed to thaw. Do not wrap the material in a moist towel and freeze it; freezing and thawing in the presence of excess water will damage the plant cells and lower the recovery of high-quality nuclei.

12.2 Preparation of Extended DNA Fibers on Glass Slides

The DNA fibers can be extended on microscope slides by any of several methods. We find that using a coverslip to drag or tease the fibers carefully across the surface of the slide seems to give the most uniform results. Dragging the suspension of lysed nuclei slowly and smoothly is crucial. We also use poly-L-lysine-coated slides obtained from Sigma. These slides are treated in a way that promotes adhesion of the DNA molecule.

1. Identify the portion of the tube containing the suspension of nuclei and debris. The nuclei tend to settle near the bottom of the tube, and the settling process can take a day or longer. The very bottom of the tube contains the settled debris, and the nuclei are often found right above it. The color of the nuclei depends on species (ranging from gray to green to brown), but very clean nuclei normally have a gray/white coloration.
2. Pipet 1–10 μL of suspension of nuclei (1–5 μL/slide, depending on the concentration of your suspension) into ~100 μL NIB (without 2-mercaptoethanol or Triton X-100) in an eppendorf tube to dilute the glycerol. Gently mix the nuclei

with the buffer and centrifuge at 1,700–2,000 × *g* for 5 min. Use a pipet to remove the NIB/glycerol solution such that only the pellet of nuclei remains at the bottom on the tube. This cleaning step can be repeated if necessary.
3. Resuspend the nuclei in PBS (the final volume is ~2 μL/slide) (PBS: 10 mM sodium phosphate, pH 7.0, 140 mM NaCl).
4. Pipet 2 μL suspension in a line across one end of a clean poly-L-lysine slide (Sigma, Poly-Prep, Cat # P0425) and air dry for 5–10 min. Completely drying the suspension would prevent efficient lysis of the nuclei (next step), so stop the drying process when enough residual solution remains to make the line of nuclei still appear slightly shiny.
5. Pipet 10 μL STE lysis buffer on top of the nuclei and incubate at room temperature for 4 min (STE: 0.5% SDS, 5 mM EDTA, 100 mM Tris–HCl, pH 7.0).
6. Slowly drag the solution down the slide with the edge of a clean coverslip held just above the surface of the slide. Take care to drag only the liquid. If the coverslip touches the slide, it will simply scrape everything off. Air dry for 10 min.
7. Fix in fresh 3:1 100% ETOH:glacial acetic acid for 2 min at room temperature.
8. Bake the slide at 60°C for 30 min. The slides are now ready for FISH.

12.3 FISH and Signal Detection

DNA probe preparation and hybridization procedures are the same as those in regular FISH protocols. We recommend using 20 μL hybridization mix per slide with a 22 × 40 mm coverslip to cover a large area on the slide. Seal the coverslip with rubber cement. After the glue dries, place the slide in an 85°C oven for 5 min in direct contact with a heated surface. Transfer the slide to a wet chamber and incubate it at 37°C overnight.

Detection of fiber-FISH signals requires at least two layers of antibodies, rather than the typical single layer used in most regular FISH experiments. Three layers of antibodies may help generate brighter signals than two layers, but using too many layers (more than three) often causes superfluous nonspecific background signal.

All antibody layers should be composed of the antibodies diluted in the appropriate buffers at the concentrations specified below. Apply 100 μL of hybridization solution to each slide and place a 22 × 40 cover slip (or a piece of parafilm of similar size) gently on the antibody solution to promote even spreading. Incubate all antibody layers in a 37°C wet chamber for at least 30 min.

12.4 Detection Procedure Using Three Layers of Antibodies

1. Peel off the rubber cement using a forcep. Dip the slides in a staining jar containing 2× SSC. Placing the jar on a slow shaker will help coax the coverslips to fall from the slides.
2.

Wash in 2× SSC	5 min
Wash in 2× SSC at 42°C	10 min
Wash in 1× PBS	5 min

3. Incubate FITC-avidin (or streptaviden) (1 μL antibody stock/100 μL TNB buffer) and/or mouse (*Mus musculus* L.) anti-digoxigenin (1 μL/100 μL). Incubate in a wet chamber at 37°C for 30 min to 1 h.

   Wash in 1× TNT (3 times) 5 min each

4. Incubate anti-avidin (or anti-streptaviden) conjugated with biotin (0.5 μL/100 μL TNB buffer) + anti-mouse conjugated with digoxigenin (1 μL/100 μL) at 37°C for 30 min to 1 h.

   Wash in 1× TNT (3 times) 5 min each

5. Incubate FITC-avidin (1 μL/100 μL TNB buffer) + rhodamine anti-digoxigenin (1–2 μL/100 μL), 37°C for 30 min.

   Wash in 1× TNT (3 times) 5 min each

6. Drain the slides, add 10–20 μL Vectashield (Vector Labs), cover with a 22- × 30-mm coverslip, and squash.
7. View your fiber-FISH results with a fluorescent microscope.

12.5 Notes

1. Antibodies

   FITC-avidin, 1 μL/100 μL buffer
   Biotin-anti-avidin, 0.5 μL/100 μL buffer
   Mouse anti-digoxigenin, 1 μL/100 μL buffer
   Digoxigenin anti-mouse, 1 μL/100 μL buffer
   Rhodamine anti-digoxigenin, 1–2 μL/100 μL buffer

2. Solutions

   TNT: 0.1 M Tris–HCl, 0.15 M NaCl, 0.05% Tween-20, pH 7.5 (make 10× stock)
   PBS: 0.13 M NaCl, 0.007 M Na_2HPO_4, 0.003 M NaH_2PO_4 (make 10× stock)

12.6 Most Frequently Asked Questions

1. Why can I not see a solid pellet of nuclei in the eppendorf tube, even after several days?
   Answer: The most likely reason is poor quality and/or recovery of nuclei from your preparation. Old plant tissues or plant tissues containing high concentrations of sugars, starch, or other polysaccharides often result in such poor samples of nuclei. You must also make sure the glycerol concentration of your sample of suspended nuclei is correct (50%).

2. Why do I not see very many fiber-FISH signals?
   Answer: A sufficient number of fibers must be available on a given slide for each hybridization reaction. The relative concentration of nuclei can be determined empirically for each stock of isolated nuclei. We find that the best way to check the concentration of DNA fibers is to stain with YOYO-1 iodide (Invitrogen). This is a simple and expedient way to check the concentration and integrity of your fibers and also simultaneously allows you to assess your ability to extend the fibers uniformly. To use this stain, first follow the steps described for extending nuclei. After the 60°C baking step, stain the fibers with 1 μL of YOYO-1 in 100 μL 1× PBS (30 min). Rinse slides twice briefly in 1× PBS, dry, add Vectashield, mount with a coverslip, and view under a fluorescence microscope. If few or no fibers are visible, use more nuclei per slide. If too many fibers appear or they are clumped together, then use less solution and make sure you drag the lysed solution slowly and evenly, without scraping the slide. YOYO-1 staining will also reveal the amount of debris in your sample of nuclei.

3. Why is the background so strong?
   Answer: Strong background signal arises most often from one of two causes: a suspension of nuclei containing too much debris and spurious binding of antibodies to the charged slides.

   To address the first possibility, make sure that, when you aliquot the nuclear suspension, you do not agitate the solution so as to stir up unwanted debris. Baking the slides will stabilize the fibers on the slides and also reduce the amount of cytoplasm present, so omitting the baking step can increase the background.

   Excess background arising from bound antibodies is more difficult to address. Some antibodies have a propensity to form more background when used sequentially than do others, and different antibodies grown in different animals may produce better or worse results.

   Experiment with increasing the stringency of the washes, decreasing the antibody concentration, and the use of antibody-blocking reagents such as BSA and/or Roche Blocking reagent. Finally, note that the layering of antibodies can increase the background signal, and we therefore recommend that only a minimal number of layers be used to ensure good contrast between probe and background signal.

4. Why are my fiber-FISH signals very weak and difficult to see with my eyes even after three layers of antibody detection?
   Answer: Strong hybridization signals result from high probe/target specificity, strong labeling, and clean/stable fibers.

   The labeled probe should be of appropriate length. A 10-kb DNA probe will produce a fiber-FISH signal that averages about 3 μm of extended fiber; this signal will consist of only two to five consecutive dots. Such small signals are difficult to distinguish from background signals, and some prior knowledge about the size of the probe can also help. In other words, you should have some idea of what you expect to see. To ensure strong annealing during the hybridization step, take care with regard to the concentration of formamide in the hybridization solution. Any deviation from the recommended 50% final concentration can significantly compromise the probe's ability to anneal precisely.

   Proper labeling of the DNA probe is critical to a successful outcome. The probe must be labeled in its entirety with labeled nucleotides distributed evenly along the entire probe sequence. An underlabeled probe will appear discontinuous on fibers, and the signal will be weak and difficult to distinguish from debris. Nick-translated probes can be checked by electrophoresis; properly labeled products should yield a smear of bands that range in size from 100 to 500 bp. If the size is too large, increase the reaction time and/or concentration of DNase I. If it is too small, decrease reaction time and/or the concentration of DNase I.

   Finally, the fibers themselves usually provide the best targets for fiber-FISH during the first 6 months after isolation. Occasionally, using stocks more than 6 months old results in poor fiber performance and poor probe retention in the FISH protocol. In this case, new stocks should be isolated.

5. I want to incorporate more colors/probes into my fiber-FISH hybridization. Is that possible?
   Answer: The number of probes that can be individually detected is limited to the number of unique filter sets available on your microscope and your ability to label each of the probes uniquely. We typically use red and green because they are the brightest and therefore easiest to see, but other fluoriphors that emit in the blue and far-red spectra have also been used with success, although they can be harder to see. Accordingly, the probes that perform the best and typically have the brightest signal should be detected in the blue or far-red to ensure visualization, whereas the probes that are in question or have a history of being difficult to see should be detected with the brighter green or red fluoriphors.

6. I don't have seed to plant seedlings, and the only plant I have is old. Can I still use it for fiber-FISH?
   Answer: Certainly, the best tissue in our opinion is young succulent tissue, but if such tissue is not available, then the youngest and greenest tissue on the plant should be sampled. Brown or dead leaves simply will not work. Decent recovery is possible from older leaves, but you may need to use more tissue than usual and more debris will therefore be present in your final suspension.

Chapter 13
Fluorescence In Situ Hybridization and In Situ PCR

James A. Birchler and Tatiana V. Danilova

Abstract The application of fluorescence in situ hybridization to chromosomes allows each member of the karyotype to be distinguished from all others. This technique can be used to detect changes in chromosomes. Individual genes and transgenes can be placed to chromosome as well. Here we describe the techniques used for chromosome identification, single-gene detection, and retroelement genome painting and the use of banding paints that cover individual chromosomes. Several applications of these techniques are discussed. Primed in situ labeling of plant chromosomes is also described.

Keywords FISH · PRINS · Chromosome · Retrotransposons · Karyotype · Meiosis · B chromosome

Contents

J.A. Birchler (✉) • T.V. Danilova
Division of Biological Sciences, University of Missouri-Columbia,
Columbia, MO 65211, USA
e-mail: birchlerj@missouri.edu

H.W. Bass and J.A. Birchler (eds.), *Plant Cytogenetics*, Plant Genetics and Genomics: Crops and Models 4, DOI 10.1007/978-0-387-70869-0_13,

13.1 Introduction

Fluorescence in situ hybridization (FISH) involves a DNA–DNA hybridization of sequences in a probe to the denatured DNA in a chromosome affixed to a slide, in which the probe can be directly or indirectly detected because a fluorescent tag is present that allows it to be visualized with fluorescence microscopy. FISH is used to label specific sites on chromosomes, to distinguish each chromosome from others, to detect transgenes or transgene arrays, and to distinguish different genomes from each other in hybrids or allopolyploids, among numerous other uses. Originally, the probe incorporated nucleotides that were conjugated with molecules that could then be detected with fluorescently labeled antibodies or that could be used for the enzymatic production of insoluble dyes at the site of hybridization (see, e.g., De Jong et al. 1999). Although these techniques work well, in our hands they exhibit a higher background than do directly labeled fluorescent probes (Kato et al. 2004, 2006). We will therefore focus on the latter in our discussions below.

13.2 Chromosome Preparations

Most often, FISH is performed on chromosomes recovered from rapidly dividing root tips that have a high mitotic index or from the pachytene stage of early meiosis, in which the chromosomes are usually morphologically distinct and not condensed to the degree that they are in somatic metaphase stages. The sampling of pachytene cells requires growing plants to near the flowering stage and some knowledge of the best sampling time for the species in question. Root tip sampling, on the other hand, can be performed on seedlings that are only a few days old and does not destroy the individual, which can be kept for further analysis. The root tips of more mature plants can also be sampled; the plant is removed from its pot, the ends of the roots are clipped, and ample water is applied. In a few days, newly grown root tips emerge that can be used for cytological analysis.

Historically, a variety of techniques have been used to arrest root tips in the metaphase stage, including colchicine, cold, and hydroxyquinoline treatments. Kato (1999) compared these techniques to a pressurized nitrous-oxide treatment, which proved far superior to the others in yielding a very large number of metaphase-arrested cells with analyzable chromosomes. The greater number of usable cells is a significant advantage for any FISH study, because potential signals observed can be confirmed in multiple cells. The nitrous-oxide treatment requires a small treatment chamber that can withstand 10 atm of pressure (Kato et al. 2006), but

many variations on the design have been demonstrated to work. The length of nitrous-oxide treatment can affect the degree of condensation of the chromosomes (Danilova and Birchler 2008).

After the tissues are arrested at metaphase, they are fixed and can be stored at −20°C for extended periods without significant detrimental effects. The material is subsequently digested with enzymes that remove the cellular structure, and the resulting mix is dropped onto slides. The chromosomes are then subjected to ultraviolet irradiation that crosslinks the chromosomes to the slides, increasing the sensitivity of FISH, presumably by holding more of the chromosomal DNA on the slide.

13.3 Probe Preparation

Probes can be prepared for FISH analysis by numerous means. As noted above, we prefer directly labeled probes or synthetically produced oligonucleotides carrying a fluorescent label. For a particular probe, the insert can be amplified from a bacterial plasmid by the polymerase chain reaction to produce sufficient amounts for the labeling reaction. Oligonucleotides labeled with a fluorochrome at one end can be purchased directly from several commercial sources.

Labeling of probes involves a nick-translation reaction. DNAse I is included in the reaction to cleave the double-stranded sequence on one strand, and DNA polymerase I is then added to repair the nicks and incorporate a new DNA strand in the region. The target sequence is tagged by inclusion of nucleotides in the reaction that have conjugated fluorochromes. When the probe is denatured and applied to chromosomes, the site of hybridization to the complementary sequences can be visualized with fluorescent microscopy.

Because a wide variety of fluorochromes is available, different colors can be incorporated into probes for different sequences. In addition, any one probe can be labeled with two different fluorochromes to produce new colors; for example, mixing red and green produces yellow fluorescence. If the target size for a probe on the chromosome is highly variable, exposure for the optimum time will probably detect only the more abundant sites. If the target sites are very different for separate sequences, then alternative fluorochromes can be used and detected in their own channels. Adjustment of the amounts of probes and the density of incorporation of the fluorochrome into the probe can optimize the system (Kato et al. 2006).

The detection of large targets (>30 kb) of repetitive arrays requires a different level of probe labeling than the detection of single genes or single transgenes (Kato et al. 2006). Large targets require less dense fluorochrome incorporation; otherwise the emission will be too bright. On the other hand, single-gene (2.5-kb) detection requires a much higher density of fluorochrome incorporation, which is achieved by use of greater amounts of DNA polymerase I in the nick-translation reaction (Kato et al. 2006; Lamb et al. 2007a; Yu et al. 2007a, b; Danilova and Birchler 2008). Texas Red is a bright fluorochrome that is superior to others for single-gene detection, although those that emit in the green range can work as well. For the localization

of small targets to chromosome, the probe for the small target can be labeled with one color, typically with Texas Red, and the chromosomes decorated with fluorochromes of various other colors – for example green, blue, and far-red (which cannot be seen but can be detected and pseudocolored) – in combinations that uniquely label each chromosome (Yu et al. 2006, 2007b). When the different channel images are merged into one, the chromosome on which the red signal of the small target lies can be identified by its color pattern.

13.4 Chromosome Painting for Karyotype Analysis

In mammalian species, chromosome sorting has allowed the development of whole-chromosome painting (Schrock et al. 1996; Speicher et al. 1996). The DNA of each separate chromosome is color-coded with different fluorochromes to produce a distinct color for each chromosome. This system has been developed further with spectral imaging in which different fluorescent spectra are detected and each is assigned a pseudocolor (Schrock et al. 1996). Such systems have yet to be developed for plant species, but an alternative approach is to use repetitive sequences that are present at specific sites on the chromosomes. A labeling system has been developed for maize that, by combining centromere repeats, subtelomere repeats, microsatellite arrays, heterochromatin repeats, and different arrays of ribosomal RNA genes, can distinguish each pair of homologues in somatic root-tip preparations (Kato et al. 2004).

13.5 Retroelement Genome Painting

The genomes of many plant species are composed of retrotransposons that are present in high copy number. Different elements experience bursts of transposition that increase their numbers in different evolutionary lineages. Retroelements expand by transcription into an RNA intermediate that is reverse-transcribed into DNA that inserts itself into new locations in the genome. These elements are bounded by long terminal repeats (LTRs) that are identical as a result of the mechanism of replication. When they are initially inserted, therefore, the LTRs are identical in sequence. Over time, the LTRs accumulate mutations that can be used to estimate their age. By this method, retroelements are suggested to have a half-life of 5–6 million years. The consequence is that different evolutionary lineages have families of retroelements that are dispersed in the genome, but they will decay as new bursts of other elements occur. As a result, chromosomes of interspecies hybrids of progenitors with divergence times of as little as a half a million years can be distinguished by the types and abundances of specific retrotransposons (Lamb and Birchler 2006; Lamb et al. 2007b).

Lamb and Birchler (2006) found that chromosomes in hybrids between maize and *Tripsacum* could be distinguished from each other by probing root-tip metaphase spreads with specific retrotransposon sequences from maize. *Tripsacum* and maize are thought to have diverged about 5 million years ago. Most of the major

retrotransposons that are so abundant in maize can easily distinguish the maize chromosomes in hybrids between the two species. Repetitive elements were isolated from *Tripsacum* that were much more abundant on the *Tripsacum* chromosomes than on the maize chromosomes. Therefore, if contrasting colors are chosen for the maize and *Tripsacum* elements, the two sets of chromosomes are visually distinct, and rearrangements can be easily detected. In a trispecies hybrid containing a genome each from maize, *Tripsacum*, and *Zea diploperennis* Iltis, Doebley, and Guzman, all three types of chromosomes can be recognized by means of contrasting retrotransposons probes. The genomes of *Z. luxurians* (Durieu and Asch.) Bird and *Z. mays* L. can also be distinguished with retroelement probes (Lamb and Birchler 2006).

Previously, different genomes in hybrids or allopolyploids were distinguished using genomic in situ hybridization (GISH) (Schwarzacher et al. 1989; Han et al. 2003). This technique uses blocking with highly repetitive DNA to allow the different low-copy sequences to be used to differentiate the chromosomes from different source species. Although this technique works well, the correct titration of blocking DNA is needed to reduce background. In retroelement genome painting, directly labeled probes are used and lower the background hybridization. As illustrated with the *Zea* example noted above, divergences of as little as half a million years can be detected by isolation and use of diverged retroelements.

13.6 Retroelement Distribution

Although the genomes of many plant species are littered with thousands of copies of different retrotransposons, the different elements are not distributed at random in the genome. The most extreme example involves the CR elements in the grass family, which are present almost exclusively at the centromeres (Ananiev et al. 1998) and continue to show activity. They are thought to have specificity for integration, perhaps through recognition of different chromatin domains. Other retroelements in maize are more abundant near the centromeres, whereas still others are more abundant at more distal locations (Lamb et al. 2007b). Some few are more or less uniformly distributed across the genome.

13.7 Single-Gene, Transgene, and Transposon Detection

High concentrations of DNA polymerase I in nick-translation labeling reactions using Texas Red fluorochromes make possible visualization of chromosome segments as short as 2–3 kb. Because many genes are at least this long, they can be localized to chromosomal position (Fig. 13.1). Using single-gene detection, one can develop a made-to-order karyotyping cocktail or use individual gene probes to confirm the identities of chromosomes labeled with repetitive sequences (Lamb et al. 2007a;

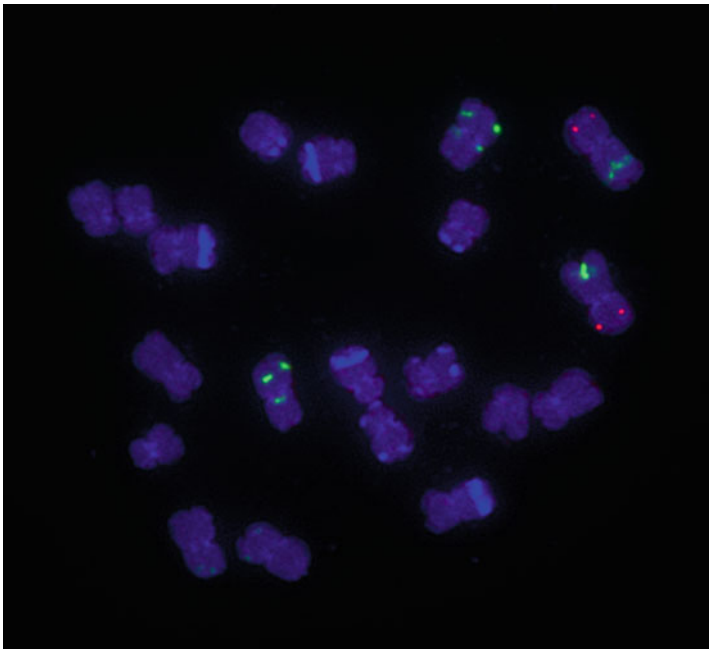

Fig. 13.1 Development of single-locus probes. The sequence of the cDNA was used to develop a probe for the *dek1* gene by RT-PCR (Lamb et al. 2007a). It hybridizes to the short arm of chromosome 1, the known location of *dek1*. Probe size is 7.0 kb; *dek1* signal is *red*; TAG microsatellite (Kato et al. 2004) is *green*. Inbred KYS maize was used for the chromosome preparation

Han et al. 2006). Most transgenes can be located to chromosomal position in this way (Yu et al. 2006, 2007a, b). This type of analysis can reveal the number of insertion sites resulting from a transformation event and the approximate genomic location.

The same principle can be used to visualize transposons that transpose by way of a DNA intermediate, because they are typically large enough (Yu et al. 2007b). Activator, Suppressor-mutator, and Mutator in maize have been tested. Transposition events for Activator and a modified Mutator (RescueMu) could be documented, in the form of cells with both a missing progenitor site and a new insertion. This approach should be useful in studying the behavior of transposons in individual cells and with a genome-wide view.

13.8 Bacterial Artificial Chromosomes as FISH Probes

In many plant species, bacterial artificial chromosomes (BACs) are used in FISH experiments (Jiang et al. 1995; Dong et al. 2000; Sadder et al. 2000; Islam-Faridi et al. 2002; Kim et al. 2002; Koumbaris and Bass 2003; Amarillo and Bass 2007). In species with few transposable elements, BACs provide sufficient probe and target length to be easily detected (Lysák et al. 2001), but in species with many such

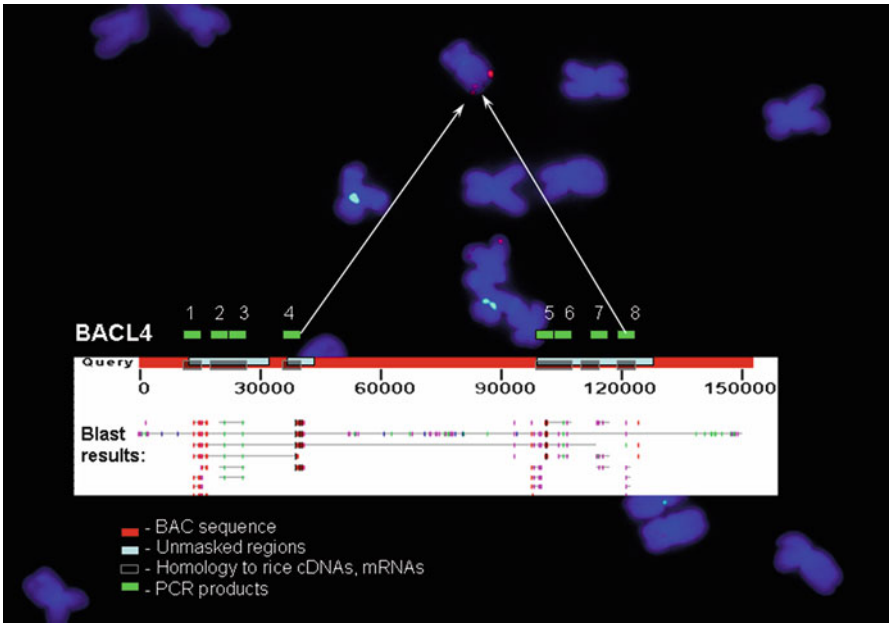

Fig. 13.2 Development of a pooled bacterial artificial chromosome (BAC) probe. The BAC-L4 (AC187803) clone sequence was used to develop a probe for chromosome arm 9L. The repeat free fragments of the BAC clone were amplified by PCR with BAC DNA as a template and used as a pooled probe. Probe size was 20.8 kb. Inbred KYS maize was used for the chromosome preparation

elements, each BAC will contain many copies of the most abundant elements and will hybridize to all chromosomes. To overcome this problem in maize, Lamb et al. (2007a) and Danilova and Birchler (2008) surveyed sequenced BACs for the unique or genic sequences. The repetitive elements were removed from consideration. The individual unique sequences were tested for hybridization to all chromosomes. For those that passed these tests of uniqueness, the collection from a BAC was pooled and used for FISH (see Fig. 13.2). Although the length of any one individual fragment is insufficient to produce a detectable signal, the pool is easily visualized, even though the individual contributors to a pool can be separated by tens of kilobases. This approach is useful for localizing unplaced BACs in the genome and for correlating the physical and cytological maps of a species.

13.9 Banding Paints

In the absence of whole-chromosome paints, "banding paints" can be produced that demark various sites along a chromosome (Wang et al. 2006; Amarillo and Bass 2007; Danilova and Birchler 2008), and under some circumstances, have greater precision than whole-chromosome paints because individual sites of interest on a

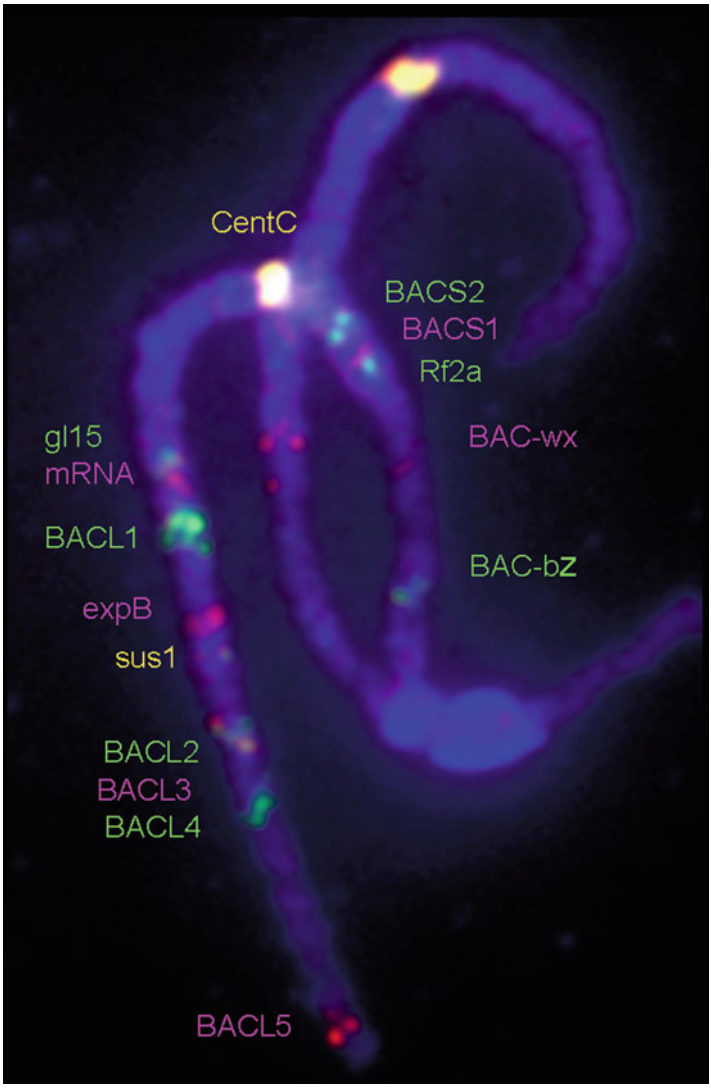

Fig. 13.3 Development of a chromosome banding paint. A series of single genes or BAC-derived probes were labeled with alternating red and green fluorochromes and hybridized to pachytene chromosomes from inbred line KYS (Danilova and Birchler 2008). The banding pattern provides known landmarks on the chromosome with which chromosomal aberrations could be detected or unplaced genes, transposons, or transgenes could be precisely positioned on the chromosome

chromosome can be more easily positioned against individual bands. Banding paints can be constructed from individual genes if they are sufficiently large to be detected or from collections of unique sequences from BACs that can be combined to form a label on the chromosome (Danilova and Birchler 2008). In species in which BACs are sequenced, such banding paints can be produced to order for a particular region of the genome or for particular chromosomes (see Fig. 13.3).

13.10 B Chromosomes

In addition to the normal chromosome set, many hundreds of plant species also harbor supernumerary or B chromosomes (Jones and Rees 1982; Jones and Houben 2003). Typically, these chromosomes behave as if they possess few functional genes and thus must have properties that foster their maintenance in populations. These accumulation mechanisms are varied but usually involve nondisjunction of the B chromosome at some point in the life cycle, such that progeny receives a greater number of these chromosomes. The properties of B chromosomes have been most thoroughly studied in maize and rye.

In maize, the accumulation results from nondisjunction of the B chromosome at the second pollen mitosis, which produces the two sperm. The sperm with the B chromosomes then preferentially fertilizes the egg, leaving the other to fuse with the polar nuclei in the process of double fertilization. An accumulation of up to about 15 B chromosomes is possible in many lines of maize without any obvious detrimental effects. Beyond that level, vigor and fertility are affected. Thus, an upper limit on accumulation prevents the continued increase in numbers of B chromosomes.

Maize B chromosomes are known to possess specific sequences that are not detectable on the normal chromosomes (Alfenito and Birchler 1993; Cheng and Lin 2003) and can be used for B-specific FISH probes, for example, a sequence that appears in and around the centromere (Alfenito and Birchler 1993; Lamb et al. 2005; Jin et al. 2005). Minor representations of this repeat also appear at other sites on the B, especially near the long-arm termini (Lamb et al. 2005). A second B-specific sequence is referred to as the CL repeat (Cheng and Lin 2003). It is present in several blocks in the long arm and at the centromeric region of the B. A third is called the Stark repeat and is heavily concentrated in a heterochromatic region on the long arm of the B (Lamb et al. 2007c). Deletion analysis reveals colocalization of the nondisjunction property to the centromeric region for which the major unique sequence remaining is the B-specific repeat (Han et al. 2006, 2007b).

The rye B chromosome has also been studied by FISH. It also contains multiple B-specific repeats (Sandery et al. 1990; Blunden et al. 1993; Wilkes et al. 1995; Houben et al. 1996). Their nature is unknown, but at least in one case, sequences that appear to lack open reading frames are nevertheless transcribed (Carchilan et al. 2007).

13.11 Endoreduplicated Endosperm Chromosomes

The endosperm results from the fusion of the two polar nuclei in the central cell of the female gametophyte with one sperm to produce a triploid tissue. Initially, the triploid nucleus replicates without cell division, forming a syncytium. Once cellularization occurs, the endosperm cells continue to divide and proliferate. In maize, about 12 days after pollination, DNA replication continues in the absence of cell division, giving rise to endoreduplicated chromosomes. Depending on the inbred

background, the replication number can reach 16 or more copies. Bauer and Birchler (2006) analyzed the structure of these chromosomes using FISH probes of B chromosome-specific and enriched sequences. The whole chromosome could be visualized under these circumstances and revealed that the replicated strands continued to adhere to each other to some degree, particularly at the centromeres and knobs, but sometimes not at scattered neighboring loci. Analysis of the copy number of different sequences suggests that the whole chromosome is replicated equally in these chromosomes.

13.12 Pollen FISH

Pollen can be subjected to FISH for visualization of specific probes in the nuclei (Shi et al. 1996a; Rusche et al. 1997, 2001; Han et al. 2006, 2007b). Typically, the reason to examine pollen is to follow the behavior of B chromosomes that are differentially partitioned into the various nuclei, as in the two sperm in maize. B-specific probes that are detected in one but not the other sperm reveal cases of nondisjunction (Shi et al. 1996a; Han et al. 2007b).

13.13 Minichromosomes

Engineered minichromosomes have been produced, by means of telomere truncation, that can serve as artificial chromosome platforms for high fidelity of gene expression and to which new genes can be added sequentially (Yu et al. 2007a). FISH can be used to reveal which chromosome has been truncated as well as to visualize the truncating transgene (Yu et al. 2006, 2007a). With these techniques, the presence of a truncated minichromosome can be determined early in the transformation process by examination of root-tip chromosomes from regenerated seedlings induced to differentiate from transformed callus or from the callus itself. FISH can also be used to follow the inheritance of small chromosomes (Kato et al. 2005; Han et al. 2007a).

13.14 Meiosis

Chromosome-painting cocktails can be applied to meiotic chromosomes (Wang and Chen 2005; Wang et al. 2006) as well as to somatic chromosomes to distinguish each of the pairs of homologues in diakinesis or metaphase (Kato et al. 2004). Individual loci have been visualized on meiotic chromosomes (Wang et al. 2006), and sorghum BACs with genes homologous to those of maize can be used to produce cytogenetic maps and to determine syntenic relationships between maize and sorghum (Koumbaris and Bass 2003; Amarillo and Bass 2007).

13.15 Primed In Situ Labeling of Plant Chromosomes

Primed in situ labeling (PRINS) is a method for physical mapping that combines PCR accuracy and sensitivity with FISH to visualize sequences on chromosomes (Koch et al. 1989, 1991; Gosden et al. 1991; Yang et al. 2001). It is based on the annealing to denatured chromosomes of short, sequence-specific unlabeled DNA, which serves as a primer for chain elongation in situ catalyzed by a DNA polymerase in the presence of labeled nucleotides. Depending on the type of modified nucleotide used, labeled chromosomal sites can be detected by means of a specific fluorescent antibody (indirect PRINS) or directly visualized by fluorescence microscopy (direct PRINS). The polymerase chain reaction can be used to amplify the sequence that has undergone primed synthesis on the chromosome (cycling PRINS or PCR-PRINS), producing an increase of signal intensity (Gosden et al. 1991; Harrer et al. 2001; Kubaláková et al. 2001).

PRINS can be faster, cheaper, more sensitive, and more accurate than FISH with probes labeled by nick translation. First, labeled probe is not needed; PRINS labeling lasts from 1 to 4 h (depending on number of cycles and method of detection). Second, unlabeled 18–35-bp oligonucleotides used as PRINS probes have better access to the chromosomal target than do long FISH probes (Pellestor et al. 2006). Moreover, they can be applied in high concentration without increasing the background noise, because only that chromosomal site will be labeled where the probe is both annealed and elongated. PRINS can therefore be used to differentiate between closely related sequences; for example, human chromosomes 13 and 21 were distinguished by labeling of centromeric α-satellite DNA when a one-base pair mismatch at the 3′ end was sufficient to distinguish them (Pellestor et al. 1994; Yang et al. 2001). Third, under optimal conditions, the ratio of incorporation of labeled nucleotides during PRINS is higher than in nick translation (Koch et al. 1989). Because chromatin DNA is highly condensed and accumulates random nicks during chromosome preparation, elongation and amplification of a long DNA sequence is difficult (Harrer et al. 2001) and depends on PCR conditions and methods used for chromosome pretreatment. The optimum DNA size for efficient extension and amplification during PRINS has been estimated to be approximately 550–1,000 bp (Gosden and Lawson 1994; Paskins et al. 1999). Therefore, location of a unique chromosomal site requires amplifying the signal by means of PCR-PRINS, indirect PRINS, tyramide signal amplification (TSA), use of multiple primers to label a longer sequence, or a combination of these methods. These approaches were used on human metaphase chromosomes to localize a 0.2–2.1-kb single-copy sequence, to identify allelic differences and subtle chromosomal rearrangements in tumor cells, and to screen mutations (Cinti et al. 1993; Kadandale et al. 2000, 2002; Harrer et al. 2001; Tharapel and Kadandale 2002; Stuppia et al. 2006; Wachtel and Tharapel 2006). The PRINS procedure can be modified to use multiple colors (Gosden and Lawson 1994; Pellestor et al. 1995; Yan et al. 2001). Fast four-color direct PRINS labeling of α-satellite DNA was applied for simultaneous detection of four pairs of human chromosomes (Pellestor 2006; Pellestor et al. 2002, 2006).

PRINS has been successfully used in some plant species (barley, wheat, rye, field bean, pea, soybean, lupine, rice, maize), mostly for repetitive DNA labeling of microsatellites, tandem repeats, telomeres, and ribosomal genes (reviewed by Macas et al. 2000; Kubaláková et al. 2001; Tatum and Rayburn 2006; Kaczmarek et al. 2007). PRINS labeling of repetitive DNA was used for banding paints of wheat, barley, and field bean chromosomes, which allows karyotyping and detection of chromosomal rearrangements (Kubaláková et al. 2000; Vrána et al. 2000), for phylogenetic studies of *Vicia* species (Macas et al. 2003, 2006) and for sex-chromosome studies in *Silene latifolia* Poir. (Hobza et al. 2006). Although PRINS labeling of plant chromosomes is not yet used routinely for detection of small single-copy sequences, some successful results have been reported; the B-hordein cluster of 10–15 genes was detected on barley chromosomes (Abbo et al. 1993) and indirect PCR-PRINS was used to detect RFLP loci in soybean (Zhu et al. 1995; Shi et al. 1996b) and single loci in lupine (Kaczmarek et al. 2007). Direct PCR-PRINS was used for localizing transgenes in rice (Saha et al. 2006). Since the late 1990s, a large number of articles and books describing the PRINS technique in detail have been published (e.g., Harrer et al. 2001; Kubaláková et al. 2001; Pellestor 2006).

Acknowledgments Research on this topic in our laboratory is supported by National Science Foundation grants DBI 0423898, DBI 0421671, and DBI 0701297.

References

Abbo S, Dunford RP, Miller TE, Reader SM, King IP (1993) Primer-mediated in situ detection of the B-hordein gene cluster on barley chromosome 1H. *Proc Natl Acad Sci USA* 90: 11821–11824

Alfenito MR, Birchler JA (1993) Molecular characterization of a maize B chromosome centric sequence. *Genetics* 135:589–597

Amarillo FIE, Bass HW (2007) A transgenomic cytogenetic sorghum (*Sorghum propinquum*) bacterial artificial chromosome fluorescence in situ hybridization map of maize (*Zea mays* L.) pachytene chromosome 9, evidence for regions of genome hyperexpansion. *Genetics* 177:1509–1526

Ananiev EV, Phillips RL, Rines HW (1998) Chromosome-specific molecular organization of maize (*Zea mays* L.) centromeric regions. *Proc Natl Acad Sci USA* 95:13073–13078

Bauer MJ, Birchler JA (2006) Organization of endoreduplicated chromosomes in the endosperm of *Zea mays* L. *Chromosoma* 115:383–394

Blunden R, Wilkes TJ, Forster JW, Jimenez MM, Sandery MJ, Karp A, Jones, RN (1993) Identification of the E3900 family, a second family of rye B chromosome B-specific repeated sequences. *Genome* 36:706–711

Carchilan M, Delgado M, Ribeiro T, Costa-Numes, Caperta A, Morais-Cecilio L, Jones RN, Viegas W, Houben A (2007) Transcriptionally active heterochromatin in rye B chromosomes. *Plant Cell* 19:1736–1749

Cheng Y, Lin B (2003) Cloning and characterization of maize B chromosome sequence derived from microdissection. *Genetics* 164:299–310

Cinti C, Santi S, Maraldil NM (1993) Localization of single copy gene by PRINS technique. *Nucleic Acids Res* 21:5799–5800

Danilova TV, Birchler JA (2008) Integrated cytogenetic map of mitotic metaphase chromosome 9 of maize: resolution, sensitivity, and banding paint development. *Chromosoma* 117:345–356

De Jong JH, Fransz P, Zabel P (1999) High resolution FISH in plants – techniques and applications. *Trends Plant Sci* 4:258–263

Dong F, Song J, Naess S K, Helgeson JP, Gebhardt C, Jiang J (2000) Development and applications of a set of chromosome-specific cytogenetic DNA markers in potato. *Theor Appl Genet* 101:1001–1007

Gosden J, Lawson D (1994) Rapid chromosome identification by oligonucleotide-primed in situ DNA synthesis (PRINS). *Hum Mol Genet* 3:931–936

Gosden J, Hanratty D, Starling J, Fantes J, Mitchell A, Porteous D (1991) Oligonucleotide primed in situ DNA synthesis (PRINS): a method for chromosome mapping, handing and investigation of sequence organization. *Cytogenet Cell Genet* 57:100–104

Han F, Fedak G, Benabdelmouna A, Armstrong K, Ouellet T (2003) Characterization of six wheat × *Thinopyrum intermedium* derivatives by GISH, RFLP and multicolor GISH. *Genome* 46:490–495

Han F, Lamb J, Birchler J (2006) High frequency of centromere inactivation resulting in stable dicentric chromosomes of maize. *Proc Natl Acad Sci USA* 103:3238–3243

Han F, Gao Z, Yu W, Birchler JA (2007a) Minichromosome analysis of chromosome pairing, disjunction and sister chromatid cohesion in maize. *Plant Cell* 19:3853–3863

Han F, Lamb JC, Yu W, Gao Z, Birchler JA (2007b) Centromere function and nondisjunction are independent components of the maize B chromosome accumulation mechanism. *Plant Cell* 19:524–533

Harrer T, Schwinger E, Mennicke K (2001) A new technique for cycling *in situ* amplification and a case report about amplification of a single copy gene sequence in human metaphase chromosomes through PCR-PRINS. *Hum Mutat* 17:131–140

Hobza R, Lengerova M, Svoboda J, Kubekova H, Kejnovsky E, Vyskot B (2006) An accumulation of tandem DNA repeats on the Y chromosome in *Silene latifolia* during early stages of sex chromosome evolution. *Chromosoma* 115:376–382

Houben A, Kynast RG, Heim U, Hermann H, Jones RN, Forster JW (1996) Molecular cytogenetic characterisation of the terminal heterochromatic segment of the B-chromosome of rye (*Secale cereale*). *Chromosoma* 105:97–103

Islam-Faridi MN, Childs KL, Klein PE, Hodnett G, Menz MA, Klein RR, Rooney WL, Mullet JE, Stelly DM, Price HJ (2002) A molecular cytogenetic map of sorghum chromosome 1: Fluorescence in situ hybridization analysis with mapped bacterial artificial chromosomes. *Genetics* 161:345–353

Jiang J, Gill BS, Wang GL, Ronald PC, Ward DC (1995) Metaphase and interphase fluorescence in situ hybridization mapping of the rice genome with bacterial artificial chromosomes. *Proc Natl Acad Sci USA* 92:4487–4491

Jin W, Lamb JC, Vega JM, Dawe RK, Birchler JA, Jiang J (2005) Molecular and functional dissection of the maize B chromosome centromere. *Plant Cell* 17:1412–1423

Jones RN, Houben A (2003) B chromosomes in plants: escapees from the A chromosome genome? *Trends Plant Sci* 8:417–423

Jones RN, Rees H (1982) *B Chromosomes,* 1st edn. Academic Press, London, New York

Kaczmarek A, Naganowska B, Wolko B (2007) PRINS and C-PRINS: promising tools for the physical mapping of the lupin genome. *Cell Mol Biol Lett* 12:16–24

Kadandale JS, Wachtel SS, Tunca Y, Wilroy RS, Martens PR, Tharapel AT (2000) Localization of *SRY* by primed *in situ* labeling in XX and XY sex reversal. *Am J Med Genet* 95:71–74

Kadandale JS, Wachtel SS, Tunca Y, Martens PR, Wilroy RS, Tharapel AT (2002) Deletion of *RBM* and *DAZ* in azoospermia: evaluation by PRINS. *Am J Med Genet* 107:105–108

Kato A (1999) Air drying method using nitrous oxide for chromosome counting in maize. *Biotech Histochem* 74:160–166

Kato A, Lamb JC, Birchler JA (2004) Chromosome painting using repetitive DNA sequences as probes for somatic chromosome identification in maize. *Proc Natl Acad Sci USA* 101:13554–13559

Kato A, Zheng Y-Z, Auger DL, Phelps-Durr T, Bauer MJ, Lamb JC, Birchler JA (2005) Minichromosomes derived from the B chromosome of maize. *Cytogenet Genome Res* 109:156–165

Kato A, Albert PS, Vega JM, Birchler JA (2006) Sensitive FISH signal detection in maize using directly labeled probes produced by high concentration DNA polymerase nick translation. *Biotech Histochem* 81:71–78

Kim J-S, Childs KL, Islam-Faridi MN, Menz, MA, Klein RR, Klein PE, Price HJ, Mullet JE, Stelly DM (2002) Integrated karyotyping of sorghum by in situ hybridization of landed BACs. *Genome* 45:402–412

Koch J, Kolvraa S, Petersen KB, Gregersen N, Bolund L (1989) Oligonucleotide-priming methods for the chromosome-specific labeling of alpha satellite DNA in situ. *Chromosoma* 98:259–265

Koch J, Hindkjaer J, Mogensen J, Kolvraa S, Bolund L (1991) An improved method for chromosome-specific labeling of satellite DNA in situ by using denatured double-stranded DNA probes as primers in a primed in situ labeling (PRINS) procedure. *Genet Anal Tech Appl* 8:171–178

Koumbaris GL, Bass HW (2003) A new single-locus cytogenetic mapping system for maize (*Zea mays* L.): overcoming FISH detection limits with marker-selected sorghum (*S. propinquum* L.) BAC clones. *Plant J* 35:647–659

Kubaláková M, Lysák MA, Vrána J, Šimková H, íhalíková J, Doležel J (2000) Rapid identification and determination of purity of flow-sorted plant chromosomes using C-PRINS. *Cytometry* 41:102–108

Kubaláková M, Vrána J, Číhalíková J, Lysák MA, Doležel J (2001) Localisation of DNA sequences on plant chromosomes using PRINS and C-PRINS. *Methods Cell Sci* 23:71–82

Lamb JC, Birchler JA (2006) Retroelement genome painting: cytological visualization of retroelement expansions in the genera *Zea* and *Tripsacum. Genetics* 173:1007–1021

Lamb JC, Kato A, Birchler JA (2005) Sequences associated with A chromosome centromeres are present throughout the maize B chromosome. *Chromosoma* 113:337–349

Lamb JC, Danilova TV, Bauer MJ, Meyer JM, Holland JJ Jensen MD, Birchler JA (2007a) Single-gene detection and karyotyping using small-target fluorescence in situ hybridization on maize somatic chromosomes. *Genetics* 175:1047–1058

Lamb JC, Meyer, JM, Corcoran B, Kato A, Han F, Birchler JA (2007b) Distinct chromosomal distributions of highly repetitive sequences in maize. *Chromosome Res* 15:33–49

Lamb JC, Riddle NC, Cheng Y, Theuri J, Birchler JA (2007c) Localization and transcription of a retrotransposon-derived element on the maize B chromosome. *Chromosome Res* 15:33–49

Lysák MA, Fransz PF, Ali HBM, Schubert I (2001) Chromosome painting in *Arabidopsis thaliana*. *Plant J* 28:689–697

Macas J, Požárková D, Navrátilová A, Nouzová M, Neumann P (2000) Two new families of tandem repeats isolated from genus *Vicia* using genomic self-priming PCR. *Mol Gen Genet* 263:741–751

Macas J, Navrátilová A, Mészáros T (2003) Sequence subfamilies of satellite repeats related to rDNA intergenic spacer are differentially amplified on *Vicia sativa* chromosomes. *Chromosoma* 112:152–158

Macas J, Navrátilová A, Koblížková A (2006) Sequence homogenization and chromosomal localization of VicTR-B satellites differ between closely related *Vicia* species. *Chromosoma* 115:437–447

Paskins L, Brownie J, Bull J (1999) In situ polymerase chain reaction and cycling primed in situ amplification: improvements and adaptations. *Histochem Cell Biol* 111:411–416

Pellestor F (ed.) (2006) *PRINS and in Situ PCR Protocols,* 2nd edn. *Methods in Molecular Biology Vol. 334*. Humana Press, Totowa, New Jersey

Pellestor F, Girardet A, Andréo B, Charlieu J (1994) A polymorphic alpha satellite sequence specific for human chromosome 13 detected by oligonucleotide primed in situ labeling (PRINS). *Hum Genet* 94:346–348

Pellestor F, Girardet A, Lefort G, Andréo B, Charlieu JP (1995) Use of the primed in situ labeling (PRINS) technique for a rapid detection of chromosomes 13, 16, 18, 21, X and Y. *Hum Genet* 95:12–17

Pellestor F, Malki S, Andréo B, Lefort G (2002) Ultra-rapid multicolor PRINS protocol for chromosome detection in human sperm. *Chromosome Res* 10:359–367

Pellestor F, Paulasova P, Andréo B, Lefort G, Hamamah S (2006) Multicolor PRINS and multicolor PNA. *Cytogenet Genome Res* 114:263–269

Rusche ML, Mogensen HL, Shi L, Keim P, Rougier M, Chaboud A, Dumas C (1997) B chromosome behavior in maize pollen as determined by a molecular probe. *Genetics* 147:1915–1921

Rusche ML, Mogensen HL, Chaboud A, Faure J-E, Rougier M, Keim P, Dumas C (2001) B chromosomes of maize (*Zea mays* L.) are positioned nonrandomly within sperm nuclei. *Sex Plant Reprod* 13:231–234

Sadder, MT, Ponelies N, Born U, Weber G (2000) Physical localization of single-copy sequences on pachytene chromosomes in maize (*Zea mays* L.) by chromosome in situ suppression hybridization. *Genome* 43:1081–1083

Saha P, Majumder P, Dutta I, Ray T, Roy SC, Das S (2006) Transgenic rice expressing *Allium sativum* leaf lectin with enhanced resistance against sap-sucking insect pests. *Planta* 223:1329–1343

Sandery MJ, Forster JW, Blunden R, Jones RN (1990) Identification of a family of repeated sequences on the rye B-chromosome. *Genome* 33:908–913

Schrock E, du Manoir S, Veldman T, Schoell B, Wienberg J, Ferguson-Smith M A, Ning Y, Ledbetter DH, Bar-Am I, Soenksen D, Garini Y, Ried T (1996) Multicolor spectral karyotyping of human chromosomes. *Science* 273:494–497

Schwarzacher T, Leitch AR, Bennett MD, Heslop-Harrison JS (1989) In situ localization of parental genomes in a wide hybrid. *Ann Bot (Lond)* 64:315–324

Shi L, Zhu T, Mogensen HL, Keim P (1996a) Sperm identification in maize by fluorescence in situ hybridization. *Plant Cell* 8:815–821

Shi L, Zhu T, Morgante M, Rafalski JA, Keim P (1996b) Soybean chromosome painting: a strategy for somatic cytogenetics. *J Hered* 87:308–313

Speicher MR, Ballard SG, Ward DC (1996) Karyotyping human chromosomes by combinatorial multi-fluor FISH. *Nat Genet* 12:368–375

Stuppia L, La Sala D, Cinti C (2006) Combined fluorescence in situ hybridization and PRINS for the analysis of the *Dystrophin* gene. *Methods Mol Biol* 334:115–132

Tatum TC, Rayburn AL (2006) PRINS-labeled knobs are not associated with increased chromosomal stickiness in the maize *st1* mutant. *J. Hered* 97:417–422

Tharapel AT, Kadandale JS (2002) Primed in situ labeling (PRINS) for evaluation of gene deletions in cancer. *Am J Med Genet* 107:123–126

Vrána J, Kubaláková M, Šimková H, íhalíková, Lysák MA, Doležel J (2000) Flow sorting of mitotic chromosomes in common wheat (*Triticum aestivum* L.). *Genetics* 156:2033–2041

Wachtel SS, Tharapel AT (2006) PRINS for mapping single-copy genes. *Methods Mol Biol* 334:33–40

Wang CJ, Chen CC (2005) Cytogenetic mapping in maize. *Cytogenet Genome Res* 109:63–69

Wang, CJ, Harper L Cande WZ (2006) High-resolution single-copy gene fluorescence in situ hybridization and its use in the construction of a cytogenetic map of maize chromosome 9. *Plant Cell* 18:529–544

Wilkes TM, Francki MG, Langridge P, Karp A, Jones RN, Forster JW (1995) Analysis of rye B-chromosome structure using fluorescence in situ hybridization (FISH). *Chromosome Res* 3:466–472

Yan J, Bronsard M, Drouin R (2001) Creating a new color by omission of 3′ end blocking step for simultaneous detection of different chromosomes in multi-PRINS technique. *Chromosoma* 109:565–570

Yang J, Schwinger E, Mennicke K (2001) Primed in situ labeling: sensitivity and specificity for detection of α-satellite DNA in the centromere regions of chromosomes 13 and 21. *Cytogenet Cell Genet* 95:28–33

Yu W, Lamb JC, Han F, Birchler JA (2006) Telomere-mediated chromosomal truncation in maize. *Proc Natl Acad Sci USA* 103:17331–17336

Yu W, Han F, Gao Z, Vega JM, Birchler JA (2007a) Construction and behavior of engineered minichromosomes in maize. *Proc Natl Acad Sci USA* 104:8924–8929

Yu W, Lamb JC, Han F, Birchler JA (2007b) Cytological visualization of DNA transposons and their transposition pattern in somatic cells of maize. *Genetics* 175:31–39

Zhu T, Shi L, Keim P (1995) Detection by in-situ fluorescence of short, single copy sequences of chromosomal DNA. *Plant Mol Biol Rep* 13:270–277

Chapter 14
Plant Cytogenetics in Genome Databases

Lisa C. Harper, Taner Z. Sen, and Carolyn J. Lawrence

Abstract Cytogenetic maps provide an integrated representation of genetic and cytological information that can be used to enhance genome and chromosome research. As genome analysis technologies become more affordable, the density of markers on cytogenetic maps increases, making these resources more useful as an information-rich visual context for research. As the accessibility of online bioinformatics and database resources grows, the primary points of access to cytogenetic data and tools will be through online resources. Here we define cytogenetic maps and distinguish them from other common map types, report and discuss the cytogenetic maps and tools currently available for plants, and describe how to access these cytogenetic resources online.

Keywords Plants · Cytogenetic maps · Genetic maps · Databases · Cytology · Chromosomes · Genetics · Recombination

Abbreviations

μm	Micrometers
BACs	Bacterial artificial chromosomes
cM	centiMorgan

L.C. Harper (✉)
USDA-ARS-PGEC, 800 Buchanan Street, Albany, CA 94710, USA
e-mail: ligule@nature.berkeley.edu

T.Z. Sen
USDA-ARS, 1025 Crop Genome Informatics Lab, Iowa State University, Ames, IA 50011, USA

C.J. Lawrence
Corn Insects and Crop Genetics Research Unit, USDA-ARS, 1034 Crop Genome Informatics Laboratory, Iowa State University, Ames, IA 50011, USA

H.W. Bass and J.A. Birchler (eds.), *Plant Cytogenetics*, Plant Genetics and Genomics: Crops and Models 4, DOI 10.1007/978-0-387-70869-0_14,

cMC	centiMcClintock
ENs	Early nodules
FISH	Fluorescence in situ hybridization
FPC	Fingerprint contig
MaizeGDB	Maize Genetics and Genomics Database
RNs	Late recombination nodules
TB	Translocations with the B chromosome

Contents

14.1 What Sorts of Chromosomal Maps Exist?

Two basic types of maps are used: recombination and physical. Recombination maps (also called genetic maps) provide measurements of meiotic crossing-over between loci, whereas physical maps report actual distances. Examples of physical maps include fingerprint contigs (FPC) of bacterial artificial chromosomes (BACs; Pampanwar et al. 2005), optical maps (reviewed by Anantharaman et al. 1997), and cytological maps. Whereas FPC and optical maps are reported in base pairs, cytological maps are reported in relative terms (described in detail below).

14.2 What Is a Cytogenetic Map?

Cytogenetic maps integrate information from cytological and genetic maps, so defining them requires clear definitions of both genetic and cytological maps.

Genetic maps are based on the percentage of recombination between markers; 1% recombination is 1 centiMorgan (cM). Genetic maps therefore accurately report the linear order of markers along a chromosome and the amount of recombination

between them, but they provide no information on physical distance between markers because the amount of crossing-over is not uniform along any chromosome.

Cytological maps are created by microscopic examination of fixed and stained condensed mitotic or meiotic chromosomes and show the positions of centromeres, knobs, chromomeres, C and G bands, Fluorescence in situ hybridization (FISH) signals, or other visible features along a chromosome. Positions are reported as percentages of total chromosome arm length from the centromere to the telomere; they can be given negative values on the short arm and positive values on the long arm. The unit of measurement is the centiMcClintock (cMC); 1% of total arm length is defined as 1 cMC. For example, position 0.83 is 83% of the distance from the centromere to the telomere of the long arm and is therefore closer to the telomere. Like cMs, cMCs represent relative units of measure; the length of 1 cMC in micrometers (μm) will be different on different chromosome arms. Measuring cytologically visible structures in cMCs has been very useful, as the absolute length of any chromosome from any species changes dramatically as chromosomes progress through the cell cycle. In addition, chromosomes fixed in ethanol:acetic acid are about twice as long as identically staged chromosomes fixed in paraformaldehyde (Wang et al. 2006); thus fixation technique affects chromosome length. For cytologically studied species, both the ratio of short-arm length to long-arm length and the position of a visible feature relative to the centromere tend to remain constant irrespective of preparation or cell-cycle stage. In the last 20 years, exciting technical advances in chromosome FISH and image analysis have made possible the determination of the positions of specific DNA sequences on cytological maps (Koumbaris and Bass 2003; Wang and Chen 2005; Wang et al. 2006). Cytological maps show no recombination data, however, and provide no information about the number of base pairs between any two cytological structures. This impediment is overcome by the combination of cytological and genetic information provided by cytogenetic maps.

Cytogenetic maps are used to report integrated data from cytological and genetic maps simultaneously (e.g., see Fig. 14.1). These maps usually take the form of a genetic map placed next to a representation of a chromosome on which the known points of intersection are indicated (e.g., see Harper and Cande 2000; Fig. 14.1a, c, d); both the cytological and genetic positions of individual markers are therefore revealed. Cytogenetic maps can also be represented as single maps drawn in proportion to the cytological map, with the measured genetic and cytological positions of genes marked on the chromosome structure directly (Fig. 14.1e). One specialized sort of cytogenetic map is the recombination nodule map, described in detail below and referred to in Fig. 14.1f.

14.3 In What Ways Are Cytogenetic Maps Useful?

The advantage of integrating information on a cytogenetic map is the enrichment of biological knowledge that results from establishment of relationships between cytological and genetic data. Perhaps the most important information gleaned from

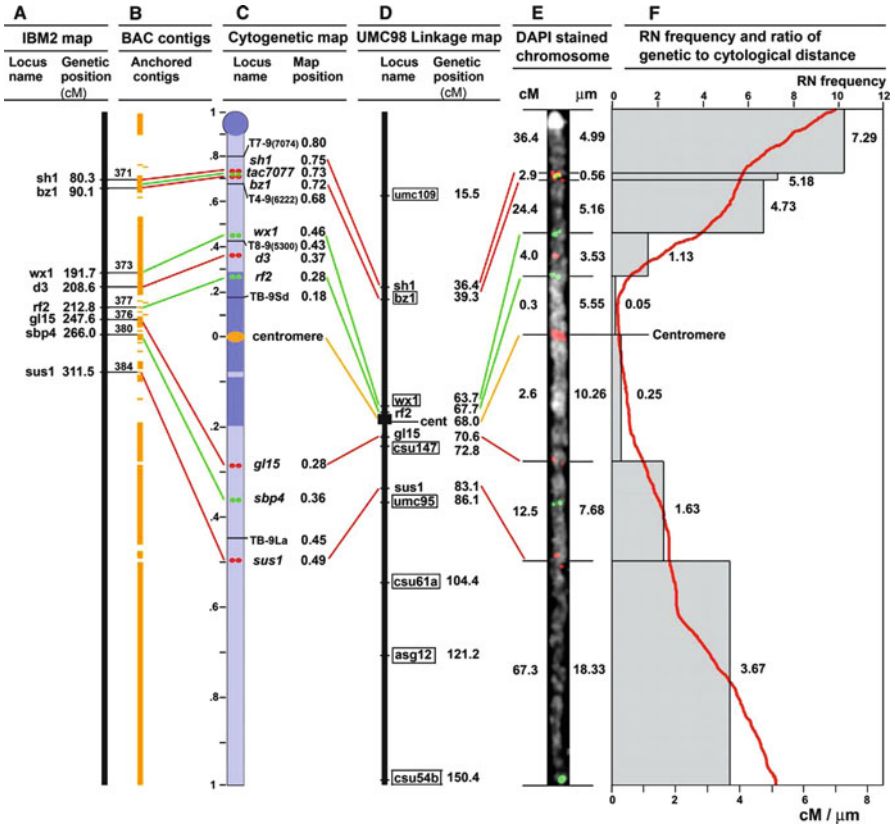

Fig. 14.1 An integrated cytogenetic map of maize chromosome 9 showing comprehensive correlation between cytological gene positions, chromosome structure, genetic maps, the bacterial artificial chromosome (BAC) fingerprint contigs (FPC), and the recombination nodule (RN) map (Wang et al. 2006). (**a**) The high-resolution genetic IBM2 map is shown in part (Maize Genetics and Genomics Database (MaizeGDB); http://www.maizegdb.org/cgi-bin/displaymaprecord.cgi?id=870753). Please note that this map is from an intermated population and that the "cM" displayed here are therefore inflated and are not comparable to those on, e.g., the UMC98 Map in (**d**). (**b**) The genetic coverage of 24 BAC contigs anchored on linkage group 9 is shown along the IBM2 map. The length of the contig corresponds to the position of its corresponding genetic locus on the IBM2 map. Six contigs are anchored to chromosome 9 by nine fluorescence in situ hybridization (FISH) probes in silico, and the serial numbers of these contigs are listed at *left*. (**c**) Ideogram of pachytene chromosome 9 of maize inbred line KYS based on HR gene FISH mapping results in the study by Wang et al. (2006). Heterochromatic and knob regions with bright DAPI staining are shown in *dark blue*. *Green* and *red circles* represent FITC and Cy3 signals, respectively, of FISH generated by the nine-gene probe cocktail. The positions of genes on the chromosome are drawn on the basis of the data in Table 3 of Wang et al. (2006). The breakpoints of several cytogenetic stocks are indicated by *horizontal lines* crossing the chromosome. The chromosomal positions of genes and breakpoints are given at *right* in centiMcClintocks (cMC). (**d**) UMC98 genetic map redrawn in part from Davis et al. (1999). *Highlighted boxes* are core bin markers (defined on line at http://www.maizegdb.org/cgi-bin/bin_viewer.cgi). (**e**) Chromosome 9, straightened as described by Wang et al. (2006). DAPI staining was converted to black-and-white images and overlaid with signal images. The genetic distances between genes, reported in centiMorgans (cM), based on the

cytogenetic maps is that the amount of recombination that occurs on average per unit length of chromosome varies widely along a whole chromosome. The most striking example of this variation is the great repression of recombination around centromeres of chromosomes in all nonholocentric organisms (Harper and Cande 2000). In Fig. 14.1, we can see that some markers, such as *rf2*, are genetically very close to the centromere (i.e., almost no recombination takes place between the *rf2* locus and the centromere; 0.3 cM on the UMC98 genetic map), yet the *rf2* locus is physically located rather far from the centromere (0.18 or 18 cMC on the short arm). For the region between the centromere and *rf2*, the ratio of genetic to cytological distance is 1.67×10^{-2} cM/cMC (i.e., 0.3 cM/18 cMC). Compare this ratio to that of a region near the center of the short arm: the ratio of the genetic to cytological distance between the *bz1* and *sh2* loci is 0.967 cM/cMC (i.e., 2.9 cM/3 cMC) on the UMC98 genetic map. The difference, standardized to cM/μm for this chromosome, can be seen in Fig. 14.1f: 0.05 cM/μm as opposed to 5.18 cM/μm – a 100-fold difference!

Cytogenetic maps show us the positions along a chromosome where genetic (meiotic) recombination occurs. Regions with high cM/cMC or cM/μm ratios have higher rates of recombination. In general, distal regions have much more recombination per unit chromosome length than proximal regions. The trend from low recombination at the centromere to high recombination can be seen in Fig. 14.1f. One ramification becomes clear when genes are cloned by walking. Walking to genes is simply high-resolution genetic mapping, followed by comparison of the genetic map to the DNA sequence. Let us say a gene of interest has been genetically mapped to a 0.1-cM region. If this 0.1-cM region is located in the distal regions of a chromosome arm, it will include much less DNA sequence (possibly 100-fold less) than if it were mapped to a 0.1-cM region near a centromere. Likewise, cytogenetic maps can be useful for estimating the lengths of gaps between loci during sequencing when only the genetic positions of given locations are known.

Another advantage of dense cytogenetic maps is that the genetic position of cytological breakpoints can be determined with more accuracy. Stocks carrying chromosomes with known cytological breakpoints are useful for genetics research designed to determine where a locus of interest resides as well as for testing the function of genes located distal to a breakpoint of interest. The problem is that determining which

Fig. 14.1 (continued) UMC98 map are listed at the *left* of the chromosome, and the cytological distances between genes, reported in μm, are shown at the *right* of the chromosome. (**f**) A comparison of RN distribution along the length of chromosome 9 and the distances in cM/μm between genes. The chromosome is represented on the *y*-axis with the short arm on *top*. The *top x*-axis is the number of RN in 0.2-μm intervals along the chromosome, and the *red line* shows the general trend of the RN distribution redrawn from Anderson et al. (2003). The *horizontal bars* represent the ratios of the genetic distances between genes (cM; the value listed to the *left* of the chromosome in (**e**)) to the cytological distances between genes (μm; the value listed to the *right* of the chromosome in (**e**)). The value for each bar is shown to the *right* of the bar. Figure and legend reprinted with permission from Wang et al. (2006), http://www.plantcell.org "Copyright American Society of Plant Biologists"

breakpoints are useful in solving a particular problem can be awfully time-consuming. More efficient use of breakpoint stocks is possible if the cytological breakpoints are integrated with genetic maps. For example, as reviewed by Lawrence et al. (2007), the genetic-to-cytological conversion can be used to simplify experiments designed to determine whether the gene product of a genetically mapped locus acts cell autonomously. In this way, integrating the cytological breakpoint positions with genetic linkage maps can enhance the application of available translocation stocks to genome research, breeding programs, and chromosome-engineering efforts.

14.4 Online Cytogenetic Resources

14.4.1 Individual Cytogenetic Projects

Many funded projects create small databases or project websites to ensure the availability of generated data to other researchers. Examples include Somatic Karyotype Analysis of the Maize Genome (http://karyotypeproject.missouri.edu/), Cytomaize (http://www.cytomaize.org/), and Functional Genomics of Maize Centromeres (http://www.plantcentromeres.org/). Project websites like these usually only persist during the funded project period, so we focus here on longer-term resources.

14.4.2 Maize: Integration of the Genetic Map and the Genetic Positions of Cytological Breakpoints in the Maize Genetics and Genomics Database in the "Genetic Map"

In maize (*Zea mays* L.), the genetic and cytological positions of breakpoints have long been the basis of maize cytogenetic mapping. Breakpoints exist in chromosome rearrangement stocks and include reciprocal translocations, inversions, translocations with the B chromosome (TB), and others (Harper and Cande 2000). A chromosome breakpoint has a consequence in the heterozygous condition: ears are semisterile, and half of the pollen is dead. This phenotype can be scored in the field and can therefore be genetically mapped. The cytological positions of breakpoints on a translocation or inversion can be determined microscopically by an experienced cytologist. In maize, this determination is usually carried out on meiotic chromosomes in pachytene. Because pachytene is also the biological stage at which crossing-over occurs, additional information about meiosis can be gleaned from the maize cytogenetic maps.

A few individuals, for example David Hoisington and Ed Coe, have integrated genetic and cytological maps in maize by collating a large number of data generated by the maize community (Maize Genetics Cooperation Newsletter by Coe 1985; Hoisington and Coe 1987). Currently, this cytogenetic map can be accessed at http://www.maizegdb.org/map.php. Another way of reaching the map is through the Maize Genetics and Genomics Database (MaizeGDB) home page (http://www.maizegdb.org/;

follow the "Maps" link under the "Search Data Centers" on the left-hand-side green box; scroll down this page to the "Genetic 2008" map). When it is updated, newer versions of the "genetic" map will also be located on this webpage. This map contains many markers that produce visible phenotypes and is a compilation of work from many individuals in the maize research community. To locate the breakpoints and their positions, you can use the cytological maps, which are available through the "Cytogenetics" link (also under "Search Data Centers" on the left-hand-side green box of the MaizeGDB home page).

14.4.3 Maize and Tomato: Recombination Nodule Maps Are Used to Infer Genetic Position from a Cytological Position and Vice Versa

A unique kind of cytogenetic map can be generated from a compilation of transmission electron microscopy data on the positions of the actual crossovers. Late recombination nodules are physical manifestations of crossovers (Baker et al. 1996; Froenicke et al. 2002; Marcon and Moens 2003; Moens et al. 2007) and can be seen in transmission electron micrographs of specially prepared pachytene chromosomes (Zickler and Kleckner 1999; Anderson et al. 2003, 2004; Moens et al. 2007). By looking at thousands of chromosomes, Stack, Sherman, Anderson, and coworkers have created chromosome maps that show the position of recombination nodules and thus the positions where crossing-over occurs in both tomato (*Solanum lycopersicum* L.) and maize (Sherman and Stack 1995; Anderson et al. 2003, 2004; Chang et al. 2007).

14.4.3.1 What Is a Recombination Nodule?

Recombination nodules are densely staining protein complexes whose occurrence is correlated with the timing and position of recombination. So-called "early recombination nodules" or "early nodules" (ENs) can be seen from leptotene through early pachytene (the stages of meiosis during which homologous chromosomes are pairing) and colocalize with RAD51, DMC1, and other important recombination proteins (Zickler and Kleckner 1999; Anderson et al. 2001; Anderson and Stack 2005; Moens et al. 2007), which have been shown to be correlated with the degree and position of the recombination initiations required for homologous pairing in meiosis (Franklin et al. 1999; Pawlowski et al. 2003). Later in meiotic prophase, "late recombination nodules" (RNs) appear as ENs disappear. RNs look different from ENs, are much less frequent (about one per chromosome arm), and are correlated with the position and frequency of crossing-over (Zickler and Kleckner 1999; Moens et al. 2007). In addition, important recombination proteins have been localized to late RNs, such as RAD51 and MLH1 (Baker et al. 1996; Froenicke et al. 2002; Moens et al. 2002; Marcon and Moens 2003). MLH1 is required specifically for crossover recombination, and MLH1 maps have been made and used in much the

same way as RN maps have been (Anderson et al. 1999; Froenicke et al. 2002; Calderon and Pigozzi 2006; Sun et al. 2006; Falque et al. 2007; Lyrakou et al. 2007). Usually, one RN is located in each chromosome arm in each meiotic nucleus during pachytene, because one crossover per arm is required to generate a chiasma, which holds homologous chromosomes together until anaphase of the first meiotic division, thus allowing for a reductional division in meiosis, which in turn permits production of haploid gametes. Genetically, a single RN represents 50 cM. Crossing-over occurs in pachytene at the four-strand stage (two homologous chromosomes, each with two sister chromatids – a bilaventbivalent). If one RN is present, one crossover between two nonsister strands has taken place, producing two recombinant chromosomes and two untouched ones (2/4 = 50% = 50 cM).

14.4.3.2 What Is an RN map?

The ultimate purpose of an RN map is to show the likelihood of a recombination occurring at any discrete position along a chromosome. To build an RN map, Anderson et al. (2003) for maize and Sherman and Stack (1995) for tomato prepared meiotic (pachytene) chromosome spreads from thousands of cells and recorded the relative and absolute position of each RN along each chromosome where individual chromosomes were identified by unique features, such as arm ratio and relative total length. To put the measurements on one map per chromosome, they averaged all chromosomes of corresponding chromosome number (e.g., all chromosomes 9s), divided the "average" chromosome into 0.2-μm bins, and counted the number of RNs in each bin. Once a large number of chromosomes had been subjected to this treatment, the frequency of RNs residing in any one bin could be determined. They observed more RNs in the distal parts of the arms than near the centromere and more in euchromatin than in heterochromatin (e.g., see Fig. 14.1d for maize chromosome 9).

Interestingly, the position of an RN along the chromosome can be converted to a recombination value in cM, on the basis that 1 RN = 50 cM (Sherman and Stack 1995; Anderson et al. 2003). For both maize and tomato, the total number of cMs in the genome calculated from the RN map is close, but not identical, to that in linkage maps created by classical genetic mapping. Potential causes of the observed differences are hypothesized, but have not been confirmed experimentally (discussed by Sherman and Stack 1995; Anderson et al. 2003, 2004; Anderson and Stack 2005).

14.4.3.3 Database Resources for the Maize and Tomato RN Maps

The maize RN maps can be viewed at http://www.maizegdb.org (click "Cytogenetics" under "Search Data Centers" in the left-hand-side green box or select "Cytogenetics" from the "Useful pages" pull-down menu at the top of each page, then select the link). There (http://www.maizegdb.org/cytogenetics.php), the "Recombination Nodule Maps 1–10" are accessible from the "Cytogenetics Maps" section. At the Recombination Nodule Map page (http://www.maizegdb.org/RNmaps.php), general information about the maps is listed beside links to the actual data by chromosome

number. These "maps" show a list of 0.2-μm chromosome segments, the number of RNs that falls within each segment, and the conversion to cM.

14.4.3.4 The Morgan2McClintock Translator

In both maize and tomato, Stack and colleagues have demonstrated that RN maps can serve as the basis for translating cytological positions to genetic map positions and vice versa (Sherman and Stack 1995; Anderson et al. 2003). As stated by Anderson et al. (2004), this process is possible because, in both species, (1) each chromosome can be uniquely distinguished in synaptonemal complex spreads, (2) each recombination nodule corresponds to a single crossover, and (3) the frequency of recombination nodules along chromosomal segments can be converted to cM values. The process for translating a genetic position to a predicted cytological location is to adjust the genetic map positions proportionally to match the cM length of the recombination nodule map and to convert the positions from genetic to cytological according to the following formulas:

For short-arm markers:

$$(a_X / A_X) \times A_{RN} = a_{RN},$$

For long-arm markers:

$$([(b_X - C_X) / B_X] \times B_{RN}) + C_{RN} = b_{RN},$$

where A is the cM length of the short arm of the chromosome, B is cM length of the long arm of the chromosome, C is the cM position of the centromere measured from the tip of the short arm, a is the cM position of a marker in the short arm, and b is the cM position of a marker in the long arm. Subscripts X and RN indicate positions extracted from the genetic and recombination nodule maps, respectively.

The predicted cytological position of a marker on the short or long arm of a pachytene chromosome can then be determined by location of the 0.2-μm interval or bin on the cumulative recombination nodule map. These conversions are automated for both maize and tomato (Lawrence et al. 2006) and can be carried out with the Morgan2McClintock Translator (http://www.lawrencelab.org/Morgan2McClintock/). This translator is a powerful tool in the generation of cytogenetic maps.

14.4.4 Maize: Fluorescence in Situ Hybridization Cytogenetic Maps at MaizeGDB

FISH can be used to find individual genes on chromosomes (see, e.g., Cabrera et al. 2002; Koumbaris and Bass 2003; Wang and Chen 2005; Jiang and Gill 2006;

Wang et al. 2006). For maize, two groups have done so. Bass and coworkers at Florida State University have used sorghum BACs containing markers highly similar to unique maize markers as FISH probes for maize chromosomes in oat-maize addition lines (Koumbaris and Bass 2003). This work has led to a dense FISH map of maize chromosome 9. Images of the cytological position of each FISH marker, and the resulting cytogenetic map, can be viewed at MaizeGDB. On the cytogenetic page mentioned above, the FSU Cytogenetic FISH 9 map can be seen in the cytogenetic map section (http://www.maizegdb.org/cgi-bin/displaymaprecord.cgi?id=892372). This map can also be accessed through the Map Data Center. The website includes images and cytological positions and allows comparisons to other maps. In addition, Wang et al. (2006) at the University of California, Berkeley, have generated a cytogenetic map of chromosome 9, which also can be accessed from the cytogenetics page at MaizeGDB.

14.4.5 Maize and Other Grasses: Comparing Cytogenetic and Genetic Maps at Gramene

The FSU cytogenetic map is also available at Gramene (http://www.gramene.org/) and can be compared to any map generated for other grasses. From the Gramene home page, go to the pull-down menu on the top bar. Under SEARCH, select "Maps." Next, select "Maize" as the species and "Cytogenetic" as the map. There, the cytogenetic map can be compared to any other map in Gramene that has markers in common with the FSU cytogenetic map.

14.4.5.1 Tomato

The tomato (*S. lycopersicum*) FISH map can be viewed from the Sol Genomics Network at http://sgn.cornell.edu/cview/map.pl?map_id=13. It can be reached in two ways: (1) at the home website (http://sgn.cornell.edu/index.pl), mouse over the "maps" link on the top of the page to reach the drop-down menu and choose "Tomato FISH map," or (2) follow the "Tomato" link under the title "SOL Species" in the box located on the right hand side, and then click on "Tomato FISH map" under the subheading "Available maps." This map combines the results of experimental work by many research groups, including those of Stack (Colorado State University), de Jong (University of Wageningen), and Cheng (Academy of Sciences in Beijing, China). The map shows euchromatin regions in light blue, heterochromatin regions in dark blue, and FISH-localized BACs in red. The chromosome representation contains links to the information about the cloned BACs and provides options for visualizing the physically mapped regions in a genome browser.

14.4.5.2 Wheat

Online cytogenetic resources for wheat are currently limited. Although wheat genetic maps can be found at GrainGenes (http://wheat.pw.usda.gov/), cytogenetic mapping is limited to deletion stocks, which are located at http://wheat.pw.usda.gov/mEST/ in the form of high-resolution pictures. The deletion breakpoints and marker positions are clearly shown, but no link is given for additional information about each marker. GrainGenes also houses a comprehensive list of wheat genetic maps at http://wheat.pw.usda.gov/ggpages/map_summary.html. In the future, GrainGenes is expected to improve data integration and representation to include more cytogenetic resources for wheat.

Other cytogenetic resources are certain to be forthcoming as cytogenetic maps become more common. As resources become available, these maps are likely to be made available on line through the model-organism and comparative databases.

References

Anantharaman TS, Mishra B, and Schwartz DC (1997) Genomics via optical mapping. II: Ordered restriction maps. *J Comput Biol* 4:91–118

Anderson LK, Stack SM (2005) Recombination nodules in plants. *Cytogenet Genome Res* 109:198–204

Anderson LK, Reeves A, Webb LM, Ashley T (1999) Distribution of crossing over on mouse synaptonemal complexes using immunofluorescent localization of MLH1 protein. *Genetics* 151:1569–1579

Anderson LK, Hooker KD, Stack SM (2001) The distribution of early recombination nodules on zygotene bivalents from plants. *Genetics* 159:1259–1269

Anderson LK, Doyle GG, Brigham B, Carter J, Hooker KD, Lai A, Rice M, Stack SM. (2003) High-resolution crossover maps for each bivalent of *Zea mays* using recombination nodules. *Genetics* 165:849–865

Anderson LK, Salameh N, Bass HW, Harper LC, Cande WZ, Weber G, Stack SM (2004) Integrating genetic linkage maps with pachytene chromosome structure in maize. *Genetics* 166:1923–1933

Baker SM, Plug AW, Prolla TA, Bronner CE, Harris AC, Yao X, Christie DM, Monell C, Arnheim N, Bradley A, Ashley T, Liskay RM (1996) Involvement of mouse Mlh1 in DNA mismatch repair and meiotic crossing over. *Nat Genet* 13:336–342

Cabrera A, Martin A, Barro F (2002) In-situ comparative mapping (ISCM) of Glu-1 loci in *Triticum* and *Hordeum. Chromosome Res* 10:49–54

Calderon PL, Pigozzi MI (2006) MLH1-focus mapping in birds shows equal recombination between sexes and diversity of crossover patterns. *Chromosome Res* 14605–612

Chang SB, Anderson LK, Sherman JD, Royer SM, Stack SM (2007) Predicting and testing physical locations of genetically mapped loci on tomato pachytene chromosome 1. *Genetics* 176: 2131–2138

Coe E, (1985) *Maize Genet Coop Newslett* 59:168–187

Davis GL, McMullen MD, Baysdorfer C, Musket T, Grant D, Staebell M, Xu G, Polacco M, Koster L, Melia-Hancock S, Houchins K, Chao S, Coe EH Jr (1999) A maize map standard with sequenced core markers, grass genome reference points and 932 expressed sequence tagged sites (ESTs) in a 1736-locus map. *Genetics* 152:1137–1172

Falque M, Mercier R, Mezard C, de Vienne D, Martin OC (2007) Patterns of recombination and MLH1 foci density along mouse chromosomes: modeling effects of interference and obligate chiasma. *Genetics* 176:1453–1467

Franklin AE, McElver J, Sunjevaric I, Rothstein R, Bowen B, Cande WZ (1999) Three-dimensional microscopy of the Rad51 recombination protein during meiotic prophase. *Plant Cell* 11:809–824

Froenicke L, Anderson LK, Wienberg J, Ashley T (2002) Male mouse recombination maps for each autosome identified by chromosome painting. *Am J Hum Genet* 71:1353–1368

Harper LC, Cande WZ (2000) Mapping a new frontier; development of integrated cytogenetic maps in plants. *Funct Integr Genomics* 1:89–98

Hoisington D, Coe E (1987) *Maize Genet Coop Newslett* 61:128–147

Jiang J, Gill BS (2006) Current status and the future of fluorescence in situ hybridization (FISH) in plant genome research. *Genome* 49:1057–1068

Koumbaris GL, Bass HW (2003) A new single-locus cytogenetic mapping system for maize (*Zea mays* L.): overcoming FISH detection limits with marker-selected sorghum (*S. propinquum* L.) BAC clones. *Plant J* 35:647–659

Lawrence CJ, Seigfried TE, Bass HW, Anderson LK (2006) Predicting chromosomal locations of genetically mapped loci in maize using the Morgan2McClintock Translator. *Genetics* 172: 2007–2009

Lawrence CJ, Schaeffer ML, Seigfried TE, Campbell DA, Harper LC (2007) MaizeGDB's new data types, resources and activities. *Nucleic Acids Res* 35:D895–D900

Lyrakou S, Mantas D, Msaouel P, Baathalah S, Shrivastav P, Chrisostomou M, Mihalopoulos Y, Hasiakos D, Baka S (2007) Crossover analysis using immunofluorescent detection of MLH1 foci in frozen-thawed testicular tissue. *Reprod Biomed Online* 15:99–105

Marcon E, Moens P (2003) MLH1p and MLH3p localize to precociously induced chiasmata of okadaic-acid-treated mouse spermatocytes. *Genetics* 165:2283–2287

Moens PB, Kolas NK, Tarsounas M, Marcon E, Cohen PE, Spyropoulos B (2002) The time course and chromosomal localization of recombination-related proteins at meiosis in the mouse are compatible with models that can resolve the early DNA-DNA interactions without reciprocal recombination. *J Cell Sci* 115:1611–1622

Moens PB, Marcon E, Shore JS, Kochakpour NK, Spyropoulos B (2007) Initiation and resolution of interhomolog connections: crossover and non-crossover sites along mouse synaptonemal complexes. *J Cell Sci* 120:1017–1027

Pampanwar V, Engler F, Hatfield J, Blundy S, Gupta G, Soderlund C (2005) FPC web tools for rice, maize, and distribution. *Plant Physiol* 138:116–126

Pawlowski WP, Golubovskaya IN, Cande WZ (2003) Altered nuclear distribution of recombination protein RAD51 in maize mutants suggests the involvement of RAD51 in meiotic homology recognition. *Plant Cell* 15:1807–1816

Sherman JD, Stack SM (1995) Two-dimensional spreads of synaptonemal complexes from solanaceous plants. VI. High-resolution recombination nodule map for tomato (*Lycopersicon esculentum*). *Genetics* 141:683–708

Sun F, Oliver-Bonet M, Liehr T, Starke H, Turek P, Ko E, Rademaker A, Martin RH (2006) Variation in MLH1 distribution in recombination maps for individual chromosomes from human males. *Hum Mol Gene*t 15:2376–2391

Wang CJ, Chen CC (2005) Cytogenetic mapping in maize. *Cytogenet Genome Res* 109:63–69

Wang CJ, Harper L, Cande WZ (2006) High-resolution single-copy gene fluorescence in situ hybridization and its use in the construction of a cytogenetic map of maize chromosome 9. *Plant Cell* 18:529–544

Zickler D, Kleckner N (1999) Meiotic chromosomes: integrating structure and function. *Annu Rev Genet* 33:603–754

Chapter 15
Practical Laboratory Exercises for Plant Molecular Cytogenetics

Scott A. Jackson, Shahryar F. Kianian, Khwaja G. Hossain, and Jason G. Walling

Abstract Practical laboratory work parallel with a lecture topic is one way to improve understanding of the subject matter. Cytogenetics deals mainly with chromosome behavior and biology. The key concepts of cytogenetics can be attached to actual experimental observations that can help students visualize the relationship of the concepts to chromosomes in practice. Many new technological developments are available to aid understanding of chromosome behavior, biology, and manipulation for plant and animal improvement. We present here a series of exercises designed to help students understand chromosome behavior during cellular divisions, chromosomal aberrations, and chromosome preparations for molecular cytogenetics, such as fluorescence in situ hybridization (FISH), genomic in situ hybridization (GISH), and even fiber-FISH. These exercises are used in several undergraduate and graduate courses. If they are to be incorporated into a cytogenetics course, we recommend that the instructor choose those that fit the course timetable and available resources.

Keywords Aneuploidy · Deletion line · EST · QTL · Radiation hybrid · SSR · Substitution line

S.A. Jackson (✉)
Department of Agronomy, Purdue University, 915 West State Street, West Lafayette, IN 47907, USA
e-mail: sjackson@purdue.edu

S.F. Kianian (✉)
Department of Plant Sciences, North Dakota State University, 470G Loftsgard Hall, Fargo, ND 58105, USA
e-mail: s.kianian@ndsu.edu

K.G. Hossain
Division of Science and Mathematics, Mayville State University, Mayville, ND 58257, USA

J.G. Walling
Department of Horticulture, University of Wisconsin, 1575 Linden Drive, Madison, WI 53706, USA

H.W. Bass and J.A. Birchler (eds.), *Plant Cytogenetics*, Plant Genetics and Genomics: Crops and Models 4, DOI 10.1007/978-0-387-70869-0_15,

Contents

15.1 Introduction

Practical cytogenetic laboratory exercises done in parallel with a lecture can help reinforce important aspects of students' understanding of chromosome behavior as well as inciting their interest in chromosome biology. Aspects of cytogenetics that seem abstract can be attached to actual experiential observations and cement the relationship of the concept with chromosomes in practice. One example is the examination of chromosomes proceeding through meiosis. Students often perceive meiosis as a rather abstract activity that results in recombined gametes, thereby increasing genetic diversity, but their understanding of how chromosomes proceed through meiosis to accomplish this end result is limited. Therefore, a series of hands-on examples that reinforce lectures can improve students learning experience and deepen their understanding of cytogenetics.

In the past, and unfortunately all too often today, lab exercises were rooted in the past. That is, the exercises consisted almost solely of chromosome preparations from cells undergoing mitosis and/or meiosis or, even worse, of simply looking at premade slides. This activity can be of some value, but to use it as the basis of an entire course will do little to create interest in the subject or to hold students attention. In the series of exercises we present here, students proceed from learning how to use a microscope to making chromosome preparations from mitotic and meiotic cells to looking at chromosome aberrations to using chromosome preparations for molecular cytogenetics, such as fluorescence in situ hybridization (FISH), genomic in situ hybridization (GISH), and even fiber-FISH. These exercises are used in several undergraduate and graduate courses. If they are to be incorporated as part of a cytogenetics course, we recommend that the instructor choose those that fit the course time-table and available resources. At the end, we present two examples of courses taught as possible scenarios (Table 15.1). A practice we have found to be very successful is to encourage graduate students to bring their own materials for use in laboratory exercises. In addition, for a graduate-level course, we have incorporated the use and identification of unknowns and written and oral reporting of findings as part of the grading system to encourage critical thinking.

Table 15.1 Schedule of topics for a laboratory course in plant molecular cytogenetics

Week	Undergraduate	Graduate
1	Basics of microscope use	Basics of microscope use and unknown assignments
2	Mitosis in onions (toluidine blue)	Mitosis in onions
3	Mitosis in onions (Feulgen)	Cereal root tips
4	Cereal root tips	Cereal root tips
5	Meiosis in *Tradescantia*	Meiosis in *Tradescantia*
6	Pollen staining	Pollen staining
7	Early meiosis in maize	Early meiosis in maize or tomato
8	Early meiosis in tomato	Collection of unknowns and beginning of analysis
9	Meiosis in cereals	Meiosis in cereals
10	Meiosis in cereals	Meiosis in aneuploids
11	Meiosis in aneuploids	GISH/FISH
12	Meiosis in mutants	Fiber-FISH
13	Polytene chromosomes	Fiber-FISH
14	Human chromosomes	Presentations and reports on unknowns

Even though much of the course and lab are centered on plants, not all the students will pursue careers in plant sciences, so we incorporate pertinent examples from insects and mammals into the series. We also include the preparation of polytene chromosomes from *Drosophila* and human chromosomes as important nonplant examples.

15.2 Laboratory Exercises

The laboratories gradually increase in complexity over the course of a semester, and we assume at least one 2-h laboratory per week for 13 weeks. We begin the first exercise with basics of microscopy, such as how to adjust, focus, and clean a microscope and how to use phase-contrast and other intricacies. We have left the content of this portion to the individual instructor, because the equipment available varies greatly from institution to institution. After familiarization with microscopes (during which students use old slides from previous classes to learn how to look for objects), we move on to mitosis, meiosis, and other topics. If unknowns are to be introduced in the course, the plants (or other material) are made available to the students at the beginning, with suitable instructions on growing or maintaining them and on what tissue to collect and when. Students are then responsible for those aspects.

A few students always have problems identifying chromosomes under a microscope and distinguishing them from cellular detritus. With early instruction and follow-up reinforcement, this problem tends to be resolved within the first few weeks of the course, and students who move on to make preparations needed by the time unknowns are ready for analysis.

15.2.1 Unknowns

The purpose of this component of the laboratory course, especially in a graduate course, is to encourage critical thinking and discussion in relation to chromosome behavior and critical cellular processes. Seeds of various mutants can be obtained from several sources (refer to http://maizecoop.cropsci.uiuc.edu/othrcntr.php for links to many of these genetic stock centers). The young plants or seeds (depending on the nature and timing of sample collection for making preparations) provided to the students at the beginning of the course fall into three categories:

15.2.1.1 Mutants

A good collection of desynaptic mutants (in which homologous chromosomes pair early but fall apart during diplotene or diakinesis) is available for barley, many of which have been backcrossed to a homogeneous 'Bowman' background (Franckowiak and Lundqvist 2001). Similar mutants are available in wheat, oat, rye, maize, and other plants. We have found the barley mutants easier to use in class for several reasons, including the number and size of chromosomes, as well as the predictable flowering time that results from the homogeneous background.

A number of asynaptic mutants (in which pairing of homologous chromosomes in meiosis I fails completely) are available, but rye and oat mutants tend to be the best for analysis because of their chromosome size (Mikhailova et al. 2001). Rice mutants can also be obtained, but are more difficult to visualize than the other cereals.

Genetic male sterile mutants (in which pollen is aborted for various reasons, even though they proceed through meiosis normally) are available in many plant species, but we again use the mutants in wheat, barley, rye, or oat for ease of observing chromosomes in meiosis and normal pairing and division throughout. Barley mutants have been backcrossed to a homogeneous 'Bowman' background, so coordinating the work on these mutants with the desynaptic ones described earlier is easier (Franckowiak and Lundqvist 2001).

15.2.1.2 Aneuploids

We routinely use monosomics, trisomics, and translocations for unknowns in this category. They are available in many plant species, and seeds can easily be obtained from various genetic stock centers (http://maizecoop.cropsci.uiuc.edu/othrcntr.php). Again cereal (wheat, barley, oat, and rye) aneuploids are our first choice for this work because of the ease with which the large chromosomes can be visualized, but maize and tomato trisomics and translocation stocks can also be used for characterization in early stages of meiosis. A critical thing to remember, as an instructor for the course, is the time to flowering of various plant species and the need to arrange for flowering to occur during the first half of the course, so that students can collect their samples for analysis.

15.2.1.3 Various Ploidy Levels

Polyploids can form the basis for some of the most interesting and challenging unknowns for students. They are available in many plant species, but again we rely on cereals because their chromosome sizes allow for easier visualization. Tetraploids of barley and rye can be used either directly as unknowns or for crossing to diploids to produce triploid progeny for analysis by students. Another option is to use various ploidy levels of wheat (diploid *Triticum monococcum* L. or *T. tauschii* (Coss.) Schmal., tetraploid *T. turgidum* L. or *T. dicoccoides* Koern., and hexaploid *T. aestivum* L.) and progeny from their crosses. In some of these crosses, hybrid necrosis or chlorosis can be an issue, but a number of lines are available that do not carry the genes and are therefore easier to use for this purpose. Chromosome pairing and fertility are some of the important factors students need to observe in these unknowns.

15.2.2 Mitosis Labs

The purpose of these exercises is to introduce the students to light microscopy, preparing chromosome squashes, and distinguishing the chromosomes from other cellular material and to reinforce concepts of chromosome behavior during mitosis.

15.2.2.1 Onion

A number of quick protocols for preparing onion root tips are available on the Internet. We follow the protocol developed by N. R. Parker (1966) called "The four-minute chromosome squash," with some minor modifications. We prefer this technique, as it takes only 3–4 min, can be carried out entirely on the slide, and produces a temporary preparation of excellent quality. Also, the cells are large, and mitotic figures are clear with a dry (about 40×) objective. Essentially, white onions (old and not red) are sprouted, resting atop beakers of a size that permits only the extreme base to touch the water. Tips from roots to 3 cm long give good results. Root tips are cut 1–2 mm behind the root cap onto clean slides. Each tip is then covered with 3–4 drops of 1N HCl and warmed gently (not boiled) over an alcohol flame. Total treatment time should be 1 min. Excess HCl is then removed, and each tip is then covered with 0.5% aqueous toluidine blue. These slides are then warmed gently over an alcohol flame without boiling. Total staining time should be 1 min. Excess stain is removed, and a drop of fresh stain is added. A coverslip is applied and the tip is then firmly squashed in folded paper towel with thumb. Coverslips should not break, and the squash should spread evenly across the slide. Good squashes can be protected from drying by various means, but we prefer making the slides permanent by the Conger and Fairchild (1953) quick-freeze method.

15.2.2.2 Wheat and Other Cereals

Wheat and triticale are used as the biological source, as they have large, easily distinguishable chromosomes, the plants are easy to grow and obtain seed for, the root tips respond well to chromosome-accumulation treatments, and the prepared slides can later be used in the FISH/GISH experiments. Each student should have preparations made from each species and should work on finding chromosomes, counting chromosomes, and describing chromosome morphology (an ideogram can be used as reference). At the beginning of each lecture, every student is given a sheet listing goals for that lab, including space to include chromosome counts, drawings, and morphological descriptions. Making chromosome squashes can get tedious for the students, so be certain to have enough equipment (especially good phase-contrast microscopes) to keep each student busy.

The protocol we use was provided to us by Dr. L. Joppa (an eminent cytogeneticist who developed many of the durum wheat cytogenetic stocks; Joppa 1993) through testing of various protocols. It works well with almost all cereals. Cereal seeds are germinated in petri plates on moist filter paper in the dark. Seeds are maintained at 22°C for 2–3 days, then at 4°C for 3 days (this treatment is critical to break residual dormancy and synchronize cell division), then at 22°C 1–2 days or until the root tips are 1–3 cm long. Two to three root tips are then cut from each seedling and placed in individual vials of a saturated solution of 1-bromo-naphthalene in tap water (this chemical is dangerous, and precautions should be taken to avoid contact with the skin or breathing of the concentrated vapors). Use a syringe or pipet to remove the solution from the middle of container. Leave for 5 h (time is critical at this stage) at 20°C. Do not stopper the vials. Wash the root tips in tap water and fix each one in 2–4 mL of a 1:1 mixture of glacial acetic acid and 95% ethanol. Stopper vials and leave overnight at 10–20°C. Pour off the fixative and put the root tips in 1N HCl at 60°C. After 10–12 min, wash the root tips briefly in tap water and place in leuco-basic fuschin. Stopper the vials and leave for 3 h. Remove the stain, replace it with 70% ethanol, and refrigerate the root tips until used. Obviously, this process cannot be completed in one lab period. Therefore, we routinely prepare the root tips up to this stage and provide these samples to the students for preparation by the following procedure.

Cut off the stained meristematic region of the root tip and place it on a slide in a dilute (0.5%) solution of aceto-carmine (one drop is sufficient). Put on the cover glass and tap with a pencil until fairly well squashed. Add aceto-carmine to the edge of the cover slip and move the cover slip with a dissecting needle to spread the cells. Place the slide on blotter paper and press excess stain from the slide. Do not press the center of the cover slip because the cells may be squeezed out; press instead around its edges.

Good chromosome preparations made by the students should be immediately stored at −80°C (or dehydrated in an ethanol series) until used in later labs. Dry ice or liquid N_2 may be needed for interim storage if a −80°C freezer is not immediately available during the lab. We have previously published detailed protocols for making chromosome squashes to be used for FISH (Walling et al. 2005). Preparation for these labs should be done months in advance – seeds must be germinated; plants

grown; root tips treated, collected, and stored; and panicles collected for use in subsequent meiotic labs. All the materials should be checked beforehand to ensure quality and availability of adequate numbers of cells at mitotic/meiotic stages.

15.2.3 Meiosis

Meiosis is probably the most difficult concept for students to grasp; therefore, the purpose of this lab is to help them cement their understanding of this most fundamental process by seeing chromosomes proceed through various meiotic stages.

15.2.3.1 *Tradescantia*

Tradescantia, commonly known as spiderwort, is a model species for study of the various stages of meiosis. The chromosomes are few (many species have only six chromosomes) and large, and nuclear cycles are timed accurately for sample collection and preparation by students (Sax 1939). Early estimates indicate that the nuclear cycle takes 6 days to go from microspore formation to metaphase in the summer and twice as long in the winter (Sax 1939). Collection of samples are the same as for any other plant species; an initial 24-h fixation of samples in 3:1 ethanol-to-acetic acid solution followed by storage in 70% ethanol solution under refrigeration. These samples can then be analyzed with the simple aceto-carmine or aceto-orcein stain (Sharma and Sharma 1994).

15.2.3.2 Pollen Fertility as a Measure of Cytological Abnormality

This simple but often overlooked method is the quickest means of evaluating possible cytological abnormalities. We like to introduce this procedure before students begin analysis of their unknowns. A number of unknowns, specifically meiotic mutants, often lead students to confused conclusions without insufficient information. We therefore use the simple method of aceto-carmine staining of pollen grains (various older samples used in analysis of meiosis can be used here) to begin discussions on the effects of meiotic aberrations on overall fertility. Trisomics and chromosome aberrations compared with parental controls are excellent samples for analysis at this stage. Further analysis of these samples for stages of meiosis later in the course will help reinforce the concept and its value in obtaining additional data on the status of unknowns.

15.2.3.3 Maize or Tomato

Maize provides ample pollen mother cells (PMCs) in the tassel, so it is an ideal system for analysis by large groups of students, but the chromosomes are small, and good preparations are difficult. Maize is used in our exercises to reinforce the

concept of preparing good meiotic samples. Pachytene analysis in maize allows the identification of knobs and, with luck, chromosomes of maize. In this type of analysis, use of samples from several maize inbred lines is important, as they show variation in the number of knobs.

Tomato provides another option for analysis of chromosomes in early meiosis (pachytene and diplotene). Again, the chromosomes are small, but interesting observations can be made about chromosome morphology or changes in number. Tomato trisomics illustrating various configuration of a trivalent association during early meiosis can form the basis of class discussions on chromosome pairing, formation of synaptonemal complexes, and crossing over (Khush 1973).

15.2.3.4 Barley, Wheat, and Triticale

Again, the easiest examples for this analysis are barley and wheat (usually tetraploid wheat or triticale). The reasons are twofold: large chromosomes and the ease of using panicles to find meiotic stages, which are distributed up and down the spike. Students seem to enjoy this particular exercise. Handouts are provided that include pictures of the various meiotic stages (premeiosis, meiosis I, meiosis II, pollen mitosis), and students are encouraged to draw the stages as they find them. This exercise can be completed in one lab period, but often requires two for the students to find all stages. Because not all the students will find all the stages, sharing of good preparations that illustrate specific meiotic stages is encouraged. Active engagement by the teacher is therefore necessary.

15.2.4 Chromosome Aberrations

One of the most exciting cytological aspects of cytogenetics is visualizing chromosome aberrations – inversions at meiosis, truncated chromosomes, translocations, and many more. Additional stocks that can help reinforce the concept of chromosome pairing during meiosis are nullisomic-tetrasomic stocks of Chinese Spring wheat (Sears 1966) and double monosomic or double ditelosomic stocks of durum wheat (*T. turgidum*, Joppa 1993). These provide excellent samples showing how univalents and multivalents differ from bivalents in meiotic behavior. Many cytogenetic stocks can be obtained from the Wheat Genetics Resource Center at Kansas State University (or *Drosophila* inversion heterozygotes can be used in combination with the polyteny lab). We often use the rye midget chromosome (Murata et al. 1992), which is from rye and necessary for fertility in a wheat-rye alloplasmic background. It is extremely small relative to the wheat chromosomes and difficult to find, but students are usually able to find it. This exercise reinforces several concepts: alloplasmic fertility restorers, chromosome breakage, and segregation in a wheat spike revealed by plump seeds. Spikes are provided in the lab to illustrate segregation of the midget chromosome as revealed by plump seeds, but the students use root-tip preparations to look for the midget chromosome.

15.2.5 Genomic In Situ Hybridization

The first molecular lab is GISH, using materials the students made in the first 2 weeks of lab – triticale mitotic spreads or D-genome chromosome substitutions in durum wheat (Joppa 1993). The objective of this exercise is to introduce the in situ technique as well as to reinforce concepts of polyploidy, specifically allopolyploidy, and chromosome differentiation at the sequence level. Preparation includes isolating and labeling rye or *T. tauschii* (D-genome donor or wheat) genomic DNA to be used as a probe for GISH. Slides containing triticale or D-genome substitution mitotic chromosome spreads are hybridized with labeled rye or *T. tauschii* genomic DNA, respectively, then counterstained so that the nonrye- or D-genome-derived chromosomes can be visualized.

In situ hybridization experiments generally require 2 consecutive days. The first is used for the hybridization and the second for washing, detection, and visualization (Jiang et al. 1996; Zhong et al. 1996). Depending on the number of students, we often break them into two groups. Half do their experiments on two consecutive days of 1 week, and the other half do the same the following week. If the number of fluorescence microscopes for visualization is limited, individuals or small groups can schedule time to use them during nonlab times. This arrangement has been very effective in accommodating everyone, although it requires more of the lab instructor's time.

15.2.6 Fluorescence In Situ Hybridization

The purpose of the FISH exercise is to introduce molecular means of mapping genes to specific chromosomes and to reinforce lecture material on nucleolus organizing regions (NORs). Among the easiest FISH targets are ribosomal gene arrays, either the NOR or the 5S rDNA genes, because these loci consist of thousands of tandemly arrayed genes that are conserved among plants and animals. FISH experiments using NOR genes as a probe result in very bright signals that are easy to distinguish from background and are thus ideal for beginners. We use rDNA probes cloned from wheat using a set of conserved primers (Tsujimoto et al. 1997). These probes are either directly labeled with a fluorophore or labeled with biotin and then hybridized to chromosome preparations from weeks 1 to 4, either mitotic or meiotic (Jiang et al. 1996; Zhong et al. 1996). Meiotic samples are especially helpful, because the students can see the chromosomes' (pairs of NOR signals) pair and align on the metaphase plate, reinforcing chromosome behavior in and during meiosis.

15.2.7 Polytene Chromosomes

The purpose of this lab exercise is to examine endoreduplication without mitosis – polytene chromosomes. The most famous example is, of course, *Drosophila*. This exercise serves a historical purpose as well, as we discuss the importance of

Drosophila in genetics and how polytene chromosomes played an important role in our ability to map genes to chromosomes and to visualize inversions and chromosome banding. Many texts and websites describe how to make polytene-chromosome preparations from *Drosophila* larvae (for example, http://www.yale.edu/ynhti/curriculum/units/1996/5/96.05.01.x.html). This is one of the easiest labs, as the chromosomes are quite large and easy to distinguish. Students take digital images of some of their better preparations as part of the exercise. The most difficult part is helping the students distinguish the salivary glands from the rest of the larval body parts, but once they find the salivary glands, the chromosome squashes are relatively easy. A useful part of the handout is early chromosome banding maps that show the students how scientists have used the banding patterns in the past (Painter 1934). The goal is for the students to use their chromosome preparations to identify the four chromosome pairs.

15.2.8 Fiber-FISH

The Fiber-FISH lab is an optional exercise that we do if time permits, and it is also a popular and easy lab. The students really seem to enjoy visualizing chromosomes at the Watson-Crick level – individual DNA fibers. The purpose is to allow the students to experience some more advanced molecular cytogenetic tools, to gain experience using digital imaging tools to measure and convert microscopic measurements to kilobase pairs of DNA and to see what fluorescently labeled DNA fibers look like.

The protocols are quite easy. Preparation for the lab includes isolating both nuclei and the DNA probes for the in situ hybridization. We generally use *Arabidopsis* nuclei and BACs, as they are easy to deal with and almost no dispersed repeats are present to complicate the interpretation of the results (Jackson et al. 1998). You can reuse the ribosomal probes that were used in previous chromosome FISH labs, as that will tie things together. The students get to see the rDNA loci on chromosomes and then see how big they really are on DNA fibers.

15.2.9 Human Chromosomes

The purpose of this exercise is twofold: first to tie classroom lectures on human chromosome biology to the laboratory and, second, to give additional experience with nonplant chromosomes. Because of health issues involved in dealing with human body fluids, we have recently been using fixed tumor cells (such as those from NeoSci, http://www.neosci.com), according to the manufacturer's protocols. Using tumor cells has the bonus of allowing the students look for chromosome aberrations relative to a standard karyotype, though their preparations are usually not of sufficient quality to allow many inferences. Standard human karyotypes should be provided to the students, and karyotypes for various chromosome abnormalities can also be provided and discussed in the context of the lab exercise.

Acknowledgments We thank the graduate and teaching assistants who have helped teach the cytogenetics laboratory at Purdue University and North Dakota State University. We also thank Drs. Jerome D. Franckowiak at North Dakota State University and Jiming Jiang at the University of Wisconsin-Madison, who previously developed much of the material presented here. Special thanks are due to our dedicated and committed cytogenetics teachers, who have helped teach a new generation about the potential of this often overlooked but powerful branch of science.

References

Conger AD, Fairchild LM (1953) A quick-freeze method for making smear slides permanent. *Stain Tech* 28:281–283

Franckowiak JD, Lundqvist U (2001) Descriptions of barley genetic stocks for 2001. *Barley Genet Newslett* 32:49–77

Jackson SA, Wang ML, Goodman HM, Jiang JM (1998) Application of fFiber-FISH in physical mapping of *Arabidopsis thaliana. Genome* 41:566–572

Jiang J, Hulbert SH, Gill BS, Ward DC (1996) Interphase fluorescence in situ mapping: a physical mapping strategy for plant species with large complex genomes. *Mol Gen Genet* 252:497–502

Joppa LR (1993) *Chromosome Engineering in Tetraploid Wheat. Crop Sci* 33:908–913

Khush GS (1973) *Cytogenetics of Aneuploids.* Academic Press, New York, London

Mikhailova EI, Sosnikhina SP, Kirillova GA, Tikholiz O, Smirnov VG, Jones RN, Jenkins G (2001) Nuclear dispositions of subtelomeric and pericentromeric chromosomal domains during meiosis in asynaptic mutants of rye (*Secale cereale* L.). *J Cell Sci* 114:1875–1882

Murata M, Nakata N, Yasumuro Y (1992) Origin and molecular structure of a midget chromosome in a common wheat carrying rye cytoplasm. *Chromosoma* 102:27–31

Painter TS (1934) A new method for the study of chromosome aberrations and the plotting of chromosome maps in *Drosophila melanogaster. Genetics* 19:175–188

Parker NR (1966) The four minute chromosome squash. *Turtox News* 46:242

Sax K (1939) An analysis of x-ray induced chromosomal aberrations in *Tradescantia. Genetics* 25:41–68

Sears ER (1966) Nullisomic-tetrasomic combinations in hexaploid wheat. In: Riley R, Lewis KR (eds) *Chromosome Manipulation and Plant Genetics.* Oliver and Boyd, Edinburgh, pp. 29–45

Sharma AK, Sharma A (1994) *Chromosome Techniques: A Manual.* Harwood Academic, Chur, Switzerland

Tsujimoto H, Yamada T, Sasakuma T (1997) Molecular structure of a wheat chromosome end healed after gametocidal gene-induced breakage. *Proc Natl Acad Sci USA* 94:3140–3144

Walling JG, Pires, JC, Jackson SA (2005) Preparation of samples for comparative studies of plant chromosomes using in situ hybridization methods. In: *Molecular Evolution: Producing the Biochemical Data, part B, Methods in Enzymology, vol. 395.* Elsevier, Amsterdam, pp. 442–459

Zhong X, Fransz PF, Wennekes-Van Eden J, Zabel P, Van Kammen A, De Jong H (1996) High-resolution mapping on pachytene chromosomes and extended DNA fibres by fluorescence in situ hybridization. *Plant Mol Biol Rep* 14:232–242

ERRATUM

Plant Cytogenetics

Hank W. Bass and James A. Birchler

H.W. Bass and J.A. Birchler (eds.), *Plant Cytogenetics*, Plant Genetics and Genomics: Crops and Models 4, DOI 10.1007/978-0-387-70869-0,

---

DOI 10.1007/978-0-387-70869-0_16

The publisher regrets that on the title page of the print and online versions of this book, Volume 9 is listed incorrectly. It should be listed as Volume 4.

Index

H.W. Bass and J.A. Birchler (eds.), *Plant Cytogenetics*, Plant Genetics and Genomics: Crops and Models 4, DOI 10.1007/978-0-387-70869-0,